

**TEXT FLY WITHIN  
THE BOOK ONLY**

**TEXT CROSS  
WITHIN THE  
BOOK ONLY**

UNIVERSAL  
LIBRARY

**OU\_164060**

UNIVERSAL  
LIBRARY









INTERNATIONAL SERIES IN PHYSICS

F. K. RICHTMYER, CONSULTING EDITOR

APPLIED X-RAYS

# INTERNATIONAL SERIES IN PHYSICS

F. K. RICHTMYER, CONSULTING EDITOR



*Bacher and Goudsmit—*

ATOMIC ENERGY STATES

*Clark—*

APPLIED X-RAYS

*Condon and Morse—*

QUANTUM MECHANICS

*Hardy and Perrin—*

THE PRINCIPLES OF OPTICS

*Hughes and DuBridge—*

PHOTOELECTRIC PHENOMENA

*Pauling and Goudsmit—*

THE STRUCTURE OF LINE SPECTRA

*Ruark and Urey—*

ATOMS, MOLECULES AND QUANTA

*Williams—*

MAGNETIC PHENOMENA





# APPLIED X-RAYS

BY

GEORGE L. CLARK, PH.D.

*Professor of Chemistry, University of Illinois*

SECOND EDITION

McGRAW-HILL BOOK COMPANY, INC.

NEW YORK AND LONDON

1932



COPYRIGHT, 1927, 1932, BY THE  
MCGRAW-HILL BOOK COMPANY, INC.

---

PRINTED IN THE UNITED STATES OF AMERICA

*All rights reserved. This book, or  
parts thereof, may not be reproduced  
in any form without permission of  
the publishers.*

THE MAPLE PRESS COMPANY, YORK, PA.

TO  
MY WIFE



## PREFACE TO THE SECOND EDITION

In the six years which have passed since the manuscript of the first edition of "Applied X-rays" was completed, the signs envisioned in 1926 of a rapid growth of pure and applied x-ray science have become accomplished facts beyond all expectations. A great group of earnest research workers all over the world has pushed out the boundaries of the science until these men themselves stand in wonderment at the progress which has been made.

Since 1926 physicists in their investigations among other phenomena of the origin of x-radiation have refined their measurements of wave lengths and energies until the Bohr theory, or in fact any mechanical model of the atom, no longer is adequate to account for experimental fact. X-ray tubes have been designed and operated successfully at millions of volts. Medical science, still confronted with the enigma of cancer, has improved vastly its knowledge, applications, and results with x-ray therapy, until the future seems certain to bring forth greater triumphs. Perhaps the branch which has made the greatest advance of all is the chemists' diffraction analysis of the fine structures of solid and liquid materials and the evolution of a new crystal chemistry scarcely dreamed of a few years ago. And industry—what has it done with a research tool which seemed promising but largely untried six years ago? No one can deny that x-ray testing and research have become important and often indispensable adjuncts to the programs of progressive industries. Baffling problems have been solved with the aid of the x-ray "supermicroscope"; improved quality of products and rational standardization of manufacturing processes have resulted; patents based on x-ray data have been issued. And yet all would agree that only the barest beginning has been made.

Confronted by such an extraordinary expansion in subject matter in a comparatively short time, it is self-evident that the task of revision resolved itself into one of a completely new creation. With the exception of a few paragraphs in the early chapters which could be retained, the book is entirely changed.

Material could be selected from a great fund of information, in contrast with the missionary effort in 1926. Lessons taught by the experimental first edition have enabled a more logical arrangement and presentation. And yet there have been retained the original plan and purpose of sketching the record of achievement and of depicting the promise for the layman in the industry and in the class room, while digging a little deeper than heretofore in the interest of clarity for the benefit of the inquisitive experimentalist in the laboratory. Again the treatment is suggestive rather than exhaustive. Several new and revised treatises on various phases of the science are now available, and from these valuable information and suggestions have been gained. A large number of original papers has been consulted. The author's series of papers on "X-ray Metallography in 1929" published in *Metals and Alloys*, and his chapter on "Some Practical Results of X-ray Researches on Colloids" in Alexander's "Colloid Chemistry," Vol. III, have served as the basis for the same topics in this book.

A list of those whose inspiration, encouragement, and suggestions have been of inestimable value in the preparation of this revision would be of formidable length. It was a fond hope of the author to include as a slight token of respect photographs of some of the great contributors to x-ray science, but regretfully on account of space limitations the plan could not be carried out. To Professor F. K. Richtmyer of Cornell University most grateful acknowledgment is given for his painstaking examination of the manuscript, his suggestions for improvement in Part I, which have been incorporated as fully as possible, and for the honor involved in his recommendation for the inclusion of this book in the International Series in Physics. Sincere thanks are due especially to graduate students at the University of Illinois, particularly Doctors Lucy Pickett, H. A. Smith, W. A. Sisson, K. E. Corrigan, and J. C. Zimmer, for their help in establishing new facts many of which are published here for the first time; to Misses Winifred Johnson, Frances Johnson, and Dorsie Baize, and Mrs. Edna Evans for efficient secretarial assistance; and to Mr. Paul Evans for his painstaking help in the preparation of illustrations and index.

GEORGE L. CLARK.

URBANA, ILLINOIS,  
September, 1932.

## PREFACE TO THE FIRST EDITION

The primary motive underlying the preparation of this book is the presentation of x-rays as a new tool for industry.

The thirty-year-old science of x-rays is now broadening from the stage of pure or academic science to that of applied or industrial science. It has already to its credit a notable record of practical achievement.

There are, therefore, several interwoven phases of the science of x-rays, none of which can be neglected in the consideration of practical applications. The spectroscopy of x-rays, involving the measurement of radiation wave lengths, has been of immeasurable assistance to the physicist in his searchings of atomic structures and of the interrelationships between matter and radiant energy. This phase of the science has found excellent expression in several books, particularly the authoritative exposition, recently translated into English, of the master experimenter and Nobel Prize recipient, Manne Siegbahn.

Scarcely more than twelve years ago, von Laue and the Braggs reasoned that the use of crystals should make it possible to measure wave lengths of x-rays, and hence that x-rays of known wave lengths might render possible the analysis of crystals of unknown ultimate structures. The complete verification of this prediction has led to the foundation of a chemical, physical, and engineering science of the solid state, which has yielded beyond all expectations exact knowledge of a previously little known subject. On this phase of the science of x-rays, again, excellent books have been written by the great pioneer Braggs, Ewald, Wyckoff, and others.

Now the science enters the industrial phase. This book aims to tell what this new tool is, how it may be used, what results it produces, why it can be applied to practical problems of everyday life and how industry is beginning to use it now. The book is the expression of a conviction that x-ray research and control methods can now and in the future be of invaluable service in the solution of problems of constitution and practical behavior of metals and alloys of every kind, of catalysts, textile fibers (cotton,

flax, jute, ramie, sisal, hemp, silk, wool, rayon), rubber, balata, gutta percha, resins, varnishes, lacquers, paints, pigments, dyes, enamels, carbon black, inorganic and organic chemicals, waxes, greases, soaps, oils, liquids of all kinds, dielectrics, storage battery oxides, colloidal metals and gels, patent leather, glass and its substitutes, gelatine, adhesives, abrasives, lime, plaster of paris, cement, ceramics, sugars, starches, biological systems, coal, gems, and numerous other substances.

I have tried to give the reader, whether he be the industrial executive or research director who is seeking to learn of a new method of attacking his problems, or the inquiring student or layman, a true and understandable survey of x-ray science as it is known to-day. This is not a handbook for the complete and precise determination by experts of wave lengths or crystal structures, but an outline of information for the intelligent inquirer who may himself never conduct a single x-ray experiment. I have hoped to make of it a missionary, which must speak an understandable language and have at hand the foundation facts to support its case.

The subject matter falls into a natural arrangement in three parts. The first eight chapters present the fundamental physics of x-rays; Chapters IX to XII cover the properties and applications of the radiation as such; the remaining chapters are concerned with the application to the study of crystalline structure.

Free usage has been made of most of the published books on x-rays. These include, besides those already mentioned, the excellent little monograph by Becker "*Die Roentgenstrahlen als Hilfsmittel für die Chemische Forschung*," Hirsch's "*Principles and Practice in Roentgen Therapy*," and the texts by de Broglie, Cermak, and Kaye. A large number of original papers, particularly the most recent contributions, have been consulted. Finally many experimental studies from my own laboratory, most of which have not been published, are included. The fact remains, of course, that in this rapidly growing science important advances have been made even during the preparation of the manuscript of this book.

I am deeply indebted, first of all, to Professor William Duane of Harvard University, pioneer and distinguished maker of light in the science of x-rays, whose inspirational guidance made possible an enthusiastic acquaintance with this research tool; also to Professors W. K. Lewis, R. T. Haslam, and W. G. Whit-

man of the Massachusetts Institute of Technology, who as engineers had the vision of x-rays in industry, and the faith to install an x-ray laboratory and to provide the facilities for the task of writing this book; to my able assistant in authorship, Mr. Robert Landis Hershey; to my associates in x-ray research, particularly Dr. R. H. Aborn, Mr. E. W. Brugmann, and Dr. Marie Farnsworth; to my friend, Mr. J. P. Kelley, author of "Workmanship in Words," who has generously examined the manuscript with a critical eye on its English; and to my wife for her never-failing encouragement and for her assistance in the reading of manuscript and proof.

GEORGE L. CLARK.

CAMBRIDGE, MASSACHUSETTS,  
*November, 1926.*





# CONTENTS

	PAGE
PREFACE TO THE SECOND EDITION. . . . .	vii
PREFACE TO THE FIRST EDITION. . . . .	ix

## PART I

### GENERAL PHYSICS AND APPLICATIONS OF X-RADIATION

#### CHAPTER I

X-RAYS, LIGHT, AND THE ELECTROMAGNETIC SPECTRUM . . . . .	3
---	---

#### CHAPTER II

THE GENERATION AND PROPERTIES OF X-RAYS . . . . .	9
---	---

#### CHAPTER III

X-RAY TUBES. . . . .	12
----------------------	----

#### CHAPTER IV

HIGH-TENSION EQUIPMENT . . . . .	40
----------------------------------	----

#### CHAPTER V

X-RAY SPECTRA. . . . .	49
------------------------	----

#### CHAPTER VI

CHEMICAL ANALYSIS FROM X-RAY SPECTRA. . . . .	82
---	----

#### CHAPTER VII

THE ABSORPTION AND SCATTERING OF X-RAYS. . . . .	91
--	----

#### CHAPTER VIII

RADIOGRAPHY. . . . .	108
----------------------	-----

#### CHAPTER IX

PHYSICAL, CHEMICAL AND BIOLOGICAL EFFECTS OF X-RAYS. . . . .	131
--	-----

## PART II

THE X-RAY ANALYSIS OF THE ULTIMATE  
STRUCTURES OF MATERIALS

## CHAPTER X

CRYSTALS AND X-RAY DIFFRACTION	171
--------------------------------	-----

## CHAPTER XI

EXPERIMENTAL X-RAY METHODS OF CRYSTAL ANALYSIS	185
--	-----

## CHAPTER XII

THE INTERPRETATION OF DIFFRACTION PATTERNS.	208
---	-----

## CHAPTER XIII

THE RESULTS OF CRYSTAL ANALYSIS: ELEMENTS AND INORGANIC COMPOUNDS	231
--	-----

## CHAPTER XIV

INORGANIC CRYSTAL CHEMISTRY: FUNDAMENTAL GEN- ERALIZATIONS FROM EXPERIMENTAL DATA	259
--	-----

## CHAPTER XV

THE STRUCTURE OF ALLOYS.	279
--------------------------	-----

## CHAPTER XVI

THE CRYSTAL STRUCTURES OF COMPOUNDS OF CARBON AND THEIR PRACTICAL SIGNIFICANCE.	307
--	-----

## CHAPTER XVII

THE INTERPRETATION OF DIFFRACTION PATTERNS IN TERMS OF GRAIN SIZE, ORIENTATION, INTERNAL STRAIN, AND MECHANICAL DEFORMATION	335
---	-----

## CHAPTER XVIII

PRACTICAL APPLICATIONS OF X-RAYS TO PROBLEMS OF METALLURGICAL INDUSTRY.	388
--	-----

## CHAPTER XIX

THE STRUCTURE OF COLLOIDAL AND AMORPHOUS MATERIALS AND OF LIQUIDS.	426
---	-----

## CHAPTER XX

THE STRUCTURE OF HIGHLY POLYMERIZED ORGANIC SUB- STANCES FOUND IN NATURE.	438
--	-----

INDEX.	463
--------	-----

**PART I**  
**GENERAL PHYSICS AND APPLICATIONS OF**  
**X-RADIATION**



## CHAPTER I

### X-RAYS, LIGHT, AND THE ELECTROMAGNETIC SPECTRUM

In 1895, during the course of some experiments with cathode rays, which are streams of electrons in evacuated tubes, Roentgen discovered the radiation which bears his name.<sup>1</sup>

The investigations of the discoverer and of other early experimenters demonstrated that there were certain striking similarities between these new rays and ordinary light.<sup>2</sup> Both x-radiation and light moved in straight lines, passed through space without apparent transference or intervention of matter, affected a photographic plate, excited fluorescence or phosphorescence in some substances, and ionized gases. Both were unaffected by electric or magnetic fields, indicating the absence of electric charges, and both exhibited polarization, or different properties in different directions at right angles to the line of propagation. Finally, convincing evidence was obtained, which has since been rigorously confirmed, that the velocities of the propagation of light and of x-rays were identical.

On the other hand, there were some respects in which x-rays and light seemed to differ. Roentgen and his contemporaries were unsuccessful in all their efforts to observe deflection of the new rays from mirrors, prisms, and lenses, to obtain diffraction by gratings, or to obtain double refraction and polarization in crystals. These phenomena in the case of light were, of course, well known. As a matter of fact, it has been within only a very few years that Duane and Patterson, A. H. Compton, Davis, Siegbahn, and others have demonstrated that x-rays may be

<sup>1</sup> The designation "x-rays" is now in more common usage among physicists and chemists in England, France, and America; but in medical science "Roentgen rays," "roentgenology," and similar terms are favored. Designation by the discoverer's name is practically universal in Germany.

<sup>2</sup> For an excellent account of the history of experimental discoveries which led to the discovery of x-rays and to the establishment of the nature of the radiation, see Wiltshire and Pullin, "X-rays Past and Present," D. Van Nostrand Company, New York, 1927.

totally reflected at very small glancing angles from mirrors, refracted in prisms, and diffracted by finely ruled parallel lines on glass or speculum metal.

According to the classical theory, derived largely by Maxwell, light consists of waves of electromagnetic origin which are propagated in the ether. Maxwell conceived of an electric field whose intensity or direction might vary periodically so as to create waves. Since action at a distance between electric charges is not instantaneous, these waves can be produced by giving an electric charge a rapid oscillatory motion. Each of these electric waves must be accompanied by a magnetic wave propagated with the same velocity; the periodically variable electric and magnetic fields must be perpendicular to each other and to the direction of propagation; hence, transverse. But such a condition is actually found in light waves, which are, therefore, electromagnetic waves. As an experimental verification, Hertz, by using oscillating electric discharges, was able to produce waves similar to light, in that they could be reflected, refracted, diffracted, and polarized. Thus all radiation throughout the spectrum finds its origin in what may be termed the unrest of electric charges.

In 1912, Laue, reasoning from the electromagnetic-wave theory, predicted that x-rays should be diffracted by crystals, which serve as three-dimensional gratings, just as light is diffracted by the finely ruled lines of an ordinary optical grating, which is essentially two-dimensional. The complete experimental verification of this prediction established beyond question the identical nature of x-rays and light. They are distinguished only by the fact that x-rays have a wide range of wave lengths shorter than those of light. Table I shows that the known x-ray range lies between 0.06 A.U., or even shorter, and 1019 A.U., thus overlapping the ranges of both  $\gamma$ -rays and ultraviolet rays. In the laboratory for crystal analysis an average wave length employed is 1 A.U. or a value about one six-thousandth the wave length of yellow light in the visible region. Not only are light and x-rays thus closely related, but also included in the electromagnetic spectrum are the  $\gamma$ -rays from radioactive disintegrations, possibly the cosmic rays, which, if they are finally proved to be like light rather than high-speed electrons, should have the shortest wave lengths thus far recognized, the ultraviolet rays, which are just shorter than visible light, the infrared or heat rays,

the long range of radio or Hertzian waves, and finally the very long electric waves such as are associated with alternating currents. All of these waves, seemingly so different in properties and produced by such vastly different methods, are actually identical in every respect except length. All have the same velocity of propagation, namely, thirty billion centimeters per second.

The spectrum of electromagnetic waves is presented in Table I. The ranges in octaves and in Ångström units (one Ångström unit, A.U., =  $10^{-8}$ , or one one-hundred-millionth of a centimeter)<sup>1</sup> and brief statements of the methods of generation and detection are included in this table.

The simple facts of the fundamental mutual similarity of electromagnetic waves and of the essential difference only in wave length suggest immediately the general practical properties and the uses which may be made of x-radiation of average wave length as compared with ordinary light. Since their wave lengths  $\lambda$  are so much shorter, or their frequencies  $\nu$  greater ( $\lambda = c/\nu$ , where  $c$  is the velocity of light), x-rays may be expected to penetrate materials which are opaque to light and to be intimately related to a far finer subdivision of matter than is possible for light waves. Even under the ultramicroscope the examination of matter with the aid of visible light rays can reach only a definite limit of size which is still far removed from that of the ultimate constituents. The ultraviolet microscope so successfully developed by Lucas<sup>2</sup> and by Barnard<sup>3</sup> discloses a fine structure which appears perfectly homogeneous under visible light rays, but here again a limit is reached. Beyond this, x-rays are able to take the investigator on to the ultimate molecules and atoms, even on to the universe within the atom, if he but interprets his information properly, the reason lying in the fact that in solid crystalline matter the spacings of the ultimate particles of mass (which may be ascertained from density, the molecular weight, and the mass of the hydrogen atom) are of the same order of magnitude as the wave length of the x-rays, namely,  $10^{-8}$  cm.

<sup>1</sup> Another unit frequently used for x-rays is 1 X.U. =  $10^{-3}$  A.U. =  $10^{-11}$  cm.

<sup>2</sup> An Introduction to Ultraviolet Metallography, *Pamphlet 1576E, Am. Inst. Mining Met. Eng.* (June, 1926), followed by several later publications.

<sup>3</sup> For the Beck-Barnard microscope and its use see Martin, *J. Roy. Soc. Arts*, **79**, 887 (1931); Wyckoff and Ter Louw, *J. Expt. Med.*, **54**, 449 (1931).



TABLE I.—RANGE OF ELECTROMAGNETIC WAVES

Type	Occur- ances	Wave length range in A.U. (1 A.U. = $10^{-8}$ cm.)	Generation	Detection
Cosmic <sup>1</sup> .....	..	0.00008—?	Cosmic condensa- tion of 4 H to 1 He and atomic syn- thesis in depths of space. (Millikan.)	Observed day and night. Uniformly in space. Pene- trate 18 ft. of lead. Discharge electro- scopes.
$\gamma$ -rays.....	..	0.01–1.4 0.06–0.5 used in radiology	Emitted w h e n atomic nuclei dis- integrate (radio- activity).	As for x-rays, but more penetrating.
X-rays.....	14	0.06–1019	Emitted by sudden stoppage of fast moving electrons.	a. Photography. b. Phosphorescence. c. Chemical action. d. Ionization. e. Photoelectric ac- tion. f. Diffraction by crystals, etc.
Ultraviolet rays...	5	136–3900	Radiated from very hot bodies and emitted by ionized gases.	Same as x-rays a to c; reflected, re- fracted, and dif- fracted by finely ruled gratings.
Visible rays.....	1	3900–7700 Violet 3900–4220 Blue 4220–4920 Green 4920–5350 Yellow 5350–5860 Orange 5860–6470 Red 6470–7700	Radiated from hot bodies and emitted by ionized gases.	Sensation of light; same as ultraviolet rays.
Infrared rays.....	9	7700– $4 \times 10^6$	Heat radiations.	Heating effects on thermocouples, bolometers, etc. Rise in tempera- ture of receiving body. Photog- raphy (special plates). Reflected, refracted, dif- fracted by coarse gratings.
Solar radiation....	..	Limiting wave lengths reaching earth 2960–53000		
Hertzian waves...	28	$1 \times 10^8$ to $3 \times 10^{14}$		
Short Hertzian....	17	$1 \times 10^6$ to $1 \times 10^{11}$	Spark-gap discharge oscillating triode valve, etc.	Cocherer. Spark across minute gaps in resonant receiv- ing circuit. Re- flected, refracted, diffracted.
Radio.....	11	$1 \times 10^{11}$ to $3 \times 10^{14}$	Same.	Cocherer. Con- version to alternating current. Recti- fication with or without heterodyn- ing and production of audible signals.
Broadcasting band	..	$2 \times 10^{12}$ to $5.5 \times 10^{12}$		Mechanical. Elec- trical. Magnetic. Thermal effects of alternating cur- rents.
Electric waves....	..	$3 \times 10^{14}$ to $3.5 \times 10^{16}$	Coil rotating in magnetic field.	

<sup>1</sup> Measurements by A. H. Compton during the summer of 1932 in various parts of the world seem to prove that cosmic rays are more intense the nearer to the earth's magnetic poles, the higher the altitude, and in daytime as compared with night. The conclusion is that cosmic rays are high-speed electrons and not rays similar to light. The theory also has been advanced that they are streams of neutrons, or particles formed from closely coupled positive and negative charges. Future progress in experimental measurements alone can settle finally the question of the nature of these rays.

In the consideration of radiation as continuous electromagnetic waves in the ether, the fact must not be dismissed that radiation also appears to be propagated in discontinuous bundles or quanta in accordance with the laws first enunciated by Planck more than a quarter century ago. In diffraction, refraction, polarization, and in phenomena involving interference, x-rays, together with all other related radiations, appear to act as waves, and  $\lambda$  has a real significance; in other phenomena, such as the appearance of sharp spectral lines and of a definite short wave-length limit of the continuous spectrum, such as the shift in the wave length of x-rays scattered by electrons in atoms, and such as the photo-electric effect, the energy seems to be propagated and transferred in quanta defined by the values of  $h\nu$ , where  $h$  is the Planck action constant, and  $\nu$  the frequency of the rays. Such a corpuscle or quantum is called a *photon*.

Radiation, however, is not alone in displaying these dual properties. Electrons long considered to be definitely corpuscular were shown first by the Americans Davisson and Germer in 1927 and later by G. P. Thomson, Rupp, and others to possess definite wave properties in that they could be diffracted by crystals in very much the same way as x-rays. The electron diffraction patterns for metal foils, for example, are formed of concentric rings just like the familiar Debye-Scherrer x-ray powder photographs, and diffraction by single crystals is observed just as it is for x-rays. From the positions of the diffraction interference maxima and the lattice spacing of the crystal it is possible to deduce the wave length of the waves causing them; this is in agreement with the theoretical expression due to de Broglie,  $\lambda = h/mv$ , where  $h$  again is the Planck constant always associated with quanta,  $m$  the mass, and  $v$  the velocity of the electron. Hence electrons behave as though guided by a train of waves. Another triumph was registered in 1930 when Dempster proved that hydrogen atoms are diffracted by crystals, so that even the combination of a proton and electron constituting the corpuscular atoms acts as though guided by a train of waves. The dual aspect of the ultimate building stones of the universe as waves and particles must, therefore, be very fundamental, although it is obviously impossible to construct a satisfactory model of electrons, radiation, or atoms. Sir William Bragg has indicated the situation in stating that we may consider these as particles on Monday, Wednesday, and Friday and as waves on Tuesday,

Thursday, and Saturday. The mathematics of the new quantum and wave mechanics so wonderfully developed by de Broglie, Born, Heisenberg, Schrödinger, Dirac, and others is alone adequate to define the atom, the electron, and radiation. Meanwhile the astronomer studies the universe of stars and suns and planets by the radiation which they emit or reflect; the physicist assigns energy levels to the electrons in the atom from a study of the radiation emitted or absorbed characteristically by the atom; the physician uses radiation to diagnose and cure disease; the biologist applies it as a vital principle in life processes; the chemist uses it to disclose the mysteries of matter and to institute chemical change; industry accepts ultraviolet rays and x-rays as great new tools of practical value; distance and isolation upon the earth are annihilated by long-wave radiation. By their own radiations and by means of radiation are all things in the universe bringing themselves to the knowledge of men.

## CHAPTER II

### THE GENERATION AND PROPERTIES OF X-RAYS

**Cathode Rays.**—The complex phenomena involved in the conduction of electricity through gases were recognized for half a century before the discovery by Roentgen of x-rays. In 1859, Plücker discovered that in a highly evacuated glass tube fitted with two metal electrodes “cathode rays” proceed in straight lines from the negative electrode or cathode. Hittorf made further advances in 1869. These rays produced fluorescence in the glass walls; they were intercepted by obstacles which cast a shadow, and they were deflected by electric and magnetic fields. Crookes believed that the rays consisted of negatively electrified particles. J. J. Thomson proved this to be the case, and found in addition that each of the particles, or electrons, as they came to be known, had a mass about one eighteen-hundredth as great as that of the hydrogen atom.

The existence of electrons as the units of negative electricity has now been established as a fact by such classic researches as those of Thomson, Rutherford, and Millikan, the latter of whom by means of measurements with minute oil droplets determined the unit charge of the electron to be  $4.774 \times 10^{-10}$  electrostatic units. Cathode rays, or streams of rapidly moving electrons, are always identical, regardless of the kind of gas or of the material of the cathode. This is but one of the evidences that electrons are a fundamental constituent of all matter and of atoms. They are spontaneously emitted by the radioactive disintegrations of heavy atoms and are called  $\beta$ -rays. They are liberated as photoelectrons under proper conditions when radiant energy—visible light, ultraviolet rays, x-rays, etc.—impinges upon matter. Glowing-hot wires produce thermionic emission of electrons; heated gases dissociate into electrons and residual ions; free electrons course through metallic conductors as a flow of electric current.

Lenard, in 1894, succeeded in bringing cathode rays out of the discharge tube through thin foil windows into the outside air.

The success of the cathode-ray tube perfected by Dr. W. D. Coolidge has led to a great increase in knowledge of the physical, chemical, and biological effects of these rays. Finally the discovery by Davisson and Germer in 1927 of diffraction of cathode rays by crystals proved that the difficulties of physics in the earlier years of this century were due to ignorance of the dual particle and wave aspects of electrons as well as light.

**Generation of X-rays.**—X-rays are emitted whenever matter is bombarded by cathode rays; in other words, the sudden stoppage of swiftly moving electrons by the atoms of matter is accompanied by the generation of x-rays. In addition to this process it will be shown that under certain conditions primary x-rays will themselves generate secondary x-rays upon being absorbed in matter. The essential parts of an x-ray generating apparatus are, therefore, (1) a source of electrons proceeding from a cathode, (2) a target or anticathode or anode in the path of the cathode-ray stream, and (3) a means of applying a potential difference between the cathode and the target which will accelerate the electrons to the requisite velocity during passage across the intervening space.

**:The Properties of X-rays.**—Many of the properties of x-rays are mentioned in Chap. I. For the purpose of a general summary of these and as an introduction to other properties which will be discussed in detail in later chapters, the following tabulation, essentially in the chronological order of discovery, will suffice.

X-rays, then, are:

1. Invisible, and pass through space without transference of matter.
2. Propagated in straight lines.
3. Unaffected by electric or magnetic fields; hence non-electrical in nature.
4. Reflected, diffracted, refracted, and polarized just as is light.
5. Propagated with a velocity of thirty billion centimeters per second, as is light.
6. Transverse electromagnetic vibrations.
7. Characterized by wide range of wave lengths (approximately 0.01 to 1000 A.U.).
8. Produced by the impact of cathode rays upon matter.
9. Capable of blackening the photographic plate.

10. Capable of producing fluorescence and phosphorescence in some substances and of coloring some stones and minerals.

11. Able to ionize gases and to influence the electrical properties of liquids and solids.

12. Differentially absorbed by matter.

13. Able to liberate photoelectrons.

14. Capable of acting photochemically, of activating catalysts in some cases, and of flocculating colloids.

15. Able to stimulate or to kill living matter.

16. Emitted in a continuous spectrum, whose short wavelength limit is determined only by the voltage on the tube.

17. Emitted also with a line spectrum characteristic of the chemical elements in the anticathode.

18. Found to have spectra characteristic of the chemical elements and of three kinds—emission, absorption, and ionization.

19. Diffracted by crystals acting as gratings in accordance with the fundamental equation  $n\lambda = 2d \sin \theta$ , to which a correction for refraction must be applied for very accurate work.

20. Diffracted by optical gratings and totally reflected at very small glancing angles.

21. Found to act in interference and related phenomena as waves; but in other phenomena as discrete quanta of energy which may be scattered by single electrons.

## CHAPTER III

### X-RAY TUBES

There are two general types of x-ray tubes which fulfil the requirements for generation outlined in the previous chapter. In the first type, the so-called gas or ion tubes, the residual gas plays an important part; in the second or electron type the tubes are exhausted of gas to such an extent that no discharge takes place when a large difference of potential is applied.

X-ray tubes are also classified according to the use to which they are put, which in turn depends upon the penetrating quality of the rays and the applied voltage.

TABLE II.—CLASSIFICATION OF X-RAY TUBES

Class	Type	Kilovolts
1. Special high-voltage tubes	Electron	3000 (Lange and Brach)
2. Deep therapy	Electron	Average 160 to 400
3. Industrial radiography	Electron	100 to 300
4. Diagnostic	{ Electron	Average 50 to 110
	{ Ion	
5. Diffraction	{ Electron	Average 25 to 50
	{ Ion	
6. Superficial therapy or Grenz ray	{ Electron	Average 10
	{ Ion	

**Gas Tubes.**—The gas tubes were the first to be developed for practical use. They still find wide application both for medical and for purely scientific purposes, but the electron tubes now in operation undoubtedly far outnumber the older type. In the gas tube, the gas molecules are split up into electrons and residual ions when the voltage is applied. These positive ions are then hurled against the cathode by the electric field, so that electrons are set free in the bombardment. The cathode-ray stream thus generated bombards the positive electrode, or anticathode, and the x-rays are produced.

The cathode-ray tube used by Roentgen in the discovery of x-rays is diagrammatically represented in Fig. 1. A flat disk served as cathode and the cathode rays impinged upon the opposite glass wall with the production of strong fluorescence, while the new rays passed through the glass. It is not surprising that it was thought that the source of the new rays resided in the fluorescence until Becquerel proved that this was not the case. The result of Becquerel's study was the discovery of radioactivity in 1896, only two months after Roentgen's discovery. Roentgen very soon constructed a tube with a special anticathode of platinum and a concave cathode for focusing the electron

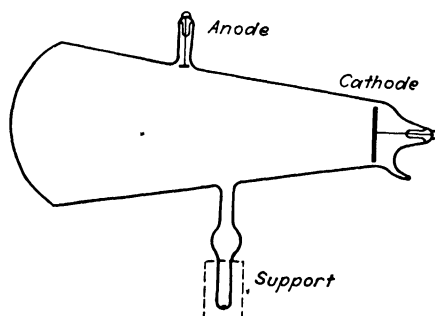


FIG. 1.—Diagram of cathode-ray tube used by Roentgen in the discovery of x-rays.

stream. Other tubes had both an anode and an anticathode bound together, with the idea that greater stability and less pitting of the anticathode would be attained.

At the present time, several manufacturers in the world still supply ion tubes of similar design, with sharp focus for medical diagnosis and for superficial therapy: the General Electric X-ray Corporation in America, Gundelach in Thüringen, C. H. F. Müller in Hamburg, Phoenix (Siemens-Reiniger-Veifa) in Thüringen, Radiologie A. G. in Berlin, Gaiffe, Gallot and Pelon in Paris, Cossor in London, and others. Some water-cooled tubes may be operated at 25 ma. for harder rays and 40 to 50 ma. for softer. Others with special radiation cooling of both electrodes may be operated momentarily up to 150 ma. The fact remains, however, that for medical purposes the electron type tube has displaced practically completely the ion tubes, largely because the former are free from complications and from the dependence of intensity and quality of the x-rays.



The older varieties of the ion tube were provided with a device with which it was possible to add small amounts of fresh gas. The "hardness" of the x-ray tube (by which is meant the penetrating quality of the x-rays produced) is determined by the amount of the residual gas, since the lower the gas pressure, the higher the voltage required for production of x-rays. During operation the hardness of the tube increases as the amount of the available gas diminishes owing to adsorption on the glass walls, etc. Consequently, in order to maintain constancy, gas must be admitted by diffusion through thin metal, or by heating or passing a spark through a small cylinder of some substance in a side tube.

Very recently, several modifications of the old gas-type tube have been made in Europe and America with such success that for many types of investigations of x-ray spectra and crystal structure these are competing favorably with the electron tubes. Seemann, Shearer, Hadding, Siegbahn, Müller, Wever, Becker, Wyckoff, and others have constructed tubes largely of metal, with interchangeable targets (iron, copper, and molybdenum usually), thin foil windows, water cooling, and permanent connections with vacuum pumps by means of which the gas pressure may be readily regulated thus eliminating special devices for controlling hardness. These tubes are very simple and rugged and may be operated with such large energy that the time of photographic exposures is greatly reduced from that normally required.

Another advantage of great importance for precise spectroscopic and diffraction work is the purity of the spectrum, since it has been found easier to build a controllable gas tube than to prevent tungsten (from the hot-cathode filament) sputtering in one of the electron type.

Probably the most familiar of the gas-type tubes for diffraction is the so-called Hadding-Siegbahn metal tube. Figure 2 shows this tube diagrammatically and Fig. 3 shows such a tube produced by the firm of Seemann. The body of the tube is entirely of metal, which permits self-protection for rays except as they pass through windows of thin foil. The entire metal part and the target are grounded and connected directly with the water mains for cooling. The cathode of aluminum, which is at high potential, is insulated through a porcelain cylinder. This cathode may be cooled with an insulated water or oil circulating system or simply by blowing compressed air through the cooling system. Tubes of this type, particularly for operation with copper targets

when long wave lengths are required, have been in successful operation in the writer's laboratory for many years. A recent improvement in the Hadding-Siegbahn tube as manufactured by Leiss is to be found in interchangeable cathodes for operation

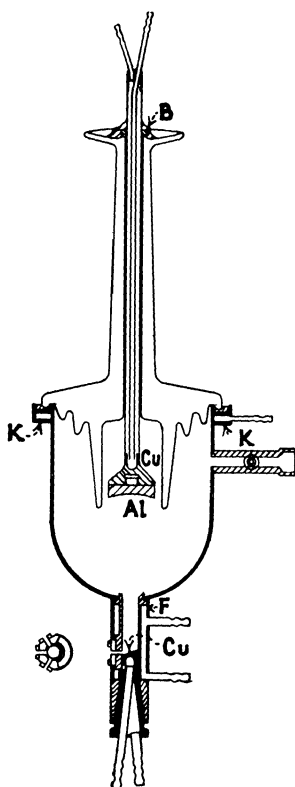


FIG. 2.—Diagram of Hadding-Siegbahn gas-type x-ray tube used in crystal analysis.

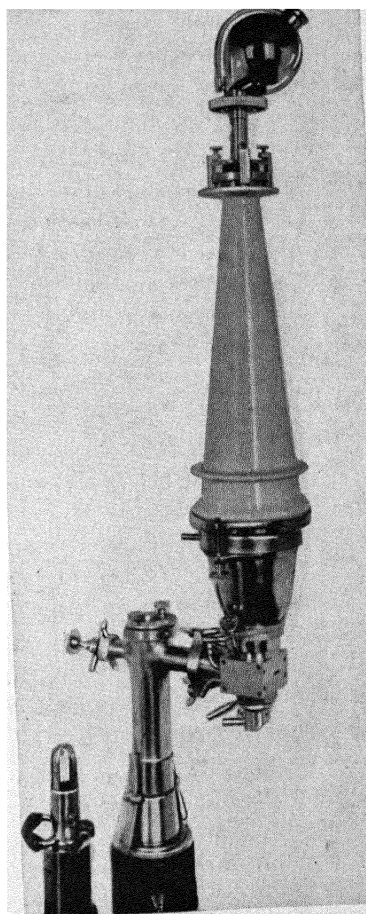


FIG. 3.—Seemann gas-type tube.

as either ion or electron tube, and a whole series of interchangeable metal targets. Four sheets of metal are mounted on the four sides of a hollow copper rod with square cross section. By rotating the rod 90 deg. the various targets may thus be brought into alignment with the cathode. A needle valve is built in as an

integral part of the tube. These tubes are ordinarily used with rectified high-tension current. Some of these tubes are so designed and operated that they are self-rectifying just as electron tubes may be, the most familiar being the Shearer tube.<sup>1</sup> A similar but even simpler and very efficient self-rectifying gas

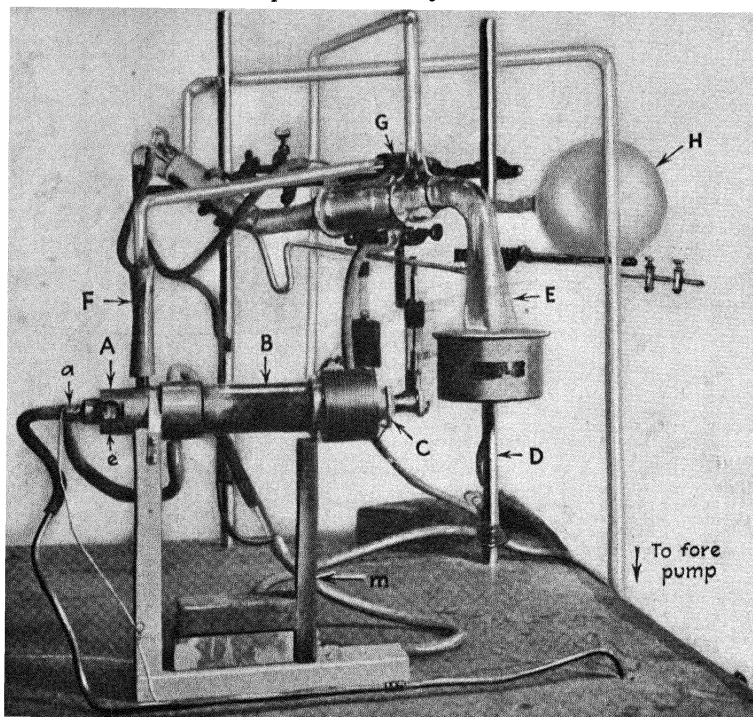


FIG. 4.—Wyckoff-Lagsdin gas-type tube with evacuative and regulative system. A, anode; B, glass tube connecting and insulating two ends (4 in. for voltage up to 40,000); C, cathode with fins for air cooling; a, interchangeable target; e, thin foil window for x-ray beam; D, automatic regulator; E, mercury diffusion pump; F, G, rubber connections for leakage; H, flask for increasing volume of system.

tube is that designed by R. W. G. Wyckoff and used almost exclusively at the Rockefeller Institute for Medical Research for biological, chemical, and physical investigations. It has also been found very satisfactory in the writer's laboratory for many purposes, particularly for long wave-length studies. Figure 4 shows the assembly of the tube and the evacuating system.<sup>2</sup>

<sup>1</sup> Manufactured by A. Hilger, London.

<sup>2</sup> WYCKOFF and LAGSDIN, *Radiology*, **15**, 42 (1930).

For continuous operation over many hours such as is desirable in diffraction work, a suitable automatic regulator of gas pressure

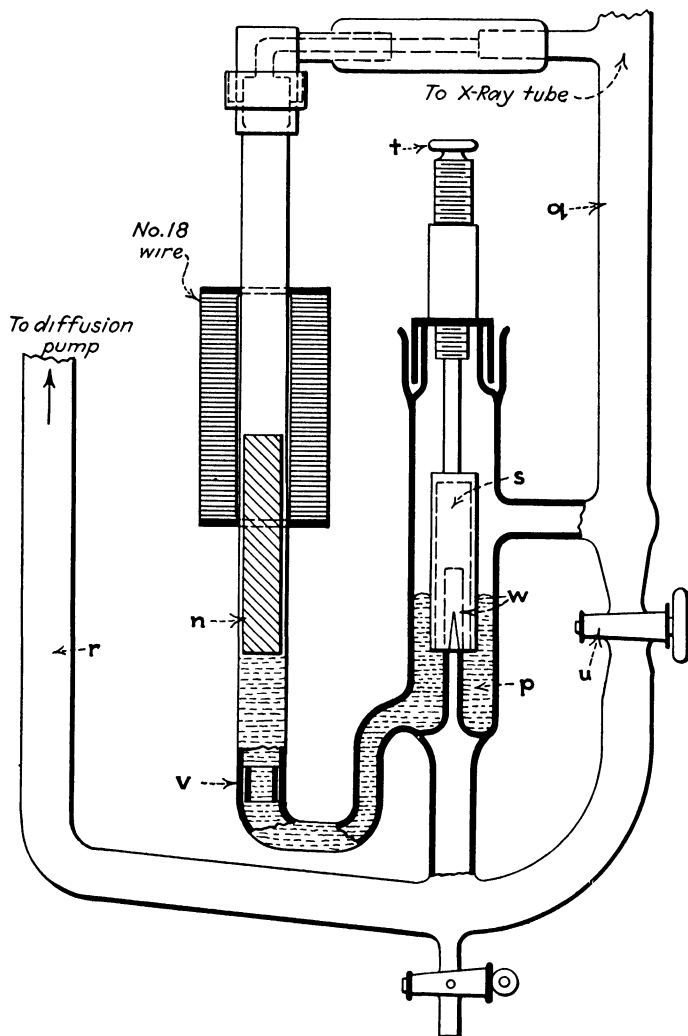


FIG. 5.—Detail of gas pressure regulator *D* of Fig. 4. Automatic regulator for gas-type tube. When the iron core *n* floating on mercury is lifted by the solenoid, the mercury level in *p* drops and connection is established between *q* and *r* through slots *w*. Adjustment is made by raising or lowering *s* and by altering the current through the solenoid.

(and thus of operation) is valuable. Such a regulator constructed by Wyckoff and Lagsdin and embodying the best features of

earlier models is shown in Fig. 5 with the circuit for operation in Fig. 6.

**Electron Tubes.** *The Coolidge Tube.*—In the electron-type tube it is necessary to have an independent source of electrons, since there is insufficient gas present to enable passage of the current. For an x-ray tube to operate with a pure electron discharge it is necessary to evacuate to the highest attainable vacuum, usually 0.01 bar or  $0.0075\mu$  of mercury. These electrons may be supplied by application of the Edison effect, *i.e.*, emission from a hot-wire cathode, or by oxides heated on the cathode, by

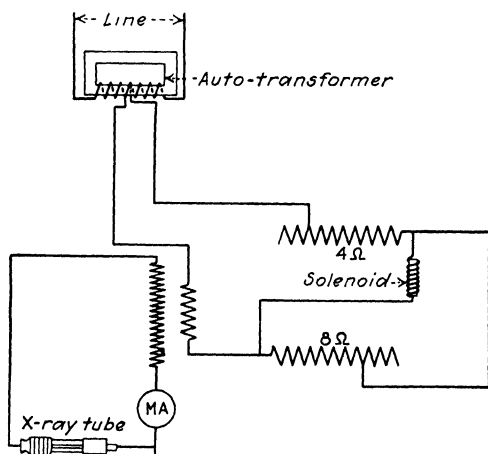


FIG. 6.—Electrical circuit suitable for the operation and control of a gas-type x-ray tube.

illumination of the cathode by ultraviolet light, or by Lilienfeld's autoelectron-emission method. The first of these is the basis of the very familiar Coolidge tube which is now being manufactured on a large scale for deep therapy, diagnosis, diffraction analysis, and superficial therapy. The original Coolidge tube consisted of a glass bulb into which were sealed a solid metal target and a spiral of tungsten wire backed by a focusing shield of molybdenum as cathode. The emitting wire was 0.216 mm. in diameter, 33.4 mm. long, and wound in a flat spiral of  $5\frac{1}{2}$  turns with a diameter of 3.5 mm. The spiral is heated to incandescence by a current of 3 to 5 amp. at 1.8 to 4.6 volts supplied in an independent circuit from storage batteries or step-down transformers. Under these conditions the wire has a temperature of 1890 to 2540° Abs. Electrons are liberated, and upon application of voltage to the

terminals of the x-ray tube they are drawn across to the target. The ordinary commercial Coolidge tubes are usually supplied with tungsten or molybdenum targets. In the "universal" type the target is not cooled and becomes white hot.

Most of the electrons in the bundle of cathode rays strike a limited portion (1 sq. cm.) of the target called the focal spot which is usually visibly defined as a pitted or etched area on the target face. The size of this spot is determined by the position of the filament in a cylindrical focusing shield of sheet molybdenum.

The necessity for cooling the target is explained by the following example: at 200 kv. and 3 ma. the kinetic energy of the electrons, which have a velocity of 220,000 km. per second as they strike the target, is transferred to the target at the rate of 150 cal./sec., or enough energy in 10 min. to raise a liter of water from 10° C. to boiling. Only about 2 per cent of this energy is transformed to x-radiation and the remaining 98 per cent goes into heat.

Obviously only metals can be used which will not melt under these conditions. In order that the energy may be dissipated, special radiators for air cooling are fixed on the end of the target arm; for continuous operation and for loads above 1 kw., water cooling of the target is resorted to. When the temperature of the target is maintained below that at which thermionic emission occurs, the terminals of the high-tension transformer producing low or moderate alternating voltages may be attached directly to the Coolidge tube, for it is then self-rectifying. Current will flow only during the half-time period during which the hot wire is negatively charged with respect to the target. If the target is at a sufficiently low temperature (during the time it is negative), there are no electrons available for the reverse current.

One great advantage of the Coolidge tube is the independence of the current through the tube and the voltage. One may be altered without affecting the other, while in gas tubes it is obvious that the number of the electrons and, hence, the current will increase with the voltage. The current in the electron type depends upon the number of electrons  $N$ , and this in turn depends upon the temperature of the hot-wire filament, by the Richardson relationship  $N = CT^2e^{-d/T}$ , where  $C$  and  $d$  are constants depending upon the metal ( $1.86 \times 10^{11}$  and  $4.95 \times 10^4$ , respectively, for tungsten), and  $T$  is the absolute temperature. On account of the building up of a space charge, since the tube current does

not increase so rapidly as does the number of electrons when the temperature of the filament is increased but the voltage held constant, a maximum or saturation current is reached at a point expressed by the equation deduced by Langmuir,

$$i_{\max.} = \frac{\sqrt{2}}{4\pi} \sqrt{\frac{e}{m}} \frac{V^{3/2}}{x^2}.$$

Here  $e$  and  $m$  are the charge and the mass of the electron,  $V$  the voltage, and  $x$  the distance between electrodes. This relationship has enabled investigators to predict correct design for tubes.

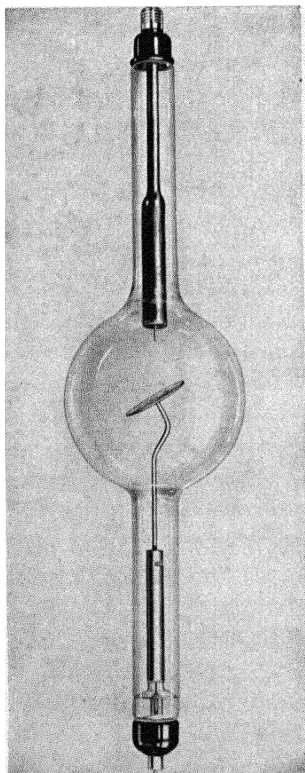


FIG. 7.—Deep-therapy tube of conventional design with thin plate target (Westinghouse).

from development of gas during operation and large currents begin to pass. Even if the operation is normal, however, with good care there is a limit to the life. The glowing filament

**Deep-therapy Tubes.**—Most of the tubes designed for deep therapy to operate up to 220 kv. under ordinary conditions retain the original Coolidge features, namely, glass bulb, spiral filament, and massive tungsten target. Thin plate targets enabling more rapid dissemination of heat are a more recent development (Fig. 7). Some prominent manufacturers are the General Electric X-ray Corporation, Westinghouse X-ray Company, Allgemeine Elektrizitäts Gesellschaft (A. E. G.) in Berlin, Phoenix in Thüringen, Radiologie A. G. in Berlin, Gaiffe, Gallot and Pelon in Paris. These tubes are pumped to the proper vacuum at the factory by the very special technique involving pumping, baking, and operation under increasing voltages in order to remove the gas which is occluded in metal parts.<sup>1</sup> Such tubes fail very often

<sup>1</sup> See TERRILL and ULREY, "X-ray Technology," pp. 49-54, D. Van Nostrand Company, New York, 1930.

vacuum tight and can be fused with glass. A photograph and diagram of a Metalix tube are shown in Fig. 9. These may be obtained in various sizes up to 240 kv. at 8 ma. with water cooling.

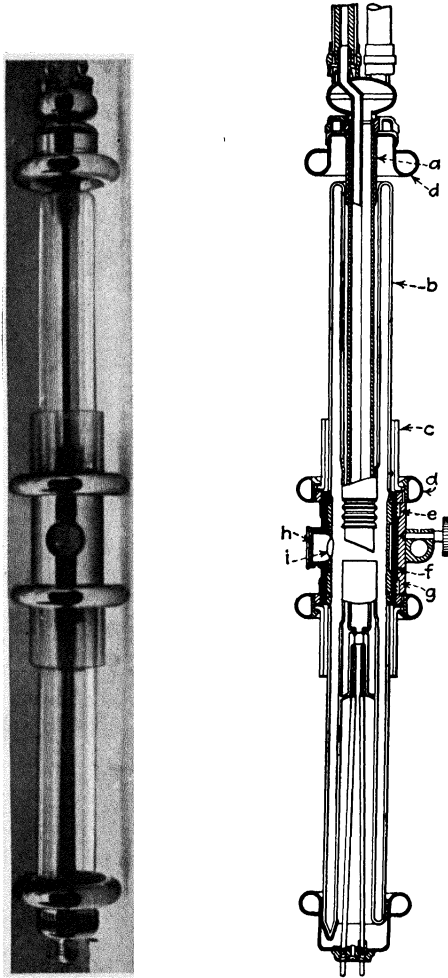


FIG. 9.—Photograph and diagram of construction of the Metalix tube, showing the central chrome-iron cylinder to which the glass anode and cathode arms are fused.

The familiar Müller Metwa therapy tube is similar to the Coolidge design except that the bulb is replaced by a chromium-steel cylinder. These tubes provide radiation in the desired direction only and require no special mountings and protection.



**Special Tubes for Very High Voltages.**—There are many points of interest in operating x-ray tubes at increasingly higher voltages. Since the effective wave length decreases as the voltage increases, the point might be reached where x-rays in the wave-length range of  $\gamma$ -rays or even cosmic rays might be generated with an output equivalent to thousands of grams of radium or with millions of times greater intensity than observed for cosmic rays. The advantage in therapy and in biological action is obvious, even supposing that the *kind* of biological action might be anticipated as independent of wave length. The intensity of radiation in the voltage range of modern deep therapy with usual filtration increases with a high power (at least third) of the voltage. The gain in intensity with mounting voltage and constant current makes possible material reductions in time of irradiation even with stronger filtration and increased distance from focal spot to patient, and a far higher percentage depth dose is attained. The physicist is also interested in the spectra of radiation excited at the highest attainable voltages and in the test of theories of atomic structure.

Serious difficulties have been encountered, however, in attempts to operate x-ray tubes of usual design at voltages very much higher than 220,000, not because power plants are not available, since 1,000,000 volts can easily be attained in commercial machines, but because of electrical phenomena within the tubes which prevent a satisfactory "life." In the first place the auto-electronic effect, or the release of electrons from metallic points or sharp edges in the electric field, produces a discharge in the tube operated above a critical voltage. Momentary currents of several amperes may pass, followed by high-frequency electric oscillations which may result in ruin of the transformer and of the x-ray tube, especially if the discharge strikes the glass walls. In less severe cases, the natural distribution of potential along the tube is affected and gas is liberated from the glass walls in certain areas. This difficulty may be counteracted, so that higher potentials may be applied safely, by careful rounding of the cathode.

The second group of phenomena which introduces difficulties is the back diffusion of electrons from the anode to the inner glass walls which become negatively charged. Next the outer glass wall becomes charged almost to the potential of the cathode, so that a high difference of potential is set up between the glass and

the anode. A stream of ions will travel from the anode, through the glass, then through the air to the metal anode cap. It has been demonstrated that gaseous electrolytic products are liberated as a result of the passage through the glass of the current, even though smaller than  $10^{-5}$  amp. The result again may be destructive discharge, depending on the potential and also the current. In order to avoid these effects so that a tube may

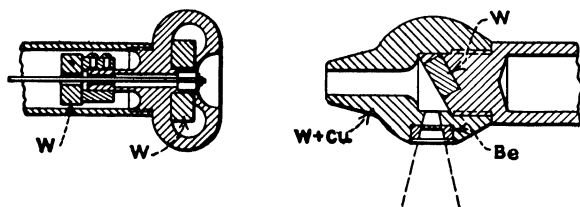


FIG. 10.—Design of electrodes in new 400-kv. deep-therapy tube (Siemens-Pantix).

operate with safety, the glass must be shielded from the secondary electrons.

A new commercial Siemens-Pantix deep-therapy tube just announced to operate at 400 kv. effective and 5 ma. embodies the rounded cathode and the shielded anode in a highly satisfactory manner.<sup>1</sup> The design of the electrodes is shown in Fig. 10, and

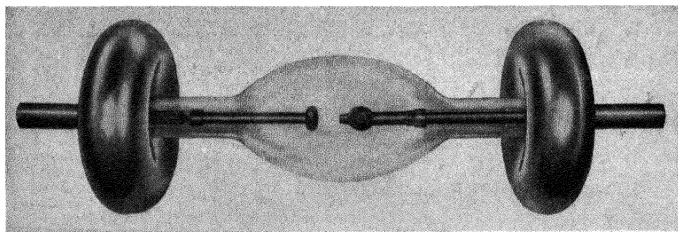


FIG. 11.—Siemens-Pantix 400-kv. deep-therapy tube with protective rings on caps.

the tube itself with protecting rings on the metallic caps is illustrated in Fig. 11. These rings involve the principle of a sphere-gap in which discharge takes place at higher potentials than between points (or small diameter caps) at the same distance. It is possible therefore to cut down the over-all length of the tube, particularly since the glass really serves as an insulator when the secondary electrons are screened off internally.

<sup>1</sup> MÜLLER and ZIMMER, *Fortschritte auf dem Gebiete der Röntgenstrahlen*, 45, 341 (1932).

Within the past year unusual interest has been aroused by the high-voltage tubes constructed by Lauritsen<sup>1</sup> at the California Institute of Technology (600,000 volts and one more recently to operate at 1,200,000 volts); by Coolidge<sup>2</sup> for the Memorial Hospital of New York (900,000 volts) operating by the cascade method (three steps of 300,000 volts each); by Tuve and associates<sup>3</sup> at the Carnegie Institution in Washington who used 15 cascades to attain nearly 2,000,000 volts; by Lange and Brasch<sup>4</sup> of Berlin (2,600,000 volts). The first three employed the usual principles of tube construction including hot-filament cathode, but with great length and special types of insulation with conducting rings. The German physicists succeeded in building a tube of alternate rings of paper, rubber, and aluminum which has been tested at 2,600,000 volts, continuing for an interval of a millionth of a second. Electrons are so speeded in this tube that they drill holes an inch deep in a brass plate. The x-rays produced penetrate lead a yard thick.

The new x-ray tube is less than a dozen feet long, despite the high voltage it withstands. It is estimated that an ordinary x-ray tube to withstand such voltages would need to be 50 ft. long.

In their work on the new-type x-ray tube Lange and Brasch discovered that the most effective tube is short and crooked, so as to break up surface leakage. For this reason they made the doughnut-like layers of paper insulation, rubber, and aluminum of different diameters inside.

Instead of using a hot-cathode source of electrons to be speeded up in the x-ray tube, the scientists actually obtained sufficient electricity for their purpose from a small porcelain tube, normally regarded as an insulator.

In Berlin a new 7,000,000-volt surge generator is being built to be used with a Lange-Brasch tube. This tube will be devoted to cancer research and physical experimentation. It is planned even to impress upon such a tube the high potentials of the natural electrical discharges in thunderstorms (these experimenters have already measured discharges in the mountains of 16,000,000 volts); if successful, there will be produced gamma rays

<sup>1</sup> *Phys. Rev.*, **32**, 850 (1928); **36**, 988, 1680 (1930).

<sup>2</sup> *Am. J. Roentgenology*, **19**, 313 (1928); **24**, 605 (1930).

<sup>3</sup> *Phys. Rev.*, **35**, 66, 1406 (1930).

<sup>4</sup> *Z. Physik.*, **70**, 10 (1931).

equivalent to a hundred thousand grams of radium, which is at least a thousand times as much radium as there is now available. When this experiment is performed, the super-x-rays obtained will equal the cosmic rays in penetration and the experiments projected should settle the question of the nature of the cosmic rays.

Spectra and biological effects from the 600,000-volt tube in Pasadena have thus far shown no unexpected or anomalous results.

**Fine-focus Tubes for Metal Radiography.**—For deep therapy a broad focus is usually desired but such a beam does not give good definition for photographic purposes. With the great increase in the industrial application of examining heavy metal castings, etc., for interior defects, high-voltage rays are required for penetration but with fine focus. The finer the focus (the smaller the focal spot), the more intense the localized energy effects in metal targets and the more serious the cooling problem becomes. Such tubes for metal radiography as a special class of the so-called deep-therapy division are now available for continuous operation at 240 kv. at 8 ma. The new 400-kv. tubes also should have excellent use in this field.

**Diagnostic Tubes.**—The essential attributes for this type of tube are as follows:

Very sharp definition of photographs or shadows of objects in the x-ray beam.

Fine focus (small focal spot).

Intermediate voltage (50 to 110), minimum wave lengths 0.25 to 0.11 A.U.).

Large currents for high intensity and greatest rapidity.

Coolidge concentrated the electron beam by means of a hemispherical shell of nickel about 25 mm. in diameter around the tungsten filament instead of the molybdenum cylinder used in deep-therapy and "universal" tubes. The anode was cooled either by radiation from external copper fins or by water cooling. The problem is, of course, the protection of the target while the largest possible current and the finest possible focus are maintained. The latest tube of conventional design for fluoroscopic work (Fig. 12) requires no radiator, since the target is a disk of tungsten with maximum surface.

The newest developments in construction of these diagnostic tubes, which apply also in general to the tubes used for diffrac-

tion with which this book is primarily concerned, may be summarized as follows:

1. Tubes of the usual Coolidge type with glass bulb and water or even radiator cooling through which currents of 150 ma. may be passed for 1 sec. are now fairly common (Fig. 13).

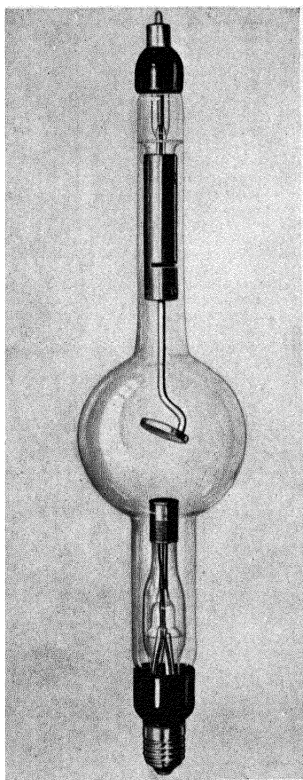


FIG. 12.

FIG. 12.—Fluoroscopic tube of conventional design (Westinghouse).

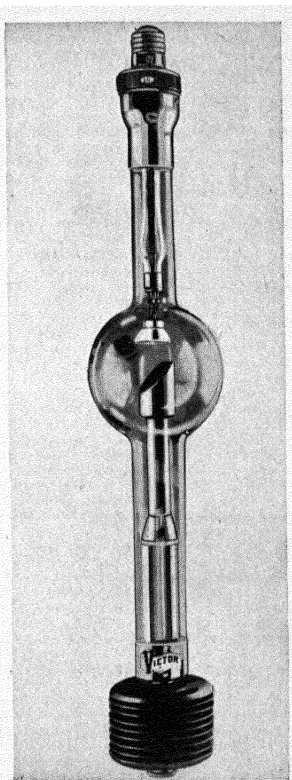


FIG. 13.

FIG. 13.—Air-cooled diagnostic tube (General Electric).

2. "Dofok" tubes (Phoenix tubes of Siemens-Reiniger-Veifa and also General Electric Coolidge tubes) have two hot spirals in the cathode, the one for fine focus and lower loads, the other for larger focus and higher loads.

3. Tubes with elongated focal spot for fine focus but high intensity. The desire to increase the load and intensity of x-radiation from such tubes in order to cut down exposure time to a minimum is opposed by the fact that greater energy input

in a small focal spot results in melting and destruction of the target. Increase in size of the focal spot in all directions causes diagnostic photographs to lose sharpness. Hence it is necessary to change the focus so that the cross section through the x-ray bundle at the focal spot is as small as possible. The line-focus filament of Goetze employed in the Media tubes of Müller is a successful solution. A long cylindrical spiral of very small

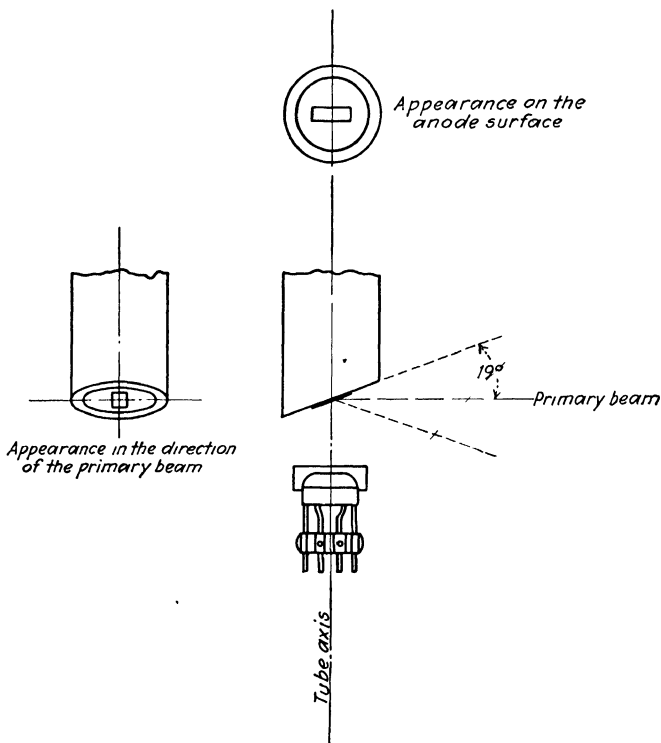


FIG. 14.—Diagram showing operation of a line-filament cathode.

diameter produces a line focal spot on the target which by virtue of length can take up a very considerable amount of energy without damage to the target. The face of the target is inclined at an angle of 71 deg. to the tube axis, so that the line focal spot in the principal direction of emergence of the x-rays appears shortened to a small point. The focal spot is actually about 2 mm. wide and 16 mm. long but from the front appears foreshortened to a spot 2 mm. square (Fig. 14). The 10-kw. Media

tube is rated at 250 ma. at 40 kv. effective for 1 sec. or 370 ma. at 40 kv. for 0.1 sec.

Another modification which serves a similar purpose is the oval focus of Kiesewetter. The "XP" General Electric tubes have a 20-deg. anode and an elongated focal spot as introduced by Benson in 1916.

4. Cone targets. For large current capacities but fine definition a Philips tube uses a target with cone-shaped hole. The filament is made of  $1\frac{1}{2}$  turns of wire and of sufficient diameter for x-rays to pass back through it. The electron stream is focused into the conical recess in the target with its larger surface but small effective focal spot.

5. Autofocus tubes of Müller are unique in that the focal spot automatically becomes larger as the current is greater. A small metal rod through the middle of the spiral filament is connected directly with the negative high-tension terminal, while the filament is connected through a high resistance so that the rod is always at negative potential to the filament. Depending upon this difference of potential determined by the tube current, the electrons will be repelled and thus increase the focal-spot area.

6. The rotating-anode tube (Philips Metalix) is a very recent and notable attempt to solve the problem of large energy input without damage to any one spot on the target. The anode, a heavy body of copper, forms the rotor of a small induction motor whose stator is a wound ring surrounding the tube. Anodes mechanically rotated through tight bearings have also been described.

7. Special tubes, particularly for dental radiography where they must be brought close to a patient or specimen, have the electrodes at right angles. Lead glass bulbs may have a window of ordinary glass opposite the target, and at 40 to 50 kv. this is sufficient protection.

8. Self-shielding tubes. For diagnostic purposes it is particularly desirable to eliminate the non-focal x-rays arising from portions of the anode outside of the focal spot and constituting 10 to 15 per cent of the beam. Coolidge was the first to solve the problem inside the tubes by surrounding the target with a molybdenum cylinder with two openings, one for the cathode rays and one for emergence of the x-rays. In this manner the diffuse cathode rays producing the extraneous rays were screened off and at the same time all the rays in directions other than that

desired. The target cap has been frequently used in commercial tubes. The General Electric X-ray Corporation self-shielding tube is rated at 100 ma. at 85 kv. for 10 sec. or 350 ma. at 55 kv. momentarily. Müller tubes are protected by an outer housing (Pertinax) and the rays emerge from a small window. The Philips Metalix tubes with chrome-steel cylinder and the Müller

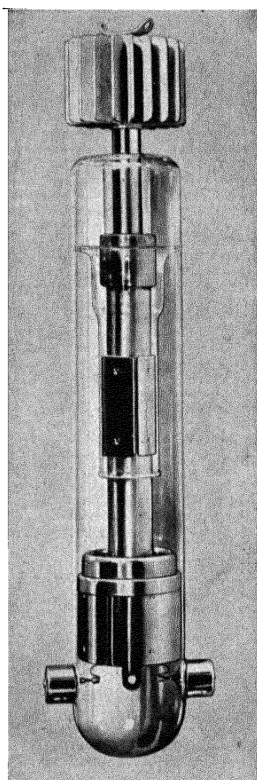


FIG. 15.

FIG. 15.—Photograph of new Westinghouse radiographic tube.

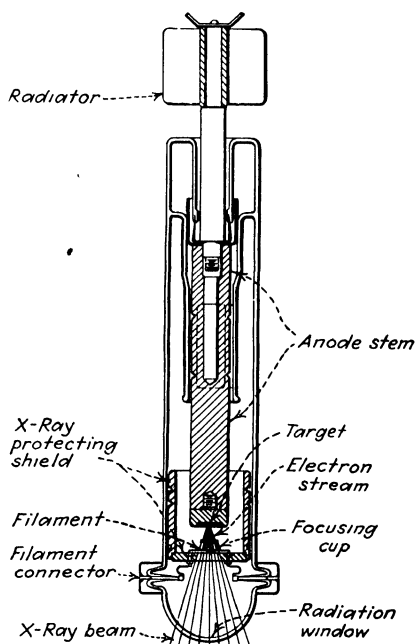


FIG. 16.

FIG. 16.—Diagrammatic construction of tube pictured in Fig. 15.

Media Metalix tubes are similar in design to the therapy tubes and are very successful for medical purposes. The new General Electric XP tubes have an independent cylindrical lead sheath and interchangeable water- and air-cooled radiators.

9. Helium- and neon-filled tubes. Following experiments by Janitsky, the Müller tubes of all varieties contain a small amount



of helium gas which is admitted after the tubes are exhausted and degassed. Westinghouse tubes contain neon. This gas, as well as helium, does not disappear upon operation of the tube like air and its high ionization potential prohibits action as an ion tube, while at the same time it permits pressure and operation to remain constant over long periods of time.

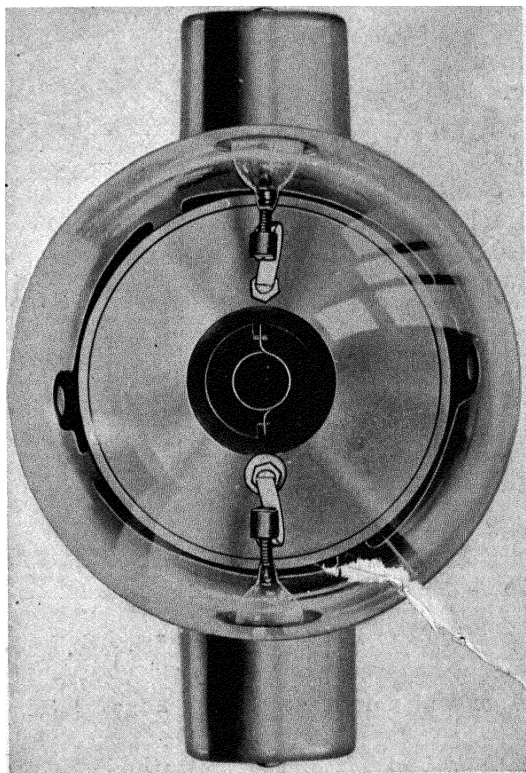


FIG. 17.—End window of Westinghouse radiographic tube showing ring filament through which x-rays from target pass.

10. "Gun"-type tubes. Westinghouse radiographic tubes have a unique construction in which the x-rays pass back through a ring filament and out of a window in the end of the tube, as illustrated in Figs. 15, 16, and 17. Pyrex glass is used throughout.

**Diffraction Tubes for Fine-structure Examination of Materials.** In this great new branch of x-ray science the diffraction of rays by a suitable grating is used as a means of discovering the ultimate fine structures of crystals and materials of all kinds.

While it was found that for determination of the gross structure of materials the medical deep-therapy or diagnostic tubes could be used, special attributes are desirable in tubes for studies of fine structure.

Moderate voltages, 25 to 50 kv.

Largest possible tube currents so as to cut down exposure times.

Continuous operation, since diffraction photographs may require many hours or days.

Medium or fine focus.

Small dimensions so that distance from target to specimen may be a minimum.

Minimum absorption of beam in desired directions.

Target usually not tungsten, but molybdenum, copper, iron, etc., and preferably easily interchangeable.

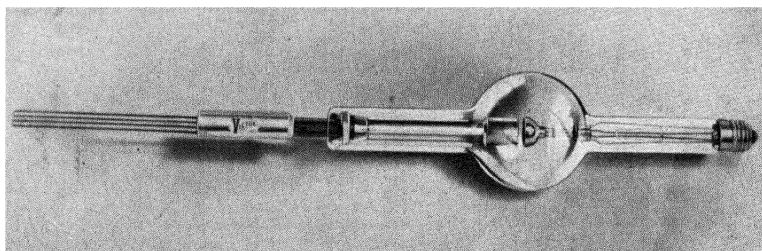


FIG. 18.—Coolidge type diffraction tube (General Electric).

Multiple beams from same target for routine examination of numerous specimens; hence flat target at right angles to cathode-ray beam from which rays at grazing angles may be defined radially.

Numerous modifications of the hot-cathode tube have been made, largely aimed at making it more adaptable for use in x-ray diffraction work with crystals, where interchangeable targets, small dimensions in order to approach as closely as possible to samples and spectroscopic apparatus, and general flexibility and ruggedness are required. Some are constructed largely of metal, some of quartz, and some of porcelain. The Coolidge water-cooled molybdenum-target tube with glass bulb is very generally used, in x-ray crystallographic investigations. It is shown in Fig. 18. The design has been carefully developed to meet many conditions which are excellently outlined in a

paper by the inventor W. D. Coolidge<sup>1</sup> with a later improvement due to Davey in which electrodes are brought much closer together. This tube is operated usually at 30,000 volts and at 20 to 30 ma. It may be connected directly with the alternating-current high-tension transformer. It is most convenient to have the positive-target end of the tube and the end of the transformer secondary at earth potential so that direct connection may be made with the water mains. A positive potential, however, may be applied satisfactorily with an insulated water system (Ford radiator and pump, thermosiphon, etc.), or even by connection with the water mains through an insulating column of water in glass or rubber tubes from 40 to 60 ft. long for ordinary city water. Since the target of this tube is perpendicular to the axis of the tube, the latter may be placed with the long axis perpendicular, and the x-rays emitted at grazing angles from the target may be defined radially around a complete circle. Hence, as many as 18 or 20 diffraction photographs may be taken simultaneously around one tube. It will operate continuously under practical conditions for several thousand hours, although the life of some tubes is less than this. Somewhat longer life is obtained by the use of rectified high tension and by intermittent use. After a time gas develops and the tube must be repumped or entirely rebuilt if the filament has burned out. A water pressure of 20 or 30 lb. is maintained, and it is essential to have automatic cutout switches (the "Mercoïd" type is best) to save the tube should the water supply fail. A ball-valve shut-off in the line can be used very satisfactorily if the pressure becomes too large and threatens to burst any rubber-tubing connections in the water-cooling system.

The best features of the diagnostic tubes in which requirements are similar have been embodied by various manufacturers, particularly Müller, Philips, and Seemann in diffraction tubes of the electron type. The most important of these are as follows:

1. Line-focus filaments for great intensity and sharp focus. In such a tube two diffraction photographs may be made simultaneously with opposite beams from the line focal spot on a target at right angles to the cathode rays.

2. Cross-focus filament (Müller) which has the same advantages as the line-focus type but four equally intense beams may be defined at right angles. Figure 19 shows the

<sup>1</sup> *J. Franklin Inst.*, **199**, 619 (May, 1925).

Müller cross-focus tube for structure determinations. Four windows of *Lindemann glass* (containing boron, lithium, and beryllium instead of silicon, sodium, and calcium in ordinary glass), through which the beam passes with little absorption, thus permit the study of four specimens simultaneously.

3. Demountable tubes. Besides the several varieties supplied by the manufacturers already pumped and permanently sealed off, it is convenient to be able to interchange targets in the same tube for diffraction research and particularly for spectroscopic analysis in which the unknown substance must constitute the target and must be mounted or pasted on a suitable backing. This, of course, means that such tubes must be pumped during operation. To one skilled in high-vacuum technique this does not present great difficulty, since equipment combining oil-backing pump, mercury-diffusion pumps in one or more stages, and liquid-air traps is well standardized.

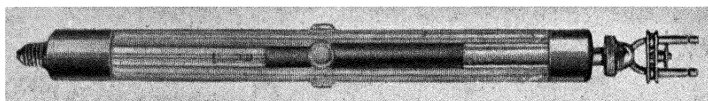


FIG. 19.—Müller diffraction tube with cross-focus filament and four Lindemann windows.

Several tubes made largely of metal are in the market and many have been designed and built in various laboratories. As probably the best examples of such a tube are the new Siegbahn tube made by Carl Leiss which may be operated as either an electron or an ion tube, and the Ott-Selmayr tube. A photograph of one of the latter in the writer's laboratory is presented in Fig. 20. The body of the tube is essentially a heavy triangular block of metal into which the electrodes are fitted at an angle of 120 deg. The cathode arm is of glass and the filaments interchangeable spiral or line focus. The targets of various metals are easily removable and interchangeable. The window of thin aluminum (or, better, beryllium) foil is only a few millimeters from the focal spot and the specimen for structure analysis can thus be placed very close to the target. The result is a tube which provides radiation of extremely high intensity.<sup>1</sup>

<sup>1</sup> For a description of this tube with improvements see Clark and Corrigan, *Ind. Eng. Chem.*, **23**, 815 (1931).

4. High-intensity tubes. X-ray apparatus and technique have been passing rapidly through the stage of development and improvement within the past very few years. The diffraction method of testing materials has been expensive, not only on account of the initial expenditure for equipment but also because of the time required for photographing a diffraction pattern—sometimes many days and always many hours. Part of the difficulty was alleviated by construction of multiple apparatus, such as the familiar and excellent General Electric unit with

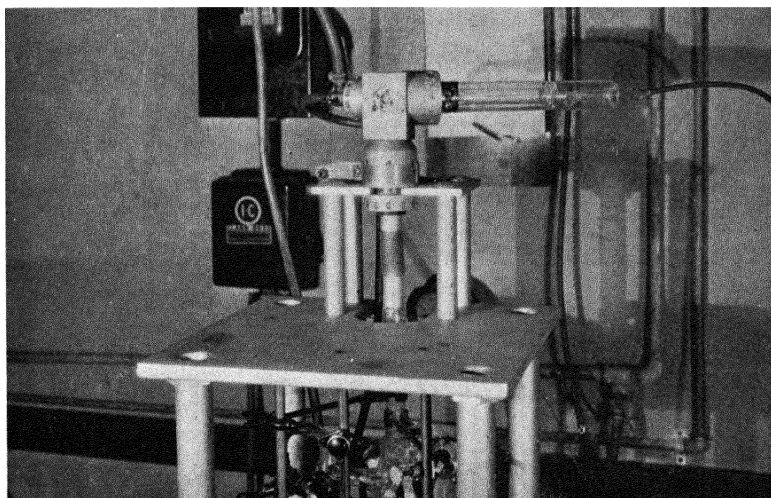


FIG. 20. Photograph of installation of high-intensity diffraction tube (Ott-Selmayr type) at the University of Illinois.

which 12 or more exposures can be made simultaneously from the same x-ray tube. This time factor, however, has precluded the possibility of using the diffraction method as an industrial control or for exhaustive studies of uniformity. Furthermore, it has been impossible to use specimens undergoing change over relatively short periods of time, unstable compounds, or specimens at very low or at high temperatures. A very logical development, therefore, has been directed toward the designing of x-ray tubes which will produce beams of so much greater intensity that times of exposure can be materially reduced.

Several workers in the diffraction field have recorded results obtained in very short periods of time. Ott published a descrip-

tion of a high-intensity tube mentioned above in 1926.<sup>1</sup> In October, 1929, Mark and von Susich<sup>2</sup> published typical results obtained with this tube in fraction of seconds, *e.g.*, a single crystal of pentaerythritol in 0.1 sec., diamond in 0.04 sec., and the progress of mercerization of cellulose at 1-min. intervals. Seemann and Schotzky<sup>3</sup> pointed out that as early as 1916–1917 Laue had shown with a Seemann x-ray tube “a complete spectral diagram” could be seen without difficulty on the fluoroscope. They showed moving picture films where the exposure times were  $\frac{1}{150}$  sec. and oscillograms for times as little as  $\frac{1}{2500}$  sec. Later the same authors<sup>4</sup> showed that the direct beam of the x-ray tube could be recorded on a film with an exposure time as short as  $\frac{1}{1,200,000}$  sec. with an x-ray oscillograph.

The purpose of investigations in the writer's laboratory has been to discover whether such tubes as the Ott-Selmayr described above are actually practicable for use in the x-ray research laboratory devoted to fine-structure studies, whether they are easily constructed and economically operated, whether they make possible fields of investigation otherwise impossible, and whether they may be expected to displace the more familiar types.

Some of the more typical experiments, selected at random are as follows:

1. The first indication of this tube's extreme intensity came while the tube was first being tested out. A thick piece of lead glass with a fluorescent screen behind it was placed in front of the window for protection and to observe the intensity of the beam. After operating for some time it was noticed that a brown spot had appeared on the glass at the point struck by the ray. When another spot was exposed a colored area the full size of the window was obtained in  $\frac{1}{2}$  hr. and a very distinct spot, the size of the focal spot, was obtained in a few minutes.

2. It was found that an ordinary fluorescent screen, ordinarily free from all after effects, would glow brightly for several minutes after the ray was turned off.

3. Laue patterns of calcite were obtained in 0.5 sec. even with a precision pinhole system only 0.020 in. in diameter.

<sup>1</sup> *Physik. Z.*, **27**, 598 (1926).

<sup>2</sup> *Naturwissenschaften*, **17**, 803 (1929).

<sup>3</sup> *Naturwissenschaften*, **17**, 960 (1929).

<sup>4</sup> *Naturwissenschaften*, **18**, 85 (1930).

4. Several independent observers have been able to see Laue patterns clearly on the fluorescent screen without special preparation of the eyes by remaining in the dark. An obvious extension is visual observation of changes in the patterns with physical or chemical changes in the specimen.

5. Diffraction spectrograms of wool (whose crystallinity is only very rudimentary) requiring on the average 4 to 5 hr., and in some cases as much as 12 hr. with other tubes, were obtained in 10 min., and in some cases in as little as 2 min. In addition these pictures, which are very difficult ordinarily to measure, were found to be clear and sharp, and in every case the exposure was accompanied by far less fogging and general scattering than with the other tubes. The central spots due to incipient fiber structure as a result appeared more clearly, and changes in these central spots could be followed more easily.

6. Liquid paraffins were investigated by cooling down and taking a short exposure. Clear pictures were obtained in intervals short enough to neglect the warming up of the sample.

7. The disintegration of a sugar crystal through the liquid phase and its subsequent charring to carbon was followed on a strip of moving picture film. This crystal was mounted on a brass pinhole and the brass heated with a hand torch. In spite of usual difficulties attending the use of motion picture film, as mentioned above, the successive patterns showed a disappearance of the Laue spots as the temperature was raised, on account of the thermal agitation of the molecules, to a point where no pattern appeared though the outer form of the solid crystal still was maintained; then followed the appearance of a liquid type of diffraction pattern, upon melting, which gave way to a pattern characteristic of carbon upon charring.

Numerous problems carried out under these most promising conditions suggest themselves and are under investigation. Meyer and Mark have shown how the mercerization process in cellulose takes place step by step by the use of a high-intensity tube. Other problems are:

1. Efflorescence, deliquescence, dehydration, etc., of crystals stepwise.
2. Unstable compounds such as  $KI_3$  for which patterns can be made in a few minutes, long before disintegration; phase rule studies of unstable alloys.
3. Crystals, tissues, and any other type of substance cooled to liquid-air temperature can be studied before sufficient warming has taken place, without special or complicated apparatus.

4. Any type of chemical reaction taking place over seconds or minutes followed as to velocity and mechanism, such as vulcanization of rubber, xanthogenation, nitration, methylation and acetylation of cellulose, polymerization of resins, setting of cements and plaster, etc., oxidation, ozonization and photochemical changes of plastics, rubber, varnish, and patent leather.

5. Steps in any process of heat treatment, as annealing of metals, and the mechanism of recrystallization; changes with gradual application of deforming forces.

6. Transitions between solid and liquid at melting points, appearance of anisotropic liquid phases, allotropic transformations, etc.

7. Experiments on structures of fresh and living tissues such as those of Clark, Bucher, and Lorenz, and of Boehm and Schotzky.<sup>1</sup> Patterns of living electrically contracted frog muscle (excited by an applied voltage to tetanus contractions) on account of the long exposure necessary have been procurable at great sacrifice. As each muscle remains fresh only  $\frac{1}{2}$  min., several hundred muscles have been required. With special tubes it has been possible to obtain photographs with a total of 2 to 6 min. with only 6 to 12 muscles.

**Superficial Therapy and Long-wave-length Tubes.**—Skin reddening or erythema develops much more rapidly with very soft x-rays than with rays of the usual range of hardness. Hence a logical development has been the design of tubes to operate at only 8 to 10 kv. corresponding to wave lengths of 1.2 to 2.0 A.U. On account of the great ease of absorption these tubes were successful only after the development of windows of Lindemann glass and of cellophane. Medically, the soft rays are known as Grenz rays for no particularly good reason. The tubes involve no unusual features of construction except in so far as the small dimensions are concerned. The Müller tube employs the cylindrical chrome-steel body of the tube as anode and the Lindemann window is thus directly opposite the cathode filament, which is screened off by a metal shield directing the electrons to the side walls.

Rays with long wave lengths have great interest from the standpoint of spectroscopy and atomic structure, and more recently for diffraction studies where very large grating spacings are involved. Clark and Corrigan<sup>2</sup> have constructed an x-ray tube and camera in a single unit for operation in vacuum, with a magnesium target supplying rays with a principal wave length of

<sup>1</sup> See Chap. XX.

<sup>2</sup> *Loc. cit*



9.86 A.U. For special studies of natural materials such as cellulose, rubber, and insulin, new information concerning

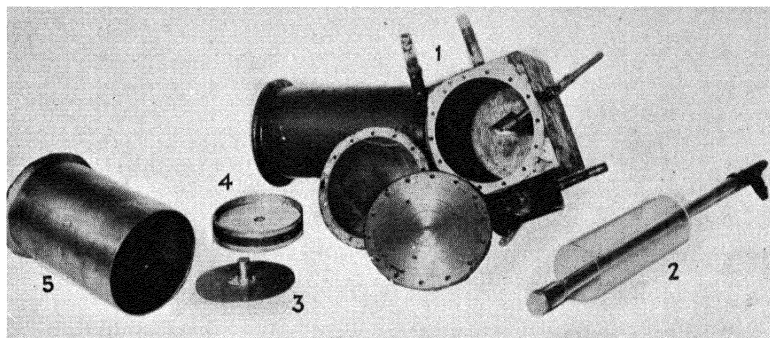


FIG. 21.—Long-wave diffraction tube (magnesium target) with integral camera (Clark and Corrigan). 1, body of tube and camera; 2, cathode; 3, pinhole system; 4, film holder; 5, camera sliding into 1.

structure has been obtained which will be considered in Chap. XX. The long-wave diffraction tube is pictured in Fig. 21.

## CHAPTER IV

### HIGH-TENSION EQUIPMENT

Of the various methods of producing the difference of potential across an x-ray tube, the alternating-current high-tension transformer is now of greatest practical importance. Static induction machines and induction coils operating on direct current with interrupters were used widely for many years after the discovery of x-rays. The latter are still to be found in many laboratories and hospitals, particularly where gas tubes operated at moderate voltages are used.

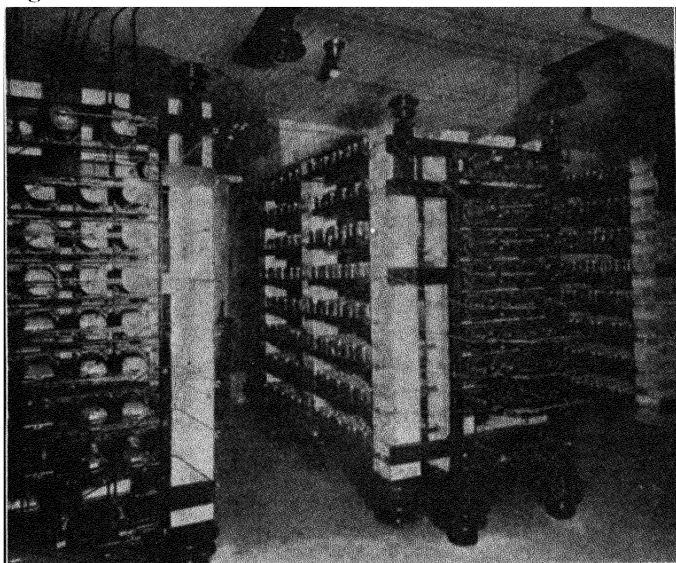


FIG. 22.—100,000-volt storage battery in Croft Laboratory, Harvard University.

**Storage Batteries.**—The high-tension storage battery is, of course, the ideal source of power, since the voltage across the tube remains perfectly constant and no rectifying devices are required. Storage batteries have the disadvantages of being very expensive, difficult properly to insulate, and dangerous to

the operator, since very large currents may be instantaneously drawn from them, and of requiring constant attention. A 43,000-volt storage battery made from test tubes gave excellent results for more than twenty years at Harvard University. With it the precision researches on x-rays by Duane and his students, particularly the most accurate evaluation of the Planck constant  $h$ , were made possible.<sup>1</sup> A new 100,000-volt plant (Fig. 22) with the cells in pint jars has much greater capacity and every possible improvement. This battery will operate a tube for two weeks before recharging is necessary.<sup>2</sup>

**Transformers.**—The usual modern equipment includes a 60-cycle oil-immersed transformer stepping up an alternating 110- or 220-volt current to the required high tension. The secondary voltage is controlled by regulating the primary-current input by resistances, autotransformers, or combinations of the two. For a filament-heating current in Coolidge type tubes, the transformer may contain a separate winding which will step down the primary voltage. For moderate voltages between 30 and 60 kv., the electron tube can rectify the alternating voltage, as explained in the description of the tubes. Usually under these conditions the positive terminal of the x-ray tube and one end of the secondary of the transformer are grounded. Most of the x-ray power units on the market are designed for therapeutic and diagnostic use at voltages up to 250 kv. These commercial machines are all similar in general operation but differ in details of design. They usually include:

A 60-cycle 110- or 220-volt alternating-current closed-core high-tension transformer.

A separate transformer for filament current (insulated storage batteries may be used).

An autotransformer for controlling input.

A device for stabilizing and controlling the tube current.

A device for rectifying the alternating high-tension current, of either a mechanical or electron-tube type.

**Rectifiers. Mechanical Type.**—The mechanical full-wave rectifiers are cross-arm arrangements revolving on the shaft of the alternating-current generator or driven by a synchronous motor. This rotating switch connects the terminals of the

<sup>1</sup> *J. Optical Soc. Am.*, **5**, 213 (1921).

<sup>2</sup> A complete description of the installation is given in a paper by Armstrong and Stifler, *J. Optical Soc. Am.*, **11**, 509 (1925).

secondary alternately to opposite ends of the x-ray tube in synchronism with the alternations of the current. Only a portion of the top of these waves is applied to the x-ray tube, since the contacts are intermittent. The tube is, therefore, excited by pulses which are alike (see Fig. 25).

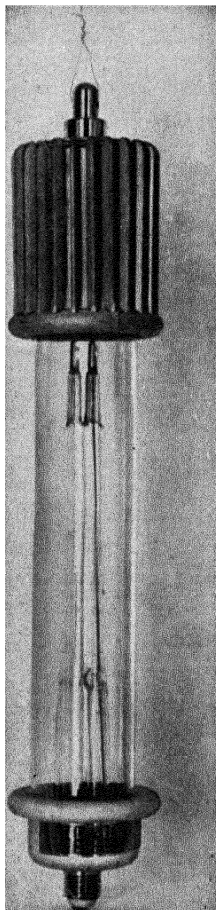


FIG. 23.—Müller  
Metalix valve tube.

*Kenotron Type.*—The Kenotron electric valve, which is a familiar type of electron-tube rectifiers, is a vacuum tube operating on the same principle as the x-ray tube. In one type a tungsten-wire filament is at the center of a coaxial cylinder of sheet molybdenum. The filament is heated by a current from storage batteries or step-down transformers. Current passes through the valve, of course, in one direction only, since the hot wire is the only source of electrons. During the time of flow of current from hot cathode to anode, a difference of potential of only a few hundred volts at the most exists. During the other half period when the cathode is positively and the anode negatively charged, the entire difference of potential on the x-ray tube is impressed on the valve tube, so that it must be constructed to withstand this. In another type the filament consists of three or more hairpin loops of wire and the anode is a cup or disk. The filament heating current is 7.8 to 8.2 amp. at 12 to 14 volts and such a tube passes a current of 300 to 400 ma. Glass tubes are made by all the prominent manufacturers. The new Müller Metalix valve tube (Fig. 23) has two metal cylinders which are fused on both sides of an insulating glass cylinder. The upper metal cylinder serves as anode with radiator fin cooling.

The heating voltage is 15 volts and the emission at 8 amp. passes 600 ma. or at 8.5 amp. 1100 ma. A new valve tube (Siemens-Supra) for operation at 400 kv. is illustrated in Fig. 24 as it appears in a complete power plant. The anode is carefully rounded, the filament has a protecting spool, and the end caps

have the protective rings. The elongated oval glass bulb is also an important feature.

Numerous types of circuits involving transformers and valve-tube rectifiers with auxiliary equipment are employed for various x-ray purposes (Fig. 25). Some of the more important may be listed as follows:

1. Self-rectifying Coolidge type x-ray tube; half-wave rectification; for diffraction and other equipment up to 60 kv. where loss in power is not so important as simplicity and economy.

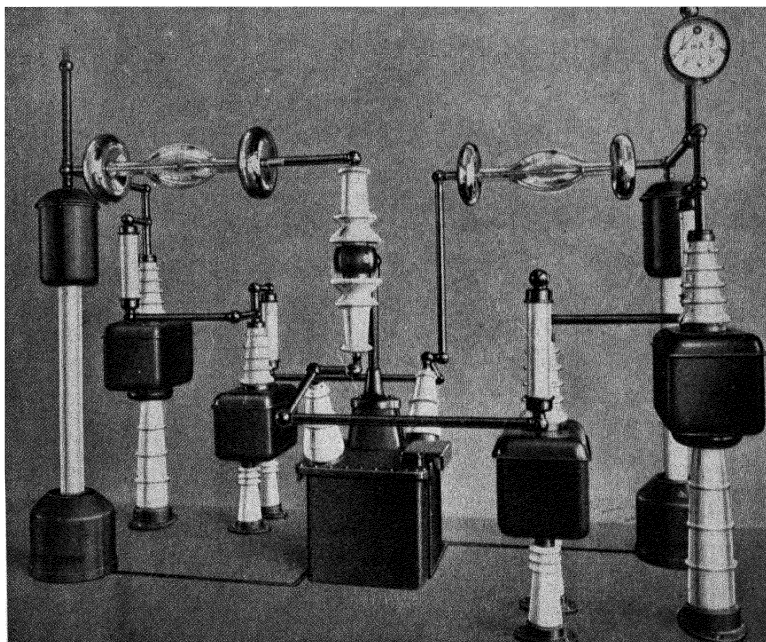
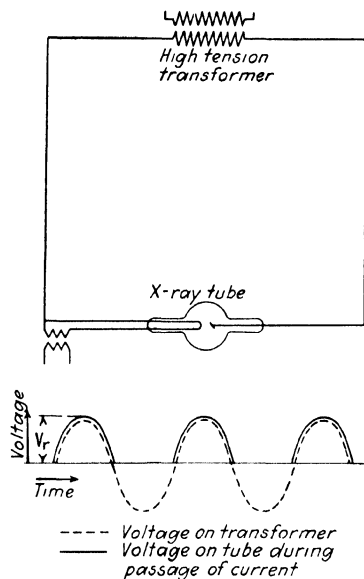


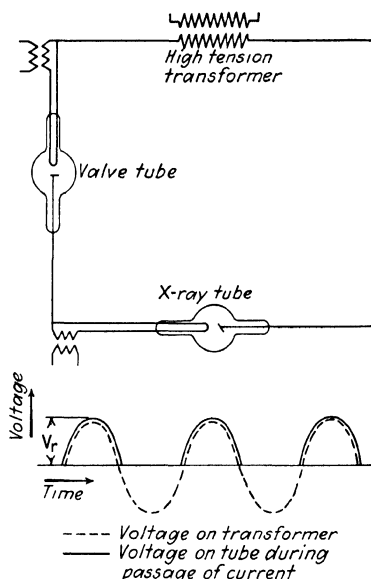
FIG. 24.—550-kv. power plant showing 400-kv. valve tubes in position with protecting rings (Siemens).

2. Single Kenotron; half-wave rectification; with or without condensers gives impulses; for use with gas- or ion-type tubes up to 80 kv. primarily. A unit of this type is shown in Fig. 26.

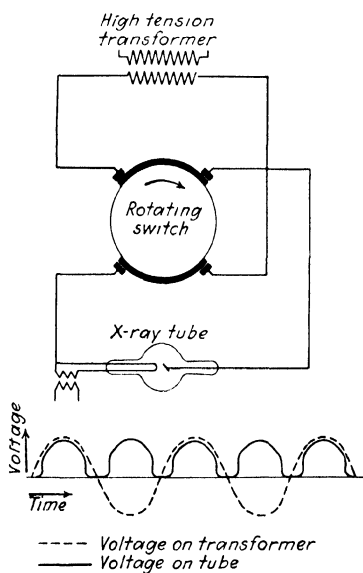
3. Two Kenotrons; full-wave rectification. The circuit is shown in Fig. 25 with condensers. If two opposed Kenotrons are connected to the end of the transformer secondary whose potential is oscillating between  $+V$  and  $-V$  then the total difference of potential across the plates of the condenser and



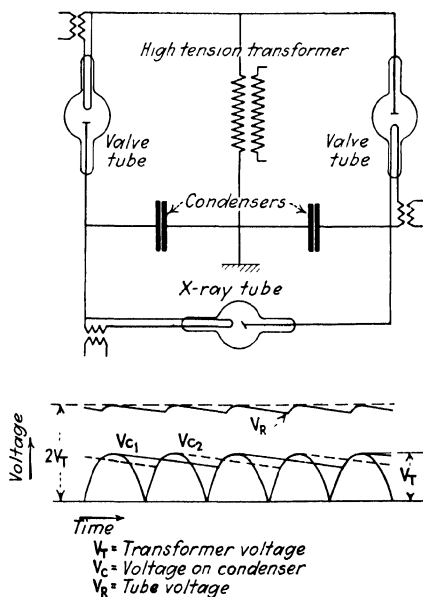
(A) Circuit for Self-Rectifying X-Ray Tube (Half-Wave)



(B) Circuit with One Valve Tube (Half-Wave)



(C) Circuit with Mechanical Rectifier



(D) Constant Potential Circuit with Two Valve Tubes

FIG. 25.—Diagram of various x-ray machine circuits showing wave form produced.

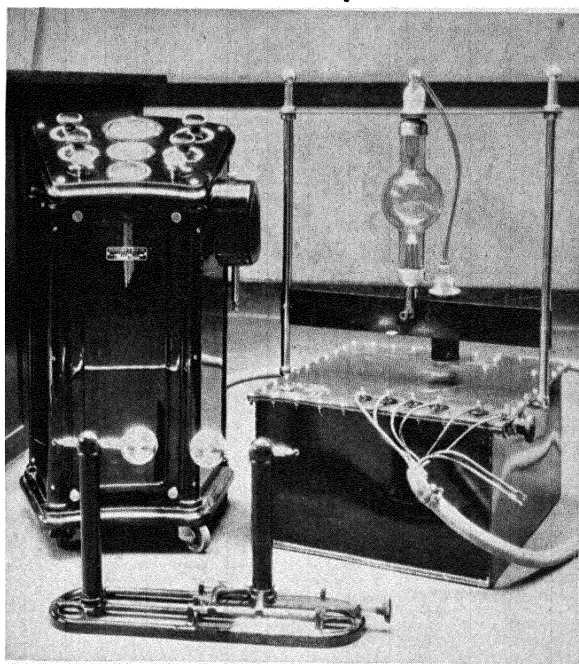


FIG. 26.—Photograph of Standard power plant with single Kenotron used in diffraction work.

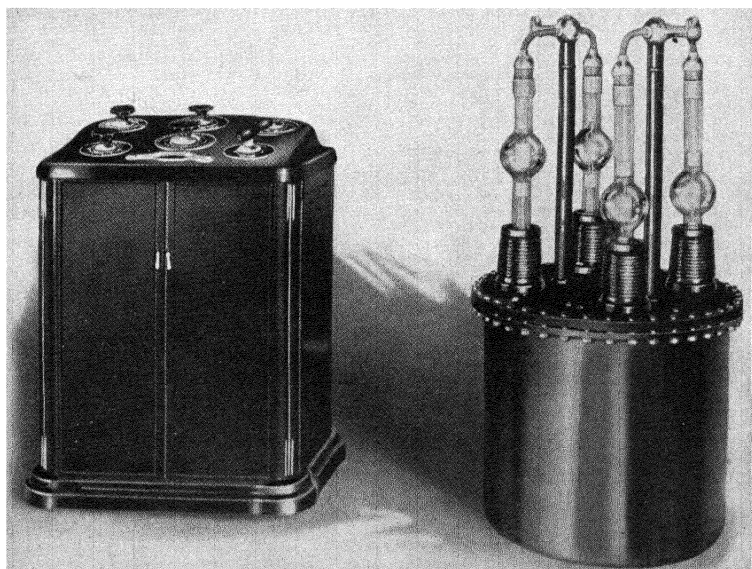


FIG. 27.—Power plant for producing radiographs in  $\frac{1}{120}$  sec. at 1000 ma. (General Electric).

the terminals of the x-ray tube will be  $+V - (-V) = 2V$ . The rectifiers must be able to withstand this voltage. Four Kenotrons give better performance. Figure 27 shows a Victor four-Kenotron apparatus with which radiographs in  $\frac{1}{120}$  sec. at 1000 ma. are obtained.

4. The most desirable is obviously a constant-potential direct-current (c.p.d.c.) machine. Only with such a condition is it possible to reproduce accurately dosages in therapy or to conduct scientific researches of the highest accuracy. Voltage and current ripples are smoothed out to less than 1 per cent. This is accomplished with 2 or 4 Kenotrons, a 500-cycle (or more) primary current, and condensers whose correct capacity depends upon the frequency. A highly satisfactory c.p.d.c. installation due to Duane at the Huntington Memorial Hospital in Boston operates on 2000 cycles with condensers of 0.0081-mf. capacity. With 60-cycle current no ordinary condenser capacity suffices to suppress the ripple, but a typical and usually unsymmetrical wave form is observed with an oscillograph. In any case this is subject to line fluctuations so that it is necessary to resort to separate generators.

**Measurement of the Voltage.**—The various methods of determining the peak or effective voltages applied to the x-ray tube are as follows:

1. Voltmeter reading of the transformer primary with known transformation ratio; a method accurate only with constant-potential apparatus.

2. Sphere gap; the method most commonly used and the simplest, but giving only very approximate readings.

3. Electrostatic voltmeter; one type consists of large balls charged with high voltage and small balls on a bifilar suspension turning in the electrostatic field. This instrument requires calibration and is then very satisfactory, not only as a measure of the voltage but also of the constancy of the potential.

4. Measurement by ammeter of the current through a very high known resistance, 10,000,000 ohms, for example.

5. Spectrometric method; this consists in determining the shortest wave length in the spectrum of a beam of x-rays reflected from a crystal of known planar spacing, and substitution of this value in the very accurate quantum equation  $V = hc/e\lambda$ , where  $V$  is the voltage (peak),  $e$ ,  $h$ , and  $c$  are constants (respectively, the charge of the electron, the Planck action constant, and the



velocity of light, so that  $hc/e = 12,350$ ), and  $\lambda$  is the short wavelength limit of the spectrum. This method is extremely accurate but, of course, requires special equipment and skilled technique. A special Seemann wedge spectrograph with spectral oscillograph is manufactured in Germany for the use of roentgenologists in determining accurate therapeutic dosage.

The importance of an accurate knowledge of the voltage, particularly in deep therapy and in quantitative studies of crystalline structures, will become apparent in later sections on intensity measurements.

**Electrical Precautions.**—The installation of x-ray equipment involves adequate protection for the operator both from the high-tension electrical power plant and leads and from the x-rays themselves. The following are recommended electrical precautions:

1. Wooden, cork, or rubber floors or coverings.
2. High-tension leads concealed in an assembled unit with outside grounded; for exterior leads, preferably metal tubes or

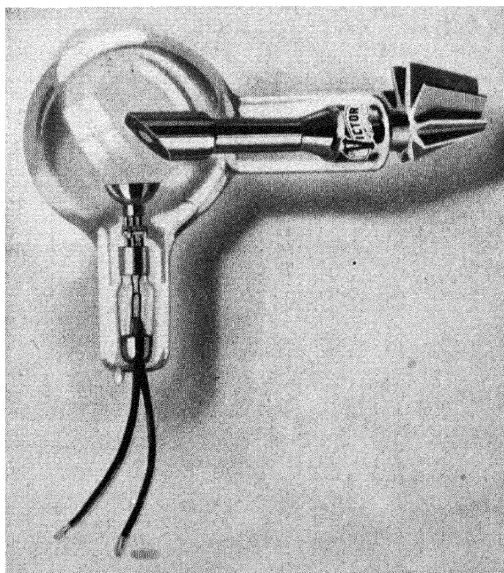


FIG. 28.—Coolidge tube used in shock-proof unit (General Electric).

rods or tightly stretched insulated wire, suspended by the best quality of shellacked silk fishline.

3. Efficient earthing of all metal parts.

4. Safety switches and fuses no heavier than absolutely necessary.

5. Magnetic circuit breakers to break contact with any unexpected surges.

6. Shock-proof equipment. One of the best recent developments in commercial medical x-ray equipment has been in shock-proof equipment. The x-ray tube of the type shown in Fig. 28 is enclosed in the transformer itself with outer grounded and lead-covered cases. Such a unit, manufactured by the General Electric X-ray Corporation, is pictured in Fig. 29.

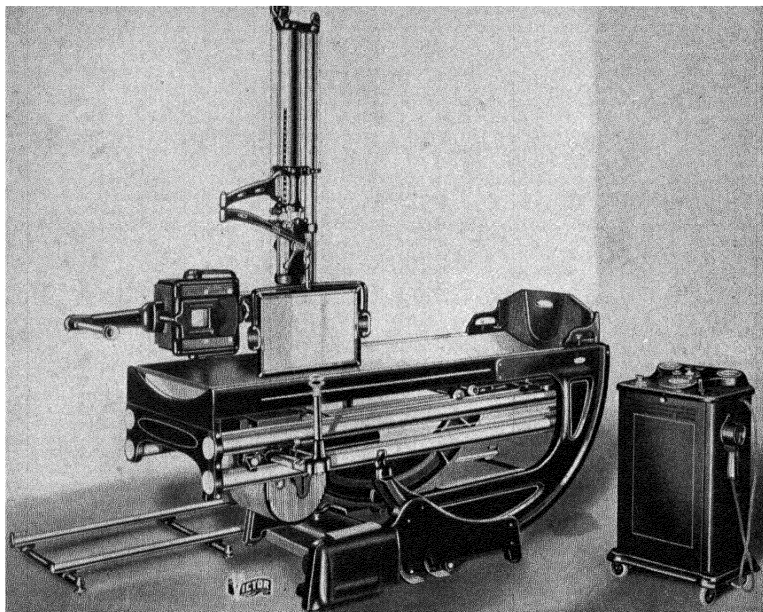


FIG. 29.—Shock-proof medical x-ray unit in which both transformer and tube are enclosed in the movable head (left center).

The protective measures to be used against the x-rays are considered in Chap. VII, page 104.

For further information concerning the electrical-engineering aspects of x-ray installations and their operation, the reader is referred to such excellent works among others as Terrill and Ulrey, "X-ray Technology," D. Van Nostrand Company, New York, 1930; Brenzinger, Janitzky, and Wilhelmy, "Allgemeine Grundlagen, Physik und Technik des Röntgenverfahrens," Thieme, Leipzig, 1931 (an excellent treatise on European equipment and practice); and literature supplied by manufacturers.

## CHAPTER V

### X-RAY SPECTRA

**Spectra from Crystals and from Ruled Gratings.**—All x-ray investigations, whether they are concerned with the radiation itself and the information thereby obtainable on chemical and biological effects and on subatomic structure or with crystalline matter whose ultimate structure is sought by means of the x-rays, involve two factors, the quantity and the quality of the x-rays. By quantity is meant the intensity of a given beam, as it is variously measured. This factor is considered in Chap. IX. By quality is meant the constitution of the beam with regard to wave length. Ordinary white light is proved to be a mixture of many rays of visible light of different wave lengths and corresponding to pure colors, because the beam is spread into a spectrum from violet to red by refraction in a prism or by diffraction by the finely ruled lines of a grating. In analogous fashion the spectrum of a beam of x-rays whose constitution previous to analysis is unknown identifies the quality.

Glass prisms or diffraction gratings consisting of finely ruled parallel lines on glass or metal can be used only under very special conditions for the spectra of x-rays, because these have wave lengths many times shorter than light. Crystals, however, are natural gratings in which parallel planes of regularly marshaled atoms are spaced from each other at distances which are of the same order of magnitude as x-ray wave lengths.

The analysis for quality is made, therefore, with the crystal spectrometer originally designed by the Braggs. It is a device upon which crystals of known interplanar spacings are mounted and rotated; the quantities measured are the angles at which the various components of the beam are reflected by the crystal planes. Upon the photographic plate or plotted from ionization-current readings is the spectrum of the beam. The analysis is complete because the whole process is governed by a simple law  $n\lambda = 2d \sin \Theta$ , where  $\lambda$  is a wave length,  $n$  is the order of the

reflection,  $d$  is the known distance between the parallel planes in the crystals, and  $\theta$  is the spectrometrically measured angle of incidence of the ray upon these planes (or  $2\theta$  the angle of diffraction or reflection).

The crystals ordinarily used in spectrum analysis are rock salt (NaCl) in which the planes parallel to the cube surface (100) planes are spaced 2.814 A.U. apart; or calcite with a spacing of  $3.029 \pm 0.001$  A.U. Gypsum, ( $d = 7.584$ ), sugar ( $d = 10.57$ ), mica ( $d = 9.93$ ), quartz ( $d = 4.247$ ), and other crystals are also used. Of these calcite is recommended as the primary standard. Siegbahn and his associates in the measurement of long wave lengths introduced the use of crystalline lauric ( $d = 27.268$  A.U.), palmitic ( $d = 35.49$  A.U.), and stearic ( $d = 38.7$  A.U.) acids and lead melissate ( $d = 87.5$  A.U.). The use of organic crystals has been practically discarded, however, in favor of the ruled gratings. The design and operation of spectrometers and the mechanism of the interaction between x-rays and crystals in accordance with the above Bragg law will be considered in Chaps. XI and XII, which are concerned with the use of x-rays in determining the structure of crystals.

It is obvious that some other method of absolute wave-length measurement is needed to substantiate thoroughly the assumptions and calculations made with crystal gratings. The fundamental grating spacing of some one standard crystal (calcite) had to be calculated as a basis for wave-length measurements of x-rays which were then applied to the determination of the grating spacings of other crystals. For calcite, a rhombohedral crystal, the distance between face planes is

$$2d_{100} = \left[ 4 \frac{V_m}{\phi(\beta)} \right]^{1/3},$$

where  $V_m$  the molecular volume  $= M/\rho N_0$  ( $M$  = molecular weight,  $\rho$  = density, and  $N_0$  is Avogadro's number or number of molecules per mole);  $\phi(\beta)$  = volume of calcite rhombohedron with unit distance between these face planes  $= (1 + \cos \beta)^2 / \sin \beta (1 + 2 \cos \beta) = 1.0962$ , with  $\beta = 101^\circ 55'$ . The most uncertain quantities are  $\rho$  and  $N_0$ ; repeated measurement has given  $\rho = 2.7102$  as most reliable and with the accepted value for  $N_0 = 6.061 \times 10^{23}$ , the grating constant comes out  $3.029 \pm 0.001$  A.U.

Several experimenters, notably Thibaud in Paris<sup>1</sup> and A. H. Compton and Bearden<sup>2</sup> in America, have made notable contributions with wave-length measurement by means of ruled optical gratings. At grazing tangential angles such gratings produce excellent diffraction spectra for x-rays and the measurement of wave length is obviously an absolute check upon crystal spectrometry. X-rays have an index of refraction  $\mu$  which is somewhat smaller than unity or

$$\mu = 1 - \delta \text{ (}\delta \text{ of the order of } 10^{-6}\text{)}.$$

It follows that a ray tangential upon a plane mirror or grating undergoes total reflection when the angle of incidence  $\theta$  is smaller than a definite limiting value  $\theta_m = \sqrt{2\delta}$ . On a photographic plate appear a central maximum for the primary beam,

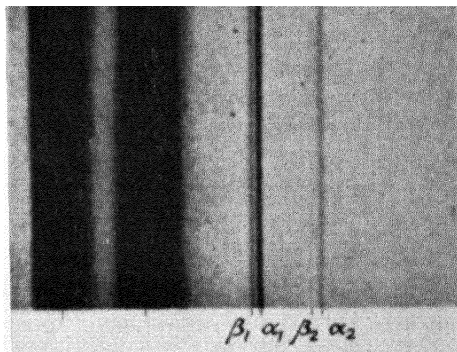


FIG. 30.—X-ray spectrum from ruled grating. *K* series of copper. (Thibaud).

another for the total reflection, the distance between these being  $2\theta$ ; finally there is observed a diffraction spectrum of sharp lines for the x-ray beam. In Fig. 30 is shown such a result for x-rays from a copper target. The measurement of these lines and calculation of the wave lengths have yielded results in approximate agreement with those derived from the Bragg expression for crystal diffraction and the value of Avogadro's constant; the difference though small presents a fundamental problem as yet unsolved. Furthermore, by means of such gratings Thibaud has bridged the gap between the x-ray and ultraviolet regions and obtained in many cases the same wave length for a chemical element from the spectrum of a beam from an x-ray tube and from an ultraviolet spark spectrum. This

<sup>1</sup> *Physik. Z.*, **29**, 241 (1928).

<sup>2</sup> *Phys. Rev.*, **37**, 1694 (1931).

region of long waves which are easily absorbed can be studied with the crystal spectrometer only in vacuum with the greatest difficulty. There are still some discrepancies, however, between crystal and ruled-grating data. The latest precision comparative measurements have been made by Bearden<sup>1</sup> with the following results:

Spectral line	Crystal $\lambda$	Grating $\lambda$
CuK $\beta$	1 38914	1 39225
CuK $\alpha$	1 53838	1 54172
CrK $\beta$	2 08017	2 08478
CrK $\alpha$	2 28590	2 29097

It is at once clear that x-rays may serve as an aid in the solution of chemical problems along two lines: (1) the analysis of the emission or absorption spectrum of a substance by means of a known crystal analyzer ( $\lambda$  unknown,  $d$  known); and (2) the determination with an x-ray beam of known wave lengths of unknown grating spacings of crystals ( $\lambda$  known,  $d$  unknown). The first yields information concerning the element which is absorbing or emitting rays; and the second, information concerning the structure of the crystal lattice. The present discussion is concerned with the first of these, and Part II with the second. The first involves largely the measurement and study of x-ray wave lengths which are characteristic of the chemical elements, hydrogen to uranium. At present the shortest characteristic wave length measured by strictly x-ray methods is 0.1075 A.U., the  $K$  absorption limit of uranium. This is the shortest possible characteristic value unless, of course, a heavier element should be discovered. Rays with much shorter wave lengths have been generated and measured but these are independent of the target metal.

**The Continuous Spectrum.**—Two kinds of x-radiation are known, (1) the general, "white," or continuous spectrum x-radiation and (2) the characteristic x-radiation, which is composed of several monochromatic rays grouped in series, with wave lengths depending upon the atomic number of the emitting element. The continuous spectrum may be generated in a tube at sufficiently low potentials over certain ranges of wave lengths without

<sup>1</sup> *Phys. Rev.*, **37**, 1694 (1931).

characteristic lines under certain conditions, but the characteristic spectrum is always superposed upon a background of the general radiation. The outstanding property of the general radiation is that the smooth curve obtained by plotting intensity against wave-length or spectrometer reading has a sharp short wave-length limit (zero intensity), which does not depend upon the material of the target of the tube but upon the voltage applied to the tube, according to the fundamental Planck-Einstein quantum equation  $Ve = h\nu_0 = hc/\lambda_0$ , where  $V$  is the constant potential,  $e$  is the charge on the electron,  $h$  the Planck action constant,<sup>1</sup>  $c$  the velocity of light,  $\nu_0$  the maximum frequency, and  $\lambda_0$  the minimum wave length occurring in the spectrum. This law was first applied to x-rays by Duane and Hunt in 1914, and it has been proved subsequently to be rigorously true, far more so than the other famous equation,  $n\lambda = 2d \sin \Theta$ .

According to this equation

$$\lambda_0 = \frac{hc}{eV_0} = \frac{6.556 \times 10^{-27} \times 3 \times 10^{10}}{1.59 \times 10^{-20} \times V_0} = \frac{12,350}{V_0},$$

where  $V_0$  is in volts. Thus at 300,000 volts, the highest now employed in deep therapy, the minimum wave length is 0.04 A.U., while Lange and Brasch's new tube at 2,600,000 volts must generate rays with a minimum wave length of 0.005 A.U., in the extreme  $\gamma$ -ray region of the electromagnetic spectrum.

It is obvious that precision researches on the general radiation spectrum should be a very exact method for evaluating the constant  $h$ ;  $\lambda_0$  can be spectrometrically evaluated from  $n\lambda_0 = 2d \sin \Theta$ ;  $V$  can be measured very accurately, particularly if the source of high potential is a storage battery, by reading the current after passage through carefully calibrated high resistances; and  $e$  is the well-known value of Millikan. The latest measurements in the laboratory of Prof. William Duane at Harvard<sup>2</sup> gave a value of  $6.556 \times 10^{-27}$  erg-sec. Several other investigators have obtained nearly the same value, which agrees well with evaluations by entirely different methods, such as the photoelectric effect.

<sup>1</sup>  $h$  has the dimensions ( $L^2mT^{-1}$ ) of a moment of momentum: [action] = [energy  $\times$  time].

<sup>2</sup> *J. Optical Soc. Am.*, **5**, 213 (1921).

Furthermore, the law of Duane and Hunt leads to the most accurate evaluation of peak voltage which is directly calculated from the sharp limit of a crystal spectrum:

$$V_0 = \frac{hc}{e\lambda_0} = \frac{12,350}{\frac{2d}{n} \sin \theta_0},$$

where  $2\theta_0$  is the experimentally measured angle of the limit.

While the short wave length of the spectrum is entirely independent of the target element, the intensity is a function of the atomic number of the target element. The relationships are, however, quite complicated and remain still in doubt. The curves rise sharply to an intensity maximum, defined roughly by  $\lambda = 1.3\lambda_0$ , and then fall away more gradually.

The question of the mechanism of the production of the general radiation is one of the most difficult in x-ray science, and a completely satisfactory answer has not been given. If cathode rays are accelerated in an x-ray tube by the voltage  $V$ , the kinetic energy  $E_k$  will be  $Ve = E_k$ . If the electrons are stopped instantaneously at the target, the kinetic energy is transformed into the maximum possible radiation energy or  $E_k = V_0e = h\nu_0 = hc/\lambda_0$ . If the stoppage of the electrons is stepwise as they penetrate the target, then the rays will have a variety of wave lengths longer than the limit. While the quantum law governs the general radiation, the explanation of the actual emission process, which can indeed be made simply upon the basis of the electromagnetic or wave theory as a forced vibration of electrons in bombarded atoms, is one of the great difficulties confronted by the modern theories of spectral emission by quantum processes.

The general radiation is of practical importance since it is employed in the Laue method of crystal analysis. In all applications at high voltages including therapy, radiography, etc., it comes prominently into play. The spectrum can be profoundly modified by filtration, inasmuch as rays of short wave lengths are absorbed far less than are those of the long wave length. The effect of filtration in the absence of characteristic effects is, then, to sharpen the curve and to shift the maximum to the shorter wave lengths, without in any way affecting the value of  $\lambda_0$ . Filtration and the measurement of effective wave length of general radiation will be considered in Chap. VII.



**Characteristic Emission Spectra.**—In addition to the continuous x-radiation, rays which have wave lengths characteristic of the anticathode elements are recognized. If the potential on the x-ray tube is sufficiently high, the spectrum of the emitted beam will show sharp lines (or peaks if the ionization current measured with an ionization spectrometer is plotted) superposed upon the continuous background. These same characteristic

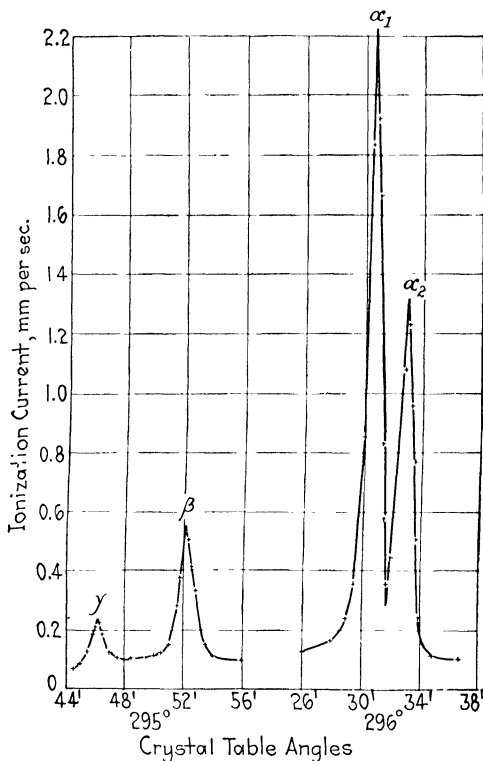


FIG. 31.  $-K$  series emission spectrum (rhodium).

x-rays are emitted as fluorescent rays if a beam of primary x-rays with sufficiently short wave lengths falls upon an absorption screen containing the same element as the tube target. The characteristic emission lines appear in groups designated as the  $K, L, M, N, O$ , etc., series (beginning with the most penetrating or shortest wave-length group), following the nomenclature of Barkla who discovered the characteristic emission in the course of his absorption measurements.

Each of the series of *emission lines* contains several definite lines of different wave lengths. Probably the most remarkable characteristic of the x-ray range of the electromagnetic spectrum is the uniform simplicity of these spectra. The *K* series of all the elements except the lightest consists of four principal lines, the  $\gamma$  (also designated  $\beta_2$ ),  $\beta$  (really a close doublet  $\beta_1$  and  $\beta_3$ ), and the doublet,  $\alpha_1$  and  $\alpha_2$ , in the order of increasing wave lengths. The typical appearance of this spectrum is shown in Fig. 31. Practically, this is the most important series, since it is now used

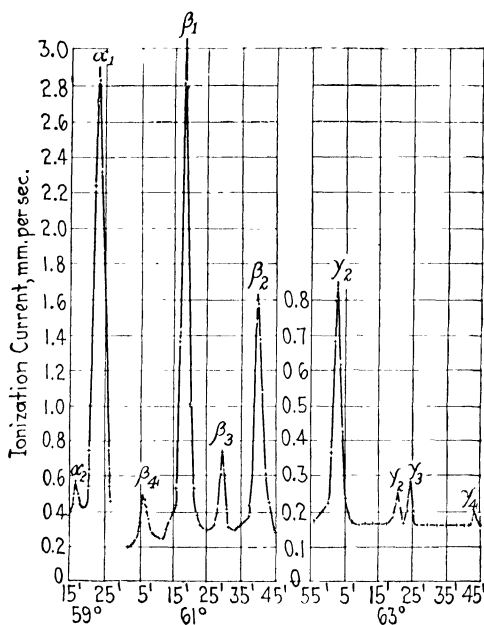


FIG. 32.—*L* series emission spectrum (tungsten).

almost exclusively in crystal analysis. The more numerous *L* series lines, illustrated in Fig. 32, are in three groups  $\gamma$ ,  $\beta$ , and  $\alpha$ , corresponding to the three *L* absorption discontinuities. About thirty have been identified. Because of the long wave lengths, measurements of the *M* and *N* series have been largely confined to the heaviest elements.

**Characteristic Absorption Spectra.**—There are also absorption discontinuities observed in x-ray spectra whenever a beam of x-rays undergoing spectroscopic analysis passes through absorbing material; the wave lengths corresponding to these discontinuities or edges are also characteristic of each of the chemical

elements. All rays with wave lengths shorter than that of a given discontinuity or edge will be absorbed by the element to a markedly greater extent than rays with wave lengths longer than this critical value. In other words, an absorbing screen which is relatively "opaque" to x-rays of a range of wave lengths up to a characteristic value is "transparent" to longer rays. Similarly, if a beam of x-rays is absorbed by a gas in which the ionization current is being measured, sharp discontinuities occur which correspond to wave lengths characteristic of the elements in the gas. A single absorption discontinuity is associated with the *K* series, three with the *L*, five with the *M*, probably seven with the *N*, and five with the *O*. Absorption bands which are observed on all photographs correspond to the *K* discontinuities of silver and bromine; the intensities as compared with the ionization curves are, of course, reversed because the absorbed energy blackens the emulsion to the greatest extent.

**The Relationship between Characteristic Emission and Absorption Discontinuities.**—It is a singular fact that all the lines in the *K* series emission spectrum are excited simultaneously when the energy conditions permit. Thus the  $\alpha$  doublet of the *K* series with definitely longer wave lengths cannot be made to appear without the  $\gamma$  and  $\beta$  lines, by adjusting the value of the voltage in the equation  $Ve = hc/\lambda_{K\alpha}$ . It is true that the spectrum obtained under such conditions will show the presence of rays with the same wave lengths as the  $K\alpha$  lines, but this spectrum is due only to general radiation and is not characteristic of the chemical element on the target. Nor will the *K* series lines appear when  $\lambda_{K\gamma}$ , corresponding to the emission line of shortest wave length, is substituted in the energy equation. An examination of the value of the wave length corresponding to the *K* absorption discontinuity for a given element serving as an absorber discloses the fact that this value is slightly shorter than the wave length of the characteristic  $K\gamma$  line emitted by this same element serving as a target. When the voltage on the x-ray tube is adjusted so that  $Ve = hc/\lambda_{K_{abs}}$ , then the entire emission series appears. It follows, also, that fluorescent x-rays can be emitted only when the primary x-ray beam contains rays with these critical wave lengths numerically the same as those which correspond to the absorption discontinuities; or shorter (*i.e.*, rays generated by a definite minimum voltage or higher). The energy represented by  $hc/\lambda_{abs}$  must be vitally related, there-

fore, to definite processes which are occurring in atoms when electrons in the cathode-ray stream strike them, or x-rays pass over them. The *L* series can be generated in three groups, since there are three quantum wave lengths or absorption discontinuities.

The effect of voltage on characteristic spectra differs markedly from that on the continuous spectrum. The latter is produced at any voltage but the short wave-length limit moves to smaller values as the voltage is increased. An emission series appears only at a critical voltage, and the only effect of a further increase of voltage is to increase the intensity of all the lines without altering them in position or in relative intensities.

#### THE EXPERIMENTAL RESULTS OF THE MEASUREMENT OF WAVE LENGTHS<sup>1</sup>

**Characteristic Absorption.**—The wave lengths of the *K* absorption limits have been measured for the elements with few

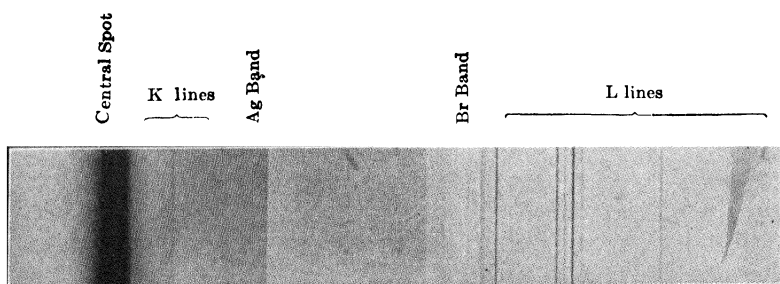


FIG. 33.—Spectrum from tungsten-target x-ray tube, showing the absorption edges of silver and bromine in photographic emulsion. (*de Broglie*.)

exceptions from magnesium (12) to uranium (92); of the three *L* limits for those from rubidium (37) to uranium (92); of the five *M* limits for tungsten (74) to uranium (92). The characteristic absorption discontinuities were observed by Barkla in his absorption measurements with screens before the discovery of the use of crystals as diffraction gratings. De Broglie in his first spectral photographs discovered the sudden changes in the blackening of the photographic plate due to the characteristic absorptions of silver and bromine in the photographic emulsion (Fig. 33); in both cases the plate was blacker on the side nearer

<sup>1</sup> For the detailed results of x-ray spectroscopy the reader is referred to "International Critical Tables," Vol. VI, pp. 36–44; Siegbahn, "Spektroskopie der Röntgenstrahlen," 2d ed., Berlin, 1931.

the zero direct-beam line, a phenomenon which accords with the definition of critical absorption wave length as the one such that the absorbing element absorbs x-rays of shorter wave length than the discontinuity to a greater extent than x-rays of longer wave length.

TABLE III.—CRITICAL ABSORPTION WAVE LENGTHS, *K* SERIES

12 Mg	9 5112	35 Br	0 9182	56 Ba...	0 3308
13 Al . .	7 9470	40 Zr	0 6874	74 W . .	0.17807
17 Cl . .	4 3938	42 Mo	0 61842	78 Pt . .	0 1581
24 Cr . .	2 0663	47 Ag	0 4852	79 Au...	0 1534
26 Fe . .	1 7405	53 I .	0 3738	82 Pb . .	0 1410
29 Cu	1 3790			92 U	0 1075

TABLE IV.—CRITICAL ABSORPTION WAVE LENGTHS, *L* SERIES

Element	$L_I$ ( $L_{11}$ )	$L_{II}$ ( $L_{21}$ )	$L_{III}$ ( $L_{22}$ )
47 Ag . . . . .	3 2474	3 5067	3 6908
53 I . . . . .	2 3839	2 5475	2 7139
56 Ba . . . . .	2 0620	2 1993	2 3568
74 W . . . . .	1 0205	1 0713	1 2116
78 Pt . . . . .	0 8921	0 9321	1 0709
82 Pb . . . . .	0 7806	0 8136	0 9500
92 U . . . . .	0 5687	0 5920	0 7216

The values in A.U. of the *K* absorption limits for a few of the more commonly used elements are as shown in Table III.

Some values of the *L* absorption limits are given in Table IV.

*M* absorption limits for thorium and uranium are given in Table V.

TABLE V.—CRITICAL ABSORPTION WAVE LENGTHS, *M* SERIES

Element	$M_{11}$ ( $M_I$ )	$M_{21}$ ( $M_{II}$ )	$M_{22}$ ( $M_{III}$ )	$M_{32}$ ( $M_{IV}$ )	$M_{33}$ ( $M_V$ )
Th .	2 388	2 571	3 058	3 552	3 721
U	2 228	2 385	2 873	3 326	3 491

**Emission Spectra.** *The K Series.*—In the wave-length region above 0.1 A.U. lie four groups of emission lines, the *K*, *L*, *M*, and *N* series. Each group in general retains the same appearance

from one element to the next, with a given line simply displaced to a shorter wave length in passing from one element to a heavier. The  $K$  series, as first photographed by Moseley in 1914, seemed to consist of two lines,  $\beta$  and  $\alpha$ , but these were later resolved into four lines  $\gamma$  ( $\beta_2$  in I.C.T.),  $\beta$ ,  $\alpha_1$ , and  $\alpha_2$ . For the light elements the spectra are more complex. The  $\beta$  line, in experiments of great precision, is further resolved into a doublet ( $\beta_1$  and  $\beta_3$ ). Very recently several more faint lines have been found in the  $K$  series; *e.g.*,  $K\beta_3$ ,  $K\beta'''$ , and  $K\eta$  are *satellites* of the line  $K\beta_1$ .<sup>1</sup> The wave-length difference between  $\alpha_1$  and  $\alpha_2$  varies from 0.0044 A.U. for tin to 0.00484 A.U. for hafnium and the remaining heavy elements.<sup>2</sup> The separation of the  $\beta$  doublet is about 0.00076 A.U. although there is a considerable variation; that of  $\gamma_\beta - \gamma_\gamma$  varies from 0.00955 A.U. for tin to 0.0048 A.U. for the elements above tungsten.

The relative intensities of the  $K$  lines have been the subject of several investigations. Duane and Stenström found the following relative values for the  $K$  lines of tungsten:

$\alpha_3$	$\alpha_2$	$\alpha_1$	$\beta_1$	$\gamma$
4	50	100	35	15

The ratio  $\alpha_1/\alpha_2 = 2/1$  seems to be generally true for practically all the elements. Allison and Armstrong<sup>3</sup> have obtained precision measurements for the following ratios: Mo- $K\beta$ /Mo- $K\alpha = 1/7.7$ ; Mo- $K\beta_1$ /Mo- $K\beta_3 = 2/1$  (the resolved doublet); Cu- $K\beta$ /Cu- $K\gamma = 42/1$ ; Cu- $K\alpha$ /Cu- $K\alpha_3\alpha_4 = 100/1$ . The appearance of lines and the relative intensities are, of course, of utmost importance in their bearing upon the structure of atoms and the levels of energy within them.

The  $K$  emission wave lengths are now known with considerable accuracy for most of the elements between carbon (6) and uranium (92). In Table VI are the most probable values for the elements most commonly employed as targets in x-ray tubes.

The lines are designated both by the Greek symbols and by the difference between two energy levels which will be explained in a later section.

<sup>1</sup> Cf. RICHMYER, *Phil. Mag*, **6**, 64 (1928).

<sup>2</sup> CORK-STEPHANSON, *Phys. Rev.*, **27**, 138, 530 (1926).

<sup>3</sup> *Proc. Nat. Acad. Sci.*, **11**, 563 (1925).

TABLE VI.—CHARACTERISTIC EMISSION WAVE LENGTHS, *K* SERIES

Element	$K - N_{21,22}$ $\gamma(\beta_2)$	$K - M_{22}$ $\beta_1$	$K - M_{21}$ $\beta_3$	$K - L_{22}$ $\alpha_1$	$K - L_{21}$ $\alpha_2$
24 Cr	2 0667( $\beta_3$ )	2 0806		2 28503	2.28891
26 Fe	1 74080( $\beta_3$ )	1 753013	1 75646	1 932076	1 936012
28 Ni	1 48561	1 49705		1 65450	1 65835
29 Cu	1 37824	1 38935		1 53739	1.54123
42 Mo	0 619698	0 630978	0 631543	0 707831	0 712105
45 Rh	0 53396	0 54449	0 54509	0 61202	0 61637
47 Ag	0 486030	0 496009	0 49665	0 55828	0 56267
74 W	0 17898	0 18422		0 20862	0 21345
78 Pt	0 15887	0 16370		0 18523	0 19004

For the lightest elements as many as twelve or more lines may appear in the *K* series instead of the usual four or five. Wentzel first claimed that these lines are due to multiple ionization of the relatively simply constructed atoms and, therefore, are related to the ordinary lines ( $\gamma$ ,  $\beta$ ,  $\alpha_1$ ,  $\alpha_2$ ) as the spark lines are to the arc lines in optical spectra. Thus an  $\alpha_3\alpha_4$  line or doublet and other “non-diagram” lines appear in all elements below zinc, in addition to the regular  $\alpha_1\alpha_2$  doublet. In the past three years great progress has been made on the interpretation of “satellite” or non-diagram lines by Richtmyer, Langer, and others as due to two-electron jumps in an atom.<sup>1</sup> The longest *K* series line recognized by “International Critical Tables” is the unresolved  $\alpha$  line of carbon, average 44.79 A.U.

It will be observed from the foregoing data that the wave length of the *K* $\gamma$  emission line is only a fraction of a per cent longer than that of the *K* absorption limit. It is a point of great interest whether there are any additional lines between *K* $\gamma$  and the limit. Larsson measured a *K* $\beta_4$  line for molybdenum at 0.61825 A.U. One of the most interesting recent discoveries in x-ray science is that of Duane in 1931. *K* series x-rays were examined by means of a Bragg spectrometer, the Moseley photographic method being employed. The incident ray and that reflected by the crystal to the photographic plate through distances of 4,725 mm. passed through long metal tubes, exhausted of air in order to reduce the absorption. The *K* $\beta$  doublet lines of molybdenum ( $\Delta\lambda = 0.00056$  A.U.), examined by photometric curves, appear separated 0.88 mm. No third line lay in the

<sup>1</sup> A complete account is found in Siegbahn, 2d ed., pp. 370–378.

immediate neighborhood of the  $\beta$  doublet. Between the  $\gamma$  line and the short wave-length limit of the series appeared a marked blackening that represented several lines close together. They were not in the position of a line reported by Leide. The new lines may be due to  $O$  electrons falling into the  $K$  level, but a better explanation is, perhaps, that the lines were produced by falls into the  $K$  level of conductivity electrons which may from time to time lie in outer atomic energy levels. Several photographs produced by long exposures showed a fainter single line, roughly halfway between the  $\beta$  and the  $\gamma$  lines. It did not correspond to a known x-ray line of any chemical element reflected in the first or second order. Ross<sup>1</sup> has also found this line which he calls  $\beta_4$  with an intensity of  $1/1000$  that of  $K\alpha$ , another,  $\beta_5$ , and two groups of still fainter lines near  $\gamma$  and  $\beta$  lines.

*The L Series.*—The complexity of the  $L$  series, which has already been referred to, prevents its extensive use for practical purposes. It is interesting to note, however, that the new elements, hafnium (72), rhenium (75), illinium (61) and (87), were all discovered by means of analysis of their  $L$  emission lines. More than twenty lines in the  $\alpha$ ,  $\beta$ , and  $\gamma$  groups have been identified for uranium; this number decreases with decreasing atomic number, as is to be expected upon the basis of atomic models in which outer shells of electrons disappear. Measurements of the tungsten  $L$  series give the following values:

TABLE VII.—WAVE LENGTHS, TUNGSTEN  $L$  SERIES

$\gamma_4$	$L_{11} - O_{21,22}$	1 02647	$\beta_7$	$L_{22} - N_{43,44}$	1 2208
$\gamma_9$	$L_{11} - N_{33}$	1 0439	$\beta_{11,12} \dots$	$\dots$	1 2354
$\gamma_3$	$L_{11} - N_{22}$	1 05965	$\beta_2$	$L_{22} - N_{32,33}$	1 24191
$\gamma_2$	$L_{11} - N_{21}$	1 06584	$\beta_3 \dots$	$L_{11} - M_{22}$	1 26000
$\gamma_6$	$L_{21} - O_{32}$	1.0720	$\beta_1$	$L_{21} - M_{32}$	1 27917
$\gamma_8$	$L_{21} - O_{11}$	1 079	$\beta_6$	$L_{22} - N_{11}$	1 2871
$\gamma_1$	$L_{21} - N_{32}$	1 09553	$\beta_4$	$L_{11} - M_{21}$	1 29874
$\gamma_5$	$L_{21} - N_{11}$	1.1292	$\beta_{11}$	$L_{11} - M_{11}$	1 3344
$\beta_9$	$\dots\dots\dots$	1 2021	$\eta \dots$	$L_{21} - M_{11}$	1.4177
$\beta_8$	$L_{11} - M_{33}$	1 2034	$\alpha_{1\dots}$	$L_{22} - M_{33}$	1 47348
$\beta_{10}$	$\dots$	1 2094	$\alpha_2 \dots$	$L_{22} - M_{32}$	1 48452
$\beta_5$	$L_{22} - O_{32,33}$	1 2125	$l.$	$L_{22} - M_{11}$	1 67505

The relative intensities of the lines  $L\alpha_1/L\alpha_2$  are  $10/1$ ; the  $\gamma$  lines are in the order  $\gamma_1:\gamma_2:\gamma_3:\gamma_4:\gamma_5:\gamma_6 = 100:14.0:22.3:7.0:3.0:2.3$ ;

<sup>1</sup> *Phys. Rev.*, **39**, 536, 748 (1932).



for the  $\beta$  lines  $\beta_1:\beta_2:\beta_3:\beta_4:\beta_5:\beta_6:\beta_7:\beta_8:\beta_9:\beta_{10} = 100:49.3:15.0:7.7:0.47:2.0:0.4:0.68:0.60$ .<sup>1,2</sup>

The  $L$  series wave lengths are known more or less completely for all the elements from vanadium (23) to uranium (92).

With remarkable ingenuity in using, as diffraction gratings in their vacuum spectrograph, crystals of palmitic and stearic acid, Siegbahn and Thoreaus made measurements upon the very long wave length  $\alpha$  and  $\beta$  lines in the  $L$  series spectra of zinc, copper, nickel, cobalt, and iron, the values ranging from 11.99 to 17.66 A.U. The longest  $L$  line recognized by I.C.T. is the  $\alpha_{1,2}$  line of vanadium at 24.200 A.U. Practically all measurements are now being made with ruled gratings rather than with organic crystals.

*The M and N Series.*—The  $M$  series was discovered by Siegbahn in 1916, and later measurements were made by Stenström and Karcher. The researches of Hjalmar with a vacuum spectrograph extended knowledge of this series in a remarkable way. In 1931, Lindberg using ruled gratings determined with great completeness and accuracy the wave length of the  $M$  series lines for elements from uranium (92) to cerium (58), with values ranging from 2.440 A.U. for the  $M_{II}O_{IV}$  line of uranium to 14.030 for the  $M_VN_{VI}$  or  $\alpha_I$  line of cerium. For tungsten the wave lengths of the strongest  $M$  emission lines are 6.076 ( $\gamma$  or  $M_{III}N_V$ ), 6.743 ( $\beta$  or  $M_{IV}N_{VI,VII}$ ), and 6.969 A.U. ( $\alpha$  or  $M_VN_{VII}$ ). Hjalmar also photographed lines belonging to the  $N$  series of uranium, thorium, and bismuth. The line at 13.805 A.U. for thorium was the longest wave length spectroscopically measured prior to the studies of Siegbahn and Thoreaus using stearic acid crystals as gratings.

**The Measurement of Long Wave Lengths by Methods Other Than X-ray Spectroscopy.**—Many investigators have attempted to measure wave lengths of the soft x-rays, particularly for the very lightest elements, by locating the discontinuities in the slope of the curves representing the photoelectric current as a function of the exciting voltage. Essentially the method consists in allowing radiation from the target of a highly evacuated x-ray tube to fall on a plate within the tube, which is connected to an electrometer. The current is kept constant and the voltage varied in steps. The various potentials corresponding to dis-

<sup>1</sup> Increasing subscripts refer to decreasing intensity.

<sup>2</sup> ALLISON and ARMSTRONG, *Proc. Nat. Acad. Sci.*, **11**, 563 (1925).

continuities in the curve are considered to be the limiting voltages for the *K* and *L* series. Important values so obtained are H-*K* 912, He-*K* 493, C-*K* 42.6–45.4, N-*K* 33.0–35.1, O-*K* 23.8–25.8, Na-*L* 35.3, Al-*L* 100, Al-*M* 326, etc.

Reference has been made on page 51 to the use of ruled gratings. Thibaud's measurements with crystal and grating were in good agreement. In the range of very long wave lengths the same lines were obtained from an x-ray tube and from an ultraviolet vacuum spark. Grating results are as follows: O-*K* $\alpha$  23.8, N-*K* $\alpha$  31.8, C-*K* $\alpha$  44.9, B-*K* $\alpha$  68.0, Fe-*L* $\alpha$  17.7, Fe-*L* $\eta$  19.6, Fe-*L* *l* 20.1, Mo-*M* 65.0, 54.9, Ta-*N* 58.3, 61.4, W-*N* 56.0, 59.0, Pt-*N* 48.0, 51.0, Au-*N* 46.8, 49.4. These values have been a powerful aid in the establishment of energy levels. Besides checking the measurements on the doublets of Ta, W, Pt and Au, del Rosario<sup>1</sup> has extended them to Hg and Ir and proved that the origins are transitions in the *N* shells, for example  $N_{IV} - N_{VI}$ , contrary to the principle of selection discussed below.

**X-ray Spectra and Chemical Valence.**—Since characteristic x-ray absorption and emission are processes in which the inner-

TABLE VIII.—PRINCIPAL AND SECONDARY ABSORPTION EDGES FOR CL AND S (LINDH)

Absorber	<i>K</i> <sub>1</sub>	<i>K</i> <sub>2</sub>	Absorber	<i>K</i> <sub>1</sub>	<i>K</i> <sub>2</sub>
Cl <sub>2</sub>	4 3938	4 3816	S monoclinic	5 0090	4 9946
HCl	4 3853		S rhombic	5 0086	4 9938
Chlorides <sup>1</sup>	4 3829	4 3600	S crystal	5 0088	4 9941
Chlorates	4 3769	4 3574	Sulfides	5 0093	Depends on metal ion
Perchlorates	4 3698	4 3478	Sulfites	4 9960	4 9881
			SO <sub>2</sub>	5 0040	4 9964
			Sulfates	4 9879	Depends on metal ion
			S <sup>++</sup> (organic)	5 0068	
			S <sup>4+</sup> (organic)	5 0019	
			S <sup>6+</sup> (organic)	4 9939	

<sup>1</sup> The different edges for chloride, chlorate, and perchlorate enable an analysis for purity of any salt.

most electrons in the atom are concerned, it is reasonable to suppose that the external or valence electrons have little or no effect upon the wave lengths. For many years it was generally agreed that the characteristic wave lengths were entirely independent of the state of chemical combination of the element; thus

<sup>1</sup> *Phys. Rev.* **41**, 136 (1932).

sulfur or manganese as elements, or exhibiting various valences in compounds, were thought to give always the same critical absorption or emission wave-length values. Precision researches, largely in the Siegbahn laboratory, have now demonstrated that for lighter elements there are small but distinct variations in these values depending upon the state of the element in the absorbing screen or target of the x-ray tube. Furthermore, a fine structure is found for the limits of certain elements. Lindh investigated both the emission lines and the absorption edges of chlorine, sulfur, phosphorus, and other elements. Wave lengths of the absorption edges of chlorine and sulfur are assembled in Table VIII ( $K_1$  and  $K_2$  principal and secondary edges, respectively). These values have been verified and extended by Stelling and others. Complete data are tabulated in the second edition of Siegbahn, "Spektroskopie der Röntgenstrahlen," pp. 278-306. Hanawalt<sup>1</sup> has made the most recent experimental study of the dependence of x-ray absorption spectra upon chemical and physical state. Spectra with a simple edge and with secondary absorption are shown in Fig. 34. Monatomic vapors exhibit no secondary structure at a distance from the main edge greater than the ionization potential. Polyatomic vapors usually have a secondary structure similar to that exhibited by the same

molecule in the solid state, but there is often additional structure observed for the solid state. The contention that completed outer electron shells are associated with the absence of secondary absorption is not verified, since Br absorption in the photographic plate and others show a secondary structure. The usual theories of secondary absorption are those of multiple electron transitions, transition of electrons in multiply-ionized atoms (Wentzel), and energies of excitation of vibrational states of "structure electrons" (Richardson). Further research and even greater experimental resolution are required for a final conclusion.<sup>2</sup>

<sup>1</sup> *Phys. Rev.*, **37**, 715 (1931).

<sup>2</sup> For a general summary with complete bibliography of 60 references see Stintzing, "Röntgenstrahlen und Chemische Bindung," *Fortschritte der Röntgenforschung*, Leipzig, p. 275, 1931.

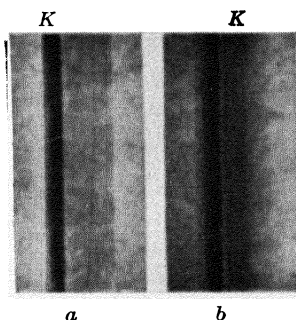


FIG. 34. —  $K$ -absorption spectra showing: *a*, simple edge; *b*, edge with secondary absorption. (Hanawalt.)

### Methods of Obtaining Homogeneous Monochromatic X-rays.

The beam of x-rays produced by any ordinary x-ray tube is obviously heterogeneous and contains many wave lengths. The general radiation is a continuous band and upon this is superposed above certain voltages the characteristic spectral series. In many applications of x-rays it is highly desirable to have a homogeneous beam of known wave length. This is particularly true for the analysis of the fine structure of materials. Even at very high voltages for deep therapy, the effort is made to homogenize the beam by filtration through sheets of metal so that dosage can be reproduced.

There is only one method of assuring a monochromatic ray, and this is the use of the double spectrometer. At a given angular setting  $\theta$  of a crystal grating with constant  $d$ , only those rays with a certain wave length  $\lambda$  can be reflected at the definite angle  $2\theta$  from the primary undeviated beam. Consequently the second spectrometer or other apparatus can be adjusted to receive the purely monochromatic beam.<sup>1</sup> Davis, Compton, Allison, and others have made excellent use of the double spectrometer to measure wave lengths accurately, to study the natural widths of spectral lines, etc. For practical purposes the method has the disadvantage that a loss in energy occurs in every reflection or diffraction process and the intensity of the radiation is thus diminished.

The second method of rendering a beam homogeneous is by the use of the characteristic absorption edges. Suppose that a molybdenum-target tube is excited at 30 kv.: the spectrum shows the  $K$  series lines superposed on the smooth general radiation curve. If, however, the first part of this band and the  $K\gamma$  and  $K\beta$  lines could be suppressed, and the  $K\alpha$  doublet left in essentially undiminished intensity, a useful "dichromatic" (since the doublet cannot be separated satisfactorily) beam would result. It is necessary only to discover an element whose  $K$  absorption edge wave length lies between the  $K\beta$  and  $K\alpha$  wave lengths of molybdenum (*i.e.*, between 0.631 and 0.708 A.U.) and use this for a filtering screen. Table III shows that zirconium has a  $K$  critical absorption wave length of 0.6874 A.U.; a thin screen interposed in the molybdenum-target beam will cut out practically completely radiation with wave lengths shorter than

<sup>1</sup> Cf. COMPTON, *Rev. Sci. Inst.*, **2**, 365 (1931); ALLISON, *Phys. Rev.*, **41**, 1 (1932).

this value but will be nearly transparent to the most intense  $\alpha$  doublet.

The following table presents some representative examples of selective absorption for obtaining homogeneous rays:

TABLE IX.—FILTERS FOR OBTAINING MONOCHROMATIC X-RAYS

Target	Lowest approximate voltage for $K$ series, kilovolts	$\lambda$ for $K\alpha$ doublet	Filter	Thickness, (millimeter)	Grams per square centimeter
Chromium	6	2 287	Vanadium		
Iron . . .	7	1 935	Manganese	0 005	0 004
Copper	9	1 539	Nickel	0 007	0 0067
Molybdenum	20	0 710	Zirconium	0 03	0 020
Silver	25	0 560	Palladium	0.03	0 036

The third method of generating a nearly monochromatic ray is largely of theoretical interest only. Reasoning from the probable mechanism of the excitation of the continuous spectrum, Duane conceived the idea of bombarding a very thin stream of mercury vapor and liquid with cathode rays so that there would be little chance for stepwise slowing up of the electrons. Under ideal conditions a single line for the short wave-length limit, instead of a continuous band, would be obtained. This ideal was very nearly realized by Duane in obtaining a very narrow sharp peak with a maximum only slightly longer than the  $\lambda_0$  defined by  $Ve = hc/\lambda_0$ .

#### GENERALIZATIONS FROM X-RAY SPECTROSCOPIC DATA

**The Moseley Law.**—The brilliant young Englishman Moseley, who was called from his remarkable researches to lose his life in the Dardanelles in 1915, was the first to recognize the essential simplicity of the  $K$  emission series. He showed that the wave lengths of a given spectral line varied *continuously* step by step in proceeding from one atomic number to the next, and not *periodically* as is the case with so many atomic properties. Even in optical line spectra there are definite relationships for chemically similar elements—doublets for the alkali metals, singlets and triplets for the alkaline earths—and spectra of increasing complexity in passing from left to right in the periodic table. The periodic properties such as these optical spectra,

atomic volumes, etc., must find their origin in the outermost parts of the atoms; the non-periodic properties such as the x-ray spectra must be ascribed to the interior. The original Moseley *K* series spectra for several neighboring elements beginning with arsenic (33) are reproduced in Fig. 35.

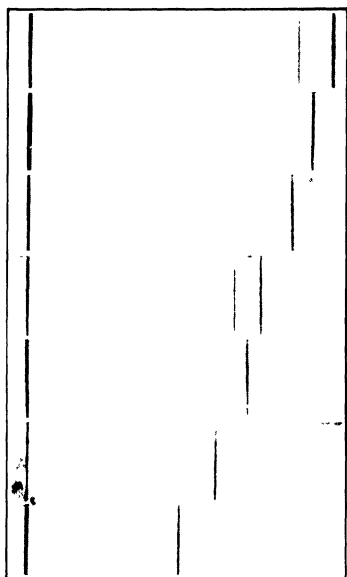


FIG. 35.—*K* series spectral lines for several neighboring elements, illustrating the continuous wave-length progression and the Moseley law.

Moseley went further and showed that if the square root of the reciprocal of the wave length (or of the frequency or of the wave number, which is the frequency divided by a fundamental frequency constant  $R$ , the Rydberg constant) of a given x-ray line,  $K\beta$ ,  $K\alpha$ ,  $L\alpha$ , etc., were plotted against atomic number, a practically straight line resulted. Precision researches have demonstrated that the curves are very slightly concave upward. For a *K* line the curve is characterized by the equation  $\sqrt{\nu/R} = \sqrt{3/4} (Z - 1)$ , where  $Z$  is the atomic number, or  $\nu = R (Z - 1)^2$

$\left(\frac{1}{1^2} - \frac{1}{2^2}\right)$ , a form which is of great significance in its analogy to that expressing the frequencies of the ultraviolet Lyman spectral series of hydrogen. Similarly an *L* series line frequency is given approximately by  $\nu = R(Z - 7.4)^2 \left(\frac{1}{2^2} - \frac{1}{3^2}\right)$ , which is

analogous to the expression for the Balmer series for hydrogen.

A remarkable extension of the Moseley law has been made in the region of optical spectra by Millikan and Bowen in their experiments with stripped atoms. Working with elements in the second horizontal row in the periodic table, they have compared the spectra of sodium, magnesium<sup>+</sup> (one electron removed), aluminum<sup>2+</sup>, silicon<sup>3+</sup>, phosphorus<sup>4+</sup>, sulfur<sup>5+</sup>, and chlorine<sup>6+</sup>, all of which, therefore, have exactly the same number of electrons and differ only in the mass and charge of the nucleus. The spectra are identical in appearance, and the square roots of

the frequencies of a given line are a linear function of atomic number. Richtmyer has demonstrated also that Moseley relationships hold true for non-diagram or satellite lines.

**Applications of the Moseley Law.**—The simplicity of the relationship between spectral line frequency and atomic number, which according to present conceptions represents the net positive charge on the nucleus, and also the number of non-nuclear electrons, suggests several valuable applications.

1. The law proves that a fundamental relationship exists among all elements from hydrogen to uranium; that these are all constructed of the same building units in definitely progressing complexity; and that if x-ray spectral lines are to be ascribed to the innermost electrons in atoms, as is indicated by the high frequencies and consequently large energy changes, these inner electrons must be essentially the same in number and disposition in all atoms, regardless of the number of electrons constituting the outer portions, or of the state of chemical combination of the element.

2. The law has been the fundamental basis upon which the discovery and identification of the recently discovered new elements has depended. Interpolation of the  $\sqrt{\nu}$ -atomic number curves, or calculation, gives the wave length which should be expected for a given *K* or *L* or *M* line in the spectrum of an unknown element. In every case the process of discovery has been the matching of experimental lines from material used as the target of an x-ray tube with the theoretical values. In this way Coster discovered hafnium (72); Tacke and Noddack masurium (43) and rhenium (75); Hopkins and his students in 1926 identified the rare earth illinium (61). In this last case the measured wave lengths of strong lines were 2.2781 and 2.0770 A.U., corresponding to the predicted values for the  $L\alpha_1$  and  $L\beta_1$  lines of the element 61, respectively, of 2.2777 and 2.0730 A.U. Finally in 1931 Papish announced the presence of element 87 in the mineral samarskite with the characteristic x-ray wave lengths  $M\alpha_1 = 4.517$ ,  $L\alpha_1 = 1.026$ ,  $L\alpha_2 = 1.038$ ,  $L\beta_2 = 0.853$ , and  $L\eta = 0.944$  A.U.

3. Qualitative and even quantitative analysis of any unknown substance is, of course, directly possible by analysis in similar fashion of the emission lines. Analytical applications of x-rays will be considered in Chap. VI.

**The Combination Principle.**—While the Moseley law gives the relationship among elements of varying atomic number from the standpoint of any given x-ray spectral line, another principle observed from experimental data gives important information concerning the relationship between lines and absorption discontinuities in different series for the same element. Thus the frequency of the  $K\beta$  line equals the sum of the frequencies of the  $K\alpha$  and  $L\alpha$  lines. The differences between the  $K$  critical absorption frequency and two of the  $L$  critical absorption frequencies equal, respectively, the frequencies of the  $K\alpha$  emission lines; and the difference between the  $K$  absorption frequency and one of the  $M$  critical absorption frequencies is equal to the frequency of the  $K\beta$  emission line; thus the differences between values of  $\nu/R$ , where  $\nu$  is the frequency and  $R$  the Rydberg constant, of the absorption discontinuities of tungsten are equal to  $\nu/R$  values for emission lines, as follows:

$$K - L_{\text{III}} = 4.367 \rightarrow K\alpha_1 = 4.3682.$$

$$K - L_{\text{II}} = 4.268 \rightarrow K\alpha_2 = 4.2693.$$

In the same way the frequencies of  $L$  and  $M$  absorption discontinuities give the frequencies of certain  $L$  emission lines. Thus the combination principle, long known in optical spectra, applies simply to x-ray spectra. In addition, Sommerfeld, Siegbahn, and others have noted important relationships between doublets in x-ray spectra. As an example may be cited the following pairs of values of the wave numbers ( $\nu/R$ ) for tungsten:

$L\eta$ .....	642 78	$L\beta_1$ . . . .	712 39	$L\gamma_6$ . . . . .	831.81
$Ll$ .....	544 03	$L\alpha_2$ .....	613 85	$L\beta_6$ . . . . .	733 76
	<hr/>		<hr/>		<hr/>
	98.75		98 54		98 05
$L\gamma_6$ .....		850 07	$K\alpha_1$ .....		4368 5
$L\beta_6$ .....		751 56	$K\alpha_2$ .....		4270 0
		<hr/>			<hr/>
		98 51			98 5

Here are at least six doublets with the same difference, which is simply that between two  $L$  absorption limits:  $L_{\text{II}} 849.59 - L_{\text{III}} 750.88 = 98.71$ . The wave-length differences corresponding to these values for each of these doublets (regular or relatively) remains practically constant for all the elements. Another type of doublet (irregular or screening) is that observed by Hertz, where the difference in  $\sqrt{\nu/R}$  values for pairs of critical absorp-



tion values ( $L_{II}$  and  $L_I$ ) is constant from one element to the next. These two types of doublets occur alternately in the structure; thus  $L_{III}$  and  $L_{II}$  are relativity,  $L_{II}$  and  $L_I$  are screening,  $M_V$  and  $M_{IV}$  relativity,  $M_{IV}$  and  $M_{III}$  screening, and so on. Such facts as these indicate at once the possibility of definite levels of energy in atoms, the differences corresponding to the frequencies of emitted or absorbed radiation, and doublets to a doubling of energy levels.

**The Facts of X-ray Spectra to Be Explained by a Theory of Atomic Structure.**—Any comprehensive theory of atomic structure must be able to account for the following facts of x-ray spectroscopy:

1. Critical absorption wave lengths.
2. Critical ionization wave lengths.
3. Sharp characteristic emission lines.
4. Grouping of spectral lines in series.
5. Critical excitation potentials for groups of lines.
6. The Moseley law, continuous, non-periodic progression in wave lengths.
7. The combination principle, regular and irregular doublets, and the relation between emission and absorption.

**The Bohr Theory of Atomic Structure.**—Before outlining very briefly the Bohr theory of atomic structure, by means of which a very useful mechanical model could be constructed and processes related to radiation clearly pictured, it must be frankly stated that the model is deficient and unable to meet the demands of the newest experimental physics. However, new quantum or wave mechanics theory, in which the mechanical model of the atom is replaced by a mathematical equation has not advanced as yet to the stage where any very satisfactory geometrical model can be visualized in terms of the facts of x-ray spectra. Hence the Bohr theory of the planetary atom still is worthy of presentation and use as a qualitative tool, particularly as it utilizes fundamental quantum laws. Sir William Bragg advises that science must not be criticized for dropping one theory in favor of another, as a carpenter is not scolded for dropping his saw to use his chisel. In a word, science can neither believe wholly in the Bohr atom nor do without it.

In addition to some of the experimental facts of x-ray spectroscopy, there were in 1916 four other great factors, which were largely unrelated and even discrepant, to be taken into considera-

tion by any theory. These were: the classical electromagnetic (wave) theory of radiation, the Planck quantum theory of radiation, the Rutherford nuclear atom, and the empirical (optical) spectroscopy of Balmer, Ritz, and Rydberg. The last factor refers to the relationships such as the following for the optical series of hydrogen: Lyman series,  $\nu_1 = \nu_0 \left( \frac{1}{1^2} - \frac{1}{n_1^2} \right)$ ,  $n_1 = 2, 3, 4, \dots$ ; Balmer series,  $\nu_2 = \nu_0 \left( \frac{1}{2^2} - \frac{1}{n_2^2} \right)$ ,  $n_2 = 3, 4, 5, \dots$ ; Paschen series,  $\nu_3 = \nu_0 \left( \frac{1}{3^2} - \frac{1}{n_3^2} \right)$ ,  $n_3 = 4, 5, 6, \dots$ ; etc., or in general  $\nu = \nu_0 \left( \frac{1}{m^2} - \frac{1}{n^2} \right)$ .

The fundamental assumptions of the original Bohr theory are as follows:

1. The atom consists of a positively charged, extremely minute nucleus which accounts for practically all the mass, and of negative electrons as satellites. The number of these electrons is equal to the net number of positive charges on the nucleus, and this number is the atomic number. The table of elements is constructed by the addition of one net positive charge and one non-nuclear electron for each element, beginning with hydrogen with one positive charge on the nucleus and one electron.

2. The atom is a dynamic system, for the electrons are in rapid orbital motion.

3. Three laws govern this atom:

- a. An Acceleration Law.*—In a simple atom like hydrogen, with the assumption that the mass of the nucleus  $M$  is infinitely great in comparison to the electron so that the electron remains in fixed position, the coulomb force of attraction between positive and negative charges is opposed by the centrifugal force required to keep the electrons revolving in a circle; in other words  $e^2/a^2 = mv^2/a$ , where  $e$  is the electric charge (+ or -),  $a$  the distance between two charges,  $m$  the mass of the electron, and  $v$  its velocity.

- b. A Momentum Law.*—The angular momentum is governed by the equation  $mva = nh/2\pi$ , where  $n$  is an integer and  $h$  is a constant. In other words, the motion of the electron is very definitely restricted to orbits whose angular moment multiplied by  $2\pi$  is equal to  $nh$ . The possible configurations under this

quantum condition are called stationary states because no radiation is emitted while the atom remains in such a state.

*c. A Frequency Law.*—While an electron is revolving in any definite orbit of definite energy  $W_1$ , it is conceived to be non-radiating, for otherwise energy would be lost and the electron would be pulled gradually into the nucleus. Another orbit  $W_2$  would correspond to a different energy level. It is only in the process of transition of an electron from one orbit to another that radiation may be emitted or absorbed; in other words, the energy difference  $W_1 - W_2 = h\nu$ , where  $\nu$  is the frequency of the radiation and  $h$  the Planck action constant. Ordinarily an atom exists in the stationary state of lowest energy but by absorption of radiation or some kinds of collisions it may be “excited” to a higher energy state. Radiation is emitted during the transition from a higher to lower state of energy.

A combination of these simple laws gives the equation

$$\nu = \frac{2\pi^2 e^4 m}{h^3} \left( \frac{1}{n^2} - \frac{1}{n'^2} \right), \text{ or } \nu = \nu_0 \left( \frac{1}{n^2} - \frac{1}{n'^2} \right),$$

where  $\nu_0$  is a fundamental constant frequency, the Rydberg constant already mentioned, and  $n$  and  $n'$  whole numbers; the equation expresses the frequencies of the spectral lines of hydrogen. There is thus immediate explanation for the empirical spectroscopic formulas of Balmer, Ritz, and Rydberg.

After the simple Bohr theory of hydrogen was announced, many corrections and additions were made. Briefly enumerated these were as follows:

1. Allowance for the mass of the nucleus (in ionized helium the mass 4 must be introduced).
2. Allowance for the revolution of the nucleus around the common center of gravity.
3. A relativity correction, taking into account the variation in mass with the velocity of electrons.
4. The introduction of elliptical orbits, in addition to Bohr's circular ones, to account for the fine structure of spectral lines. These orbits, in order to have energies which differ from those of the circular ones and thus to account for the complexity of apparently single lines, must undergo precession around the nucleus.
5. The most striking characteristic of the quantum theory of atomic structure is the frequent occurrence of integers and half

integers; it is essentially a theory of numbers which are combined in all possible ways. The types of elliptical orbits, upon which the electrons in the complicated atoms revolve, may be characterized by quantum numbers  $n$ ,  $k$ ,  $j$ . The number  $n$  is related to the size of the orbit,  $k$  to its shape, and  $j$  to its position in the atoms relative to other electronic orbits. For convenience a particular orbit is referred to as  $n_{kj}$ . The larger the value of  $n$  the more loosely is the electron bound to the atom.<sup>1</sup> Thus the innermost electron "shell" consists of a single circular orbit  $1_{11}$ , the second of two ellipses,  $2_{11}$  (most eccentric) and  $2_{21}$ , and a circle  $2_{22}$ , and so on.

6. By combination of x-ray, spectroscopic, and chemical information the complete arrangement of electrons in various shells or orbits has been derived, most satisfactorily in 1925 by Stoner and Main-Smith, for all the elements from hydrogen to uranium. As an example may be cited the structure for the rare gases of the atmosphere, which, except helium, always have eight outside electrons:

- 2. He  $1_{11}(2)$ .
- 10. Ne  $1_{11}(2)$ ;  $2_{11}(2)$ ;  $2_{21}(2)$ ;  $2_{22}(4)$ .
- 18. A  $1_{11}(2)$ ;  $2_{11}(2)$ ;  $2_{21}(2)$ ;  $2_{22}(4)$ ;  $3_{11}(2)$ ;  $3_{21}(2)$ ;  $3_{22}(4)$ .
- 36. Kr  $1_{11}(2)$ ;  $2_{11}(2)$ ;  $2_{21}(2)$ ;  $2_{22}(4)$ ;  $3_{11}(2)$ ;  $3_{21}(2)$ ;  $3_{22}(4)$ ;  $3_{32}(4)$ ;  
 $3_{33}(6)$ ;  $4_{11}(2)$ ;  $4_{21}(2)$ ;  $4_{22}(4)$ .
- 54. Xe, same as Kr and in addition  $4_{32}(4)$ ;  $4_{33}(6)$ ;  $5_{11}(2)$ ;  $5_{21}(2)$ ;  
 $5_{22}(4)$ .
- 86. Rn, same as Xe, and in addition  $5_{32}(4)$ ;  $5_{33}(6)$ ;  $6_{11}(2)$ ;  $6_{21}(2)$ ;  
 $6_{22}(4)$ .

This system explains many chemical and spectroscopic facts, the similarity in such homologous elements as Li, Na, K, Rb, and Cs, the chemical similarity of the triads Fe, Co, Ni; Ru, Rh, Pd; and Os, Ir, Pt; and the place of the 14 rare earths (57 to 71). Here the successive electrons are added in the  $4_{43}$  and  $4_{44}$  orbits, previously unoccupied, though electrons are being added in the fifth shell beginning with rubidium, atomic number 37.

**The Explanation of the Facts of X-ray Spectroscopy by the Bohr Atom.**—It is now certain that the fundamental orbit of the x-ray  $K$  series is a one-quantum orbit ( $n = 1$ ), that of the  $L$  series a two-quantum orbit ( $n = 2$ ).

The existence of individual, widely separated spectral series leads directly to the fundamental conception that a number of

<sup>1</sup> A third subquantum number takes into account electron spin.

electron groups are present in the atom which differ considerably from each other with respect to orbital energy and the distance between the electrons and the nucleus. Therefore, a single series arises from the transition of an electron from one of the outer groups (*e.g.*, the *L*, *M*, or *N* groups) to one of the inner groups (*e.g.*, the *K* group). The fine structure of the individual lines is due to the energy differences within a definite group; *e.g.*, the  $K\alpha_1$  and  $K\alpha_2$  lines are to be explained by transitions from two somewhat different *L* orbits to a single *K* orbit.

The energies of the various orbits or shells or levels are designated by the  $h\nu$  values of the experimentally measured critical limits,  $1K$ ,  $3L$ , and  $5M$ , and presumably  $7N$ ,  $5O$ , and  $3P$ , discussed on page 56. As a matter of fact, these are the energies required to lift an electron in its particular orbit out of the atom. For this reason the various levels may be designated either by reference to the letter *K*, *L*, etc., or to the quantum number  $n_{k,l}$ , or now even to the terms used analogously in optical spectra; for example, the following are synonymous:

<i>K</i>	<i>L<sub>I</sub></i>	<i>L<sub>II</sub></i>	<i>L<sub>III</sub></i>	<i>M<sub>I</sub></i>	<i>M<sub>II</sub></i>	<i>M<sub>III</sub></i>	<i>M<sub>IV</sub></i>	<i>M<sub>V</sub></i> .
$1_{11}$	$2_{11}$	$2_{21}$	$2_{22}$	$3_{11}$	$3_{21}$	$3_{22}$	$3_{32}$	$3_{33}$ , etc.
$1s$	$2s$	$2p_2$	$2p_1$	$3s$	$3p_2$	$3p_1$	$3d_2$	$3d$ .

The orbital energy is expressed by  $\sqrt{U/Rch} = Z^*/n$  where *U* is the orbital energy of an electron, *R* is the Rydberg constant, *c* the velocity of light, *n* the principal quantum number, and  $Z^*$  the effective nuclear charge; this is less than the true nuclear charge *Z* by virtue of the screening effect upon the electron in question, which other electrons of the atom with interpenetrating orbits exert upon the full attractive force of the positive nucleus. When  $Z^*/n$  is plotted against *Z*, the curves show that  $Z^*$  in the different levels, particularly for heavier atoms, does not vary in the same way with increasing *Z*. It is considerations such as these, indicating when electrons are added to a new shell before an underlying one is completed, which have led to the assignment of complete electron structures to all the elements; measurements of energy levels from experimental values of x-ray critical absorption limits have been one of the most valuable contributions.

The Bohr theory, therefore, explains the facts of x-ray spectra as follows:

1. *Critical Absorption Limits.*—Energy required in primary radiation quantum, or collision with cathode rays, to lift electrons from a given energy level out of atom.

2. *Critical Ionization.*—The frequency is the same as that of critical absorption, since only with energies greater than those corresponding to this frequency can ionization and electric current increase occur.

3 and 4. *Sharp Emission Lines in Series.*—When a  $K$  electron is removed,  $L$  electrons may fall into the vacancy producing  $K\alpha_1$  and  $K\alpha_2$  from two of the three  $L$  levels corresponding to circular and elliptical orbits. The  $K\beta$  doublet results from the transition of electrons from two of the five  $M$  levels, and  $K\gamma$ , an unresolved doublet, from transition from two  $N$  levels. If electrons in the  $L$  level are removed, the  $L$  series results by the transition from the higher  $M$ ,  $N$ , etc., levels to the  $L$  level. With three  $L$  and five  $M$  levels there are thus possible 15 lines from this one type. However, not all the lines so predicted appear. The spectra are governed by a partly empirical rule of selection which states that  $n$  in the quantum number  $n_{k,j}$  must change, that  $k$  must change by one unit and that  $j$  may change by one unit or remain unchanged. Recently a number of “forbidden” lines have been discovered, but they are very faint. Newly measured lines of very long wave length whose origins are transitions *within* the  $N$  shell ( $\Delta n = 0$ ) have been mentioned on page 64. Energy-level diagrams have been constructed for all the atoms to show how spectral lines in x-ray and optical regions are related to these transitions. Optical spectral lines are produced, of course, by electronic changes between the orbits farthest removed from the center. The complete energy-level diagram, as designed by Meggers, Foote, and others, is given in Fig. 36; each point represents an orbit characterized by an  $n_{k,j}$  value, and the lines joining these points represent electron transitions resulting in spectral lines. The diagram is a remarkably terse and complete expression of the origin of radiation and its relationship to atomic structure. It is independent of conceptions of orbits and the mechanism of electron jumps so holds useful in spite of deficiencies in the Bohr model of the atom.

5. *Critical Excitation Potentials.*—The  $K$  series lines are not excited separately but appear together only when the kinetic energy of the bombarding electron stream in the x-ray tube is equal to or greater than the value given by the equation  $E_k = Ve = h\nu_{K_{abs.}}$ . Similarly  $K$  series secondary fluorescent x-rays are excited only by primary rays with energies equal to or greater than  $h\nu_{K_{abs.}}$ . Only under these conditions is it possible

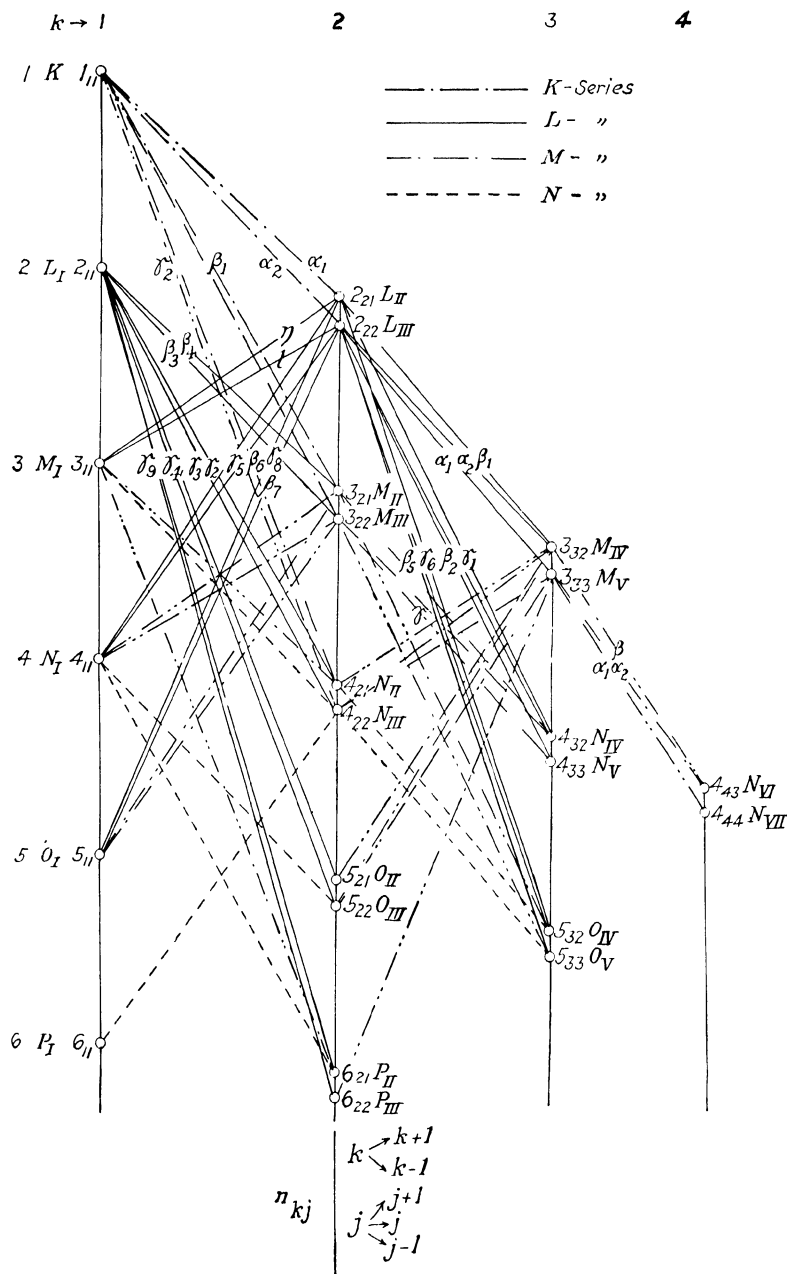


FIG. 36.—Complete energy-level diagram, showing the origin of x-ray spectral lines. (From Siegbahn, "Spectroscopy of X-Rays.")

to impart sufficient energy to the *K* electron to remove it entirely from the atom (not to the *L* or *M* levels, for example). The vacancy is supplied then by an *L*, *M*, or *N* electron; the new vacancy is filled from a still more distant shell. The atom returns to a neutral state by a process which, in general, takes place as a series of steps; but jumping over several steps and even the direct return of an outer electron to the *K* ring is not unusual.

6. *The Moseley law* is a consequence of the fact that the innermost levels in atoms, which take part in the production of x-rays, are all similarly constituted as regards number and disposition of the electrons.

7. *The combination principle* is a direct consequence of different energy levels with definite values. The same wave-number difference may be obtained by several combinations of the wave numbers of critical absorption limits and emission lines, when these are pictured as distinct jumps from lower to higher levels or *vice versa* (Fig. 36). The principle thus affords several checks for numerical evaluation of the energy levels.

**Happenings to an Electron in an X-ray Tube.**—In the light of the foregoing considerations of atomic structure, evidently at least four things can happen to an electron which is hurled at the anode in an x-ray tube:

1. It can be reflected from the anode surface.
2. It can pass through one or more atoms. The electric fields in the interior of the atom diminish the speed of the electron so that it loses part of its energy. This has been imparted to the atom whose kinetic energy is increased; thus the lost electron energy has been transformed not only into x-rays but also into *heat*, and the temperature of the anode rises. The slowed-up electron then may pass through another atom with further diminution in speed and so on until it is stopped.

3. It is stopped completely by impact with the atom nucleus. In this case only is the initial electron energy transformed completely to radiation as  $E_k = h\nu$  with a continuous spectrum as explained above. The stoppage in steps explains why from an x-ray tube operating at absolutely constant potential rays of different wave lengths are emitted. It is evident that x-rays are generated not only upon the surface of the anode but also in the interior of the metal. The thickness of the layer in which x-rays arise depends on the voltage and on the anode material;



with a tungsten target this is only about 0.001 mm. or a layer 2000 tungsten atoms deep.

4. In its impact on an atom in the anode the electron which has traveled from the cathode may eject an electron out of its energy level (or quantum orbit) in this atom either to another level, thereby producing an excited atom or entirely out of the atom, thereby producing an ionized atom. Characteristic x-rays are emitted as the atom returns to the normal state. The electron proceeds with smaller kinetic energy to any one of the four possible occurrences just enumerated.

**X-rays and the New Quantum Theory.**—Heisenberg<sup>1</sup> cites the following as the most important experiments from which may be deduced concepts of present physics:

a. Wilson photographs by the cloud-track method showing that  $\alpha$  and  $\beta$  rays may be regarded as streams of minute particles.

b. Diffraction of  $\beta$  rays or electrons, showing wave-like properties, discovered by Davisson and Germer in 1927.

c. The diffraction of x-rays showing form of wave motion, and the photoelectric ejection of electrons when x-rays strike matter, showing corpuscular properties.

d. The Compton-Simon experiment, in which x-rays passing through supersaturated water vapor are scattered by molecules, producing both recoil electrons and photoelectrons, the first by a collision of a photon (light particle) with an electron in a molecule and the second as a result of the collision of this photon moving in a new direction with a second molecule.

e. Collision experiments of Franck and Hertz leading to the conclusion that atoms in a gas through which a beam of slow electrons passes can assume only discrete energy values and "stationary states" as originally postulated by Bohr.

In simplest terms the essential facts involved underlying the new theories which have displaced the Bohr model are as follows:

1. Matter, including free electrons, and radiation possess a remarkable duality of character, since they sometimes exhibit the properties of waves, at other times those of particles. A phenomenon cannot be a form of wave motion and be composed of particles at the same time. It is experimentally certain only

<sup>1</sup> "Physical Principles of the Quantum Theory," University of Chicago Press, Chicago (1930).

that light sometimes behaves as if it possessed some of the attributes of a particle, but there is no experiment which proves that it possesses all the properties of a particle; similar statements hold for matter and wave motion.

2. Language is incapable of describing processes occurring within atoms, for it was invented to express the experiences of daily life which consist of processes involving exceedingly large numbers of atoms. Furthermore, it is almost impossible to modify language so as to describe these atomic processes, since words can only describe things of which we can form mental pictures and this ability is a result of daily experience. Mathematics is not subject to this limitation.

3. Contradictions between theory (Bohr) and experiment have led to the necessity of demanding that no concept which has not been experimentally verified should be involved in scientific formulations.

4. The principle of uncertainty shows among other things that the position and velocity of an electron (say in an orbit) cannot be known simultaneously. Determinism is dropped out of the latest formulations of theoretical physics.

5. The new theory removes discrepancies between the orbit theory and the facts of spectroscopy, particularly fine structure. The power of the new quantum mechanics in giving better understanding of events on an atomic scale is becoming increasingly evident. The structure of the helium atom, the existence of half-quantum numbers in band spectra, the continuous spacial distribution of photoelectrons, and the phenomenon of radioactive disintegration are items which baffled old theories but are successfully accounted for by the new.

6. As nearly as may be visually conceived, the new model of the atom spreads the electron from a point charge moving in orbits to diffuse shells of negative electricity with increasing density the closer to the nucleus. Hence the orbits are smudged, in the words of G. P. Thomson, but the electrons retain in a sense their individuality. However, Dirac regards waves or particles of light or electrons as two useful abstractions for describing the same physical reality but he warns the student against combining them into a mechanism that behaves like familiar things.

7. The Bohr atom is, therefore, welcomed today as an indispensable model, expected to remain so for many years to come,

and admitted to be inadequate. Even the most advanced mathematical physicists still speak of "orbits" and "electron jumps." Nor has the final word been said with the new mathematical models.

8. Finally, in the words of Jeans, "the Great Architect of the Universe now begins to appear as a pure mathematician."

## CHAPTER VI

### CHEMICAL ANALYSIS FROM X-RAY SPECTRA

Since definite x-ray wave lengths, both emission and absorption, are characteristic of the chemical elements, it follows that x-ray spectroscopy may find practical application in qualitative and quantitative analysis. The Moseley law, of course, is of splendid assistance, more particularly in the qualitative discovery of new elements in complex mixtures, since the wave lengths for these elements may be accurately predicted.

The five general procedures employed in analysis are as follows:

1. Measurement of primary spectral emission lines (*K* or *L* or *M* series) in which the unknown substance undergoing analysis is made the target of an x-ray tube.

2. Measurement of secondary fluorescent emission lines in which the unknown is so placed on some device inside the x-ray tube that it is screened from the cathode rays but directly irradiated by the primary x-ray beam.

3. The same except that the unknown is irradiated outside the x-ray tube; on this account the intensities are greatly decreased and the time required for photographic registration of the spectrum increased.

4. Measurement of wave lengths of characteristic absorption edges in which the unknown serves as an absorbing screen.

5. Use of a cathode-ray tube with thin windows for passage of rays, with bombardment of unknown outside and spectrographic analysis of x-rays generated.

**Apparatus.**—The essential apparatus for analysis comprises the x-ray tube and power plant and a crystal spectrograph. Special demountable tubes are required for methods 1 and 2. In the first case the sample must be pasted or fused on a cooled metal surface serving as anode. The tube so prepared is then pumped continuously. Any of the demountable electron or ion tubes described in Chap. III are used. For method 2 either a second target or some other special holder is required inside the

tube which must then be pumped. One of the best designs due to Stintzing is shown in Fig. 37. Both the vertical cone-shaped anode opposite the hot-filament cathode and the fluorescent-ray plate, horizontal left, are rotated. Another tube for method 2 which has been used with great success by Coster, Hevesy, and others is shown in Fig. 38.

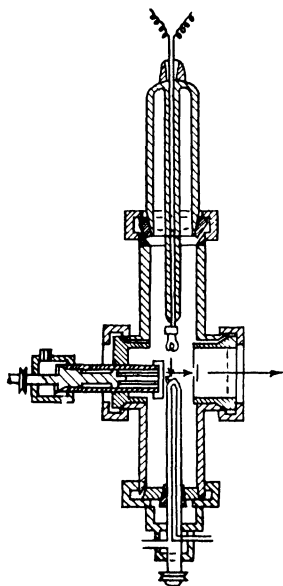


FIG. 37.

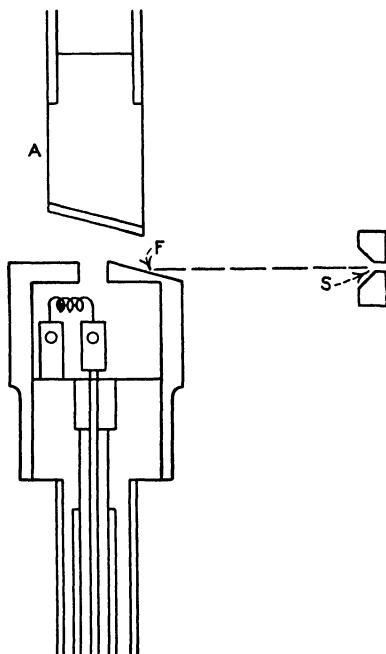


FIG. 38.

FIG. 37.—X-ray tube for chemical analysis by secondary fluorescent rays (Stintzing).

FIG. 38.—X-ray tube for chemical analysis by secondary fluorescent rays (Hevesy).

For methods 3 and 4 any standard x-ray tube with ordinary targets can be used, operated at requisite voltages for the excitation of the secondary radiation. Vacuum spectrographs are very largely used for analyses, particularly where minute amounts of substances are involved. Standard equipment such as shown in Fig. 39 is available in which the high vacuum of the tube is separated from the moderate vacuum of the spectrograph by aluminum foil. A calcite crystal with cleavage face as reflecting plane is used as grating. Registration of the spectra is

almost always photographic, although measurement of ionization currents with the ionization chamber spectrometer is easily

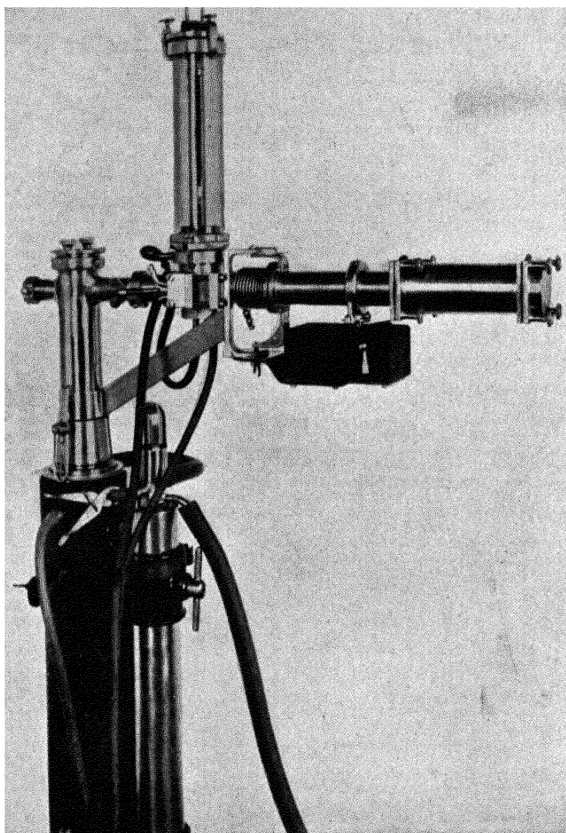


FIG. 39.—Seemann high-vacuum spectrograph shown attached to x-ray tube (vertical).

possible without vacuum. The crystal is best oscillated over a small angle by means of a motor and heart-shaped cam.

#### ADVANTAGES OF X-RAY ANALYSIS

1. Over chemical methods.

- a. Analysis of extremely minute amounts—triumph of discovery of elements 72, 43, 75, 61, and 87 (Papish 1931).
- b. Analysis of rare earths, platinum metals, etc., where separations are difficult or impossible.

- c. Material used in any available form without special preparation and independent of chemical combination and without loss; hence valuable for rare metals, gems, etc.
  - d. Greater safety, since no separation of elements is involved; hence much less work and great saving of time.
  - e. Permanent record on plates, largely independent of personal equation.
2. Over optical spectroscopy.
- a. The great simplicity of x-ray spectra, particularly the *K* series emission, as compared with the great complexity of optical spectra (notably iron).
  - b. Absolute independence of x-ray spectra (number of lines and relative intensities) from excitation conditions; optical spectra are affected by differences in arc and spark spectra, changes in capacity and induction of the current for ultraviolet causing disappearance or strengthening of lines, etc.
  - c. Independence of x-ray spectra from chemical combination or valence, since only atoms and not molecules are involved; optical spectra are affected by kind of chemical combination, band spectra of molecules, presence of foreign substances, etc.

#### DISADVANTAGES

1. Cannot be used for analysis of lightest elements, since characteristic wave lengths are too long for measurement by usual crystal gratings; the practical limit is calcium ( $Z = 20$ ).

2. Somewhat expensive and special equipment, much of it commercially available only in Europe.

3. Very special technique, including selection of proper voltage, etc., for accurate quantitative analysis.

4. Somewhat limited accuracy for quantitative work involving comparison of line intensities with standards. The line intensities are not proportional strictly to the weight proportions of elements in the preparation for several reasons noted below. Intensities also depend on the particle size of the substance undergoing analysis, and minimum size is essential for true values.

5. Selective volatilization of constituents of mixture from focal spot of target for primary emission method, with erroneous results; this difficulty is partly alleviated by rotating the anode in order to present fresh surface, or by using the fluorescent-spectra methods.

6. Great decrease in intensities and prolongation of time for fluorescent-spectra methods.

7. A serious difficulty for quantitative analysis is the effect of absorption edges on emission lines; if in a mixture one element has one characteristic absorption edge of longer wave length than the emission lines of other constituents of the mixture, these lines will be selectively absorbed. Such difficulties are avoided, when standardizing substances are used, by not mixing but by using a rotating target with the samples contiguous and excited to emission separately but, of course, registering on the same photographic plate. The effect of the absorption edges of silver and bromine in the plate must be taken into account also.

8. Line coincidence<sup>1</sup> may occur and cause difficulties; avoided only by greater resolution of spectra and use of higher orders of reflection.

9. Appearance of foreign lines, such as mercury, from diffusion pump; tungsten from metal sputtered in target from hot cathode, fluorescent metal lines from slits, traces of material from previous experiments on surface of anode, etc.; these can be checked with blank runs of apparatus.

10. In certain mixtures characteristic rays of one element can be excited by the characteristic rays of another element and thus produce a strengthening of intensity of lines for the first. Gunther, Stransky, and Wileke observed that a mixture of chromium and copper in the ratio of 46:54 appeared to have the ratio 60:40 on account of characteristic rays of chromium excited by copper rays. Dilution with ground quartz produced true results.

11. Varying sensitivity of the photographic emulsion to different wave lengths; long-wave lines are blacker in proportion to intensity than shorter.

**Qualitative Analysis.**—For the case of qualitative analysis of materials most of the foregoing disadvantages of the x-ray method are unimportant and the method is straightforward for the analysis, particularly of rare earths and alloys of every kind. The fluorescent method which has been hampered by low intensities and long exposure times is coming into almost universal use with the advent of high-power tubes producing very intense radiation.

**Quantitative Chemical Analysis.**—Methods of quantitative analysis using the emission spectrum have been described by Coster, Stintzing, Gunther and Wileke, Hevesy, Glocker, Goldschmidt, and others. In general these methods depend upon the comparison of the intensities of corresponding spectral lines of two neighboring elements in the periodic table, the assumption being made that the intensities of, say, the *K* lines of two such elements would be the same because of the similar electronic configurations, provided the elements were present in the same amounts on the anticathode, and provided also that the excess of the potential on the tube over the potential required to excite these lines was great compared with the difference between the characteristic excitation potentials of the two lines. (In the first approximation the intensity of a spectral line is proportional to the second power of the difference between the potential used and the characteristic potential.)

<sup>1</sup> GLOCKER, "Materialprüfung mit Röntgenstrahlen," p. 119, Berlin (1927).



The actual procedure in all these methods consists in determining, photographically, the emission spectrum of a mixture containing an unknown amount of the element for which the determination is being made and a known amount of the reference element. The intensities of the two corresponding lines of these two elements which have been chosen for comparison are then measured, and the elements are then, on the previous assumptions, present in amounts proportional to the intensities of their respective lines; or the amount of the reference material may be changed until the two intensities are equal, when their atomic amounts are also equal.

The differences in the methods mentioned are mainly differences in the technique of measuring the line intensities. Coster used a Siegbahn spectrograph and measured the relative line intensities with a Moll microphotometer. Gunther and Willeke used spectrograms made with very small times of exposure, the lines being hardly visible to the eye. By using a microscope of 800 magnification, they then directly counted the reduced silver grains in the film. The choice of the time of exposure is very delicate with this procedure, for too long a time causes agglomeration of the grains, making counting inaccurate and difficult. Stintzing mentions the use of a microphotometer and also suggests a simpler method. He proposes the use of several superimposed photographic plates to record the spectrogram, the intensities of the several lines being indicated by the number of films they penetrate.

Coster and Nishina, indeed, found the assumption of equal intensity of the lines for equal atomic concentration to be valid only under certain conditions. For instance, in analyzing zirconium ores for hafnium, tantalum was added as the reference element, and correct results obtained if the tantalum was used as the dioxide. If, however, the pentoxide was used, the tantalum lines were  $2\frac{1}{2}$  times as weak as the assumption would predict. Furthermore, the presence of only a small amount of  $\text{Lu}_2\text{O}_3$  caused the dioxide to give results similar to those obtained with the pentoxide. These differences led Coster and Nishina to the adoption of an entirely empirical method in which any two lines near each other in the photographic plate may be used. Thus Hevesy and Jantzen used the  $\text{Lu-L}\beta_1$  line and the  $\text{Hf-L}\beta_2$  lines, which are 0.004 A.U. apart, in analyzing for hafnium. The method of Coster and Nishina has been used for the analysis of a

large number of zirconium ores for their hafnium content. The determinations are said to have been made to 0.1 per cent with an accuracy of 10 per cent.

Because of the inherent difficulties of the emission-spectrum method, Glocker and Frohnmayer have developed a method which depends upon the relative intensities of the general radiation on each side of a characteristic absorption discontinuity of the element for which the analysis is being made. An ordinary Coolidge tube may be used; the sample may be in a number of different forms and may even be used without change if necessary. A photographic absorption spectrum is obtained in the usual way and the relative intensities determined by a microphotometer; or an absorption spectrum may be determined by using an ionization chamber. The relation between the intensities and the amount of the element in the sample is given in general by the equation

$$\frac{I_2}{I_1} = e^{-cp},$$

where  $I_2$  is the intensity of the radiation leaving the absorption screen on the short-wave-length side of the discontinuity, and  $I_1$  is the intensity of the long-wave side;  $c$  is a coefficient which must be experimentally determined, and  $p$  is the amount of element present.

The following data include values of  $c$  and of the smallest mass,  $m$ , in milligrams per square centimeter for the production of

TABLE X.—MINIMUM MASS OF ELEMENTS REQUIRED FOR ABSORPTION EDGE

Element	$c$ $K$ edge	$c$ $L_I$ edge	$m$ $K$ edge	$m$ $L_I$ edge
42 Mo	69		0.7	
47 Ag	45		1.1	
50 Sn	34		1.5	
51 Sb	31		1.6	
56 Ba	24		2.1	
58 Ce	22.5		2.2	
74 CV	8		6.0	
82 Pb	5.7		9.0	
90 Th	3.2	50	16.0	0
92 U		45		1.1

a true absorption edge (5 per cent intensity difference in two sides).

This method has been used by Glocker and Frohnmayer in the successful analysis of barium in glass, antimony in a silicate, salt mixtures of antimony, barium, and lanthenum, bismuth in alloys, etc. It cannot be used to advantage for elements below molybdenum.

Hevesy<sup>1</sup> has made a very careful study of the factors which determine the results by analysis with fluorescent secondary rays. Characteristic primary rays ordinarily give six or seven times more intense secondary rays than rays with a continuous spectrum. For greatest intensity a metal must be chosen for target whose characteristic rays are 0.15 – 0.20 A.U. shorter than the absorption bands of the elements undergoing analysis.

Especial attention also has been paid to the distorting effects upon emission-line intensity of absorption edges of a foreign element between comparison lines, or lines of a foreign substance between the edges of the elements being compared, etc. The general conclusion is that the comparison element should be chosen so that the lines and absorption edges are as near as possible to those of the element being determined. The following table is an example of correct choice:

TABLE XI.—COMPARISON ELEMENTS FOR QUANTITATIVE ANALYSIS

Element analyzed	Line $\lambda$ , A.U.	Edge $\lambda$	Comparison element	Line $\lambda$	Edge $\lambda$
Pt	$L\alpha_1$ 1 310	1 070	Ta	$L\beta_3$ 1 303	1 058
In	$L\alpha_1$ 3 764	3 313	Cd	$L\beta_1$ 3.730	3 322
Cd	$L\alpha_1$ 3.948	3 496	Ag	$L\beta_1$ 3.927	3 505
Mo	$L\alpha_1$ 5.394	4 914	Cb	$L\beta_1$ 5 480	5 012
Rb	$L\alpha_1$ 7.303	6 841	Si	$K\alpha_1$ 7 109	6 731
Ge	$K\beta_1$ 1.126	1.115	Ta	$L\alpha_1$ 1 135	1 112
Zn	$K\beta_1$ 1.293	1 281	Hf	$L\beta_2$ 1 324	1.293
Ni	$K\beta_1$ 1 497	1.489	Er	$L\beta_2$ 1 511	1 480
Ti	$K\beta_1$ 2.509	2 494	Cs	$L\beta_2$ 2 506	2.466
S	$K\beta_1$ 5.021	5 012	Mo	$L\beta_2$ 4 909	4 904
Al	$K\beta_1$ 7 941	7 947	Br	$L\beta_1$ 8.108	7.727
Mg	$K\beta_1$ 9 535	9 511	As	$L\beta_1$ 9.394	9 300

<sup>1</sup> "Chemical Analysis by X-rays and Its Applications," McGraw-Hill Book Company, Inc., New York, 1932.

Fortunately the distorting effect is appreciable only when there is a considerable amount of a foreign element present; in ordinary cases it may be neglected without seriously affecting the quantitative analysis. An important application of secondary-ray analysis is that of complex minerals down to 0.1 per cent of a constituent or even 0.001 mg. of any element. Another is in tests of preparations for purity, in which concentration of impurities of 1 part in 10,000 may be found. Eddy, Gaby, and Turner<sup>1</sup> were able to find 1 part of iron in 300,000 parts of zinc.

<sup>1</sup> *Proc. Roy. Soc. (London)*, **124**, 249 (1929); **127**, 20 (1930).

## CHAPTER VII

### THE ABSORPTION AND SCATTERING OF X-RAYS

The fact that x-rays are absorbed in matter in accordance with definite laws is, of course, of very great practical importance. Differential absorption by heterogeneous matter of varying density is the fundamental basis of the entire science of radiography both in medical diagnosis and in the examination, for example, of metal castings for defects, inclusions, pipes, gas pockets, etc. The laws of absorption determine the protection which x-ray workers must utilize against the harmful effects of the x-rays. Similarly, absorption must precede any effects of x-rays upon chemical action or biological functions.

X-ray science owes much to absorption measurements, since, properly interpreted, they give valuable information upon atomic structure. They were the sole method of investigating the quality of x-rays from the time of Roentgen's discovery down to 1913 when Laue and the Braggs introduced crystal analysis. By absorption measurements with screens of various materials Barkla discovered the absorption and emission of x-rays with wave lengths which are characteristic for each chemical element.

**The Absorption Coefficients.**—In traversing matter of all kinds, x-rays are absorbed in accordance with the usual exponential equation  $I = I_0 e^{-\mu x}$  where  $I$  is the intensity after passage through homogeneous matter of thickness  $x$ ,  $I_0$  is the initial intensity, and  $\mu$  is the absorption coefficient. One of the most useful applications of this formula is the expression of absorption properties in terms of the "half-value thickness"  $H$  or that which diminishes the intensity of a parallel bundle of rays to one-half the

initial value; thus  $\frac{1}{2} = e^{-\mu H}$ ,  $H = \frac{\log 2}{\mu} = \frac{0.69}{\mu}$ . When the intensity of a monochromatic beam of x-rays is plotted against the thickness of absorbing material (presupposing no characteristic absorption effects), a curve of the form illustrated in Fig. 40 is obtained. If values of  $\log I$  are plotted against  $x$ , a linear relationship holds, as shown in Fig. 41, always provided that the

beam is strictly homogeneous. The slope of the line is an indication of quality or wave length: the steeper the slope, the softer the ray.

Practically always, however, the absorption formula appears as

$I = I_0 e^{-\frac{\mu}{\rho} \rho x}$  where  $\rho$  is the density, and  $\mu/\rho$ , the mass-absorption

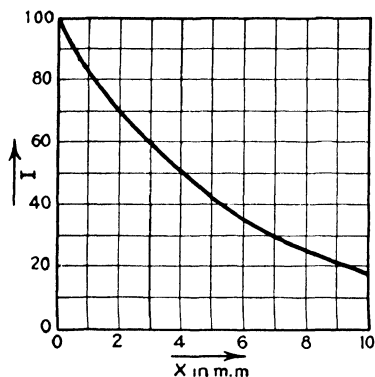


FIG. 40.—Intensity of x-rays plotted as a function of thickness ( $x$ ) of an absorbing screen.

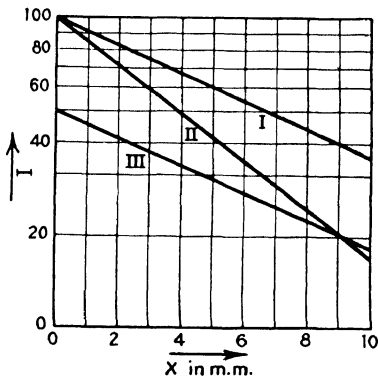


FIG. 41.—Semilogarithmic graph for absorption of x-rays; I and III represent beams with the same wave length but different initial intensities, while II has the same initial intensity as I but a longer wave length.

coefficient, denotes the absorption by a screen of such thickness that it contains unit mass per square centimeter. Only in this way is it possible to compare rationally the absorption coefficients of different substances and the properties of the atoms themselves. This  $\mu/\rho$  is a simple function of atomic number while  $\mu$  is not. The mass coefficient is independent of physical state, state of aggregation, and temperature and for chemical compounds is in the first approximation additive from the mass coefficients of the constituent elements. By multiplying  $\mu/\rho$  by the absolute mass of an atom, which is the atomic weight  $A$  divided by the Avogadro number  $N_0 = 6.063 \times 10^{23}$ , the atomic-absorption coefficient is obtained. Since this refers to a screen which contains 1 atom per square centimeter, it leads to some interesting information concerning atomic structure.

It is now definitely established that  $\mu/\rho$  is really the sum of two coefficients  $\tau/\rho$ , the true or fluorescent-ray mass-absorption coefficient, and  $\sigma/\rho$ , the mass-absorption coefficient due to scattering. The latter is usually much smaller in value than the coefficient for

the absorption due to fluorescence. For light elements  $\sigma/\rho$  has a practically constant value of 0.17 independent of the wave length for intermediate ranges. For heavier elements its experimental value changes in a complicated fashion. Some representative values for  $\mu/\rho$  and  $\sigma/\rho$  are as follows:

TABLE XII.—VALUES OF  $\mu/\rho$  AND  $\sigma/\rho$ 

Elements	$\mu/\rho$		$\sigma/\rho$	
	$\lambda = 0.12 \text{ A.U.}$	$\lambda = 0.71 \text{ A.U.}$	$\lambda = 0.12 \text{ A.U.}$	$\lambda = 0.71 \text{ A.U.}$
C	0 151	0 68	0 14	0 18
Al	0 18	5 35	0 14	0 20
Cu	0 46	53 7	0 18	0 29
Ag	1 60	28 5	0 35	0 47
Pb	5 2	140 0	0 67	0 82

In all cases  $\sigma/\rho$  has a very small value for very short wave lengths. Barkla obtained the approximately constant value of 0.2 in his pioneer experiments. When this value is equated with the J. J. Thomson theoretical value of scattering by electrons in accordance with the classical wave theory, the result comes out that the number of electrons per atom is half the atomic weight. Subsequent developments have proved that this deduction is only approximate.

The true or fluorescent coefficient may be written as a function of the cube of the wave length, *i.e.*,  $K\lambda^3$ . The atomic-fluorescent coefficient of absorption refers to a process of actual transformation of x-rays in the absorbing screen. It is a function of both the atomic number  $Z$  and the wave length; thus  $\tau/\rho \cdot A/N_0 = CZ^4\lambda^3$  (law of Bragg and Peirce).  $C$  for each element is constant only over certain ranges and then changes abruptly at wave lengths which are characteristic of each element; the same is true of  $K$  in

$$\mu/\rho = \tau/\rho + \sigma/\rho = K\lambda^3 + \sigma/\rho.$$

The latest values<sup>1</sup> of the constants for six metals in the equations for the mass-absorption coefficients above,  $K_K$ , and below,  $K_L$ , the first discontinuity (the characteristic  $K$  absorption), are given in Table XIII.

<sup>1</sup> RICHTMYER, *Phys. Rev.*, **27**, 1 (1926).

TABLE XIII.—VALUES OF CONSTANTS IN ABSORPTION EQUATION

	Mo(42)	Ag(47)	Sn(50)	W(74)	Au(79)	Pb(82)
$K_K$ .....	375	545	595	1870	2230	2570
$K_L$ .....	50	70	90	330	395	476
$K_K/K_L$ .....	7.5	7.8	6 6	5 65	5.65	5 40
$\tau_A(10^{-21})$ .....	13.3	11.0	8 90	3 19	2 57	2 37

Of especial interest are the precise equations deduced by Duane and Mazumdar for aluminum and copper which are so commonly used as filters for x-rays:

$$\text{Al}, \frac{\mu}{\rho} = 15.5\lambda^3 + 0.147;$$

$$\text{Cu}, \frac{\mu}{\rho} = 193\lambda^3 + 0.13.$$

Allen<sup>1</sup> has found that the empirical formula

$$\frac{\mu}{\rho} = C\lambda^{2.92} \frac{Z^4}{(A/N_0)} + \frac{\sigma}{\rho}$$

where  $A$  is the atomic weight and  $N_0$  the Avogadro number, applied to his experimental results on carbon, paraffin, sulfur, and 16 metal elements from aluminum to uranium for wave lengths 0.56 to 0.08 A.U. (the important range in therapeutic uses of x-rays) gives values of  $\sigma/\rho$  which increase with atomic number, becoming about 1 for heavier elements. The values of  $C$  for all values of  $Z$  and for values of  $\lambda$  from 0.08 to 1.0 A.U. are 0.0132 for the so-called  $K$  (or hardest) series of x-rays and 0.00181 for the  $L$  series.

Another empirical formula, suggested by A. H. Compton, has the form

$$\mu/\rho = (C\lambda^3 Z^4 \times 0.32Z)/(A/N_0).$$

Since the mass-absorption coefficient of a chemical compound may be represented as the sum of the coefficients for each of the atomic species present in the compound, the equation may be written in the summation form

$$\mu/\rho = (\text{compound}) = (C\lambda^3 \Sigma Z^4 + 0.32 \Sigma Z)/\Sigma(A/N_0).$$

<sup>1</sup> ALLEN, *Phys. Rev.*, **27**, 266 (1926).



In precision researches by Havighurst<sup>1</sup> this equation has been found to agree excellently with experimental results on various powdered salts containing elements with atomic numbers greater than 5. Measurements by Windgarth on some of the same salts in solution are also in agreement.

Jönsson has utilized the idea of absorption coefficient "per electron"

$$\mu_e = \frac{\tau}{\rho} \cdot \frac{A}{N_0 Z} = \frac{\tau_{at}}{Z} = C(Z \cdot \lambda)^{f(Z, \lambda)},$$

where  $A$  is the atomic weight,  $N_0$  the Avogadro number, and  $Z$  the atomic number. Out of this has come a universal absorption curve<sup>2</sup> in which

$$\log [(\mu_e)_K \times N_0] = \log \left[ \left( \frac{\tau}{\rho} \right)_K \times \frac{A}{Z} \right]$$

is plotted against  $\log (Z\lambda)$ . This linear graphical method is surprisingly accurate and is applied directly if  $\lambda$  is smaller than the  $K$  absorption limit; if  $\lambda$  lies between  $\lambda_K$  and  $\lambda_{L_1}$  the numerical value from the curve must be multiplied by  $\nu_{L_1}/\nu_K$ , etc.

**Mechanism of Absorption.**—When a beam of x-rays impinges upon matter, the radiation energy is partly transformed, as already indicated, and partly scattered. Figure 42 indicates the principal phenomena which have been identified, though others have some experimental proof.<sup>3</sup>

**Fluorescent Characteristic X-rays.**—The energy of these secondary rays is accounted for in the term  $\tau/\rho$  in the mass-absorption equation  $\mu/\rho = \tau/\rho + \sigma/\rho$ . Upon analysis with a spectrometer the rays are shown to be identical with those which would be emitted if the absorber element were used as an x-ray tube target, in that the line spectra in the  $K$ ,  $L$ ,  $M$ , etc., series are obtained with the same wave lengths. This presupposes that if the  $K$  series spectrum appears, the exciting primary beam must contain rays with a frequency equal to or greater

<sup>1</sup> *Proc. Nat. Acad. Sci.*, **27**, 477 (1926).

<sup>2</sup> KIRCHNER, *Allgemeine Physik der Röntgenstrahlen*, "Handbuch der Experimentalphysik," Vol. XXIV, Part 1, p. 252.

<sup>3</sup> The most complete and recent treatise on the whole subject is to be found in Kirchner, *Allgemeine Physik der Röntgenstrahlen*, "Handbuch der Experimentalphysik," Vol. XXIV, Part 1.

than that which is characteristic of the  $K$  critical absorption limit of the absorber element. Fluorescent x-rays are unpolarized.

Primary x-ray quanta with an energy equal to or greater than  $h\nu_{\text{absorber } K \text{ limit}}$  remove electrons from characteristic levels in the atom just as effectively as the cathode rays in an x-ray tube.

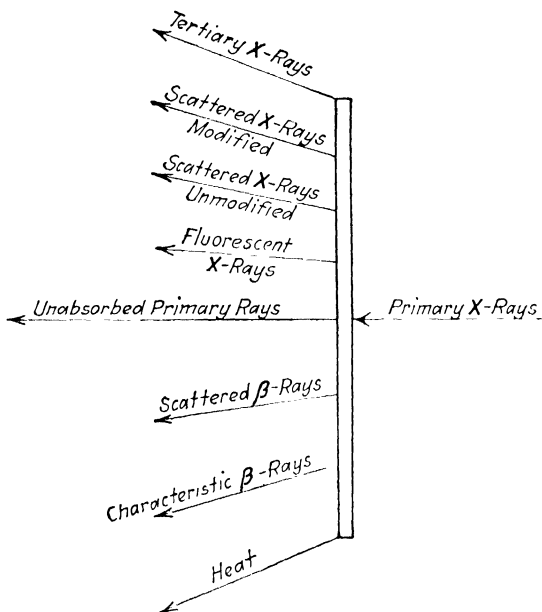


FIG. 42.—Phenomena occurring when x-rays impinge upon matter.

**Scattered X-rays Unmodified.**—These rays have the same wave lengths as the primary beam; for instance, if the primary beam contains the tungsten characteristic rays, then the spectrum of the scattered x-rays will show the tungsten lines; thus reflection from crystals is essentially a special case of scattering. If the primary x-rays are transferred in energy quanta, the scattering is produced by atoms or groups of atoms which are too massive to be sensibly affected by the radiation quantum. These rays are polarized, usually completely; thus no reflection from a crystal occurs, when the primary rays are linearly polarized, if the direction of the reflected ray coincides with the electric vector of the incident ray.

**Scattered X-rays Modified by the Compton Effect.**—One of the great contributions in physics in recent years was the discovery by Compton and by Debye that the spectra of scattered

rays, characteristic of the primary rays and not of the secondary radiators, show not only lines with the same wave length as those in the primary beam but also, on the long wave-length side of these lines, other lines which indicate that in the process of scattering a distinct change has occurred. These modified lines were shown to be quantitatively explained upon the basis of a purely quantum phenomenon. A primary quantum of x-radiation energy  $h\nu_0$  strikes an electron and imparts to it a certain amount of kinetic energy resulting in recoil. The radiation quantum is changed in its direction and proceeds with an energy  $h\nu$ , smaller by the amount involved in the recoil of the electron. Consequently the wave length will be longer. The so-called shift from the unmodified wave length is expressed by the equation  $\delta\lambda = (h/mc)(1 - \cos \phi) = 0.0242(1 - \cos \phi) =$

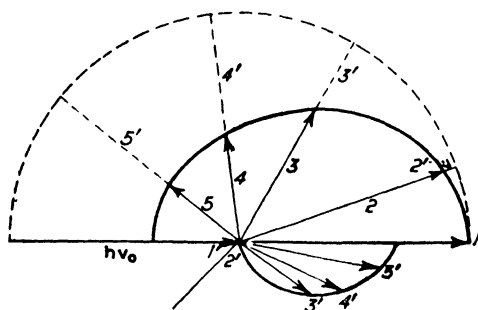


FIG. 43.—Diagram showing Compton effect.

$\gamma$  vers  $\phi$ , where  $\phi$  is the angle between the incident and the scattered ray. At  $\phi = 90$  deg., the shift will therefore be 0.0242 A.U. This increase in wave length is, therefore, independent of the wave length and of the scattering element and depends only on the angle  $\phi$ .

The Compton effect is well illustrated in the diagram in Fig. 43. Here  $h\nu_0$  is the primary quantum scattered by the electron  $e$ . The length of the arrow  $h\nu_0$  measures the energy magnitude. According to classical or unmodified scattering, the scattered quanta will always have the same  $h\nu_0$  value independent of the direction. This can be represented by the dotted semicircle with radii  $h\nu_0$ . Actually there is a wave-length change and this is represented for five directions 1, 2, 3, 4, 5, as full lines, the lengths  $h\nu$  being smaller the greater the scattering angle, and the energy changes being the vector difference between the dotted

and full positions of each radius. This energy change is accounted for in the kinetic energy of the recoil electrons represented by the arrows in the smaller curve;  $1'$  is 0 because for the scattering angle 0 deg. no energy is available;  $2'$ , which is too small to show, corresponds to 2,  $3'$  to 3, etc.

The ratio of the intensities of modified and unmodified rays in the Compton effect, however, varies with the atomic number of the radiator element, from  $\infty$  for lithium (all energy modified) to 5.48 for carbon, 1.91 for sulfur, 0.51 for iron, 0.21 for copper, and decreasing values for heavier elements to practically zero for lead. The Compton effect has been the subject of considerable controversy, as the result of which careful researches by numerous investigators throughout the world have established it as a fact and as a powerful support to the conception of radiation energy in quanta. No such change in wave length has been observed in the reflection of x-rays by crystals, or in the scattering of rays of light. As independent proof the tracks of the recoil electrons have been photographed by C. T. R. Wilson's cloud-expansion method.

The energy distribution

$$E_{\text{kinetic}} = h\nu \cdot \frac{\alpha \text{ vers } \phi}{1 + \alpha \text{ vers } \phi} = h\nu \cdot \frac{2\alpha \cos^2 \Theta}{(1 + \alpha)^2 - \alpha^2 \cos^2 \Theta}$$

where  $\alpha = \gamma/\lambda$ , is verified experimentally.

It is interesting to calculate how much energy is involved in the recoil electrons for a practical case of irradiation of the human body from a tube at 200 kv. (average wave length 0.04 A.U.):

$$E_{\text{kinetic}} = h(\nu_0 - \nu).$$

If the average increase in wave length ( $\phi = 90^\circ$ ) is 0.024 A.U.,

$$E_k = h\left(\frac{c}{\lambda_0} - \frac{c}{\lambda_0 + 0.024}\right); \text{ expressing } E \text{ in volts the recoil electrons}$$

have a velocity of about 50 kv. Thus  $50/200$  or 25 per cent of each quantum in the human body goes into the energy of recoil electrons. For rays generated at 200 kv., 2.5 per cent of the x-ray energy in each part of a tissue is transformed into the energy of photoelectrons. Of the fraction of primary energy which is scattered (12 per cent), 3 per cent (25 per cent of 12 per cent) goes into recoil-electron energy.

**Scattered and Characteristic  $\beta$ -rays.**—X-rays which are impinging upon the surface of a secondary radiator eject photo-

electrons. If the radiation is monochromatic (frequency  $\nu$ ), then the kinetic energy of some of the liberated (scattered) electrons will be  $E_k = h\nu$ , independent of the secondary radiator. The electrons are those so loosely bound in the atoms that the work required for their removal is negligible. In addition, however, other photoelectrons are ejected with kinetic energies which depend upon the particular kind of atom from which they are liberated; hence, their removal has involved a certain amount of work  $W$ . If a beam of these electrons is analyzed by causing them to bend in a magnetic field, then all electrons with the same value of  $E_k = h\nu - W$  will register a sharp spectral line on a suitably disposed photographic plate. By means of these characteristic  $\beta$ -ray spectra, de Broglie showed that the energy necessary to eject an electron from an inner atomic shell, which is involved in the correction term  $W$ , is simply the quantity of energy representing the energy levels  $K, L, M, N$ , etc., which is in turn measured by the frequency values of the critical absorption limits. These  $\beta$ -ray spectra, therefore, constitute another important method of measuring energy levels. In one photograph for photoelectrons ejected from a silver plate irradiated by the  $K$ -radiation of tungsten (and of course producing the secondary fluorescent silver  $K$ -radiation), de Broglie obtained six lines, corresponding to six different kinetic energies. He showed that these were:

1.  $h\nu_{\text{AgK}\alpha} - L_{\text{Ag}}$  (where  $L_{\text{Ag}}$  is the energy required to remove an  $L$  electron from the silver atoms, or  $h\nu_{\text{AgLabs}}$ ).
2.  $\begin{cases} h\nu_{\text{AgK}\alpha} - M_{\text{Ag}}; \\ h\nu_{\text{AgK}\beta} - L_{\text{Ag}}. \end{cases}$
3.  $h\nu_{\text{AgK}\beta} - M_{\text{Ag}}.$
4.  $h\nu_{\text{W}\text{K}\alpha_2} - K_{\text{Ag}}.$
5.  $h\nu_{\text{W}\text{K}\alpha_1} - K_{\text{Ag}}.$
6.  $h\nu_{\text{W}\text{K}\beta} - K_{\text{Ag}}.$

More recently Robinson and his associates<sup>1</sup> have made notable contributions to the field of magnetic spectra of secondary electrons. By means of greatly improved experimental methods the values of energy levels have been determined for many of the chemical elements, including measurement of absorption limits in the range of long wave lengths in which the crystal-grating method is impracticable. This new work has also included

<sup>1</sup> For further detailed information see "International Critical Tables," Vol. VI, p. 2. The data of Robinson, together with all references, are given in Siegbahn, "Spektroskopie der Röntgenstrahlen," 2d ed., pp. 413-428.

measurement of energy levels in multiply-ionized atoms. The magnetic spectra not only yield energy values of secondary electrons which are ejected from inner levels by action of the primary x-rays; the secondary fluorescent x-rays generated in the radiator are also effective in liberating electrons. The process may be pictured as follows: a  $K$  electron is ejected through the agency of the primary x-rays, followed by the transition of an  $L$  electron, for example, to fill the vacancy. Normally a  $K\alpha$  ray is emitted as a consequence of liberation of energy. However, this energy so released can be transformed in the atom into forms other than the quantum of radiation. For example, the transition  $L \rightarrow K$  may lead to the ejection of an  $M$  electron with a kinetic energy represented by the difference between the first energy ( $L \rightarrow K$ ) and the work required to remove this  $M$  electron from the atom. This work is greater than that which normally corresponds to the  $M$  level, because an electron is missing from an inner level with the result that there is diminished screening of the positive nucleus. Therefore the work of separating an outer electron is equal to that required normally for the element of next higher atomic number. Such processes have been experimentally verified in Robinson's work.

**Atomic Structure from Intensity of Scattering by Gases.**—One of the most promising recent developments in physics has been the use of data from the scattering of x-rays by gases to determine electron distribution in atoms and to test data calculated from wave mechanics. Compton<sup>1</sup> has shown that the density of electrons is represented by a Fourier integral of the form

$$U(r) = Zr \int_0^\infty B \sin(\pi r x) dx,$$

where  $U(r)$  represents the number of electrons per Ångström unit at a distance  $r$  from the center,  $Z$  is the atomic number,  $B$  (depending on intensity of scattering)  $= 2\pi x \left\{ \frac{S-1}{Z-1} \right\}^{\frac{1}{2}}$ , where

$S$  is the scattering per electron at  $x = 4/\lambda \sin(\phi/2)$ .

Wollan<sup>2</sup> has determined the distribution in helium, neon, and argon and found the curves for  $U(r)$  against  $r$  in good agreement

<sup>1</sup> *Phys. Rev.*, **35**, 925 (1930).

<sup>2</sup> *Phys. Rev.*, **37**, 862; **38**, 15 (1931); see also JAUNCEY, *ibid.*, **38**, 1.

with similar curves derived from waves mechanics. For neon the data actually are able to separate the *K* and *L* electrons, as shown in Fig. 44.

**Filtration.**—The x-ray beams directly from a tube target are not of greatest usefulness as they are. The rays contain a large proportion of very soft components which are absorbed in the uppermost layers of any absorbing substance. For medical diagnosis and deep therapy they are obviously useless; particularly as they may cause harmful skin reactions because the absorption per unit volume for the soft rays is relatively so great. The necessity presents itself in medical and other uses of working

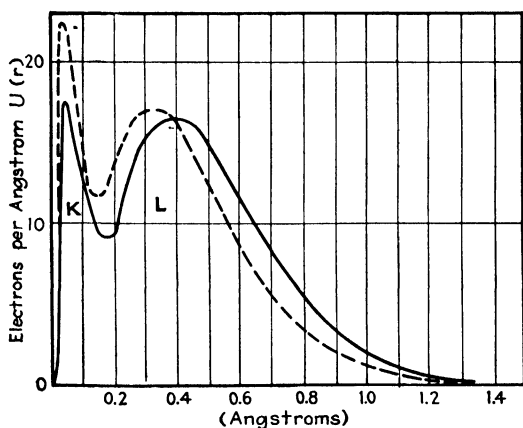


FIG. 44.—Electron distribution in neon gas as derived from experiments on x-ray scattering (Wollan.)

with the most nearly homogeneous rays possible, namely, those for which the relative ratios of components of various wave length do not change during penetration of the irradiated object. The effect of filtration is illustrated by the following example: A mixture of rays consisting of 3 parts, soft, hard, and very hard constituents with equal intensity is filtered through 5 mm. of aluminum. For the very hard ray,  $\mu = 0.405$ , 80 per cent penetrates through, for the hard ray,  $\mu = 1.08$ , 60 per cent, and for the soft,  $\mu = 6.75$ , only 4 per cent. Thus out of a continuous heterogeneous mixture actually generated, a beam less and less heterogeneous and with greater and greater average hardness (shorter wave length) results from greater filtration. Actual experimental results showing the effect of passage through 1, 5,

and 10 mm. of aluminum are illustrated in Fig. 45. When the absorption results are plotted logarithmically as in Fig. 46, it is

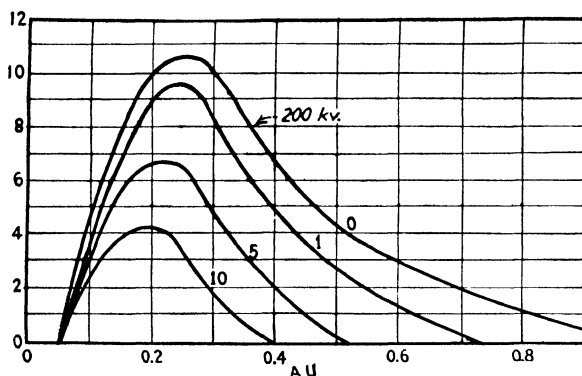


FIG. 45.—Curves showing effect of filtration of heterogeneous x-ray beam through 1, 5, and 10 mm. of aluminum.

seen that the slope of the curve for small thicknesses changes continuously instead of being constant as is true for monochromatic rays (Fig. 41), showing that the quality of the beam is changing. Finally a point is reached where the curve becomes linear and below this homogeneity

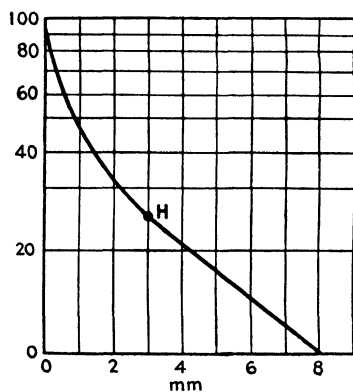


FIG. 46.—Semi-logarithmic curve illustrating the homogenizing of a beam of x-rays by filtration through copper (compare with Fig. 41 for monochromatic rays).

point no further change in quality occurs. This does not mean that the beam is monochromatic or even homogeneous when filtered through other materials. A beam generated at 200 kv. and filtered through 1 mm. of copper behaves as though it were homogeneous when passed next through water or the human body, for the curve is linear; but the same filtered beam passed through more copper is by no means homogeneous.

These different behaviors are, of course, determined by the relation between values of  $\mu$  and  $\sigma$ . Hence filtration for the purposes of homogenizing is easily accomplished with a substance of higher atomic number than that of the object or body in which the rays are to remain homo-



geneous. In general medical practice copper is used as the homogenizing filter and aluminum as the test filter. If the radiation is homogeneous in aluminum, it will be so in the human body.

**Measurement of Quality by Absorption Methods.**—Since absorption depends so definitely upon the nature of the absorber or filter and upon the wave length of the ray, a practical measurement of the quality or hardness of an x-ray may be based upon it; for example, by comparing the absorption power of layers

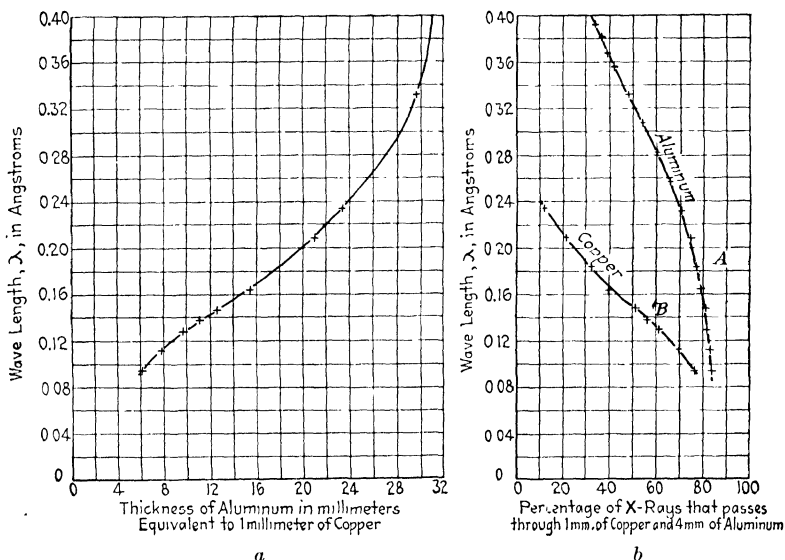


FIG. 47.—Methods of evaluating effective wave length of a heterogeneous beam of x-rays. (Duane.) (a) Curve showing the thickness of aluminum having the same absorbing power as 1 mm. of copper for a beam of heterogeneous x-rays; (b) curves showing the percentage absorption in 1 mm. of copper and in 4 mm. of aluminum as a function of wave length.

of aluminum to that of fixed thicknesses of silver, as judged by the fluorescent or photographic power of the emergent ray, a scale may be constructed and used without reference to wave lengths. Roentgen himself used such a device, and the Benoist penetrometer, consisting of a thin silver disk 0.11 mm. thick, surrounded by 12 numbered aluminum sectors from 1 to 12 mm. thick is still widely used, particularly in the measurement of dosage in x-ray therapy.

In many cases an x-ray beam with a variety of wave lengths may be used, and the simple absorption equations cannot be

used directly. Duane has suggested, however, the determination of the "effective" wave length, or the wave length of a monochromatic ray which has the same absorption under given conditions as the whole polychromatic beam. An experimental curve has been constructed, based upon the fact that the thickness of aluminum which has the same absorbing power as a given thickness of copper depends upon the wave length of the radiation; for soft or long wave-length x-rays the thickness of aluminum must be large, and for hard x-rays small. Experimentally, the percentage of the beam absorbed in 1 mm. of copper is first measured by the ionization produced in a gas, or by the effect on a fluorescent screen or photographic plate; then the absorption in increasing thicknesses of aluminum is measured until it has the same value as for the copper. The wave length as a function of this equivalent thickness is read from a graph such as is shown in Fig. 47*a*. Another method consists in the successive measurements of absorption in 1 mm. of copper and 4 mm. of aluminum. The wave length may then be read from the curves in Fig. 47*b*.

**Protection from X-rays.**—The definite laws which govern the absorption of x-rays also permit an exact determination of the thickness of protecting material which must be employed in all work with these rays in order to prevent dangerous physiological effects such as burns and anemia. Of the more readily available materials, lead is the best for protective purposes. Table XIV, from the work of Kaye and Owen, lists the thicknesses of lead in millimeters which are equivalent to 1 mm. of several protective materials in common use for x-rays generated by a Coolidge tube operated at 100,000 volts.

TABLE XIV.—PROTECTIVE POWERS OF MATERIALS RELATIVE TO LEAD

Lead glass	0 12 to 0 20
Lead rubber	0 25 to 0 45
Bricks and concrete	0 01
Woods	0 001
Barium sulfate plaster	0 05 to 0 13
Steel	0 15

Adequate protection is a factor of vital importance which must be considered in the installation of x-ray equipment. Undue exposure to the radiation may lead to a lowering of the white blood-corpuscle count (leukopenia), to low blood pressure and anemia, as well as to the skin burns which were so fatal to

the early workers. For those engaged in x-ray researches a dental film carried in the pocket for 2 weeks will give a quick index of excessive exposure; if it is then definitely fogged, protection should be increased. Blood-corpuscle counts at intervals are advisable. Shortening the hours of work and increasing the amount of fresh air and recreation are effective in removing symptoms. A "tolerance dose" which the human body may withstand without ill effects has been determined as  $1 \times 10^{-5}$  r<sup>1</sup>/sec. for 200 working hours per month.<sup>2</sup>

An International Safety Committee under the auspices of the International Congress of Radiology has functioned for several years in standardizing requirements for adequate x-ray protection. As higher and higher voltages are being used in therapy, such standards become increasingly important. A new advisory committee formed in the United States has prepared a unified and detailed set of safety recommendations (x-ray and high-tension protection, storage of inflammable film, etc.).<sup>3</sup>

The following minimum equivalent thicknesses of lead for protection are recommended as adequate:

TABLE XV

X-rays Generated by Peak Voltage Not in Excess of (Kilovolts)	Minimum Equivalent Thickness of Lead, Millimeters
75	1 0
100	1 5
125	2 0
150	2 5
175	3 0
200	4 0
225	5 0
300	9 0
400	15 0
500	22 0
600	34 0

In the x-ray laboratory at the University of Illinois which is devoted primarily to researches on ultimate structures of materials, the x-ray tubes are enclosed in lead-lined containers through which are adjusted the necessary slits and pinholes. Sheet lead  $\frac{1}{8}$  in. thick gives a large factor of safety for a molybdenum-target tube operated at voltages up to 30,000 volts, and a

<sup>1</sup> The "r" unit of dosage is defined on p. 163.

<sup>2</sup> MUTSCHELLER, *Am. J. Roentgenology*, **13**, 65 (1925).

<sup>3</sup> Bureau of Standards, *Handbook 15* (1931).

thickness of  $\frac{1}{4}$  in. suffices for tungsten-target tubes operated at voltages up to 150,000 volts. The new metal self-shielding x-ray tubes, which permit passage of rays only through very small windows, also simplify the matter of protection of the research worker. For radiographic examination of metals and in x-ray therapy, the rays from a tube cannot be so narrowly defined, and it is sometimes essential to line an entire room with sheet lead and to place the control instruments outside the room. Such equipment may be seen at the Watertown Arsenal and in the Physics Department of the Massachusetts Institute of Technology.

**Some Practical Applications of Absorption Measurements.**—Aside from the value of characteristic absorption edges in qualitative and quantitative analysis (Chap. VI), the simple exponential law  $I = I_0 e^{-\mu x}$  is the basis from which valuable information may be obtained. Filtration, for the purpose of homogenizing beams for therapy, and the determination of quality and effective wave length have been considered already.

Other possibilities which have found interesting practical use are as follows:

1. Determination of the true thickness  $x$  of various specimens. As an example may be selected the classification of hides and finished leather. Because of the biological variable, constant quality and thickness are out of the question and mechanical micrometric methods are ineffective. For such a classification the beam from an x-ray tube, which is operated so that wave length will be compatible with absorbing power of a specimen (soft rays for leather), is passed through a specimen and the intensity  $I$  as well as the initial intensity  $I_0$  is measured, best from the ionization current produced in a gas, which in turn is measured by the deflection of an electrometer or electroscope. The brightness of a fluorescent screen or darkening of a photographic plate could also be employed. With constant  $I_0$  and  $\mu$  for the given material it follows that the values of  $x$  from one sample to another may be ascertained with great accuracy. Other known examples are glass lenses, thin metal foils, paper, paint and varnish films.

2. Uniformity of gage. Variations in thickness in a sample of material are, of course, indicated by irregular results when the sample is moved around in the x-ray beam.

3. Composition of mixtures and solutions. In such cases quantitative analysis of the unknown composition of two or

more substances mixed as powders or melted together, or dissolved, may be made if standard measurements of absorption as a function of known composition are available for comparison. Aborn and Brown<sup>1</sup> showed that the amount of lead tetraethyl in gasoline could be determined by measurement of the absorption of x-rays, generated under standard conditions, in a standard thickness of the solution and comparison with standard experimental curves showing absorption as a function of lead tetraethyl concentration. This method is, of course, best adapted for pairs of substances whose absorbing powers are widely different. Alloy composition, amount and uniformity of distribution of impregnating agents in wood, heavy metal content of glass, loading of silk fibers with tin dioxide, concentration of colloidal metal sols, and fillers in rubber are among the examples of this process.

4. Determination of porosity. The actual absorption measurements of a substance of certain apparent thickness depend, of course, on whether the substance possesses maximum density or whether the density is affected by a porosity, even microscopic, so that the absorbing power is smaller than the value predicted for the measured thickness. Charcoals, drying agents such as magnesium perchlorate, sodium silicates, and other substances have been studied in this way.

5. Detection of counterfeit coins; differentiation of true and imitation gems, such as diamonds, and of soft and lead glass; and other similar test in which specimens may be compared side by side have depended upon the absorption laws for x-rays. The advantage is found in the extreme rapidity with which identification can be made, presupposing the availability of suitable apparatus.

6. Finally, the examination of all materials for gross interior structure, the discovering particularly of inhomogeneities and imperfections, depends upon the differential absorption of x-rays. This constitutes the familiar and extremely important and practical science of radiography to which the next chapter is devoted.

<sup>1</sup> *Ind. Eng. Chem.*, analytical ed., Vol. I, p. 26 (1929).

## CHAPTER VIII

### RADIOGRAPHY

Although x-rays, because of their short wave lengths are able to penetrate matter, still they are differently absorbed by different substances; that is to say, all materials are not equally transparent to x-rays. These facts are the basis of the science of radiography. Broadly defined, the experimental technique consists in passing a beam of x-rays through the object to be examined and, by means of a fluorescent screen or photographic plate, recording the varying intensities of the emergent beam and thus obtaining a shadow picture of the interior of the object. Probably the first practical uses of x-rays were of a radiographic nature, and radiography today is a most useful tool to the medical and industrial diagnosticians.

### MEDICAL DIAGNOSIS

In the discovery and location of internal defects of the human body, radiography has become indispensable. The use of x-rays to examine fractured bones preparatory to setting, to study conditions of the teeth as an index to subsequent treatment, and to locate bullets, swallowed pins (Fig. 48), and the like has become so routine that everyone is acquainted with it. Not so well-known, perhaps, are the uses of x-rays in the diagnosis of tumors, of incipient tuberculosis of the lungs and joints, of diseases of the alimentary tract, of stones in the kidney and the gall bladder, and of diseases of the liver and the pelvic organs.

In the examination of the alimentary tract the use of barium sulfate or bismuth salts or emulsions and other similar agents, mixed with the food to produce opacity in the part to be examined, has become a science in itself. Similarly, the injection of gases and iodized oil into affected parts enables these to be thrown into relief for diagnosis from radiographs. The application of such schemes is continually extending the field of x-rays in medical diagnosis, and wider and wider applications are certain to be found.

An exceedingly interesting outgrowth of medical diagnosis has been the x-ray photography of mummies taken through wrappings. Some very interesting anatomical comparisons of ancient Egyptians with modern man have been made possible and the same evidences of disease and malnutrition in bone structures obtained as are common today. The Field Museum

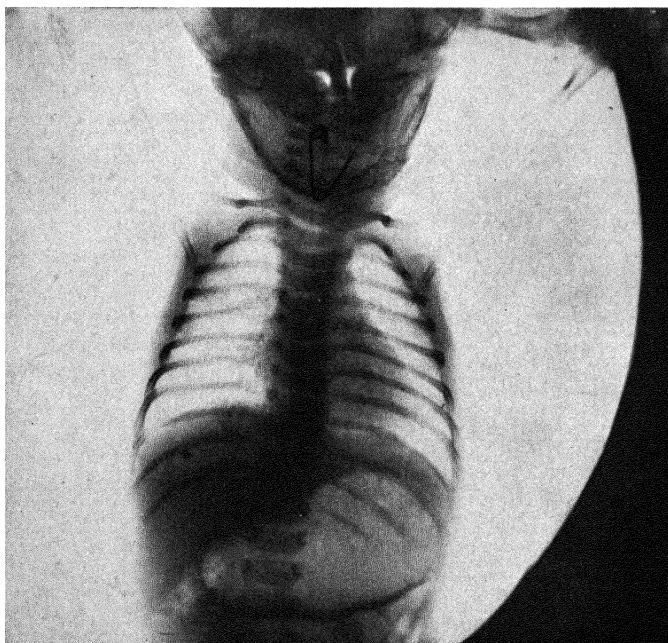


FIG. 48.—Typical medical diagnostic radiograph for location of foreign bodies.

including one in which the ancient embalmer had perpetrated a hoax entirely unsuspected from the exterior of the mummy by connecting the head and the legs with a stick since the trunk of the body is entirely missing.

Still other applications are the fitting of shoes; identification of skeletons by radiographs of the skull which are as highly individualistic as finger prints; scientific studies of the diet as it affects bone and tooth structures of rats and test animals, or produces rickets; and identification of cause of diseases in fish such as the knot-head carp in the Illinois River radiographed in the writer's laboratory.

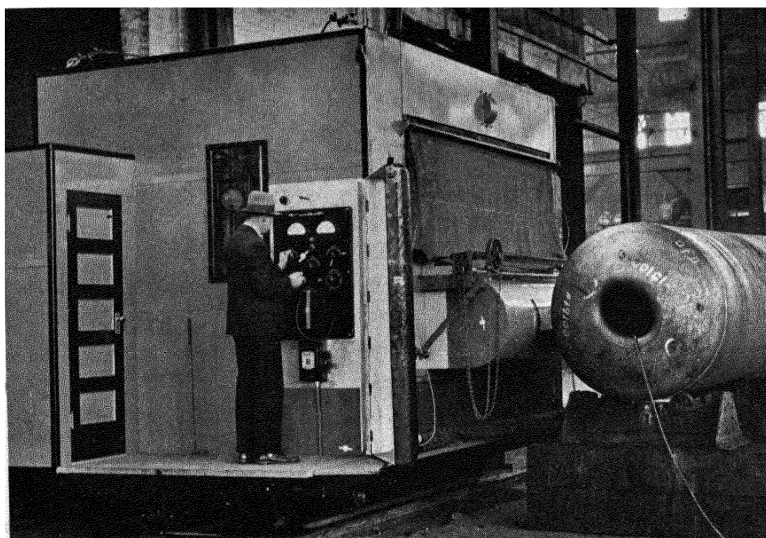


FIG. 49.—Exterior view of modern industrial x-ray installation for radiographic examination of welded pressure vessels. (*Courtesy Henry Vogt Machine Company, Louisville, Ky.*)

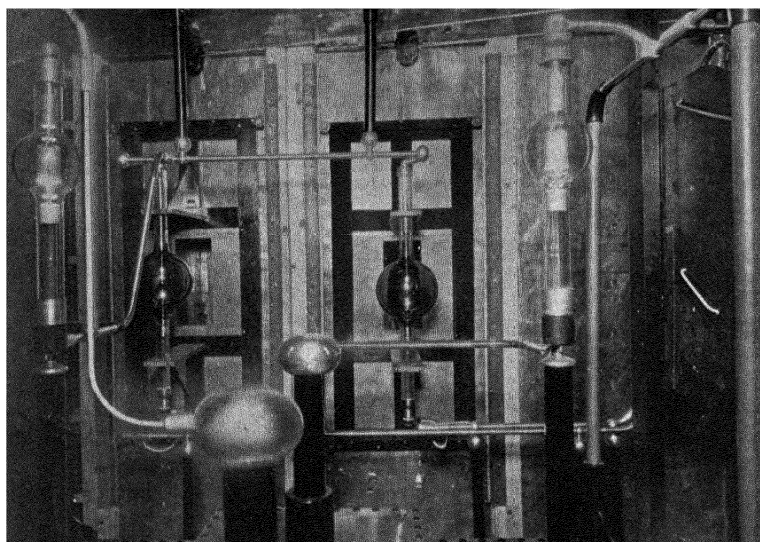


FIG. 50.—Interior view, showing two x-ray tubes and two Kenotrons, of new installation for metal radiography. (*Courtesy General Electric X-Ray Corporation.*)



## INDUSTRIAL DIAGNOSIS

Just as the inside of the opaque human body may be observed on the photographic film or fluorescent screen by virtue of the differential absorption of penetrating x-rays, and without damage, so also may any metal object be radiographed for the purpose of determining the gross structure and the presence of inhomogeneity or defect. The immeasurable importance of this information is evident in terms of the satisfactory behavior or failure of metal or other objects of practical utility and of the safety of human life which is so frequently involved.

**General Principles and Technique of Radiography Applied to Industrial Materials.**—1. The

technique for preparing radiographic pictures is comparatively simple. A tungsten-target x-ray tube of the Coolidge or Metalix hot-filament type is ordinarily employed. The filament is heated to incandescence by a separate circuit and this constitutes the cathode in the high-tension circuit, with the target as the anode. A closed-core, oil-immersed, high-tension transformer which may produce up to 300 kv. is almost invariably the modern equipment. The alternating high-tension current is rectified by mechanically rotating disks or by vacuum-tube Kenotrons. The targets may be water-cooled by an insulated circulating system and thus enable the passage of large currents through the tubes. Since radiographic exposures are usually of short duration, x-ray tubes of the universal type, in which the targets become hot, are ordinarily employed. The object which is to

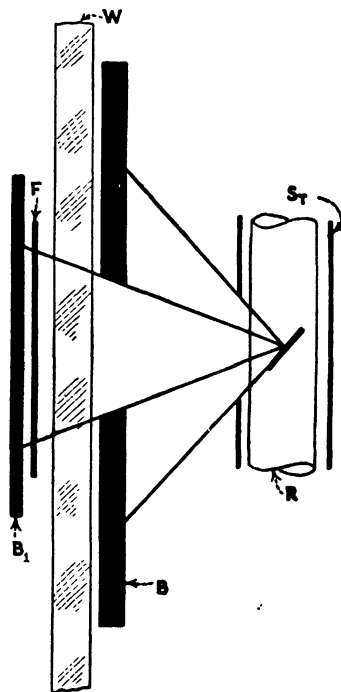


FIG. 51.—General arrangement for photographic radiography. *R*, x-ray tube; *S<sub>T</sub>*, protecting cylinder; *B*, diaphragm; *W*, specimen; *F*, photographic plate; *B<sub>1</sub>*, lead screen.

be radiographed is placed at some distance from the tube so that the rays proceeding from the focal spot on the target are essentially from a point source. Radiographs are merely shadow pictures

produced by radiation traveling in straight lines from a point source. The most recent types of industrial installation for the examination of high-pressure vessels are shown in Figs. 49 and 50.

2. Registration of the radiograph is either photographic or visually observed on the fluorescent screen (calcium tungstate usually, or barium platinocyanide, zinc silicate, cadmium tungstate, etc.). The general arrangements for the two methods are shown in Fig. 51 for the photographic method and in Fig. 52 for visual observation. In the latter case a mirror is arranged so that the observer will not be in the direct path of the x-rays.

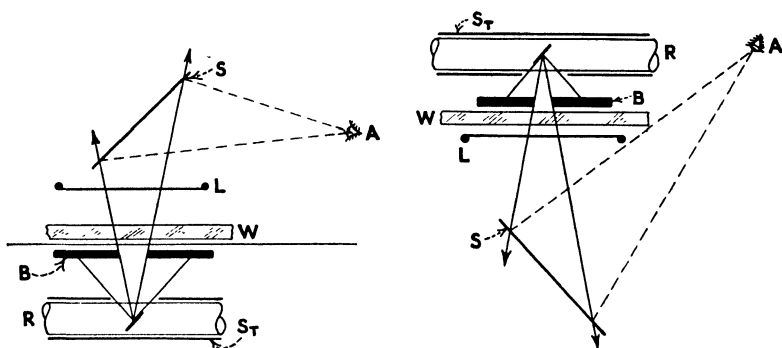


FIG. 52.—Two arrangements for x-ray fluoroscopy; *R*, x-ray tube; *S<sub>T</sub>*, protecting cylinder; *B*, diaphragm; *W*, specimen; *L*, fluorescent screen; *S*, mirror for observation of fluorescent image without direct exposure to x-rays; *A*, eye.

3. For each material and each thickness there is a certain optimum voltage for excitation of the x-ray tube: *e.g.*, 80 kv. for 4 cm. Al, 110 kv. for 10 cm. Al, 200 kv. for 6 cm. Fe, 230 kv. for 6 cm. brass.

4. Secondary and scattered radiation plays a large part in the results obtained and, for the certain identification of small imperfections in an object on the plate, must be eliminated. A grid such as a Bucky diaphragm consisting of narrow strips of lead or other metal edgewise with free space between each strip is often placed between the object and the plate. The primary rays pass straight through the gaps between these strips, while the secondary rays at various oblique angles from the specimen are entirely cut off. Such diaphragms must be moved slowly across the plate. Secondary rays also arise from the walls of the room and other objects, so that the film must be thoroughly protected by covering the back and edges with sheet lead.

5. Tubes with the sharpest possible focal spots are necessary for sharp definition and contrast on photographs at the boundaries of portions indicating different densities.

6. Careful photographic technique must be employed in order to assure distinction between the smallest differences in blackening of the plate. Experiment has indicated that the optimum blackening is  $S = 0.7$  to  $0.9$  ( $S = \log \frac{L_0}{L}$ , the photometrically measured light intensities before and after passage through the photographic layer). The normal eye can detect with certainty a minimum blackening difference between adjacent areas of 0.02.

7. The amount of exposure is defined by the product of the milliamperage through the x-ray tube and the time of exposure in

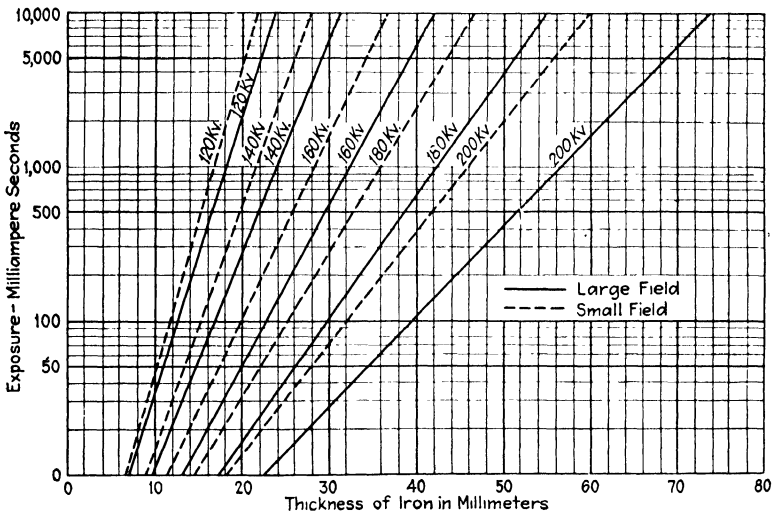


FIG. 53.—Exposure chart for radiography of iron or steel specimens.

seconds. Very complete and useful data have been obtained by Berthold<sup>1</sup> for iron, aluminum, copper, and brass. The chart for iron in thickness up to 80 mm. is reproduced in Fig. 53. This shows the log of milliampere seconds (m.a.s.) against thickness of iron in millimeters, for voltages from 120 to 200 kv. for both small field (less than 3 cm.<sup>2</sup>) and large field (50 to 100 cm.<sup>2</sup>), focal distance 50 cm., two intensifying screens with Agfa films, absolute blackening 0.7.

<sup>1</sup> "Grundlagen der technischen Röntgendurchstrahlung," Leipzig, 1930.

8. For practical use of the fluorescent observation, at least a dose  $5 \times 10^{-3} r^1$  per second must fall upon the screen.

9. The practical limits of penetration and satisfactory radiographic examination of aluminum, iron, and copper are listed in Table XVI for the following conditions: 200 kv. non-pulsating, 15 ma., 50 cm. focal distance, two intensifying screens, Agfa film, blackening  $S = 0.7$ , without screens for eliminating scattered radiation.

TABLE XVI.—LIMITS OF THICKNESS IN MILLIMETERS FOR RADIOGRAPHIC EXAMINATION

Element	Photographic, small field		Photographic, large field		Fluorescent screen, small field	Fluorescent screen, large field
	10 min	60 min.	10 min.	60 min.		
Aluminum . .	240	280	355	415	120	175
Iron . . .	59	70	73	86	30	40
Copper .	39	46	46	56	20	25

Berthold has conducted experiments with a Phoenix tube up to 350 kv. in order to determine what advantage would be gained

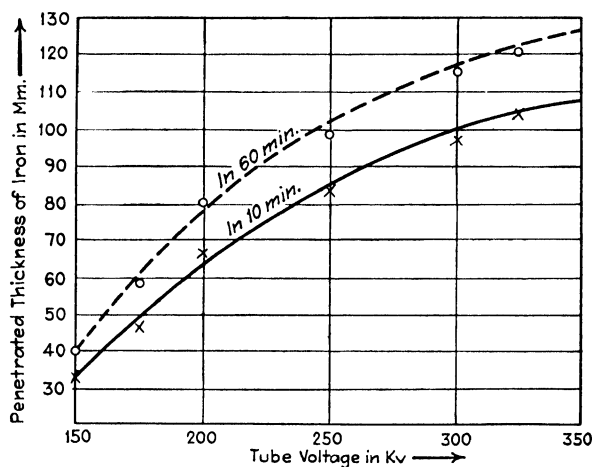


FIG. 54.—Curves illustrating penetration of iron as a function of tube voltage. (Berthold.)

by such unusual technique over more common procedures. The results are graphically shown in Fig. 54. Increasing voltages

<sup>1</sup> The  $r$  unit of x-ray quantity or intensity is considered on p. 163, in the next chapter.

have increasingly smaller increments in the limit of penetration, so that above 300 kv. the increase in material thickness limit of iron is inappreciable. With these very short wave lengths, scattering and recoil coefficients become very important in relation to the true absorption coefficient.

10. The limit of recognition of inhomogeneities in a material of certain thickness is practically measured by the smallest sharply defined difference in thickness of this same material which can be recognized. Blowholes and gas pockets have little or no absorbing power, so that this definition accurately holds for such cases. This limiting difference in blackening of a film is of the order of 2.4 per cent.

Thus:  $I = I_0 e^{-\mu x_1}$ ,

For a 10 per cent difference in blackening,

$$\frac{I}{I_0} = 0.976 = e^{-\mu x_1},$$

$$\frac{I_1}{I_2} = e^{-\mu x_2} = 0.89$$

$$\mu x_1 = 0.024.$$

$$\mu x_2 = 0.115.$$

Since  $\mu$  is constant,  $x_2/x_1 = 4.8$ . By means of such absorption calculations, taking into account scattering which serves to obscure the sharpness of delineation of defective areas, it is possible to calculate the limits of failure recognition and experimentally verify these data, such as are shown in Table XVII.

TABLE XVII.—REQUIREMENTS FOR RECOGNITION OF FAILURE RADIOGRAPHICALLY

Kilo-volts	Material thickness, millimeters			Smallest thickness difference, millimeters			Per cent of irradiated material		
	Al	Fe	Cu	Al	Fe	Cu	Al	Fe	Cu
80	72	..	..	0 42	.	.. .	0 6		
120	173	23	12.7	2 7	0 11	0 058	1 6	0 48	0 46
160	247	41	25	12	0 30	0 14	4 9	0 73	0 56
180	290	54	34	30	0 55	0 25	10	1.0	0 73
200	355	73	46		1 20	0 49		1 6	1 05

Conditions: Milliampere seconds 9000 (10 min. at 15 ma), field < 100 cm.<sup>2</sup>, 50 cm. focal distance, constant non-pulsating potential, blackening 0.7, no scattered ray screen, film with two intensifying screens

For observation of inhomogeneities on the fluorescent screen, a difference in brightness of two adjacent areas of the shadow

must be 15 per cent, and a blowhole or gas pocket in aluminum, iron, or copper must be 5 to 7 per cent of the total thickness of sound metal for certain conclusions.

11. Special technique is required for specimens of irregular shape in order that parts of the radiograph will not be over- or underexposed. Cylindrical bars or other specimens with circular parts should be placed in suitable holders of the same material so that the x-ray beam will pass through a constant thickness. Immersion in liquids, such as methylene iodide, having nearly the same opacity to x-rays as the piece to be examined, removes this difficulty. Otherwise, sheet lead of varying thickness, lead shot, lead oxide paste, barium sulfate paste, and other absorbing materials can be used with irregularly shaped pieces and for the prevention of the undue fogging of the film by scattered radiation or halation from direct rays at the edges of the specimen.

12. Intensifying screens have played a most important part in bringing this branch of radiography to its present high state. The ordinary calcium tungstate screens are usually employed. It may be mentioned here that a metal screen may also be used, lead foil being sometimes employed. The intensifying factor of such screens is lower than that of calcium tungstate screens; they have, nevertheless, some advantages over the tungstate screen. They absorb some of the secondary radiation from the under side of the piece being examined and, hence, reduce the fogging of the film; they produce finer-grained and, hence, more sharply defined images and are, therefore, especially useful for the examination for fine cracks in the metal. For thick pieces, where a higher intensifying factor than a lead screen provides is necessary (*i.e.*, above 2 in.), the two kinds of screens may be used together with the lead one next to the film. Metal screens may find an increasing usefulness as higher-powered tubes come to be used for thicker sections, because of their ability to reduce fogging.

13. The microphotometer has come into increasing usefulness for quantitative interpretation of radiographs on films, since the curves indicate at once the relative densities and hence dimensions of any imperfection. An example from the tests of Schwarz is shown in Fig. 55. The microphotometer is an instrument which has become practically indispensable for any kind of x-ray photographic work. The general principle of its operation is as follows: A light of constant intensity passes through the film

which is moved slowly and at constant speed. The light of varying intensity, depending upon the density of the photographic layer, then falls upon a delicate thermocouple (thermopile, photoelectric cell, etc.) which is connected with a galvanometer.

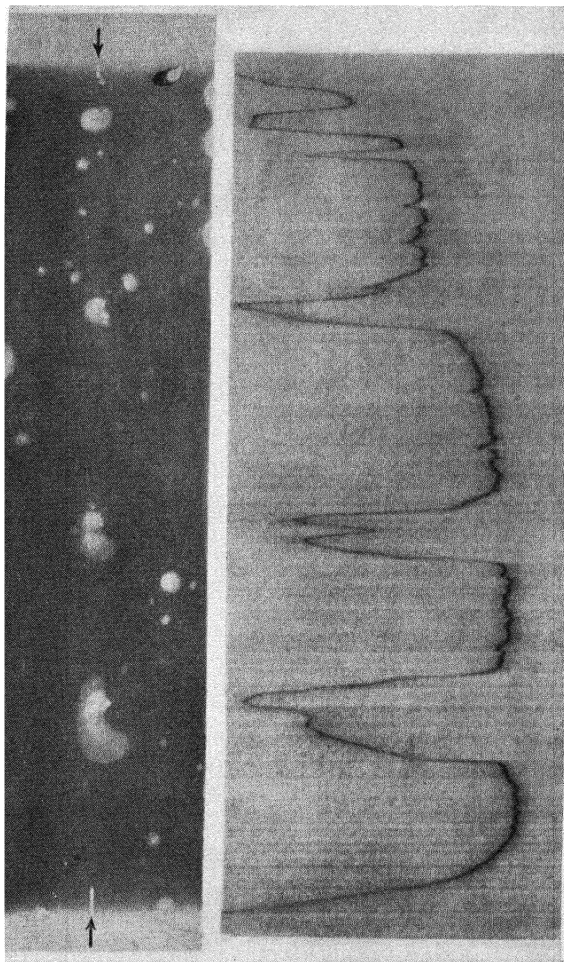


Fig. 55.—Radiograph of defective steel with microphotometer curve to enable quantitative study. (Schwarz.)

The deflections of the mirror which are a function of the thermoelectric current, the light intensity, and the photographic density, are then indicated by causing a reflected beam of light to register on sensitized paper on a slowly moving drum.

Spectral lines on the film are thus converted into peaks and the completed curve gives a method of quantitative measurement.

An instrument of special design in the writer's laboratory is shown in Fig. 56. The microphotometer is useful in the following types of investigation:

a. Accurate measurement of wave length and of relative intensities of spectral lines; indication of resolution of doublets, etc. The photometric curves measure position, fine structure, intensity from height of peak, and inherent breadth of lines.

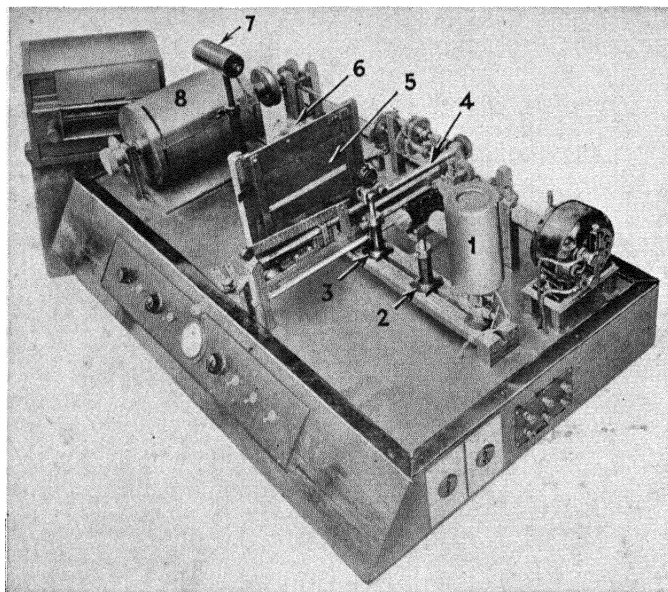


FIG. 56.—Microphotometer for quantitative measurement for x-ray spectra, diffraction patterns and radiographs. 1, constant source of light; 2, slit; 3, lens; 4, driving screw for slow movement of film holder; 5, film holder for moving film over narrow beam of light; 6, sensitive silver-bismuth thermocouple registering intensity of light transmitted through successive positions of film; 7, galvanometer lamp (galvanometer not shown); 8, rotating drum for sensitized paper (cover removed) registering deflections of galvanometer mirror.

b. Indispensable in quantitative chemical analysis, for which line intensities or height of absorption edges must be accurately compared with standards; indications of very faint foreign lines, etc.

c. Quantitative representation of radiographs.

d. Position and intensities of lines in diffraction photographs.

e. Indispensable in measurement of colloidal-particle size from widths of diffraction lines.



*f.* All other cases where automatic graphical measurement of a photographic plate in film would be useful.

14. Stereoscopic radiography for industrial diagnosis is often as valuable as it is in medical diagnosis. The depth and angular disposition of an inhomogeneity in any material may be ascertained much more certainly. Two radiographs are made, in each of which the tube has been shifted about 1.25 in. on either side of the center of the object. The two films are then viewed in the stereoscope which fuses the two pictures into one with the appearance of three dimensions.

### PRACTICAL APPLICATIONS OF RADIOGRAPHY

**1. Metal Castings.**—This is the most important application of x-ray radiographic diagnosis simply because of the wide use of castings and because of the uncertainty of gross structure with empirically developed foundry practice. The following defects may be radiographically detected on the interior of castings without in any way destroying or marring the specimens, although the diagnosis may be confirmed by “post mortem” incisions:

Gas cavities.

Due to gases liberated from the hot metal.

Due to gases from the mold.

Sand inclusions.

Slag inclusions.

Pipe or shrinkage cavities.

Porosity.

Due to small gas cavities.

Due to small shrinkage cavities.

Cracks.

Metal segregations.

Figure 57 shows the interior gross structure of a steel casting 1.25 in. thick which is characterized by every type of defect noted above, particularly gas cavities, non-metallic inclusions, and shrinkage cavities. The photographic reproduction is a negative and the spots of smaller absorbing power show up darker than the surrounding metal. Figure 58 shows typical gas cavities in cast steel 1 in. thick and Fig. 59 demonstrates with remarkable clearness the presence of internal cracks entirely unsuspected in cast steel 1.5 in. thick. These radiographs have been supplied through the generous cooperation of Dr. H. H. Lester of the Watertown Arsenal, a leading authority on metal radiography.

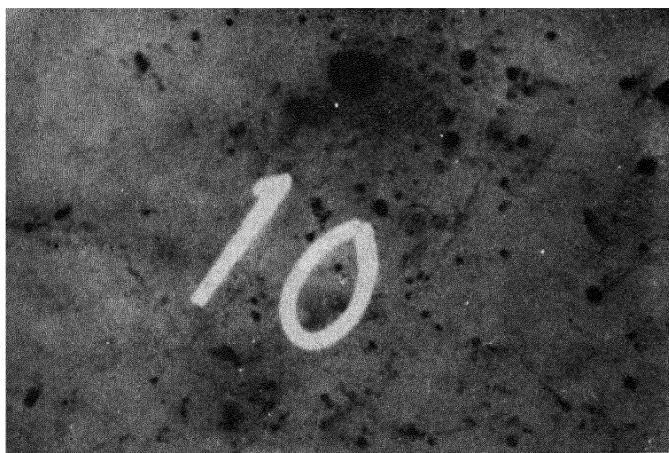


FIG. 57.—Interior gross structure of a steel casting with all types of defects.

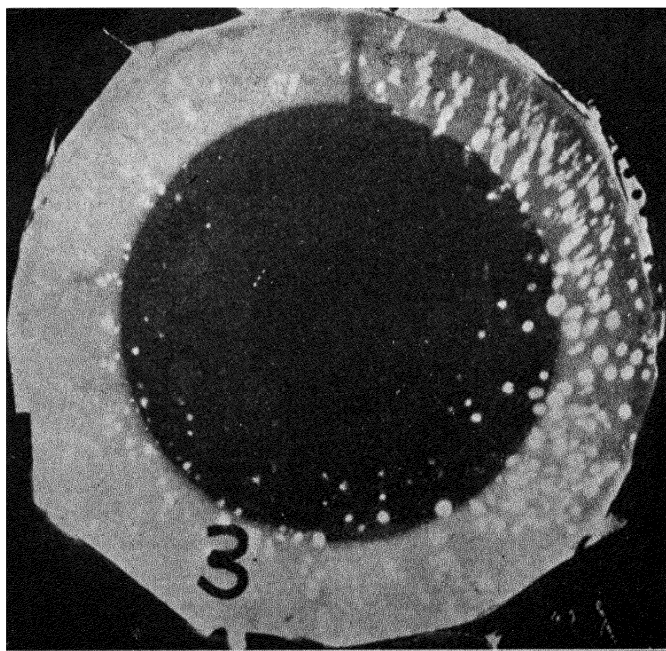


FIG. 58.—Radiograph of cast steel showing blowholes. (*Lester.*)

It is now possible with commercially available equipment to radiograph satisfactorily 3.5 in. of steel, while the Woolwich Arsenal in England reports penetration of 4.5 in. of steel showing an internal flaw 0.3 in. in diameter. The limiting thickness of metal is at present determined by the inability of available x-ray tubes to withstand voltages higher than about 280 kv.

The value of the x-ray method of inspection of castings to insure soundness and safety in operation is readily apparent.

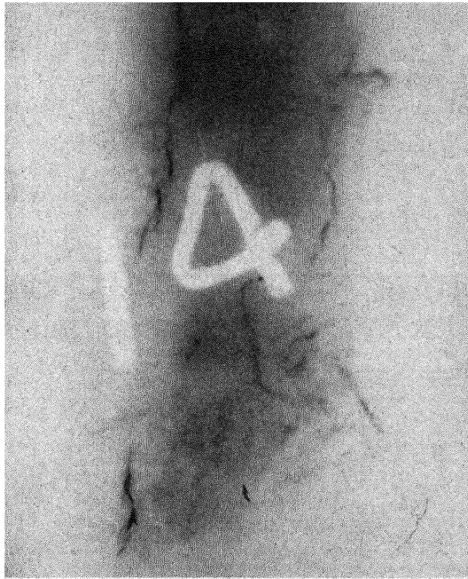


FIG. 59. --Radiograph of cast steel showing internal cracks.

The method may seem too expensive to utilize in the examination of every piece, but even in such cases it may be employed to tremendous advantage in the derivation of a proper foundry technique and changes in the design of core and mold or in the process of gating. Many progressive foundries have adopted this practice, although the great majority still cling to the old empirical methods and uncertainty whether a casting will survive or fail. On the other hand, it is the part of wise economy often to radiograph every unit of cast metal in an installation or every piece which is intended for expensive machining operations. An outstanding example in which extensive radiographic tests were used as specification for acceptance of parts is that of the high-

pressure steam installation in the Edgar power plant of the Boston Edison Company at Weymouth, Mass. The pipe and fittings for the 1200-lb. steam line and the cast shell of a 3000-kw. steam turbine were all examined and many rejections were made upon the basis of the radiographs before acceptance. The justification lies in the fact that not a single failure or break of any kind has occurred since installation, even though the conditions represented are extreme. Examples of this type are being multiplied rapidly at the present time and radiography must be considered an indispensable and thoroughly scientific testing and control method in the foundry industry. The Aluminum Company of America, for example, has considered as a sound and necessary investment the installation in all plants of radiographic equipment for the examination of aluminum and other light-alloy castings.<sup>1</sup>

**2. Welds.**—Closely allied to the problem of testing metal castings for soundness is that of welds. Here again there is no

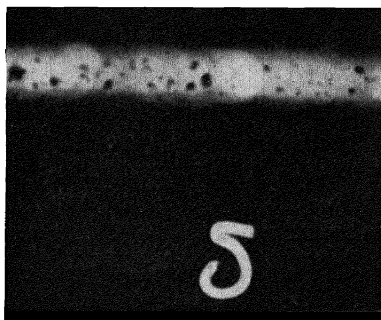


FIG. 60.—Radiograph of defective weld.

positive assurance by the usual methods that a weld has been made perfectly. With the agency of x-rays the smallest defects, such as pipes or gas inclusions, are indicated directly, with the result that a vast improvement in the technique of welding has taken place in the space of a very few years. Welds are now made with certainty of safety where they would never have been attempted previously. Figure 60 shows the actual condition of a typical weld which appeared perfect on the outside. The radiography of welds in locomotive parts subjected to vibrations and stress is widely used, particularly in Germany. In Fig. 61 is shown standard equipment on a German railroad for testing welds of locomotive fire boxes.<sup>2</sup> The writer recently advised the installation of an x-ray plant by a large manufacturer for the continuous inspection of welded rod to be used in

<sup>1</sup> See FINK and ARCHER, A.S.S.T. 1929; 108 references to radiographic applications are given.

<sup>2</sup> HERR, "Ergebnisse der technischen Röntgenkunde," Vol. I, p. 181. Leipzig, 1930.

the drilling of oil wells. Here is a case where these rods hundreds of feet long depend entirely upon the strength of the weakest welded joint, for with a break the rod falls to the bottom of the well. Consequently, the manufacturer did not dare to market the product without the assurance of sound joints. Since the rodding was only about 1 in. in diameter, it was found possible to use visual inspection with a fluorescent screen as the welded pieces moved along on a belt. The inspector was protected from the radiation by observation of the screen by means of a series of mirrors arranged in baffle fashion through heavy lead glass.

A very comprehensive radiographic, macro- and micrographic study of butt and lap welds of all kinds is reported by Lefring.<sup>1</sup>

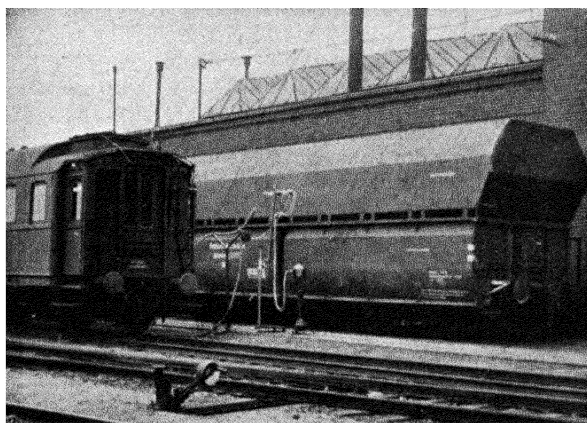


FIG. 61.—Standard x-ray equipment on a German railroad for radiographic examination of locomotive parts and welds.

The failures are divided into bonding and layer deficiencies and gas pores. Such a study, of course, leads directly to establishment of the best possible technique.

**3. Automotive and Aircraft Parts.**—It may be truthfully stated that the remarkable dependability of automobile and aircraft motors in races and endurance flights such as those of recent months may be ascribed primarily to the assurance of soundness promoted by radiographic testing. This is particularly true for propellers, in which soundness is absolutely necessary. Not only internal defects but also *surface* cracks which have escaped attention are immediately detected. Pistons

<sup>1</sup> "Ergebnisse der technischen Röntgenkunde," Vol. II, p. 313, Leipzig, 1931.

have been surprisingly prone to disclose serious though unsuspected defects. All parts of an airplane may be inspected with x-rays from the cast cylinders to the spark plugs and the wooden framework. And where the safety of life is so utterly dependent upon sound mechanism and faithful performance

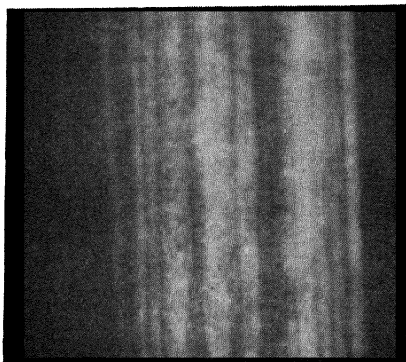


FIG. 62.—Radiograph of rolled sheet steel containing slag inclusions.

it would seem little short of criminal not to use this positive method of specification and selection.

**4. Rolled and Drawn Metal.**—Figure 62 is the radiograph of a rolled sheet of steel containing slag inclusions which have

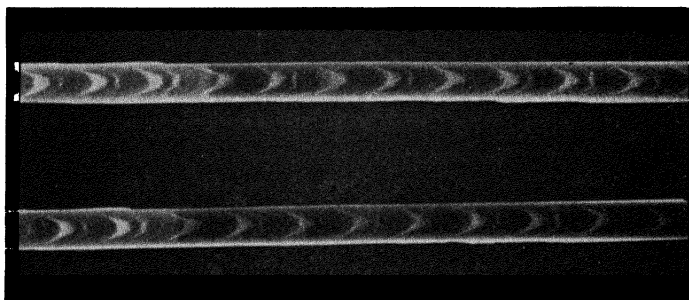


FIG. 63.—Radiograph of overdrawn aluminum rod.

been fibered with the metal in the rolling process. The very poor quality of such a sheet is clearly demonstrated by entire failure in forming operations. Figure 63 shows how an aluminum rod is affected by extreme cold drawing. The structure is such as to render the specimen worthless.

**5. Miscellaneous Applications of Metal Radiography.**—Among a large number may be mentioned the inspection of insulated

wires and cables and coated metals for breaks, of metal tubes and capillaries for clogging, of intricate assembled objects for proper adjustment of parts, of projectiles for proper location of caps and fuses as well as for complete filling by explosive, of gun barrels for rifling and defects, of molten metals inside furnaces for melting point and surface tension (Fig. 64), of ball bearings and of all fencing foils at the University of Illinois for soundness, of electric insulators for the presence of metallic particles, of metal radio transmission tubes for proper position of grid and filament, of all sorts of sheets suspected of corrosion, and of steel Dewar flasks used for liquid air or oxygen, where corrosion may

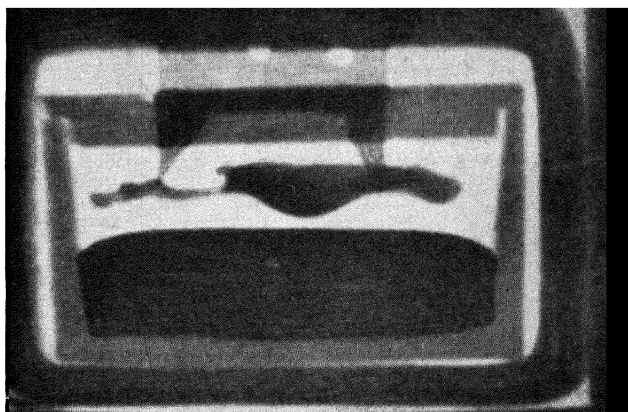


FIG. 64.—Radiograph through furnace showing solid and liquid copper in equilibrium at the melting point. (*Libman.*)

result in great decrease in wall thickness. This last test is a standard procedure in the German railway shops.<sup>1</sup>

**Miscellaneous Practical Applications.**—Besides innumerable metal products, numerous other practical applications of radiography have been made and some of these are briefly enumerated:

Arc electrodes for soundness.

Coal for classification as to foreign mineral content (Fig. 65), and for control of cleaning by flotation (Fig. 66).

Rubber tires for imperfect bonding to cords.

Reclaimed rubber for nails and other foreign bodies.

Golf balls for centering of core.

Complicated glass, hard rubber, and bakelite pieces of various kinds with internal seals, etc., for improper fabrication.

<sup>1</sup> SCHWARZ, *loc. cit.*

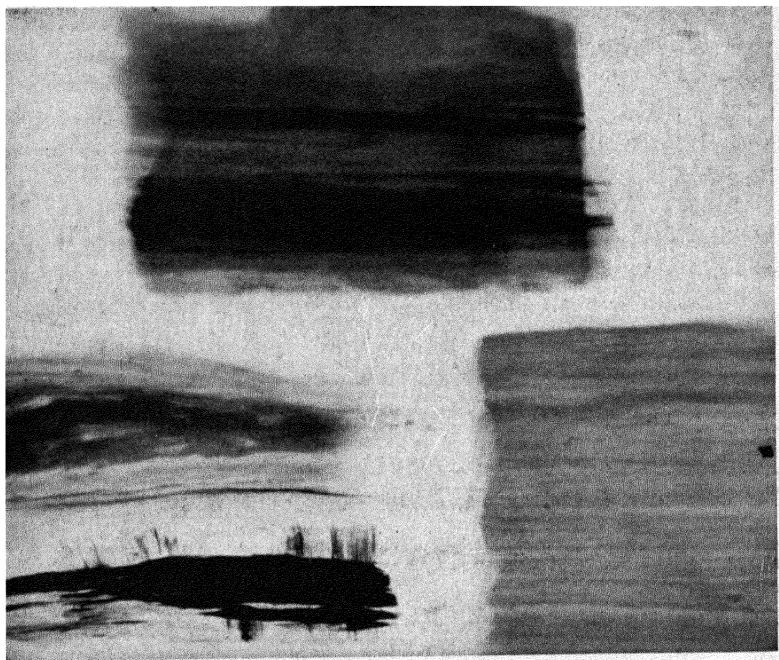


FIG. 65.—Radiographs of coal lumps showing nearly pure coal (lower right) contrasted with samples containing inclusions. (*Clark and Mitchell.*)

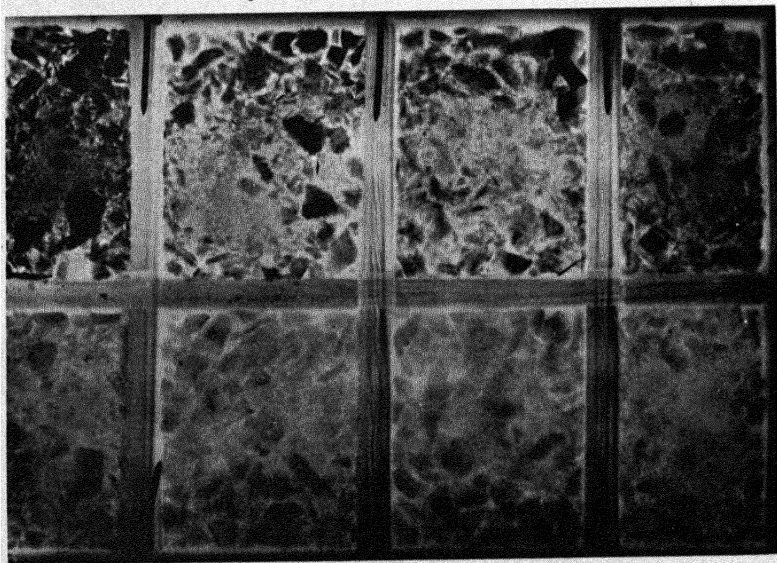


FIG. 66.—Radiograph showing steps in cleaning of coal by flotation. Upper left, maximum content of impurities; lower right, nearly pure coal.



Wood for cracks, wormholes, rot, knots, embedded nails, etc., as employed in aircraft frames, special lumber, telephone poles, etc.

Railway ties for compression or erosion under the plates (after soaking in mercuric chloride solution to increase x-ray absorption).

Shells and cartridges for improper filling.

Porcelain insulators, thermocouple tubes, spark plugs, etc., for internal cracks (Fig. 67).

Location of pipes and wires in building walls.

Contraband goods in trunks with false bottoms, and suspicious packages for bombs, etc.

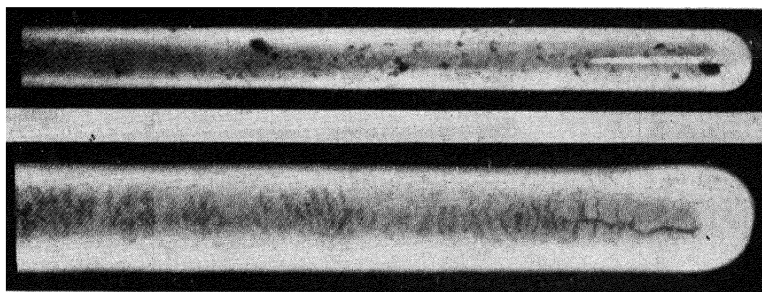


FIG. 67.—Radiographic detection of defects in porcelain tubes. (Courtesy Cloud S. Gordon Company.)

**X-rays and Art.**—One of the most striking applications of x-rays has been in the field of art. A well-established branch of radiography is now that of the examination of old paintings and art objects for evidences of retouching, or of original paintings covered over with others, and for distinguishing true masterpieces from copies. Important court cases have been decided upon the base of the x-ray evidence. The old paint pigments consisted of inorganic substances which are heavily absorbing to x-rays as compared with modern organic dyes. Excellent x-ray laboratories are now to be found at the Fogg Art Museum of Harvard University, Metropolitan Museum of New York, and the museums at Chicago, Philadelphia, Minneapolis, and elsewhere. An example is reproduced in Fig. 68 from the paper by Dr. Alan Burroughs,<sup>1</sup> an outstanding authority on this subject. The x-ray photograph represents a portion of the painting "Mars and Venus" by Veronese. The painting shows the head of

<sup>1</sup> *Smithsonian Rept.*, 529 (1927).

Venus upright while the x-ray photograph shows two heads, the one more inclined to the right having been painted out very likely by the master himself.



FIG. 68.—Typical result of application of radiography in examination of old paintings; from "Mars and Venus" by Veronese. The head at the right was painted out and disclosed only by x-rays. (*Burroughs, Smithsonian Report, 1927.*)

**The Cost of Radiographs.**—Several attempts have been made to estimate the cost of radiographic examination of materials in order to justify its adoption as an industrial method of testing, control, and research. The cost, of course, depends on many factors, among which are the nature, size of the specimens, the number per hour, amortization, and overhead. Fink and Archer estimate an average cost of \$2 per square foot of film, although for several small specimens on one film this may fall to well below \$1. In other cases for very large specimens the cost may well rise to much higher values. Berthold has made the most extensive calculations for German practice and has constructed a series of curves of basic cost against specimen thickness for three kinds of apparatus operating at 120, 180, and 200 kv. and for aluminum, iron, and copper. A few data read from these

graphs for the cost of 1 RM (about 24 cts.), to which must be added the cost of photographic materials, are as follows:

Metal	Kilovolts	Thickness, millimeters
Al. . . . .	120	145
Al . . . . .	180	248
Fe . . . . .	120	16.5
Fe . . . . .	180	43.5
Fe . . . . .	200	62.5
Cu . . . . .	120	10
Cu . . . . .	180	26.5
Cu . . . . .	200	39

The indications, therefore, point to a considerably lower cost now than in the past, due to the newer high-power tubes, standardized equipment, and technique. However, it is probably still too expensive for ordinary routine examination of every unit, except when safety is involved or where the pieces are especially valuable, or the raw material is to be subjected to expensive fabrication.

**Radiography by the Use of Gamma Rays.**—The presentation of this subject would be incomplete without mention of the

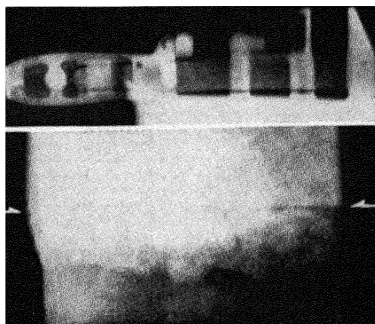


FIG. 69.—Radiographs of wrench and defective weld, with  $\gamma$ -rays. (*Mehl and associates.*)

remarkable radiographic results obtained by Mehl and his associates with the  $\gamma$ -rays from radium emanation. Since the wave lengths of  $\gamma$ -rays are shorter than x-rays as generated under practical conditions, it follows that they should penetrate thicker sections. Successful photographs were made through 10 in. or

more of steel, utilizing only a small bulb of radium emanation at a certain distance from the specimen and a photographic film. Exposures of 10 or 12 hr. were necessary but, of course, this is not a serious handicap, since no attention is required. The method is very promising for the examination of structures in position and because of the extreme simplicity and absence of all machinery. The  $\gamma$ -radiographs of a wrench and a weld are shown in Fig. 69.

## CHAPTER IX

### PHYSICAL, CHEMICAL, AND BIOLOGICAL EFFECTS OF X-RAYS

#### I. SOME PHYSICAL EFFECTS

**Ionization.**—Of physical phenomena the ionization of gases through which x-rays pass is the best known and probably the most fundamental. It was recognized soon after the discovery of x-rays and has ever since been the subject of much extensive and intensive study. Although C. T. R. Wilson, with his beautiful cloud-condensation experiments, was able to demonstrate the mechanism of the ion formation some years ago, accurate information concerning the variation in ionization with changes in the gas and x-ray conditions has become available only very recently and is even now incomplete.

When the x-rays pass through the gas, they liberate photoelectrons (which, as will be explained, are known to cause the ionization); they excite those characteristic radiations of the gas whose critical absorption frequencies are less than the frequency of the incident x-ray beam; they produce scattered radiation of the frequency of the incident beam; and they may produce recoil electrons and the accompanying secondary radiation (Compton effect). Ionization experiments are usually conducted so that the ionization is measured by the electric current passing through the ionized gas, under a definite potential difference. The gas is held in an ionization chamber between two electrodes which are connected to the source of electric potential. Many of the early experiments were valueless because the incident radiation was allowed to impinge upon these electrodes, where it caused secondary phenomena similar to those mentioned above and consequently altered the electrode potential. It is obvious that the secondary radiation excited in the gas, even when the electrodes are protected from the incident beam, may cause like disturbances. The difficulty of measuring ionization—and ionization only—is very great.

The mechanism of the ionization is now agreed to be the following: The high-speed photoelectrons released by the x-ray beam have too much kinetic energy to be at once absorbed by adjacent molecules, and they consequently break down the molecules with which they come in contact into pairs of ions. Thus they progressively dissipate their kinetic energy until it becomes so small that the electron is absorbed either by a molecule to form a negative ion or by a positive ion to cause neutralization. All this was very excellently shown by the experiments of C. T. R. Wil-

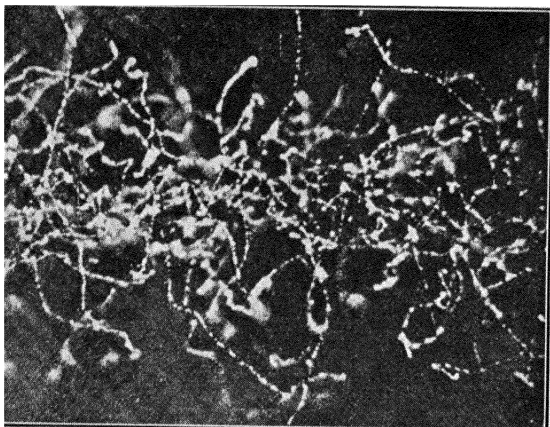


FIG. 70.—Tracks of  $\beta$ -rays liberated in gas by x-rays. (C. T. R. Wilson.)

son who, by condensing water on the ions at the moment of formation and simultaneously photographing them, was able to obtain actual photographic records of the paths of the photoelectrons. One of Wilson's photographs is reproduced in Fig. 70.

Thus it would be expected that in a layer of gas insufficiently thick to absorb the x-ray beam completely, the degree of ionization would be proportional to the density of the gas or, if the temperature were constant, to the pressure on the gas, provided the x-ray beam remained unchanged. This has been borne out by experiment, Crowther and Owen having found the ionization to increase proportionally with pressure, and Crowther having shown that temperature over a range from  $-180$  to  $+148^{\circ}$  C. has no effect on ionization if the density is kept constant. It is reasonable to assume that, after the density became sufficiently great to absorb the x-ray beam completely, no further increase in ionization with increasing density would be observed. There are, however, no high-pressure experiments to test this point.

The relative ionization of the gases, except hydrogen and possibly ethyl bromide, is not changed by a change in wave length of the incident ray, so long as the range over which the wave length changes does not include a characteristic absorption discontinuity for any of the gases.

Several recent experiments seem to prove quite satisfactorily that within certain wave-length limits, at any rate, ionization is independent of the wave length of the exciting x-ray beam,

TABLE XVIII.—RELATIVE IONIZATION PRODUCED IN VARIOUS GASES BY HETEROGENEOUS X-RAYS

Gas or vapor	Density relative to air = 1	Ionization relative to air = 1	
		Soft x-rays	Hard x-rays
Hydrogen, H <sub>2</sub> ...	0 07	0 01	0 18
Carbon dioxide, CO <sub>2</sub> ...	1 53	1 57	1 49
Ethyl chloride, C <sub>2</sub> H <sub>5</sub> Cl ...	2 24	18 0	17 3
Carbon tetrachloride, CCl <sub>4</sub> ...	5 35	67	71
Nickel carbonyl, Ni(CO) <sub>4</sub> ...	5 90	89	97
Ethyl bromide, C <sub>2</sub> H <sub>5</sub> Br ...	3 78	72	118
Methyl iodide, CH <sub>3</sub> I...	4 96	145	125
Mercury methyl, Hg(CH <sub>3</sub> ) <sub>2</sub> .	7 93	425	

TABLE XIX.—RELATIVE IONIZATION PRODUCED IN VARIOUS GASES BY HOMOGENEOUS X-RAYS

Element emitting characteristic radiation	Ionization relative to air = 1					
	H <sub>2</sub>	O <sub>2</sub>	CO <sub>2</sub>	SO <sub>2</sub>	C <sub>2</sub> H <sub>5</sub> Br	CH <sub>3</sub> I
Fe	0.00571	1 37	1 58	11 3	41.2	
Ni .....		1.35	1 55	11 6	.....	162
Cu .....	0 00573	1 38	1 55	11 8	42	152
Zn .....	0 00570	1.42	1 54	11.5	41 6	
As .....	0.00573	1.27	1 51	11.7	42.2	158
Se.....	.....	1.31	1 53	11 8	41.7	
Sr.....	.....	1.28	1 53	11 8	153	
Mo.....	.....	1.28	1 54	11.5	213	188
Ag.....	.....	1 32	....	....	272	198
Sn .....	0.04	1.29	....	....	335	205
Sb .....	.....	1 28				
I .....	.....	..	..	....	.....	211
Ba .....	.....	.	.	.	.	251

provided that the number of photoelectrons liberated is the same (see page 192).

Kulenkampff and Kircher and Schmitz have calculated the energy necessary for the production of one pair of ions in the ionization of air, and the former finds it to be 35 volts, while the latter find 21 volts. The energy is here expressed as the number of volts necessary to impart to a single electron a kinetic energy equal to the energy in question. Kulenkampff's value is the more likely and is generally accepted. The Compton effect explains the lower value. Recoil, or Compton, electrons in addition to the photoelectrons are excited by the shorter wave lengths, and these electrons, though having little ionizing power, absorb much of the energy in the x-ray beam; longer waves excite only the photoelectrons, which produce the ionization.

The ionization of gases by x-rays is much used in measuring x-ray intensity. A more complete description of such use will be found on page 161.

**The Effect of X-rays on the Electrical Conductivity of Solids and Liquids.**—Although there have been few experiments directly aimed at studying ionization in solids and liquids, it is certain that the increase in electrical conductivity of certain solid dielectrics when exposed to x-radiation is exactly the same phenomenon. This effect has been known for many years and has been studied in several different dielectrics. The experiments have generally been found to be in good agreement. The most exhaustive experiments are reported by Roos,<sup>1</sup> who studied sulfur, paraffin, hard rubber, and amber.

The conductivity of sulfur was found to increase rapidly to a constant and reproducible value, if the raying was not continued over a period of more than about 2 min. In such cases, also, the conductivity fell to its original value almost immediately after the raying was discontinued. If, however, the dielectric was exposed to the rays for a somewhat longer period of time, the conductivity first rose, then gradually fell off, and did not drop immediately to its original value after cessation of the raying. It was found that the current through the sulfur was proportional to the voltage imposed for the whole range of voltages employed. These results are in agreement with those of Grebe,<sup>2</sup> who used potentials up to 200 volts. Both experimenters found

<sup>1</sup> *Z. Physik.*, **36**, 18 (1926).

<sup>2</sup> *Z. Physik.*, **17**, 295 (1923).



that the effect was also proportional to the x-ray intensity, a result also obtained by many of the early experimenters (see Roos's paper for references).

The influence of x-ray wave length on this effect was studied by both Grebe and Roos by comparing the ionization produced in air with the increase in conductivity. Grebe found the ratios of the currents through the ionization chamber to the current through the sulfur to be equal for different waves and, from this fact and from the discovery that the ratio of the absorption coefficients for air and sulfur remains constant for wave lengths less than the *K* absorption discontinuities, he concluded that the change in conductivity of sulfur was due to a kind of internal photoelectric effect, similar to the effect that produces ionization in air.

The action of paraffin, hard rubber, and amber strengthens this conclusion; for while the same relationship between x-ray intensity and the effect holds for them as for sulfur, they also show definite saturation currents, just as does air, though no such current was found for sulfur.

After this saturation current is reached, it is no longer permissible to speak of the change in conductivity of the dielectric but rather of the change in ionization. It is also interesting to note that Gudden and Pohl,<sup>1</sup> who studied the effects of ultraviolet light on the electrical properties of crystals, came to the conclusion that these were the results of an internal photoelectric effect. It may be concluded that those solids which are strong dielectrics undergo an ionization exactly similar to that of gases. Indeed it is probable that this phenomenon is of fundamental importance in every direct effect of radiation, and that a more complete knowledge of it will lead to a better understanding of the many and diverse ways in which x-rays react upon matter.

The fact that saturation currents can be reached for amber, hard rubber, and paraffin make these dielectrics more suitable for practical insulation in x-ray apparatus than sulfur, unless protection is provided against the x-radiation. Thus for thin insulator layers the conductivity of sulfur is appreciably higher than that of the others. In this connection it is interesting to notice that Grebe found in his experiments that monoclinic sulfur was approximately three times as conductive as rhombic sulfur when radiated with the same beam.

<sup>1</sup> Several papers in *Z. Physik.* (1920-1924).

An effect somewhat similar to the one just discussed is the well-known change in the electrical resistance of selenium crystals, when illuminated with ordinary light, ultraviolet rays, or x-rays. Although McMahon found that an increase in pressure on the crystal increased the effect, the change in sensitivity with wave length has not been determined.<sup>1</sup> This phenomenon of resistance decrease, which must find its explanation ultimately in the peculiarities of the structure of the selenium crystal, has been explained upon the basis of several hypotheses, one of the most promising being that of resonance. By this theory the electrons in the crystal which have radiation frequencies in approximate correspondence with the frequency of the exciting radiation are temporarily loosened from their atomic bonds and become available for the transfer of electricity. In a practical way this phenomenon has found some application in estimating x-ray intensity.

The conductivity ( $C$ ) of insulating liquids exposed to x-rays has been investigated a few times. A few typical results are as follows for

$$C = 10^{-4} \text{ ohm}^{-1} \text{ cm}^{-1};$$

Carbon tetrachloride 8, carbon disulfide 20, amylene 14, benzene 4, liquid air 1.3, petroleum ether 15, vaseline oil 1.6.<sup>2</sup>

**The Excitation of Luminescence in Irradiated Substances.**—The excitation of luminescence in many substances, when irradiated by x-rays, is a property which has played an important role in the history of the science. As a matter of fact, the fluorescence of neighboring objects led to Roentgen's discovery of the radiation.

The phenomenon depends upon the ability of substances to absorb the rays and transform the energy into radiation of longer wave lengths in the ultraviolet or visible regions.

Schuhknecht<sup>3</sup> was the first to study the fluorescence of materials under x-rays, with the quartz spectrograph. Because of the excellence of his work, the results are presented in Table XX, showing the spectral regions and the wave lengths of the intensity maxima, in A.U.

Schuhknecht observed that the spectral distribution of the luminescence was profoundly influenced by minute amounts of

<sup>1</sup> *Phys. Rev.*, **16**, 558 (1920).

<sup>2</sup> "International Critical Tables," Vol. VI, p. 6.

<sup>3</sup> *Ann. Physik*, **17**, 717 (1915).

TABLE XX.—WAVE LENGTHS OF FLUORESCENT LIGHT EXCITED BY X-RAYS

	Region, A.U.	Position of maximum, A.U.
Fluorspar.....	3640-2400	2840
Fluorspar and iron spar	3900-2310	2800
Scheelite (Ca tungstate)	4800-3750	4330
Zinc sulfide.....	5090-4120	4500
K platinoeyanide....	4900-4120	4500
Ba platinoeyanide....	5090-4420	4800
Ca platinoeyanide.....	5090-4550	4800
U NH <sub>4</sub> fluoride.....	4400-3800	4100
X-ray tube glass	5090-3000	3750

impurities, as is well known for fluorescence under visible light.

Nichols and Merritt<sup>1</sup> found that the intensity distribution in a fluorescent band was independent of the exciting radiation, x-rays, ultraviolet light, or cathode rays. More recently Wick<sup>2</sup> has studied the fluorescence of uranium salts, and Newcomer<sup>3</sup> that of about five hundred chemical compounds (mostly organic). The latter found sodium bromide very strongly fluorescent in the ultraviolet, and benzoic acid and naphthalene and their derivations in the yellow green.

All workers with x-rays are probably familiar with the fact that when the radiation strikes the eyes, there ensues a sensation of luminescence which may continue for several seconds after the exciting source is removed. This latter phenomenon is an example of *phosphorescence*; with x-rays phosphorescence, in general, is usually more pronounced than with light because of the deeper penetration of the former, and hence of a greater volume effect. Gases and many solids are phosphorescent. Even powdered rock salt is easily visible in a darkened room for a half hour or more after its exposure to x-rays.

There are several practical uses of fluorescence under x-rays. The property may be used to differentiate between chemical substances, *e.g.*, diamond and a glass substitute. It may serve

<sup>1</sup> *Phys. Rev.* (1), **21**, 247 (1905); **28**, 349 (1909).

<sup>2</sup> *Phys. Rev.* (2), **5**, 418 (1915).

<sup>3</sup> *J. Am. Chem. Soc.*, **42**, 1997 (1920).

as the basis of invisible inks and identification marks on objects which are developed under a beam of x-rays. It may be used as a means of measuring intensities of x-rays, as discussed later in this chapter. It is the basis of the science of fluoroscopy or visual radiography, as outlined in Chap. VIII. Tarada in 1915 used a fluorescent screen in order to see Laue diffraction patterns of crystals; more recently Hauser and Mark have proved by such a visible examination that the diffraction pattern of stretched rubber appears instantaneously; with the advent of high-power x-ray tubes diffraction patterns may be easily visually observed. The property of fluorescence may be utilized to intensify x-ray photographic exposure, as will be shown in a subsequent paragraph.

Finally, the newest and most remarkable application of fluorescence of substances irradiated by x-rays is that discovered by McDonald and associates in cancer researches in Philadelphia.<sup>1</sup> Living cells comparatively resistant to the direct action of x-rays were treated with solutions of organic compounds which fluoresce in the ultraviolet range when irradiated with x-rays. Under the action of these ultraviolet rays (2000 to 2500 A.U.) the cells were observed to become violently agitated and then killed in an astonishingly short interval of time as the result of specific photochemical action on the nucleus. This discovery is recognized as one of major importance in the further development of x-ray therapy.

*Fluorescent Intensifying Screens.*—A very practical use of the property of fluorescence is the intensifying screen, used with photographic films in x-ray radiographic and crystal diffraction applications in order to cut down the time of exposure, sometimes to a twentieth of the usual value. For these screens calcium tungstate serves best because of its intense blue-violet fluorescence. The screens are usually placed behind the photographic plate or film, and the fluorescent portions add their action on the sensitive emulsion to the direct x-ray effects. Unless care is used, difficulties with the screens may arise as follows:

1. If the calcium tungstate is not pure, the screen may have an appreciable hangover or phosphorescence. In the writer's laboratory some of the best commercial screens have produced a distinct effect on a photographic plate for as long as 3 months

<sup>1</sup>Reported at the Denver meeting of the American Chemical Society, August, 1932.

after their exposure to x-rays. Hence, this extraneous action of previously used screens may lead to misinterpretation of newly obtained x-ray photographs.

2. Unless the screen is very carefully prepared for uniform particle size and is placed in the closest proximity to the sensitive emulsion, it may reduce the definition of the photograph by broadening the image. This effect is observed easily, even when only the thickness of the glass of a photographic plate separates the emulsion and the luminescent image.

3. The intensity of fluorescence depends upon the wave lengths; although quantitative data on this point are lacking, de Broglie<sup>1</sup> showed that a screen had no intensifying effect upon rays with wave lengths of 1.25 A.U. but displayed a gradual increase in

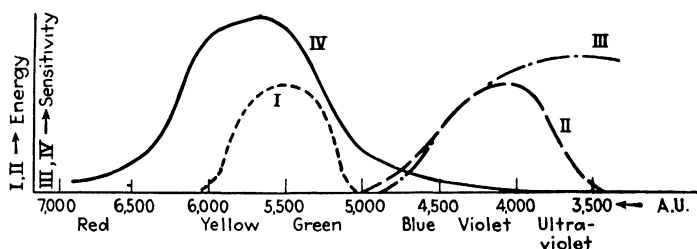


FIG. 71.—Curves showing spectral ranges of maximum sensitivity of the eye and photographic plate, to which should correspond, respectively, the fluorescent screen and the intensifying screen. I, fluorescent screen; II, calcium tungstate intensifying screen; III, silver bromide of photographic emulsion; IV, human eye.

effectiveness up to the critical absorption wave length of tungsten at about 0.179 A.U., at which point, corresponding to greater absorption, a sharp increase occurred for the shorter wave lengths. For this reason fluorescence cannot serve satisfactorily as a means of measuring x-ray intensities.

An interesting comparison is given in Fig. 71 of the spectral ranges of sensitivity of the eye, the fluoroscope screen (containing as the most important constituent zinc silicate), the silver bromide emulsion, and the calcium tungstate photographic intensifying screen. Very properly the first two and the last two show sensitivities over the same spectral range.

## II. CHEMICAL EFFECTS OF X-RAYS

There are several points of interest in the study of the chemical effects of x-rays which may be enumerated as follows:

<sup>1</sup> *Compt. rend.*, **177**, 849 (1920).

1. Pure photochemistry, the mechanism and rate of reactions, the stability of chemical bonds, etc.

2. Light thrown on therapeutic effects by study of chemical changes.

3. Discovery of reactions which could be used as suitable dosimeters for quantity or intensity of radiation.

The casual observer could well believe that x-rays by virtue of their penetration and energy should have innumerable profound chemical effects, but as a matter of fact the examples of considerable chemical change are extraordinarily few in number. Systems which undergo change in ultraviolet light are apparently unaffected. The photographic effect, a few oxidation-reduction reactions, and some condensations of organic compounds are almost unique among the large number of experiments already empirically tried. However, the hope remains that other chemical effects may be discovered which might serve the purpose even of a convenient dosimeter.

**The Mechanism of Chemical and Biological Action.**—It has already been indicated that absorption of radiation energy must precede any physical, chemical, or biological effects which may be observed. In pure absorption the energy of an x-ray quantum is transformed to that of electrons (photoelectrons) liberated from atoms, together with the net potential energy of the irradiated atom (ionization). In the latter case the atom remains in the ionized condition only a very short time ( $10^{-9}$  sec.); one of the electrons in the outer orbits falls into the vacancy created by the photoelectron. In so doing, the potential energy of the ionized atoms becomes the energy of secondary characteristic rays. The ionized action by virtue of its changed condition can also enter into chemical reactions. Since secondary characteristic rays produced by return of the ionized atom to the normal state are softer than the primary rays, especially so in the human body on account of the light elements, they will be easily absorbed by one of two processes. The quantum of radiation may leave the mother atom and be absorbed by a neighboring atom, or it may actually remain in the mother atom so that its energy is used for the liberation of a second electron (photoelectron of the second kind). This effect or process of inner absorption can also be considered as a radiationless transition of an electron to a deeper orbit, in which the energy difference is imparted as kinetic energy to another electron.

The photoelectrons account for the second portion of the energy following absorption of a primary quantum (or x-ray photon). The variations in velocities as determined in  $\beta$ -ray spectra have already been considered and it follows that the kinetic energy will have nearly the same value of the primary x-ray quantum for light elements or for outer electrons of heavier atoms, in which the work required to free the electron is small. The photoelectron is now free to liberate secondary electrons by impact with atoms, which, of course, have lower velocities, thereby ionizing the atoms, or the impact may serve only to lift the electron to a higher energy level in the atom which becomes therefore excited.

Still another mechanism in the absorption of x-rays by atoms in molecules is the transformation into heat. An increase in energy of motion of atoms in molecules in position results in nothing more than local elevation in temperature. Of course in an irradiated body the transformed x-ray energy is so small that a measurable increase in temperature is almost impossible to observe. The phenomenon is of interest in the light of Dessauer's point-heat theory of biological action.

It is certain that in a biological or chemical medium the photoelectrons possess large initial velocity with a velocity distribution corresponding to the x-ray spectrum. The fate of the photoelectrons is widely varied but in general it is the same as that observed for the impact of cathode rays on the anticathode of the x-ray tube (see page 78). Between the first and last (heat) steps in the chain of transformations the widest variety of effects must be possible.

These high-speed electrons can bring into reactive form by impact other atoms and molecules which have been absolutely unaffected by the primary radiation quanta; in fact the proportion of atoms and molecules activated by the photoelectrons may be very much larger. This mechanism differs from the chemical effects of ordinary light in which energy suffices only to excite atoms by lifting electrons to higher energy levels. X-rays also differ from ordinary light in that they may *have chemical action* because of scattering and recoil electrons and yet undergo no fluorescent absorption, a process unknown for light.

Besides the process of true absorption, the energy of a quantum of x-radiation can also be transformed into electron kinetic

energy—that of the recoil electrons in the Compton effect. The velocity of these is considerably smaller than that of the photoelectrons and, of course, depends on the scattering angle. Their chemical and biological effects are consequently smaller. However, it must be noted that at 200 kv. 2.5 per cent of the x-ray energy goes into photoelectrons and 3 per cent into recoil electrons. At higher voltages the latter figure becomes even more significant.

**Experimental Tests of Theories of Chemical-reaction Mechanism.**—The above theory of chemical action due very largely to Glocker has been subjected by him and by others to experimental test. Glocker and Risse<sup>1</sup> have studied the decomposition of hydrogen peroxide and potassium persulfate in very dilute solutions. The amounts decomposed corresponded to the energy of the secondary electrons liberated in the system during passage of x-rays; 70,000 cal. (electrons in motion) are required to decompose 1 mole of  $\text{H}_2\text{O}_2$  in  $\frac{1}{600}$  normal solution and 2.45 times as much for potassium persulfate. The dependence of chemical effect upon x-ray wave length is a question entirely of how much energy during passage of an x-ray beam of certain wave length through matter of certain composition is transformed into the energy of secondary electrons. Taking into account the complications of scattered and fluorescent rays which may form secondary electrons, Glocker and Risse have obtained complete verification of the theory, and further substantiation has been obtained by other workers for other systems.

In general, the exact mechanism and kinetics of chemical reactions, though due to activation by electron impact, have been explained only in a very few instances. The photographic action is unusually simple, in that the silver and bromine ions are converted endothermically into neutral atoms through the energy of the secondary electrons. The evolution of hydrogen chloride from chloroform is the best example of a reaction where far greater change is observed than can be accounted for by electron impact. It is, therefore, a chain reaction: a residual chloroform molecule disturbed by electron impact can react with an unchanged chloroform molecule, the product of this reaction with another unchanged chloroform molecule, and so on. Such reactions, together with side reactions with atmospheric oxygen, account for the extreme sensitiveness toward x-rays of iodoform solutions in chloroform. Because of the common mechanism

<sup>1</sup> *Z. Physik.*, **48**, 845 (1928); *Z. physik. Chem. (A)*, **140**, 133 (1929).



some chemical effects of x-rays would be expected to be the same as those with ultraviolet light, but not necessarily the same as thermal reactions. Barium azide decomposes into nitride with x-rays but never with heat.

**The Photographic Effect.**—In their action on the photographic plate x-rays seem similar to ordinary light, for there are no known plates sensitive to x-rays which are not also sensitive to the visible radiation. Examination of microscopic sections through the sensitive layer of exposed plates has shown, however, that x-rays, unlike light, produce an equal distribution of grains of reduced silver throughout the whole thickness of the layer. Consequently a greater blackening of the plate, when exposed to x-rays, can be obtained by increasing the thickness of the sensitive layer. Here, indeed, is found the chief difference between ordinary photographic films or plates and those manufactured for x-ray use; the latter are provided with a thicker sensitive layer and are usually “duplitized,” or coated on both sides with the sensitive silver bromide emulsion.

The laws of the blackening of photographic plates have been quite thoroughly studied. The frequency and intensity of the incident rays and the time of exposure are the important factors. Rays of differing frequencies do not have an equal quantitative effect. Kulenkampff has made calculations, based on some new intensity and ionization measurements, which appear to show that equal blackening will result from equal energy absorption regardless of wave length. Furthermore, rays of frequencies higher than the critical absorption frequencies of bromine and silver are very highly absorbed and produce a large photographic effect, while rays of slightly lower frequency produce a relatively lower effect, though the incident intensities may be the same.

With monochromatic rays of constant intensity, the blackening is approximately linear with time, for short periods of time. With longer exposures the blackening increases less rapidly than this proportionality demands and finally, with very long exposures, approaches a constant value. Over a certain range, then, Bunsen's law, that equal products of time and intensity produce equal blackening, is fulfilled. A long exposure with a low intensity, however, produces a less blackening than a shorter exposure at a correspondingly higher intensity.

Eggert has worked out with great care the optimum conditions for practical photography in radiography. Films are classified

TABLE XXI.—PARTIAL LIST OF THE CHEMICAL EFFECTS OF X-RAYS

System	Reaction	Energy relations	Reference
Potassium permanganate . . .	Decolorized, reduced $MnO_2$ formed	. . . . .	CHAMBERLAIN, <i>Phys. Rev.</i> , <b>26</b> , 525 (1925)
Iodic acid. . . . .	Reduced	. . . . .	CHAMBERLAIN, <i>Phys. Rev.</i> , <b>26</b> , 525 (1925)
Sulfurous acid . . . . .	Oxidized to sulfuric acid	. . . . .	CHAMBERLAIN, <i>Phys. Rev.</i> , <b>26</b> , 525 (1925)
Ferrous sulfate . . . . .	Oxidized to ferric sulfate	0.0027 mg. $FeSO_4$ per cubic centimeter per 1000 r. Independent of wave length between 0.204 and 0.765 A.U.	FRICKE and MORSE, <i>Phil. Mag.</i> , <b>7</b> , 129 (1929)
Oxyhemoglobin. . . . .	Methemoglobin	Independent of wave length 50 per cent transformed by 56,000r	FRICKE and PETERSON, <i>Am. J. Roentgenology and Radium Therapy</i> , <b>17</b> , 611 (1927)
Iodoform in chloroform . . .	Iodine liberated	Depends on solvent	GLOCKER and RISSE, <i>loc. cit.</i>
Hydrogen peroxide . . . . .	Water	70,000 cal. mol. from photo-electrons	GUNTHER <i>et al.</i> , <i>Z. Elektrochem.</i> , <b>34</b> , 616 (1929)
Chloroform } . . . . .	HCl, HI	. . . . .	ECCERT and NODDACK, <i>loc. cit.</i>
Iodoform	Silver	1 quantum $\rightarrow$ 1000 silver atoms	PATTERN and SMITH, <i>Trans. Roy. Soc. Can. Inst.</i> , <b>22</b> , 221 (1928)
Silver bromide. . . . .	Silver	. . . . .	
Ammonium thiocyanate.	Dark red	. . . . .	

Mercuric chloride and potassium oxalate.	$2\text{HgCl}_2 + \text{C}_2\text{O}_4^{2-} \rightarrow \text{Hg}_2\text{Cl}_2 + 2\text{Cl}^- + 2\text{CO}_2$	$6 \times 10^5$ mole per ion pair	ROSEVEARE, J. Am. Chem. Soc., <b>52</b> , 2612 (1930)
Mercuric chloride + ammonium oxalate (Eder's Solution)	$\text{Hg}_2\text{Cl}_2$ precipitated evolved	0.58 mg. mercury per 840 r	WYCKOFF and BAKER, Am. J. Roentgenology and Radium Therapy, <b>22</b> , 551 (1929)
Sucrose.....	Solution inverted, crystals turned reddish brown	6.5 per cent change in 2 per cent solution in 40 hr.	QUIMBY and DOWNES, Radiology, <b>14</b> , 468 (1930)
Amino acids..	Cystine unchanged, tyrosine changed in phenol group	Proportional to dosage	REINHART and TUCKER, Radiology, <b>12</b> , 151 (1929)
$\alpha$ -acetoxy mercuri- $\beta$ -methoxy hydrocinnamic ethyl ester.	Mercury liberated	0.293 mg. mercury precipitated by 28,500 r	STENSTROM and LOHMANN, J. Biol. Chem., <b>79</b> , 673 (1928)
Aldehydes . . . . .	Condense with ketones	Markedly catalyzed by x-rays	CLARK, PICKETT, and JOHNSON, Radiology, <b>15</b> , 245 (1930)
Potassium iodide . . . . .	Iodine liberated	Amount decomposed linear with dosage in absence of oxygen; larger unit in presence of oxygen	CLARK, PICKETT, and JOHNSON, loc. cit.
Potassium nitrate.....	Reduced to $\text{KNO}_2$	Proportional to dosage $5.58 \times 10$ molecules per r, 0.2 molecule per ion pair	CLARK, PICKETT, and JOHNSON, loc. cit.
Methylene blue.....	Decolorized; change measured spectrophotometrically; best concentration 0.0016 mg. per cubic centimeter; acetone, etc., inhibit change	Change not proportional to dosage	STENSTROM and LOHMANN, Radiology, <b>16</b> , 332 (1931)
			CLARK, PICKETT, and JOHNSON, loc. cit.
			CLARK and FITCH, Radiology, <b>17</b> , 285 (1931)

TABLE XXI.—PARTIAL LIST OF THE CHEMICAL EFFECTS OF X-RAYS.—(Continued)

System	Reaction	Energy relations	Reference
Aromatic colors .....	127 examples studies; tetraphenyl methane, alazarine, anthracine, indigo types promising	. . . . .	CLARK and FITCH, <i>loc. cit.</i>
Thioglucose, etc.....	In presence of acceptor such as silver on a developed photographic paper easily reduced forming $\text{Ag}_2\text{S}$ ; no reaction without x-rays	Very efficient; new light on biological effects	Unpublished

according to their threshold sensitivity and the steepness of gradation of the blackening—log time curve and the double emulsions and use of intensifying screens improve these. The photographic blackening effect depends on voltage. Under the same conditions the exposure time is smaller the harder the rays. The same blackening, for example, is obtained at 25 kv. in 25 m.a.s., 50 kv. in 3.2 m.a.s., and 80 kv. in 1.6 m.a.s. For radiography, however, the best contrast and less disturbance due to scattered rays but longer exposure time are obtained with soft x-rays. Proper technique, therefore, involves using the lowest voltage consistent with a practicable exposure time. Intensifying screens (shortening time but decreasing definition) and screens to eliminate scattered rays improve contrast.

As a chemical effect the blackening of the photographic film has been quantitatively studied.<sup>1</sup> For a wave length 0.45 A.U. about one thousand silver atoms are set free per quantum as compared to one silver atom per quantum of ordinary light. Of course, the absorption of a quantum takes place on one molecule of silver bromide so that the additional action is accounted for by secondary electrons. The Einstein equivalence law is not obeyed, since the x-ray quantum is about ten thousand times greater than a light quantum and yet has only one thousand

 TABLE XXII.—PHOTOLYSIS OF  $\text{KNO}_3$ 

Experiment	Exposed area, centimeter squared	Thickness of layer, centimeters	Weight of 0.001 <i>N</i> thio, grams	Incident energy per centimeter squared per second, <i>r</i>	Energy absorbed per centimeter squared per second, <i>r</i>
1	15.48	1.62	0.4117	2.56	0.80
2	15.90	1.04	0.2702	2.32	0.490
3	12.91	1.12	0.2291	2.40	0.535

Total energy absorbed (10 hr.)	Molecules reacting per	Molecules per ion pair ( <i>M/N</i> )	Energy, calories per mole
445,680 <i>r</i>	$5.58 \times 10^{11}$	0.2–0.3	$1.31 \times 10^7$
280,476 <i>r</i>	$5.83 \times 10^{11}$	0.2–0.3	$1.25 \times 10^7$
248,400 <i>r</i>	$5.58 \times 10^{11}$	0.2–0.3	$1.31 \times 10^7$

<sup>1</sup> EGGERT and NODDACK, *Z. Physik.*, **43**, 222 (1924).

times greater chemical effect. The discrepancy is due to scattering of energy as heat. The dependence on wave length is determined by the number of absorbed quanta, *i.e.*, the absorbing properties of the photographic plate or film.

Energy calculations have been made for several chemical systems; these may be illustrated for the case of the photolysis of potassium nitrate, studied by Clark and Pickett. These calculations depend upon ionization, or the formation of ion pairs.

Fairbrother makes the assumption that a given amount of radiation will produce approximately the same number of ion pairs in a dilute aqueous solution as are produced in the same weight of air, inasmuch as the atomic numbers of air and water are not very different. To allow for relative densities of air and dilute solution, a factor of about 1000 is involved. If this assumption is adopted, the number of molecules of potassium nitrate which react for each ion pair may be calculated, as follows:

$$\frac{\text{Total energy}}{\text{Charge on electron}} = \text{ion pairs per cubic centimeter in air} = \frac{10^{10}}{4.774} = 2.1 \times 10^9 \text{ ion pairs per cubic centimeter in air, or approximately } 2 \times 10^{12} \text{ ion pairs per cubic centimeter in the solution;}$$

$$\frac{\text{Molecules reacting}}{\text{Ion pairs}} = \text{molecules per ion pair.}$$

Using the data given above, the values for the latter are between 0.2 and 0.3 for this endothermic decomposition of potassium nitrate. The number of molecules per ion pair may be calculated independently from the energy in calories per mole and the work required to form one ion pair (35 volts):  $(1.313 \times 10^7 \text{ cal./mole KNO}_3) / (23,000 \times 35 \text{ cal./mole ion pairs})$ , or approximately 0.1 molecule of potassium nitrate per ion pair. This is in satisfactory agreement with the value calculated above, considering experimental difficulty, and with the order of magnitude to be expected thermodynamically.

In order to express results in terms of absolute energy, the absorption coefficients and the fraction of the absorbed energy which is converted into the kinetic energy of electrons and thence into the work of formation of ions must be known. The absorption coefficient 0.228, as calculated from the above data, agrees very closely with the value for absorption of the same wave

length in water interpolated from a series of values given by Glocker. The fraction of the total absorbed energy converted into work of formation of ions is the ratio of the values of the absorption coefficients for the energy given to recoil and photoelectrons to that of the total absorption coefficient. Using values recorded by Glocker, this fraction for the effective wave length used is 0.263.

The absorbed energy as measured in  $r$  may be converted into ergs by the use of the formula proposed by Rump<sup>1</sup> and Kulenkampff's experimental value of 35 volts as the work required to form one ion pair in air

$$\frac{E}{i} = \frac{\epsilon}{0.36} \left( \frac{\rho}{\tau + \sigma_r} \right),$$

where  $E/i = 1944$  ergs/ $r$ ,  $\rho$  = density,  $\epsilon = 35$  volts, and  $\tau + \sigma_r$  = absorption coefficient attributed to recoil and photoelectrons.

Thus the total energy absorbed in experiment 1 is  $445,680 \times 1944$  ergs, the fraction 0.263 of which is transformed into work of ionization. At the same time  $4.117 \times 10^{-7}$  mole of potassium nitrate is transformed. Thus the energy rate is  $1.313 \times 10^7$  cal./mole of reactant.

The heat of decomposition of potassium nitrate calculated from band spectra of oxygen and thermochemical data is  $1.03 \times 10^5$  cal./mole. Thus it seems evident that not more than 0.8 per cent of the energy absorbed and utilized in formation of ions in the solution appears as chemical dissociation of the molecule of potassium nitrate.

With these results is to be contrasted the very efficient photochemical-chain reaction between mercuric chloride and potassium oxalate, studied by Roseveare. The energy efficiency in this case is 1.32 cal./mole or  $0.91 \times 10^{-16}$  erg per molecule; since it takes 35 volts or  $56 \times 10^{-12}$  erg to produce an ion pair, there are  $6 \times 10^5$  molecules reacting per ion pair.

**The Flocculation of Colloids by X-rays.**—The action of x-rays in flocculating colloids, now a well-recognized phenomenon, is another subject which appears promising for the research worker. Fernau<sup>2</sup> noticed the coagulation of cerous hydroxide,  $\text{Ce}(\text{OH})_2$ ,

<sup>1</sup> *Z. Physik*, **43**, 254 (1927).

<sup>2</sup> *Kolloid Z.*, **33**, 89 (1923).

sols under x-radiation, and a similar effect in the case of albumin sols. Here again the effects can be produced by hydrogen peroxide and ozone, and the production of these is supposed to be the first step in the coagulation. The positively charged  $\text{Ce}(\text{OH})_2$  is then coagulated by the electrons released when the hydrogen peroxide reverts to water. Wels and Thiele<sup>1</sup> found that aggregate formation in globulin solutions occurred on either side of the isoelectric point and, hence, is independent of the charge which the molecules bear. Dognon reported a peculiar phenomenon in the flocculation of gum-mastic suspensions. Whereas homogeneous rays caused flocculation, a heterogeneous beam caused very little or none.

Crowther and Fairbrother<sup>2</sup> have performed numerous experiments on colloid flocculation and dispersion under x-radiation. They contend that positively charged colloids are coagulated. Clark and Pickett, however, found that colloidal lead was stabilized to a slight extent. This metallic sol is of unusual interest because of the discovery by Blair-Bell in England that injection into the tissue before therapeutic irradiation resulted in a much greater effect than observed for tissues alone. This might be due to secondary radiation from the heavy metal particles, or to a specific chemical effect. Clark and Pickett have experimentally demonstrated that the latter must be true, since colloidal gold, equally efficient in production of secondary rays, has no beneficial effect whatever. These authors have also shown that the flocculation of clay slips by x-rays, measured by viscosity changes, is a direct function of the amount of organic protein matter present. The whole matter of flocculation or dispersion of colloids under x-ray treatment is of greatest importance in its bearing on the therapeutic effect on cancers. At present the results are still so conflicting, due to large effects of impurities, sensitiveness to hydrogen-ion concentration, and other unknown eccentricities such as internal photoelectric action, that no definite conclusions or rules can be established.

**The Effects of X-rays on the Activity of Catalysts.**—The effects of x-rays on catalytic reactions have been studied in the decomposition of hydrogen peroxide by platinum and catalase, and in

<sup>1</sup> *Arch. ges. Physiol. (Pflüger's)*, **209**, 49.

<sup>2</sup> *Phil. Mag.* (7), **4**, 325 (1927) **6**, 385 (1928); *Brit. J. Radiology*, **1**, 121 (1928).



the production of sulfuric acid by contact of sulfur dioxide and oxygen with platinum.

Schwarz and Friedrich<sup>1</sup> studied the decomposition of  $\text{H}_2\text{O}_2$  under x-ray influence and found that the rate of decomposition was decreased. Subsequently, Schwarz and Klingenfuss<sup>2</sup> studied the catalytic oxidation of  $\text{SO}_2$  by contact platinum, which had been x-rayed. They found a temporary increase in activity of the catalyst. The increased activity toward  $\text{SO}_2$  was explained as due to a photolytic action on the moisture present, producing an activated form of oxygen or a peroxide, which then becomes the oxidizing agent.

Clark, McGrath, and Johnson<sup>3</sup> studied the effect of x-rays on contact platinum catalysts for the  $\text{SO}_2$  oxidation. Some experiments were made with thoroughly dried gases and very little conversion was obtained, whether the catalyst had been previously rayed or not. The conversion in these cases was constant at about 3.25 per cent for both rayed and unrayed catalysts.

Experiments with moist gases and those in which the catalyst was rayed in the presence of moisture showed, however, a decided increase in the catalyst activity. Thus for a run after the first irradiation of the catalyst, the conversion at a constant temperature of  $300^\circ \text{C}$ . increased from 88 to 94 per cent. After about five hours the activity dropped very markedly to something less than the original value, subsequently increased to about the original value, and then slowly decreased, until the conversion became constant at about 84 per cent. A second 3-hr. irradiation of the same catalyst produced another increase in activity, but only to about 87 per cent, followed by fluctuations similar to those described for the first run.

After raying, the catalyst always contained more oxygen as measured by the amount of iodine liberated from potassium iodide solution.

**Coloration of Glass and Minerals.**—It is a well-known fact that x-ray tubes made of glass containing manganese are colored violet after the tube has been in use for some time. Lead glass is colored brown. Barium platinocyanide and some other platinum compounds undergo color changes probably by a process of dehydration under x-ray illumination. The extent of this color

<sup>1</sup> *Ber.*, **55B**, 1040 (1922).

<sup>2</sup> *Z. Elektrochem.*, **28**, 472 (1922); **29**, 470 (1923).

<sup>3</sup> *Proc. Nat. Acad. Sci.*, **11**, 646 (1925).

change is used as a means of estimating intensity in x-ray therapy. Some substances, *e.g.*, fluorspar, undergo a change, but exposure to sunlight effects the return of the original color.

Bayley<sup>1</sup> has investigated a large number of alkali halides with respect to this change. Most of them showed a temporary coloration, though some did not. The colors faded logarithmically with time, upon exposure to sunlight. Halite, which was colored amber and showed an absorption band from 0.3 to 1.3 $\mu$  with a maximum at 0.46 $\mu$ , and silvite, which showed a similar band at 0.55 $\mu$ , faded most rapidly when illuminated with rays whose wave lengths corresponded roughly to these maxima.

Dauvillier<sup>2</sup> has pointed out that these effects are always associated with ions. The x-rays release electrons, which attach themselves to positive ions; the neutral atoms, so formed, probably form colloidal aggregates which cause the color change, while the subsequent illumination by light restores the electrons to their original positions. In a few cases, such as the conversion from red to green oxide of chromium, colloidal phenomena are evidently not involved.

This change in color with exposure to x-radiation has been employed in the production of colored candles, of artificial amethysts from manganese glass, of special pieces of glassware, and it is perhaps the irony of progress that the purple-glass windows, so colored by years of exposure to sunlight and often so highly prized by antiquarians, can be produced cheaply, rapidly, and genuinely by x-radiation.

**The Transformation of Metastable into Stable Solid States by X-rays.**—In their remarkable studies of the allotropic modifications of sulfur trioxide Smits and Schoenmaker<sup>3</sup> attempted to demonstrate the differences between the icelike form, the low-melting asbestos-like form, and the high-melting asbestos-like form, by photographing the x-ray crystal diffraction patterns. The films were identical, the pattern being that of the stable third form. The radiation thus converts metastable to stable modifications. On distillation of a portion of the intensively dried, high-melting, asbestos-like form, different states having abnormally low vapor pressures and abnormally high initial melting points were obtained, thus showing that this particular

<sup>1</sup> *Phys. Rev.*, **24**, 495 (1924).

<sup>2</sup> *Compt. rend.*, **171**, 627 (1922).

<sup>3</sup> *J. Chem. Soc.*, **1926**, 1120, 1603.

form behaves as a mixture of pseudo-components which have very different vapor pressures and melting points. At room temperature these states do not alter but at 50° changes take place in the direction of inner equilibrium. The x-ray diffraction patterns for the unchanged state and that changed at 50° were identical. It was proved experimentally that the x-rays actually effect a *very rapid increase in vapor pressure* to a value exactly that of the high-melting, asbestos-like form in inner equilibrium. An entirely new field of investigation is opened in this work and in that of Cohen on the metastable states.

### III. BIOLOGICAL EFFECTS OF X-RAYS

It has been indicated that in all experiments designed to determine the direct action of x-rays, the variables are difficult to control. In the study of the action of x-radiation on living matter, certainly the most interesting and important both practically and theoretically, the additional variable of life produces complexities which have so far defied satisfactory interpretation. This statement made in 1926 in the first edition of this book must still stand in 1932. As Dr. James Ewing<sup>1</sup> in his masterly Caldwell lecture, "Tissue Reactions to Radiation," put it: "Ultimate knowledge of the mode of action of radiation still eludes our grasp." Speaking of action on human tissues, he says:

More than a decade ago one could trace in detail the nuclear and cytoplasmic reactions following irradiation, the preliminary hyperemia, cell liquefaction and necrosis, the appearance of phagocytic cells, the growth of granulation tissue, the extreme overgrowth of lymphocytes and plasma cells, the healing by supple scar tissue. . . . The very voluminous contributions of the past decade have served to clarify many details . . . but no new and fundamental principles of reaction have been established.

The subject, by its enormity and by the vast number of largely uncontrolled and unrelated observations recorded in the literature, ranging all the way from a single-cell nucleus to a complete human system, is appalling, particularly in light of the urgent need to have the ultimate knowledge which will permit accurate, scientifically founded radiation therapy.

For many years, the supposed rule gained wide circulation that small dosages tend to activate and stimulate various functions and chemical reactions in biological colloidal systems,

<sup>1</sup> *Am. J. Roentgenology and Radium Therapy*, **15**, 93 (1926).

while larger dosages destroy, either instantly or after a latent period. This idea has been tested on seeds, eggs, single cells, and organisms of every imaginable kind. It found practical applications in the destruction of tobacco-worm larvae, cotton-boll weevil, the flour weevil (*tribolium confusum*), etc. The experimental evidence for stimulation with small doses is extremely meager and the rule is considered now invalid. A measure of acceleration in cellular metabolism has been observed repeatedly but this is proved to be a transient phase of reaction invariably followed by inhibition of function and cellular degeneration.<sup>1</sup> Again as the result of primary degeneration of certain radiosensitive cells a secondary and indirect stimulation may sometimes be observed. It has been demonstrated very recently<sup>2</sup> that x-rays do not kill cancer cells instantly, but accelerate the process of normal living and dying characteristic of each cell.

Numerous studies have been made on bacteria. Among these Clark and Boruff<sup>3</sup> found that x-rays act like sterilizing agents on cultures of *B. coli* (from sewage) and *Erythrobacillus prodigiosus* (from bread mold), in that the curves are characteristic sterilization or death-rate curves, showing that the total counts decrease logarithmically with time. *B. coli* showed no mutations with less than lethal dosages but the other organism showed a tendency toward lack of ability to produce its characteristic red pigment, although this is recovered in 12 hr. when a white colony is transferred to an agar slant. Wyckoff and Luyet<sup>4</sup> have shown that yeasts can be injured without being killed outright, and that injury is followed by development of an extraordinarily large number of two-celled colonies which on prolonged incubation ultimately die without further budding.

**Genetics and X-rays.**—One of the most important new developments has been in the study of mutations after the irradiation of parent organisms. In 1927, Prof. H. J. Muller of the University of Texas discovered that when fruit flies (*Drosophila*) were irradiated, the processes of evolution were speeded up over 1500 per cent. The second generation of offspring showed abnormalities such as rudimentary wings, no wings, white eyes, etc. These sensational results were the inspiration for further researches all

<sup>1</sup> DESJARDINS, *Science*, **75**, 569 (1932).

<sup>2</sup> ISAACS, *Science News Letter*, **22**, July 9, 1932.

<sup>3</sup> *Science*, **70**, 74 (1929).

<sup>4</sup> *Radiology*, **17**, 1171 (1931).

over the world in this field of genetics, on other insects, worms, mice, rats, larger animals, roses, corn, and many other plants. In all cases the effect of x-rays on the chromosomes has been fully substantiated. Obviously these dosages were smaller than those producing death. The obvious application is to the human race. Before these discoveries x-rays were being rather widely, and entirely ignorantly, used by some physicians for the purpose of producing sterility. The condition, however, is ordinarily temporary only; the first generation after such treatment may appear normal, but what abnormalities might appear in succeeding generations can only be guessed. Certainly as a means of birth control x-rays are to be most surely shunned, except as recommended and applied by men of unquestioned authority.

Among diseased cells which show a pronounced sensitiveness to the action of x-rays are those of hyperplastic connective tissue and young rapidly growing cells of the embryonal type.

**The Effect of X-rays on Tissue.**—As inquiries into the ultimate nature of the action of rays upon tumor and normal tissue cells become more fundamental in terms of physics and chemistry, they become less satisfying in terms of biology. Since such tissues are not merely aggregates of cells but are highly complex systems of related and interdependent structures, purely chemical or physical data can never explain their behavior. And yet it is highly important to review briefly a few of these observations.

First, the cell and nuclear membranes become more permeable.

The marked swelling of irradiated nuclei and the ballooning of the cytoplasm are most easily and probably correctly interpreted as an increased capacity of these structures to absorb water, through an altered cell membrane. The nature of this cell change escapes us, but again assuming the simplest cause, one must suppose that intracellular chemical changes produce new electrolytes by decomposition of salts, proteins, and fats and that water is drawn in by simple osmosis.

One of the gross effects is the actual closing of blood vessels and a disturbance of the vascular supply. Unfortunately there are no simple chemical studies comparing normal with heavily irradiated tissue. Again, radiation inhibits cell ferments. Hussey has shown that simple solutions of pepsin or trypsin are inhibited in action. Theories of splitting or ionization of cell constituents, of colloidal coagulation by points of radiation heat (Dessauer),

increase in hydrogen-ion concentration, alterations in the dispersion phase, changes in the electric charge of the colloidal constituents, disintegration of lipoids, changes in albumin, increase<sup>1</sup> in the ratio  $Q = K(H_2PO_4 + HPO_4)/Ca$  are among the observations and theories which may be laying the basis for the solution of the problem. Certain it is that tissues must be considered as a whole.

There is, however, a dominating fact which has become a recognized law in radiology, namely, the specific sensitiveness of each kind of cell to radiation. According to Desjardins,<sup>2</sup> although the factors responsible for such specificity have not yet been determined, the sensitiveness peculiar to each kind of cell appears to be related to the natural life cycle. Thus the lymphocytes, whose metabolic cycle is the shortest, are also the most radiosensitive, and the nerve cells, whose life cycle is longest, are also the most resistant to irradiation.

General average values of the sensitivity coefficients of normal tissues to x-radiation of medium hardness, referred to the skin as unity, are assembled in Table XXIII.<sup>3</sup>

TABLE XXIII.—RELATIVE SENSITIVITY OF A NORMAL TISSUE TO RADIATION OF MEDIUM HARDNESS (SKIN = 1.0)

Leucocytes:	Blood vessels:
2.5 Lymphocytes	1.5 Endothelium (intima)
2.4 Polynuclear	
Epithelial cells of salivary glands	Dermal structures:
Germinal cells:	1.4 Hair papillae
2.3 Ovarian	1.3 Sweat glands
2.2 Testicular	1.2 Sebaceous glands
Blood-forming organs:	1.1 Mucous membrane
2.1 Spleen	1.0 Skin
2.0 Lymphatic tissue	0.9 Serous membrane
1.9 Bone marrow	Viscera:
Endoerines:	0.8 Intestine
1.8 Thymus	0.7 Liver, pancreas
1.7 Thyroid	0.6 Uterus, kidney
1.6 Adrenal	Connective tissue:
	0.5 Fibrous tissue
	0.4 Muscle, fibrocartilage
	0.3 Bone
	0.2 Nerve tissue
	0.1 Fat

<sup>1</sup> KROETZ, *Biochem. Z.*, **151**, 449 (1926).

<sup>2</sup> *Loc. cit.*

<sup>3</sup> HIRSCH, "Principles and Practice of Roentgen Therapy," p. 240, American X-ray Publishing Company, New York, 1925.

**X-ray Therapy.**—X-ray therapy is indicated when it is desirable to produce the following effects.<sup>1</sup>

1. Stimulation. It is now doubtful if there is a true stimulative effect. The change due to a so-called stimulating dose may be really processes of repair following an injury caused by irradiation. Treatment of skin diseases characterized by sluggishness or dryness, or of glands deficient in function, has given conflicting results.

2. Inhibition of the growth or function of glands and cells. Differentiated cells such as those composing glands and hair follicles, physiologically active cells, young cells, cells about to divide, lymphoid tissue, and tissue of embryonic type are all markedly radiosensitive. This fact is the fundamental basis of therapy. Skin diseases characterized by hyperactivity of the glands, hyperthyroidism, diseases which can be cured by checking ovulation, leukemia, and many other conditions are successfully treated by irradiation.

3. Solution of hyperplastic connective tissue, such as in uterine fibroids.

4. Reduction of lichenification. The effect of x-rays on overgrowth of cells of the epidermis is due to inhibition of cell division and activity.

5. Anodyne effect. The relief of itching has been very frequently accomplished. The relief of pain, except when due to a lesion which can be cured by irradiation, is less certain, though many writers have reported an analgesic effect upon neuralgic pain.

6. Reduction of inflammation. There is a favorable experience in treatment of carbuncles, pneumonia in certain stages, erysipelas, etc. The rate and mode of reaction of inflammatory lesions indicate that the rays act chiefly by destroying the infiltrating lymphocytes, the exceptional sensitiveness of which has already been pointed out. Evidently these cells contain protective substances which enable them to neutralize bacterial or other toxic products which give rise to the inflammation; when the cells are destroyed by irradiation these protective substances are liberated and become immediately available for defensive purposes.

7. Destruction of fungi.

<sup>1</sup> ERSKINE, "Practical X-ray Treatment," Bruce Publishing Company, Milwaukee, 1931.

## 8. Destruction of benign and malignant tumors.

Desjardins<sup>1</sup> summarizes this subject in part as follows:

The specific sensitiveness of different kinds of cells constitutes the most important single factor in the treatment of neoplasms. The value of roentgen rays or radium in different varieties of tumor depends mainly on this feature. The susceptibility of tumors to irradiation agrees closely with the radiosensitiveness of normal cells of the same kind as those from which the tumors are derived and of which they are largely composed. Thus, the inordinate hyperplasia of lymphoid structures which characterizes Hodgkin's disease, lymphosarcoma, and lymphatic leukemia retrogresses under irradiation at the same rate as normal lymphocytes are known to be destroyed by similar exposure. In fact, so striking is the parallel that irradiation is now being used daily as a means of distinguishing such conditions when their clinical features do not permit absolute identification. In some cases, indeed, the radiotherapeutic method of diagnosis is more accurate and dependable than microscopic examination.

Knowledge of the relative radiosensitiveness of different cells has enabled Ewing and others to distinguish a group of bone tumors from other neoplasms which affect the skeleton. Ewing has designated this tumor as endothelial myeloma, because endothelial cells are a prominent feature. Among the malignant tumors of bone they are the most sensitive to irradiation. In fact, the other malignant growths which attack bone can hardly be said to have any sensitiveness; rather they are noteworthy for their resistance. Endothelial myeloma, on the contrary, is distinctly sensitive, and large tumors of this kind melt away with astonishing rapidity. The only other bone tumor which is radiosensitive is the usually benign giant-cell tumor, but its reaction to irradiation is unlike that of any malignant neoplasm. Instead of being followed by rapid or slow, but steady regression, irradiation of such growths causes them to swell and become tender. The patient and the uninitiated physician may naturally conclude that exposure to the rays has stimulated the tumor to increased growth, and the limb may be unnecessarily sacrificed. Such inflammatory reaction is a transient phase which lasts two or three weeks and is followed by slow regression and repair of the tumor by deposition of new bone. This characteristic reaction of giant-cell tumor constitutes at once a valuable means of identification and treatment and furnishes additional evidence that tumors of this kind, at least at the outset, are not true neoplasms but chronic inflammatory lesions.

Many other examples might be mentioned, but the foregoing are sufficient to illustrate the important bearing on medical diagnosis and

<sup>1</sup> *Loc. cit.*



treatment of the radiosensitiveness of cells and tissues. Heretofore, for some reason, biologists have seldom made use of radiation for experimental purposes. As soon as they begin to realize its possibilities, they will find in the method a means of acquiring much valuable information, and such increase in knowledge will help to extend the diagnostic and therapeutic applications.

The most recent important contributions to our knowledge of the mechanism of cancer is that of McDonald of the University of Pennsylvania.<sup>1</sup> As a result of careful researches it is definitely established that, in order to have a cure for cancer, conditions must be produced which will accomplish the following:

1. Alter glycogenolysis towards normal from the cancer type; in tumor tissue for every 13 sugar molecules attacked, 12 are split up into lactic acid and 1 oxidized, while in normal tissue this ratio is 1:1; hence the cancer cell as an energy adapter follows a different mechanism from normal.

2. Produce conditions of biological equilibrium towards normal from the alkaline state (pH 7.47 or 8.7 per cent more alkaline in internal untreated cancer blood plasma; the more alkaline, the quicker the disease kills).

3. Reduce high blood glucose.

4. Produce a calcium-like effect (cancer cells have less calcium than normal).

5. Reduce or prevent a potassium-like effect (the virulence of the tumor increasing with potassium content).

These remarkable facts so newly established should give a clue to the satisfactory treatment of cancer by x-rays or  $\gamma$ -rays. The mechanism, aside from specific radiosensitiveness of cells, by which radiation is accomplishing these necessary changes and others still unknown, remains largely a mystery. But in the meanwhile, in spite of ignorance and inefficiency, x-rays are proving one of mankind's greatest aids and hopes in the evolution of the most important problem of our time, namely, cancer. The literature abounds with case reports of cures, some even for the advanced stages of the disease. In other cases where cure is hopeless, comfort and alleviation of pain and prolongation of life are made possible. However, the underlying principle of successful cancer treatment by radiation therapy is early diagnosis. People must be educated not only to the

<sup>1</sup> *Science*, **74**, 55 (1931).

desirability but to the necessity of complete physical examination, in which x-rays shall be applied in their other great medical province, that of radiographic diagnosis. Internal cancer may be well advanced without the disclosure of symptoms; and yet a radiographic examination alone may show its presence.

The earlier the discovery of such a condition, the greater the probability of a genuine cure under the careful and intelligent ministrations of a trained roentgenologist. Ignorantly used, however, this great therapeutic agency may actually become a curse.

#### IV. THE MEASUREMENT OF X-RAY INTENSITY OR DOSAGE

Besides the measurement of quality or wave lengths of an x-ray beam, which has been discussed in Chap. V, the measurement of the intensity of x-rays is of importance to all x-ray workers, whether in the pure science or in its applications. The physicist must know the energy distribution in the x-ray spectrum and must have a ready and accurate method of measurement of the absolute intensity if he is to discover the underlying natural laws he seeks. The x-ray spectroscopist and the student of crystal structure need reliable intensity measurements if they are to obtain the utmost benefit from their data. The roentgenologist requires a simple and easily usable method to estimate x-ray dosage. Intensity is measured not as radiation energy directly, but by means of the following effects: heat, ionization, darkening of the photographic plate, other chemical effects, fluorescence, color change, change in the conductivity, and certain biological effects such as skin erythema, killing of *Drosophila* eggs, etc.

**Heat Methods.**—If a small beam of x-rays is allowed to impinge upon a metal block of such size that practically complete (97 per cent or more) absorption of the beam occurs, the net effect of the absorption will be an increase in the heat content of the block. That is to say that essentially all secondary rays, photoelectrons, etc., are absorbed in the block and their energy is converted into heat. This fact is the basis of present methods of accurately determining the total energy content of an x-ray beam. Such methods have been used to study the distribution of energy in the x-ray spectrum, the dependence of intensity upon the potential on the x-ray tube and upon the current through the tube, the relation between the energy input to the tube and the

x-ray energy produced, the relation between energy, wave length, and ionization, and the relation between energy and photographic darkening.

The instruments employed generally consist of two elements, one heated by x-rays and one by electricity, which are balanced, by several different methods, against each other; the electric energy input is measured directly and, since the heat effects in the two elements are the same, is equal, after the instrumental corrections have been applied, to the x-ray energy input.

Terrill<sup>1</sup> has used the method to determine the total energy of x-rays from a tungsten-target tube excited by constant potential direct current at 30 to 100 kv. The total output of the tube was thus found to be from 0.00025 to 0.00192 times the input. Plotted against the square of the voltage these values give a straight line to 69.3 kv. where a change of slope occurs, probably due to the selective absorption of the target itself.<sup>2</sup>

All these heat-measuring devices require the most careful construction and manipulation, the chances of experimental error being very great as the measured effects are usually very small; hence, they are not available for routine intensity measurements.

**Ionization.**—Except for heat methods involving complete absorption, the actual extent of various other effects of x-rays including ionization depends on radiation intensity and also on wave length and on this account a different fraction of the initial radiation with varying intensity for different wave lengths is transformed in the irradiated medium into other energy forms. The action is independent of wave length only when the beam of given initial intensity, inclusive of secondary rays arising therefrom, is completely absorbed in the irradiated material. Hence the ionization current is a measure of the absorbed, not the incident, radiation intensity. The difference in the dependence of the sensitiveness of different methods of measurement upon the wave length is demonstrated in Fig. 72. If different homogeneous rays fall simultaneously with equal intensity upon an air ionization chamber, a fluorescent screen, and a photographic plate, the brightness of the screen changes much less with wave length than the ionization current; the photographic

<sup>1</sup> *Phys. Rev.*, **28**, 438 (1926).

<sup>2</sup> The *K* series tungsten rays are generated only above 69.3 kv.

sensitiveness changes with sudden jumps at 0.49 and 0.91 A.U. Since these wave lengths coincide with the discontinuities in absorption coefficients of silver and bromine, the two effective constituents of the photographic emulsion, the photographic action is closely connected with absorption. Hence the action of the rays changes with wave length in the same way as the intensity of the absorbed portion of the incident rays changes; exceptions occur in the rays of very short wave x-rays when the

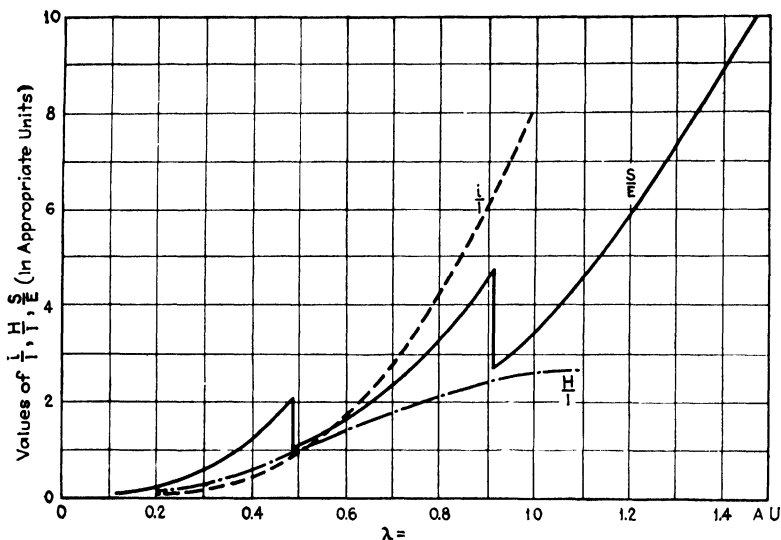


FIG. 72.—Effects of x-rays of different wave lengths.

$$\begin{aligned} \frac{i}{I} &= \frac{\text{ionization}}{\text{incident ray intensity}}; \\ \frac{H}{I} &= \frac{\text{fluorescent screen brightness}}{\text{incident ray intensity}}; \\ \frac{S}{E} &= \frac{\text{photographic blackening}}{\text{incident ray energy}}. \end{aligned}$$

Compton effect is appreciable and in the case of the excitation of characteristic fluorescent rays of the irradiated material. The general rule holds for each known physical and chemical effect: that the effect changes with wave length in the same way as the fraction of the incident radiation energy transformed into the energy of photoelectrons and Compton electrons. The values may be calculated for certain chemical compositions of a material from physical data (absorption coefficient, recoil coefficient, etc.) and Glocker has found excellent agreement between theory and experiment for ionization.

The aim of practical dosage measurement, particularly for therapy, must consist in the selection of a radiation effect which can be measured and which changes with wave length in the same way as a given biological reaction, *e.g.*, skin erythema. Repeated experimentation has proved convincingly that a complete parallelism between skin erythema and air ionization exists independent of the quality of the radiation. Since the absorption coefficient depends not only on wave length but also upon the density and upon the atomic number of the elements constituting a material, so it is to be expected that air consisting of the light elements oxygen and nitrogen should possess the same absorption properties as tissues consisting of organic compounds of carbon, nitrogen and oxygen, or water. At the second International Congress of Radiology in 1928, therefore, the measurement of air ionization was accepted as the basis of international dosage measurement, and a definition was given of the unit of dosage, designated the roentgen unit and written as "*r*," as follows:

The *absolute unit of the x-ray* dose, one roentgen or *r*, is obtained from that x-ray energy which, when the secondary electrons are fully utilized and secondary radiation from the wall of the chamber is avoided, under standard conditions 0° C. and 760 mm. of mercury pressure, produces in 1 c.c. of atmospheric air such a degree of conductivity that the quantity of electricity measured at saturation current equals 1 electrostatic unit.

The physical dose is the electron energy (kinetic energy of photoelectrons and Compton electrons) liberated by the action of x-rays in a volume element of an irradiated body during the time of exposure divided by the size of the volume element.

Glocker<sup>1</sup> has proposed a change in the definitions of the roentgen unit, to provide for the entire range of wave lengths. The absorption edge of argon found in air at 3.86 A.U. has the consequence that the absorption of x-rays in air changes discontinuously at this wave length and the dose measured for wave lengths greater than 3.86 A.U. is 18-20 per cent too small—whereas the same phenomenon does not take place in tissues or water. Glocker, therefore, suggests that carbon dioxide gas be substituted for air in the definition.

Several types of ionization chambers have been designed for the determination of intensities in therapy, even in absolute

<sup>1</sup> *Radiology*, **17** (in press).

units. The Duane ionization chamber or iontoquantimeter is one of especial merit. It consists simply of a series of aluminum sheets about 5 cm. long and 2 cm. broad held parallel to each other and 5 mm. apart by hard-rubber frames. Alternate sheets are connected together, thus forming a small condenser with layers of air between the sheets. The condenser is joined in a simple electric circuit with a battery and sensitive galvanometer which is calibrated by means of a Weston standard cell and resistance. By comparison of the deflection with the known current to the deflection produced by the current produced by the ionization of air by the x-ray beam in the chamber of known volume, the intensity of the beam in  $r$  units may be calculated. Glasser at the Cleveland Clinic, Taylor at the Bureau of Standards, and others have designed large air ionization chambers for standardization purposes.

Friedrich has introduced the use of an ionization chamber made of horn, the chemical elements in which are those found in the body, containing only 1 c.c. This has the advantage that intensities in absolute units may be read on a scale of the deflecting electroscope. Dauvillier has devised a spherical gas chamber containing xenon as the absorbing gas. Several other similar devices of bakelite, graphite, etc., are manufactured by equipment builders.

An unusually simple and efficient portable instrument is the Victoreen  $r$ -meter, consisting of a small ionization chamber rigidly connected with a string electrometer, the scale of which is calibrated in international units. The chamber is exposed for 1 min. to the rays and the scale read, the figure being  $r$  per minute. This instrument also serves readily in all kinds of absorption measurements including the determination of effective wave length.

Meanwhile, by using a properly designed ionization chamber and by recording simply the ionization-chamber current as the index of intensity, the method becomes very valuable for many kinds of work, particularly in the analysis of crystal structure by the ionization spectrometer (see p. 190), where only a relative measure of intensity is needed. The ionization chamber should be large enough completely, or nearly completely, to absorb the rays; the electrodes must not be exposed to the incident rays; a gas of quite heavy molecular weight is most satisfactory, methyl iodide or ethyl bromide being often used. Sulfur dioxide

has also been used; air usually does not show enough effect. The use of heavy gases is also helpful in insuring complete absorption of the rays without the use of excessively large pressures or large chambers.

There are several accepted ways of measuring the current through the ionization chamber. Some experimenters use an electroscope and time the fall of the leaf. Others use a quadrant or string electrometer; recently it has been suggested that the current might be amplified by the use of three-element electron, or ordinary radio, tubes; and indeed such an arrangement has been developed by the Siemens and Halske Company<sup>1</sup> in Germany in an instrument designed to measure dosage in x-ray therapy, usually in conjunction with the small Friedrich ionization chamber. This amplifies the current to such a magnitude that it may be measured by a microammeter. The General Electric Company has developed also a special amplifying tube for this purpose (see page 193). In every case the potential across the chamber is provided by a battery of electric cells and must be high enough to insure reaching the saturation current through the chamber. A potential of 90 volts is usually sufficient.

**Photographic Methods.**—The limitations in the photographic method for determining absolute or even relative intensities have already been indicated on page 143. The wide variation in the speed of different emulsions, the complications introduced by the absorption edges of silver and bromine (Fig. 29), and the dependence of blackening on voltage are some of the difficulties.

**Other Chemical Methods.**—Table XXI (page 144) lists a few chemical reactions which have been suggested as dosimeters and have been calibrated in *r* units. The most promising and practical of these are:

Mercuric chloride + ammonium oxalate (Eder's solution) → precipitate of mercurous chloride (calomel) which may be weighed; 0.58 mg. mercury per cubic centimeter for 840 *r* (1 threshold erythema dose).

Oxidation of ferrous sulfate to ferric sulfate; 0.0027 mg. FeSO<sub>4</sub> per cubic centimeter per 1000 *r*.

<sup>1</sup> VON HAUSER, K. W., R. JAEGER, and W. VAHLE, "Siemens and Halske Catalogue, Röhrengalvanometer," Siemens and Halske Company.

Both of these reactions are relatively simple but will scarcely compete as dosimeters with commercial ionization equipment.

**Fluorescent Methods.**—For measuring intensity of x-rays by fluorescence methods, the fluorescence of a screen is compared with the fluorescence produced by a standard radiation. This is obviously a comparative method and is open to the objections that the fluorescing salt becomes “tired” under the action of the rays, and that the screen may not be of uniform fluorescing power. The objections to using fluorescence methods to determine absolute intensity are that the relation between fluorescence and the x-ray intensity is unknown and that certain rays will excite a characteristic fluorescence. Further shortcomings of fluorescent screens are covered on page 139 in the present chapter. The method is not used except in medical work, and then rarely.

**Coloration Methods.**—With the medical profession the color change in barium platinoeyanide “pastilles” as an index of intensity has been utilized. The pastille is placed at a specified distance from the anticathode of the tube and the color matched against a set of standards. The color changes from yellow green to brown, and periodic comparison with the standard indicates the total energy absorbed. The method gives hardly more than qualitative information since wave lengths of all kinds are measured by a surface-color change. Exposure to light brings the pastille to its original color.

**Selenium-cell Method.**—Furstenau has developed a selenium-cell method of measuring intensity which is used in x-ray therapy. This is dependent upon the fact that x-rays cause a change in the electrical resistance of selenium. The method is only qualitative, and the cells must be frequently checked against a standard, since they change characteristics during usage.

**Biological Methods.**—The method of estimating dosage from skin reddening or erythema is familiar to all x-ray workers. This can never serve as an accurate method because of the widely varying sensitivity of the skin of different individuals to radiation. Glasser and Portmann<sup>1</sup> compiled data from 40 clinics on the number of  $r$  units for average erythema reaction in deep therapy. These varied from 500 to 1,250  $r$ , or an average of 930. The threshold value of erythema is commonly taken to be 840  $r$ .

<sup>1</sup> *Radiology*, **14**, 346 (1931).



A much more accurate "biological ionization chamber," as designated by Wood<sup>1</sup> are *Drosophila* (fruit fly) eggs. Invariably 50 per cent of the eggs are killed by 180 *r* and 90 per cent by 500 *r*. The points for the effect of radium fall directly on the curve experimentally determined for the percentage of eggs hatching as a function of *r*-units.

<sup>1</sup> *Radiology*, **12**, 461 (1929).



**PART II**  
**THE X-RAY ANALYSIS OF THE ULTIMATE**  
**STRUCTURES OF MATERIALS**



## CHAPTER X

### CRYSTALS AND X-RAY DIFFRACTION

**The Solid State of Matter.**—Knowledge of the crystalline state of matter was decidedly limited prior to the discovery by Laue and the Braggs that x-rays could be applied to the analysis of the internal structure of crystals. The great and relatively aged science of crystallography had been built up to the conclusion, from careful observations with microscopes and optical goniometers, that apparently almost all true solids were really crystals, either single entities with pairs of parallel bounding surfaces disposed in definite geometric fashion at angles which could be measured, or aggregates of these single crystals. While regularity of exterior appearance indicated some kind of regular internal arrangement of unit building material, whatever that might be, yet without experimental methods of investigation and without adequate conceptions of atomic and molecular structure and the forces holding atoms and molecules together, physicists and chemists were unable to find points of useful contact with the essentially applied geometric science of crystallography. Concerning the gaseous and liquid states of matter, much more was known in the sense that their behavior could be explained by simple hypotheses. They are characterized by disordered arrangement of atoms or molecules which are relatively free to move, even in liquids. Since all directions are alike, it is possible to calculate with considerable accuracy the behavior of gases and liquids in very practical phenomena. Chemists have worked very largely with gases and liquids because the freedom of motion of the molecules has permitted reactions more readily. But in solids great complications arise because the atoms and molecules are bound together tightly by their mutual forces. It is evident that the exercise of these forces should tend to produce regularity of arrangement. X-ray analysis has shown that such a regularity does exist in practically every solid substance.

The great practical importance of scientific knowledge of the ultimate structure of solids, which are crystals in the natural state, is self-evident, when consideration is given to the definition of desired physical and chemical properties. The strength of steel girders, the corrosion of aluminum alloys, the wearing properties of case-hardened steel, the plasticity of lime, the dielectric capacity of materials, the lubricating properties of long-chain paraffins or of graphite, the stretching of rubber, the covering power of pigments, and innumerable other practical phenomena of everyday life—all depend upon ultimate crystalline structure. Bragg has shown clearly that as a matter of fact the only properties of solid bodies which are not directly and obviously related to crystal structure are those, few in number, which depend upon atomic characteristics alone, such as weight. With few exceptions every aspect of the behavior of a solid substance depends on the *mode of arrangement* of its atoms and molecules.

A clear distinction must be made relative to the ultimate crystalline structure of materials. Sir William Bragg speaks in the following inimitably clear fashion of the three types of assemblage:

The simplest is that of the single atom as in helium in the gaseous state, in which the behavior of every atom is on the whole the same as the behavior of any other. The next is that of the molecules, the smallest portion of a liquid or a gas which has all the properties of the whole; and lastly, the crystal unit, the smallest portion of a crystal (really the simplest form of a solid substance) which has all the properties of the crystal. There are atoms of silicon and oxygen, there is a molecule of silicon dioxide, and a crystal unit of quartz containing three molecules of silicon dioxide. The separate atoms of silicon and oxygen are not silicon dioxide, of course, in the same way the molecule of silicon dioxide is not quartz; the crystal unit consisting of three molecules arranged in a particular way *is* quartz.

The first aim of the x-ray analysis of crystals is to determine the arrangement of the atoms and molecules in the crystal unit, and to account for the properties of the crystal in terms of that arrangement. The interference of x-rays in gases and liquids has made possible more recently fine-structure determination even for these states.

**Fundamentals of Crystallography.**—In Part I attention has been given primarily to the fundamental properties of x-rays which are to be used subsequently simply as a tool in the analysis of fine structure of matter. The crystal grating of known con-

stant by which it is possible to analyze x-radiation and measure wave lengths has been taken more or less for granted. It is now appropriate to take the radiation for granted and to inquire into the reasons for the satisfactory action of crystals as gratings and for the fact that the analysis of x-ray spectra from each crystal leads directly to the interpretation of how a particular crystal is built from ultimate atomic units.

Entirely apart from x-ray data a systematic science of crystallography has been developed which serves as the basis for rational

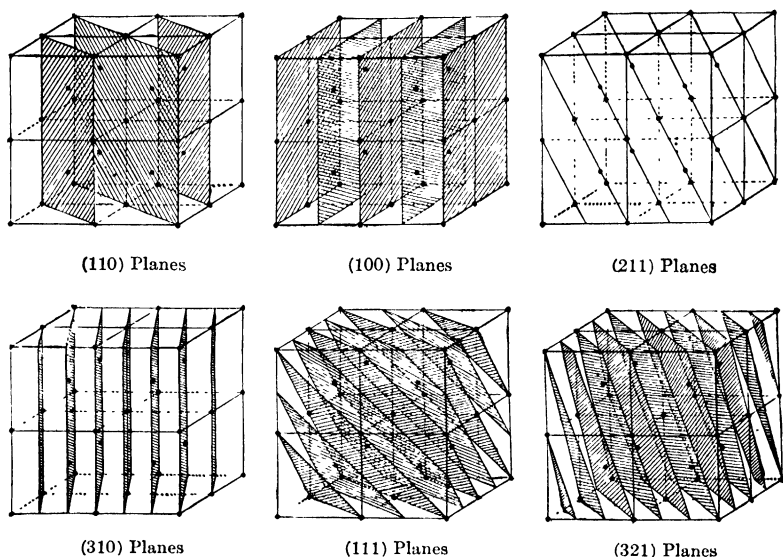


FIG. 73.—Typical sets of parallel planes in a cubic lattice.

interpretation of x-ray data. The steps in the development of this information may be summarized briefly as follows:

1. The important properties of a crystal visible to the eye are the planar bounding faces and the symmetry. The first logical step is to measure the *angles* between faces with the goniometer. In order to express then the positions in space of these planes relatively to each other, it is essential to derive a system of coordinates. The planes may then be indexed in terms of their intercepts upon the axes of a system of coordinates; upon each axis a unit distance is chosen and then the distances from the origin of the given plane along the three axes are measured; the reciprocals of these intercepts are then the indices of the plane.

Thus a plane intersecting the  $X$ -axis at unit distance from the origin and parallel to the  $Y$  and  $Z$  axes has the intercepts 1,  $\infty$ ,  $\infty$  and the indices 100 (see Fig. 73). Other cubic faces have the indices (010) and (001) and the planes which bisect diagonally

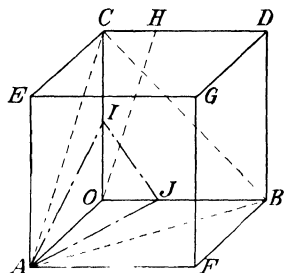


FIG. 74. Directions and planes in a cubic lattice.

the cube faces are (110), (101), and (011). In addition there are the similar planes with negative indices where the intercepts are in other quadrants. A single specific plane or crystal face is usually designated with parenthesis, thus (100), a family of

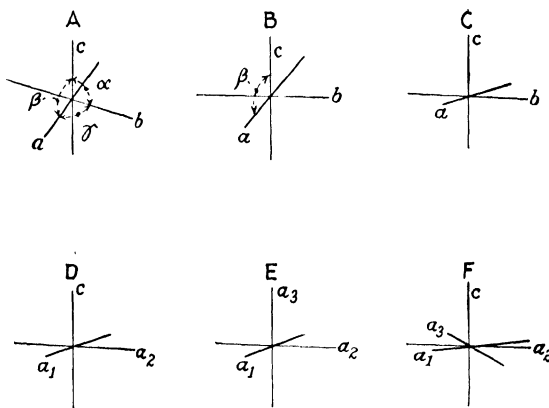


FIG. 75.—The coordinate axes of crystal systems. (A) Triclinic,  $a \neq b \neq c$ ,  $\alpha \neq \beta \neq \gamma \neq 90^\circ$ . (B) Monoclinic,  $a \neq b \neq c$ ,  $\alpha = \gamma = 90^\circ$ ,  $\beta \neq 90^\circ$ . (C) Rhombic,  $a \neq b \neq c$ ,  $\alpha = \beta = \gamma = 90^\circ$ . (D) Tetragonal,  $a = b \neq c$ ,  $\alpha = \beta = \gamma = 90^\circ$ . (E) Cubic,  $a = b = c$ ,  $\alpha = \beta = \gamma = 90^\circ$ . (F) Hexagonal,  $a = b \neq c$ ,  $\alpha = \beta = 90^\circ$ ,  $\gamma = 120^\circ$ .

parallel planes  $\langle 100 \rangle$  or 100, and a direction or normal to a side of parallel planes  $[100]$  (Fig. 74); if the faces of a crystal are completely developed then the form is designated  $\{100\}$  to include the six cubic faces, etc. A crystal in the cubic system may have the form  $\{100\}$ , cubic shape, or  $\{111\}$ , an octahedron. In Fig. 73



are shown six of the various sets of planes into which a cube may be imagined to be sliced up.

Now an immense amount of experimentation has proved that all angle measurements and indexing of plane faces are accounted for by seven systems of coordinates (Fig. 75). In other words, there are seven crystal systems: triclinic, monoclinic, orthorhombic, tetragonal, hexagonal, rhombohedral (often classed under hexagonal), and cubic. As an example of these relationships whereby a crystal is characterized, the case of tetragonal tin (Schiebold) is represented in Fig. 76. The outer form of a single crystal is represented on tetragonal axes,  $a, a, c$ ,  $\alpha = \beta = \gamma = 90^\circ$ . The most characteristic faces are designated  $p$  the

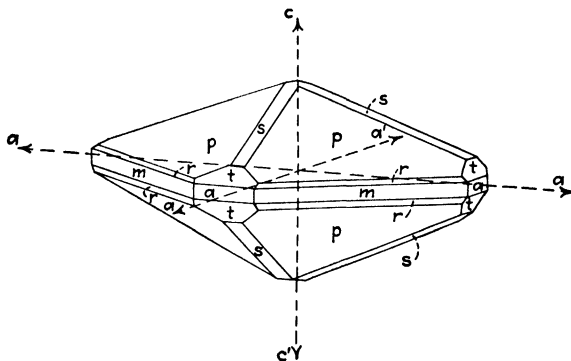


FIG. 76.—Diagram of faces of a single crystal of white tin, after Schiebold (see text for method of indexing face planes).

indices being  $(111)$ ,  $(1\bar{1}1)$ ,  $(\bar{1}\bar{1}1)$ ,  $(\bar{1}11)$ ,  $(11\bar{1})$ ,  $(1\bar{1}\bar{1})$ ,  $(\bar{1}\bar{1}\bar{1})$ ,  $(\bar{1}1\bar{1})$ , or the form  $\{111\}$ . The other faces can also be symbolically represented, so that the crystal habit is completely described as follows:

$$\begin{aligned} p &= \{a, a, c\} = \{111\}; & r &= \{a/3, a/3, c\} = \{331\}; \\ & & m &= \{a:a:\infty c\} = \{110\}; \\ s &= \{a, \infty a, c\} = \{101\}; & t &= \{a/3, \infty a, c\} = \{301\}; \\ & & a &= \{a:\infty a:\infty c\} = \{100\}. \end{aligned}$$

From the angle between the faces  $s:a = 68^\circ 54'$ , the axial ratio can be calculated to be  $a:c = 1:0.3857$ .

Another important property is illustrated by this figure, namely, that several faces intersect in parallel edges—*stats*, *prmrp*, etc. The aggregation of all faces or planes which intersect with parallel edges is called a *zone* and the common

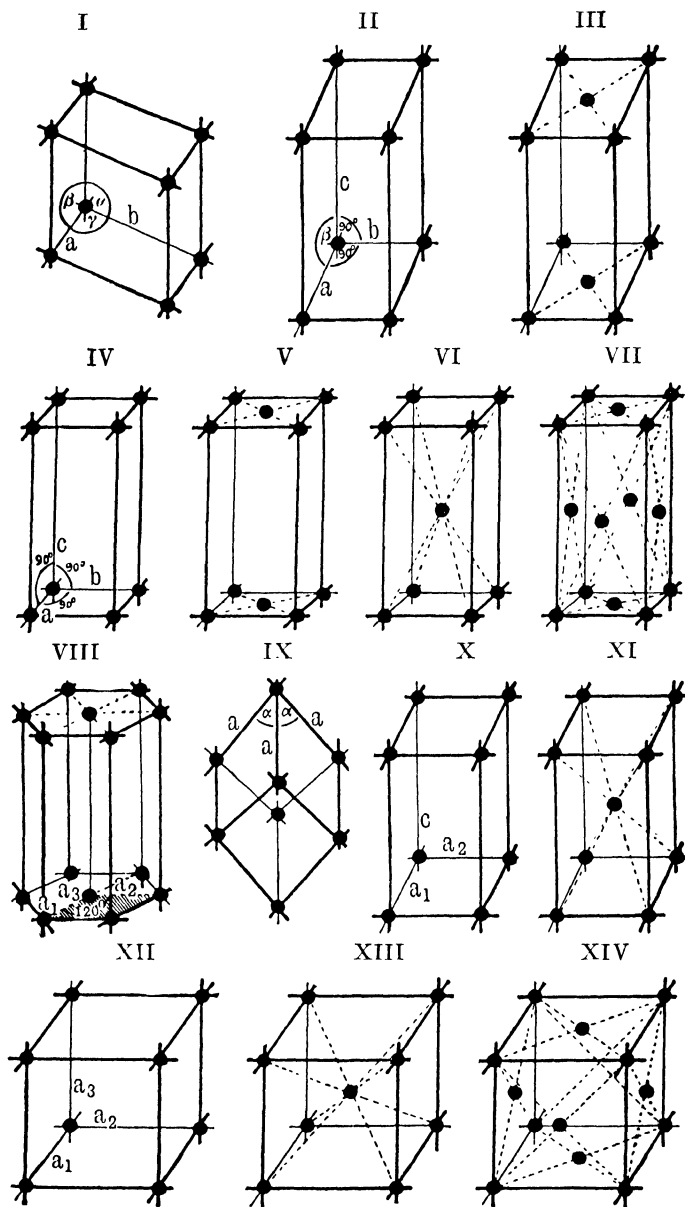


FIG. 77.—Space lattices. I, triclinic; II, simple monoclinic; III, end face-centered monoclinic; IV, simple rhombic; V, end face-centered rhombic; VI, body-centered rhombic; VII, face-centered rhombic; VIII, hexagonal, IX, rhombohedral; X, simple tetragonal; XI, body-centered tetragonal; XII, simple cubic; XIII, body-centered cubic, XIV, face-centered cubic.

edge direction a zone axis. It follows that every possible crystal face must belong to at least two crystallographic zones.

2. As a further result of the experience of two hundred years it is now definitely assured that the indices of all the plane faces of crystals are always small whole numbers (*i.e.*, 100, 321, 568, etc.)—the law of rational indices. If this is true, then only a definite *lattice* in three dimensions formed by the intersection of three sets of parallel planes can explain the rational intersections on axes. These lattices are, of course, considered to be built on the above seven systems of coordinates, and there are 14 of these spacial patterns geometrically possible (Fig. 77).

3. To the systematic classification into seven crystal systems, the experimentally founded law of rational indices and the consequent hypothesis of space lattices, may be added other types of information enabling an approach to the subject of symmetry. Some of these are velocity of solution of different crystal faces, etch figures, birefringence, optical activity, piezo- and pyroelectric properties. In general, it might be expected that two crystals, which gave identical measurements of angles between faces indicating identical disposition of planes, should also have identical properties. It soon becomes evident, however, that the formal classification of crystals thus made has not been extended far enough. Mark<sup>1</sup> points out that angle measurements class both barium antimonyl tartrate and calcium molybdate as tetragonal, but this in no sense explains why one has optical activity and the other has not. Account, therefore, must be taken of different symmetries.

4. The symmetry of an object is an expression of the fact that the object has equal properties in different directions. Two positions of a crystal, in which the equivalent directions may be brought into coincidence, say by a simple rotation around an axis, are not distinguishable by any physical-chemical means. Now the following symmetry operations may be performed to bring equivalent points in space into coincidence:

*a.* Axes of symmetry (cyclic operation). Points in crystals may have one-, two-, three-, four-, or six-fold axes by which is meant coincidence of equivalent points by rotation of 360 (every point has this identity operation), 180, 120, 90, or 60 degrees. The fact that there is no five- or seven-fold axis (although five-

<sup>1</sup>*Z. Metallkunde*, **20**, 342 (1928).

fold symmetry is found in nature in starfish) is further indication of a space-lattice structure.

b. Plane of symmetry (mirror operation), in which points on one side of a plane are mirror images of points on the other.

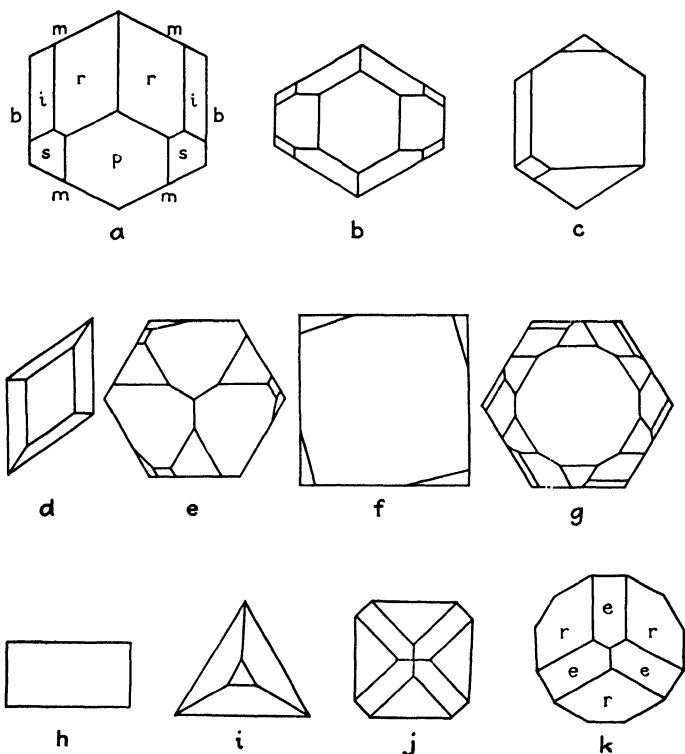


FIG. 78.—Ornamental figures illustrating crystal symmetry. (After Schiebold.) a, plane of symmetry, hornblende; b, two planes of symmetry, aragonite; c, ornament with a plane of symmetry; d, two-fold axis of symmetry, gypsum; e, three-fold axis of symmetry, quartz; f, four-fold axis of symmetry, wulfenite; g, six-fold axis of symmetry, apatite; h, ornament with mirror and rhythmic symmetry; i, planes of symmetry and three-fold axis, tourmaline; j, planes of symmetry and four-fold axis, tinstone; k, planes of symmetry with three-fold rhythmic symmetry, calcite.

c. Center of symmetry or a combined rotation and reflection across a plane perpendicular to the axis.

These symmetry elements are well illustrated by the ornamental figures selected by Schiebold, shown in Fig. 78. The symmetry planes, axes, and center for a cube are illustrated in Fig. 79.

When now these symmetry operations are combined in every possible way, using the seven systems of coordinates, it develops that there are 32 point-groups which define 32 crystal classes in terms of symmetry. A combination of goniometric and physical measurements makes it possible to classify crystals as to system and as to the finer subdivision of class or point-group. But it is to be observed that this is still a macroclassification, and the idea of the lattice, except as an explanatory hypothesis, or of the ultimate units from which crystals are built, does not enter in.

5. The final step in the further refining of classification of crystals was taken as a result of the work of Schoenflies in 1890, with the three-dimensional lattice theory and the idea of atoms at the points of the lattice as a basis. In other words, by combining the 32 classes of symmetry around a point with translation in three directions to other equivalent points, arranged according to a definite spacial pattern (the lattice), at a distance of the order of  $10^{-8}$  cm. or atomic dimensions apart, other symmetry operations involving this translation become evident, namely, two-, three-, four-, and six-fold *screw*

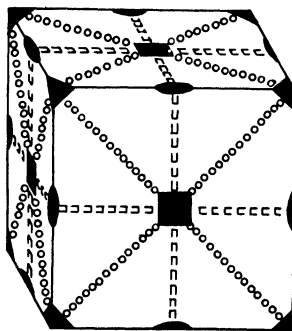


FIG. 79.—Symmetry axes in a cubic crystal; squares, four-fold; triangles, three-fold; ellipses, two-fold.

axes of symmetry, involving rotations about and translations along an axis, and glide planes of symmetry in which a figure is brought into coincidence by reflection in a plane combined with translation of a definite length and direction in the plane. These were called by Schoenflies "microscopic symmetry elements." When these are included in the process of placing each of the 32 point-groups at the points of the 14 lattices, the result is a total of 230 combinations or space-groups. The definition of a crystal by its space-group is unique. A recent extension of the space-group theory by Weissenberg takes into account the existence in space of the molecule (in the sense of Avogadro) defined as "island point-group," "dynad," and "micro-building unit."

It is obvious in the macroclassifications depending upon reflections of visible light by different faces, and other physical measurements, why this final refinement depending upon the arrangement in space of atoms, and the differentiation between

axes and screw axes of symmetry, was impossible. Herein lies the great province of x-rays, as first predicted by Laue in 1913, with wave lengths of the same order of magnitude as these lattice spacings. X-ray studies of fine structure have thoroughly confirmed the geometrical theory of space-groups, so that now, *vice versa*, the theory of space-groups is an indispensable aid in the interpretation of x-ray spectra obtained from any given crystal in terms of the ultimate fine structure of that crystal.

**X-ray Diffraction by Crystals.**—If crystals are built up of atoms and molecules marshaled in definite rows and in parallel planes with their mutual forces restraining them to relatively fixed positions in the rigid solid, and if x-rays are scattered by atoms, then these crystals are potential three-dimensional diffrac-

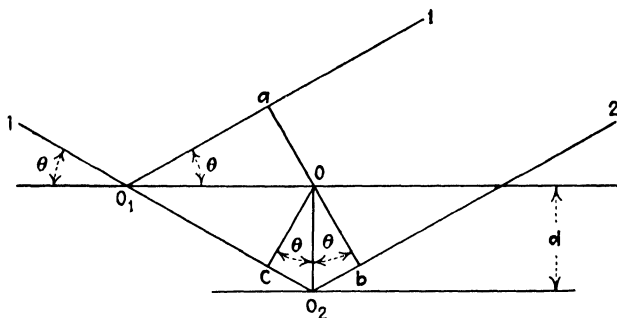


FIG. 80.—Derivation of Bragg law.  $n\lambda = 2d \sin \theta$ .

tion gratings for x-rays. Such was the prediction in 1913 of Laue, after he had accepted the work of Schoenflies and Federov leading to the conception of space-groups and had calculated from the density, molecular weight, and weight of the hydrogen atom that the distances between regularly disposed particles of mass in crystals must be of the same order as the wave length of x-rays ( $10^{-8}$  cm.). Friedrich and Knipping verified the prediction using a crystal of zinc blende. The original analysis by Laue was of considerable mathematical complexity but the Braggs were able to reduce the interaction between x-rays and crystals to terms of great simplicity, by considering primary x-rays to be reflected by the face of a crystal. As a matter of fact, the mechanism is far more complicated, since planes and atoms far below the "reflecting" surface are concerned, and since the emergent "secondary" x-rays have been emitted as a consequence of electronic changes in the atoms across which the

primary beam passes. Experiments have shown that the whole phenomenon appears to be simple reflection of the primary beam in accordance with a simple equation  $n\lambda = 2d \sin \Theta$ . The simple relations among  $\lambda$ ,  $d$ , and  $\Theta$  are at once seen from Fig. 80, which shows the incident beam  $I$  reflected at  $O_1$  and  $O_2$ . The line  $ab$  is perpendicular to the reflected rays  $O_11$  and  $O_22$ . The length of path  $O_1O_2b$  is greater than the length of the path  $O_1a$  by the length of the broken line  $cO_2b$ , the line  $Oc$  being perpendicular to  $O_1O_2$ . The length of the broken line  $cO_2b$  is, obviously,  $2d \sin \Theta$ . The condition that there should be a reflected beam is, therefore, that the reflected train  $O_22$  shall be exactly one wave length or an integer multiple of wave lengths  $n$  behind the train  $O_11$  or that

$$n\lambda = 2d \sin \Theta.$$

This is the fundamental equation of x-ray spectroscopy and of the analysis of structure of crystalline materials. For ordinary purposes it may be considered as rigorous; slight departures from it, observed particularly at higher orders of reflection, are due entirely to refraction, for  $\delta$ , in the expression for refractive index  $\mu = 1 - \delta$ , is not zero but of the order of  $10^{-6}$ .

Regardless of the experimental method of analysis (considered in the next chapter), the information vouchsafed by interference patterns of crystals is essentially the same. This is the determination of a series of values of  $d$  for different sets of planes by use of the Bragg equation. Now if a crystal is really a lattice, it follows that planes of three sets in the principal directions will enclose a small unit cell—the smallest possible subdivision which has the properties of the visible macrocrystal and which by repetition or translation of itself in all directions actually builds the crystal. It is the size of this fundamental architectural unit which may be determined directly from the experimental values of  $d_1$ ,  $d_2$ , and  $d_3$ —the respective edge lengths of the small parallelepiped. This presupposes some previous information about the crystallographic system, whether the axes are at right angles or not, or are of equal length or not. As previously indicated, this may easily be obtained by goniometer measurements of angles between faces. But if optical data are not available, the angles between the axes and axial ratios may be measured by reflection of x-rays from a crystal mounted on a goniometer head just as readily as by the optical

method. Assuming this to be the process employed, the steps in analysis are as follows:

1. Goniometric determination of crystallographic system.
2. Determination of dimensions and volume of unit cell.
3. Determination of the number of atoms or molecules in each unit cell. This involves a measurement of the density of the crystal and the use of the volume of the unit cell in the following formula:

$$n = \frac{\rho V}{Mm},$$

where  $n$  is the number of atoms (of an element) or molecules per unit cell;  $\rho$  is the density;  $V$  is the volume of the unit cell ( $d^3$  for a cubic crystal, or in general

$$V = abc \sqrt{\sin^2 \alpha + \sin^2 \beta + \sin^2 \gamma - 2 \cos \alpha \cos \beta \cos \gamma},$$

where  $a$ ,  $b$ , and  $c$  are edge lengths, and  $\alpha$ ,  $\beta$ , and  $\gamma$  the angles enclosed by the edges);  $M$  is the atomic or molecular weight, and  $m$  is the absolute weight of the hydrogen atom ( $1.663 \times 10^{-24}$  g.).

4. Further classification as far as possible according to symmetry observed, measurement of the intensities of lines, appearance or non-appearance of certain reflections, and the identification of interference maxima with the indices of planes.

5. Application of the theory of space-groups. Each of these space-groups is characterized by certain diffraction criteria, such as the apparent halving of spacings due to non-appearance of odd order ( $n = 1, 3, 5$ , etc.) interferences. Screw axes and glide planes can be detected; for a screw axis causes all orders of reflection from the plane normal to it to disappear except that corresponding to a multiple of the screw translation, as, for example, in quartz with a trigonal screw axis only the third, sixth, ninth, etc., orders appear. Glide planes halve whole sets of planes  $hko$ , where  $h + k$  is odd. A great service has been performed by Astbury and Yardley<sup>1</sup> in tabulating and graphically representing these criteria.

6. Determination of the symmetry of the molecule from the space-group of the crystal, the number of entirely unsymmetrical molecules theoretically required, and the number of molecules per unit cell actually found.

<sup>1</sup> *Phil. Trans. Roy. Soc. (London)*, **224A**, 221 (1924).



7. An analysis of the structure factor from intensity measurements, defining the positions within the unit cell of the diffracting centers, and even of the symmetry and positions of atoms in molecules if these are the lattice units. This is the most difficult, least direct, and yet the most interesting stage in crystal analysis. Briefly put, the process consists in assuming certain values for parameters and upon the basis of known laws of scattering and interference in calculating from these the theoretical intensity of reflections from a set of planes. These results are compared with observed intensities, and the process of trial and error continued until there is an agreement. Bernal has likened the process to the solution of a cross-word puzzle. The cell and space-group provide the square and pattern, the atoms the letters, and the intensities the clues.

8. A coordination and test of the completed structure with other known physical and chemical properties, such as atomic or ionic radii, optical activity, polarization, etc.

**Types of Information Obtainable from X-ray Diffraction Data.**—From the foregoing development of the subject it might be concluded that the lattice-type and unit-cell dimensions of crystals, together with the consequent explanation of certain properties, are the only facts to be gained from x-ray diffraction data. Suppose that we know that a whole series of samples of metal has exactly the same lattice structure, characteristic of iron or copper, etc. Is there any further differentiation possible upon the basis of x-ray diffraction patterns?

The dependence of x-ray interferences upon the condition as well as the kind of lattice makes it possible to detect very minute changes in atomic position or in lattice constituents. Consequently a fund of purely scientific and technological information is obtained from this fine-structure method which is almost universal in its scope.

Following is a tabulation of the principal types of information, each of which will receive discussion:

- a. Crystalline or non-crystalline.
- b. Crystallographic system, space-group, unit-cell dimensions, parameters of atoms or molecules.
- c. Deduction of crystal unit (atom, ion, molecule), of size of unit, of type of binding, and of general properties of solid to be expected.

- d.* Chemical identity, chemical and crystallographic changes and stability.
- e.* Allotropic modifications.
- f.* Type and mechanism of alloy formation.
- g.* Single crystal or aggregate.
- h.* Crystallographic orientation of single crystal or of grains in aggregate.
- i.* Random or fibered aggregate and relative degree of preferred orientation in intermediate stages.
- j.* Grain size in an aggregate (particularly in colloidal range).
- k.* Internal strain or distortion.
- l.* Extent of deformation and mechanism of fabrication in rolling, drawing, etc.
- m.* Analysis of effect of heat treatment, grain growth, control and mechanism of recrystallization, and the establishment of scientifically correct annealing technique.
- n.* Differentiation between surface and interior structure.

## CHAPTER XI

### THE EXPERIMENTAL X-RAY METHODS OF CRYSTAL ANALYSIS

The several methods of analysis of crystal structure by x-rays involve the following essential differences: single crystals or powders; monochromatic or polychromatic x-rays; photographic or ionization-current registration; and reflection or diffraction from a single set of parallel planes, or from many different sets simultaneously. It is evident, therefore, that the information obtained will differ somewhat, depending upon the combination of these variables. The proper selection of the method for the material under investigation, and for the type of information wanted, is of utmost importance. To this end the five more important methods have been compared and contrasted in tabular form (Table XXIV) under the heads: kind of x-rays, beam definition, sample (single crystal or powder), mounting, method of registration, pattern, interpretation, chief usefulness, modifications. Representative photographs or ionization-current curves obtained by each method are shown in figures indicated in the table.

**Special Notes on Apparatus.** 1. *The Laue Method.*—The experimental equipment here is relatively so simple, as shown in Fig. 81, that little additional explanation is required. Typical symmetrical and unsymmetrical Laue patterns are illustrated in Figs. 82 and 83. The design and construction of the pinhole for defining the beam are most important. With a single orifice, of course, a pinhole image of the target is obtained by the pinhole camera effect. The longer the collimator, which is simply a pinhole in a solid block or two apertures in metal plates separated by a fixed distance, the more nearly parallel is the x-ray beam. The diameter of the pinhole is of importance from the standpoint of detail in the diffraction pattern. The interferences become sharper the smaller the diameter. This is well illustrated in Fig. 84 for patterns of an aluminum wire (not a single crystal) taken respectively with pinholes of diameters 0.060, 0.040, and

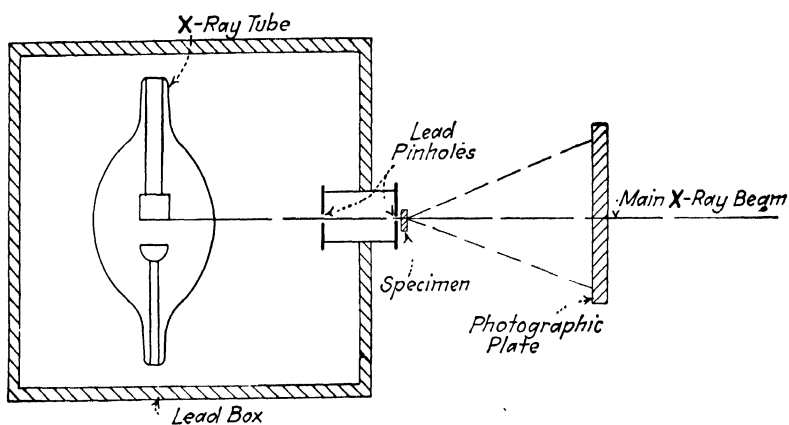


FIG. 81.—Diagram of the Laue and monochromatic pinhole x-ray methods.

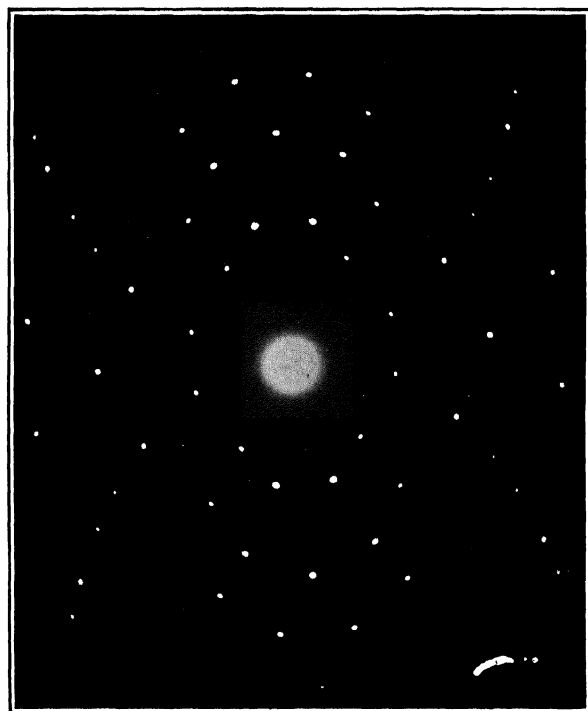


FIG. 82.—Symmetrical Laue photograph of an iron crystal.

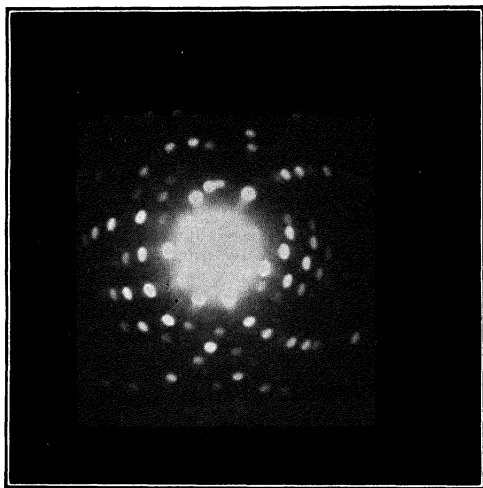


FIG. 83.—Unsymmetrical Laue photograph of an iron crystal.

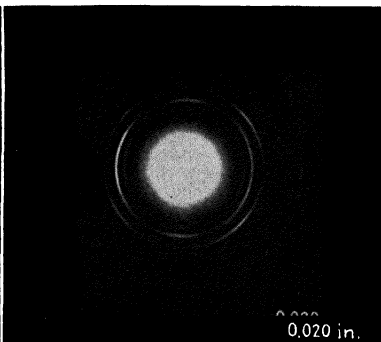
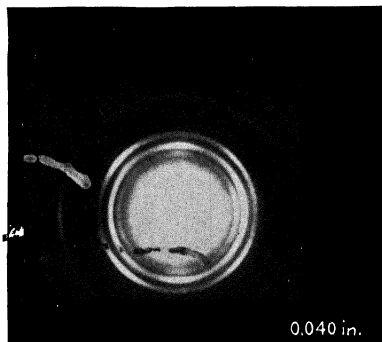
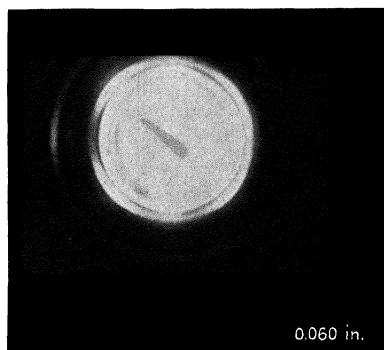


FIG. 84.—Diffraction patterns for aluminum wire showing effect of pinhole diameter.

TABLE XXIV.—EXPERIMENTAL DIFFRACTION METHODS

Method	Laue	Bragg	Rotating crystal (Schiebold-Polanyi)	Powder (Hull-Debye-Scherrer)	Monochromatic pinhole (Fiber)
X-ray beam . . . Beam definition . . .	Polychromatic Pinhole (Fig. 81 without filter)	Monochromatic Slit	Monochromatic Pinhole usually; also wedge with knife edge on crystal face	Monochromatic Hull, slit; Debye-Scherrer pinhole	Monochromatic Pinhole (Fig. 81 with fil- ter)
	Single crystal	Single crystal or film of oriented molecules	Single crystal	Powder or random ag- gregate	Any—fibers particularly
	Fixed according to defi- nite crystal direction	Oscillation; reflection from face or transmis- sion, successive settings of angle in ionization spectrometer (Fig. 85)	Rotated or oscillated over fixed angle around principal axis, mount- ing on goniometer head for proper orientation (Fig. 88)	Fixed, in small tubes, threads, wires, ribbons, etc	Fixed with fiber axis ori- ented, over pinhole and beam transmitted per- pendicular
Usual registration	Flat photographic film	Flat or cylindrical film; ionization chamber	Flat or cylindrical film with crystal at center	Narrow film bent in arc with specimen at center	Flat film, perpendicular to beam
Pattern . . .	Symmetrical spots each from different set of planes and particular value of $d, \lambda, \theta$ (Fig. 82)	Line spectrum from sin- gle set of planes (Figs. 31, 32, 33)	Diffraction spots lying on layer lines, parallel horizontal with cylin- drical film, and hyper- bolas with flat film (Fig. 89)	Line spectrum, each line corresponding to differ- ent sets of planes (Fig. 97)	For random aggregate concentric rings (Fig. 96) or diagram 360 deg. in azimuth; for fibers layer line pattern like rotating single crystal (Fig. 98)
Interpretation . . .	Calculation of spacings according to spots Assignment of indices with assistance of stere- ographic or gnomonic projections. Estima- tion of relative intensi- ties	Calculation of spacings for set of planes involv- ed in particular orienta- tion ( $n\lambda = 2d \sin \theta$ ) and thence from three experiments size of unit crystal cell Determina- tion of missing or- ders, etc., in aiding to- ward structure factor	Measurement of identity period from layer lines by $I = n\lambda/\sin \mu_n$ and exact size of unit cell Straight-forward in- dexing of diffraction spots on layer line Comparison with space- group criteria	Calculation of spacings for lines. In simpler cases assignment of in- dices from $\sin^2 \theta$ data, and unit-cell dimen- sions. Measurement of line breadths for par- ticle size	Same as for powders. Identity period along fiber axis from $I =$ $n\lambda/\sin \mu_n$ . Orienta- tion of planes in all fiber particles from po- sitions of interference maxima on Debye- Scherrer rings

TABLE XXIV.—EXPERIMENTAL DIFFRACTION METHODS.—(Continued)

Method	Laue	Bragg	Rotating crystal (Schiebold-Polanyi)	Powder (Hull-Debye-Scherrer)	Monochromatic pinhole (Fiber)
Chief uses	Symmetry, indices, and intensities for assignment of space-group Practical determination of orientation as of large grains with respect to surface of sheet	Occasionally used to determine or check lattice spacing, for all films of long-chain carbon compounds	Commonly used for determining uniquely crystal structure and constitution where single crystals are available	Used in the great majority of cases (single crystals unavailable) for crystalline structure, allotropy, qualitative and quantitative analysis, purity, grain size from line breadths, etc.	Same for powders or random aggregates. Determination of actual state of any specimen, such as degree of fiber-ing, internal strain, etc., and of the effect of any process such as working or heat treatment; thus for the control of industrial processes and as a method of specification
Modifications...	Unsymmetrical patterns (Fig. 83)	...	Special goniometers (Weissenberg, etc.) described in text (Figs 90-95)	Bohlin-Westgren method has slit, flat sample, and film on same circumference permitting focus and rapid exposure by reducing absorption of rays in specimen to a minimum (Figs 100, 101)	Cylindrical film with axis perpendicular to beam or coaxial with beam. Reflection from surface at fixed angle (Fig 99); back reflection (described in later section)

0.020 in. On the other hand, the time of exposure increases with increase in length or decrease in diameter. Voltages are usually not higher than 60,000 volts, since higher values merely complicate the range of wave lengths which in this method are unknown except in so far as there is a short wave-length limit corresponding to each voltage, so that in the interpretation of the patterns all lower values of  $\lambda$  can be at once eliminated.

The average length of exposure with ordinary equipment for a Laue photograph of a single crystal without heavily absorbing elements is 30 min. to 1 hr. The new high-powered tubes described on page 35 enable reduction of time to a matter of seconds or minutes.

2. *The Bragg Method (Spectrometry).*—Since the Bragg method of crystal analysis involves direct angular measurements of  $\theta$ , the use of monochromatic radiation, and reflection from a single set of planes, the significance of the results is readily understood in terms of the preceding development. By successive resetttings of the crystal so that the planar distances for various set of planes, which have a common zone axis, are ascertained, it is usually possible to arrive at something like a complete structure; the difficulty arises in the tedious repetition of measurements and the accurate orientation of the crystal specimen on the spectrometer.

Because of the great value of intensity data in this method, the ionization method is preferable for the investigation of an unknown structure. The ionization spectrometer consists essentially of a crystal table, which rotates about the axis of the spectrometer with reference to a fixed scale graduated in degrees and minutes; readings to seconds of arc may be made by means of a vernier or with microscopes with micrometer eyepieces. A separate movable arm carries the ionization chamber, whose angular position can be read on a second concentric scale. Two or more slits define the x-ray beam impinging on the crystal, and another slit is adjusted in front of the ionization chamber.

The ionization chamber is simply a container for a gas or vapor and two electrodes; reflected x-rays ~~passing into the gas~~ ionize it; with a sufficient difference of potential between the electrodes, a current results, which is measured by the speed of discharge of a gold-leaf electroscope or the deflection per second of a quadrant electrometer. In an experiment the ionization chamber is adjusted so as to receive the reflection from the



crystal face. Then the crystal and ionization chamber are moved step by step (the latter at twice the rate of the former), and the ionization current measured for each step. When the ionization current is plotted against the angle  $\theta$ , or angular scale reading, a

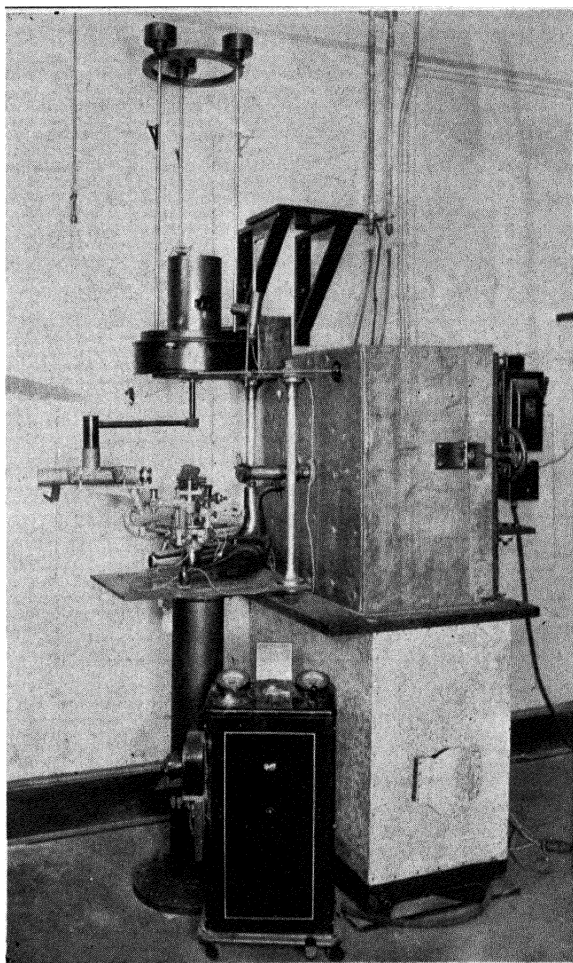


FIG. 85.—Precision ionization spectrometer with quadrant electrometer.

curve is obtained showing the characteristic peaks, which appear as spectral lines if a photographic plate is substituted for the ionization chamber.

The theory of ionization and the practical utilization of air ionization as a measure of x-ray dosage in tissues have been

considered in Chap. IX. Recently Allison and Andrew<sup>1</sup> made an experimental test of the ionization-chamber method of measuring the relative intensities of x-ray spectrum lines. With suitable precautions it was proved that the saturation current obtained from a given volume of any gas is proportional to the fraction of the x-ray beam transformed into  $\beta$ -rays within it, provided the  $\beta$ -rays come to the end of their ionizing range within the volume.

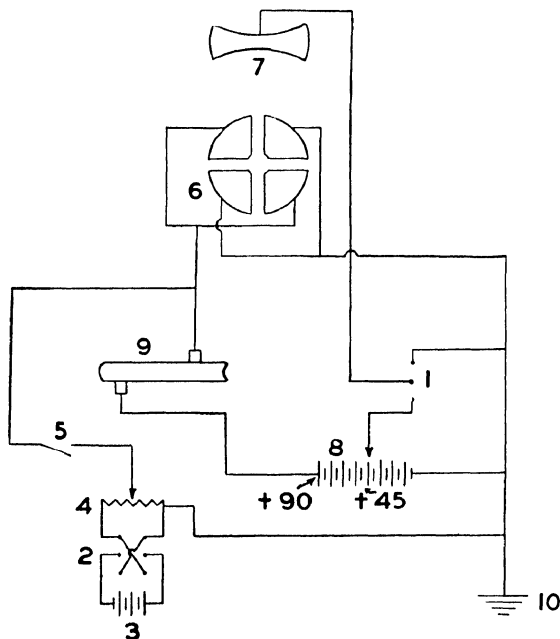


FIG. 86.—Potentiometric control of quadrant electrometer used to measure ionization currents.

1, Single-pole, double-throw switch for charging needle; 2, Reversing switch for potentiometer circuit; 3, 2-volt 20-amp.-hr. storage cell; 4, 400-ohm general radio potentiometer; 5, Earthing key controlled by silk fishline for distance; 6, Quadrant electrometer fixed quadrants; 7, Movable needle of electrometer; 8, Dry-cell radio "B" battery (90 to 150 volts); 9, Ionization chamber; 10, Earth.

The photograph of a precision spectrometer equipment in the writer's laboratory is reproduced in Fig. 85. Upon the spectrometer, built (by the Société Genévoise d'Instruments de Physique) with circular scales which may be read to 0.2 sec. of arc, is mounted an ionization chamber of the original Duane design, consisting of a long glass tube, containing a cylindrical electrode

<sup>1</sup> *Phys. Rev.*, **38**, 441 (1931).

connected with a battery and a central insulated-rod electrode running along the axis of the tube and connected with a pair of quadrants in an electrometer. The electrical connections of the system are shown diagrammatically in Fig. 86. The electrometer is of the Compton-Stryker type with sputtered quartz fiber suspension; it has proved eminently satisfactory. A source of light is reflected by the mirror upon a large scale upon the side of the wall, so that extremely accurate readings of the speed of deflection are possible. The make-and-break switch consists of two fine longitudinal platinum wires, stretched on stirrups which are supported on quartz rods and make contact at right angles; from the standpoint of stray and induced e.m.f.s. the arrangement is by far superior to any other. The quadrant or string electrometer may be used as null instruments, so that readings of potential are made by inducing such an opposite charge on the collecting system as to return the needle to the neutral position.

Numerous attempts have been made to displace the quadrant electrometer, string electrometer, or gold-leaf electroscope as measuring devices for ionization currents. Fonda and Collins<sup>1</sup> have described an amplifying system for ionization currents employing a new four-element vacuum tube characterized by a very high input resistance. The deflection of the galvanometer is taken directly as a measure of the relative intensities of the x-rays entering the chamber.

Many modifications of the Bragg spectrometric method have been made; chief among these are the remarkably precise instruments of Siegbahn, who has preferred the photographic method originally developed by de Broglie. Depending upon the range of wave lengths to be used, a somewhat different type of spectrometer has been devised by this master experimenter; the vacuum type for the spectroscopy of very soft x-rays, which are easily absorbed in air, is perhaps of the greatest interest and importance. These spectrographs are fully described in Siegbahn's book.

For the photographic registration the setting of crystal angles by hand is inconvenient and a mechanical method of oscillating the crystal over a certain angle is desirable. This consists of a cam and small motor. A spectrograph for use on a multiple diffraction unit is shown in Fig. 87. The crystal is mounted flat on the circular table which is oscillated in a vertical plane,

<sup>1</sup> *J. Am. Chem. Soc.*, **53**, 113 (1931).

since slits are horizontal in such units. This Bragg spectrograph is applicable not only for single crystals but for all thin films of long-chain organic compounds in which parallel diffracting planes are built up from molecules oriented perpendicular or at some definite angle to the planes (see Chap. XVI).

The photographic modification of the Bragg method in which diffraction from only a single set of planes is registered is, of course, only a special case of the general single-crystal spectroscopy in which a crystal is oscillated or rotated in the x-ray beam.

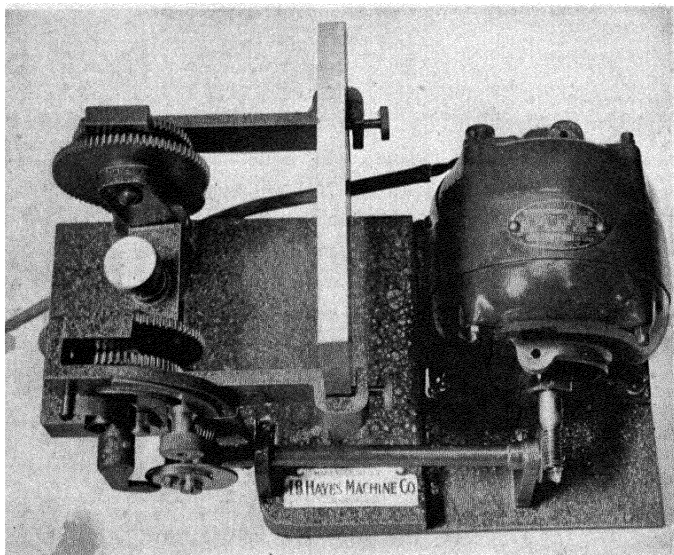


FIG. 87.—Oscillating spectrograph for Bragg method.

The simultaneous registration of all possible reflections from a crystal rotated around an axis produces the so-called complete spectral diagram. This technique is considered separately under the rotation method.

The ionization spectrometers have been primarily used with known crystals for the accurate evaluation of wave lengths, energy levels, etc. The double spectrometer in which a purely monochromatic beam is formed by reflection from a crystal is a special modification for very refined physical measurements, spectrum line breadths, resolution of doublets, etc. For the accurate measurement of intensities of reflections from both single crystals and powders, which is so important for the com-

plete analysis of crystalline structure, no instrument can compare with the ionization spectrometer. The best experimental measurements of the so-called  $F$  curves for various atoms have been made by Wyckoff and his associates. The method and results will be considered in the next chapter.

*Rotation Method.*—The most powerful method of crystal analysis is undoubtedly the rotation method which is known in several modifications. Ordinarily the single crystal is mounted and rotated around a principal axis. Three such photographs around the principal axes make possible almost complete informa-

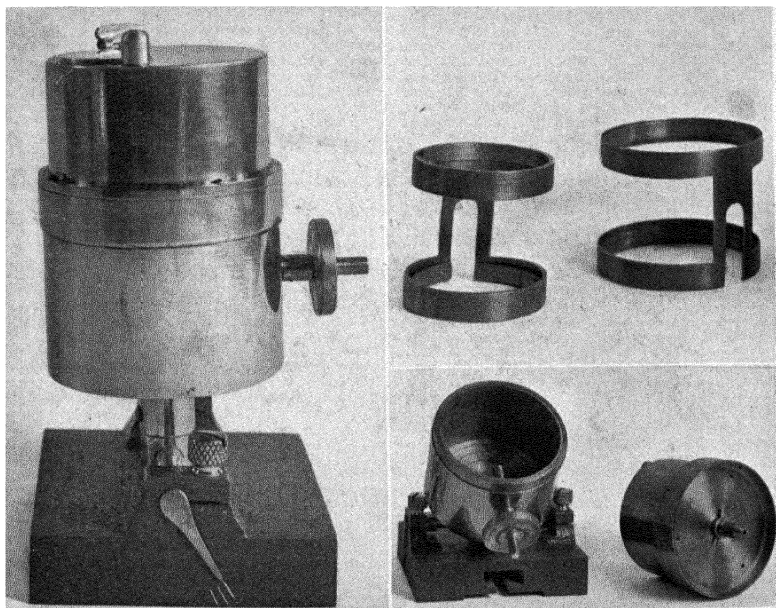


FIG. 88.—Two views of camera for rotating crystal and Debye-Scherrer powder diffraction methods. Left, complete camera; upper right, film holders of two sizes; lower right, adjustable case with pinhole and clock work top for rotation of specimen held in chuck.

tion. In the usual method a stationary film is used, either flat at a fixed distance from the crystal or preferably bent on the circumference of a circle with the crystal at the center. A satisfactory design of rotation camera or spectrograph is shown in Fig. 88 either for special units or for commercial multiple apparatus. Frequently it is desirable to mount the crystals on a goniometer head by means of which the angles between axes

may be measured. If, for example, a rational layer line pattern for the rotation method is obtained for one orientation of an

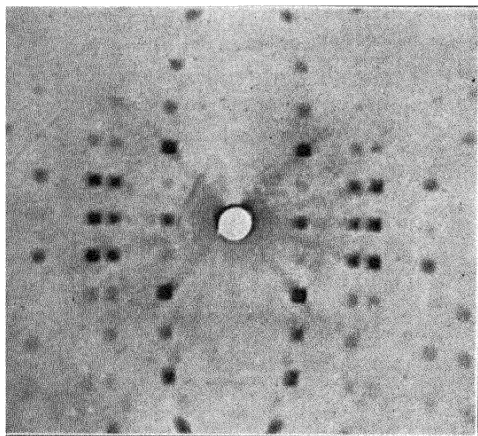


FIG. 89.—Complete diagram (Seemann-Schiebold-Polyani) for benzil crystal taken with a Müller spectrograph. (*Hilger.*)

orthorhombic crystal another will be obtained when the crystal is shifted 90 deg. and again rotated, and still another after it is shifted 90 deg. in the third direction. In all cases a complete

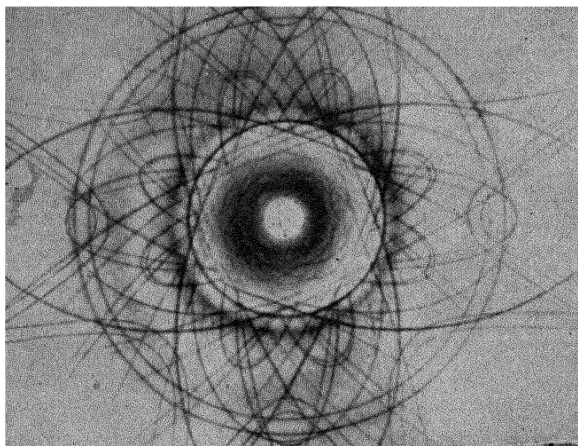


FIG. 90.—Complete spectrum pattern of rock-salt crystal by Seemann wide-angle method

spectral diagram for all possible reflections from a given crystalline zone (the rotation axis) is obtained, such as appears in Fig. 89. By a special modification employing a widely divergent

fan-shaped beam Seemann has obtained patterns of the type shown in Fig. 90.

A complete diagram for rotation around 360 deg. is, of course, the summation of a series of diagrams which may be prepared by oscillating the crystal over fixed angles, 1 to 20 deg., 20 to 40 deg., etc. The apparatus employs the heart-shaped cam described under the Bragg method. This interpretation of a complex rotation pattern is often greatly simplified by these oscillation diagrams.

Aside from the arrangement of the photographic film and the method of mechanically rotating or oscillating the crystal,

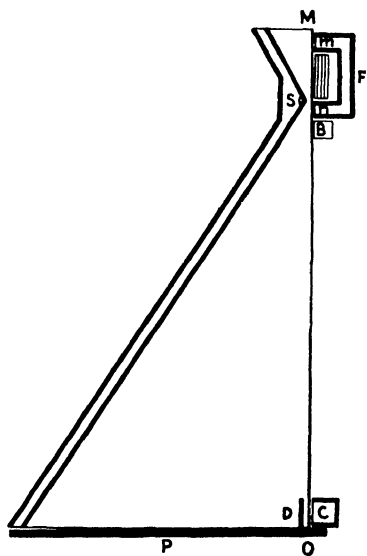


FIG. 91.—Principle of slitless spectrograph with specimen mounted between *m* and *n*.

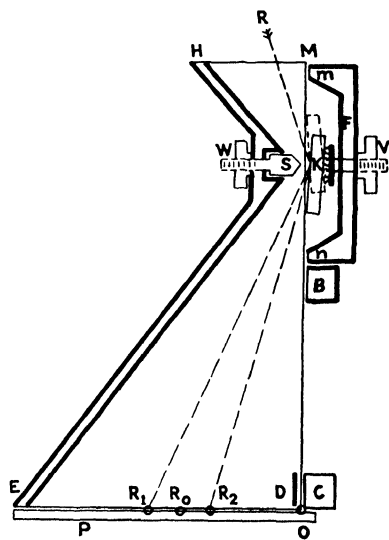


FIG. 92.— Principle of wedge spectrograph with wedge at *S*.

the principal variable in the simple method is the method of beam definition. Here as in the Bragg spectrometer the most common equipment is a pair of slits for rendering the rays parallel. These are made of lead, lead alloy, gold, or even brass for softer rays. For only very small crystals the slits may be so short as actually to be pinholes, as is the case of the rotation camera pictured in Fig. 88. The smaller the slit width or pinhole diameter, the sharper are the interferences. There are also the so-called slitless spectrographs which have been devised by Seemann and others for widely divergent rays. The slitless

method is illustrated in Fig. 91, and the wedge spectrograph in Fig. 92. These methods make it possible to bring the crystal very close to the x-ray source and thus permit very rapid photographic exposures. A very complete comparison between the various methods of beam definition is given by Seemann.<sup>1</sup>

For increasing accuracy and sensitiveness special modifications of the rotation method are employed as follows:

- a. Displacement of the film parallel to the direction of the axis of rotation of the crystal (Weissenberg goniometer).
- b. Displacement of the plate or film parallel to the  $x$ -axis (Dausar).

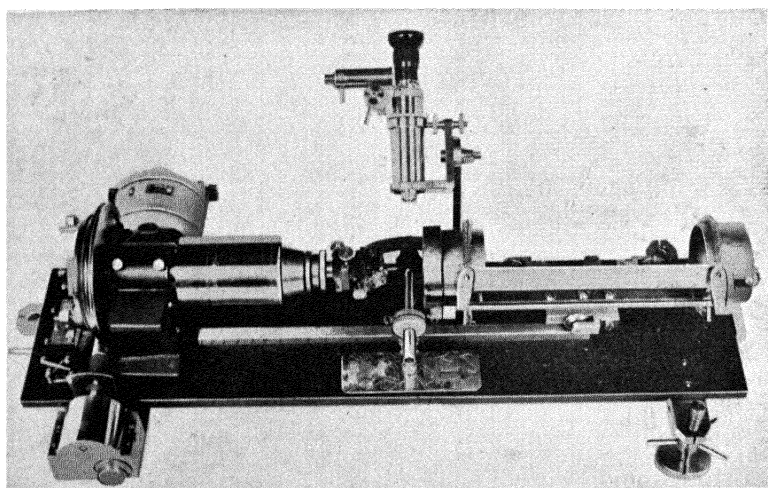


FIG. 93.—Weissenberg-Seemann goniometer.

- c. Displacement of the film parallel to the direction of the primary beams (Kratky).

- d. Rotation of the photographic plate or film around the  $z$ -axis (Seemann, Mark, and Wigner).

- e. Rotation of the plate around the  $y$ -axis (primary beam) (Schiebold).

- f. Displacement of two photographic plates ~~in directions~~ parallel and perpendicular to the axis of rotation.

Of these the first is most generally employed, largely because of the simplicity of interpretation and because of the availability of an excellent commercial instrument. Figure 93 shows such a

<sup>1</sup> *Ann. Physik*, 5, 6, (1930).



Weissenberg goniometer as designed by Bohm and built by Seemann. The cylindrical film, coaxial with the rotating crystal fragment, is gradually displaced during the exposure in the direction parallel to the axis. The principle of the apparatus is shown diagrammatically in Fig. 94, and in Fig. 95 is reproduced a diffraction pattern; the line spectrum above is that obtained by the ordinary rotation method. In the Weissenberg diagram the spectra of the various surfaces of the zone of rotation are not superimposed but are arranged in hyperbolas which enable relatively simple assignment of indices. When several lattice planes are equivalent, such as  $(110)$ ,  $(\bar{1}10)$ ,  $(\bar{1}\bar{1}0)$ ,  $(1\bar{1}0)$  in a rhombic crystal, and have the same lattice spacing  $d$  and the same diffraction angle  $2\theta$ , they will all register on a stationary film the same interference point, whereas in this modification with moving film each set of planes will register its own interference lying on a vertical line.

#### The Diffraction of X-rays by

**Powders.**—Thus far the consideration of the reflection or diffraction of x-rays by crystals has assumed essentially single crystals. On account of the fact that so many interesting chemical substances, including practically all metals, cannot be obtained in the form of sufficiently large single crystals, one of the great contributions to x-ray science has been the discovery, independently by Debye and Scherrer in Europe and by Hull in America, that fine powders, or crystalline aggregates of all kinds, may be analyzed for ultimate crys-

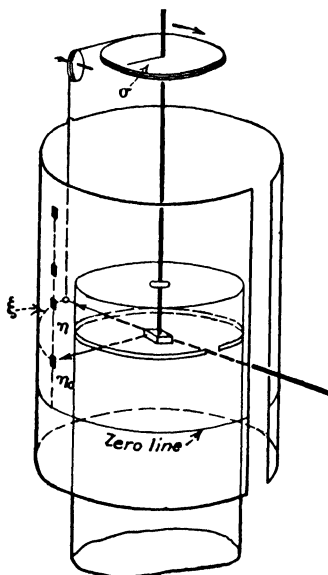


FIG. 94.—Principle of operation of the Weissenberg goniometer.

talline structure in a most satisfactory way. The diffraction depends upon the fact that in a fine powder the grains are arranged in an entirely chaotic manner. There should be enough particles in this array, turned at just the right angle to the incident primary beam of monochromatic x-rays, to enable strong reflection from one set of parallel planes; other particles turned at another angle will produce reflection from another set of planes (the same set in

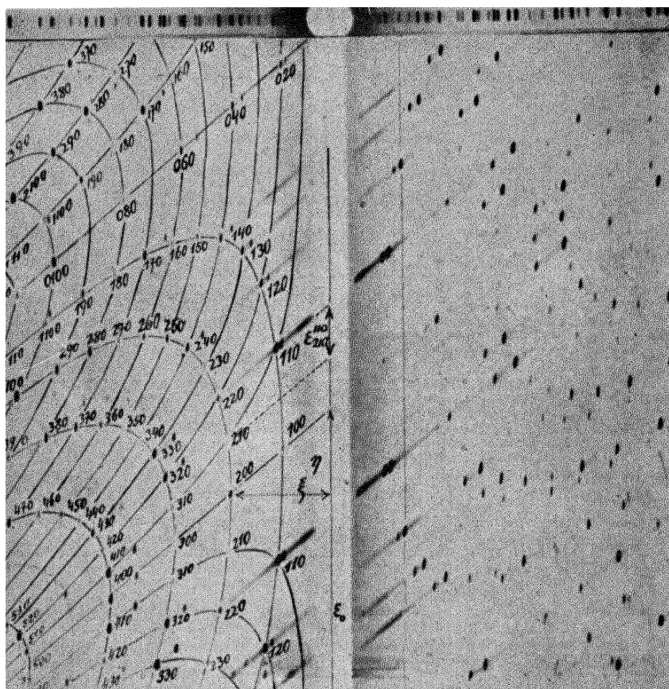


FIG. 95.—Typical Weissenberg diagram compared with ordinary rotation spectrum above.

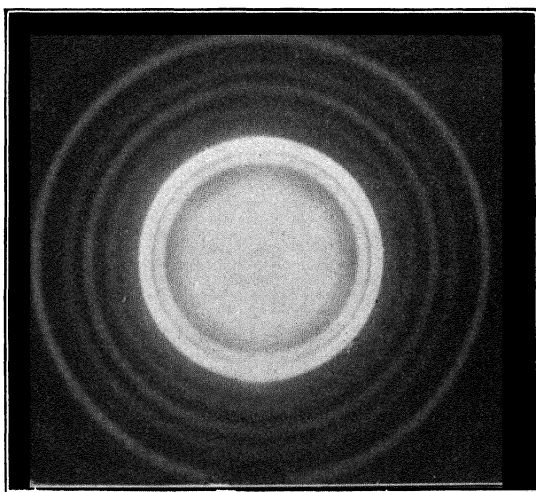


FIG. 96.—Monochromatic pinhole diagram of steel ribbon showing continuous rings.

many particles cooperating). Thus a beam passing through a powder specimen will fall upon a perpendicular flat photographic film (Fig. 81) as a series of concentric rings (Fig. 96), each uniformly intense throughout, and corresponding to one set of planes of spacing  $d$ . A horizontal section cut through this diagram has, therefore, the appearance of a line spectrum (Fig. 97). This same result may be obtained by bending a narrow

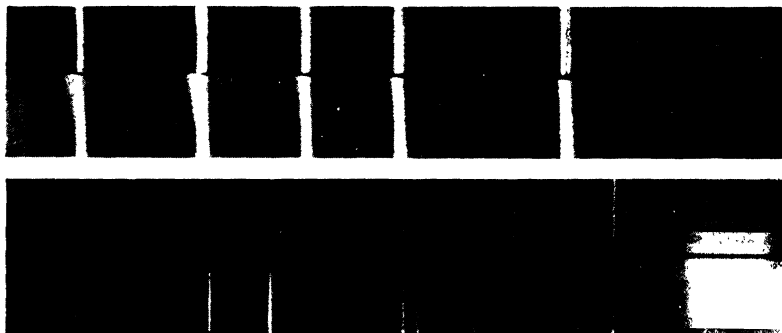


FIG. 97.—Powder diffraction patterns for  $\alpha$ -iron (body-centered cubic) and platinum (face-centered cubic).

film in a cassette on the circumference of a circle, at the center of which is the specimen. In the so-called Debye-Scherrer camera, now purchasable on the market, the film is bent around 360 deg. and the beam, defined by pinholes, passes through a hole in the

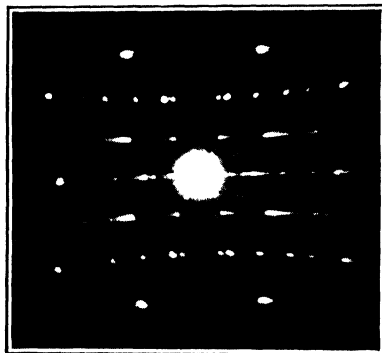


FIG. 98.—Monochromatic pinhole diagram of chrysotile (asbestos) showing almost perfect fiber structure.

film; in other modifications where larger dispersion is desired, the film may occupy only a quadrant or semicircle. In contrast a pinhole pattern for a fiber, instead of a random aggregate, is shown in Fig. 98.

The sample may have one of various forms, the essential point being random orientation of grains; powders of 200-mesh or smaller size may be placed in fine capillary tubes of glass or celluloid, pasted by collodion on ribbons or threads, or pressed into slabs. Metals may be used in the form of fine wires or as small beveled plates with the beam grazing the blunt knife-edge at a small angle and passing through a sharp edge. Reflection from the surface of a sample at a fixed angle with respect to the x-ray beam can be used, as illustrated in Fig. 99.

For powders of heavily absorbing substances such as lead it is desirable to use a non-crystalline diluent such as gum tragacanth or powdered starch. A complete table of proper proportions

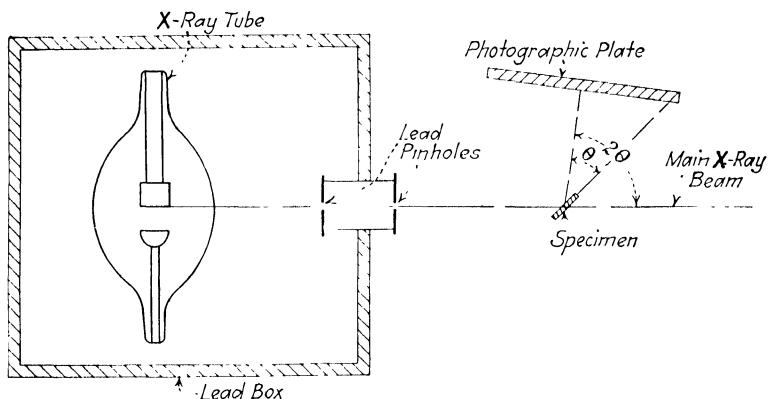


FIG. 99.- Diagram of surface reflection method.

has been worked out by Davey. The volume of the diluting material with 1 volume of a chemical element varies from 1 for elements 10 to 26, 3 for 18 to 28, 5 for 29 to 44, 6 for 36 to 46, 7 for 47 to 53, 8 for 54 to 57, and 9 to 10 on up to 92.

On account of the complexity of the spectrum it is desirable that the beam of x-rays should be as nearly monochromatic as possible. With molybdenum rays the zirconium filter eliminates all but the  $K\alpha$  doublet, and a nickel filter serves for copper, etc. (see page 66).

The accurate measurement of the crystal powder spectrum lines is, of course, of great importance in analyses of unknown mixtures. Where semicircular cassettes or cylindrical cameras are used, the undeflected beam strikes the center of the film and diffraction lines are registered on both sides of this zero position. Uncertainties as to this are eliminated by measuring from one

line to the corresponding line on the opposite end of the film. If, however, the zero position is at one end of the film as in the case of quadrant cassettes, greater resolution is possible but it is often necessary to run a calibrating spectrum for known pure crystal powders such as sodium chloride on the same film, either mixed with the unknown or placed in half of the small capillary tube. Since the spacings for each of these lines are accurately known and, hence, the necessary displacement on the film, the zero position may be accurately determined as well as all evidences of film shrinkage and inaccurate alignment of the specimen.

By its very nature the powder method requires more energy to produce a suitable photograph than is necessary for single crystals; consequently a greater time of exposure is required and this may well run into a hundred hours or more for some substances on usual apparatus. High-powered x-ray tubes, of course, can be used to advantage. The Seemann-Bohlin camera (Fig. 100) employs a divergent beam of x-rays and a

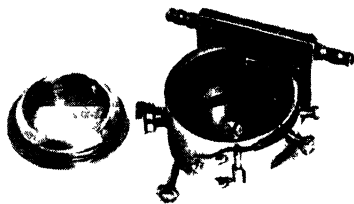


FIG. 100.—Seemann-Bohlin powder diffraction camera, with slit, specimen and film on same circumference, similar to type used in studies of alloys by Westgren and coworkers.



FIG. 101.—Pattern for sheet steel with Seemann-Bohlin camera.

focusing principle. Here the focal spot of an x-ray tube, the specimen in the form of a ribbon or flat surface, and the photographic film are on the circumference of the same circle. Spectra such as illustrated in Fig. 101 are registered very rapidly and the method has proved of greatest value in technical examination of materials such as alloys, not only at room temperatures but also at low and high temperatures.

**Multiple Apparatus.**—The most familiar and useful apparatus for metallurgical and chemical applications is the multiple General Electric diffraction apparatus. This consists of a transformer operating at a fixed potential of 30,000 volts, with

an enclosed filament transformer, an operating switchboard with filament current stabilizer, a water-cooled molybdenum-target self-rectifying Coolidge tube, a slit system which permits 12 simultaneous exposures radially around the vertical tube at a grazing angle of 5 deg. upon the target, and quadrant cassettes for the Hull powder method. Interchangeable slits and pinholes made of bakelite impregnated with lead oxide give the apparatus greater elasticity, since oscillating reflection spectrographs (Fig.

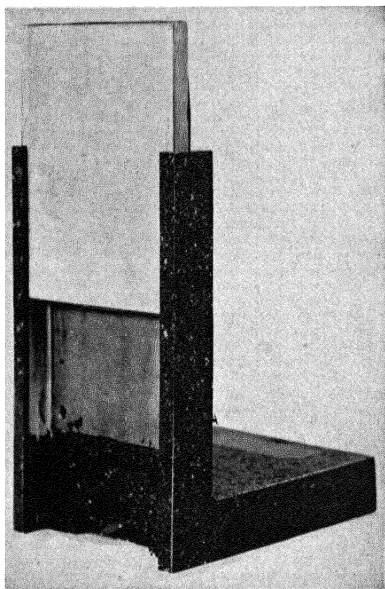


FIG. 102.—Flat cassette and holder for pinhole method used with multiple apparatus.

87), flat cassettes (Fig. 102), and other specially constructed devices may also be mounted. In the writer's laboratory every one of the methods including modifications may be used on the General Electric apparatus. Figure 103 shows the table top with quadrant cassettes for the powder method and a spectrograph combining the Bragg method (oscillation of the specimen) and the pinhole surface reflection method (diagrammatically shown in Fig. 99). A new multiple-diffraction unit designed and constructed in the writer's laboratory is shown in Fig. 104. It is distinguished by a small lead-covered bakelite

cylinder around the x-ray tube, external pinholes adjustable in all directions (as shown in Fig. 105, looking down from above), and an integral control switchboard.

A new Philips "Metalix" crystal analysis unit weighing only 54 lb. is shown in Fig. 106. The Metalix tube and two Debye-Scherrer cameras are shown in position.

Another ingenious universal spectrograph which, however, cannot be used with the General Electric apparatus, is the Müller-Hilger instrument. It has interchangeable parts which adapt it for all of the methods of crystal analysis. As shown in Fig. 107 *a*, *b*, *c*, it is set up respectively for the Bragg method (oscillating

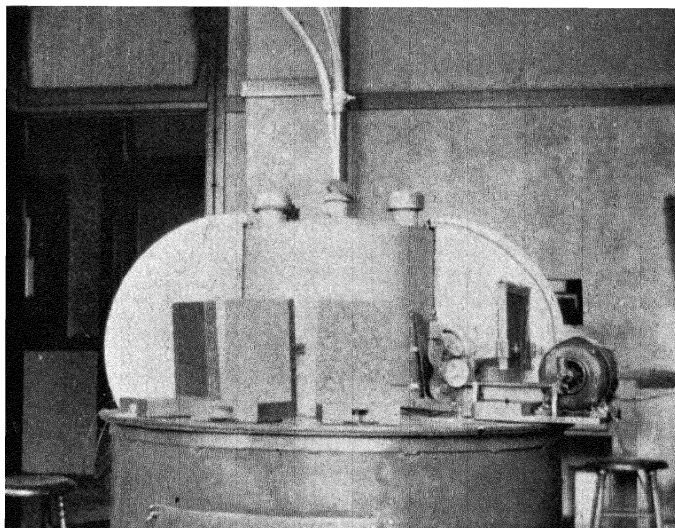


FIG. 103.—Top of General Electric multiple-diffraction apparatus with various types of cassettes in position.



FIG. 104.—New multiple-diffraction unit with Standard transformer and integral control board designed and built at the University of Illinois.

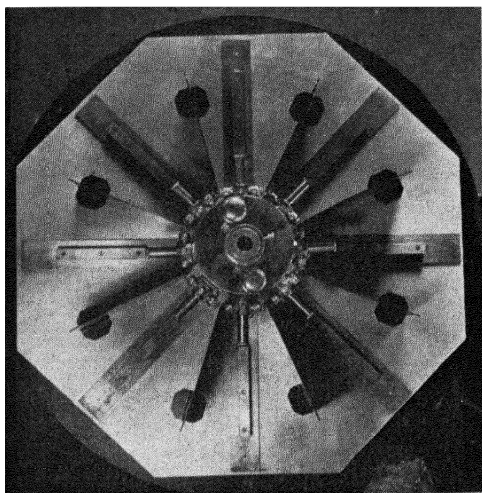


FIG. 105.—Multiple-diffraction unit illustrated in Fig. 104 as viewed from above, showing completely adjustable pinholes and slits.

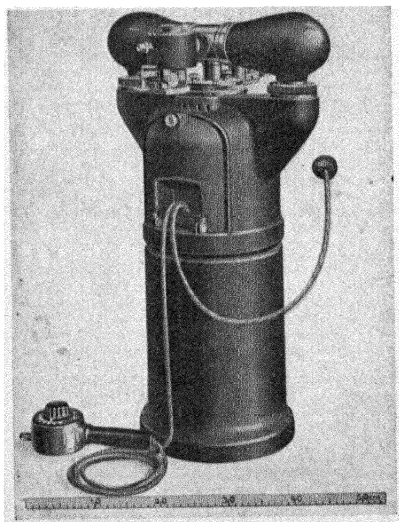


FIG. 106.—Philips Metalix diffraction apparatus with Metalix tube in horizontal covering and two Debye-Scherrer cameras; weight 54 lb.



crystal), for the Laue and rotating crystal methods (showing the goniometer head), and for the Debye-Scherrer powder method.

Numerous spectrographs and cameras of all types combining special features have been described in the literature, particularly

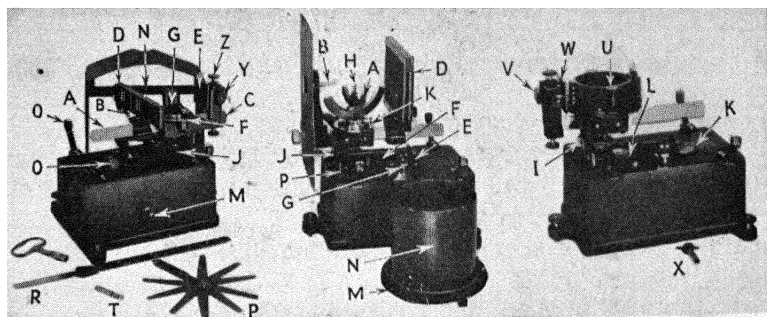


FIG. 107.—Muller-Hilger Universal Spectrograph as set up respectively for Bragg, Laue and rotating-crystal, and Debye-Scherrer powder methods.

those of German design and manufacture. Many of these, such as the Seemann spectrograph, are most ingeniously combined with steel mercury vapor pumps and demountable x-ray tubes. A diagram of a typical unit is shown in Fig. 39, page 84.

## CHAPTER XII

### THE INTERPRETATION OF DIFFRACTION PATTERNS

Once the diffraction effects from any material have been observed by one or more of the experimental methods described in the preceding chapter, the interpretation must be made as the step in x-ray science which requires most knowledge and experience. The problem may involve the complete structural analysis of an unknown crystalline substance by the successive steps which are outlined on page 182. Or again the interpretation may involve the *condition* of a substance of known structure in terms of grain size and orientation, internal strain, purity, or other properties listed on page 183 concerning which information is vouchsafed by diffraction patterns. Exhaustive treatment of the matter of interpretation is obviously impossible in this book but the attempt is made in this chapter to consider briefly, first, the most fundamental aspects of the general subject, the position of interferences, and their intensities; second, characteristic details of measurement of patterns from each of the most important experimental diffraction methods for structural analysis; and, finally, the interpretation of the exact condition of any specimen whose ultimate crystalline structure may be known.

#### 1. The Positions of Diffraction Interferences from Crystals.—

As explained in Chap. X, the simple law which governs all diffraction phenomena is  $n\lambda = 2d \sin \Theta$ , where  $n$  is an integer, the order of the reflection,  $\lambda$  is the wave length,  $d$  is the distance between the set of planes at an angle  $\Theta$  with respect to the incident beam. Thus for a known wave length  $\lambda$ , the ratio  $d/n$  can be calculated for any diffraction spot or line, independent of any assumptions as to the grating structure, since the experimental measurement in diffraction science is that of  $\Theta$ ; actually the measurement is made not of the angle of incidence but of the angle of diffraction  $2\Theta$ . This relationship is easily seen when it is understood that a beam of x-rays impinging on the face of a crystal at the angle  $\Theta$  will appear to be reflected from this face at the equal angle  $\Theta$  between the face and the beam, but the total

angle between the undiffracted primary beam and the reflected or diffracted beam will be  $2\theta$ . On a flat film placed at right angles to the primary beam the displacement of the interference from the zero primary beam ( $a$ ) divided by the known distance from specimen to film ( $b$ ) gives  $2\theta = \tan^{-1} a/b$ . From this  $\sin \theta$  is obtained and the calculation for  $d/n$  (usually  $d/1$ ) is made. For a film bent on the circumference of a circle with the specimen at the center,  $x/r = 2\theta_n$  in radians, or  $360x/2\pi$ , where  $x$  is the displacement of the interference on the film and  $r$  is the effective radius of the curved film.

If it is known that the crystal is cubic, a single measurement of the spacing of planes parallel to the cube face  $d_{100}$  (or  $a_0$ ) on the spectrometer leads at once to the volume of the unit cell; if orthorhombic, three measurements of  $d_{100}$ ,  $d_{010}$ ,  $d_{001}$ , are made at right angles, etc. However, in most of the methods numerous other interferences appear which must be identified before complete analysis is possible, or the crystal system may be unknown and must be deduced from the x-ray data. It is evident that all the  $hkl$  planes in a crystal must be related in such a way that all the spacings can be calculated in terms of a fundamental value  $a_0$  together with information concerning axial ratios and angles. By the method of direction cosines or by pure lattice geometry it can be easily shown<sup>1</sup> that for a cubic crystal

$$n\lambda = \frac{2a_0}{\sqrt{h^2 + k^2 + l^2}} \sin \theta,$$

where  $a_0$  is the lattice constant or length of the unit cube edge, and  $h, k, l$ , the indices of any planes. Hence

$$d_{hkl} = \frac{a_0}{\sqrt{h^2 + k^2 + l^2}}.$$

If an unknown crystal is cubic, all the diffraction interferences must be related in this way; the usual method is therefore to correlate calculations with experimental values. In the same way equations may be derived for all other simple lattices. In general

$$n\lambda = 2d_{hkl} \sin \theta_n = \frac{2a_0}{\sqrt{F(hkl; abc; \alpha\beta\gamma)}} \sin \theta_n,$$

where  $abc$  are unit lengths in three dimensions, and  $\alpha\beta\gamma$  are axial

<sup>1</sup> WYCKOFF, "The Structure of Crystals," 2d ed., p. 78.

TABLE XXV.—CALCULATION OF INTERPLANAR SPACINGS,  $d_{hkl}$ 

System	$a:b:c$	$\alpha, \beta, \gamma$	$d_{hkl}$
Cubic. ....	1:1:1	$\alpha = \beta = \gamma = 90^\circ$	$\frac{a_0}{\sqrt{h^2 + k^2 + l^2}}$
Tetragonal. ....	1:1:c	$\alpha = \beta = \gamma = 90^\circ$	$\frac{a_0}{\sqrt{h^2 + k^2 + (l/c)^2}}$
Orthorhombic. ....	a:1:c	$\alpha = \beta = \gamma = 90^\circ$	$\frac{b_0}{\sqrt{(h/a)^2 + k^2 + (l/c)^2}}$
Hexagonal. ....	1:1:c	$\alpha = \beta = 90^\circ, \gamma = 120^\circ$	$\frac{a_0}{\sqrt{\frac{4}{3}(h^2 + hk + k^2) + (l/c)^2}}$
Rhombohedral. ....	1:1:1	$\alpha = \beta = \gamma = 90^\circ$	$\frac{a_0 \sqrt{1 + 2 \cos^3 \alpha - 3 \cos^2 \alpha}}{\sqrt{(h^2 + k^2 + l^2) \sin^2 \alpha + 2(hk + hl + kl)(\cos^2 \alpha - \cos \alpha)}}$
Monoclinic. ....	a:1:c	$\alpha = \gamma = 90^\circ, \beta \neq 90^\circ$	$\frac{b_0}{\sqrt{\frac{(h/a)^2 + (l/c)^2 - \frac{2hl}{ac} \cos \beta + k^2}{\sin^2 \beta}}}$
Triclinic. ....	a:1:c	$\alpha \neq \beta \neq \gamma \neq 90^\circ$	$\frac{b_0}{\sqrt{\frac{h/a}{k} \frac{h/a \cos \gamma \cos \beta}{l/c \cos \alpha} + \frac{1}{\cos \beta} \frac{h/a \cos \beta}{k \cos \alpha} + \frac{1}{l/c} \frac{\cos \gamma}{\cos \beta} \frac{h/a}{\cos \alpha}}}$

angles. Table XXV lists the formulas for  $d_{hkl}$  in convenient form.

From the mathematical expressions  $n\lambda$  may be calculated by substituting the values of  $d_{hkl}$  in  $n\lambda = 2d \sin \theta$ . For the cubic system therefore

$$n\lambda = \frac{2a_0}{\sqrt{h^2 + k^2 + l^2}} \sin \theta_n.$$

Squaring,

$$n^2\lambda^2 = \frac{4a_0^2}{h^2 + k^2 + l^2} \sin^2 \theta_n,$$

$$\sin^2 \theta_n = \left( \frac{n^2\lambda^2}{4a_0^2} \right) (h^2 + k^2 + l^2).$$

All the possible values of  $\sin^2 \theta_n$  may then be calculated when the cube edge length  $a_0$  and the wave length are known, assigning all values of  $hkl$ . These values are then compared with the experimental  $\sin^2 \theta$  values for the interferences appearing on the pattern and the crystallographic system is thus established. The interferences may be those on different photographs for different zones or all on the same film as in the powder method.

It is clear that with decreasing symmetry the number of possible interference maxima increases. The derivation of the quadratic form from the x-ray data therefore becomes different except in the cases of highest symmetry. In a cubic lattice it is possible to have 48 planes of the same form ( $hkl$ ) where  $h$ ,  $k$ , and  $l$  are all different, with the same spacing, and hence cooperating to produce only a single interference maximum; whereas in the triclinic lattice there are 24 different spacings and hence 24 reflection lines or spots corresponding to these  $hkl$  planes. Theoretically possible maxima may overlap and thus render derivation of the quadratic form and the crystal system practically impossible.

**Modes of Atomic and Molecular Arrangement from Intensity Data.**—While the  $d_{hkl}$  equations just considered give the positions of all the possible reflections for a given lattice, and no crystal of a given system can produce any additional interferences, it does not follow that they will all appear. Whether they all appear, or what are the possible reflections, is determined by the arrangement of atoms in the unit crystal cell. This is the most important aspect of the general problem of the effects of all variables on intensities.

Consider a series of planes all alike in a single crystal. If reflection is observed, the path difference from successive planes is  $2\pi$  or an integral multiple. The ratio of the amplitude of the wave scattered in a given direction by the electrons in the atom to that which would be scattered by a single electron in similar circumstances is designated by  $F$ . Now consider two parallel planes, one bearing  $P$  and the other  $Q$  atoms, and disposed from each other at a fraction  $a/x$  of the lattice constant or distance between  $P$  planes, and  $Q$  planes. The contribution from  $P$  planes with path difference  $2\pi n$  will be  $F_P$  and from the  $Q$  planes  $F_Q$ . The secondary x-ray waves from  $P$  and  $Q$  have a phase difference. If  $Q$  planes are exactly halfway between  $P$  planes, then waves from them will be exactly out of phase with waves from  $P$  when  $n$  is odd. The resulting amplitude or *structure factor*  $F'$  or  $\Sigma$  is the difference of the contributions from  $P$  and  $Q$  atoms or  $F_P - F_Q$ . It is a function, of course, of atomic numbers of  $P$  and  $Q$  and also of  $x$ . If other interleaving planes are present, the phase relationships between the waves from the various sequences of parallel planes may be very complicated but  $F'$  is determined by a summation of the  $F$  values,  $F_P, F_Q, F_R$ , etc., for each of the atoms modified by a phase factor  $\phi_P, \phi_Q, \phi_R$ , etc., expressing the distance of the atomic plane from the parallel geometric plane (e.g.,  $a/x$ ). From optics it can be shown that the square of the structure factor  $F'$  is the sum of squares of cosine and sine terms: or

$$F'^2 = A^2 + B^2,$$

where

$$A = F_P \cos \phi_P + F_Q \cos \phi_Q + F_R \cos \phi_R, \text{ etc.}$$

$$B = F_P \sin \phi_P + F_Q \sin \phi_Q + F_R \sin \phi_R, \text{ etc.}$$

For a cubic crystal simple equations for planes show that

$$\phi_P = 2\pi n (hx_P + ky_P + lz_P), \text{ etc.,}$$

where  $2\pi n$  is the phase difference between waves from geometrically like planes which reinforce, and the parallel plane passes through the atomic coordinate position  $x_P y_P z_P$ . Hence for crystals containing parallel planes of  $P, Q$ , and  $R$  atoms

$$A = F_P \cos 2\pi n (hx_P + ky_P + lz_P) + F_Q \cos 2\pi n (hx_Q + ky_Q + lz_Q), \text{ etc.}$$

$$B = F_P \sin 2\pi n (hx_P + ky_P + lz_P) + F_Q \sin 2\pi n (hx_Q + ky_Q + lz_Q), \text{ etc.}$$

From wave optics an experimental form may also be written

$$F' = F_P e^{2\pi ni(hx_P + ky_P + lz_P)} + F_Q e^{2\pi ni(hx_Q + ky_Q + lz_Q)} \text{ etc.}$$

If a lattice cell has two atoms of the same kind with coordinates  $xyz$  and  $x^1y^1z^1$ , the intensity of the interference from the planes  $hkl$  will be proportional to  $F'^2$ . If the atoms have the coordinates  $000$  and  $\frac{1}{2}\frac{1}{2}\frac{1}{2}$  (cubic as for iron, tungsten, etc.)

$$F' = e^{2\pi ni0} + e^{\frac{2\pi ni(h+k+l)}{2}} = 1 + e^{\pi ni(h+k+l)},$$

the structure factor for a body-centered lattice of an element (Fig. 108). Now when  $h + k + l$  is an even number, the latter factor will be 1 and  $F' = 2$ ; if  $h + k + l$  is an uneven number,

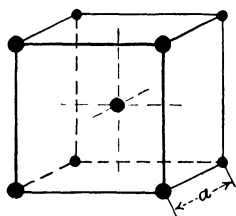


FIG. 108.—Body-centered cubic lattice (tungsten type).

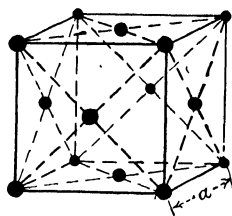


FIG. 109.—Face-centered cubic lattice (copper type).

$F' = 0$ . Thus all reflections will be missing on the diffraction pattern for planes, the sum of whose indices is an uneven number.

First the expression  $\sin^2 \theta = \frac{n\lambda}{4a_0^2} (h^2 + k^2 + l^2)$  gives all the possible reflections for the cubic lattice, while the structure factor  $F' = 1 + e^{\pi ni(h+k+l)}$  shows which of these will be missing from the particular variety of the cubic lattice known as body centered; *e.g.*, 100, 111, 210, 221, etc., will be absent.

For the face-centered cubic lattice (aluminum, copper, gold, etc.) the four atoms in the unit cell have the coordinates (see Fig. 109)  $000$ ,  $\frac{1}{2}\frac{1}{2}0$ ,  $\frac{1}{2}0\frac{1}{2}$ ,  $0\frac{1}{2}\frac{1}{2}$ . Thus

$$F' = 1 + e^{\pi ni(h+k)} + e^{\pi ni(h+l)} + e^{\pi ni(k+l)}.$$

If all three indices  $hkl$  are even numbers (including 0) or all odd numbers,  $F' = 4$  and the interferences will appear. If, however, the indices are mixed, partly odd and partly even numbers,  $F' = 0$  and interferences for these planes 001, 011, 012, 112, 122, 003, 013, 023, etc., will not appear.

To consider one more example we may select the cesium chloride type lattice, body-centered cubic with two kinds of atoms (Fig. 108) with  $P$  at 000 and  $Q$  at  $\frac{1}{2} \frac{1}{2} \frac{1}{2}$

$$F' = F_P(1) + F_Q e^{\pi i(h+k+l)};$$

when  $h + k + l$  is an even number  $F' = F_P + F_Q$  (for a lattice with only one kind of atom  $F' = 1 + 1$ ), while for  $h + k + l$  an odd number  $F' = F_P - F_Q$ . It is at once evident that if the scattering powers of  $P$  and  $Q$  were approximately the same, or in other words the effective atomic number the same as in  $\text{Cs}^+ \text{I}^-$  crystals, for  $h + k + l$  an odd number  $F' = F_{\text{Cs}^+} - F_{\text{I}^-} = 0$ , and thus reflections will be totally missing where they would be observed for  $\text{CsCl}$  or  $\text{CsBr}$ .

In this way structure factors may be derived for all the various lattice types and the atomic positions in the unit crystal cells properly interpreted. It is possible to ascertain the value of  $F'$  accurately from intensity data but the actual values of  $F'$ 's which contribute to  $F'$  and which measure the atomic scattering powers are still incompletely known. However, even with limited experimental data astonishingly satisfactory practical results are being obtained. Wyckoff has undertaken the task of determining the  $F$  curves for the atoms and lists the values so far available.<sup>1</sup> If all electrons in an atom were at the exact center point and scattered independently, the  $F$  curve would have a constant value equal to the number of electrons. But actually the electrons are distributed in space around this center and  $F$  must decrease as the diffraction angle  $2\theta$  increases. In order to calculate  $F$  values the fundamental intensity equation is applied.

The work of Darwin, Compton, Bragg, James, Bosanquet, Hartree, and others has led to the following formula for the absolute intensity  $\rho$  of integrated reflection by the face of an imperfect crystal:<sup>2</sup>

$$\rho = \frac{E\omega}{I} = \frac{1}{2\mu} n^2 \lambda^3 F^2 \frac{e^4}{m^2 c^4} \frac{1}{\sin 2\theta} \frac{1 + \cos^2 2\theta}{2} e^{-B \sin^2 \theta}.$$

<sup>1</sup> "Structure of Crystals," 2d ed., p. 100.

<sup>2</sup> Diamond is the only crystal which has given reflections agreeing with theoretical deductions for ideally perfect crystals, the intensity varying with the first power of  $F$ . In most cases the reflections are too intense but correspond to those from an ideally imperfect or mosaic crystal. It is for this case that the equation is derived. The majority of crystal specimens lie somewhere between the two ideal conditions.



Here  $E\omega/I$  is the experimental measurement on the ionization spectrometer,  $E$  the total ionization,  $\omega$  the angular velocity of the crystal in radians per second, and  $I$  the power of the incident x-ray beam (obtained by measuring a known crystal). The other symbols in the above formula are:  $\mu$  = linear absorption coefficient of the crystal;  $n$  = number of unit crystal cells in 1 c.c.;  $\lambda$  = the x-ray wave length;  $e$  and  $m$  = charge and mass of the electron;  $c$  = velocity of light;  $\Theta$  = the angle of incidence; and  $e^{-B \sin^2 \Theta}$  is the Debye factor, a correction term for temperature effects usually small and included in  $F$ . The symbol  $F$  stands for the ratio of the amplitude of the wave scattered by all atoms in the unit cell in the given direction, as compared with the wave scattered by a single electron in similar circumstances. Mathematically this can be stated:

$$F = Z \int_{D/2}^{D/2} p(z) \cos\left(\frac{2\pi n z}{D}\right) dz,$$

where  $Z$  is the atomic number,  $D$  is the grating space, and  $p(z)dz$  is the probability that an electron will lie at a height between  $Z$  and  $Z + dz$  above the atomic layer. The value of  $F$  varies with the direction of the incident and scattered x-ray beam as above explained and hence  $F$  curves against  $\sin \Theta/\lambda$  are plotted. The contribution of each atom to the scattered wave will depend on the arrangement of the electrons in the atom, and the combination of these contributions into a single scattered wave will depend on the relative positions of the atoms in the unit cell. In practice, therefore, the values of  $F'$  for a number of crystal planes are calculated from the observed intensities by x-ray reflection; from these values the atomic positions may be directly deduced. For example, in rock salt  $F' = F_{Na} - F_{Cl}$  for planes with all odd indices, such as the cube diagonal planes 111, and for other planes  $F' = F_{Na} + F_{Cl}$ . These lead directly to the curves for  $F_{Na}$  and for  $F_{Cl}$ .

It is evident from all the foregoing discussion that the actual intensity of a given x-ray diffraction interference depends upon a number of factors. A general expression is as follows:

$$I \propto H D \frac{P}{L} F^2 \text{ or } H e^{-B \sin^2 \Theta} \frac{1 + \cos^2 2\Theta}{\sin^2 \Theta \cos \Theta} F^2.$$

$F$  is the structure factor just considered.  $H$  is the cooperation factor taking into account the number of equivalent planes of

the same kind which cooperate to produce a single diffraction maximum varying from 2 for triclinic to 48 for  $(hkl)$  planes in certain cubic crystals.  $D$  is the Debye factor taking into account the increasing oscillations of atoms from a mean plane or position with temperature and is equal to  $e^{-B \sin^2 \theta}$  where  $B$  is a constant  $\alpha T/\lambda^2$  with  $\alpha$  calculated from the theory of specific heat.  $P$  is a factor which takes into account polarization of scattered radiation and is equal to  $1 + \cos^2 2\theta$ .  $L$  is the Lorentz factor taking into account overlapping reflections or departures from sharp reflections at the angle  $\theta$  and is expressed by  $\sin^2 \theta \cos \theta$ .

Two other effects on intensities have particular bearing on the discrepancies which have been observed between calculated and observed reflection intensities from actual crystals. These have been termed *primary* and *secondary extinction*. The first is the abnormally great absorption of an incident x-ray beam resulting from the fact that crystal fragments act as perfect crystals and upper layers of atoms shield the lower layers of the same homogeneous fragment from the intensity of the primary beam. Secondary extinction is a loss in intensity due to the fact that reflection from atomic planes in the interior of imperfect crystals is decreased by reflections from the tiny crystals making up the imperfect crystal nearer the surface. These effects are avoided by finely powdering the crystal before intensity measurements for  $F$  values are made.

Finally, the most recent method employed in analyzing diffraction effect is that of Fourier series, although the applications to periodic wave motions in sound and light have long been known. The suggestion was made by Bragg in 1915 and worked out by Duane first in 1925 with further development by Havighurst, Compton,<sup>1</sup> and others. If the amplitude of reflection in a number of orders is measured experimentally, a curve representing the electron distribution in sheets parallel to the geometric planes can be constructed by adding together the terms of the mathematical Fourier series. Such an equation has the form

$$Np(z) = N/d + 2(F_1'/d) \cos 2\pi z/d + 2(F_2'/d) \cos 4\pi z/d + 2(F_3'/d) \cos 6\pi z/d + \dots \text{etc.},$$

where  $N$  is the number of electrons in the atom,  $p(z)$  is the probability that one will be in a plane at the distance  $z$  from a

<sup>1</sup> For the best treatment see Compton, "X-rays and Electrons," New York, 1926.

geometrical plane,  $d$  is the interplanar spacing, and the  $F$ 's are measured from reflection intensities in several orders. The curves calculated from the above equation for electrons per A.U. plotted against height above a given plane have given good pictures of electron distributions in simple cases.<sup>1</sup> Extension of the series to three dimensions enables calculation of electron

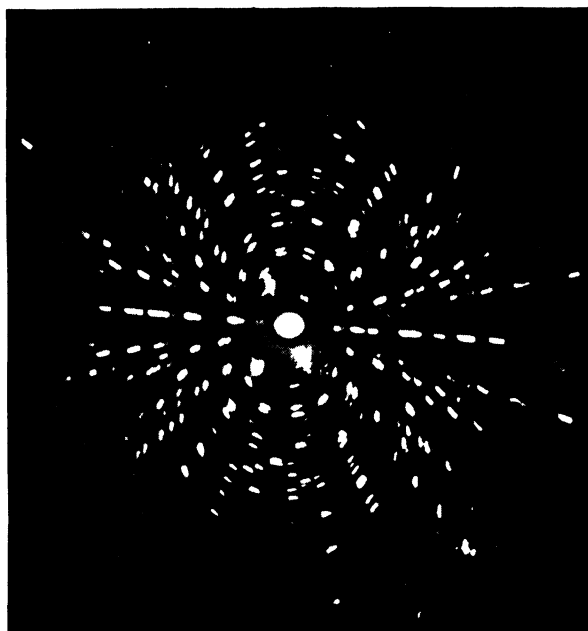


FIG. 110.—Laue pattern of single crystal of carborundum.

density along a given line in a crystal, and by this same method the variation in electron density in an *atom* from the center along the radius has been calculated. These are called  $U$  curves. Extensions to electron distribution in atoms of gases and liquids as well as solids from the intensities of scattering have been mentioned on page 100. Agreement of wave-mechanics calcula-

<sup>1</sup> As an excellent recent example of the application of the Fourier method may be cited Wyckoff's analysis of single crystal spectrometric data for urea, *Z. Kryst.*, **81**, 102 (1932). The  $F$  values of  $\text{NH}_2$  agree with those of  $\text{NH}_4$  in  $\text{NH}_4\text{Cl}$ ; the experimental C + O curve is practically identical with the sum of the carbon curve from graphite and the oxygen curve from metallic oxides.

tions with these data has given strong support to the newest atomic theories.<sup>1</sup>

**The Interpretation of Laue Photographs.**—The growing usefulness of this historically first method for obtaining information, even as to the probable space-group characteristics of a crystal, makes desirable some further comment upon interpretation, although detailed discussion is to be found in the several technical treatises on crystal analysis. A single Laue photograph taken alone yields only a limited amount of information. It appears as a series of spots (Fig. 110) whose loci are symmetrically disposed ellipses, passing through the central direct beam image if the primary beam has passed through the crystal parallel to a principal axis. The galaxy of spots is an indication of the ability of the many families of planes, each at a certain angle  $\Theta$  with respect to the primary x-ray beam, to pick out, from the assortment of rays of different wave lengths, the particular one for reflection according to  $n\lambda = 2d \sin \Theta$ . The symmetry is a proof of the orderly arrangement within the crystal, suggested by the external crystalline form. Thus if the beam passes parallel to a cubic axis, with fourfold symmetry, the pattern has a fourfold symmetry.

The spots<sup>2</sup> on any ellipse correspond to reflections taking place at a number of faces which have a common zone axis (*i.e.*, a row of atoms through which various planes pass). If the incident rays are inclined at an angle  $\Theta$  to the zone axis, the reflected rays will also make an angle  $\Theta$  with this axis, so that all the rays lie on a circular cone whose axis is that of the zone. The direction of the incident rays also lies on this cone; consequently the loci of the reflected spots are situated on the ellipse formed by the intersection of the cone with the photographic plate. Important zones of the crystal structure correspond to those ellipses which are densely packed with spots in the Laue diagram. The symbol of the zone which corresponds to each ellipse can be found and, since each spot may be considered as lying at the intersection of two ellipses, the plane which reflects it can be identified by cross-multiplication of the zone symbols.

<sup>1</sup> An exhaustive treatment of the present status of the whole subject of atomic structure factors is given by Ehrenberg and Schäfer, *Physik. Z.*, **33**, 97 (1932), and especially Wollan, *Rev. Mod. Phys.* **4**, 205 (1932).

<sup>2</sup> BRAGG and BRAGG, "X-rays and Crystal Structure," p. 279.

It is much more convenient, however, to use a system of projection in the assignment of indices to spots. The stereographic method converts the ellipses into circles. In Fig. 111 a crystal is at the center of a sphere which touches the photographic plate at the point  $N$ , where the direct beam  $SN$  is intercepted by the plate. The cone of reflected rays about any zone axis will cut the sphere in a circle which can be projected on the plate. A reflected spot appears on the plate at  $R$ . A line from  $S$  through  $Q$ , where the ray cuts the sphere, meets the plate at  $R'$ , the projection of  $R$ . This spot will be on a circle with the projections of the other spots originating from planes with a common zone axis.

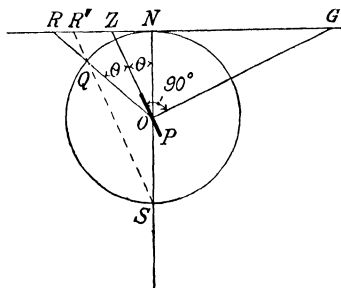


FIG. 111.—Method of stereographic projection.

A stereographic projection of potassium chloride is shown in Fig. 112. The Laue pattern of this simple cubic crystal is characterized by spots with perfectly regular distribution of intensities, at every intersection of circles. The Laue pattern for sodium chloride, on the other hand, differs in that the spots which

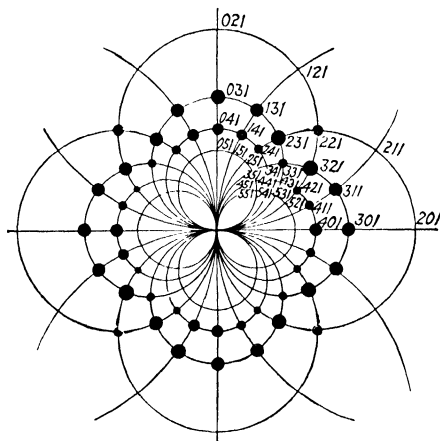


FIG. 112.—Stereographic projection of Laue pattern of KCl.

for KCl have odd and even indices (*e.g.*, 341) are absent. Thus the face-centered cubic lattice for which the structure factor predicts this very fact may be assigned as the underlying arrangement of the heavier chlorine atoms in rock salt.



ratios; for a rhombohedral or hexagonal close-packed lattice, it will be parallelograms with an angle of 120 deg. between sides, and so on. The indexing of the planes corresponding to each spot is usually not difficult, particularly when the axis of a crystal is normal to the plane of projection, say the  $Z$  or  $l$  index. This will then always be  $l$ , and  $X$  and  $Y$  (or  $h$ ,  $k$ ) can be read directly from the coordinates on the network. Thus for a cubic crystal in which the  $Z$  axis is perpendicular to the plane of pro-

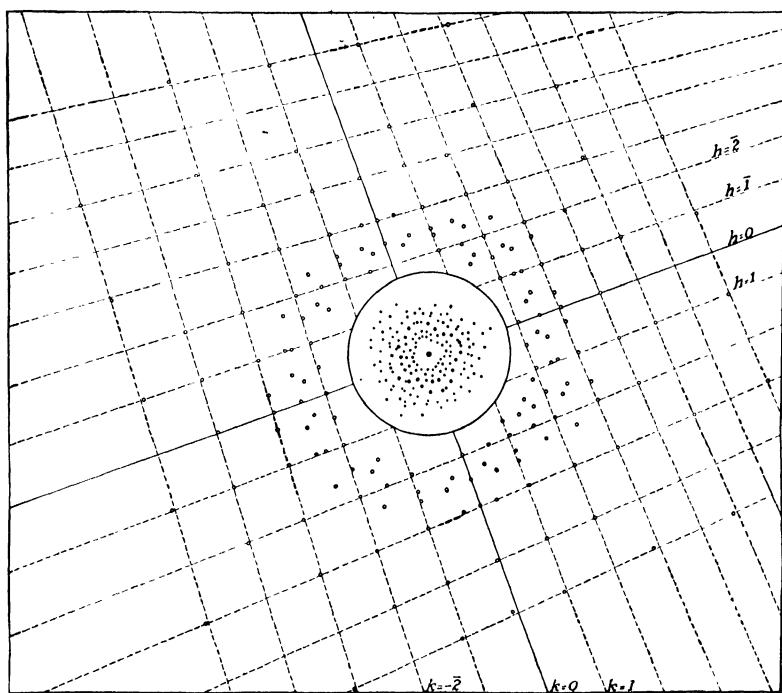


FIG. 114.—Gnomonic projection of an unsymmetrical Laue pattern of KI.

jection, or paper, a spot two squares to the right of the center and one square up would have the indices 211; a spot two to the right and one-half down is 412 [ $2 \times (2, \frac{1}{2}, 1)$ ], and so on.

Wyckoff has used, with great success, unsymmetrical Laue photographs, obtained by inclining one of the crystal axes to the beam. Such a result with a crystal of iron is reproduced in Fig. 83 which is to be compared with the symmetrical diagram in Fig. 82. In Fig. 114 is shown the gnomonic projection for such a photograph of a potassium iodide crystal.

The dimensions of the unit cell may be sometimes estimated from these data, and, of course, for cubic crystals the values of  $n\lambda$  for each spot are given by  $\sin \theta$  and  $a_0$  and  $hkl$  from the

$$\text{equation } n\lambda = \frac{2a_0}{\sqrt{h^2 + k^2 + l^2}} \sin \theta_n.$$

The fact that general radiation is employed, however, is always a complication. At moderate voltages, 50,000 kv., the maximum intensity in the spectrum is at 0.48 A.U., the characteristic absorption wave length of the silver in the emulsion. If the voltage is known,  $\lambda_{\min.}$  is, of course, at once established and this at once limits the possibilities of interpretation of Laue spots and eliminates some of the alternative possible unit crystal cells.

Intensity data from Laue patterns are not accurately determined but simply classed relatively by visual comparison on the photographic negative. Numerous complications are involved as explained earlier and in addition absorption in the crystal. However, the Laue data even though very approximate are sometimes very important, since by this method alone are reflections from planes of high indices and complicated structure registered. The greatest usefulness of the method therefore lies in conjunction with other methods with which quantitative information can be easily obtained.

**The Interpretation of Bragg Spectrum, Rotation, and Oscillation Patterns.**—When a single crystal is rotated around one of its principal crystallographic axes in the path of an x-ray beam defined by pinholes or slits, a very characteristic pattern is registered on the photographic film. It is called a layer line diagram because the interference maxima all lie on horizontal layers or lines. If a flat film is used, these lines are hyperbolas above and below a straight equatorial line. On a cylindrical film bent on the circumference of a circle at the center of which is the crystal the layer lines are straight lines parallel to the equator. Representative photographs are shown in Figs. 115 and 116. It follows that all the interference maxima lying on these layer lines are produced by planes with the same zone axis, namely, the common crystallographic and rotation axis. The spectrum is therefore "complete." The familiar Bragg spectra are, of course, produced by only one set of planes, the experimental arrangement of slits and crystal being such that other planes cannot register. The lines or spots lying on the equator of the



oscillation or rotation pattern therefore are really the "Bragg principal spectrum."

As explained in the preceding chapter, the angles between principal axes may be determined in many cases by reorienting the crystal on its goniometer head until sharp layer line diagrams are obtained. With three such rotation patterns corresponding to the three principal axes, the dimension of the unit crystal cell may be directly deduced. These patterns have the great advantage that one lattice spacing, namely, that for the atomic planes along the rotation axis, may be measured independently of any assumption as to crystal system or planar indices. It is necessary only to

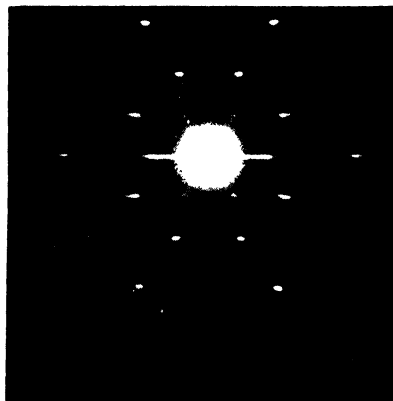


FIG. 115.—Typical rotation pattern (chrysotile) on flat film showing layer lines as hyperbolas.

measure the distances  $e_1, e_2 \dots e_n$  of the vertices of the hyperbolas on the tangent film (or the straight layer lines on a film which had been bent on a cylinder coaxial with the specimen) from the central zero point of the main beam. The distance



FIG. 116.—Typical rotation pattern (3,3—diamino-dimesityl) on cylindrical film.

from specimen to film,  $a$ , being known, the diffraction angles  $\mu_1, \mu_2 \dots \mu_n$  (Fig. 117) may be calculated, since the tangents are  $e_n/a$ . The identity period or spacing along the rotation axis is then simply calculated from

$$I = n\lambda/\sin \mu_n,$$

where  $n$  is the number of the layer line (1, 2, 3, etc.). Then

identically the same value is obtained from all the layer lines. Three such values of  $I$  for each of the principal axes give the size of the unit cell.

The process of assigning indices to the interference maxima lying on the layer line is usually straightforward. Thus on the

equatorial line the index  $h_3$  in  $h_1h_2h_3$  is zero; in other words all indices must be  $h_1h_20$ ;  $h_2$  must be 1 on the first horizontal layer

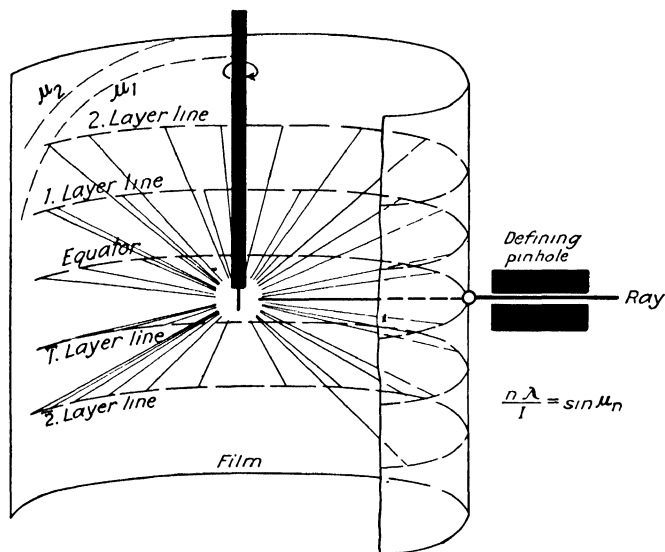


FIG. 117.—Diagrammatic representation of the rotation method.

line, 2 on the second, etc. These maxima lie not only on horizontal layer lines but also on vertical loci which are zone curves

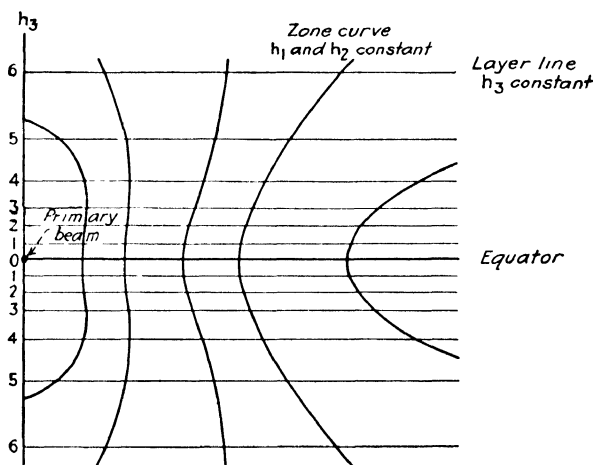


FIG. 118.—Diagram of two types of layer lines on rotation patterns.

(Fig. 118). Schiebold calculated these two types of layer lines (*Schichtlinien*) of the I and II kind. Thus if the first maximum

on the equator is due to 100 planes, then the spot on the first layer line lying on the common vertical zone curve is 101; if the second spot on the equator is 110, the spot above or below it on the first layer line and the second zone curve is 111. It is at once evident that oscillation photographs taken over a fixed angle are much simpler to interpret than a composite pattern made for a complete rotation around 360 deg. The matter of interpretation may become very complex, of course, if the number of maxima on a rotation pattern is large, or if the axis of rotation or oscillation is not a principal crystallographic axis. Fortunately these cases in practical crystal structure analysis are rare. However, rigorous methods of indexing have been worked out by Schiebold<sup>1</sup> and Bernal<sup>2</sup> employing the conception of the reciprocal lattice<sup>3</sup> and graphical nets. Inasmuch as the great majority of experimental results can be interpreted by the very simple means described above, these more rigorous procedures will not be presented here, and the reader is referred to the original articles.

Besides giving direct information concerning the crystallographic system, and the dimensions and shape of the unit cell together with the number of atoms or molecules per unit cell, these spectrum photographs permit space-group assignment. When the interference maxima have been identified with the planar indices, the presence or absence of possible reflections can at once be noted and the criteria for a specific space-group set up.

The advantages of the Weissenberg modification of the rotation method, in which the film is moved parallel to the axis of rotation, have already been noted. An important equation for the interpretation of these patterns is  $\sigma = \frac{1}{R}\Delta\eta - \frac{\Delta\xi \cdot 90^\circ}{\pi a}$  where  $\sigma$  is the angle between lattice plane normals,  $R$  is the translation of the films in millimeters during a revolution of 1 deg.,  $\Delta\xi$  the difference in abscissas of two interference points,  $\Delta\eta$  the ordinate difference, and  $a$  is the distance of the crystal from the photo-

<sup>1</sup> SCHIEBOLD, *Fortschritte Mineral., Kryst. Petro.*, **11**, 113 (1923).

<sup>2</sup> BERNAL, *Proc. Roy. Soc. (London)*, **113A**, 117 (1926).

<sup>3</sup> In the reciprocal lattice originally worked out by Ewald, *Z. Kryst.*, **56**, 129 (1921), the points, each of which represents a plane of the crystal, lie along normals through the origin to these planes at distances inversely to the spacings  $d_{hkl}$ . The mathematical calculations are greatly simplified obviously by representing planes as points.

graphic film. Since only one layer line is used in the Weissenberg goniometer, the assignment of indices as illustrated in Fig. 95 is usually not difficult, particularly when a pattern with stationary film is used in conjunction. The great power of the method, of course, lies in the separation of interferences for planes of the same indices which would normally cooperate to produce the same diffraction maximum. Any overlapping interferences which render intensity estimation difficult can thus be separated.

**The Interpretation of Powder Spectra.**—This subject is practically completely covered in the first part of this chapter under the discussion of the positions and intensities of interferences. In this method there is simultaneous registration of all sets of planes due to the random distribution of fine grains. If the crystal system and unit-cell dimensions are known from independent measurements with single crystals, the assignment of indices is not difficult, since  $d_{hkl} = \frac{a_0}{\sqrt{F(hkl; abc; \alpha\beta\gamma)}}$  or for the cubic system  $d_{hkl} = \frac{a_0}{\sqrt{h^2 + k^2 + l^2}}$ . Under the discussion of intensities and structure factors a differentiation was found for

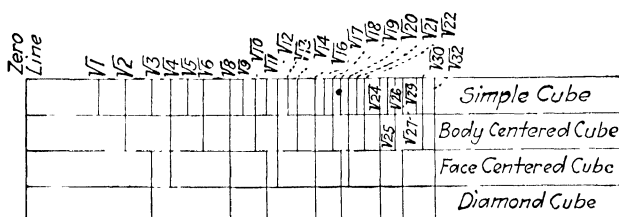


FIG. 119.—Diagrammatic representations of powder spectra for cubic lattices.

simple, body-centered, and face-centered cubic lattices depending upon non-appearance of reflections for certain planes. The structure factor clearly indicates that if all possible values of  $hkl$  appear the crystal is simple cubic; for the body-centered lattice the sum of  $hkl$  indices must be even and 110, 200, 211, 220, 310, 222, 321, 400, etc., will appear, and for the face-centered cubic lattice the indices must be all odd or all even as in 111, 200, 311, 222, 400, etc. The powder spectra are illustrated in a diagram in Fig. 119. It will be noticed that even for the cubic system lines related to  $\sqrt{7}$ ,  $\sqrt{15}$ ,  $\sqrt{23}$ ,  $\sqrt{28}$ ,  $\sqrt{31}$ , etc., are absent, since in  $\sqrt{h^2 + k^2 + l^2}$  no sum of squares of integers will give these

numbers. If values of  $a_0$ , etc., are unknown, trial and failure methods may be successfully used. Thus for a cubic crystal

$$d_{hkl} = \frac{a_0}{\sqrt{h^2 + k^2 + l^2}} = \frac{n\lambda}{2\sin\Theta_n}$$

$$\frac{4a_0^2 \sin^2 \Theta_n}{\lambda^2} = (h^2 + k^2 + l^2)n^2.$$

Any two powder spectrum lines must have  $\sin^2 \Theta_n$  values which will be in the ratio of whole numbers, since  $(h^2 + k^2 + l^2)n^2$  is always an integer and  $a_0$  and  $\lambda$  are constant. For other systems the ratio will not be that of whole numbers. In systems of lower symmetry than cubic (in which only the cube edge length need be known) the calculations from quadratic equations listed in Table XXV may become increasingly difficult, particularly when the crystal system is unknown. Numerous criteria have been set forth but most useful probably is the graphic method of Hull and Davey<sup>1</sup> for the hexagonal, rhombohedral, tetragonal, and partially the orthorhombic systems. For each system the logarithms of the spacing  $d$  calculated for each set of planes are plotted against axial ratios. The experimental data are plotted to the same logarithmic scale and then moved over the graph until a match is found, thus identifying system and axial ratios as well as planar indices for each interference.

The following facts are obvious in the interpretation of these line crystal spectra:

1. Only definite lines in a definite pattern correspond to a pure crystalline substance.
2. Foreign lines indicate the presence of other crystalline substances as impurities; each entity produces its own spectrum if present in sufficient quantity (above 0.2 to 1 per cent usually) and the comparison of intensities is a method of quantitative analysis.
3. Solid solution is indicated by no change in the pattern of lines of a pure constituent, but in a shift in position of the lines, toward smaller angles (nearer the zero main beam) if the lattice is expanded by the addition of foreign atoms, or to larger angles if contracted. In many cases the lattice spacing is linearly related to atomic percentage of constituents of a solid solution alloy, as will be illustrated later.

<sup>1</sup> For example, *Phys. Rev.*, **17**, 266, 549 (1921).

4. The powder method may be made very accurate in evaluating the lattice constant of a pure substance and from this the ideal density of the material. The value for tungsten so obtained has been of utmost value in vacuum-tube applications where tungsten filaments are employed.

5. The widths of the diffraction lines serve as a means of determining grain size in the specimen as will be demonstrated in a later section.

6. Any departure of the powder or aggregate from purely random arrangement, which results in continuous diffraction

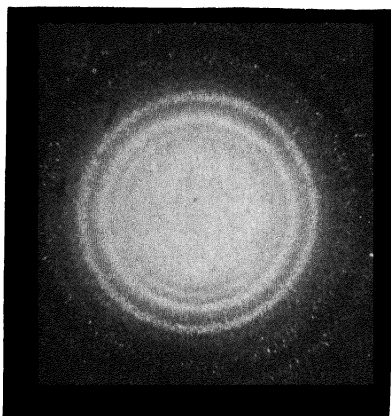


FIG. 120.—Pinhole pattern illustrating effect of large grain size (black diamond or carbonado used in mining drills) with pattern characteristic of an aggregate of diamond crystals.

circles or lines of uniform intensity, is manifested by the patterns. Thus if the grains are too large to permit the probability of random arrangement, the lines become spotted and dashed due to reflection from individual grains (Fig. 120). In general, the grain diameter must be smaller than  $10^{-3}$  cm. to prevent this. Most metals with grains which will pass through a 200-mesh sieve will give uniform lines. Again if the grains are sufficiently small but are oriented in some preferred

direction, as by some deforming force, some lines may become shortened or disappear or assume localized intensity maxima. This process of fibering will be now considered.

**The Monochromatic Pinhole Method.**—Figure 98 taken by the monochromatic pinhole method is reproduced as an example of the structure of a natural fiber, asbestos. This mineral is not a single crystal, since otherwise it would give a Laue pattern of symmetrical spots. But neither is it constituted of grains in random arrangement, since this would mean a pattern of concentric uniformly intense rings. It may be seen, however, that circles may still be drawn through the diffraction maxima, although the more prominent loci are hyperbolas. These would be parallel straight horizontal lines (as in Fig. 116) if a cylindrical film had been used instead of a flat one. In this mineral, there-

fore, the grains are oriented in a common direction with respect to the fiber axis. The pattern is typical of a fibered aggregate. It should be noted that the pattern obtained by rotating a crystal around a principal axis is a layer line diagram exactly like that produced by a fiber without rotation. With a fiber, of course, only one such result is obtainable, while with a single crystal three patterns corresponding to rotations around the three principal axes are possible. Now a fine-grained aggregate may be made fibered by rolling or drawing in one direction, as shown by Fig. 121 for cold-drawn aluminum wire. The desirability of a pattern 360 deg.

in azimuth is at once apparent if the degree of fiber-  
ing is to be estimated and if the actual location of the symmetrically placed maxima is to be used in the determination of the mechanism of deformation by mechanical work as explained in a later section. A fiber diagram has a great advantage over an ordinary powder pattern and this is that a measurement of a lattice

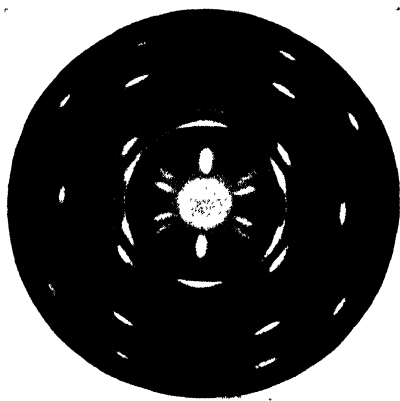


Fig. 121.—Fiber diffraction pattern for cold-drawn aluminum wire.

spacing, namely, the atomic plane periodicities along the fiber axis, may be made independently of any assumption as to crystal system or planar indices. It is necessary only to measure the distances  $e_1, e_2, e_3 \dots e_n$  of the vertices of the hyperbolas (or of the straight layer lines on a film which had been bent on a cylinder coaxial with the specimen) from the central zero point of the main beam. Knowing the distance from specimen to film,  $a$ , the diffraction angle  $\mu_1, \mu_2 \dots \mu_n$  may be calculated, since the tangents are  $e_n/a$ . The identity period or spacing along the fiber axis is then simply calculated from  $I = n\lambda/\sin \mu_n$ , where  $n$  is the number of the layer line (1, 2, 3, etc.). Thus identically the same value is obtained from all the layer lines. For the other lattice spacings it is necessary, of course, to interpret the pattern exactly as in the powder method since the Debye-Scherrer circles may still be evident. The degree of perfection of preferred orientation is,

of course, indicated at once by the patterns, since there may be a continuous transition between the concentric circles for a random aggregate and the sharp horizontal layer lines for perfect fibering.

While this method has come to be most generally associated with the fiber state, it follows that it is only a special case of the Laue method and of the powder method. It is generally employed in all of the metallurgical studies involving fibering in fabrication, internal strain, annealing, and recrystallization.

**The Complete Determination of Crystal Structure.**—From the results of one or more of the crystal-structure methods interpreted as briefly outlined in this chapter the complete analysis of a given crystal in terms of the exact coordinates in space even of the ultimate atoms in molecules may be made. The steps in this procedure have been outlined on page 182. Actually a considerable training and experience are required for the analysis of the more complicated substances which now occupy the attention of x-ray scientists, since probably nearly all of the simplest types of crystals have now been studied. The attempt will not be made here to carry through a complete analysis from experimental data, since this is not intended to be a technical handbook and since the chief interest is in generalization from results to date. However, in the chapter on organic compounds, the procedure employed by Mrs. Lonsdale in her painstaking and classical analysis of the shape of the hexamethyl benzene molecule will be outlined. All of the next chapter dealing with results, of course, has depended on carrying through analyses in the stepwise fashion already referred to.



## CHAPTER XIII

## THE RESULTS OF CRYSTAL ANALYSIS: ELEMENTS AND INORGANIC COMPOUNDS

**The Chemical Elements.**—By the methods of x-ray analysis outlined in the preceding chapter about 65 of the known chemical elements (the discovery of the last of the 92 was announced in November, 1931) have been assigned definite lattice structures in the solid state. Pure metals are, of course, chemical elements;

	0	1	2	3	4	5	6	7	8		1	2	3	4	5	6	7	8								
1	H																		He							
2	He	Li	Be																	Be	B	C	N	O	F	Ne
3	Ne	Na	Mg																	Mg	Al	Si	P	S	Cl	Ar
4	Ar	K	Ca	Sc	Ti	V	Cr	Mn	Fe	Co	Ni	Cu	Zn	Ga	Ge	As	Se	Br	Kr							
5	Kr	Rb	Sr	Y	Zr	Cb	Mo	Mn	Ru	Rh	Pd	Ag	Cd	In	Sn	Sb	Te	I	Xe							
6	Xe	Cs	Ba	<i>5f1</i>	Hf	Ta	W	Re	Os	Ir	Pt	Au	Hg	Tl	Pb	Bi	Po	At	Rn							
7	Rn	—	Ra	Ac	Th	Pa	U	—	—	—	—	—	—	—	—	—	—	—	—							
		6	La	Ce	Pr	Nd	Il	Sm	Eu	Gd	Tb	Dy	Ho	Er	Tu	Yb	Lu									

## KEY







	Face-centered cubic		Hexagonal close-packed
	Body-centered cubic		Diamond type
	Arsenic type		Selenium type

FIG. 122.—Periodic table of chemical elements showing crystal structures.

every metal except a few of the rarest in nature may be classified now according to the pattern by which its atoms form crystals, and according to the numerical values which define the unit crystal cell. Fortunately for practical purposes most of the metals are grouped in a very few crystal systems, the majority being face-centered and body-centered cubic and hexagonal close

TABLE XXVI.—LATTICE TYPES OF THE ELEMENTS

Type element	Space lattice	Space-group	Type symbol (Ewald-Hermann)	Figure number	Elements and modifications	Atomic coordinates	Z = atoms per unit cell	Most important planes	Coordination number
Copper	Face-centered cubic FCC	$O_h^{15}$	A 1	109	Ag, Al, A, Au, Ca, $\beta$ -Ce, $\beta$ -Co, Cu, $\beta$ -Fe, Ir, Kr, Ne, $\beta$ -Ni, Pb, Pd, Pt, Rh, Sr, Th, $\beta$ -Ti, Xe Ba, Cb(Nb), $\alpha$ -Cr, Cs, $\alpha$ -Fe, K, Li, Mo, Na, Rb, Ta, Tl, V, $\alpha$ -W	$000, \frac{1}{2}, \frac{1}{2}, 0, \frac{1}{2}$ $0, \frac{1}{2}, 0, \frac{1}{2}, \frac{1}{2}$	4	111, 100, 110	Atom at 000 $12 [\frac{1}{2}, \frac{1}{2}, 0]$ 6 [100]
Tungsten ( $\alpha$ )	B o d y-centered cubic BCC	$O_h^{15}$	A 2	108	Cs, $\alpha$ -Fe, K, Li, Mo, Na, Rb, Ta, Tl, V, $\alpha$ -W	$000, \frac{1}{2}, \frac{1}{2}, \frac{1}{2}, \frac{1}{2}$	2	110, 100, 111	Atom at 000 $8 [\frac{1}{2}, \frac{1}{2}, \frac{1}{2}]$ 6 [100]
Magnesium	Hexagonal close-packed HCP	$D_{6h}^{14}$	A 3	123	Be, Cd, $\alpha$ -Ce, $\alpha$ -Co, $\alpha$ -Ni, $\beta$ -Cr, Er, Hf, Ca, Mg, Os, Re, Ru, Ta, $\alpha$ -Ti, Zn, Zr C (diamond), Ge, Si, $\alpha$ -Sn (gray)	$000, \frac{2}{3}, \frac{2}{3}, \frac{1}{4}$	2	0001, 11 $\bar{2}$ 0 11 $\bar{2}$ 1, 11 $\bar{2}$ 2 1010, 1011	Atom at $\frac{1}{3}$ $\frac{2}{3}, \frac{1}{4}, 6[100]$ 6 $[\frac{1}{3}, \frac{2}{3}, \frac{1}{2}]$ 6 $[\frac{1}{3}, \frac{2}{3}, \frac{1}{2}]$ 4
Diamond (carbon)	Two interpenetrating FCC	$O_h^{17}$	A 4	124	$\beta$ -Sn (white)	As in A 1 with $000$ and $\frac{1}{4}, \frac{1}{4}, \frac{1}{4}$ as origins in turn	8	110, 100, 112 111	4, 2, 4, 8 4, 8, 4, 2 3, 6, 1
$\beta$ -Tin (white)	Double BC tetragonal	$D_{4h}^{19}$	A 5		Indium	$000, 0, \frac{1}{2}, \frac{1}{4}, \frac{1}{4}, \frac{1}{2}, \frac{1}{2}$ $000, \frac{1}{2}, \frac{1}{2}, \frac{1}{2}, \frac{1}{2}$ $000, \frac{1}{2} + \Delta, \frac{1}{2} + \Delta, \frac{1}{2} + \Delta$	4	010, 110, 112 000, 101	2, 4, 6
Indium	BC tetragonal	$D_{4h}^{17}$	A 6		As, Bi, P (black), Sb		2	110, 112, 110, 100, 111	2, 4, 6
Arsenic	BC Rhombohedral (deformed simple cubic)	$D_{3d}^{15}$	A 7		Se, Te		2		2, 3, 6
Selenium (hexagonal)	Hexagonal (deformed simple cubic)	$D_{3h}^{14}$ or $D_{3d}^{15}$	A 8		Graphite (C)	$000, 00, \frac{1}{2}, \frac{1}{3}, \frac{2}{3}$ $\frac{1}{3}, \frac{2}{3}, \frac{1}{3}, \frac{2}{3}, \frac{1}{2} + \frac{1}{2}$ $(p < 0.02)$ $\frac{1}{3}, \frac{2}{3} \pm u, \frac{2}{3}, \frac{1}{3}$ $\frac{1}{2} \pm u$ Complex	3	10 $\bar{1}$ 1, 01 $\bar{1}$ 2 0001	6 (5 in one layer)
Graphite (carbon)	Hexagonal	$D_{6h}^{14}$	A 9	141	Hg		4	0001, 10 $\bar{1}$ 0, 11 $\bar{2}$ 0, 1011, 1121	2, 3, 6
Mercury	Rhombohedral	$D_{3d}^{15}$	A 10		Ga		4	110, 111, 110	6
Gallium	Tetragonal (simple)	$D_{4h}^{16}$	A 11						

TABLE XXVIa.—NEW UNCLASSIFIED TYPES FOR INCOMPLETELY ANALYZED STRUCTURES

(See Table XXVII for details)

Type element	Space lattice	Space-group
Iodine. . . . .	Rhombic	$V_h^{18}$
$\alpha$ -Manganese, $\gamma$ -chromium	BCC (special)	$T_d^3$
$\beta$ -Manganese	Cubic	$O^6, O^7$
$\alpha$ -Nitrogen	Cubic	$T^4$
$\beta$ -Tungsten . . . .	Cubic	$O^2$ or $O_h^3$
Sulfur . . . . .	FC rhombic	$V_h^{24}$
Se (monoclinic) . . .	Monoclinic	$C_{2h}^2$
Parahydrogen . . .	Hexagonal	?
Oxygen . . . . .	BC rhombic	?
White phosphorus	Cubic	?

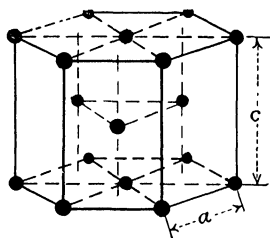


FIG. 123.—Hexagonal close-packed lattice (zinc type).

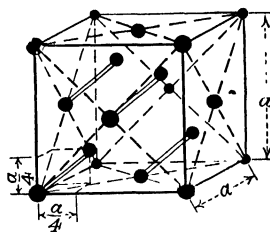


FIG. 124.—Tetrahedral cubic lattice (diamond type).

packed. In addition, some of the metallic as well as non-metallic elements crystallize in more than one modification, iron being an outstanding example. In Fig. 122 the periodic table of elements is used as a basis for a graphical representation of lattice types. These types are further listed and defined in Table XXVI and finally Table XXVII presents in detail the most recent and reliable data for the elements alphabetically arranged.<sup>1</sup>

<sup>1</sup> From an excellent and painstaking summary by Neuberger, *Z. Kryst.*, **80**, 103 (1931). This paper gives complete formulas for calculating distance between atoms, atomic radius, atomic volume, packing density, volume of the unit cell, etc.

TABLE XXVII.—LATTICE CONSTANTS, 1932

Element and modification	Atomic number	Atomic weight, 1931	Density (roentgenographic)	Space lattice space-group lattice type	Number of atoms per unit cell	Edge lengths $a, b, c$	Axial angles	Atomic radius, $r_A$ in Å U.	Remarks
Aluminum, Al . .	13	26.97	2.699	FCC $O_h^s$ A 1	4	$a = 4.0402 \pm 0.0004$		1.428	
Antimony, Sb . .	51	121.76	6.67	Rhombohedral $D_{2d}^s$ A 7	2	$a = 4.501 \pm 0.003$	$\omega = 57^\circ 3'$	1.449	Simple rhombohedral
					8	$a = 6.226 \pm 0.004$	$\omega = 87^\circ 24'$		FC rhombohedral
Argon, A . . .	18	39.94	1.65	FCC $O_h^s$ A 1	4	$a = 5.42 \pm 0.02$		1.191	At $40^\circ$ Abs.
Arsenic (metallic), As.	33	74.93	5.71	Rhombohedral $D_{2d}^s$ A 7	2	$a = 4.151$	$\omega = 53^\circ 49'$	1.254	Simple rhombohedral
					8	$a = 5.599$	$\omega = 84^\circ 18'$		FC rhombohedral
Barium, Ba	56	137.36	3.59	BCC $O_h^s$ A 2	2	$a = 5.015 \pm 0.003$		2.171	
Beryllium, Be	4	9.02	1.83	Hexagonal $D_{6h}^s$ A 3	2	$a = 2.28$ $c = 3.61$		1.11	
Bismuth, Bi	83	209.00	9.72	Rhombohedral $D_{2h}^s$ A 7	2	$a = 4.749 \pm 0.005$	$\omega = 57^\circ 16'$	1.556	Simple rhombohedral
					8	$a = 6.578 \pm 0.007$	$\omega = 87^\circ 34'$		FC rhombohedral

TABLE XXVII.—LATTICE CONSTANTS, 1932.—(Continued)

Element and modification	Atomic number	Atomic weight, 1931	Density (roentgenographic)	Space lattice space-group lattice type	Number of atoms per unit cell	Edge lengths $a, b, c$	Axial angles	Atomic radius, $r_A$ in A. U.	Remarks
Cadmium, Cd	48	112.41	8.64	Hexagonal $D_{6h}^4$ A 3	2	$a = 2.973 \pm 0.003$ $c = 5.606 \pm 0.006$		1.486	
Calcium, Ca . . .	20	40.07	1.53	FCC $O_h^3$ A 1	4	$a = 5.56$		1.96	
Carbon, C Diamond . . . . .			3.511	FCC $O_h^7$ A 4	8	$a = 3.5597 \pm 0.001$		0.770	At 18° C.
Graphite . . .	6	12.000	2.19	Hexagonal $D_{6h}^4$ A 9	4	$a = 2.48$ $c = 6.78$		0.71	
Cerium, Ce $\alpha$ . . .			6.78	Hexagonal $D_{6h}^4$ A 3	2	$a = 3.65$ $c = 5.91$		1.81	
$\beta$ . . .	58	140.13	6.89	FCC $O_h^3$ A 1	4	$a = 5.12$		1.81	
Cesium, Cs . .	55	132.81	1.98	BCC $O_h^9$ A 2	2	$a = 6.05 \pm 0.03$		2.62	At 100° Abs

TABLE XXVII.—LATTICE CONSTANTS, 1932.—(Continued)

Element and modification	Atomic number	Atomic weight, 1931	Density (roentgeno- graphic)	Space lattice space-group lattice type	Number of atoms per unit cell	Edge lengths <i>a</i> , <i>b</i> , <i>c</i>	Axial angles	Atomic radius, <i>r<sub>A</sub></i> in A U.	Remarks
Chromium, Cr <i>α</i> . . . . .	24	52.01	7.20	BCC <i>O<sub>h</sub><sup>9</sup></i> A 2	2	<i>a</i> = 2.878 ± 0.003	. . . . .	1.246	
			6.07	Hexagonal <i>D<sub>6h</sub><sup>4</sup></i> A 3	2	<i>a</i> = 2.717 <i>c</i> = 4.418	. . . . .	1.354	
			7.51	BCC <i>T<sub>d</sub><sup>3</sup></i> <i>α</i> -Mn type	58	<i>a</i> = 8.717	. . . . .	0.522 1.021 1.164, 1.222	
Cobalt, Co <i>α</i> . . . . .	27	58.94	8.65	Hexagonal <i>D<sub>6h</sub><sup>4</sup></i> A 3	2	<i>a</i> = 2.514 ± 0.005 <i>c</i> = 4.105 ± 0.008	.	1.256	
			8.67	FCC <i>O<sub>h</sub><sup>3</sup></i> A 1	4	<i>a</i> = 3.554 ± 0.005	. . .	1.256	
			8.93	FCC <i>O<sub>h</sub><sup>3</sup></i> A 1	4	<i>a</i> = 3.608 ± 0.001	. . .	1.275	
Erbium, Er . . .	68	167.64	7.49	Hexagonal <i>D<sub>6h</sub><sup>4</sup></i> A 3	2	<i>a</i> = 3.74 <i>c</i> = 6.09		1.86	

TABLE XXVII.—LATTICE CONSTANTS, 1932.—(Continued)

Element and modification	Atomic number	Atomic weight, 1931	Density (roentgenographic)	Space lattice space-group lattice type	Number of atoms per unit cell	Edge lengths $a, b, c$	Axial angles	Atomic radius, $r_A$ in A.U.	Remarks
Gallium, Ga. . .	31	69.72	6.02	Tetragonal $D_{4h}^{16}$ A 11	8	$a = 4.51$ $c = 7.51$	.	1.24	
Germanium, Ge .	32	72.60	5.32	FCC (diamond) $O_h^7$ A 4	8	$a = 5.647$		1.222	
Gold, Au. . . .	79	197.2	19.301	FCC $O_h^5$ A 1	4	$a = 4.0702 \pm 0.0006$		1.439	
Hafnium, Hf .	72	178.6	13.09	Hexagonal $D_{6h}^4$ A 3	2	$a = 3.200 \pm 0.002$ $c = 5.077 \pm 0.005$		1.569	
Hydrogen, H <sub>2</sub> (para).	1	1.0078	0.089	Hexagonal ?	4	$a = 3.75$ $c = 6.11$			At 2° Abs 2 H <sub>2</sub>
Indium, In . . . .	49	114.8	7.43	Tetragonal FC $D_{4h}^{17}$ A 6	4	$a = 4.58$ $c = 4.86$		1.62	
Iodine, I <sub>2</sub>	53	126.93	4.92	Rhombohedral $V_h^{18}$ characteristic type	8	$a = 4.795 \pm 0.004$ $b = 7.255 \pm 0.007$ $c = 9.780 \pm 0.009$		1.351 1.769	4I <sub>2</sub> groups

TABLE XXVII.—LATTICE CONSTANTS, 1932.—(Continued)

Element and modification	Atomic number	Atomic weight, 1931	Density (roentgenographic)	Space lattice space-group lattice type	Number of atoms per unit cell	Edge lengths $a, b, c$	Axial angles	Atomic radius, $r_A$ in A.U.	Remarks
Iridium, Ir...	77	193.1	22.80	FCC $O_h^3$ A 1	4	$a = 3.823 \pm 0.002$		1.351	
Iron, Fe $\alpha$ . . . . .  $\gamma$ . . . . .	26	55.84	7.868	BCC $O_h^3$ A 2	2	$a = 2.86106 \pm 0.00003$		1.2389	At 22° C. $\beta$ and $\delta$ -Fe same
			8.15	FCC $O_h^3$ A 2	4	$a = 3.562 \pm 0.003$		1.259	At room temperature (extrapolated)
Krypton, Kr	36	82.9	3.13	FCC $O_h^3$ A 1	4	$a = 3.63$		1.28	At 1100° C.
						$a = 5.59$		1.97	At 20° Abs
Lanthanum, La.	57	138.90	6.30	Hexagonal $D_{6h}^4$ A 3	2	$a = 3.72$ $c = 6.06$		1.86	
Lead, Pb	82	207.21	11.33	FCC $O_h^3$ A 1	4	$a = 4.941 \pm 0.002$		1.747	
Lithium, Li	3	6.940	0.55	BCC $O_h^3$ A 2	2	$a = 3.46 \pm 0.02$		1.50	At 100° Abs.



TABLE XXVII.—LATTICE CONSTANTS, 1932.—(Continued)

Element and modification	Atomic number	Atomic weight, 1931	Density (roentgenographic)	Space lattice space-group lattice type	Number of atoms per unit cell	Edge lengths $a, b, c$	Axial angles	Atomic radius, $r_A$ in $\text{\AA}$ U	Remarks
<b>Magnesium, Mg.</b>	12	24.32	1.74	Hexagonal $D_{6h}^{14}$ A 3		$a = 3.203 \pm 0.002$ $c = 5.196 \pm 0.003$	.....	1.594	
<b>Manganese, Mn</b> $\alpha$ . . . . .			7.47	BCC $T_d^2$ characteristic type	58	$a = 8.894 \pm 0.005$		0.532 1.042 1.188 1.247	At room temperature
	25	54.93	7.25	Cubic $O_h$ or $O_h^7$ characteristic type	20	$a = 6.300 \pm 0.003$	.	1.184 1.265	At room temperature
			7.21	Tetragonal FC $D_{4h}^{17}$ A 6	4	$a = 3.774 \pm 0.005$ $c = 3.526 \pm 0.008$	.	1.291	At room temperature (extrapolated)
<b>Mercury, Hg</b>	80	200.61	14.29	Rhombohedral $D_{3d}^{15}$ A 10	1	$a = 2.997$	$\omega = 70^\circ 32'$	1.498	Simple rhombohedral, at $227^\circ \text{Abs.}$
					4	$a = 4.578$	$\omega = 98^\circ 13'$		FC rhombohedral
<b>Molybdenum, Mo</b>	42	96.0	10.231	BCC $O_h^9$ A 2	2	$a = 3.1401 \pm 0.0003$	.	1.360	
<b>Neon, Ne.</b> . . . .	10	20.18	1.44	FCC $O_h^5$ A 1	4	$a = 4.52$	.	1.60	At $5^\circ \text{Abs}$

TABLE XXVII.—LATTICE CONSTANTS, 1932.—(Continued)

Element and modification	Atomic number	Atomic weight, 1931	Density (roentgenographic)	Space lattice space-group lattice type	Number of atoms per unit cell	Edge lengths $a, b, c$	Axial angles	Atomic radius, $r_A$ in Å U	Remarks
Nickel, Ni $\alpha$ .....	28	58.69	8.90	Hexagonal $D_{6h}^{14}$ A 3	2	$a = 2.66$ $c = 4.29$			Hexagonal form by Bredig glow-discharge method; non-magnetic, transformed to cubic at 300° C
			8.90	FCC $O_h^8$ A 1	4	$a = 3.517 \pm 0.001$		1.234	
Niobium, Nb (Columbium, Cb).	41	93.5	8.56	BCC $O_h^8$ A 2	2	$a = 3.303 \pm 0.002$		1.430	
Nitrogen ( $\alpha$ ), N <sub>2</sub> ...	7	14.008	1.02	Cubic $T_d$ characteristic type	8	$a = 5.66$		0.53	At 21° Abs. 4 N <sub>2</sub>
Osmium, Os	76	190.9	22.72	Hexagonal $D_{6h}^{14}$ A 3	2	$a = 2.724 \pm 0.002$ $c = 4.314 \pm 0.004$		1.335	
Oxygen, O <sub>2</sub>	8	16.0000	1.46	Rhombic BC ? ?	4	$a = 5.50$ $b = 3.82$ $c = 3.44$			At 21° Abs.
Palladium, Pd	46	106.7	12.06	FCC $O_h^8$ A 1	4	$a = 3.879 \pm 0.002$		1.371	

TABLE XXVII.—LATTICE CONSTANTS, 1932.—(Continued)

Element and modification	Atomic number	Atomic weight, 1931	Density (roentgenographic)	Space lattice space-group lattice type	Number of atoms per unit cell	Edge lengths $a, b, c$	Axial angles	Atomic radius, $r_4$ in A.U.	Remarks
Phosphorus, P White			2.22	Cubic $D_{3d}^6$	16	$a = 7.17$	.....		At 238° Abs. 4 $P_4$ dimorphous
Metallic	15	31.02	2.68	Rhombohedral $D_{3d}^3$	2	$a = 5.14$	$\omega = 34^\circ 7'$	0.87	Simple rhombohedral
				$A 7$	8	$a = 5.96$	$\omega = 60^\circ 47'$		FC rhombohedral
Platinum, Pt ...	78	195.23	21.485	FCC $O_h^3$	4	$a = 3.9142 \pm 0.0004$		1.384	
Potassium, K ...	19	39.104	0.85	BCC $O_h^3$	2	$a = 5.333 \pm 0.005$		2.309	
Rhenium, Re.	75	186.31	20.77	Hexagonal $D_{6h}^4$	2	$a = 2.765 \pm 0.003$ $c = 4.470 \pm 0.004$		1.373	
Rhodium, Rh ....	45	102.9	12.431	FCC $O_h^3$	4	$a = 3.7944 \pm 0.0004$		1.341	
Rubidium, Rb.	37	85.45	1.58	BCC $O_h^3$	2	$a = 5.62 \pm 0.03$		2.43	At 100° Abs.

TABLE XXVII.—LATTICE CONSTANTS, 1932.—(Continued)

Element and modification	Atomic number	Atomic weight, 1931	Density (roentgenographic)	Space lattice space-group lattice type	Number of atoms per unit cell	Edge lengths $a, b, c$	Axial angles	Atomic radius, $r_A$ in A.U.	Remarks
Ruthenium, Ru	44	101.7	12.48	Hexagonal $D_{6h}^4$ A 3	2	$a = 2.695 \pm 0.002$ $c = 4.273 \pm 0.004$		1.341	
Selenium, Se Hexagonal			4.87	Hexagonal $D_{3h}^4$ or $D_{3d}^5$ A 8	3	$a = 4.337 \pm 0.005$ $c = 4.944 \pm 0.005$		1.158	
Monoclinic	34	79.2	4.51	Monoclinic $C_{2h}^2$ ?	32	$a = 11.50$ $b = 8.98$ $c = 8.977$	$\beta = 90^\circ 57'$		4 Ses
Silicon, Si . . . . .	14	28.06	2.32	FCC (diamond) $O_h^7$ A 4	8	$a = 5.418 \pm 0.006$		1.173	
Silver, Ag . . . . .	47	107.880	10.501	FCC $O_h^5$ A 1	4	$a = 4.0776 \pm 0.0006$		1.441	
Sodium, Na . . . . .	11	22.997	0.99	BCC $O_h^9$ A 2	2	$a = 4.24 \pm 0.02$		1.83	At 100° Abs.
Strontium, Sr.	38	87.63	2.57	FCC $O_h^5$ A 1	4	$a = 6.075 \pm 0.004$		2.148	

TABLE XXVII.—LATTICE CONSTANTS, 1932.—(Continued)

Element and modification	Atomic number	Atomic weight, 1931	Density (roentgenographic)	Space lattice space-group lattice type	Number of atoms per unit cell	Edge lengths $a, b, c$	Axial angles	Atomic radius, $r_A$ in Å U	Remarks
Sulphur, S...	16	32.06	2.01	Rhombohedral $V_h^{2,4}$	128	$a = 10.61$ $b = 12.87$ $c = 24.56$			Molecular lattice
Tantalum, Ta...	73	181.36	16.94	BCC $O_h^8$ A 2	2	$a = 3.281 \pm 0.003$		1.421	
Tellurium, Te...	52	127.5	6.23	Hexagonal $D_{3d}^4$ or $D_{3h}^6$ A 8	3	$a = 4.495$ $c = 5.912$	..	1.439	
Thallium, Tl $\alpha$ .....	81	204.39	11.85	Hexagonal $D_{6h}^{14}$ A 3	2	$a = 3.450$ $c = 5.520$	...	1.702	
$\beta$ .....			11.88	FCC $O_h^3$ A 1	4	$a = 4.841$		1.711	
Thorium, Th...	90	232.12	11.73	FCC $O_h^3$ A 1	4	$a = 5.074 \pm 0.002$		1.794	
Tin, Sn $\alpha$ (gray)...	50	118.70	5.81	FCC (diamond) $O_h^3$ A 4	8	$a = 6.46$		1.40	
$\beta$ (white)...			7.29	Tetragonal BC $D_{4h}^{19}$ A 5	4	$a = 5.818 \pm 0.003$ $c = 3.174 \pm 0.003$	..	1.508	

TABLE XXVII.—LATTICE CONSTANTS, 1932.—(Continued)

Element and modification	Atomic number	Atomic weight, 1931	Density (roentgenographic)	Space lattice space-group lattice type	Number of atoms per unit cell	Edge lengths $a, b, c$	Axial angles	Atomic radius, $r_A$ in $\text{\AA}$	Remarks
Titanium, Ti	22	47.90	4.46	Hexagonal $D_{6h}^4$ A 3	2	$a = 2.951 \pm 0.004$ $c = 4.692 \pm 0.004$		1.450	
Tungsten, W	74	184.0	19.273	BCC $O_h^9$ A 2	2	$a = 3.1583 \pm 0.0003$		1.368	
			18.97	Cubic $O^2$ or $O_h^3$ characteristic type	8	$a = 5.04$		1.26	
Uranium, U . .	92	238.14	19.47	BCC $O_h^9$ A 2	2	$a = 3.43$		1.49	
Vanadium, V .	23	50.95	6.16	BCC $O_h^9$ A 2	2	$a = 3.011 \pm 0.003$		1.304	
Xenon, Xe . .	54	130.2	3.64	FCC $O_h^9$ A 1	4	$a = 6.18 \pm 0.02$		2.18	At 100° Abs.
Zinc, Zn . . .	30	65.38	7.20	Hexagonal $D_{6h}^4$ A 3	2	$a = 2.649 \pm 0.003$ $c = 4.930 \pm 0.005$		1.324	
Zirconium, Zr .	40	91.22	6.53	Hexagonal $D_{6h}^4$ A 3	2	$a = 3.223 \pm 0.002$ $c = 5.123 \pm 0.003$		1.583	

**Inorganic Compounds.**—Several hundred inorganic compounds have now been subjected to crystal-structure examination and more or less complete analysis by x-rays.<sup>1</sup> These data are readily available for reference in the International Critical Tables, Vol. 1, Wyckoff's "The Structure of Crystals," 2d ed., New York (1931), and especially in the monumental "Strukturbericht" of Ewald and Hermann which appeared serially in the *Zeitschrift für Kristallographie* and in book form late in 1931. Hence, only the general types and relationships need be considered here. Ewald and Hermann's type classification evidently will be adopted as a standard so this method is followed here. The list does not include a hundred or more compounds which have been subjected to crystal analysis but for which results are still incomplete owing to extreme structure complexity, such as some of the natural silicates or to very complex or poorly defined chemical formulas. Alloys are considered separately in Chap. XV.

A general impression to be gained by such a table is that the field of inorganic chemistry is a hopelessly complex one from the structural standpoint. Thus for the various classes of compounds there are the following definitely classified different types, to which must be added numerous highly characteristic structures for individual compounds:

$AB$ .	.....	13
$AB_2(A_2B)$	.. . . .	16
$A_xB_y$ . . . . .	. . . . .	8
$A_x(mB)_y, A_x(mB_2)_y$	. . . . .	5
$A_x(mB_3)_y$	. . . . .	8
$A_x(mB_n)_y$	..	20

The 878 pages of the "Strukturbericht" are eloquent evidence of the industry and ingenuity of x-ray diffraction research workers all over the world whose interest lies in trying to discover *how* nature builds its vast number of chemical compounds. They have succeeded in finding already 70 definite architectural plans according to which one or more compounds are constructed, plus as many more which are not so definitely known. Out of the complexity a great step forward has been made in the classification alone. Similarly constituted compounds of chemically similar elements tend to crystallize in the same way. Certainly

<sup>1</sup> In the valuable "Tables of Cubic Crystal Structure," by Knaggs, Karlik and Elan (Hilger, London, 1932) there are listed 513 cubic elements and compounds, and 156 cubic alloys.

TABLE XXVIII.—RÉSUMÉ OF CRYSTAL STRUCTURES OF INORGANIC COMPOUNDS  
I. Binary Compounds AB

Type	Typical compound	Lattice	Space group	Number of mols	a	Others
B 1 .	NaCl	Simple cubic	$O_h^5$	4	5 628	(Li, Na, K, Rb) (F, Cl, Br, I); CsF; $NH_4Cl$ , Br, I; Ag(F, Cl, Br); (Mg, Ca, Sr, Ba, Cd, Mn, Fe, Co, Ni)O; (Mg, Ca, Sr, Ba, Pb, Mn)S; (Mg, Ca, Sr, Ba, Pb, Mn)Se; (Ca, Sr, Ba, Sn, Pb)Te; (Sc, Ti, Zr, V, Nb)N; (Ti, Zr, V, Nb, Ta)C; LiH (Cs, $NH_4$ , Tl) (Cl, Br, I); TlSb, TlBi, CuZn, AgZn, AuZn, CuPd, AlNi, etc.
B 2 . . .	CsCl	BCC	$O_h^1$	1	4.110	
B 3 . .	ZnS (zinc blende)	Diamond cubic	$T_d^2$	4	5 42	Cu(Cl, Br, I); (Be, Zn, Cd, Hg) (S, Se, Te); AlP, GaP, AlAs, GaAs, AlSb, GaSb, InSb, SnSb, CSi $NH_4F$ , BeO, ZnO, ZnS, CdS, MgTe, CdSe, AlN, AgI
B 4	ZnS (wurtzite)	Hexagonal	$C_{6v}^4$	2	$\begin{cases} a = 3.84 \\ c = 6.28 \end{cases}$	
B 5	Carborundum III	Hexagonal	$C_{6v}^4$	4	$\begin{cases} a = 3.095 \\ c = 10.09 \end{cases}$	
B 6	Carborundum II	Hexagonal	$C_{6v}^4$	6	$\begin{cases} a = 3.095 \\ c = 15.17 \end{cases}$	
B 7 .	Carborundum I	Hexagonal	$C_{3v}^5$	15	$\begin{cases} a = 3.095 \\ c = 37.95 \end{cases}$	
B 8 . . .	Nickel arsenide, NiAs	Hexagonal	$D_{6h}^4$	2	$\begin{cases} a = 3.61 \\ c = 5.03 \end{cases}$	(Fe, Co, Ni)S; (Fe, Co, Ni)Se; (Co, Ni)Te; NiAs, (Cr, Mn, Fe, Co, Ni)Sb
B 9 .	Cinnabar, HgS (deformed NaCl lattice)	Hexagonal		3	$\begin{cases} a = 4.14 \\ c = 9.49 \end{cases}$	
B 10 . . . .	$PH_4I$	Tetragonal	$D_{4h}^7$	2	$\begin{cases} a = 6.34 \\ c = 4.62 \end{cases}$	
B 11 .	PbO (red)	Tetragonal	$D_{4h}^7$	2	$\begin{cases} a = 3.98 \\ c = 5.01 \end{cases}$	(Pb, Sn, Pd)O
B 12	BN	Same as A9 (Graphite)	$D_{6h}^4$	4	$\begin{cases} a = 2.51 \\ c = 6.69 \end{cases}$	
B 13 .	Millerite, NiS	Rhombohedral	$C_{3v}^5$	3 (chains)	5 65	



TABLE XXVIII.—RÉSUMÉ OF CRYSTAL STRUCTURES OF INORGANIC COMPOUNDS.—(Continued)  
II. Compounds  $AB_2$  or  $A_2B$

Type	Typical compound	Lattice	Space group	Number of mols	a	Others
C 1.....	Fluorite, $CaF_2$	Cubic	$O_h^{15}$	4	$a = 5.451$	(Ca, Sr, Ba, Cd, Pb)F <sub>2</sub> , SrO <sub>2</sub> , (Ce, Cr, Zr, Th, U)O <sub>2</sub> , Li <sub>2</sub> O, Li <sub>2</sub> S, Na <sub>2</sub> S, Cu <sub>2</sub> S, Cu <sub>2</sub> Se, Mg <sub>2</sub> Si, Mg <sub>2</sub> Sn, Mg <sub>2</sub> Pb
C 2(1)...	Pyrites, FeS <sub>2</sub>	Cubic	$T_h^{16}$	4	5.404	(Mn, Fe, Co, Ni, Ru, Os)S <sub>2</sub> , PtAs <sub>2</sub>
C 2(2)...	CO <sub>2</sub>	Cubic	$T_h^{16}$	4	5.63	CO <sub>2</sub> , N <sub>2</sub> O
C 3...	Cuprite, Cu <sub>2</sub> O	Cubic	$O_h^{14}$	2	4.26	Cu <sub>2</sub> O, Ag <sub>2</sub> O, Pb <sub>2</sub> O
C 4.....	Rutile, TiO <sub>2</sub>	Tetragonal	$D_{4h}^{14}$	2	$\begin{cases} a = 4.58 \\ c = 2.95 \end{cases}$	(Mg, Zn, Mn, Fe, Co, Ni)F <sub>2</sub> (Ti, Sn, Pb, V, Sb, Te, Mo, W, Mn, Ru, Os, Ir)O <sub>2</sub>
C 5	Anatase, TiO <sub>2</sub>	Tetragonal	$D_{4h}^{19}$	4	$\begin{cases} a = 4.24 \\ c = 9.37 \end{cases}$	(Cd, Pb)I <sub>2</sub> ; (Mg, Ca, Cd, Mn, Fe, Co, Ni)-(OH) <sub>2</sub> ; Ti(S <sub>2</sub> , Se <sub>2</sub> , Te <sub>2</sub> ); Zr(S <sub>2</sub> , Se <sub>2</sub> ); SnS <sub>2</sub>
C 6.....	CdI <sub>2</sub>	Hexagonal (layer lattice)	$C_{3d}^{13}$	4	$\begin{cases} a = 6.84 \\ c = 3.15 \end{cases}$	MoS <sub>2</sub> , WS <sub>2</sub>
C 7...	Molybdenite, MoS <sub>2</sub>	Hexagonal	$D_{6h}^{14}$	2	$\begin{cases} a = 12.30 \\ c = 4.89 \end{cases}$	$\alpha, \beta, SiO_2, GeO_2$
C 8.....	Quartz SiO <sub>2</sub>	Hexagonal	$D_6^{15}, D_6^{14}$	3	$\begin{cases} \alpha \begin{cases} a = 5.03 \\ c = 8.22 \end{cases} \\ \beta \begin{cases} a = 5.01 \\ c = 5.47 \end{cases} \end{cases}$	
C 9...	$\beta$ -cristobalite (SiO <sub>2</sub> )	Cubic	$O_h^{17}$	8	7.12	
C 10...	$\beta$ -tridymite (SiO <sub>2</sub> )	Hexagonal	$D_{6h}^{14}$	4	$\begin{cases} a = 4.5 \\ c = 7.3 \end{cases}$	H <sub>2</sub> O, ice
C 11.....	CaC <sub>2</sub>	Tetragonal	$O_{4h}^{17}$	2	$\begin{cases} a = 3.87 \\ c = 6.37 \end{cases}$	(Ca, Sr, Ba, La, Ce, Pr, Nd)C <sub>2</sub>
C 12.....	CaSi <sub>2</sub>	Rhombohedral	Same as A7	2	10.4	MoSi <sub>2</sub> , WSi <sub>2</sub>
C 13.....	HgI <sub>2</sub>	Tetragonal	$D_{4h}^{15}$	2	$\begin{cases} a = 4.36 \\ c = 12.36 \end{cases}$	

TABLE XXVIII.—RÉSUMÉ OF CRYSTAL STRUCTURES OF INORGANIC COMPOUNDS.—(Continued)

Type	Typical compound	Lattice	Space group	Number of mols	<i>a</i>	Others
C 14	MgZn <sub>2</sub>	Hexagonal	<i>D</i> <sub>6h</sub> <sup>4</sup>	4	$\begin{cases} a = 5.15 \\ c = 8.48 \end{cases}$	
C 15	Cu <sub>2</sub> Mg	Cubic	<i>O</i> <sub>h</sub> <sup>7</sup> (spinel)	8	7.03	
C 16	CuAl <sub>2</sub>	Tetragonal	<i>D</i> <sub>4h</sub> <sup>18</sup>	4	$\begin{cases} a = 6.052 \\ c = 4.878 \end{cases}$	
C 17 . . .	Fe <sub>2</sub> B	Tetragonal	<i>V</i> <sub>4</sub> <sup>11</sup>	4	$\begin{cases} a = 5.078 \\ c = 4.233 \end{cases}$	( <i>B</i> in center of tetrahedron of Fe)
C 18	Marcasite, FeS <sub>2</sub>	Rhombic	<i>V</i> <sub>h</sub> <sup>12</sup>	2	$\begin{cases} a = 3.35 \\ b = 4.40 \\ c = 5.35 \end{cases}$	FeS <sub>2</sub> , FeAs <sub>2</sub> , FeSb <sub>2</sub>
C 19	CdCl <sub>2</sub>	Rhombohedral	<i>D</i> <sub>3d</sub> <sup>5</sup>	1	6.35	(Mg, Zn, Cd, Mn, Fe, Co, Ni)Cl <sub>2</sub>
III. Compounds <i>A<sub>m</sub>B<sub>n</sub></i>						
D 1 .	NH <sub>3</sub>	Cubic	<i>T</i> <sub>h</sub> <sup>4</sup>	4	5.15	NH <sub>3</sub> , NIa <sub>3</sub>
D 2	CoAs <sub>3</sub>	Cubic	<i>T</i> <sub>h</sub> <sup>3</sup>	8	8.18	
D 11 .	SnI <sub>4</sub>	Cubic	<i>T</i> <sub>h</sub> <sup>6</sup>	8	12.23	SnI <sub>4</sub> , GeI <sub>4</sub>
D 31 .	Hg <sub>2</sub> Cl <sub>2</sub>	Tetragonal	<i>D</i> <sub>4h</sub> <sup>17</sup>	2	$\begin{cases} a = 4.45 \\ c = 10.89 \end{cases}$	Hg <sub>2</sub> (Cl <sub>2</sub> , Br <sub>2</sub> , I <sub>2</sub> )
D 41 .	Diborane, B <sub>2</sub> H <sub>6</sub>	Same as AlO (Hg)			$\begin{cases} a = 4.54 \\ c = 8.69 \end{cases}$	B <sub>2</sub> H <sub>6</sub> , C <sub>2</sub> H <sub>6</sub>
D 51	Corundum, Al <sub>2</sub> O <sub>3</sub>	Rhombohedral	<i>D</i> <sub>3d</sub> <sup>6</sup>	2	$\begin{cases} a = 5.12 \\ c = 13.93 \end{cases}$	α-Al <sub>2</sub> O <sub>3</sub> , Fe <sub>2</sub> O <sub>3</sub> , Cr <sub>2</sub> O <sub>3</sub> , Ti <sub>2</sub> O <sub>3</sub> , V <sub>2</sub> O <sub>3</sub> , α- Ga <sub>2</sub> O <sub>3</sub> , Rh <sub>2</sub> O <sub>3</sub>
D 52 . . .	La <sub>2</sub> O <sub>3</sub>	Hexagonal	<i>D</i> <sub>3d</sub> <sup>2</sup>	1	$\begin{cases} a = 3.93 \\ c = 6.12 \end{cases}$	La <sub>2</sub> O <sub>3</sub> , Ce <sub>2</sub> O <sub>3</sub> , Pr <sub>2</sub> O <sub>3</sub> , Nd <sub>2</sub> O <sub>3</sub>
D 61 .	Sb <sub>2</sub> O <sub>3</sub>	Cubic	<i>O</i> <sub>h</sub> <sup>7</sup>	16	11.06	As <sub>2</sub> O <sub>3</sub> , Sb <sub>2</sub> O <sub>3</sub> (as molecules of As <sub>2</sub> O <sub>3</sub> , Sb <sub>2</sub> O <sub>6</sub> )

TABLE XXVIII.—RÉSUMÉ OF CRYSTAL STRUCTURES OF INORGANIC COMPOUNDS.—(Continued)

Type	Typical compound	Lattice	Space group	Number of mols	<i>a</i>	Others
<i>D</i> 81	FeZn <sub>10</sub>	Cubic (body-centered three times as large minus two atoms)	<i>O<sub>h</sub><sup>9</sup></i>	52	<i>a</i> = 8.93	
<i>D</i> 82	Cu <sub>12</sub> Zn <sub>8</sub>	Cubic (body-centered three times as large minus two atoms)	<i>T<sub>d</sub><sup>3</sup></i>	52	<i>a</i> = 8.85	Cu <sub>12</sub> Zn <sub>8</sub> , Ag <sub>3</sub> Zn <sub>8</sub> , Ag <sub>3</sub> Cd <sub>8</sub> , Au <sub>3</sub> Zn <sub>8</sub>
<i>D</i> 83	Cu <sub>3</sub> Al <sub>4</sub>	Simple cubic	<i>T<sub>d</sub><sup>1</sup></i>	52	8.70	
<i>D</i> 84	Cu <sub>31</sub> Sn <sub>8</sub>	Cubic, incompletely known			8.955	Na <sub>31</sub> Pb <sub>8</sub>

IV. Compounds with Two- and Three-atom Radicals $A_x(mB)_y$ , $A_x(mB_2)_y$						
<i>F</i> 1	CoAsS	Cubic	<i>T<sub>h</sub><sup>4</sup></i>	4	5.60	KCN, CoAsS, NiAsS, NiSbS
<i>F</i> 11	Hg(CN) <sub>2</sub>	Tetragonal	<i>V<sub>d</sub><sup>12</sup></i>	8	$\begin{cases} a = 9.67 \\ c = 8.92 \end{cases}$	
<i>F</i> 51	$\begin{cases} NaHF_2 \\ CsICl_2 \end{cases}$	Rhombohedral	<i>D<sub>3d</sub><sup>2</sup></i>	1	.	NaHF <sub>2</sub> , Na <sub>3</sub> N <sub>3</sub> , Ca(CN) <sub>2</sub> , CsICl <sub>2</sub>
<i>F</i> 52	KHF <sub>2</sub>	Tetragonal	<i>D<sub>4h</sub><sup>15</sup></i>	4	$\begin{cases} a = 5.67 \\ c = 6.81 \end{cases}$	KHF <sub>2</sub> , KN <sub>3</sub> , KCN
<i>F</i> 61	Chalcopyrite, CuFeS <sub>2</sub>	Tetragonal	<i>V<sub>d</sub><sup>3</sup></i>	1	$\begin{cases} a = 3.726 \\ c = 5.194 \end{cases}$	

TABLE XXVIII.—RÉSUMÉ OF CRYSTAL STRUCTURES OF INORGANIC COMPOUNDS.—(Continued)  
V. Compounds with Four-atom Radicals  $A_x(mB_3)_y$

Type	Typical compound	Lattice	Space group	Number of mols	$a$	Others
G 1	Calcite, $\text{CaCO}_3$	Rhombohedral	$D_3^6$	2	$\begin{cases} a = 6.361 \\ b = 4.94 \\ c = 7.94 \end{cases}$	(Ca, Mg, Zn, Mn, Fe) $\text{CO}_3$ , $\text{NaNO}_3$ (Ca, Sr, Ba) $\text{CO}_3$
G 2	Aragonite, $\text{CaCO}_3$	Rhombic	$V_h^{16}$	4	$\begin{cases} a = 6.56 \\ b = 5.40 \\ c = 3.80 \end{cases}$	$\text{NaClO}_3$ , $\text{NaBrO}_3$ (Fe, Mg) $\text{TiO}_3$ , $\text{LaCBO}_3$
G 3	$\text{NaClO}_3$	Cubic	$T^4$	4	5.40	$\text{KIO}_3$ , $\text{RbIO}_3$ , $\text{NaCBO}_3$ , $\text{KCBO}_3$ , (Ca, Sr, Ba)- $\text{TiO}_3$ , $\text{CaZrO}_3$ , $\text{CaSnO}_3$ , $\text{YAlO}_3$ , $\text{LaAlO}_3$ , $\text{LaGaO}_3$ , $\text{KMgF}_3$ , $\text{KZnF}_3$ , $\text{KNiF}_3$ , $\text{CsCdCl}_3$ , $\text{CsHgCl}_3$
G 4	Ilmenite, $\text{FeTiO}_3$	Rhombohedral	$C_{3v}^2$	2	3.80	
G 5	Perovskite, $\text{CaTiO}_3$	Cubic	$O_h^1$	1		
G 11	Dolomite, $\text{CaMg}(\text{CO}_3)_2$	Rhombohedral	$C_{3v}^2$	1	6.00	(Ca, Sr, Ba, Pb)(NO) $_2$
G 21	$\text{Pb}(\text{NO}_3)_2$	Cubic	$T_h^6$	4	$\begin{cases} a = 7.84 \\ b = 9.21 \\ c = 9.17 \end{cases}$	
G 31	Beryl, $\text{Be}_3\text{Al}_2(\text{SiO}_3)_6$	Hexagonal	$D_{6h}^2$	2		

VI. Compounds with Five and More Atom Radicals  $A_x(mB_n)_y$

H 1	$\text{CaSO}_4$	Rhombic	$V_h^{17}$	4	$\begin{cases} a = 6.22 \\ b = 6.96 \\ c = 6.97 \end{cases}$	(NH $_4$ , K, Rb, Cs, Tl) $\text{ClO}_4$ , $\text{KMnO}_4$ , (Sr, Ba, Pb) $\text{SO}_4$
H 2	$\text{BaSO}_4$	Rhombic	$V_h^{16}$	4	$\begin{cases} a = 8.85 \\ b = 5.44 \\ c = 7.13 \end{cases}$	$\text{ZrSiO}_4$ , $\text{YPO}_4$
H 3	Zircon, $\text{ZrSiO}_4$	Tetragonal	$D_{4h}^{19}$	4	$\begin{cases} a = 6.58 \\ c = 5.93 \end{cases}$	

TABLE XXVIII.—RÉSUMÉ OF CRYSTAL STRUCTURES OF INORGANIC COMPOUNDS —(Continued)

Type	Typical compound	Lattice	Space group	No of mols	<i>a</i>	Others
H 4	CaWO <sub>4</sub>	Tetragonal	C <sub>4h</sub> <sup>6</sup>	4	$\begin{cases} a = 5.24 \\ c = 11.38 \end{cases}$	NaIO <sub>4</sub> , KIO <sub>4</sub> (Ca, Ba, Pb)(MoO <sub>4</sub> ), (Ca, Ba, Pb)(WO <sub>4</sub> )
H 11	Spinel, Al <sub>2</sub> MgO <sub>4</sub>	Cubic	O <sub>h</sub> <sup>7</sup>	8	8.09	Including all spinels, Fe <sub>3</sub> O <sub>4</sub> , etc. K <sub>2</sub> Zn(CN) <sub>4</sub> , K <sub>2</sub> Cd(CN) <sub>4</sub> , K <sub>2</sub> Hg(CN) <sub>4</sub> , etc.
H 12	Olivine, Mg <sub>2</sub> SiO <sub>4</sub>	Rhombic	V <sub>h</sub> <sup>16</sup>	4		(Mg, Fe) <sub>2</sub> SiO <sub>4</sub> ; (Mg, Ca)SiO <sub>4</sub> , Al <sub>2</sub> BeO <sub>4</sub>
H 13	Phenactite, Be <sub>2</sub> SiO <sub>4</sub>	Rhombohedral	C <sub>3h</sub> <sup>2</sup>	6	7.68	Li <sub>2</sub> MoO <sub>4</sub> , Li <sub>2</sub> WO <sub>4</sub> , Be <sub>2</sub> SiO <sub>4</sub> (Zn, Mn) <sub>2</sub> SiO <sub>4</sub> , Li <sub>2</sub> BeF <sub>4</sub>
H 14	LiKSO <sub>4</sub>	Hexagonal	C <sub>6</sub> <sup>6</sup>	2	$\begin{cases} a = 5.13 \\ c = 8.00 \end{cases}$	
H 15	K <sub>2</sub> PtCl <sub>4</sub>	Tetragonal	D <sub>4h</sub> <sup>1</sup>	1	$\begin{cases} a = 6.99 \\ c = 4.13 \end{cases}$	K <sub>2</sub> PtCl <sub>4</sub> , K <sub>2</sub> PdCl <sub>4</sub> , (NH <sub>4</sub> ) <sub>2</sub> PdCl <sub>4</sub>
H 21	Ag <sub>3</sub> PO <sub>4</sub>	Cubic	O <sub>h</sub> <sup>3</sup>	2	5.99	Ag <sub>3</sub> PO <sub>4</sub> , Ag <sub>3</sub> AsO <sub>4</sub>
H 22	KH <sub>2</sub> PO <sub>4</sub>	Tetragonal	V <sub>h</sub> <sup>12</sup>	4	$\begin{cases} a = 7.43 \\ c = 6.97 \end{cases}$	KH <sub>2</sub> PO <sub>4</sub> , (NH <sub>4</sub> )H <sub>2</sub> PO <sub>4</sub>
H 31	Granite, Al <sub>2</sub> Ca <sub>3</sub> (SiO <sub>4</sub> ) <sub>3</sub>	Cubic	O <sub>h</sub> <sup>10</sup>	8	11.83	R <sub>3</sub> <sup>IV</sup> R <sub>2</sub> <sup>III</sup> (SiO <sub>4</sub> ) <sub>3</sub>
H 41	K <sub>2</sub> CuCl <sub>4</sub> ·2H <sub>2</sub> O	Tetragonal	O <sub>4h</sub> <sup>14</sup>	2	$\begin{cases} a = 7.45 \\ c = 7.88 \end{cases}$	[K, Rb, (NH <sub>4</sub> ) <sub>2</sub> ]CuCl <sub>4</sub> ·2H <sub>2</sub> O
H 42	Alum, KAl(SO <sub>4</sub> ) <sub>2</sub> , H <sub>2</sub> O	Cubic	T <sub>h</sub> <sup>6</sup>	4	12.11	NH <sub>4</sub> Al, NH <sub>4</sub> Fe, KAl, KCr, RbAl, CsAl, TlAl alums
H 51	Cyanite, Al <sub>2</sub> SiO <sub>5</sub>	Triclinic	C <sub>1</sub> <sup>1</sup>	4		
H 61	K <sub>2</sub> PtCl <sub>6</sub>	Cubic	O <sub>h</sub> <sup>5</sup>	4	9.73	(NH <sub>4</sub> ) <sub>2</sub> SiF <sub>6</sub> , Cs <sub>2</sub> CeF <sub>6</sub> , K <sub>2</sub> SnCl <sub>6</sub> , (NH <sub>4</sub> ) <sub>2</sub> SnCl <sub>6</sub> , (NH <sub>4</sub> ) <sub>2</sub> PbCl <sub>6</sub> , K <sub>2</sub> PtCl <sub>6</sub> , (NH <sub>4</sub> ) <sub>2</sub> PtCl <sub>6</sub> , Rb <sub>2</sub> PdCl <sub>6</sub> , [Ni(NH <sub>3</sub> ) <sub>4</sub> ](Cl <sub>2</sub> , Br <sub>2</sub> , I <sub>2</sub> ), [Co(NH <sub>3</sub> ) <sub>6</sub> ](Cl <sub>2</sub> , I <sub>2</sub> , ISO <sub>4</sub> , BrSO <sub>4</sub> , ISeO <sub>4</sub> ), [Co(NH <sub>3</sub> ) <sub>6</sub> ](H <sub>2</sub> O)] (ISO <sub>4</sub> , BrSO <sub>4</sub> )
H 62	K <sub>2</sub> Sn(OH) <sub>6</sub>	Rhombohedral	D <sub>3d</sub> <sup>5</sup>	1	5.67	(K, Rb, (NH <sub>4</sub> ) <sub>2</sub> )Pt(SCN) <sub>6</sub>
H 63	K <sub>2</sub> Pt(SCN) <sub>6</sub>	Hexagonal	D <sub>3d</sub> <sup>1</sup>	1	$\begin{cases} a = 6.77 \\ c = 10.45 \end{cases}$	
H 64	Ni(NH <sub>3</sub> ) <sub>6</sub> (NO <sub>3</sub> ) <sub>2</sub>	Cubic	T <sub>h</sub> <sup>6</sup>	4	10.96	Ni(NH <sub>3</sub> ) <sub>6</sub> (NO <sub>3</sub> ) <sub>2</sub> , Zn(BrO <sub>3</sub> ) <sub>2</sub> ·6H <sub>2</sub> O
H 71	(NH <sub>4</sub> ) <sub>2</sub> AlF <sub>6</sub>	Cubic	T <sub>h</sub> <sup>6</sup>	4	8.40	(NH <sub>4</sub> ) <sub>2</sub> (AlF <sub>6</sub> , FeF <sub>6</sub> , MoO <sub>4</sub> F <sub>3</sub> ); Co(NH <sub>3</sub> ) <sub>6</sub> [I, (ClO <sub>4</sub> ) <sub>3</sub> ]

the number of atoms in the molecule is of great importance; the size and shape of atoms and groups or the electron configurations would surely be a determining factor; the type of forces which hold the units in position in space must be considered. It is the province of the new science of crystal chemistry to take the great mass of experimental data which show *how* crystals are built and try by means of classification and correlation to generalize and answer the question *why* a compound assumes the lattice structure which it does. What is it that causes simple binary compounds  $AB$  to have about 13 ways of crystallizing? What determines the fact that some of the dioxides crystallize like calcium fluoride and others like rutile? These and other questions which naturally arise are the subject of the next chapter on crystal chemistry.

**Some Practical X-ray Researches on Inorganic Substances.**—In order to identify a substance *as it exists in a particular solid crystalline form*, either alone or in mixtures, the chemist, mineralogist, ceramist, jeweler, or manufacturer must have recourse to optical methods or to x-ray diffraction results. In many problems the latter alone can be applied to practical problems. Several patents and patent litigations have been based solely and convincingly on x-ray results. It is possible here to enumerate only a few of the general problems which have been successfully attacked. By way of suggesting further applications it is necessary to point out only that any problem of qualitative or even quantitative analytical identification of a substance in terms of the actual formula and crystalline forms, purity, chemical change, etc., is a potential x-ray investigation, entirely apart from the scientific value of unique space-group determinations.

1. *Qualitative Separations.*—The identity of the sulfides in the tin subgroup and of such compounds as  $\text{HgNH}_2\text{Cl}$ , the invariable presence of crystalline  $\text{BiOCl}$  in  $\text{Bi}_2\text{S}_3$ , and numerous other similar problems have been investigated. A vast field for diffraction research still lies in classical qualitative analysis.

2. *Complex Formation.*—Many examples might be cited of studies of suspected complexes formed by inorganic compounds. For example, the compound dimethyl barium carbonate which is definitely reported in the literature is found to produce a diffraction pattern identical with that of pure barium carbonate.

Purple of Cassius is found to be a colloidal mixture, rather than a compound.

3. *True and False Hydrates*.—A true hydrate possesses a crystal lattice just as definite and characteristic as any pure anhydrous compound. Many so-called hydrates with stoichiometric composition give patterns which indicate appropriate mixtures of lower and higher hydrates. Again some unsuspected cases of hydrate formation, such as the pentahydrate of sodium silicate, produce patterns proving their true identity.

4. *Unsuspected Chemical Reactions*.—Among many which might be cited are: formation of barium carbide catalytically

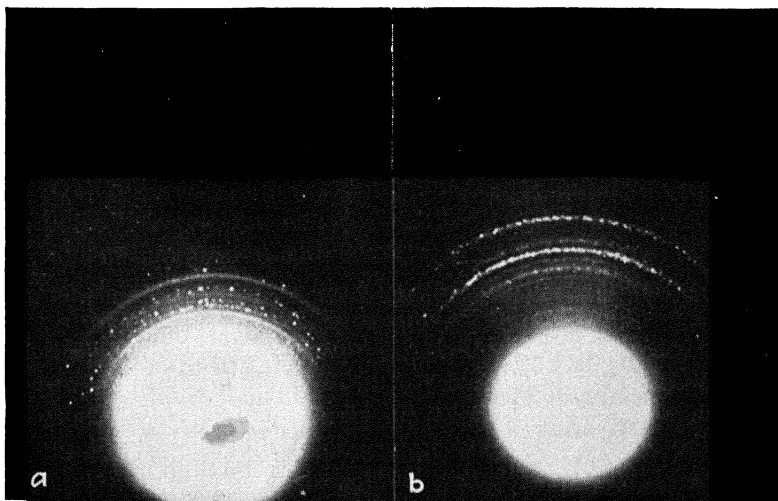


FIG. 125.—Reflection spectrograms from lead storage-battery plates ( $\text{Cu-K}\alpha$  radiation) showing lines for lead oxides, sulfate, etc. *a*, positive; *b*, negative.

from barium oxide and carbon in thermally emitting electrodes at temperatures far below those predicted; formation of mercurous chloride by absorption of mercuric chloride on charcoal; reduction of zinc oxide in methanol catalysts and formation of brass with copper; and identification of the composition and chemical charges in lead storage-battery plates as related to performance. Reflection patterns with copper radiation for used positive and negative battery plates (Fig. 125) show clearly the types of lead oxides, presence of lead sulfate, grain size, addition agents, etc.

5. *Inclusions in Metals*.—Proof of existence and analysis of nature are possible without dissolving or destroying a metal specimen.

6. *Mineralogy*.—This has become one of the greatest inorganic applications of diffraction analysis, particularly since the great steps forward in interpretation of silicate structures. An entire monograph upon this subject could be written, since possibly two hundred minerals have been already uniquely analyzed. The interest lies not only in identification and classification even to evaluation of commercial ores, as a great aid to optical mineralogy, but to chemical questions of variations in composition, and in geological questions of origin. The great library of standard diffraction patterns for all minerals made by Professor Winchell at the University of Wisconsin is an example. Aside from unique analyses of crystal structures of asbestos minerals, mentioned in connection with silicates in this chapter, Clark and Anderson<sup>1</sup> made a study of eighty specimens from mines all over the world, and found the diffraction patterns often so distinctive as to indicate the origin. The effects of acid and heat treatment were also characteristically depicted in patterns. Clark and Ally<sup>2</sup> found for five chrome ores from different localities, that the length of the edge of the unit cube ranged from 8.283 to 8.179, varying inversely with the  $\text{Al}_2\text{O}_3$  content of the ore. The theoretical densities also were calculated from the "average" molecular weights and x-ray data.

The spinels both natural and synthesized have been the subject of several investigations as regards identification and for the bearing on generalizations of crystal chemistry. The following data on these cubic crystals were obtained in precision measurements on carefully synthesized spinels, by Clark, Ally, and Badger.<sup>3</sup>

TABLE XXIX.—LATTICE DIMENSIONS (A.U.) OF SYNTHETIC SPINELS

Element	Aluminates	Chromites	Ferrites
Zn . . . . .	8 062 $\pm$ 0 001	8 296 $\pm$ 0 002	8 423 $\pm$ 0 001
M . . . . .	8.086 $\pm$ 0.003	8 305 $\pm$ 0 001	8 366 $\pm$ 0 001
Fe. . . . .	8 119 $\pm$ 0 002	8 344 $\pm$ 0 003	8 374 $\pm$ 0 003
Mn . . . . .	8 271 $\pm$ 0 002	8 436 $\pm$ 0 001	8 457 $\pm$ 0 002

The analysis of silicate minerals, which presented greatest difficulties until the rational assumption of coordination structures

<sup>1</sup> *Ind. Eng. Chem.*, **21**, 924 (1929).

<sup>2</sup> *Am. Mineralogist*, **17**, 66 (1932).

<sup>3</sup> *Am. J. Sci.*, **22**, 539 (1931).



was introduced, will be discussed in the next chapters. For specific results reference may be made to such excellent summaries as that of W. L. Bragg,<sup>1</sup> Schiebold on feldspars,<sup>2</sup> and numerous papers published in the past two years.

An excellent mineralogical research combining x-ray, chemical, and microscopic methods has been conducted recently on phosphate rock and apatite-like substances.<sup>3</sup> American continental phosphate rock consists of submicrocrystalline fluorapatite,  $\text{Ca}_{10}\text{F}_2(\text{PO}_4)_6$ , with excess of fluorine and some sodium. The compounds  $\text{Ca}_{10}(\text{OH})_2(\text{PO}_4)_6$ ,  $\text{Ca}_9(\text{H}_2\text{O})_2(\text{PO}_4)_6$ , and  $\text{Ca}_{10}\text{CO}_3(\text{PO}_4)_6 \cdot \text{H}_2\text{O}$ , all of which are identified in natural or artificial mixtures by means of diffraction patterns, form extensive series of solid solutions with fluorapatite some members of which occur in geologically recent rocks. Tricalcium phosphate hydrate,  $\text{Ca}_9(\text{H}_2\text{O})_2(\text{PO}_4)_6$ , gives a pattern like apatite, disappearing after heating at  $900^\circ \text{C}$ .; it comprises phosphate rock from Curacao while hydroxy fluorapatite,  $\text{Ca}_{10}(\text{F}, \text{OH})_2(\text{PO}_4)_9$  is found native in Pacific islands.

7. *Bone*.—In connection with the research on phosphate rock just described it was proved that animal bone free from organic matter is a carbonate apatite,  $\text{Ca}_{10}\text{CO}_3(\text{PO}_4)_6 \cdot \text{H}_2\text{O}$ , isomorphous with fluorapatite. Oxyapatite,  $\text{Ca}_{10}\text{O}(\text{PO}_4)_6$ , is formed by heating bone to constant weight at  $900^\circ \text{C}$ . Upon fossilization the carbonate group and the water molecules are replaced by fluorine.

8. *Zeolites, Permutites, Ultramarines, Etc.*—The permutites, or zeolitic silicates, are a group of remarkable aluminosilicates in which alkali atoms may be exchanged with other metallic atoms. They are the familiar agents used in water softeners, as hydraulic agents accelerating the setting of Portland cement, and as substances which can take up or lose water without affecting the solid form in any apparent manner. The ultramarines, a group of famous pigments, are closely related to the permutites, containing sulfur in addition, and having similar atom-replaceable properties. The extraordinary properties make the problem of structure especially interesting and valuable. X-ray researches

<sup>1</sup> *Faraday Soc. Mon.*, Crystal Structural and Chemical Constitution, p. 291 (1929).

<sup>2</sup> *Ibid.*, p. 316.

<sup>3</sup> HENDRICKS, HILL, JACOB, and JEFFERSON, *Ind. Eng. Chem.*, **23**, 1413 (1931).

by Jaeger<sup>1</sup> on permutites, minerals sodalite, nosean, garnet, etc., and ultramarines, and in the writer's laboratory on a whole series of natural and synthetic cement accelerating agents have thrown interesting light on the problem. Ultramarines give powder diffraction patterns identical with those of hauyne or nosean, ( $\text{Na}_{10} \text{Al}_6 \text{Si}_6 \text{O}_{32} \text{S}_2$ ), apparently for a cubic lattice,  $a_0 = 9.11$  A.U. One fact immediately becomes apparent, namely, that it is impossible to attribute to any appreciable number of the atoms in the molecule any definite fixed place in the unit cell. Sodium, aluminum, and sulfur atoms are "wandering" constituents, just as are the water molecules in zeolites. The sodium ions are situated in a cavity, 2.66 A.U. between six oxygen atoms, and thus have room to move freely in it and be easily replaced by Li, K, Ag, Tl and  $\text{NH}_4$ , Zn, Mn, Ca, etc., ions with smaller diameters, or even larger ions, when the substance is brought into contact with solutions containing other ions. In the middle of the unit crystal cell is a large cavity with an edge length of 3.7 A.U. in which the wandering constituents may easily move, and into which water and solutions may easily pass. The walls of these cavities are electrically charged. This fact may help to fix electrically charged ions or water molecules. It is clearly evident that x-ray research has been necessary in order to clear up the puzzle of these peculiar substances although there is not yet agreement among all x-ray investigators. It is possible that these structures account for the selective absorbent power of the soil, containing, as it does, permutites, and to the remarkable stimulating power of traces of zinc and manganese on plant growth, as well as the predominant part of calcium.

9. *Gems and Pearls*.—Numerous applications of diffraction analysis have been made to the identification and structure and perfection of natural and synthetic gems, particularly with Laue patterns. The distinction between a fine pearl and one cultivated with a mother-of-pearl nucleus is easily made without injury to the specimen from a diffraction pattern, since the typically crystalline center is disclosed at once.

10. *Cement*.—The analysis of the constitution and structure of cement is a problem of great importance and difficulty. Fundamental x-ray studies beginning with structures of single pure constituents have been under way for several years at the Bureau of Standards and elsewhere. In a recent investigation by Brown-

<sup>1</sup> *Ibid.*, p. 320.

millers and Bogue<sup>1</sup> 28 samples were examined and the results found to agree with chemical and microscopical data; tricalcium silicate and  $\beta$ -dicalcium silicate are the most abundant constituents, while calcium oxide up to  $2\frac{1}{2}$  per cent is seldom found. Much remains to be done on setting, hydration, effects of addition agents, and aging.

11. *Lime*.—The plasticity of lime is directly related to the appearances of additional diffraction lines, corresponding to  $\text{Ca(OH)}_2$  and  $\text{CaCO}_3$  in  $\text{CaO}$ , and to unchanged  $\text{CaCO}_3$  in  $\text{Ca(OH)}_2$ . Evidently calcium carbonate may coat some of the grains of oxide and slow down the rate of hydration, thus decreasing plasticity.

12. *Ceramics*.—There are so many practical applications of the diffraction method to ceramic materials that it is not surprising that fruitful results have been obtained already. Merely as an indication of these results and of possibilities for further usefulness, there will be cited a few examples of researches carried out in the x-ray laboratory at the University of Illinois.

In an investigation of the effect of heat on china clays,<sup>2</sup> it was found that the chief crystalline constituent of the clay was kaolinite, whose lattice was destroyed upon dehydration. Mullite was formed at  $950^\circ\text{C}$ ., and in Georgia clay free alumina was present from  $950$  to  $1100^\circ\text{C}$ . and cristobalite at temperatures above  $1200^\circ\text{C}$ .

The x-ray method is of value in the detection of the various forms of silica in silica refractories, as found in a study of the zonal structure of silica brick from the roof of a basic open-hearth furnace.<sup>3</sup> After use to the point of fusion in an open-hearth furnace, the silica brick still retains quartz formation with increasing tendency towards cristobalite the higher the temperature.

The identity of crystalline compounds present in sheet-steel enamels as opacifiers<sup>4</sup> is easily determined.  $\text{SnO}_2$  is the primary opacifying compound when it is used in any mixture;  $\text{Sb}_2\text{O}_5$  when commercial  $\text{Sb}_2\text{O}_3$  or sodium antimonate are the primary agents; sodium silicofluoride, fluorspar, and cryolite aid in the development of opacity when used with the above compounds, although no diffraction lines for them appear. When used alone, however,

<sup>1</sup> *Concrete*, **38**, 85, 89 (1931).

<sup>2</sup> McVAY and THOMPSON, *J. Am. Ceram. Soc.*, **11**, 829 (1928).

<sup>3</sup> CLARK and ANDERSON, *Ind. Eng. Chem.*, **21**, 781 (1929).

<sup>4</sup> ANDREWS, CLARK, and ALEXANDER, *J. Am. Ceram. Soc.*, **14**, 634 (1931).

they produce opacity, NaF from cryolite and  $\text{CaF}_2$  from fluorspar. Interesting cases of solubility, dissociation, and oxidation are thus involved in these.

The problem of the constitution and structure of glasses will be considered in later chapters dealing with grain size, colloids, and liquids.

## CHAPTER XIV

### INORGANIC CRYSTAL CHEMISTRY: FUNDAMENTAL GENERALIZATIONS FROM EXPERIMENTAL DATA

The complexities which confront the crystal analyst when he attempts to generalize on the modes of crystal construction have been amply demonstrated by the data of the preceding chapter. In spite of the immensity of the field, however, a brilliant chapter in science is being written by the Braggs, Fajans, Pauling, Bernal, and particularly Goldschmidt. From their work it is possible to advance a theory of why crystals are built as they are, which not only explains at least the simpler types of structures already known semiquantitatively but enables even the prediction of new structures and properties. Five years ago when the first edition of this book appeared no chapter with the above heading could have been written. The concepts of the new wave mechanics have assisted materially in these developments, and great further progress may be expected of this infant branch of chemistry. The fundamental unit to be considered in these structural inquiries is, of course, the atom, which may be now pictured roughly (see page 79) as a nucleus surrounded by shells of diffuse negative electricity, which is denser the nearer the nucleus. Each shell is thought of as composed of a set of Bohr orbits on the older theory. Thus the atom has a size, and since it certainly is not rigid it must have a certain degree of compressibility and deformability. It has been amply demonstrated many times that the chemical and crystallographic properties of atoms depend on the size and particularly on the condition of the outer shell of electrons. Each ion or atom in a compound must be considered as forming a lattice of its own, the interpenetration of the various lattices resulting in the structure of the compound.

**1. Types of Crystals in Terms of Bonding Forces.**—A careful survey of all crystal-structure data leads to the conclusion that all crystalline substances may be classed under four principal types according to the types of combination of atoms into molecules and solid crystals: ionic or heteropolar, homopolar (sharing

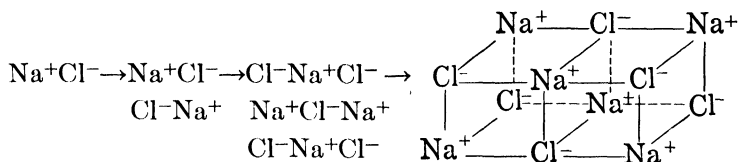
TABLE XXX.—CLASSIFICATION OF CRYSTALS

Crystal type	Crystal units	Type of binding	Characteristic properties				Typical crystals
			Optical	Electrical	Thermal	Mechanical	
Ionic.....	Simple and complex ions	Electrical attraction between ions of opposite signs ( $e/r^2$ ) balanced by repulsion of negative outer shells ( $\frac{-e}{r_0}$ )	Transparent; absorption in visible color if present is due to atoms	Moderate insulators in high fields; conduct by transfer of ions	Early high melting point; ionization occurs in liquid and vapor	Hardness increasing with higher ionization. Tendency to fracture by cleavage	NaCl CaF <sub>2</sub> CaCO <sub>3</sub> K <sub>2</sub> SO <sub>4</sub> (NH <sub>4</sub> ) <sub>2</sub> PtCl <sub>6</sub>
Silicate.....	O <sup>-2</sup> or F <sup>-</sup> ions Sc <sup>3+</sup> or Be <sup>2+</sup> or Al <sup>3+</sup> and other positive ions	Weak to moderate polarization	In short infrared due to complex ions In long infrared due to crystal lattice Refractivity due to positive ions	When polarization is slight they dissolve with ionization in ionizing solvents (water); when stronger are insoluble	Very high melting points, glasses formed on cooling of melt	Very hard with tendency to cleave or fracture conchoidally	Olivine, Mg <sub>2</sub> SiO <sub>4</sub> Cyanite, Al <sub>2</sub> SiO <sub>5</sub> Garnet, R <sub>3</sub> Al <sub>2</sub> Si <sub>3</sub> O <sub>12</sub> Spinel, Al <sub>2</sub> MgO <sub>4</sub> Corundum, Al <sub>2</sub> O <sub>3</sub>
Homopolar ...	Atoms of the fourth group and groups on either side of it	Homopolar bonds throughout or strongly polarized ionic binding	Transparent with high refractivity or opaque metalloidal	Diamond is a perfect insulator. The others conduct metalloidally. Very insoluble	Very high melting points with tendency to vaporize except in more metalloidal	Very hard Hardness less for metalloidal types	Diamond, C Zinc Blende, ZnS Wurtzite, ZnS Carborundum, CSI

Molecular . . .	Inert gas atoms Non-polar and polar molecules	Van der Waal's forces or resid- ual electric fields between molecular poles	Transparent optical prop- erties due to molecules and similar to gas and liquid phases	Insulators ex- cept when very polar; soluble in non-ionizing (molecular) solvents except when polar	Melting point very low with neutral atoms, rises with heav- ier molecules and polar molecules	Very soft, hard- ness increasing with polarity of molecules Deformation plastic	Argon, A CO <sub>2</sub> Ice H <sub>2</sub> O Paraffins, C <sub>n</sub> H <sub>2n+2</sub> Calomel, Hg <sub>2</sub> Cl <sub>2</sub>
Layer . . . .	Strongly polariz- ing and easily polarized ions	In layers . Homopolar or polarized ionic Between layers molecular	As homopolar	Various, similar to both molec- ular and homo- polar	Various, similar to both molec- ular and homo- polar	Cleaving readily in layers which are soft and flexible	Graphite, C CdI <sub>2</sub>
Metallic. . . . .	Positive ions and electron gas	Electrical attraction between posi- tive ions and electron gas	Opaque (due to free electrons) with selective reflection in in- frared	Conductors, conductivity inversely proportional to number of free electrons. Sol- uble in acids where H <sup>+</sup> ions absorb free electrons	Moderate to very high melt- ing points Long liquid interval	Moderate hardness increased by alloying. Elas- tic but yield by glide plane slipping when overstressed	Copper, iron Iron, sodium Zinc
Metalloidal . .	Metal atoms and atoms of the sulfur and arsenic type	Mixture of homopolar ionic and me- tallic binding	Opaque metallic or transparent with high re- fractivity and color	Medium to bad conductors Soluble only with decompo- sition	Tendency to vaporize or decompose at high tem- peratures	Moderately hard to soft Properties a mixture of those of other types	Nickel arsenide, NiAs Fahlert <sub>z</sub> , R <sub>12</sub> Sb <sub>2</sub> Pyrites, FeS <sub>2</sub>

of electron pairs), molecular, and metallic. This does not mean to say that the division lines are clear-cut, for many substances may be thought of as in the transition zone between two or more types. Bernal has therefore added three of the most important intermediate classes: silicates, layer lattices, and metalloids. The fundamental classification and properties have been assembled by Bernal<sup>1</sup> as shown in Table XXX.

**2. Important Concepts and Definitions in Classification of Crystals.** *a. Ionic or Heteropolar Combination.*—There remains little doubt that in a large number of crystals the atoms are really ions in the familiar chemical sense and that they are held together in space with requisite rigidity by electrostatic forces of attraction between positively and negatively charged particles, inversely as the square of the distance. When the outer electron shells of + and - ions are in close proximity, however, a repulsion sets in inversely at about the ninth power of the distance between them. Thus in a crystal like rock salt a condition is easily reached like



and so on, till the whole single crystal is thus constructed. Thus sodium chloride diffracts x-rays in a way which leads to the assignment of a structure in which each sodium ion is not bound to a single chlorine ion as in the simple chemical molecule (vapor state) but exerts its attraction on six equidistant chlorine neighbors, and each chlorine ion is surrounded by six sodium ions. Thus each ion tends to surround itself with as many oppositely charged ions as possible. In the electrically neutral crystal there are not pairs of sodium and chlorine atoms or ions, but simply an equal number of oppositely charged ions. In a sense, the chemical molecule seems to be lost sight of and proper formulas would seem to be  $\text{Na}_6\text{Cl}$  and  $\text{NaCl}_6$ . However, an analogy cited by Sir William Bragg serves to clarify the situation. Several couples of men and women go in to dinner and are seated at a circular table. Each man now has a lady on either side and the identity of the original couple is obscured though by no means destroyed on account of the seating arrangement.

<sup>1</sup> *Encyclopedia Britannica*, 14th ed., Vol. 23, p. 857.



All physical and chemical properties, all knowledge concerning the scattering of x-rays since the original interpretations by Debye of experiments on lithium fluoride, all calculations from intensity data on electron distribution (see pages 100 and 211), and all mechanical data on breaking strengths of perfect crystals<sup>1</sup> are in agreement that the lattice units in solid salts are ions and that the bonding forces are electrostatic.

*b. Polarization.*—It is certain that ions are of very different sizes and it follows that some curious effects might be obtained by combining, for example, a small highly charged positive ion with a larger diffuse negative ion such as  $S^{=}$ . This ion would be not only attracted but actually distorted, since the negative shell would be pulled toward the small positive ion and the nucleus repelled. This phenomenon which has been demonstrated in numerous ways particularly by Fajans is called polarization. Increasing polarization gradually merges with homopolar binding.

*c. Homopolar Combination.*—In terms of modern theories of valence this means that atoms are held together by sharing electrons, usually in pairs called covalences. The stable diatomic molecules such as  $H_2$ ,  $O_2$ ,  $N_2$ , etc., and  $H_2O$ ,  $CO_2$  are built up in this fashion in order to complete the various quantum electron shells. In organic molecules the carbon atoms form long chains by homopolar bonds. The best example is in diamond where each carbon atom is sharing electron pairs with four others, so that this linking is extended indefinitely in all directions to the limits of the crystal itself which thus may be considered a single solid molecule. The word "adamantine" has been ascribed to this class by Bernal.

*d. Molecular Combination.*—Organic compounds form the great class of crystals whose pattern units are the whole molecules in which, in turn, the atoms are linked together by pairs of electrons held in common. While in the ionic lattice the identity of the single molecule of potassium chloride, for example, is somewhat obscured (though by no means destroyed) by the division of the bonding forces of one atom among six neighbors, in the molecular lattices the molecule of the chemists' formula and of the gaseous phase is built essentially unchanged into the solid structure. By virtue of the residual stray fields of the electrically neutral molecules, it is possible for one molecule to lie up against

<sup>1</sup> See JOFFE, "The Physics of Crystals," McGraw-Hill Book Company, Inc., 1928.

another and form the regularly built-up solid. Thus there are two molecules of naphthalene in the unit crystal cell. Because the stray forces holding the molecules in their fixed position cannot compare in intensity with the strong polar or non-polar bondings between atoms, the substance easily melts or throws off single whole molecules in the process of sublimation. This type of combination will be considered in detail in Chap. XVI on the structure of organic crystals. In the case of electrically neutral inert gas atoms, the residual attraction is effective only at very close distances and consequently except at lowest temperature the substance remains a gas. Molecular lattices are also to be found among inorganic compounds, notably solid HCl,  $\text{SnI}_4$ ,<sup>1</sup> and the cubic forms<sup>2</sup> of arsenious and antimonious oxides.

*e. Metallic Combination.*—Metallic combination occurs when atoms tend to lose electrons very easily. The positive ions are then held together by an electron gas produced from the discarded electron now no longer bound to particular atoms.

*f. Coordination and Primary and Secondary Valence Forces.*—The various types of lattices enumerated in Chap. XIII for inorganic compounds are distinguishable by their coordination numbers as originally defined chemically by Werner, or the number of neighbors possessed by each ion; thus the following simple coordination types for the compounds AB and  $\text{AB}_2$  may be recognized:

AB. 1: single molecules and molecular lattices.

2: double molecules, molecular chains.

3: BN type.

4: diamond type lattices of zinc blende and zinc oxide.

6: NaCl and NiAs types.

8: CsCl type.

$\text{AB}_2$ . 2 and 1: single molecules and molecular lattices.

4 and 2:  $\alpha$  and  $\beta$  quartz, cristobalite, tridymite, cuprite.

6 and 3: anatase, rutile, brookite, layer lattice  $\text{CdI}_2$ .

8 and 4: fluorite.

Each of these types is characterized by a definite energy stability, which may be deduced theoretically and the constants evaluated from compressibility and related data.<sup>3</sup>

<sup>1</sup> DICKINSON, *J. Am. Chem. Soc.*, **45**, 958 (1923).

<sup>2</sup> BOZORTH, *ibid.*, **45**, 1621–1629 (1923).

<sup>3</sup> Cf. BORN, "Problems of Atomic Dynamics," p. 176, Massachusetts Institute of Technology, 1926.

The point of greatest interest to chemists, possibly, is the complete verification by x-ray analysis of the remarkable Werner theory. This holds not only in the case of primary coordination of oppositely charged ions but also for the so-called secondary valence compounds, in which electrically neutral molecules, such as ammonia in the amines or water in the hydrates, may be chemically bound by molecules of ionogens. For the compound  $\text{Ni}(\text{NH}_3)_6\text{Cl}_2$ , for example, Werner postulated that the six ammonia molecules should be held around the central nickel ion at the corners of an octahedron. By x-ray analysis Wyckoff found this indeed to be the case for the complex ammonia complex compounds, potassium chloroplatinate ( $\text{K}_2\text{PtCl}_6$ ), zinc bromate hexahydrate, etc. Dickinson<sup>1</sup> studied potassium chloroplatinite,  $\text{K}_2\text{PtCl}_4$ , and found again the four chlorine atoms equidistant around the platinum atom in the same plane. Upon these grounds primary and secondary valences are no longer separable sharply from each other. Even when neutral ammonia molecules are bound by nickel atoms, there is a sharing of electron pairs, both being present originally in the nitrogen atom. In the alkali polyhalides such as  $\text{CsI}_3$ , the ionic lattice consists of singly positively charged cesium atoms and a group or radical  $\text{I}_3$ , retained intact, the iodine atoms being held in a string probably by the sharing of only single electrons.<sup>2</sup>

*g. The Sizes and Shapes of Atoms and Ions.*—Since the dimensions of the crystal unit cells of the elements containing a definite number of regularly arranged atoms may be determined with great accuracy, by simple deductions it is possible to determine the distance of nearest approach of two atoms and the radius of the atom. By radius is, of course, meant the sphere of influence of the very open structure of electrons in diffuse shells around a minute nucleus which constitute the atom; however, the electrical forces holding atoms and ions in position are so strong as to render solids very little compressible, and, hence, the atoms *act* usually like solid spheres in the crystallographic sense. These radii, calculated from the best available crystal-structure data, are tabulated in Table XXVII in the preceding chapter. As has long been known, the atomic radii, as well as volumes, are distinctly a periodic function of atomic number.

<sup>1</sup> *J. Am. Chem. Soc.*, **44**, 2404 (1922).

<sup>2</sup> CLARK, *Am. J. Sci.*, **7**, 109 (1924).

TABLE XXXIa.—EMPIRICAL ION RADII (GOLDSCHMIDT, 1926) AND  
THEORETICAL ION RADII (PAULING, 1927)

	1- H	O He	1+ Li	2+ Be	3+ B	4+ C Maximum	5+ N Maximum						
Goldschmidt, empirical...	1 27	1 22	0 78	0 34	.....	0 2	0 1-0 2						
Pauling, theoretical ...	2 08	.....	0 60	0 31	0 20	0 15	0 11						
2- O	1- F	O Ne	1+ Na	2+ Mg	3+ Al	4+ Si	5+ P	6+ S					
Goldschmidt, empirical	1 32	1 33	0 98	0 78	0 57	0 39	0 3-0 4	0 34					
Pauling, theoretical ..	1 40	1 36	0 95	0 65	0 50	0 41	0 34	0 29					
2- S	1- Cl	O A	1+ K	2+ Ca	3+ Sc	4+ Ti	5+ V	6+ Cr	1+ Cu	2+ Zr	3+ Ga	4+ Ge	6+ Se
Goldschmidt, empirical	1 74	1 81	1 92	1 33	1 06	0 83	0 64	0 3-0 4	.....	0 83	0 62	0 44	0 3-0 4
Pauling, theoretical...	1 84	1 81	.....	1 33	0 99	0 81	0 68	0 52	0 96	0 74	0 62	0 53	0 42
2- Se	1- Br	O Kr	1+ Rb	2+ Sr	3+ Y	4+ Zr	5+ Cb	.....	1+ Ag	2+ Cd	3+ In	4+ Sn	
Goldschmidt, empirical...	1 91	1 96	2 1	1 49	1 27	1 06	0 87	0 69	1 13	1 03	0 92	0 74	
Pauling, theoretical ....	1 98	1 95	.....	1 48	1 13	0 93	0 80	0 70	1 26	0 97	0 81	0 71	
2- Te	1- I	O Xe	1+ Cs	2+ Ba	3+ La	4+ Ce	.....	.....	1+ Au	2+ Hg	3+ Tl	4+ Pb	
Goldschmidt, empirical...	2 11	2 20	2 3	1 65	1 43	1 22	1 02	.....	.....	.....	1 12	1 05	0 84
Pauling, theoretical ..	2 21	2 16	.....	1 69	1 35	1 15	1 01	.....	1 37	1 10	0 95	0 84	

TABLE XXXIb.—SEVERAL EMPIRICAL ION-RADII ACCORDING TO  
GOLDSCHMIDT AND PAULING

	1+	1+	2+	2+	2+	2+	2+	2+	3+	3+	3+	3+	3+	3+	3+	3+	3+
	NH <sub>4</sub>	Tl	Mn	Fe	Co	Ni	Pb	Ti	V	Cr	Mn	Fe	Rh				
Goldschmidt, empirical	1.43	1.49	0.91	0.83	0.82	0.78	1.32	0.69	0.65	0.64	0.70	0.67	0.68				
Pauling, empirical	...	1.44	0.80	0.75	0.69	0.69	1.21										
	3+	3+	3+	3+	3+	3+	3+	3+	3+	3+	3+	3+	3+	3+	3+	3+	3+
	La	Ce	Pr	Nd	II	Sm	Eu	Gd	Tb	Dy	Ho	Er	Tm	Yb	Cp		
Goldschmidt, empirical	1.22	1.18	1.16	1.15		1.13	1.13	1.11	1.09	1.07	1.05	1.04	1.04	1.00	0.99		
	4+	4+	4+	4+	4+	4+	4+	4+	4+	4+	4+	4+	4+	4+	4+	4+	4+
	V	Mn	Nb	Mo	W	U	Ru	Os	Ir	Te	Pr	Tb	Th				
Goldschmidt, empirical	0.61	0.52	0.69	0.68	0.68	1.05	0.65	0.67	0.66	0.89	1.00	0.89	1.10				
Pauling, empirical	0.59	0.50	0.67	0.66	0.66	0.97	0.63	0.65	0.64	0.81	0.92	...	1.02				

Numerous methods have been employed to calculate the radii of ions, but the most widely accepted values today are those of Goldschmidt, empirically determined from crystal-structure data and from Wasastjerna's values (optical)  $F^- = 1.33$  and  $O^- = 1.32$  A.U. Pauling has calculated theoretical radii from quantum-mechanics considerations and the agreement in general is excellent. The values are shown in Tables XXXIa, b, c.

TABLE XXXIc.—RADII OF ANIONS

	$F^-$	$Cl^-$	$Br^-$	$I^-$	$O^-$	$S^-$	$Se^-$	$Te^-$
Goldschmidt	1.33	1.81	1.96	2.20	1.32	1.74	1.91	2.11
Pauling	1.36	1.81	1.95	2.16	1.40	1.84	1.98	2.21

It may be seen at once that the size of the positive ions in the same periodic group increases with atomic number, whereas it decreases in the same periodic series with increasing charge which tends to tighten the structure. In negative ions the increased size due to repulsion of the extra electrons is balanced by the greater electric field, so that doubly charged negative ions are no larger, and sometimes smaller, than singly charged ions. The tightening effect of increased charges is shown by comparing  $K^+Cl^-$  and  $Ca^{++}S^-$ ; although all four ions have 18 electrons, the interatomic spacing for KCl is 3.14 A.U. and for CaS 2.84 A.U.

**3. The Laws of Formation of Ionic Crystals.**—Goldschmidt's first law of formation of ionic crystals is as follows: the crystal structure of a substance is determined by the ratios of numbers, the ratio of sizes and polarization properties of its components, which may be ions, atoms or atomic groups. The sizes of ions are obviously the most important property, since the coordination numbers which define crystal-structure types depend upon the

Transition in lattice type	Change in coordination number	Decrease in distance, per cent
$CsCl \rightarrow NaCl$ . . . . .	8 $\rightarrow$ 6	3
$NaCl \rightarrow ZnS$ . . . . .	6 $\rightarrow$ 4	5.8
$CaF_2 \rightarrow TiO_2$ (rutile) . .	8, 4 $\rightarrow$ 6, 3	3

packing radii. The influence of the coordination on distances in ionic lattices is shown in the table on p. 268. Thus the fewer the neighbors around an ion, the shorter the ionic distance, the charges being kept constant. Goldschmidt has shown from simple geometry that in order to arrange a certain number of spheres  $B$  so that they will touch around a central sphere  $A$ , the following ratios must hold:

Number spheres $B$	Arrangement	Limiting $R_A/R_X$
2	Opposite	
3	Equilateral triangle	0.15
4	Cube diagonal (tetrahedral)	0.22
4	Square	0.41
6	Cube normals (octahedral edges)	0.41
8	Cube diagonals (octahedral)	0.73

Such simple relationships which determine possible arrangements in space for given ratios of radii hold true in remarkable fashion for the packing of ions in crystals.

The way in which atomic diameter influences structure can be seen from the simplest ionic structure of the type  $AB$ , with equal numbers of ions of opposite signs. The simplest of these is the structure of rock salt, where sodium and chlorine ions occupy alternate corners of a cubic lattice. The coordination number is 6:6; *i.e.*, each sodium has six chlorine neighbors and *vice versa*. Actually, the chlorine ions are so large compared to the sodium that they form an octahedron that encloses it almost completely. Simple geometry shows that this can only be the case if  $R_A$  (radius of positive ion):  $R_B$  (radius of negative ion) = 0.73. This relation holds for all halides of the alkaline metals with the exception of the chloride, bromide, and iodide of cesium where the ratios  $R_A/R_B$  are 0.91, 0.84, and 0.75 respectively. Now these last three are the only alkaline halides which do not belong to the sodium chloride type but to the cesium chloride type. Here the coordination number is 8:8 and there is, so to speak, more room for the larger cesium ion inside the cube of chlorine ions. Where  $R_A:R_B$  is very small, the factor of polarization comes in, and the structure ceases to be ionic and becomes adamantine or molecular.

If we pass to the next simpler series,  $AB_2$ , a similar situation occurs. Where  $R_A:R_B$  is greater than 0.73, the structure is of the fluorite type (see Fig. 126). Here the coordination number is 8:4, the calcium ions being surrounded by a cube of eight fluorine ions just as the cesium by the chlorines. A number of compounds (see Type C1 in Table XXVIII) belong to this type, which includes the fluorides of the alkaline earths and the dioxides of zirconium, thorium, praseodymium, cerium, and uranium. If  $R_A:R_B$  lies between .73 and .41, a structure is formed analogous to rock salt. This is the rutile structure (see Fig. 127). Here the coordination number 6:3 cannot be satisfied in the cubic system and the octahedron of oxygen ions is placed on its side in a tetragonal structure. The two other forms of  $TiO_2$ , anatase and

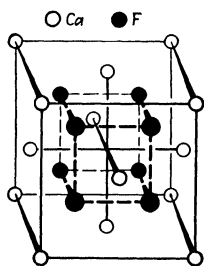


FIG. 126.—Lattice model for fluorite ( $CaF_2$ ).

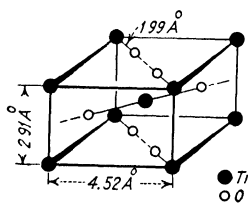


FIG. 127.—Lattice model for rutile ( $TiO_2$ ).

brookite, are also built with the same coordination but with the octahedra distorted and differently placed. A large number of substances belong to the rutile structure: the fluorides of Mg, Mn, Co, Fe, Ni, Zn and the dioxides of Mn, V, Ti, Ru, Ir, Os, Mo, W, Cb, Sn, Pb, and Te.

When  $R_A:R_B$  lies between .41 and .22 the coordination number is 4:2, which is approaching a homopolar structure. This is the case for the different forms of silica ( $SiO_2$ ), cristobalite, tridymite, and quartz. Though apparently different, these structures have the essential point in common that they are built from silicon ions completely surrounded by four oxygens in a tetrahedron. Each oxygen is shared between two tetrahedra and the different forms of structure are merely due to different arrangements of these tetrahedra. Thus the polymorphism of silica is not due to any change in the molecule.

Such considerations as these may be extended even to the ionic compounds with complex cations such as  $Ni(NH_3)_6^{++}$  and



to atomic radicals such as sulfate, nitrate, chlorates, etc. The work of Zachariasen on the compounds  $\text{ABO}_3$ ,  $\text{A}_2\text{BO}_4$ , etc., is especially noteworthy. In anhydrous  $\text{Na}_2\text{SO}_4$ , the  $\text{SO}_4$  ion is a perfect tetrahedron, and  $\text{NaO}_6$  a deformed octahedron, with each tetrahedron sharing two edges with an octahedron.<sup>1</sup>

**4. Layer Lattices.**—The most important influence, next to the size of the ions, in determining how a compound shall crystallize is the phenomenon of polarization, which includes all alterations which particles show under the influence of electric forces. The simplest case is the formation of a dipole under the influence of an electric field. The negative iodide ion is a typical polarizable ion. Cadmium iodide, by analogy with related compounds and the transition  $\text{CdF}_2 \rightarrow \text{CdI}_2$  and by consideration of the ratio of ionic radii  $R_{\text{Cd}^{++}}/R_{\text{I}^-}$ , would be expected to have a rutile structure, but instead it forms a distinctive type of its own. The coordination arrangement is such that any cadmium ion is surrounded symmetrically by six iodine ions rhombohedrally, but each iodine ion is in contact with three cadmium ions *on one side*, an ideal condition for polarization. The structure is built up in layers with the sequence iodide ion-cadmium ion-iodide ion layers being repeated. In each layer there is really a giant ionic molecule as large as the extension of the layer, whereas the layers are held together by secondary forces, which accounts for the very prominent cleavage. Of course, graphite is a prominent example among the elements. The transitions  $\text{TiO}_2 \rightarrow \text{TiS}_2$  and  $\text{SnO}_2 \rightarrow \text{SnS}_2$  also result in changes to layer lattices.

**5. Isomorphism, Morphotropism, Polymorphism.**—Goldschmidt's great contributions have been the result of his experimental method of substituting one ion for another in compounds and observing what change in structure occurred. It is clear that analogy in size of ions is the most important attribute contributing to isomorphism. This accounts for unsuspected cases of isomorphism such as lead and strontium, and magnesium and cobalt or nickel, salts, and for lack of isomorphism among salts far more nearly related chemically, such as salts of magnesium and calcium and even of sodium and potassium. In general, one atom or ion may be replaced by another without destroying the crystalline arrangement when the ionic distances do not differ by more than 10 per cent. This is also the degree of disarrange-

<sup>1</sup> *Z. Kryst.*, **81**, 92 (1932).

ment thermally possible before a crystalline arrangement of planes is destroyed by melting; thus the isomorphic and thermal tolerances are the same. When by chemical substitution the limit of homogeneous deformation is surpassed, a new atomic arrangement in space takes place; such a process Goldschmidt calls morphotropism. This occurs in the series of dioxides when the ratio  $R_A/R_B$  reaches 0.7 and in numerous other series of compounds in which stepwise substitutions are made to points where sudden changes in properties occur. Polymorphism, the phenomenon in which the same substance under different thermodynamic conditions may have different crystal structures, is simply a case of morphotropism brought about not by substitution but by thermodynamic alteration (temperature, pressure, directed force, etc.) so that the substance is no longer isomorphous with itself. These are but a few simple examples of the rational explanations of crystal chemistry based on x-ray crystal-structure data.

Goldschmidt has gone even further and used a model principally employing substitution of ions of the same size and shown that  $\text{TiO}_2$  is like  $\text{MgF}_2$ ,  $\text{ThO}_2$  like  $\text{CaF}_2$ ,  $\text{SrTiO}_3$  like  $\text{KMgF}_3$ ,  $\text{BaSO}_4$  like  $\text{RbBF}_4$ ,  $\text{Zn}_2\text{SiO}_4$  like  $\text{Li}_2\text{BaF}_4$ . Thus the properties of a very difficultly prepared salt may be anticipated by the study of a substituted model more easily available.

**6. Application of Crystal Chemistry Laws to Prediction of Properties.**—Goldschmidt has shown that the hardness and related cohesive properties of ionic crystals depend directly upon the electrostatic forces between ions. The hardness of crystals increases with decreasing distance between the ion centers, the charge being kept constant; and the hardness increases with increasing ionic charge when the distance is kept constant: for example,

Property	MgO	CaO	SrO	BaO	NaF	MgO	ScN	TiC
Distance	2 10	2.40	2 57	.	2 13	2 10	2 23	2 23
Hardness	6 5	4.5	3 5	3 3	3.2	6.5	7 to 8	8 to 9

Partial correlations have been made between ionic structure and optical properties,<sup>1</sup> compressibility,<sup>2</sup> expansion coefficients, elastic constants, cohesion, etc.

<sup>1</sup> See for example WOOSTER, In Relation between Double Refraction and Crystal Structure, *Z. Kryst.*, **80**, 495 (1931).

<sup>2</sup> See Bridgman's great book "The Physics of High Pressure," 1931.

**7. The Structure of Silicates.**—One of the most brilliant recent achievements in diffraction analysis is the series of remarkable studies of the complex silicates, which for a time defied complete interpretation on account of formulas which seemed unrelated to the usual valence laws of chemistry. A large number of ionic crystals which are of neither the simple nor complex ionic types are thus grouped together as the intermediate silicate type though not all contain silicon. W. L. Bragg was the first to show that the great complexities were dispelled when it was realized that these compounds consist essentially of the relatively larger oxygen ions in close-packed arrangement, either cubic or hexagonal. These ions are held together by strongly charged metallic ions which fit into the spaces between them. In tetrahedral spaces are to be found the smallest and most highly charged ions,  $\text{Si}^{++++}$ ,  $\text{Be}^{++}$ ,  $\text{Ti}^{++++}$ ,  $\text{Al}^{+++}$ ,  $\text{Mg}^{++}$ ,  $\text{Fe}^{++}$ , etc. Larger ions, such as  $\text{Ca}^{++}$ ,  $\text{Na}^{+}$ , and  $\text{K}^{+}$ , introduce distortion into the structure. The symmetry of the particular silicate adjusts itself to fit these ions with minimum distortion, with the result that the unit crystal cells are large and complicated because of low symmetry. W. L. Bragg summarizes the features of the great work done under his guidance as follows:<sup>1</sup>

a. Whatever the silicon to oxygen ratio, silicon always is situated within the tetrahedral group of four oxygen atoms, which is very constant in form from crystal to crystal.

b. The structures are typical coordination structures—four oxygens at the corners of a tetrahedron, six of an octahedron, etc. The whole structure may be regarded as a fabric of which these groups are the stitches, the groups being joined together by sharing oxygen atoms.

c. The coordination numbers among silicates are  $\text{Be}^{++}$  4,  $\text{B}^{+++}$  3, 4,  $\text{Na}^{+}$  6, 8,  $\text{Mg}^{++}$  4, 6, 8,  $\text{Al}^{+++}$  4, 5, 6,  $\text{Si}^{++}$  4,  $\text{Ca}^{++}$  6, 7, 8,  $\text{Sc}^{+++}$  6,  $\text{Ti}^{4+}$  6,  $\text{Mn}^{++}$  4, 6, 8,  $\text{Fe}^{++}$  4, 6, 8,  $\text{Fe}^{+++}$  6,  $\text{Zn}^{++}$  4,  $\text{Zr}^{4+}$  8,  $\text{Ba}^{++}$  6, 12.

Pauling<sup>2</sup> has gone still further in discovering general principles of structures. The entire group of coordinated anions around each cation is to be considered as polyhedron (see Fig. 128). The presence of shared edges, and particularly of shared faces, in a

<sup>1</sup> *Faraday Soc. Mon.*, Crystal Structure and Chemical Constitution (March, 1929).

<sup>2</sup> *J. Am. Chem. Soc.*, **51**, 1010 (1929).

coordinated structure decreases its stability (since the positive ions would be brought into unusually close proximity): the effect is large for cations with large valence and small coordination number and is especially large in case the radius ratio  $R_A/R_B$  approaches the lower limit of stability of the particular polyhedron.

In limited space it is impossible to give a just picture of the great progress which has been made possible by means of these

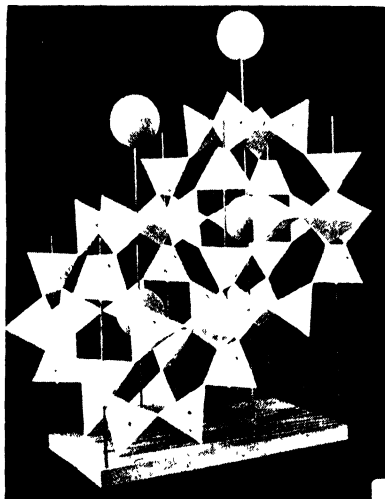


FIG. 128.—Photograph of a model illustrating coordination structures of complex compounds, and representing sodalite,  $\text{Na}_4\text{Al}_3\text{Si}_3\text{O}_{12}\text{Cl}$ . (Pauling.) The spheres indicate chlorine ions, and the tetrahedra have an oxygen ion in each corner and silicon or aluminum at the center.

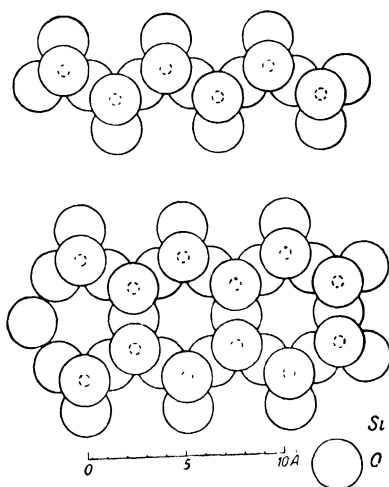


FIG. 129.—Silicon-oxygen chains in pyroxene (diopside), above; and double chains in amphibole, below. Mica is built from a further extension of these chains into a sheet.

simplifying conceptions. The service to chemistry, geology, and mineralogy is immeasurably great. Only a single example need be cited to show what simple relationships are now found to hold for substances which seemed hopelessly complex only a short time ago. The essential feature of diopside, a typical metasilicate with the formula  $\text{CaMg}(\text{SiO}_3)_2$ , is that each silicon atom is surrounded tetrahedrally by four oxygen atoms in the usual way. Two of these atoms are common to neighboring groups and two are not. The tetrahedra are linked by their corners into *endless chains* parallel to the  $c$  axis of this monoclinic crystal as shown in Fig. 129. It is incidental that the  $\text{SiO}_4$  groups are cemented sideways by

calcium and magnesium ions. Bragg and Warren, soon after the analysis of diopside, noted certain similarities with asbestos. Analysis has indicated that the  $\text{SiO}_4$  single chains in diopside are now *double* chains in asbestos. Splitting can occur parallel with these double-linked chains. Now this process may continue until a whole sheet or network of the  $\text{SiO}_4$  groups is made possible by sharing oxygens. This is mica whose cleavage in thin sheets is so familiar.

**8. General Relationships of Structure and Properties of Crystalline Metals.**—The following conclusions may be drawn from a consideration of the data obtained by x-ray analysis of crystalline structure of metals:

a. The periodic arrangement of elements is, in general, carried over into the types of crystalline structures; there is an easily observed tendency for elements in the same periodic column or family to crystallize in the same way. There are notable exceptions, as, for example, the discovery in the writer's laboratory that calcium and strontium are face-centered cubic and barium is body-centered cubic.<sup>1</sup> Other complexities are the unusual structures of  $\alpha$  and  $\beta$  manganese, which have remarkable analogues among the alloys, and the cases noted above of entirely distinctive structures for white tin, etc.

b. As noted in a preceding section, evidence, including the interpretation of the new quantum mechanics, points to the fact that true crystalline metals are built up from positive ions in an electron gas. This electron gas, so-called, is a primary determining factor. In ordinary ionic lattices for chemical compounds in which electrostatic forces between positive and negative ions hold these at the points of the lattice, the elements magnesium, cobalt, nickel, and zinc are very similar, whereas in metallic crystals the similarity is retained only for cobalt and nickel.

c. New evidence seems to indicate that metals are a state of matter rather than a type; in other words, at sufficiently high temperatures and pressures such as may be attained on the interior of the stars, all elements and compounds may become metals in the sense of the fundamental properties such as conductivity by electron transport.

<sup>1</sup> CLARK, KING, and HYDE, *Proc. Nat. Acad. Sci.*, **14**, 617 (1928); **15**, 337 (1929); *J. Am. Chem. Soc.*, **51**, 1709 (1929). Also EBERT and HARTMANN, *Z. anorg. allgem. Chem.*, **179**, 418 (1929).

d. The ratios in which metal atoms combine are often not capable of explanation on the basis of usual chemical rules but may be accounted for geometrically on the basis of coordination. In the series  $\text{Cd}_2\text{Li}$ ,  $\text{Cd}_6\text{Na}$ ,  $\text{Cd}_{11}\text{K}$ , the proportion of cadmium increases with the atomic volumes of Li (21 A.U.<sup>3</sup>), Na (48 A.U.<sup>3</sup>), and K (72 A.U.<sup>3</sup>). Similarly miscibility or non-miscibility may be almost entirely a matter of atomic radii.

The best method of arriving at definite conclusions as to the relation between characteristic properties and structure is to observe the transformations of one type of crystal structure into another in series of comparable alloys. This logic has been used by Westgren and by Goldschmidt to derive important generalizations from a seemingly hopelessly complicated field. Some of these will be noted in the next chapter on alloys. It is certain that, for metals, atomic weights or atomic numbers are relatively far less important in determining the type of crystalline structure than the average concentration of valence electrons. In other words, the most important factors are the polarization properties of the atoms. Goldschmidt<sup>1</sup> draws an analogy between a radical such as ammonium ( $\text{NH}_4$ ), which acts as a *polynuclear pseudo-atom*, and a single metal crystal, no matter how large, which is also a *polynuclear pseudo-atom* on account of the common electron shell (gas) around the positive kernels. In terms of modern theories of the structure of matter, this accounts for all those properties characteristically associated with the metallic state—allotropy, transformations, common behavior in polyphase systems, the solubility of hydrogen in solid metal crystals<sup>2</sup> (in the form of hydrogen kernels), the electron emission from heated metals as an ionization leaving the whole metal crystal as a *macroscopic cation*, electron isomerism, and passivity. Even molten metals are polynuclear pseudo-atoms, and only in vaporization do the single atoms regain their individuality.

e. As might be anticipated, the problem of the metallic state is rendered so difficult by the fact that there are so many *degrees* of what may be termed metallic properties. It is impossible to find, for example, where metallic combination leaves off and homopolar begins, just as is true for the transition from ionic to homopolar combination in silicates. There is recognized, how-

<sup>1</sup> *Ber.*, **60**, 1263 (1927); *Trans. Faraday Soc.*, **25**, 253 (1929).

<sup>2</sup> Also helium in platinum, with x-ray evidence of compound formation; cf. Damianovitch and Trillat, *Compt. rend.*, **188**, 991 (1929).

ever, a class of half metals found in the *B* periods of the periodic table (Al, Zn, Ga, Ge, As, Cd, In, Sn, Sb, Hg, Tl, Pb, Bi). They are distinguished from true metals in part as follows:

(1) Their structures are such that each atom is surrounded by  $8-n$  neighbors where  $n$  is the group number of the element in the periodic system (Hume-Rothery); in other words each atom has as many neighbors as there are number of electrons required to fill up the rare gas shells. This leads to two-atom molecules for the halogens, chains for selenium and tellurium, layers for As, Sb, and Bi, and to the diamond structure for Ge and Sn.

(2) True metals conduct electricity less readily in molten condition, while the half metals are characterized by the reverse.

(3) Closest packing in crystal lattices is ordinarily absent in half metals. They can ordinarily dissolve only traces of the true metals, since an atom can be replaced only by one of similar electron configuration, while true metals can readily dissolve half metals if there is not too great a discrepancy in atomic dimensions.

(4) Half metals are strongly diamagnetic (as is also true in the alloy structures); the atoms themselves (vapor) may be paramagnetic but the behavior of the solid indicates the great structural effect. Very weak diamagnetism persisting after melting must reside in bonds of homopolar nature. Very strong negative susceptibility is also a structural property.

(5) Electrical conductivity is at a minimum for stoichiometric combinations of half metals, but a maximum for true metals.

(6) The compounds of the true metals with P, As, Sb, Bi, Si (Ge, Sn, Pb), S, Se, Te and with H, B, C, and N(O, F) are distinguished at least for the first two groups as simple ionic, while the compounds with the transition metals, half metals, and heavy metals are homopolar or metallic.

In a masterly paper on the problem of the metallic state, J. D. Bernal<sup>1</sup> summarizes the evidence concerning the metallic bond as follows:

1. It must be capable of acting between identical atoms and at the same time between atoms of very different constitution (as in intermetallic compounds), the only limit being that the majority of atoms concerned should be metallic.

2. It should be undirected, as is shown by its identity and almost equal efficacy in the liquid state, and unsaturated; *i.e.*, it

<sup>1</sup> *Trans. Faraday Soc.*, **25**, 367 (1929).

should permit always of the highest coordination number sterically possible. This number in some alloys rises as high as 16.

3. Its force must vary inversely as some high power of inter-nuclear distance as shown by its extreme weakness in the alkaline metals, with low melting points and very large atomic volumes, by the high value of the thermal energy of titanium, and by the low atomic volume of the platinum group. There must be some difference between the forces concerned with thermal and mechanical effects.

4. In equilibrium with this force of attraction there must be a force of repulsion which is an atomic property as shown by the *constancy of atomic volume* in alloy formation. (This is the most difficult fact to explain on the theory that conductivity electrons belong to the lattice, as a whole, and not to single atoms.)

5. The bond must allow a transfer of electrons from one atom to another to account for the electrical properties.

Notable efforts have been made in recent months by Bernal, Slater, Mott, and others to take these factors into account in attempting to define the metallic state upon the basis of wave functions combining what amounts to both free and bound electrons. The great progress which has been made, the great mass of experimental observations on metals, half metals, alloys, etc., and the need of further development of modern wave mechanics are clearly indicated in two very recent publications by Bernal<sup>1</sup> and by Hume-Rothery<sup>2</sup> which present the entire subject of the metallic state as it is now known.

<sup>1</sup> "Fortschritte der Röntgenforschung in Methods und Anwendung," pp. 200-239, Leipzig, 1931.

<sup>2</sup> "The Metallic State," Oxford University Press, New York, 1931.



## CHAPTER XV

### THE STRUCTURE OF ALLOYS

**1. Types of Alloys.**—The phenomena which occur when two metals are melted together and allowed to cool have long been known. Microscopic, thermal, dilatometric, and electrical methods have demonstrated the formation of “mixed crystals” or solid solutions, of eutectic mixtures, and of chemical compounds. In binary alloys all of these conditions are found in various combinations.

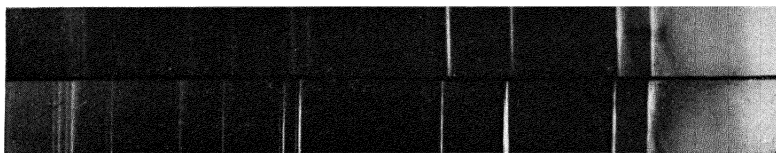


FIG. 130.—Powder diffraction patterns illustrating solid solution: upper,  $\alpha$ -brass, 80 per cent copper, 20 per cent zinc; lower, pure copper.

*a. Alloys Formed by a Continuous Series of Solid Solutions (Substitutional).*—In such alloys the atoms of one kind of metal which is being alloyed with another replace the atoms of the latter at the lattice points. In most cases this is a simple process but in other cases, as in copper-aluminum alloys, complex substitution may involve replacing three by two atoms, etc.

Microscopic evidence: only one kind of crystals appears in any specimen ranging from one pure component to the other.

Thermal evidence: smooth continuous curve in phase diagram between pure components. Very slow cooling or careful annealing to permit diffusion is necessary to assure that all the crystals separating from the liquid phase are uniform in composition since two “nicks” appear in cooling curves.

X-ray evidence: only one type of diffraction pattern throughout, the only variation being a change in the lattice parameter. Figure 130 shows how the diffraction lines for a pure metal are shifted for a solid solution.

Requirements: only two metals which have the same lattice structure (*i.e.*, both face-centered cubic, for example) can form

a continuous series of solid solutions. All pairs of metals with common lattice structure do not form continuous series (*e.g.*, aluminum-gold).

Additivity relations: Vegard's law of additivity states that in a binary system forming a continuous series of solid solutions the lattice parameters are linearly related to atomic percentage of one of the components. In other words, upon a straight line joining the numerical values of the edge lengths of the unit crystal cells of the two pure metals, lie all the lattice values for all possible solid solutions of the two metals.

Examples investigated by x-rays: gold-copper, gold-silver, gold-palladium, nickel-copper, tungsten-molybdenum, cobalt-nickel, nickel-palladium, iron-vanadium, platinum-palladium, potassium-rubidium, strontium-calcium (unpublished), etc.

*b. Substitutional Solid Solution over Limited Ranges.*—It follows, of course, that other systems which do not form a continuous series of solid solutions will show substitutional mixed crystals over limited ranges of *B* in *A* and *A* in *B*.

*c. Interstitial Solid Solution.*—The alloying atoms do not substitute for atoms of the original metal but enter the empty lattice spaces between the atoms; the best example is carbon in iron.

X-ray evidence: the symmetry and the positions of the x-ray interferences of one of the fine metals may be entirely unaffected. With the entrance of new atoms in the interstices, of course, the relative intensities will be definitely affected.

*d. Systems with a Eutectic.*—Microscopic evidence: mechanical mixture of two kinds of crystals usually identified as the pure components.

Thermal evidence: liquidus curve sharply discontinuous with separation of crystals at lower temperature than that for the pure metals or intermediate mixtures.

X-ray evidence: diffraction patterns for both metals superposed.

Example: lead-silver alloys. In an alloy with 1 per cent silver, pure lead crystals will first separate until a composition of 2.5 per cent silver is reached, whereupon at 304° C. both lead and silver crystals separate together in constant ratio.

*e. Systems with Compound Formation.*—Microscopic evidence: doubtful, two kinds of crystals, unless the specimen has the exact constitution corresponding to a definite chemical compound.

Thermal evidence: maximum in the melting point curve.

X-ray evidence: limited solid solutions of  $A$  in  $B$  and  $B$  in  $A$ , or lattices of both  $A$  and  $B$ , compound  $A_xB_y$  with different characteristic lattice, and solid solutions or mechanical mixtures of  $A$  and  $A_xB_y$  and  $B$  and  $A_xB_y$ .

Example: in the system lead-magnesium (Sacklowski), x-ray data show a series of mixtures, from 0 to 81 per cent lead, of magnesium, and the compound  $PbMg_2$ ; at 81 per cent lead a face-centered cubic lattice for  $PbMg_2$  with an edge length of 6.76 A.U., and at higher lead contents, mixtures of lead and  $PbMg_2$  lattices.

The elements may be arranged according to the ease with which foreign atoms enter the lattices:

Group I, first kind: Cu, Ag, Au, and the Fe, Pd, and Pt triads. Group II, second kind: Li-Be, Na-Al, K-V, Pb-Cb, Cs-Ta, Zn-Ce, Cd-Sn, Hg-Bi, non-metals, half metals (B, Si, As, Sb), rare gases, and hydrogen.

Alloys of metals of the first kind form generally continuous solid solutions or wide ranges of solubility; intermediate compounds if any are of the overstructure type, appearing only after careful tempering.

Alloys between metals of types I and II are characterized by a great array of intermediate phases, *e.g.*, copper-zinc or brass (Fig. 131). Those phases which are rich in the metal of the first kind have a greater range of homogeneity than the others.

Alloys between metals of the second kind, between metals and half metals or non-metals, are similar to the last class, although the greater the loss of metallic character, the more definite the chemical compound with no solution phenomena.

*f. Systems with Superstructures.*—Intermediate types between the foregoing principal types are, of course, to be expected, such as the solid solubility of a compound in the lattice of a pure metal. Or a foreign atom entering the two kinds of mixed crystals (substitutional and interstitial) may take up special positions and actually enlarge the lattice or lower the symmetry. Such a lattice is really a true compound. It is distinguished from the other compounds by the fact that it represents very slight deformation of the lattice of the pure metal; it is distinguished from a true solid solution or mixed crystal, in that new or superstructure lines appear in the x-ray patterns in addition to those characteristic of a pure metal, or in that normally single lines



appear to be split. The surprising list of examples is shown in Table XXXII. These superstructure types do not usually appear with ordinary melting practice, but only after careful tempering.

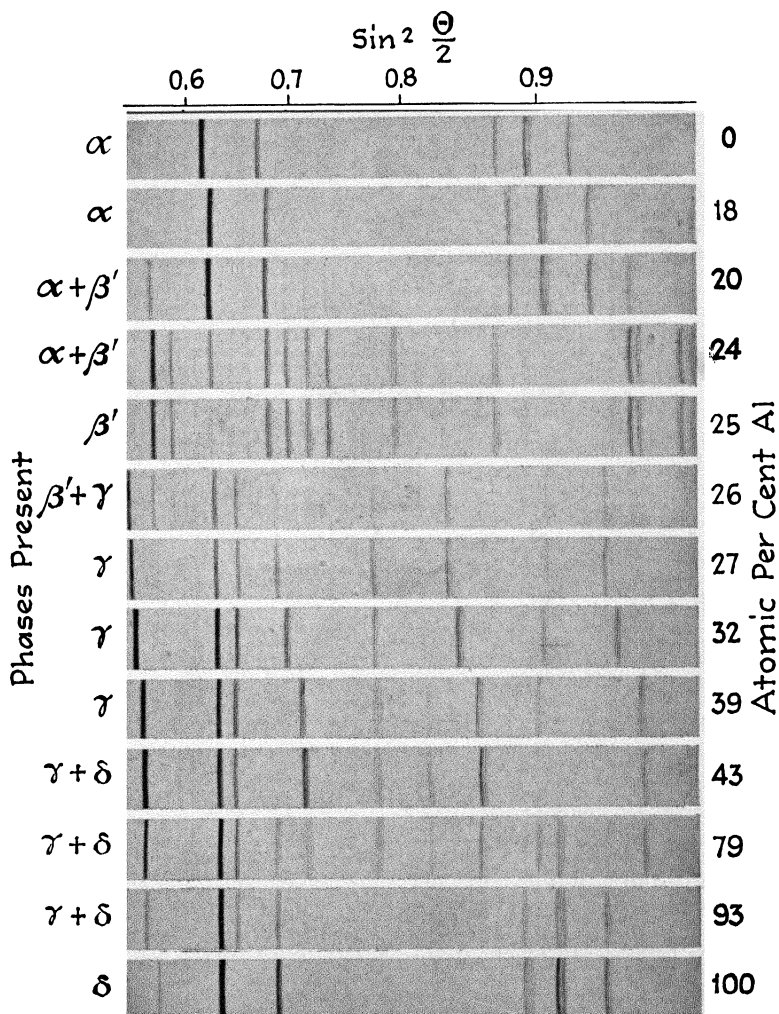


FIG. 132.—Powder photographs of silver-aluminum alloys. (Westgren and Bradley.)

**2. X-ray Results on Alloy Systems.**—The lattice types of the alloy compounds have been classified on the arrangement of Ewald and Hermann's "Strukturbericht" in Table XXXII. All of the types *B*, *C*, and *D* have been listed in the classification of

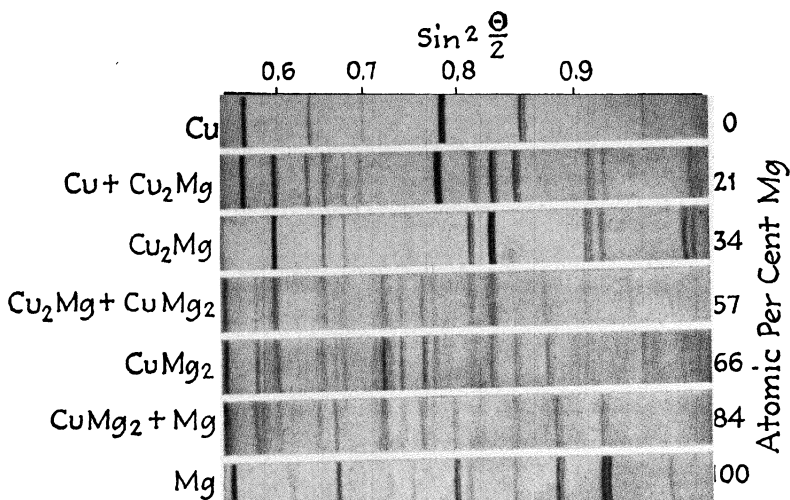


FIG. 133.—Powder photographs of copper-magnesium alloys. (Runquist, Arnfelt, and Westgren.)

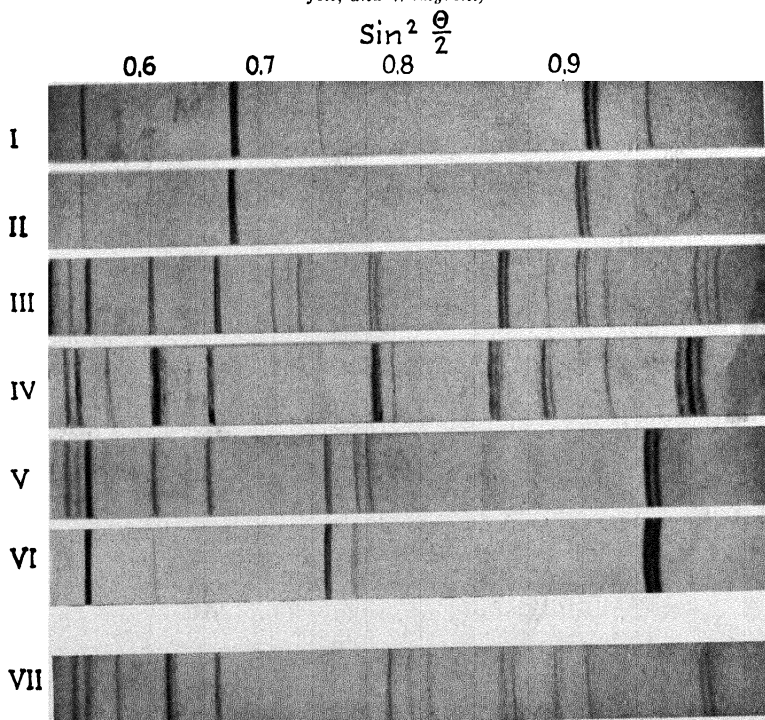


FIG. 134.—Powder photographs of metals and alloys of the iron-tungsten and iron-molybdenum systems. I, Fe; II, Fe, saturated with W; III, Fe<sub>2</sub>W; IV, Fe<sub>3</sub>W<sub>2</sub>; V, Fe<sub>3</sub>W<sub>2</sub> + W; VI, W; VII, Fe<sub>3</sub>MO<sub>2</sub>.

inorganic compounds (Table XXVIII, page 246). A new type  $L$ , however, has been devised to account for the substitutional alloys of the superstructure types and  $L^1$  for the interstitial superstructure types.

While it is evident that a great many papers have been published particularly in the past two years and that most of the present information on the metallic state, valence, atomic structure, and general analogies have been obtained from a knowledge of how metals combine, still the great part of the field is unexplored. First in the field of alloy structure and constitution stands Prof. A. F. Westgren of Stockholm, who, with Dr. G. Phragmen and other coworkers, has carried out a series of

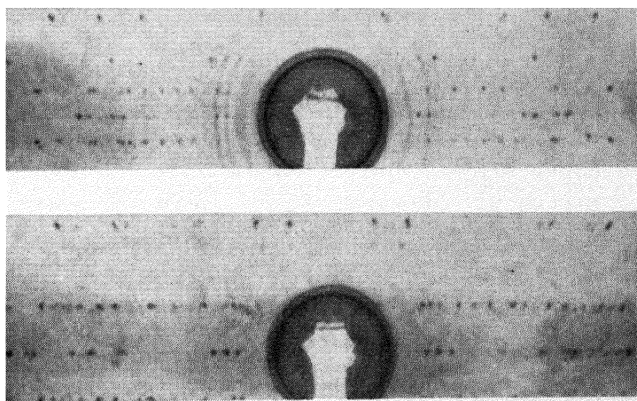


Fig. 135. Rotation patterns around two axes for single crystal of  $\text{CuMg}_2$ .

experimental researches with x-ray methods which finds no superior in science. In the Stockholm laboratory have been perfected all the standard methods of analysis and interpretation. In the face of widespread doubt and criticism there were reported the large unit cells of  $\gamma$ -brass (52 atoms),  $\delta$ -bronze (416 atoms),  $\alpha$ - and  $\beta$ -manganese, etc., only to demonstrate that these results were correct. It is one of the privileges of x-ray workers to pay tribute to the untiring skill and invaluable contributions of Professor Westgren. Diffraction patterns made in the Westgren researches, on the systems silver-aluminum, copper-magnesium, and iron-tungsten and iron-molybdenum are reproduced in Figs. 132, 133, and 134, respectively. The camera used was of the focusing type with slit, specimen, and film on the same circumference, similar to the Seemann-Bohlin instrument shown in Fig. 100. Single crystal patterns for  $\text{CuMg}_2$  are shown in Fig. 135.

TABLE XXXII.—CLASSIFICATION OF ALLOYS  
Alloys related to type A1 (face-centered cubic): substitution superstructures

L 10	Tetragonal	$D_{4h}^1$	A1 distorted along a 4-fold axis	CuAu
L 11	Rhombohedral	$D_{3d}^5$	A 1 distorted along a 3-fold axis	PtAu
L 12	Cubic	$O_h^1$	A 1 with regulated substitution; planes with mixed indices double A1	AuCu <sub>3</sub> , PtCu <sub>3</sub> , PdCu <sub>3</sub>
L 13	Cubic	$O_h^7$	Superstructure; 100, 110 same as A1 planes with 3 odd indices doubled	CuPt
L 10	Cubic	$O_h^1$	Planes 3 odd indices same as in A 1; mixed indices planes doubled	Fe <sub>4</sub> N

Alloys related to type A 2 (body-centered cubic)

B 2	Cubic		CsCl structure	CuPd, CuBe, Cu- Zn, AgMg, Ag- Zn, AgCd, AuZn, NiAl
L 21	Cubic	$O_h^8$	Substitution superstructures; planes of even and two odd (110) indices same as A 2, of one odd and 2 even (100) doubled; all odd (111) quad- rupled	Cu <sub>2</sub> AlMn (Heu- sler alloy)
L 22	Cubic	$O_h^9$	Substitution superstructure; cube edge three times A 2 cell; contains 54 atoms	Sb <sub>2</sub> Th
L 20	Tetragonal	$D_{4h}^{17}$	Interstitial superstructures A2 interferences for 100, 110 split into two and others into three; 111 simple	Martensite $\alpha$ — Fe + 6 at. per cent C

Other alloy types in Table XXVIII

B 2	(Cubic CsCl structure)	CuPd, CuBe, CuZn, AgMg, AgZn, AgCd, AuZn, NiAl
B 8...	(Nickel arsenide)	AuSn
C 1	(Fluorite)	Mg <sub>2</sub> Si, Mg <sub>2</sub> Sn, Mg <sub>2</sub> Pd
C 14...	Hexagonal	MgZn <sub>2</sub>
C 15	Cubic	Cu <sub>2</sub> Mg
C 16	Tetragonal	Cu <sub>2</sub> Al
C 17	Tetragonal	Fe <sub>2</sub> B
C 18	Rhombic	FeS <sub>2</sub> (marcasite), FeAs <sub>2</sub> , FeSb <sub>2</sub>
D 81, 82, 83, 84	.....	Fe <sub>3</sub> Zn <sub>10</sub> , Cu <sub>3</sub> Zns, Cu <sub>3</sub> Al <sub>4</sub> , Cu <sub>31</sub> Sn <sub>8</sub>

#### BRIEF SUMMARY OF CONCLUSIONS FROM X-RAY DATA ON ALLOYS

Ag-Al:  $\alpha$  (Al in solution in Ag to about 19 per cent);  $\beta'$  (Ag<sub>3</sub>Al, complex cubic with 20 atoms per unit cell);  $\gamma$  (27 to 43 per cent Al, hexagonal close-packed);  $\delta$  (Al, no Ag dissolving).

Ag-Au: Continuous solid solution very nearly obeying Vegard's law.

Ag-Bi: No compounds; Bi in Ag to 5.5 per cent, expanding Ag lattice.



- Ag-In:  $\text{Ag}_3\text{In}$  (hexagonal close-packed).
- Ag-Pd: Continuous solid solution.
- Ag-Sb: Sb in Ag to 6 per cent; 11 to 16 per cent Sb, hexagonal close-packed;  $\text{Ag}_3\text{Sb}$  (rhombohedral).
- Ag-Sn: 0 to 11 per cent Sn in Ag;  $\text{Ag}_{6,7}\text{Sn}$ ,  $\epsilon$  and  $\epsilon'$  ( $\text{Ag}_3\text{Sn}$ ) (hexagonal close-packed).
- Ag-Zn: Like Cu-Zn.
- Al-Sb:  $\text{AlSb}$  (type *B* 3).
- Au-Cd:  $\gamma$ -phase like Au-Zn.
- Au-Hg: 0 to 15 per cent Hg in Au; 25 per cent Hg, hexagonal; two other phases at 50 to 60 and 65 to 70 per cent Hg.
- Au-Pd: Continuous solid solution.
- Au-Sb:  $\text{AuSb}_2$ , cubic.
- Au-Sn:  $\text{AuSn}$  (*B* 8 type), and  $\text{AuSn}_2$ ,  $\text{AuSn}_4$ , and another intermediate compound (16 atomic per cent Sn) with hexagonal lattice.
- Au-Zn: Like Cu-Zn, and Ag-Zn except two additional phases:  $\gamma'$  (75 atomic per cent Zn,  $\text{AuZn}_3$ , cubic, 32 atoms per cell, ordinary temperature);  $\gamma''$  (77.7 atomic per cent Zn, high temperature, cubic similar to  $\gamma'$ ).
- Cd-Hg: Two phases 0 to 20 per cent Hg (Cd lattice); 36 to 65 per cent Hg (tetragonal body-centered).
- Co-Cr: 30 per cent Cr in Co, 25 per cent Co in Cr, intermediate heterogeneous.
- Cr-C: See page 303.
- Cu-Ag: Incompletely miscible, no compounds; no silver lines below 6 per cent Ag and no Cu lines above 70 per cent Ag.
- Cu-Al:  $\alpha$  (solution of Al in Cu to 20 per cent *A* 1),  $\beta$  ( $\text{Cu}_3\text{Al}$  stable at high temperatures, cubic superstructure),  $\delta$ ,  $\epsilon$ ,  $\eta$ , ( $\gamma'$ ) (all similar, *D* 83,  $\text{Cu}_9\text{Al}_4$ );  $\theta$  ( $\delta$ ),  $\text{CuAl}_2$  (type *C* 16);  $\kappa$  ( $\epsilon$ ), solution Cu in Al in very small amounts.
- Cu-Al-Mn { Heusler alloys;  $\alpha$ ,  $\beta$ ,  $\delta$  ( $\gamma'$ ) structures of Cu-Al, while Mn pro-  
Cu-Sn-Mn } duces superstructures in  $\beta$ .
- Cu-Au: Continuous solid solution nearly obeying Vegard's law;  $\text{AuCu}$  (type *L* 10) and  $\text{AuCu}_3$  (type *L* 12) superstructures with very slow cooling or tempering.
- Cu-Be:  $\alpha$  (15 per cent Be in Cu);  $\gamma$  ( $\text{CuBe}$ , type *L* 20);  $\delta$  ( $\text{CuBe}_3$ ).
- Cu-Co: 5 per cent Co in Cu, 8 per cent Cu in Co. Co always cubic in alloys, hexagonal when pure.
- Cu-Mg: Cu lattice expands 3.608 to 3.624 when saturated;  $\text{Cu}_2\text{Mg}$  (*C* 15);  $\text{CuMg}_2$  (rhombohedral); Mg dissolves no Cu.
- Cu-Mn: Cu dissolves 30 per cent Mn with increase in *a*.
- Cu-Ni: Continuous solid solution.
- Cu-Pd: 38 atomic per cent Pd in Cu, 50 per cent Cu in Pd; compounds  $\text{CuPd}$  (type *L* 20); superstructure  $\text{Cu}_3\text{Pd}$  from copper phase in tempering (type *L* 12).
- Cu-Sb:  $\text{Cu}_3\text{Sb}$  like  $\text{Cu}_3\text{Sn}$ ;  $\text{Cu}_2\text{Sb}$  like  $\text{Fe}_2\text{As}$ .
- Cu-Si:  $\alpha$ , Cu lattice;  $\beta$  (high temperature) 14.5 atomic per cent Si, hexagonal close-packed,  $a = 2.588$ ,  $c = 4.176$  A.U.;  $\gamma$  (low temperature) 17 at. per cent Si, cubic same as  $\beta$ -Mn,  $a = 6.210$  A.U.,  $\text{Cu}_6\text{Si}$ ;  $\delta$  (high temperature) 18 at. per cent Si, deformed  $\gamma$ -brass type;  $\epsilon$  (low temperature) 21

at. per cent Si, body-centered cubic,  $a = 9.694$  A.U. 76 atoms per unit cell,  $\text{Cu}_{16}\text{Si}_4$ ;  $\eta$ , 25 at. per cent Si, hexagonal nearly same as cubic  $\beta$ -brass type.

Cu-Sn (bronze):  $\alpha$  (0 to 8 per cent Sn in Cu);  $\beta$  (15 per cent Sn, quenched from 700 deg. BCC);  $\gamma$  ( $D$  84,  $\text{Cu}_{31}\text{Sn}_8$ );  $\epsilon$  ( $\text{Cu}_3\text{Sn}$ , hexagonal close-packed with superstructure);  $\eta$  CuSn ( $B$  8 with superstructure  $a' = 5a$ ); Sn (white Sn dissolves no Cu).

Cu-Zn (brass):  $\alpha$  (solid solution, types  $A$  1-0 per cent Zn,  $a = 3.61$ ; 38 per cent Zn,  $a = 3.69$ ).  $\beta$  and  $\beta'$  ( $\text{CuZn}$ , type  $L$  20: 46 to 48 per cent Zn,  $a = 2.945$ );  $\gamma$  ( $\text{Cu}_5\text{Zn}_8$ , type  $D$  82, 61 per cent Zn,  $a = 8.85$ );  $\epsilon$  (type  $A$  3, 80 per cent Zn,  $a = 2.745$ ,  $c = 4.294$ ; 86 per cent Zn,  $a = 2.761$ ,  $c = 4.286$ );  $\eta$  (type  $A$  3, solid solution Cu in Zn; 96 per cent Zn,  $a = 2.67$ ,  $c = 4.92$ ; 100 per cent Zn,  $a = 2.66$ ,  $c = 4.94$ ). See Fig. 131.

Cu-Zn-Al:  $x\text{Cu}_5\text{Zn}_8.y\text{Cu}_9\text{Al}_4$ .

Fe-As:  $\alpha$  (0 to 4 per cent As);  $\epsilon$  ( $\text{Fe}_2\text{As}$ , tetragonal  $D'_{4h}$ );  $\eta$  ( $\text{FeAs}$  rhombic, deformed NiAs structure).

Fe-B:  $\text{Fe}_2\text{B}$  ( $C$  16 type).

Fe-Bi: Completely insoluble in each other.

Fe-C: See page 296 for iron-carbon alloys.

Fe-Co: 80 per cent Co in  $\alpha$ -Fe; in FCC-Co 11 per cent Fe; hexagonal Co only with traces of Fe.

Fe-Cr: Continuous solid solution obeying Vegard's law.

Fe-Mn:  $\gamma$ -Fe in  $\gamma$ -Mn, continuous series of mixed crystals; 35 per cent  $\gamma$ -Fe in  $\beta$ -Mn ( $730^\circ\text{C}$ .); 37 per cent  $\gamma$ -Fe in  $\alpha$ -Mn ( $490^\circ\text{C}$ .);  $\epsilon$  phase, 12 to 23 at. per cent Mn; solubility of Mn in  $\alpha$ -Fe very small.

Fe-Mo: Limited solubility; compound  $\text{Mo}_2\text{Fe}_3$  (hexagonal, 8 molecules per cell).

Fe-N:  $\alpha$  (pure  $\alpha$ -Fe,  $\text{N}_2$  insoluble);  $\gamma'$  ( $\text{Fe}_4\text{N}$ , type  $L'10$ ),  $\epsilon$  (hexagonal packing Fe atoms);  $\zeta$  ( $\text{Fe}_2\text{N}$ , rhombic).

Fe-Ni: Twenty-five per cent Ni in  $\alpha$ -Fe; 65 per Fe in Ni.

Fe-P:  $\alpha$  (0 to several per cent P with no change in lattice of Fe);  $\epsilon$  ( $\text{Fe}_3\text{P}$ , tetragonal  $S_4^2$ );  $\zeta$  ( $\text{Fe}_2\text{P}$  hexagonal);  $\eta$  ( $\text{FeP}$ ?).

Fe-Sb:  $\alpha$  (0 to 3 per cent Sb);  $\epsilon$  ( $\text{FeSb}$ , type  $B$  8);  $\zeta$  ( $\text{FeSb}_2$  rhombic type  $C$  18);  $\eta$  (pure Sb, no Fe dissolving).

Fe-Si:  $\alpha$  (0 to 30 per cent Si with decrease in lattice from 2.861 to 2.815); above 13 per cent Si superstructure ( $L$  21),  $\gamma$  (with 4.8 per cent Si and above  $\gamma$ -phase of Fe non-existent);  $\epsilon$  ( $\text{FeSi}$ , cubic),  $\zeta$  ( $\text{FeSi}_2$  tetragonal);  $\eta$  (pure Si, dissolving no Fe).

Hg-Sn: Tetragonal tin dissolves no Hg; 7 to 8 per cent Sn in Hg hexagonal.

Mg-Al: Limited mutual solubility.

Mg-Cd: No x-ray trace  $\text{MgCd}_2$ ; superstructure at 50 at. per cent Mg,  $a^1 = 6a$ ,  $c^1 = 3c$  of Mg.

Mg-Si:  $\text{Mg}_2\text{Si}$  (type  $C$  2).

Mg-Sn: }  
Mg-Pb: } Three phases, pure metals and  $\text{Mg}_2\text{Sn}$ ,  $\text{Mg}_2\text{Pb}$  (type  $C$  1).

Mg-Zn: Three intermediate compounds;  $\text{MgZn}_2$  ( $C$  14 type).

Mo-C: 30 to 39 per cent C, hexagonal close-packed Mo atoms.

Mo-W: Continuous solid solution.

Na-Cd:  $\text{NaCd}_2$ .

Na-Pb: several compounds with complex structures;  $\text{Na}_4\text{Pb}$  really  $\text{Na}_{31}\text{Pb}_8$  cubic, 78 atoms per unit cell, related to  $\gamma$ -brass structure.

Ni-Al:  $\text{NiAl}$  (*L* 20 type).

Ni-Cr: Sixty-four per cent Ni in Cr, 65 to 85 per cent Cr rhombohedral phase.

Pd-H:  $\text{Pd}_2\text{H}$  (face-centered cubic metal atoms dissolve more H up to  $\text{PdH}$ ),  $a$  (Pd) = 3.89;  $a$  (maximum H content) = 4.02 to 4.07; lose H in air to stable  $\text{Pd}_2\text{H}$ .

Sn-Pb: 0 to 3.6 per cent Sn in Pb; both lattices beyond.

Sn-Sb: 55 per cent Sb, *B* 1 type with doubled cube edge.

Tl-Pb: Tl dissolves little Pb, 4 per cent Pb giving both lattices; Pb dissolves 80 per cent Tl.

Tl-Sb:  $\alpha$  (0–8 per cent Sb in  $\alpha$ -Tl);  $\beta$  (soln. of Sb in  $\beta$ -Tl);  $\gamma$  ( $\text{Tl}_7\text{Sb}_2$ , type *L* 22);  $\delta$  (Sb, with only small solubility of Tl).

W-C:  $\text{W}_2\text{C}$  cubic, WC (hexagonal lattice).

Zn-Al: Solubility Zn in Al: 2.7 per cent 25°; 5.2 per cent, 100°; 7.4 per cent, 150°; 9.4 per cent, 200°; 13.4 per cent, 250°. Both lattices beyond.

Zn-Hg: Two solid phases 0 to 6 per cent, 12 to 35 per cent Hg (hexagonal close-packed).

**3. The Mechanism of Solid Solution.**—The two types of solid solution may be distinguished by density measurements, as illustrated by the following example from the work of Westgren and Phragmen:

Austenitic steel with 12.1 per cent manganese and 1.34 per cent carbon has a face-centered cubic lattice with  $a = 3.624$  A.U. The two possibilities are that these alloying elements are substitutes for iron atoms, or that the manganese atoms are substitutional and the carbon interstitial. The average atomic weight, calculated from the atomic weights of three elements, iron, manganese, and carbon, in given percentages is given by

$$A = \frac{100}{\frac{86.56 (\%) }{55.85 (\text{at. wt. Fe})} + \frac{12.1 (\%) }{54.93 (\text{at. wt. Mn})} + \frac{1.34}{12 (\text{at. wt. C})}} = 53.13.$$

Substituting this in the density formula (see page 182)

$$\rho = n \frac{\text{Mn}}{\text{volume unit cell}} = \frac{4 \times 53.13 \times 1.65 \times 10^{-24}}{(3.624 \times 10^{-8})^3} = 7.36.$$

This is the density, therefore, on the substitutional basis.

For the other case the average atomic weight for iron and manganese is 55.74. To each 55.74 grams (iron + manganese) are added interstitially  $\frac{1.34}{98.66} \times 55.74 = 0.757$  gram of carbon.

The average atomic weight is therefore  $55.74 + 0.757 = 56.497$  and

$$\rho = \frac{4 \times 56.497 \times 1.65 \times 10^{-24}}{(3.624 \times 10^{-8})^3} = 7.83.$$

The actual experimental density is 7.83, proving that the second alternative of interstitial carbon is correct.

The interstitial type of solid solution is usually unstable and limited to only a few per cent of one component (the solubility of carbon in iron is about 0.1 per cent in body-centered and 1.7 per cent in face-centered cubic). Heat treatment may destroy this condition. There has been much conjecture as to whether the interstitial carbon atoms in iron alloys are fixed in position or are free to move. In a paper on the absence of allotropy in pure iron, Yensen shows how the thermal agitation of atoms is large at high temperatures and how the small carbon atoms may travel from one cube to another. If the concentration is low enough no distortion may result, but with increasing concentrations the lattice may change over because of distortions to face-centered cubic, in which the solubility is greater. At still higher concentrations (6.67 per cent) exceeding the powers of the  $\gamma$ -iron, the compound cementite  $\text{Fe}_3\text{C}$  is formed. Similarly nitrogen which has a maximum solubility of 0.5 per cent in  $\alpha$ -iron may cause the lattice transformation and then the formation of  $\text{Fe}_4\text{N}$ . Oxygen with a maximum solubility of 0.2 per cent may behave similarly.

**4. The Distinction between "Chemical Compound" and "Solid Solution."**—From the x-ray point of view the most interesting phases of alloy research are the intermetallic compounds and the solid solutions. The question which is still frequently agitated is just what is the boundary line between the two. Westgren and Phragmen, outstanding masters in the x-ray science of alloys, some years ago made the following differentiation: "In an ideal solid chemical compound, structurally equivalent atoms are chemically identical. In an ideal solid solution, all atoms are structurally equivalent."

In the case of iron-nickel alloys, for example, the forces of combination of a definite number of nickel atoms with iron are not sufficiently strong to overcome the forces of diffusion. There is a geometric chance, however, for the compounds  $\text{Fe}_3\text{Ni}$  (20 per cent nickel, face-centered cubic),  $\text{FeNi}$  (51 per cent), and

FeNi<sub>3</sub> (76 per cent). Efforts have been made to identify these among the series of alloys, based upon Tammann's theory, but without avail; hence they may be regarded as very weak compounds or merely as stages in the continuous solid solutions. In one sense, an intermetallic compound may be regarded as a solid solution in which the forces of combination are stronger than those of diffusion. CuAl<sub>2</sub>, FeSi, and FeSi<sub>2</sub> have been clearly considered as chemical compounds, on the basis that structurally equivalent atoms are chemically identical. The explanation of the fact that the composition of such phases as these corresponds

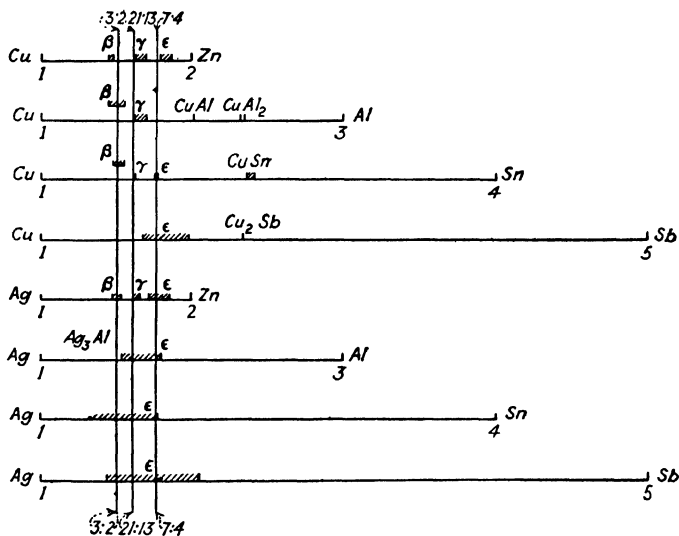


FIG. 136.—Graphical representation by Westgren and Phragmen of structural analogies and common ratios of total number of valence electrons to total number of atoms, for some copper and silver alloys.

to simple stoichiometric proportions is sought therefore in the crystal structures. However, more recently some cases have been found where the composition corresponds with constant and simple stoichiometric proportions without reference to regularity in the crystal structure. Westgren and Phragmen<sup>1</sup> point out the case of Ag<sub>3</sub>Al which has a crystal structure apparently isomorphous with β-manganese, even to the relative intensities of x-ray interferences (see the pattern for the γ phase, Fig. 132). Preston<sup>2</sup> has shown that the 20 atoms of manganese

<sup>1</sup> *Trans. Faraday Soc.*, **25**, 379 (1929).

<sup>2</sup> *Phil. Mag.* (VII), **5**, 1198 (1928).

in the unit cell are divided into two groups, one containing 12 and the other 8 equivalent atoms. Now in  $\text{Ag}_3\text{Al}$  the 15 silver atoms cannot all be unequivalent to aluminum atoms, and any possible division of the two kinds of atoms into unequivalent groups will yield entirely different intensity relationships from those in  $\beta$ -manganese. The inevitable conclusion, therefore, is that the silver and aluminum atoms are distributed *at random* and approximately uniformly over the two groups of structurally equivalent atomic positions. From the standpoint of constant and simple stoichiometric proportions  $\text{Ag}_3\text{Al}$  is a chemical compound; from the standpoint of crystal geometry and the earlier definition of Westgren and Phragmen it is not. The explanation of proportions must, therefore, be sought elsewhere than in structural equivalence, and probably in the ratio of valence electrons to atoms as explained later.

**5. Analogies and Generalizations from the Study of Alloys.**—It is always the method of science to try to find a thread of generalization or correlation running through a mass of experimental facts. Alloy formation seems at first sight to be hopelessly complex, but x-ray investigations primarily in the laboratory of Westgren have disclosed orderly processes and relationships where other methods have fallen short. Some of these analogies summarized in a paper by Westgren and Phragmen,<sup>1</sup> together with more recent developments, are briefly outlined in the following paragraphs.

a. In 1926 W. Hume-Rothery<sup>2</sup> suggested that the  $\beta$  phases of the system Cu-Zn, Cu-Al, and Cu-Sn are analogous in structure. As their compositions correspond approximately to the formula  $\text{CuZn}$ ,  $\text{Cu}_2\text{Al}$ , and  $\text{Cu}_3\text{Sn}$ , he also put forward the hypothesis that their structural similarity might be due to the fact that in each case the ratio of valence electrons to atoms is 3:2. X-ray investigations have confirmed the assumption that the said phases have the same type of structure.<sup>3</sup> In each case the atoms occupy the points of a body-centered cubic lattice. In the  $\beta$ -Cu-Sn-phase the Cu and Sn atoms seem to be distributed at random over the lattice points, but in  $\beta$ -Cu-Zn and  $\beta$ -Cu-Al the different kinds of atoms are mainly oriented in networks of their own, forming what may be denominated "super-lattices." Phases of this structure

<sup>1</sup> *Trans. Faraday Soc.*, **25**, 379 (1929).

<sup>2</sup> HUME-ROTHERY, *J. Inst. Metals*, **35**, 295 (1926).

<sup>3</sup> WESTGREN and PHRAGMEN, *Phil. Mag.* (VI), **50**, 331 (1925).

PERSSON, *Naturwissenschaften*, **16**, 613 (1928).

WESTGREN and PHRAGMEN, *Z. anorg. Chem.*, **175**, 80 (1928).

have been found in several binary alloys of Cu, Ag, and Au with other metals and, in fact, they all occur at concentrations making the ratio of valence electrons to atoms about 3:2.

b. In many cases a phase ( $\gamma$ ) of a complicated cubic structure has been found, having usually 52, but in some cases  $8 \times 52$ , *i.e.*, 416, atoms in its elementary cube. When Cu, Ag, or Au is combined with a bivalent (Zn, Cd . . . ) the homogeneity range of this phase corresponds to formulas of the type  $\text{Cu}_3\text{Al}$ . In these phases there are 21 valence electrons to 13 atoms. The type of phase present in the Cu-Sn system has an extremely narrow range of homogeneity. It is homogeneous at 32.6 per cent Sn,<sup>1</sup> as shown by Heycock and Neville,<sup>2</sup> corresponding to  $\text{Cu}_{31}\text{Sn}_8$ , which gives again 21 valence electrons to 13 atoms.

c. Phases of the systems Fe-Zn, Co-Zn, Ni-Zn, Rh-Zn, Pd-Zn, Pt-Zn, Ni-Cd also give the same diffraction pattern as  $\gamma$ -brass and correspond to the ratio 21:13 if zero valence is assigned to the transition (Group VIII) elements.

d. The close-packed hexagonal structure ( $\epsilon$ ), an atomic grouping which seems, moreover, to be connected with a certain concentration of valence electrons  $\frac{3}{4}$ , is also commonly present in these systems.

e. Figure 136 gives a survey of the occurrences of analogous phases in some binary Cu and Ag alloys. The homogeneity ranges of the intermetallic phases in the different systems are here indicated on one and the same scale, denoting the concentration of valence electrons. As will be seen, the homogeneity intervals of analogous phases all include, or come very close to, certain common concentration values indicated by vertical lines in the figure.

f. In some cases when in an alloy the ratio of valence electrons to atoms is 3:2 and a phase having a body-centered cubic lattice might thus have been expected, the atoms have instead been found to be grouped in the same way as in  $\beta$ -manganese. Just as this metal differs from its neighboring elements in respect to crystal structure, these intermetallic phases, for some reason, form exceptions to the general rule. A phase of this kind is found in the Ag-Al system.<sup>3</sup> Its range of homogeneity is so narrow that it may be denoted by a mere line in the equilibrium diagram. Its composition corresponds to  $\text{Ag}_3\text{Al}$ , from which it is evident that its ratio of valence electrons to atoms is 3:2. Other good examples are  $\text{Au}_3\text{Al}$  and  $\text{Cu}_3\text{Si}$ .

g. In order to explain the facts of structures of binary alloys it is evident that the most important factor is the number of valence electrons per atom. Electron configurations in metal atoms and molecules in the vapor state are known from spectroscopic work but not for solids

<sup>1</sup> GLOCKER, "Materialprüfung mit Röntgenstrahlen," p. 281 Berlin 1927.

<sup>2</sup> HEYCOCK and NEVILLE, *Phil. Trans.*, **202**, 1 (1904).

BERNAL, *Nature*, **122**, 54 (1928).

<sup>3</sup> WESTGREN and BRADLEY, *Phil. Mag.* (VII), **6**, 280 (1928).

unless new work on the fine structure of spectra of very soft x-rays bears out present promise of enabling energy-level determinations. The number of valence electrons per atom in metals is most easily determined from magnetic susceptibilities. In a crystal like diamond with homopolar or electron-pair bonds the coordination number is equal to the valence or number of outermost electrons—in the case of carbon four. In a metallic bond, however, the coordination number, usually 8 or 12, is greater than the valence number of the atom, so that it is not possible to assign a certain pair of bonding electrons to a certain pair of atoms. Thus each of the bonding electrons in a metal lattice must encircle in the course of time all the atoms in the lattice in the same way, and thus transport an electric current through the lattice. These are the valence electrons in metallic bonding. It does not follow that all the electrons which belong to the outermost shell in the free atom act as valence electrons in the crystalline combination, for some of these must fall back into the second outermost shell, which in many metallic elements is uncompleted, when the atoms combine with a metallic bond.

*h.* A general rule as stated by Dehlinger<sup>1</sup> is as follows: When in the fusion of two metals with different valence electron number per atom (for example, Cu, 1 and Zn, 2) concentrations are reached at which the resulting average valence electron per atom (or the ratio of the total number of electrons to the number of atoms) varies markedly from a whole number, an intermetallic compound is formed.

*i.* Upon the basis of the foregoing generalizations it is possible to classify binary alloys in a new and fundamental way, as follows:

I. Metallic compounds of metals with *different* valence electron numbers.

1. Body-centered cubic lattice ( $\beta$ ) with the average valence electron number  $3\frac{1}{2}$ ; *examples*: CuZn, Cu<sub>3</sub>Al, Cu<sub>5</sub>Sn, CoAl, etc., where the numbers are Cu1, Zn2, Al3, Sn4, Co0.

Similar lattices related to  $\beta$ -Mn with number  $3\frac{1}{2}$  as for Ag<sub>3</sub>Al and Cu<sub>5</sub>Si.

2.  $\gamma$ -phase with average valence electron number  $2\frac{1}{3}$ , as in Cu<sub>5</sub>Zn<sub>8</sub>, Cu<sub>9</sub>Al<sub>4</sub>, Cu<sub>31</sub>Sn<sub>8</sub>, Fe<sub>5</sub>Zn<sub>21</sub>, etc.

3. Hexagonal  $\epsilon$  phase with number  $\frac{7}{4}$ , as in CuZn<sub>3</sub>, Cu<sub>3</sub>Sn, Ag<sub>3</sub>Al<sub>3</sub>, etc.

4. Other compounds, as CuPd, Ag<sub>5</sub>Sb, FeZn<sub>8</sub>, Cu<sub>2</sub>Mg, Mg<sub>2</sub>Cu, etc.

II. Alloys of metals with equal numbers of valence electrons without compounds.

1. With continuous series of mixed crystals, as Ag-Au, Au-Cu, Mn-Ni, Mn-Co, Mn-Fe, Ni-Co, Ni-Fe, Co-Fe, Pt-Ir, Pt-Rh, Au-Ni, Cu-Mn, Cu-Ni, Ag-Pd, Au-Pt, Au-Pd, Cu-Pt, Cu-Pd, Fe-Pt, Ni-Pt, Bi-Sb.

2. With intervals of non-miscibility in the solid state, as Ag-Cu, Ag-Pt, Au-Mn, Au-Co, Au-Fe, Cu-Co, Mg-Cd, Cd-Hg, Pb-Sn.

<sup>1</sup> *Z. Elektrochem.*, **38**, 149 (1932).



3. With intervals of non-miscibility in both liquid and solid states, as Ag-Mn, Ag-Ni, Ag-Co, Ag-Fe, Ag-V, Cu-Fe.
4. Superstructure phases observed for some of these systems: Au-Cu, Cu-Pd, Cu-Pt, Mg-Cd, Ni-Mn, Fe-V, Fe-Cr, Au-Pt, Ag-Pt.
- III. Alloys of metals with apparently different valence electron numbers but forming no compounds: Sn-Al, Pb-Tl, Pb-Sb, Sn-Bi.
- IV. Alloys of metals with apparently the same electron numbers but forming compounds (usually with non-metallic properties): MgZn<sub>2</sub>, CdSe, HgTe, GaAs, InSb.
- V. Compounds with unknown numbers of valence electrons: Fe<sub>2</sub>W, Fe<sub>3</sub>W<sub>2</sub>, Fe<sub>3</sub>Mo<sub>2</sub>, Co-Cr, Ni-W.

j. Miscibility and compound formation in metals depend much less on radius ratios than is true for polar salts (see page 268). Abnormal cases may involve specific influence of atomic kernels, including abnormally strongly bound valence electrons in Hg, Tl, Pb, etc., accounting for superconductivity, and the especially small influence of the kernel in silver so that this metal is similar to the alkali metals in many properties.

k. Westgren<sup>1</sup> has shown that the divergence of the transition elements of Group VIII of the periodic system from other metals is manifested in three ways: these elements alone are able to form phases with NiAs structure; when combined with hydrogen, boron, carbon, or nitrogen they give products with metallic properties, which is not the case with other elements; and in the  $\beta$  and  $\gamma$  phases of alloys with Zn, Cd, Al, etc., they appear to have zero valence in maintaining the ratios 3:2 and 21:13.

**6. The Systematization of Iron Alloys.**—From the viewpoint of crystal chemical generalizations the iron alloys form a unique series on account of the complications introduced by the polymorphic phases. Sufficient x-ray data are now at hand so that some remarkable relationships have been observed by Wever.<sup>2</sup> All the many iron alloys may be classified under four types: (a) open  $\gamma$ -field, illustrated by the iron-nickel system in Fig. 137. (b) the closed  $\gamma$ -field illustrated by iron-chromium; (c) the expanded  $\gamma$ -field (iron-carbon); and (d) the contracted  $\gamma$ -field (iron-boron). Figure 138 shows a periodic arrangement of the atoms and the description as to which type of binary alloy is formed. The open  $\gamma$ -field for alloys with metals of Group VIII, the closed  $\gamma$ -field in the center of the periodic table and insolubility for elements of Groups I and II are clearly apparent. That these differences are due primarily to atomic dimensions

<sup>1</sup> *J. Franklin Inst.*, **212**, 577 (1931).

<sup>2</sup> WEVER, *Ergebnisse der technische Röntgenkunde*, **2**, 240 (1931).

is shown by Fig. 139. The elements with largest atomic radii are insoluble in iron, and those with smallest radii are most soluble and form alloys which are characterized by open or expanded  $\gamma$ -field, while intermediate elements narrowed the  $\gamma$ -phase.

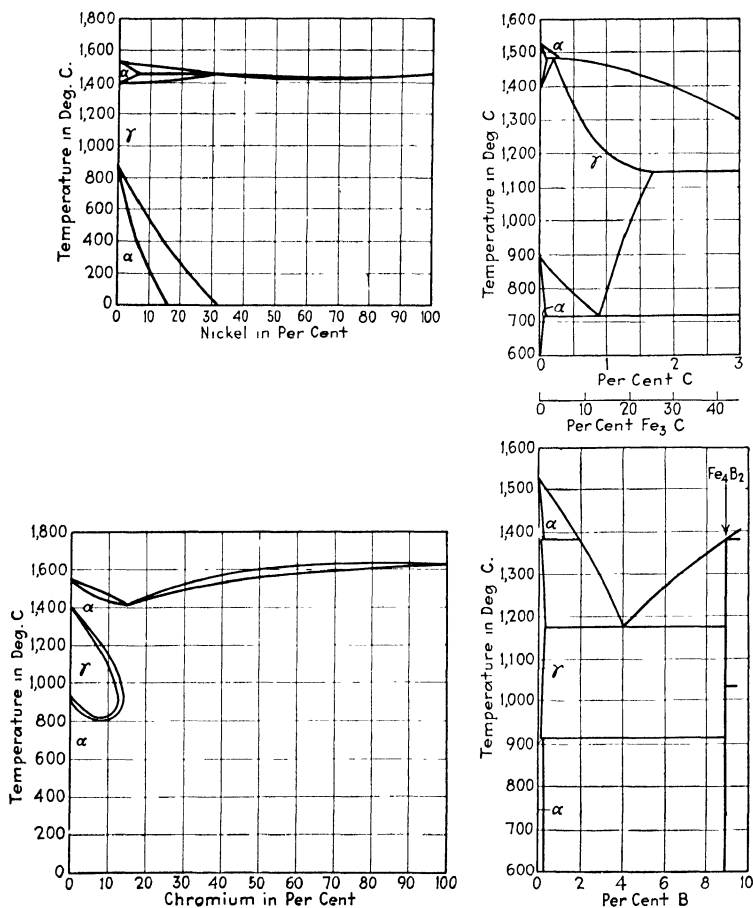


FIG. 137.—Classification of binary iron alloys.

Such generalizations are highly gratifying and rapid progress may be expected in classifying similarly other systems of binary alloys.

**7. Steel (Fe-C Alloys).**—The most important possible application of x-ray analysis to the structure of alloys is, of course, to the series of iron-carbon alloys. There are several reasons for this, aside from the practical utility of steel. The equilibrium diagram is one of great complexity because of the great variety

of forms involving the four allotropic forms of pure iron; hence, there has been among metallurgists for a great many years the widest divergence of opinion concerning the actual constitution of many of the iron-carbon phases. The x-ray has been eagerly sought for a final answer to these mooted problems; while it has already given many hopeful signs, the results are still insufficient to more than open the subject.

The facts established by x-ray analysis of steel may be briefly summarized as follows:

*a. Austenite*, formed by quenching Fe-C alloys from above the  $A_3$  transformation point, has the structure of  $\gamma$ -iron (face-

	$\alpha$ I b		$\alpha$ II b		$\alpha$ III b		$\alpha$ IV b		$\alpha$ V b		$\alpha$ VI b		$\alpha$ VII b		$\alpha$ VIII		b
I															1H		2He
II	3Li ▲		4Be ▲			5B ○	6C □		7N □		8O		9F				10Ne
III	11Na ▲		12Mg ▲			13Al ○	14Si ●		15P ●		16S ○		17Cl				18A
IV	19K ▲		20Ca ▲		21Sc	22Ti ●		23V ●	24Cr ●		25Mn ■		26Fe	27Co ■	28Ni ■		
V		29Cu □		30Zn □	31Ga	32Ge ●		33As ●		34Se		35Br					36Kr
VI	37Rb ▲		38Sr ▲		39Yt	40Zr ○		41Nb ●	42Mo ●		43Ma		44Ru ■	45Rh ■	46Pd ■		
VII		47Ag ▲		48Cd ▲	49In	50Sn ●		51Sb ●		52Te		53I					54Xe
VIII	55Cs ▲		56Ba		58Ce ○	72Hf		73Ta ●	74W ●		75Re		76Os ■	77Ir ■	78Pt ■		
IX		79Au □		80Hg ▲	81Tl	82Pb ▲		83Bi ▲		84Po		85-					86Rn
X	87-		88Ra ▲		89Ac	90Th		91Pa		92U							

● Open  $\gamma$ -Field      □ Expanded  $\gamma$ -Field      ▲ Insoluble  
 ● Closed  $\gamma$ -Field      ○ Contracted  $\gamma$ -Field

FIG. 138.—Periodic table showing effects of chemical elements in binary iron alloys.

centered cubic). Carbon causes an enlargement of the lattice. Westgren and Phragmen found the dimensions of the unit cell to be 3.629 A.U. for a saturated solution (1.7 per cent) quenched from 1100° C., and 3.606 A.U. for a specimen containing 0.9 per cent C quenched from 750° C. A specimen containing 12.1 per cent Mn and 1.34 per cent C had a parameter 3.624 A.U. As already explained, the carbon atoms are placed interstitially. The carbon may be atomically and irregularly dispersed or the atoms may be more definitely arranged, in the sense that an atom of  $\gamma$ -iron may be replaced by a complex of an iron combined with one or more carbon atoms. In other words, austenite is a solid solution of carbon or  $\text{Fe}_3\text{C}$  (cementite) in  $\gamma$ -iron.

*b. Cementite.*—The only definite compound formed by iron and carbon,  $\text{Fe}_3\text{C}$ , crystallizes in the orthorhombic system. The unit parallelepiped has the dimensions 4.518 by 5.019 by 6.736 A.U. or the axial ratios 0.671: 0.753: 1. This compound is found

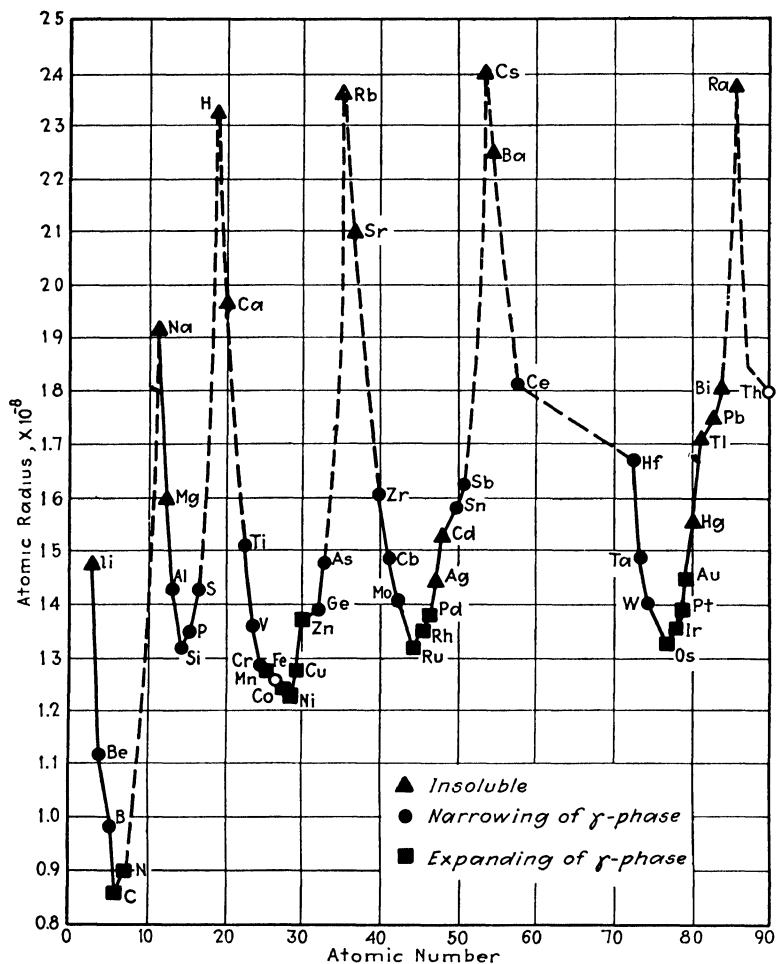


FIG. 139.—Curve showing effect of atomic radius upon formation of binary iron alloy.

in *pearlite* (the eutectoid mixture of  $\alpha$ -iron and cementite formed by slow cooling of austenite from the transformation point), *troostite* ( $\alpha$ -iron and cementite in colloidal dispersion), *sorbite*, and in the massive spheroidal condition. Meteoric cohenite has the same structure.

*c. Ferrite* has the body-centered cubic structure of pure  $\alpha$ -iron. Carbon has a very limited solubility in it, since the diffraction lines for the numerous specimens have the same position as for pure electrolytic  $\alpha$ -iron. A widening of the lines and the disappearance of the resolution of doublet lines may be taken as an indication of a slight increase (up to 0.3 per cent) in the lattice, but non-uniformly, since pure iron dimensions are still indicated.

*d.  $\beta$ -Iron.*—There is no x-ray evidence of  $\beta$ -iron, since there is no structural discontinuity between  $\alpha$ - and  $\gamma$ -iron.

*e. Martensite.*—This interesting constituent found in hardened steel has received more attention than any other phase of x-ray analysis of alloys. Martensite is formed and retained at room temperatures when the  $\gamma$ - $\alpha$  transformation is delayed by sufficiently rapid cooling until a temperature of 300° C. is reached. The cooling may be slower in the presence of retarding elements such as nickel and manganese. The simple facts were first established that martensite gives the spectrum of  $\alpha$ -iron and that the diffraction lines are broad and diffuse.

More careful technique in the preparation of samples and in photographing diffraction spectra has served to clarify the problem. Fink and Campbell<sup>1</sup> found evidence in drastically quenched eutectoid and hypereutectoid steels of a body-centered tetragonal structure. This was not uniform with lower carbon contents, but with 1.5 per cent carbon the value of  $a$  was 2.85 A.U. and of  $c$ , 3.02 A.U. (body-centered cubic  $\alpha$ -iron,  $a = 2.86$  A.U.). It was found to be less stable at low temperatures than the  $\gamma$ -iron lattice and disappeared on tempering at 100° C. Bain then showed that the face-centered cubic lattice can be considered as a body-centered tetragonal lattice with an axial ratio of  $\sqrt{2}$  and  $a = 2.54$  and  $c = 3.60$  A.U. Of this, the body-centered cubic lattice would be a special case with axial ratio 1. Hence, the martensitic tetragonal structure might represent an arrested stage in transformation from face-centered cubic ( $\gamma$ ) to body-centered cubic iron ( $\alpha$ ). This discovery was confirmed by Seljakow, Kurdjumow, and Goodtzow,<sup>2</sup> who showed further that the axial ratio  $c/a$  increases with carbon content at constant heating and quenching conditions and with the temperature before quenching at constant carbon content. Honda

<sup>1</sup> *Trans. Am. Soc. Steel Treating*, **9**, 717 (1926).

<sup>2</sup> *Z. Physik*, **45**, 384 (1927).

and Sekito<sup>1</sup> found still later that the outer layer of quenched carbon steel contains a body-centered tetragonal lattice,  $\beta$ -martensite, and the inner portion a body-centered cubic lattice,  $\alpha$ -martensite, with a gradual change in the axial ratio from 1.07 to 1. Upon annealing, the tetragonal structure gradually changes to cubic without passing through a stage of an intermediate axial ratio. Kurdjumow and Kaminskii,<sup>2</sup> however, maintain that the tetragonal structure exists on the interior of quenched specimens. There is some difference of opinion also concerning the actual positions of the carbon atoms (although it is most probable that two carbon atoms substitute for one iron atom) and concerning the exact mechanism of the transformation from face-centered cubic to body-centered tetragonal and then to body-centered cubic structures. At any rate, it may be concluded that martensite is a supersaturated solid solution of carbon in  $\alpha$ -iron, although austenite is also almost invariably indicated by its diffraction pattern, and that the intermediate tetragonal structure together with inherent complex strains accounts for hardness. The variable parameters of course could account for the very diffuse x-ray diffraction interferences as well as distortion or very small grain size.

**8. The Problem of Hardness.**—Six views have<sup>3</sup> been presented to account for the hardness of martensite: (a) solid solution, (b) supersaturated solid solution, (c) fineness of grains, (d) distorted space lattice, (e) presence of minute particles of carbide, and (f) internal strains. These reduce to two general phenomena associated with hardness: (1) distortion and (2) slip resistance by the keying action of small particles.

Bernal<sup>4</sup> points out that a pure metal crystal, when stressed, yields not by cleavage or fracture but by the formation of glide planes in which layers of atoms slip over each other with little loss of energy. It is possible that in the ideal case of an absolutely pure metal with infinitely small stress it would lose no energy at all in gliding. Its behavior would, in fact, be that of a liquid, and a pure metal crystal would only differ from a liquid by the regular ordering of its atoms. Actually, however,

<sup>1</sup> *Science Repts. Tôhoku Imp. Univ.*, **17**, 743 (1928); *J. Study Metals*, **5**, 380 (1928).

<sup>2</sup> *Nature*, **122**, 475 (1928); *Z. Physik.*, **53**, 696 (1929).

<sup>3</sup> SAUVEUR, *Trans. Am. Inst. Mining Met. Eng.*, **73**, 859 (1926).

<sup>4</sup> *Trans. Faraday Soc.*, **25**, 370 (1929).

when a certain amount of gliding has taken place, a hardening sets in which prevents further gliding. This hardening is almost certainly due to a distortion of the lattice elements. What appears to be an exactly similar distortion is produced by the presence of foreign atoms in solid solution. (It is, of course, to these properties of hardening by cold working and alloying that metals owe their technical importance.) The distortion of the lattice manifests itself in a variety of ways; as well as the mechanical hardening there is always a very large increase in the electrical resistance, but what shows most clearly the nature of the change is the x-ray evidence. In a strained or impure metal crystal the reflection of a monochromatic ray in a crystal plane, instead of occurring extremely sharply over a width of a few seconds of arc, occurs more and more diffusely as the strain is increased. This is an indication that the atoms no longer lie in absolutely plane parallel layers but that there is a more or less irregular displacement of certain atoms from the average planar position. A similar but periodic displacement is produced by the temperature vibration of the atoms, and indeed on looking at an x-ray photograph of a metal which shows very blurred lines it is impossible without further information to know whether they are due to impure crystals, distorted crystals, or hot crystals. It is probable that the effects which Dr. Kapitza<sup>1</sup> has found in high magnetic fields are due to a similar distortion of the lattice. It is possible that solid solutions do not represent stable states but metastable ones; that given sufficient atomic mobility, or

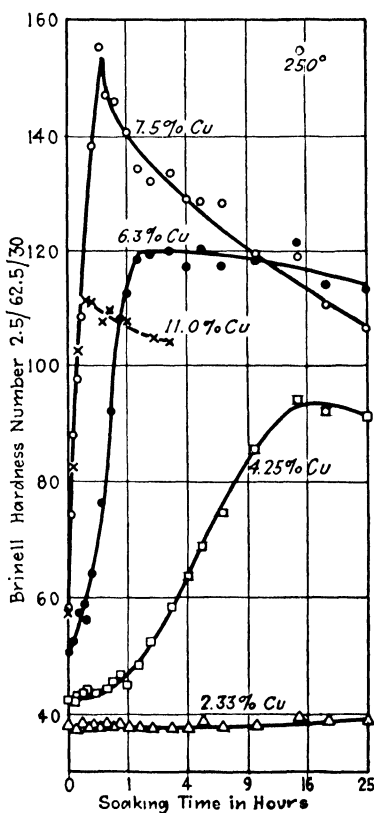


FIG. 140.—Curves showing age-hardening of copper-silver alloys.

<sup>1</sup> *Proc. Roy. Soc. (London)*, **123**, 292 (1929).

sufficient time, all solid solutions would separate out into their constituent compounds, or form regular superstructures. From this point of view the solid solution is a mere regular form of a glass.

**9. Age-hardening.**—Several alloy systems, notably Al-Cu-Si (duralumin), Au-Cu (intermediate state of AuCu), Ag-Cu, Cu-Be, Cu-Fe, low-carbon (armco) iron, etc., are characterized by hardening with time after a heat treatment. Figure 140 shows the variation of hardness with time of mixed crystals of silver and copper as measured by Agnew, Hanan, and Sachs.<sup>1</sup> The alloy was quenched from 770° C. and then held at a temperature of 250° C. This age-hardening has great technical significance, since an alloy of steel in light metals may be formed while in easily worked condition and then the product subsequently strengthened is hardened with aging. Difficulties are, of course, encountered even at room temperatures if steel sheets, for example, are not used for a considerable period after manufacture so that they will form far less easily. The phenomenon of age-hardening therefore has been subjected to numerous investigations. If gold-copper mixed crystals containing about 50 atomic per cent gold with entirely random distribution of atoms above 425° are cooled, an intermediate state can be observed from x-ray patterns. The unit cell has the tetragonal form (AuCu) of the final equilibrium state but in a part of the lattice the copper and gold atoms have definite arrangement and in the remainder are completely random. This inhomogeneous irregularity is to be distinguished from the true homogeneous substitutional solid solution type. The intermediate state is characterized by great hardness. By long heating under 428° the much softer, entirely definitely arranged tetragonal state is reached. Diffraction lines for CuAl<sub>2</sub> have been observed after long heat treatment of duralumin. The theory of hardness has been based on the conception of separation of very small colloidal particles which tend to key slip on planes. However, newer x-ray researches seem to demonstrate that at the point of greatest hardness no new lattice is necessarily observed. There may be a slight broadening of x-ray lines, such as might be produced in very slight deformation, but no change in lattice dimension of the old lattice is observed as ought to be expected from concentration changes, due to separation of a new phase. Upon the basis of magnetic meas-

<sup>1</sup> *Z. Physik.*, **66**, 350 (1930).



urements on copper-iron specimens Tammann has presented the hypothesis that, before the separation of a new phase, some kind of grouping within the coherent old lattice of the chemically different atoms occurs which in an unknown manner causes increase in hardness. This agrees with the actual observation of inhomogeneous atomic distribution in the intermediate state of AuCu and with the most recent observations on duralumin at maximum hardness by Hengstenberg and Wassermann<sup>1</sup> of increase in line intensity and decrease of fogging due to scattering. The dependence on temperature of the age-hardening process is still unexplained.

**10. Alloy Steels.**—The success attendant upon the complete interpretation of the highly complex x-ray diffraction patterns obtained with alloy steels within the past two years has been truly amazing. A rationally scientific explanation can now be given to the properties of various alloy steels in terms of ultimate constitutions and structure. Ranges of stability of phases are defined and predictions of the constitution and properties of new alloys are non-empirically made. A very few of all the facts which x-rays have disclosed are enumerated simply as an indication of achievements and possibilities, other results being briefly noted in the tabular summary of alloys:

a. The identification in the iron-tungsten system of  $\text{Fe}_2\text{W}$  (hexagonal) and  $\text{Fe}_3\text{W}_2$  (trigonal, 40 atoms per unit cell) and of  $\text{Fe}_3\text{Mo}_2$  corresponding to  $\text{Fe}_3\text{W}_2$  in the iron-molybdenum system (Fig. 134).<sup>2</sup>

b. Studies of the iron-chromium-carbon system and stainless steel<sup>3</sup> with the following conclusions:

(1) Iron and chromium form a continuous series of solid solutions.

(2) Phases in the Fe-Cr-C system:

$\alpha$ -metal.

$\gamma$ -metal.

Cementite  $(\text{Fe}, \text{Cr})_3\text{C}$  in which chromium may rise to 15 per cent.

Cubic chromium carbide  $(\text{Cr}, \text{Fe})_4\text{C}$  in which chromium may be substituted by iron up to 25 per cent.

Trigonal chromium carbide  $(\text{Cr}, \text{Fe})_7\text{C}_3$  with iron up to 55 per cent.

Orthorhombic chromium carbide  $(\text{Cr}, \text{Fe})_3\text{C}_2$  with only a few per cent of iron substituting.

<sup>1</sup> *Z. Metallkunde*, **23**, 114 (1930).

<sup>2</sup> ARNFELT, Carnegie Scholarship Memoirs, Iron and Steel Inst., Vol. XVIII, p. 1 (1928).

<sup>3</sup> WESTGREN, PHRAGMEN, and NEGRESKO, *J. Iron and Steel Inst.*, **117**, 383 (1928).

(3) In annealed ball-bearing steel the chromium is contained in cementite. "Double carbide" causing rejection, due only to unequal distribution of cementite.

(4) Carbide in stainless steel is cubic chromium carbide saturated with iron (35 per cent).

(5) Steel for dies (17 per cent nickel, 11 per cent chromium, 2 per cent carbon) contains trigonal chromium carbide with more than half of the chromium substituted by iron.

(6) Ferro-chromium (60 per cent Cr, 5 per cent C) peritectic alloy of cubic chromium carbide with iron substituting partially,  $\alpha$ -metal, and some trigonal carbide.

c. The identification in high-speed steel of a true double carbide  $\text{Fe}_4\text{W}_2\text{C}$ , face-centered cubic,  $a = 11.04$  A.U., containing 112 atoms per unit cell.<sup>1</sup>

d. The identification and proof of  $\text{Fe}_4\text{N}$ , important in case hardening of iron by nitrogen, with the iron on a face-centered cubic lattice,  $a = 3.789$  A.U. and the nitrogen at the center.<sup>2</sup>

**11. Crystal Structure and Magnetism.**—The fact that  $\alpha$ -iron is magnetic and  $\beta$ -iron non-magnetic, though x-rays detect no structural discontinuity between these, seems to indicate that magnetic properties are not functions of the arrangement of atoms in space. However, Persson<sup>3</sup> in Westgren's laboratory has recently demonstrated that the magnetic Heusler alloys (copper-manganese-aluminum) always show the x-ray diffraction lines of the  $\beta$ -phase. In this the basic lattice is body-centered cubic, upon which is superposed a face-centered cubic lattice of aluminum atoms with twice the dimensions of the basic lattice. Hence the unit cube contains 16 atoms, of which 12 are copper + manganese and 4 aluminum. The formula  $(\text{Cu}, \text{Mn})_3\text{Al}$  is substantiated by the x-ray results. It is further essential that the concentration of manganese must be above a limiting value in order that magnetic properties may develop. In other words, the pattern for the  $\beta$ -phase may appear for non-magnetic specimens if manganese is insufficient. Further work will be awaited with interest.

**12. X-ray Studies of the Mechanism of Corrosion of Alloys.**—One of the most remarkable recent examples of the application of x-ray diffraction methods to metallurgical problems is the study made by Graf and Glocker<sup>4</sup> of the mechanism of corrosion of single crystals of gold-copper alloys. Carefully prepared

<sup>1</sup> WESTGREN and PHRAGMEN, *Trans. Am. Soc. Steel Treating*, **1928**, 539.

<sup>2</sup> HÄGG, *Nature* (Sept. 1, 1928).

<sup>3</sup> *Naturwissenschaften*, **16**, 631 (1928).

<sup>4</sup> *Metallwirtschaft*, **11**, 77 (1932).

specimens were analyzed by the rotation method, the patterns showing the characteristic solid solution and superstructure phases of this system. After etching with strong oxidizing agents, the specimen produced the interferences for pure gold in a surface layer oriented exactly like the original alloy layer. Thus with the removal of the less noble copper atoms from the mixed crystal lattice the remaining gold atoms apparently had grouped together into a pure gold crystal layer with entirely different lattice spacing from that of the underlying unattacked alloy. Weak oxidizing agents, sulfur-containing compounds, and corrosive gases had the effect of producing an outer layer of alloy much richer in gold than the original crystal. When gases attacked the surface at high temperatures, at which atoms diffuse easily, the copper atoms could all reach the surface and escape from the protective action of the gold atoms, so that the corrosion zone was pure gold. In order to explain these results a definite mobility of the gold atoms after the copper atoms are removed from the lattice is necessary, either by a direct way in which the gold atoms in unstable configuration are brought to new and stable lattice positions by the action of outer one-sided lattice forces in the layer, as in the case of weak oxidizing agents, sulfurizing compounds and gases at low temperatures; or indirectly by diffusion at higher temperatures or by ionization in the corrosive liquid agent such as a strong oxidizing agent. In the latter case the gold atoms exceed the wave potential which holds them in place in the solid lattice and they escape as ions. They return to the lattice by imparting the ionic charge to the remaining neutral, less noble, copper atoms in the interface between solid and solution, and thus displace them to form a copper-free gold layer. By attack of other agents at low temperatures only the copper atoms are ionized and separated from the lattice. The gold atoms left behind are sufficiently mobile in their unstable positions to regroup under the action of the one-sided lattice forces. A small fraction of copper atoms which had been completely surrounded and protected by gold atoms remains in the layer as is readily ascertained from the diffraction patterns. An interesting further observation has to do with limits of resistance to corrosion as a function of alloy composition. Tammann has stated certain rules, based on experiment, concerning these limits at which corrosive attack can occur in alloys. Resistance to corrosion begins at a remarkably definite content

of the noble metal component. Depending on the corrosive agent the various resistance limits correspond to contents of  $n/8$  mole of the noble component. In the present case of gold-copper alloys, resistance to attack of weak oxidizing, sulfur-containing, and gaseous agents begins at 25 atomic per cent of gold ( $\frac{2}{8}$  mole), and the corrosion zone is a gold-rich solid solution. The alloy with 50 atomic per cent of gold ( $\frac{4}{8}$  mole) is the resistance limit for strong oxidizing agents, and the corrosion zone is pure gold. As a result of these observations a complete picture of corrosion and resistance mechanisms is afforded—all based upon the interpretation of x-ray diffraction patterns.

## CHAPTER XVI

### THE CRYSTAL STRUCTURES OF COMPOUNDS OF CARBON AND THEIR PRACTICAL SIGNIFICANCE

The examination of the crystals of organic substances represents the newest phase of the still infant science of x-ray crystal analysis. This hesitancy among experimenters is in one sense surprising, inasmuch as the organic chemist long ago introduced the simplifying and logical conceptions of spacial arrangements of atoms which have been the strength of the science as compared with the great complexities with which inorganic chemists have been confronted; on the other hand, crystallographic examination has shown that the great majority of organic compounds crystallize in the very classes of low symmetry whose diffraction effects are the most difficult to interpret; and good crystals for analysis are usually impossible to obtain. It stands to the matchless credit of Sir William Bragg, always in leadership, that he undertook the problems fearlessly. His skill in combining x-ray data with other authentic information, to show that whole molecules instead of atoms are the units placed at the points of the lattice and to arrive at a final solution of structural problems, has given to organic chemistry the solid experimental facts of structure which have been hoped for.

Sir William Bragg<sup>1</sup> speaks of another point of interest in these compounds as follows:

Apart from the interest in determining structures of this kind, there is also the question of the "minor" ties which bind the molecules together; not so much the ties that bind the atoms together in the molecule. The ties which bind molecule to molecule are perhaps of a different and weaker nature and yet must be of immense importance in the constitution of the world, for after all a great deal of nature's work is done at moderate temperatures and simply by the laying of one molecule against another.

**The Carbon Structures.**—The structure of the compounds of carbon must find ultimate prototypes in the structure of crystalline carbon; of this there are two varieties: the diamond,

<sup>1</sup> *Chem. Ind.*, **45**, 245 (1926).

crystallizing in the tetrahedral cubic system with each carbon very definitely at the center of four other equidistant carbons at the corners of a tetrahedron; and graphite, with a lower hexagonal symmetry. "Puckered" six-carbon rings are easily identified in the diamond lattice (Fig. 141). After considerable controversy Bernal<sup>1</sup> succeeded in proving from x-ray data that the carbon atoms in graphite are flattened into a plane so that three of the carbon neighbors remain at somewhat

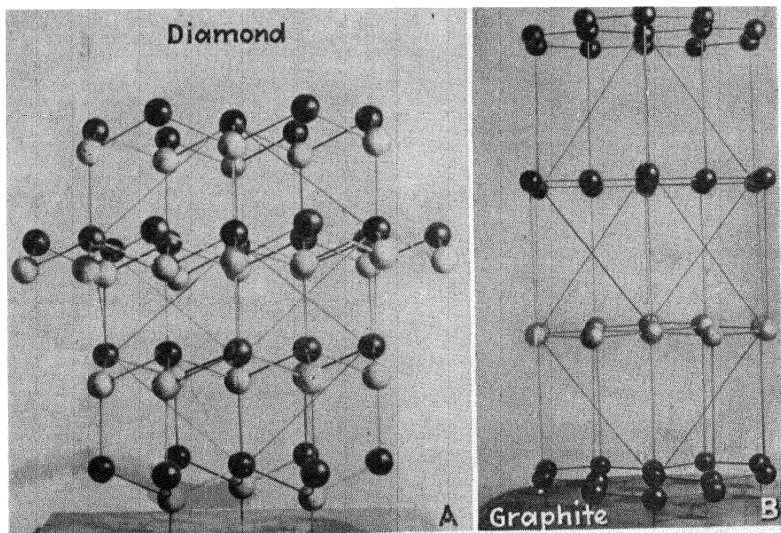


FIG. 141.—Comparison of crystal models of diamond and graphite. (Courtesy Central Scientific Company.)

smaller distance from the central atom than in the diamond tetrahedra (1.42 A.U. as against 1.54 A.U. in diamond), and the fourth is at a greater distance (3.40 A.U.) in the next layer (Fig. 141). In other words, in graphite the atom has three strong bonds coplanar or very nearly so with itself, and one weak bond at right angles to these bonds. This bond may be easily ruptured so that one layer will slide over another to account for the lubricating properties of graphite. The peculiar lamellar structure also enables special types of reactions to occur as shown by Hofmann and Frenzel.<sup>2</sup> Graphite reacts with alkali metals to form stoichiometric compounds of the type  $C_8K$  and  $C_{16}K$ . X-ray diffraction data show no change in the distance between

<sup>1</sup> *Proc. Roy. Soc. (London)*, **106A**, 749 (1924).

<sup>2</sup> *Kolloid-Z.*, **58**, 8 (1932).

carbon atoms in the same layers, but the distance between layers increases from 3.38 A.U. in graphite to 5.34 in  $C_8K$ . Treatment with mercury regenerates graphite. In graphitic acid this distance between layers is 6 A.U. which increases to 11 A.U. by swelling with water.

One of the most interesting questions in the whole science has been whether the carbon atoms in ring compounds, *e.g.*, aromatic series, lie in one plane, as in graphite and as the organic chemist has represented structures on paper, or are staggered as in diamond. A satisfactory answer to this question has been given only very recently; even yet it cannot be maintained that the shape of the benzene ring found for some compounds is necessarily the same in all aromatic compounds. A few of the important steps leading to the final conclusion will be outlined.

**The Structure of the Benzene Ring.** *a. Bragg Analysis of Naphthalene and Anthracene.*—The first selections for complete crystal analysis were naphthalene and anthracene, since solid benzene cannot be easily prepared. Bragg found for the dimensions of the unit prisms of these monoclinic crystals, each containing two molecules, the following:

Naphthalene,  $a = 8.34$ ,  $b = 6.05$ ,  $c = 8.69$ ,  $\beta = 122^\circ 49'$ .

Anthracene,  $a = 8.7$ ,  $b = 6.1$ ,  $c = 11.6$ ,  $\beta = 124^\circ 24'$ .

The  $a$  and  $b$  axes are very nearly the same, but the  $c$  axis is considerably longer for anthracene than for naphthalene. This difference in the  $c$  axis suggested the difference in the length of the two molecules, since anthracene is represented as three contiguous benzene rings and naphthalene as two. Bragg then assumed that the closed rings of six carbon atoms, which were definitely known to exist in diamond, were carried over essentially unchanged into benzene, naphthalene, and anthracene. The difference in length between the two, 3 A.U., was exactly accounted for by the extra ring in anthracene. The constancy of the cross sections of the two cells results from the fact that it is determined not by the length but by the breadth and thickness of a single ring and, hence, is a measure of the space necessary for side-by-side linking of the two molecules in each unit cell. Furthermore, the theoretical length of the naphthalene molecule, 6.65 A.U., agrees with the length of the  $c$  axis, 8.69 A.U., if allowance of 1 A.U. is made for a hydrogen atom at each end. Further consideration showed that the two molecules in the unit cell were

arranged so that one is the mirror image of the other. In the monoclinic prismatic class, there must exist a plane of symmetry, a twofold axis perpendicular to the plane and, hence, a center of symmetry. If the molecules lack symmetry, then there must be four of them in the cell, one obtained by rotation of another around 180 deg., and the two from the first pair by reflection in the plane of symmetry. Hence, the molecules must have a center of symmetry, since only two are found. The cleavage of these crystals is easily accounted for as coming only in the direction where hydrogen atoms from *different* adjacent molecules touch; in all other directions the strong forces due to the carbon atoms are involved.

*b. Miscellaneous Aromatic Compounds.*—Structure investigations on fully halogenated benzene derivatives have not been particularly successful from the standpoint of elucidating the structure of the nucleus itself. The compounds  $C_6Cl_6$ ,  $C_6Br_6$ , and  $C_6I_6$  were found to be centrosymmetrical and monoclinic, just as naphthalene, anthracene, and benzene were observed to be centrosymmetrical. The tendency, of course, was to incline towards the puckered nucleus.

Diphenyl was found to crystallize<sup>1</sup> in the monoclinic system with the space-group  $C_{2h}^{15}$ . The indications were that it is centrosymmetrical. Presumably then the rings are not flat, for in that case the molecule would be expected to have at least a plane of symmetry which it did not seem to have. This conclusion was based on the fact that there were two molecules per unit cell in the crystal, while four asymmetrical molecules are required by the space-group. It is clear, of course, that failure to realize that only the minimum molecular symmetry is fixed by the crystal symmetry may lead to erroneous interpretations as Hendricks and Hilbert<sup>2</sup> have shown. The explanation proposed by Bergmann and Mark<sup>3</sup> for the possible isomerism of some derivatives of fluorene prepared by Schlenk and Bergmann is based on an assumed puckered benzene ring which was incorrectly said to be required by molecular symmetries of compounds. Geometric isomers of fluorene and optical isomers of diphenyl derivatives

<sup>1</sup> HENGSTENBERG and MARK, *Z. Kryst.*, **70**, 285 (1929).

CLARK and PICKETT, *J. Am. Chem. Soc.*, **53**, 167 (1931).

<sup>2</sup> *J. Am. Chem. Soc.*, **53**, 4280 (1931).

<sup>3</sup> *Ber.*, **62**, 750 (1929).



can be explained with the flat benzene ring, since these need not be coplanar in the same molecule.

*c. The Structure of Hexamethylbenzene.*—The classical research by Mrs. Lonsdale<sup>1</sup> on hexamethylbenzene has done most to clear up the controversy. She demonstrated rigorously from x-ray diffraction data that in this compound the benzene nucleus is flat and that the carbon atoms in the methyl group also lie in this same plane. The choice of compound was particularly fortunate, since only one molecule per unit triclinic cell is found and the intensity data may be very directly interpreted. The direct x-ray information on axial lengths and angles is as follows:

$$\begin{array}{ll} a = 9.010 \text{ A.U.} & \alpha = 44^{\circ}27' \\ b = 8.926 \text{ A.U.} & \beta = 116^{\circ}43' \\ c = 5.344 \text{ A.U.} & \gamma = 119^{\circ}34' \end{array}$$

The facts that  $a$  and  $b$  are nearly equal and that the angle between them is nearly  $2\pi/3$  immediately suggested hexagonal structure. The factors in the (001) zone should repeat themselves closely throughout the series of planes (100)  $\rightarrow$  (010), (010)  $\rightarrow$  ( $\bar{1}\bar{1}0$ ), ( $\bar{1}\bar{1}0$ )  $\rightarrow$  ( $\bar{1}00$ ). This was tested by a comparison of structure factors which were calculated from the observed intensities by the formula

$$F' \propto \sqrt{I} \div \left( \Sigma F e^{-m} \times \sqrt{\frac{0.15 + \cos^2 2\theta}{\sin \theta}} \right),$$

where  $(0.15 + \cos^2 2\theta)$  is the measure of the polarization factor for Mo  $K\alpha$ -radiation;  $F$  is the scattering power of the atoms and  $e^{-m}$  is the temperature factor. Two sets of calculations were made corresponding to  $F$  values for diamond (Ponte) and graphite (Bernal), respectively. These proved conclusively the hexagonal arrangement and the graphite arrangement; there was a marked similarity in the intensities of various orders from the (001) cleavage plane and those from the corresponding cleavage plane of graphite. The structure factor was also larger than for any other plane in the crystal and almost independent of the order of reflections, proving that the carbon atoms lay in or near the (001) planes. The factors for planes (340), ( $4\bar{7}0$ ), and ( $\bar{7}30$ ) also were very large and these gave a further clue, since these were small spacing planes and therefore any deviation of the atoms from these planes would cause a more rapid falling off of structure fac-

<sup>1</sup> *Proc. Roy. Soc. (London)*, **A123**, 494 (1929).

tor than would a similar movement away from a plane of larger spacing. In other words, the carbon atoms must lie at or near the intersections of these planes. There are 36 such intersections and only 12 carbon atoms. Since, however, there is an hexagonal arrangement in the (001) zone, the problem was greatly simplified. Mrs. Lonsdale calculated structure factors for the first six orders of the (100) plane for each possibility and the true arrangement at once derived.

The immediate deductions are as follows:

- (1) The molecule exists in the crystal as a separate entity.
- (2) The benzene carbon atoms are arranged in ring formation.
- (3) The ring is hexagonal or pseudohexagonal in shape.

In order to answer the question as to the sizes of the atoms in the rings and the dimensions of the ring itself, and whether or not the ring is plane, variations of three kinds are made from the positions of the atoms established: (a) a variation of atomic dimensions, (b) a variation in directions along which atoms lie (ring rotation), and (c) shifting of atoms perpendicular to the (001) plane, or a puckering of the benzene ring. The effect of each kind of variation upon the structure factors was then determined and compared with experimental results, with the following further deductions.

- (4) Diameter of the nuclear carbon atom  $1.42 \pm 0.03$  A.U.

Diameter of the side-chain carbon atom  $1.54 \pm 0.12$  A.U. (diamond). The aromatic nucleus is therefore exactly like graphite in dimensions.

- (5) Only the plane ring gives anything like agreement with observations, again as in graphite.

- (6) The side-chain carbon atoms are attached radially to their respective nuclear atoms and lie in the plane of the ring.

- (7) Three of the valences of aromatic carbon are coplanar certainly, but no direct information is afforded concerning the fourth except that it must be so disposed as to give the ring as a whole a center of symmetry. This condition eliminates the Kekule static model with three double bonds.

*d. Further Recent Information Concerning the Benzene Nucleus.*—Since the analysis of hexamethylbenzene, renewed interest has been taken in the questions of the shape of the benzene nucleus. The fact that in  $C_6(CH_3)_6$  it corresponds so closely in structure to the graphite type of ring indicates that very little deformation can have taken place. The expectation is that in fully substi-

tuted derivatives the structure of the nucleus should remain similar. However, some symmetry has been lost, for the graphite ring possesses true hexagonal symmetry while the benzene derivatives are only centrosymmetrical.

Banerjee<sup>1</sup> has made a careful reinvestigation of naphthalene and has shown that the intensity data are consistent with perfectly flat rings. Hendricks and Hilbert<sup>2</sup> have shown that in meta-dinitrobenzene the carbon and nitrogen atoms are all in the same plane. The failure of attempts to form meta or para rings of benzene compounds indicates that the valences are not easily deformed in direction and that the benzene ring is very rigid. Dhar<sup>3</sup> has subjected diphenyl to complete analysis, including structure factor data from intensities, and proved that the rings are flat and lie in one plane and that the molecules are inclined to cell faces. The distance between rings in the molecule is 1.48 A.U., which is a mean of 1.42 (in graphite) and 1.54 in aliphatic linkages.

There is still uncertainty as to whether cyclohexane and reduced compounds have plane or puckered rings. The *cis*-forms of  $C_6H_6Cl_6$  and  $C_6H_6Br_6$  have greater symmetry than benzene and the halogen atoms belonging to one molecule lie in two planes. In naphthalene tetrachloride and dichloronaphthalene tetrachloride, one ring remains unreduced and retains aromatic character, while the other has been reduced and might be puckered. Considerably more research is required to discover whether the aromatic character is bound up with a graphitic arrangement or whether this can persist when aromatic properties are lost. If the ring is flat in reduced derivatives, then the aromatic nature must depend more on the fourth valence bond than on the configuration of the bond.

One interesting question is this: In derivatives with flat rings a considerably higher symmetry might easily be expected for the crystal lattice than is actually observed. Even hexamethylbenzene has only triclinic symmetry. This would seem to indicate that the lower symmetry of the molecular arrangement in space is due to the hydrogen atoms in some way or to a distortion of the ring so slight as not to affect the structure factors markedly for the flat ring. Of course, reliable interpretation of data on

<sup>1</sup> *Nature*, **125**, 456 (1930); *Indian J. Phys.*, **4**, 557 (1930).

<sup>2</sup> *Loc. cit.*

<sup>3</sup> *Indian J. Phys.*, **7**, 43 (1932).

crystallized benzene is still lacking. In the derivatives with more than one nucleus (naphthalene, diphenyl, etc.) the rings may be flat but still not coplanar.

Some light on these questions is afforded by electron diffraction studies on benzene, cyclohexane, etc., vapors. The data best agree with a plane hexagonal ring with edge length 1.42 A.U. for benzene and a puckered ring with edge length 1.54 A.U. for cyclohexane. Just what happens when these molecules are condensed into crystals with a lower symmetry is still doubtful.

There are evidences from both x-ray and electron diffraction, of course, that the aliphatic carbon atom is tetrahedral or sphenoidal. Only in methane,  $\text{CCl}_4$ , or other fully substituted derivatives is the regular tetrahedron maintained. If the carbon atom is unsymmetrically loaded with halogen atoms, for example, tetrahedral symmetry is lost. But even  $\text{CBr}_4$  crystallizes in two forms: tetrahedral symmetry at low temperatures and bi-molecules (monoclinic) at higher temperatures with deformation of the single molecules and a loss in symmetry.

**The Results of Crystal Analysis of Organic Compounds.**—Six years ago all x-ray data on organic compounds could be considered in very little space, and in fact the International Critical Tables, Vol. I, listed only about fifteen organic compounds for which space-groups had been assigned. With the great improvements in technique and in methods of interpretation a very large number of organic compounds have now been analyzed for crystalline and molecular structures with results just as complete and convincing as the examples already cited. Ewald and Hermann have classified these into 26 main types already, with many others still to be fit into the scheme. Little would be gained in this book by presenting these experimental data, since even tabulation would be greatly extended, and since they are to be found in full in the "Strukturbericht." Consequently only some general conclusions of general interest to the chemist will be considered briefly.

1. *Inorganic Types with Organic Substituted Radicals.*—The alkyl ammonium halides, principally studied by Wyckoff and Hendricks, are the chief representatives. In almost every case a very clear relationship exists between the structure of the compound and the simpler compound in which a metal atom has been replaced by a radical. For example, triethylammonium iodide is like wurtzite ( $\text{ZnS}$ ), with the radical replacing Zn atoms;

the length of the chain, of course, causes a large decrease in the axial ratio. Tetramethylammonium iodide is similarly related to phosphonium iodide (type *B10*), methylammonium iodide to rock salt, and methylammonium chloride to cesium chloride. A very curious result is that in these latter two cases the chains which replace one of the ions in the simple salts evidently must be linear rather than zigzag, in order to account for observed symmetry and spacings. Several derivatives of hexachloroplatinates and hexachlorostannates, in which these ions are octahedrally coordinated, also have structures which might be predicted from the results on metal ion salts of these complex anions. The chief interest, of course, is in the effect on the symmetry of the ammonium group by substituting various combinations of alkyl groups.

2. *Symmetrical Methane Derivatives.*—The tetrahedral form of these compounds is the point of greatest interest. Methane crystallizes in the face-centered cubic lattice of parallel  $\text{CH}_4$  tetrahedra; tetramethyl methane has the diamond cubic structure, and tetraiodomethane is a simple cubic lattice of parallel tetrahedra. X-ray and electron diffraction researches have shown clearly the distortion of the tetrahedra which results when the hydrogen atoms are unsymmetrically replaced by halogens or other groups. Even carbon tetrabromide, which crystallizes in two modifications with a tetrahedral molecule for the lower temperature modification, loses symmetry at higher temperatures and forms a monoclinic lattice from bi-molecules. In tetranitromethane, although cubic, one of the nitro groups evidently differs from the other three in space and the formula is perhaps correctly written  $\text{O}=\text{N}-\text{O}-\text{C}(\text{NO}_2)_3$ .

Pentaerythritol,  $\text{C}(\text{CH}_2\text{OH})_4$ , a tetragonal crystal, probably has the distinction of having been investigated more repeatedly than any other organic compound. It illustrates the case in which very slight differences in interpretation of x-ray and optical data lead to widely different molecular structures. In the early work it was concluded that the carbon atoms were all coplanar or formed a flat pyramid. Further work has demonstrated that it is impossible from the x-ray data to distinguish between symmetry classes  $\text{C}_4$  or  $\text{S}_4$  (tetrahedral). Researches on crystal growth and solution, etch figures, pyro- and piezoelectricity have given preponderance to the tetrahedral molecule and the space-group  $\text{S}_4^2$ . Besides pentaerythritol, the tetracetate and tetranitrate are

also body-centered tetragonal with the same symmetry class but they differ in the orientation of the center molecule with respect to the molecules at the corners of the unit cell. The compounds  $C(C_6H_5)_4$ ,  $Si(C_6H_5)_4$ ,  $Ge(C_6H_5)_4$ ,  $Sn(C_6H_5)_4$ , and  $Pb(C_6H_5)_4$  all have the same tetrahedral molecular structure and lattice as pentaerythritol tetranitrate.

3. *Unsymmetrical Methane Derivatives without Chain Character.* Chief representatives of this class thus far studied are iodoform, urea and its derivatives, and some formates. In iodoform the iodine atoms form an hexagonal packing of spheres. The carbon and hydrogen atoms enter octahedrally the holes in this lattice work, so that the molecule  $CHI_3$  forms the unit. In urea  $OC(NH_2)_2$ , the molecule consists of a central atom circumscribed by an almost equilateral triangle of one O and two N atoms. There are thus chains of the molecules parallel to the  $c$  axis or networks perpendicular. Thiourea is orthorhombic with four molecules per unit cell, instead of tetragonal with two molecules per cell for urea, and the carbon atoms are surrounded by the sulfur and two nitrogen atoms in the form of a flat pyramid. The nitrogen atoms are equivalent, so that the correct formula in

the solid state is  $S=C\begin{matrix} \nearrow NH_2 \\ \searrow NH_2 \end{matrix}$  and not  $HS-C\begin{matrix} \nearrow NH_2 \\ \searrow NH \end{matrix}$ .

4. *Short Aliphatic Chains with Symmetry about a Central C—C Linkage.*—Numerous compounds of this type have been investigated, of chief interest being ethane and its derivatives, and oxalic, maleic and fumaric, and tartaric acids and their derivatives. Ethane,  $C_2H_6$ , and diborane,  $B_2H_6$ , crystallize alike with hexagonal cell (type  $D_{4h}$ ). The dimensions for the former are  $a = 4.46$ ,  $c = 8.19$  A.U., distance C—C in the same molecule 1.55 A.U., C—C, different molecules, 3.5 A.U., distance molecule center to center 4.46 A.U. Of the derivatives  $C_2Cl_6$ ,  $C_2Br_6$ ,  $C_2H_4Br_2$  (two modifications),  $C_2H_5F$ ,  $C_2Cl_3Br_3$ , and  $C_2H_4(CH_3)_2$  (two modifications) are isomorphous-orthorhombic, space-group  $V_h^{16}$ ;  $C_2(CH_3)_4Br_2$  and  $C_2Br_4(CH_3)_2$  have isomorphous tetragonal structures;  $C_2(CH_3)_5OH$  is orthorhombic with eight molecules per unit cell. Further work is required to understand exactly the distortions of carbon tetrahedra caused by substituent groups and the temperature conditions of stability of polymorphic forms.

Fumaric acid is distinguished from its isomer maleic acid in showing six molecules per unit cell, an unusual case of association

or polymerization. Outstanding among early work are Astbury's analyses of *d*-tartaric acid and *dl*-tartaric acid (racemic acid).<sup>1</sup> The first is monoclinic,  $a = 7.70$ ,  $b = 6.04$ ,  $c = 6.20$  A.U., and  $\beta = 100^\circ 17'$ , with two molecules to the unit cell; the second is triclinic,  $a = 14.82$ ,  $b = 9.74$ ,  $c = 4.99$  A.U.,  $\alpha = 82^\circ 20'$ ,  $\beta = 122^\circ 50'$ , and  $\alpha = 111^\circ 52'$ , with four molecules to the unit cell. Cleavage occurs in the [100] direction where the OH groups touch.

The power of both crystals and solutions of tartaric acid to rotate the plane of polarized light is to be found in a spiral arrangement of the atoms. In the crystal two such spirals exist, one connected with the four central carbon atoms of the molecule, and the second resulting from the way in which the molecules are combined in the crystal unit. These two spirals are in opposite directions, so that the rotatory power of the solid is determined by the difference. In solution, of course, the second spiral structure is absent and the rotatory power depends only on the central carbon atoms. In racemic acid spirals are exactly balanced, so that there is internal compensation.

5. *Short Aliphatic Chains without Symmetry around a Central C—C Linkage*.—Examples of this classification are metaldehyde, aldehyde ammonia, acetamide, basic beryllium salts of fatty acids, and other metal salts including acetylacetone compounds of trivalent metals. These last are isotrimorphic:  $\alpha$ , monoclinic,  $\beta$ , rhombic, and  $\gamma$ , rhombic. The iron compound of the  $\gamma$ -modification has 16 molecules per unit cell of the unusually large dimensions  $13.68 \times 15.74 \times 33.0$  A.U.

6. *Highly Polymerized Organic Compounds*.—These substances usually of natural origin, such as cellulose and rubber, will be considered in Chap. XX.

7. *Derivatives of Benzene*.—These have already been considered in sufficient detail to indicate the nature of the benzene nucleus. Reference should be made to Ewald and Hermann's "Strukturbericht" for numerous interesting details for a large number of derivatives.

8. *Special Ring Compounds*.—Hexamethylenetetramine  $C_6H_{12}N_4$  was probably the first organic compound to be subjected to a complete structure determination.<sup>2</sup> It is cubic space-group  $T_d^3$  with two molecules per unit cell. The N and C atoms

<sup>1</sup> *Proc. Roy. Soc. (London)*, **102**, 506; **104**, 219.

<sup>2</sup> DICKINSON, and RAYMOND, *J. Am. Chem. Soc.*, **45**, 22 (1923).

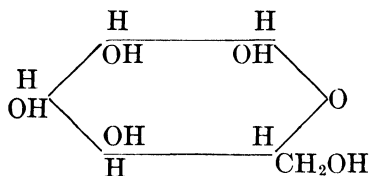
form molecules of the same configuration as those of  $(\text{Sb}_2\text{O}_3)_2$  (type D61) but the lattice is body-centered instead of diamond;  $a_0 = 7.02$  A.U., the distance C—N in a molecule 1.58, C—C between two molecules 3.37.

9. *Sugars*.—The principal x-ray research on sugars has been carried on by Hengstenberg and Mark,<sup>1</sup> Sponsler and Dore,<sup>2</sup> Marwick,<sup>3</sup> and Astbury and Marwick.<sup>4</sup>

Essential data are tabulated as follows:

Carbohydrate	System	Dimensions of unit cell				Density
		<i>a</i>	<i>b</i>	<i>c</i>	$\beta$	
Natural cellulose.	Monoclinic	8 3	10 3	7 9	84°	1 52
Cellulose hydrate	Monoclinic	8.14	10 3	9 14	62°	1.56
Cellobiose . . . . .	Monoclinic	5.0	13 2	11 1	90°	1 556
Sucrose . . . . .	Monoclinic	11.0	8.7	7 65	103 5°	1 588
Mannose. . . . .	Orthorhombic	7.62	18 18	5.67	.	1 501
Glucose ( $\alpha$ - <i>d</i> ) . . . .	Orthorhombic	10 40	14 89	4 99	.	1 544
Fructose ( <i>d</i> ) . . . . .	Orthorhombic	8 06	10 06	9.12	.	1 598
Sorbose . . . . .	Orthorhombic	6 12	18 24	6 43	.	1 654

Astbury and Marwick have pointed out that the small variation in density of these saccharoses suggests an approximate close packing of some molecular unit, and by further calculation of cross-sectional areas it becomes apparent at once that the dimensions of this unit—the sugar ring and its side chain—impress themselves in the various unit cells. For mannose as an example, the ring may be drawn



The molecular dimensions so deduced are 7.27, 5.64, and  $2 \times 4.58$ . Thus probably the sugar ring takes about 4.5 A.U. in thickness or normal to the ring (being puckered), about 5.5 A.U.

<sup>1</sup> *Z. Kryst.*, **72**, 301 (1929).

<sup>2</sup> *J. Am. Chem. Soc.*, **53**, 1639 (1931).

<sup>3</sup> *Proc. Roy. Soc. (London)*, **A131**, 621 (1931).

<sup>4</sup> *Nature*, **127**, 12 (1931).



across the ring horizontally, *i.e.*, in the direction of the chains in cellulose, and 7.5 A.U. across the ring vertically, in the direction of the side chain  $\text{CH}_2\text{OH}$ .

**Long-chain Compounds.**—Out of the x-ray studies of the aliphatic series, conducted largely by Müller and Shearer in Bragg's laboratory and by Trillat and Thibaud in de Broglie's laboratory, have come some of the most striking results of the science; these have been achieved in the face of such difficulties as the inability to use the simpler compounds (which are liquid), or to obtain single crystals of the higher members of the series, thus necessitating the use of the powder method except in a few cases.

The great simplifying phenomena discovered in the study of the higher paraffin hydrocarbons, acids, esters, salts or soaps, ketones, etc., were that the unit cells into which the molecules, long pictured by chemists as chains, are packed, have one side which is very much longer than the others, and that this side grows in a uniformly constant manner as the number of carbon atoms increases. This dimension must, therefore, correspond to the length of the molecule. The two other dimensions remain nearly constant throughout the series; hence, they must correspond to the essentially constant cross section of a chain of carbon atoms.

For the usual diffraction experiments in which single crystals are not obtainable, a small flake of the substance is flattened on a glass or metal backing, or melted or poured on a flat surface and placed on an oscillating-type spectrograph. On the film is obtained a single strong line repeated through many orders, corresponding to the long dimension and varying with the number of carbon atoms, and lines corresponding to the smaller side spacings. The x-rays measure the perpendicular distance between successive identical planes in the crystal; since the principal spacing increases a constant amount for each addition of a  $\text{CH}_2$  group, the conclusion is that the molecules are parallel and either perpendicular (in which case the interplanar spacing measures the actual molecule length) or inclined at a constant angle to these reflecting planes. Bragg uses the picturesque analogy of a carpet as a layer, the pile of the carpet as the molecules, and a stack of carpets as the crystal.

This oriented film in a sense, therefore, acts like a single crystal which is oscillated in an x-ray beam and reflections from a set of planes registered by the Bragg method in accordance with  $n\lambda =$

$2d \sin \theta$  (see page 180). The simultaneous appearance of the side spacings proves the powder nature of the specimen. Hence the oriented film consists of many crystal grains oriented exactly alike with respect to one axis but at random *around* this axis.

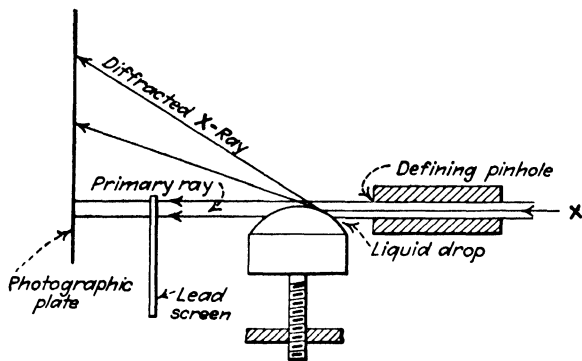


FIG. 142.--The tangent drop diffraction method.

Another technique which has been used with great success by Trillat and by the writer is the use of a curved surface upon which the molecules of a film may orient. Inasmuch as the x-ray

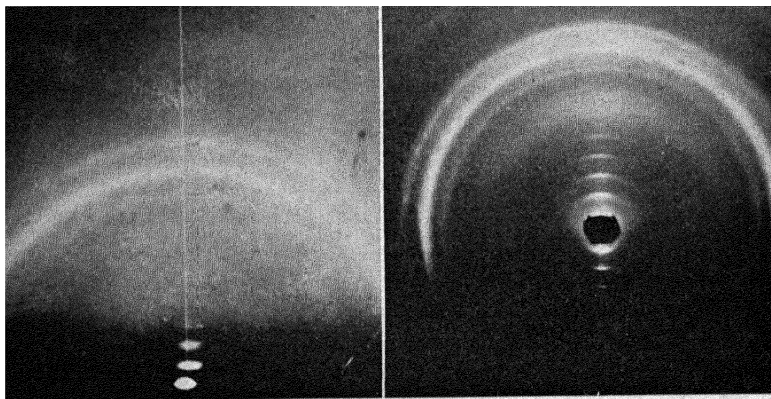


FIG. 143.—Patterns for thin films of paraffin wax. Left, on glass plate and oscillation spectrograph; right, on mercury drop. The short lines or arcs at small angles are interferences in various orders for molecular length, while the long Debye-Scherrer rings correspond to molecular cross section.

beam may strike this spherical surface tangentially at a whole series of angles, one position will be correct for reflection from the long spacings of the film. Hence oscillation of the specimen is obviously unnecessary. This method is illustrated in Fig. 142.

Typical patterns for the same paraffin wax sample, respectively by the method of oscillating a film on a flat plate and of orienting a film on a mercury drop, are illustrated in Fig. 143. Orientation of film on water, metals, molten liquids, etc., will be considered in a later paragraph.

*Paraffin Hydrocarbons.*—In order fully to understand the results obtained from films of the hydrocarbons, a complete

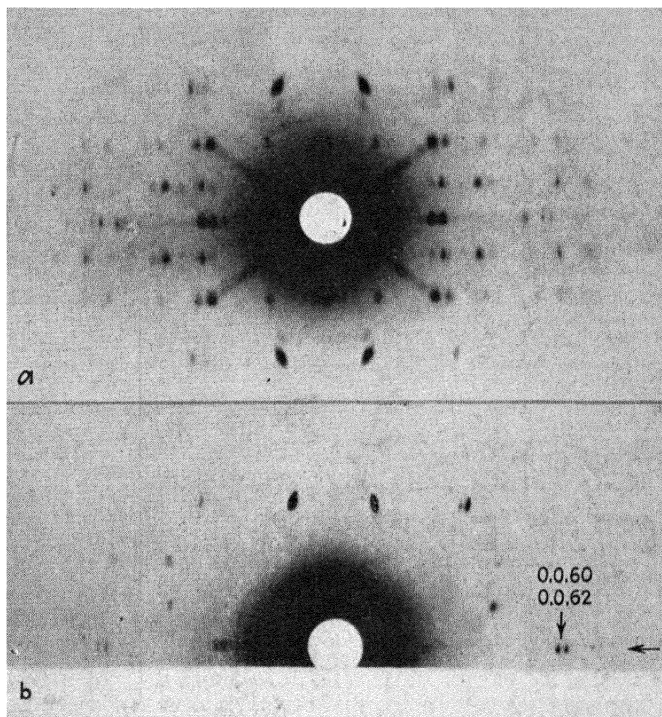


FIG. 144.—Rotation spectra for single crystal of  $C_{29}H_{60}$ , showing sixty-second-order reflection. (Müller.)

structure determination obviously was necessary and, of course, this required a single crystal which could be analyzed by the rotation method. Müller<sup>1</sup> succeeded in obtaining a single crystal of  $C_{29}H_{60}$  and in completing a remarkably able analysis. A rotation photographic around the  $a$  axis and another showing 0, 0,60 and higher reflections are reproduced in Fig. 144. The crystal is orthorhombic with the space-group  $V_h^{16}$ ; the unit cell

<sup>1</sup> *Proc. Roy. Soc. (London)*, **120A**, 437 (1928).

containing four molecules has the dimensions:  $a = 7.45$ ,  $b = 4.97$ ,  $c = 77.2$  A.U. It is evident therefore that two molecules end to end are placed along the  $c$  axis, since a spacing  $d_1$  of 38.6 A.U. is observed by the powder (thin-film) method together with  $d_2 = 4.13$ ,  $d_3 = 3.72$ ,  $d_4 = 2.98$ ,  $d_5 = 2.48$ , and  $d_6 = 2.35$ . These all correspond to the planar indices in the single crystal analysis respectively of 002, 110, 200, 210, 020, and 120. The analysis further shows that the  $\text{CH}_2$  groups of the chain molecule

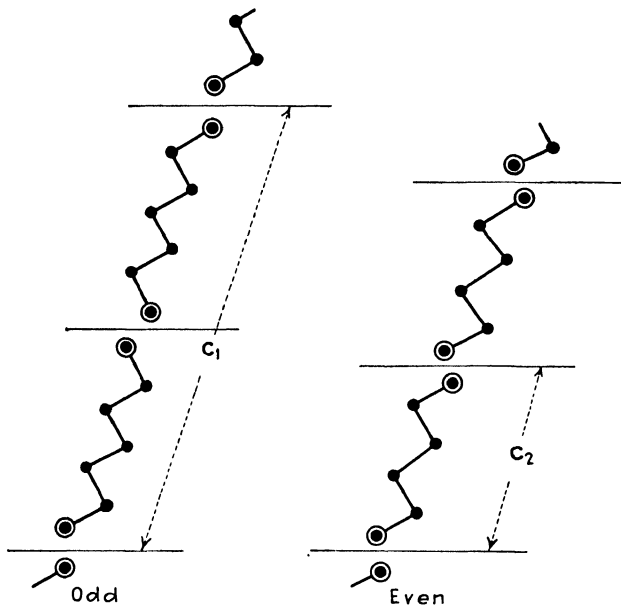


FIG. 145.—Diagram of long-chain compounds with odd and even numbers of carbon atoms.

lie equally spaced on two parallel rows, the lines between successive centers thus forming a zigzag with an angle somewhat less than  $92^\circ$ . (slightly distorted tetrahedral angle). The distance between two consecutive scattering centers on either row of the crystal molecule, *i.e.*, from  $(\text{CH}_2)_0$  to  $(\text{CH}_2)_2$  on one row, or from  $(\text{CH}_3)_1$  to  $(\text{CH}_3)_3$  on the other, is 2.537 A.U., or the increment per  $\text{CH}_2$  to the total length is 1.27 A.U. A gap of 3.09 A.U. exists between the ends of two consecutive molecules in the crystal.

Hengstenberg<sup>1</sup> obtained results also for crystals of  $\text{C}_{35}\text{H}_{22}$  which gave unit-cell dimensions of  $a = 7.43$ ,  $b = 4.97$ ,  $c = 46.2$

<sup>1</sup> *Z. Kryst.*, **67**, 583 (1928).

A.U. (single-chain length). Because of great intensity of the thirty-sixth and thirty-seventh orders, the vertical component of distance between neighboring carbon atoms must be 1.27 A.U. as Müller found.

Of principal interest in these studies is the significance of the zigzag chain in explaining the well-known alternations in properties for substances containing odd and even numbers of carbon atoms. Müller's interpretation<sup>1</sup> is shown most clearly in Fig. 145. In the odd molecule the pattern repeats itself every second

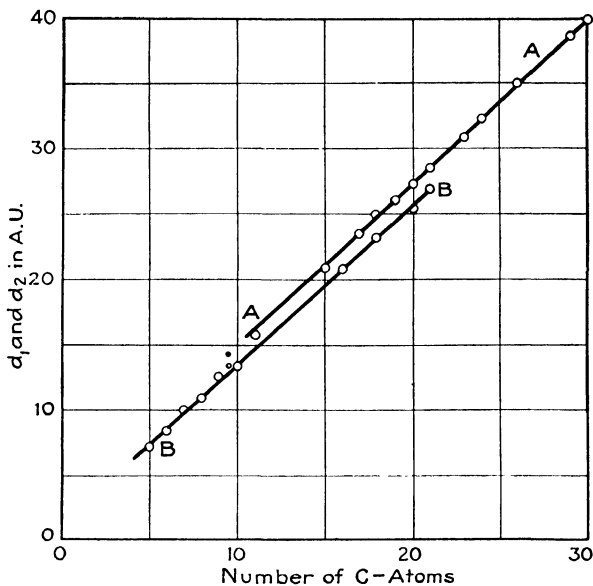


FIG. 146.—Plot for normal paraffin hydrocarbons showing relationship of two modifications.

molecule along the direction  $c$ , while in the even all successive molecules are identically situated. It would be expected in the actual crystal therefore that two molecules would lie along the  $c$  axis for odd-numbered chains and only one molecule in crystals containing even-numbered molecules. This prediction has been fully verified for dicarboxylic acids where the end groups are  $\text{COOH}$  instead of  $\text{CH}_3$  in the paraffins.

In order to test the effect of even and odd hydrocarbons, Müller investigated<sup>2</sup> a number of normal paraffins ranging from

<sup>1</sup> *Proc. Roy. Soc. (London)*, **A124**, 317 (1929).

<sup>2</sup> *Proc. Roy. Soc. (London)*, **A127**, 417 (1930).

$C_5H_{12}$  to  $C_{30}H_{62}$  at liquid-air, room, and nearly melting temperatures. The higher members of the paraffin series crystallize in the normal form as found for  $C_{29}H_{60}$ , irrespective of whether the carbon content is an even or odd number. Thus for these *long* chains the effects of the end groups are not sufficient to differentiate the two series as predicted from Fig. 145. Differences in the behavior of even and odd members begin to appear, however, when the carbon content decreases.  $C_{22}H_{46}$ ,  $C_{20}H_{42}$  and  $C_{18}H_{38}$  exist in two alternative structures, the normal one near the melting point and another structure at lower temperatures. The change from the normal form into another one also occurs in the series of odd members between  $C_{11}H_{24}$  and  $C_9H_{20}$ . The results are expressed graphically in Fig. 146, in which the long spacings, varying from 7.35 A.U. for  $C_5H_{12}$  to 40.0 A.U. for  $C_{30}H_{62}$ , are plotted against the number of carbon atoms. There are two straight lines, the upper representing the normal crystal structure, the lower the second form appearing at low temperatures. In spite of this complication, the fact is demonstrated that these chains have a constant increment in length of 1.25 A.U. per carbon atom and that the x-ray spectrum is a powerful method of identifying any member of an homologous series and of determining molecular weight. Hengstenberg's values of 46.2 A.U. for  $C_{35}H_{72}$  and 78.2 A.U. for  $C_{60}H_{122}$  are consistent.

X-ray diffraction results with ordinary paraffin waxes are of unusual interest. In spite of the fact that these waxes may contain as many as 18 or 20 different hydrocarbons, both normal and branched-chain isomers, a single diffraction spacing corresponding to molecular length is obtained, together with the usual side spacings. Clark<sup>1</sup> first made x-ray measurements on a series of commercial waxes of varying melting points with the following results:

Wax melting point, degrees Fahrenheit	$d_1$	Number of C atoms indicated
135	39.42	29 0
130	38.58	28 5
125	35.22	26 0
120	34.38	25 0

<sup>1</sup> *Science*, **66**, 136 (1929).

The spacing obtained varied, however, depending upon the method of preparing the specimen film (from 36.64 to 40.20 A.U. for the 135° wax), and especially the time given for molecular orientation. Furthermore, the presence of addition agents in very small amounts served to change the long spacing. Obviously, possibilities of polymorphism, changing predominance of one molecular species over all others in the mixture, and changing tilts of molecules to the diffracting planes may explain the variations.

Clark and Smith<sup>1</sup> next studied series of samples from carefully fractionated paraffin waxes derived from midcontinent petroleum.

Some representative data are tabulated for one of the series.

Fraction	A	B	C	D	E	F
Melting point, degrees Centigrade	59 9	55 2	47 1	40 5	35.2	29 4
Refractive index, 80° C	1 4303	1 4306	1 4330	1 4550	1 4359	1 4380
Molecular refraction	122 7	122 8	126 5	129 8	128 4	125 0
Specific gravity	0 770	0 773	0 779	0 783	0 786	0 792
Solubility in $C_7H_{14}Cl_2$ (14°, g for 100 c c) . . . .	0 115	0 218	0 82	2 4	5 7	70 3
Molecular weight	366	367	379	389	385	377
Average value of $n$ in $C_nH_{2n+2}$ indicated	26	26	27	27 6	27 4	26 8
X-ray identity period, $d_1$	42 3	39 2	42 3	42 3	45 8	50 3
Number of carbon atoms.	31	29	31	31	34	38
Number of orders of reflection	6	4	2	2	1	1
Molecular weight from $d_1$	464 5	430 9	464 5	464 5	503 8	552 8

Some conclusions are as follows:

- No fraction is a single pure compound.
- In fractions from the same wax the identity periods corresponding to the predominating molecular length follow no regular order with melting point; thus the largest spacing was obtained with the fraction with lowest melting point.
- The number of orders of diffraction caused by the oriented molecules varies directly with the melting point of the fraction. This indicates that with the lower melting fractions the degree of perfection of orientation of the molecules becomes less, probably owing to the interference of an increasing number of molecules with lower orienting tendency. Excellent agreement between observed and calculated molecular refractions proves that

<sup>1</sup> *Ind. Eng. Chem.*, **23**, 697 (1931).

these molecules must also belong to the paraffin series and are probably branched-chain molecules in view of the small variation in the observed molecular weight compared with large variation in melting point. This is further indicated by the fact that the side-spacing diffraction maxima corresponding to molecular cross sections become increasingly diffuse from  $A$  to  $F$ .

*d.* Molecular weights calculated from the x-ray data are about 25 per cent higher than values by the ebullioscopic method. This indicates that besides containing the molecules indicated by the identity period every fraction is also made up of lower molecular weight paraffins, either shorter straight chain or isoparaffins or both.

*e.* In 16 fractions only five spacings are observed corresponding to the values for pure hydrocarbons with 29, 31, 34, 38, and 42 carbon atoms by interpolation on the straight-line plot of  $d_1$  against  $n$ .  $C_{38}H_{78}$  and  $C_{42}H_{86}$  were recognized as constituents of paraffin wax for the first time.

*Aliphatic Acids.*—The principal spacings vary from 6.66 A.U. for crystallized acetic acid,  $C_2H_4O_2$  (Saville), to 82.0 A.U. for one modification of lacceroic acid,  $C_{32}H_{64}O_2$  (Thibaud, powder method). The layers in any one acid have double the spacing displayed by the paraffin with the same number of carbon atoms; hence they are two molecules thick with COOH groups together at the ends of two oppositely turned molecules. Until the remarkable photographs of Prins and Coster, showing as many as 34 orders for palmitic acid, it was believed that the odd orders were generally more intense than the even. These new results prove that this is true to about the ninth order at which point even and odd intensities become equal; beyond this the even orders become more intense, reaching a maximum at the sixteenth. The thirty-fourth order spectral line is much stronger than any of the adjacent lines indicating a distinct periodic phenomenon in the fact that the spacing for one molecule (35.6 A.U.) is thirty-four times the increment for a  $CH_2$  group. The precision measurements of Trillat prove that the large lattice spacings (and hence the lengths of the molecules) for the fatty acids vary in proportion to the number of carbon atoms, but group the acids into two series, one for those containing an even number, the other for those containing an odd number of carbon atoms.



In addition the researches of Piper, Malken and Austin,<sup>1</sup> Thibaud,<sup>2</sup> deBoer,<sup>3</sup> and others have demonstrated that there is a definite polymorphism of the higher fatty acids, each acid from palmitic ( $C_{16}$ ) up, whether containing even or odd carbon atoms, having two forms. One form is obtained by melting the acid and forming a thin layer, the other by evaporating a solution.

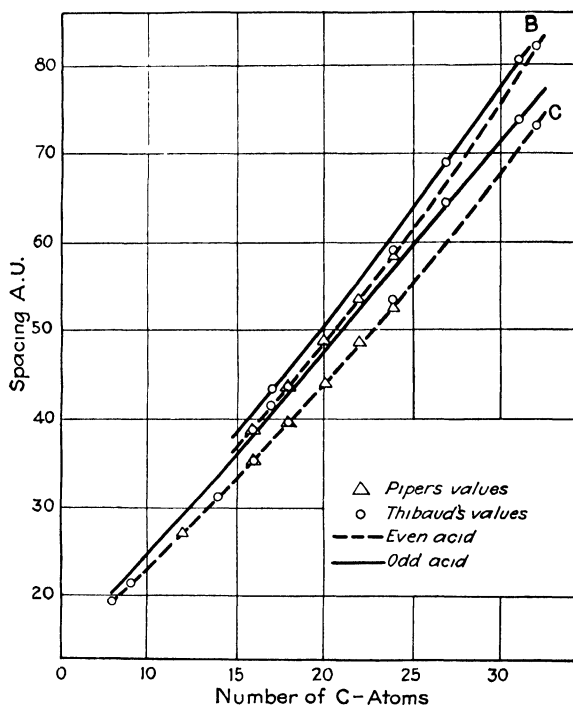


FIG. 147.—Graph for normal aliphatic acids showing effect of even and odd numbers of carbon atoms, and of *B* and *C* modifications.

These are called, respectively, the *C* or  $\alpha$  and the *B* or  $\beta$  forms. An *A* or  $\gamma$  form with still larger principal spacing appears very rarely. A graphical representation of the variation of the spacings corresponding to molecular length with the number of carbon atoms thus requires at least four curves: odd acids *B* and *C*, and even acids *B* and *C*. The best data are plotted in Fig. 147. The increase of the chain's length per carbon atom is, respec-

<sup>1</sup> *J. Chem. Soc.*, **129**, 2310 (1926).

<sup>2</sup> *Compt. rend.*, **184**, 24, 96 (1927); **190**, 945 (1930); *Nature*, **119**, 852 (1927).

<sup>3</sup> *Nature*, **119**, 50, 635 (1927).

tively, 1.327 and 1.146 A.U. for the *B* and *C* forms of the odd acids and 1.21 and 1.10 A.U. for the even acids. The polymorphic transitions occur at definite temperatures and are accompanied not only by a change in spacing but also in refractive index. Some representative data are as follows:

Acid	<i>B</i> Spacing	<i>C</i> Spacing	Transition temperature
C <sub>11</sub> H <sub>22</sub> O <sub>2</sub> .....	30 1	25 4	17 (deBoer)
C <sub>13</sub> H <sub>26</sub> O <sub>2</sub> .....	35 1, 31 5	29 8	32
C <sub>15</sub> H <sub>30</sub> O <sub>2</sub> .....	39 7, 35 9	34 4	44
C <sub>17</sub> H <sub>34</sub> O <sub>2</sub> .....	40 2	38 7	54
C <sub>12</sub> H <sub>24</sub> O <sub>2</sub> .....	30 6	27 4	10 (Thibaud)
C <sub>14</sub> H <sub>28</sub> O <sub>2</sub> .....	35 0	31 2	25
C <sub>16</sub> H <sub>32</sub> O <sub>2</sub> .....	39 3	35 6	40
C <sub>18</sub> H <sub>36</sub> O <sub>2</sub> .....	43 95	39 9	55
C <sub>16</sub> + C <sub>18</sub> acids	41 6	37 6	40 < T < 55
C <sub>27</sub> H <sub>54</sub> O <sub>2</sub> . . . . .	69 0	64 0	82 5

Excellent complete analyses of single crystals have been made on stearic acid and derivatives by Müller,<sup>1</sup> and on lauric acid by Brill and Moyer,<sup>2</sup> and partial analyses on several others.

Both the C<sub>12</sub> and C<sub>18</sub> acids are monoclinic with four molecules per unit cell and with double molecules lying with their long direction almost parallel to the *c* axis. The zigzag aliphatic acid

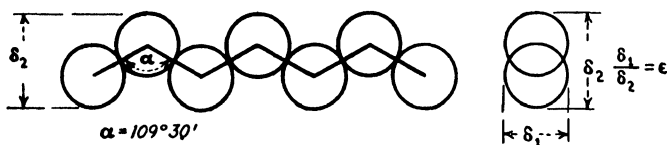


FIG. 148.—Form of zigzag carbon chain and cross section.

chain can be represented essentially as an elliptical rod with a ratio of axes of 0.64 as represented in Fig. 148.

*Other Acids.*—Oleic, with one double bond, linolic with two, and linolenic with three when in thin layers on polished lead, demonstrate according to Trillat how chemical change may be followed by x-ray patterns. New lines appear as oxygen is absorbed at the double bonds. When the latter two become hard and dry, the x-ray spectra disappear as is the case with linseed oil.

<sup>1</sup> *Proc. Roy. Soc. (London)*, **114**, 542 (1927).

<sup>2</sup> *Z. Kryst.*, **67**, 570 (1928).

Patterson<sup>1</sup> studied a series of phenyl normal saturated fatty acids. While benzoic acid is a purely aromatic acid, from  $\epsilon$ -phenyl-caproic acid ( $n = 5$ ) onwards, the side chain tends to predominate and the substances tend to be like the aliphatic acids. The lower acids thus represent the stage in which the properties go over from aromatic to aliphatic and these variations are quite complicated.

The di-acids (succinic, adipic, pimelic, suberic, azelaic, etc.) diffract x-rays in the predicted manner from oriented films. Since there are two COOH groups in each molecule, the layers are only one molecule thick; the spacing of a  $C_8$  di-acid, for example, multiplied by four gives the observed spacing of the  $C_{16}$  fatty acid (with two molecules per layer).

An alternation is observed in the films between chains with even and odd numbers of carbon atoms. Caspari<sup>2</sup> prepared single crystals and found the effect greatly pronounced in complete-structure analyses. In the following table the data are assembled for the unit-cell dimension of the monoclinic unit cell ( $c$ ) corresponding to molecular length, the number of molecules per cell ( $z$ ), and for comparison the principal spacings obtained by Henderson from films of the acids.

Acid	Number of C atoms	$c$	$Z$	$d$ (film)
Adipic .....	6	10 02	2	6.90
Pimelic .....	7	22 12	4	7 65
Suberic . . . . .	8	12 56	2	9.05
Azelaic . . . . .	9	27 14	4	9 56
Sebacic .. . . .	10	15 02	2	11.20
Brassylic . . . . .	13	37 95	4	13 3
Hexadecanedicarboxylic	18	25 10	2	

Part of the discrepancy between single-crystal and film data may be due to polymorphism which has been observed for such di-acids as malonic, succinic, and glutaric by Latour.<sup>3</sup> However, these acids substantiate the theory of Müller as to the effect of even and odd chains on properties.

<sup>1</sup> *Phil. Mag.*, **3**, 1252 (1927).

<sup>2</sup> *J. Chem. Soc.*, **1928**, 3235.

<sup>3</sup> *Compt. rend.*, **193**, 180 (1931).

*Esters.*—Ordinarily there is a normal decrease in intensity; the layers are one molecule thick; this is true except for acetates  $\text{CH}_3\text{COO}(\text{CH}_2)_n\text{CH}_3$  with much greater spacings, suggesting doubling from the active double-bonded oxygen atom, while methyl esters  $\text{CH}_3(\text{CH}_2)_n\text{COOCH}_3$  are normal; the increase per carbon atom is 1.22 A.U.

*Soaps.*—The layers are one molecule thick, and the spacing is independent of the metal for any one acid. By the ingenious method depending upon the fact that the fatty acids on a lead support will form the lead soaps, Trillat has obtained the spectra for a series from the acetate,  $\text{C}_2$ ,  $d = 12.6$  A.U. to the lacceroate  $\text{C}_{32}$ ,  $d = 92.0$  A.U., the largest lattice spacing thus far measured. The increment per carbon atom is 1.3 A.U.

For a whole series of potassium salts, Piper<sup>1</sup> observed two different types with different lattice spacings, one for freshly prepared specimens and one for the same specimen after standing exposed in air which proved to be the acid salt. The acid-salt molecules evidently are perpendicular to the diffracting layer and the neutral-salt chains at an angle of  $54^\circ 54'$ .

*Ketones.*—In general for  $\text{CH}_3(\text{CH}_2)_m\text{CO}(\text{CH}_2)_n\text{CH}_3$  the layers are one molecule thick, but for ketones with the CO group separated from the end only by a methyl group, double spacings occur, indicating activity of the  $\text{COCH}_3$  group comparable with  $\text{COOH}$  for acids; the compound methyl heptadecyl ketone has double the spacing of the isomeric propyl pentadecyl ketone; the intensities of the normal di-ketones (oxygen in the middle of the chain) are strong in the odd orders and weak in the even, exactly as with acids, except that one molecule of a ketone acts like two molecules of the acid; if the oxygen atom is one-third along the chain, the third, sixth, ninth, etc., orders disappear; the increase in spacing per carbon atom is 1.3 A.U.

The following conclusions and practical applications from the x-ray analysis of long-chain compounds may be drawn:

1. *Molecular Form.*—The molecules are confirmed as the long chains known to the chemists. The substances are truly crystalline, since the side spacings are observed, although some of the soaps are obtainable in the mesomorphic smectic state (see Chap. XIX). The increments in spacing, per  $\text{CH}_2$  group added, are on the average either 1.05 or 1.27 A.U. In diamond an addition of a carbon atom to the zigzag chain lying in one plane increases the

<sup>1</sup> *J. Chem. Soc.*, 1929, 234.

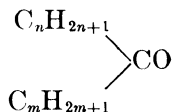
length 1.26 A.U.; hence, for paraffins, ketones, etc., the increment is the same as in diamond, and the molecules may be considered as perpendicular to the layers; for acids, etc., with smaller increments, molecules tilted at about 30 deg. may be the explanation. Weight to this explanation is given by the fact that measurements on single crystals of stearic acid show an angle of 30.3 deg. between the  $c$  axis and the normal to the  $c$  plane in the unit monoclinic prism.

2. *Polymorphism*.—The parallel arrangement of molecules and the tilt may be determined by preparation and working of the samples. Particularly with lower members of the series, depending on whether flakes are pressed on flat surfaces or the substance is melted and solidified in a film, different spacings are obtained. Polymorphism is very common, though previously unsuspected, in many series of compounds.

3. *Molecular Weight*.—The simple x-ray photographs may be used to determine molecular weights by interpolation of the observed spacing on the straight line relating number of carbon atoms to the interplanar spacing. Pure hydrocarbons will give results which fall on the curve while mixtures will not; isomers are clearly differentiated as they fall on different curves. This matter is complicated for normal saturated acids with four curves necessary.

4. *Isomerism*.—The position of ketonic oxygen atoms is accurately determinable in any compound from data on the intensities because of its greater scattering power for x-rays and the resultant effect upon the intensities of various orders.

5. *Structural Formula*.—Alternative possible formulas may be tested; for example the ketones may be



or  $\text{C}_n\text{H}_{2n+1}.\text{COC}_m\text{H}_{2m+1}$ , the length of the first being  $n + 1$  or  $m + 1$ , and of the second  $n + m + 1$  carbon atoms; the second is proved correct.

6. *Film Formation*.—Numerous physical properties are explained; *e.g.*, the comparatively strong black spot of very thin soap films is truly crystalline in the sense that it consists of a double layer of oleic acid molecules, with their carboxyl ends

turned in toward each other. The thickness of a layer of double molecules determined by x-ray diffraction corresponds to the various measurements on the thickness of the black spot and to the length of the molecule adsorbed in surface films.

7. *Chemical Analysis*.—Natural materials such as paraffin wax, glyceryl margarate, hydrogenated soy-bean oil, spermaceti, chinese wax, ceresin, lecithin, etc., all give lines and may be analyzed. Mixtures pressed together give lines for all constituents but, when melted together, may give lines for only one constituent which may actually be present in only a minor quantity.

8. *Lubrication*.—Flakiness, greasiness, and lubricating properties are due to layer formation and ease of movement of one layer over another, particularly if methyl groups on the ends are in contact. Thin stratified layers of lubricant may thus be more effective than thicker unoriented layers.

9. *Chemical Reactions*.—These long-chain compounds are the best for following the course of chemical reactions. Small quantities of the acids melted on metals show superposed spectra of the acid and the soap formed by interaction with the metal base; the latter spectra are intense with lead, tin, and antimony; less intense with iron, copper, and bismuth; faint with nickel, zinc, and molybdenum; and absent with aluminum, palladium, platinum, and gold. The absorption of oxygen at the double bonds of lead oleate, formed by painting a film of oleic acid on lead, may be followed perfectly by the gradual appearance of new spectrum lines and the disappearance of the oleate lines.

10. *Spectroscopy of Soft X-rays*.—The large spacings characteristic of these stratified organic compounds made possible the spectroscopic measurement of long-wave lengths and the bridging of the gap between ultraviolet and x-rays. Ruled gratings are used now more commonly for these researches.

11. *Molecular Orientation at Surfaces and Interfaces*.—Finally, the theory of orientation of molecules at surfaces and interfaces, long well-known as the result of surface energy studies of Hardy, Harkins, Langmuir, N. K. Adam, and others could be subjected to the most rigorous direct experimental test by the methods discovered for the study of these long-chain organic compounds. In general, the x-ray study of the structure of thin films, surface and interfacial layers has fully substantiated the conception of definite molecular orientations such as fatty acid

molecules at the surface of water standing upright with the polar carboxyl group turned into the water. Obviously, monomolecular films cannot serve as diffraction gratings but the results obtained with layers only a few molecules thick fully substantiate the picture. A wide variety of experiments have been conducted to show orientation. The excellent results obtained from very thin films on mercury drops have been noted already. Trillat<sup>1</sup> in a second paper reports a whole series of ingenious investigations on the surface structure of entirely solidified drops of fatty acids, diacids, paraffins, and triglycerides, of films of these substances

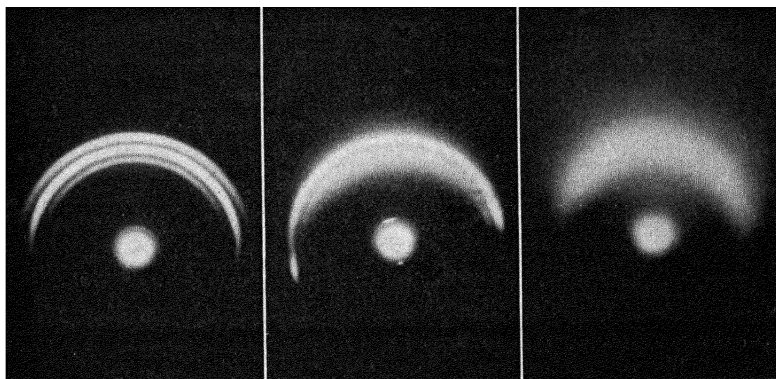


FIG. 149.—Diffraction patterns showing molecular orientation in surfaces. Left, surface of solidified drop; center, surface of molten drop with invisible film cooled by jet of air; right, surface of liquid drop.

obtained by cooling the surface of a liquid drop, the remainder being molten, and of films obtained by cooling in contact with heated water. An x-ray beam defined by a horizontal slit strikes tangentially upon the surface in each case. The appearance on the diffraction photograph of the interferences in several orders corresponding to the molecular lengths at once proves that the chains must be preferentially oriented at interfaces between solid or liquid substance and air, and between water and air. Figure 149 shows a series of patterns for paraffin made in the writer's laboratory by J. N. Mrgudich. Especially interesting is the second one made as follows: the paraffin is melted in a small cup by means of a carefully controlled current through a resistance wire in contact with the cup. A blast of air was directed on the surface so as to form a transparent film on the molten drop. The

<sup>1</sup> *Ann. phys.*, **15**, 455 (1931).

pattern shows a liquid halo and in addition sharp interferences for the oriented film. The orientation theories are thus entirely substantiated. Not only is this true of long organic molecules, but even in surface "skins" of other substances. Surface reflection x-ray photographs have demonstrated conclusively an oriented molecular structure approaching the crystalline condition in the surface of cast-glass cylinders, while a nearly amorphous glass pattern is obtained for the interior. Organization and orientation seem to be inherent tendencies of matter, given the proper conditions of molecular mobility, or assisted by some mechanical unidirectional force such as stretching or drawing into a fiber. The orientation of molecules thus observed is true whether in the solid or liquid state. For example, molten lead oleate on metallic lead backing gives nearly as sharp interferences as a solidified film.



## CHAPTER XVII

### THE INTERPRETATION OF DIFFRACTION PATTERNS IN TERMS OF GRAIN SIZE, ORIENTATION, INTERNAL STRAIN, AND MECHANICAL DEFORMATION

**The Scope of X-ray Diffraction Information.**—In the subject-matter thus far developed in this book in Part II, particular application of fundamental principles has been made to the analysis of crystalline constitution or ultimate structure. It has been shown that such analyses of solids may involve the use of single crystals or of specimens composed of many fine grains usually in random orientation. The various experimental methods employing either single crystals or aggregates have been outlined in Chap. XI. It has also been indicated that numerous other types of information besides ultimate crystalline structure may be obtained from the interpretation of the x-ray diffraction patterns. It is at once apparent that a whole series of specimens may give identically the same known crystal pattern characteristic of body-centered cubic  $\alpha$ -iron, and yet from the standpoint of *practical behavior* these specimens may vary enormously. If, then, x-rays told us only that all the specimens were  $\alpha$ -iron, they would perform a notable service but fall far short of the greatest usefulness. Fortunately, by means of these rays it is possible to make fundamental and subtle distinctions between the specimens, which all have the same unit crystal cell, far beyond the powers of any other testing agency, and thus scientifically to account for actual behavior in service, and to enable rational establishment of manufacturing processes which will assure a desirable combination of properties in terms of a desirable structure. It is this information concerning grain size, internal strain, fabrication, heat treatment, etc., which is the newest contribution of x-ray science and at the same time the most important from the actual industrial point of view. In this chapter consideration will be given to the fundamental interpretation of x-ray patterns in terms of some of these properties, while Chap. XVIII will be devoted largely to

actual examples and achievements of the x-ray method in metallurgical industry.

**Grain Size.** 1. *X-ray Evidence of Grain Size.*—In Figs. 82 and 96 are shown the x-ray diffraction patterns for two extremes of grain size of  $\alpha$ -iron, respectively, a single crystal grain and a random aggregate of very small grains. The former is distinguished by a symmetrical array of Laue spots, the latter by a series of concentric, continuous Debye-Scherrer rings. Both patterns are definitely characteristic of crystalline  $\alpha$ -iron and, in addition, each characterizes a particular condition of grain size. Of course, there may be every possible gradation in grain size between the extremes and also extending to grain sizes in the colloidal range smaller than represented by Fig. 96. In general, it may be stated that specimens with grains larger than  $10^{-3}$  cm. in diameter produce a fairly uniform peppering of diffraction spots which grow larger and fewer in number as the grain size increases or the number of grains in the path of an x-ray beam of constant cross section decreases. In the region of  $10^{-3}$  cm. these spots begin to lie on Debye-Scherrer rings as in Fig. 120 if the  $K\alpha$ -doublet of the radiation is present so as to exceed all other rays in intensity (*i.e.*, approaching monochromatic rays). As the size still further decreases, the spots lying on rings decrease in size and increase in number until individual spots can no longer be distinguished and the diffraction rings appear of continuously uniform intensity and have maximum sharpness. There is a range of particle sizes between  $10^{-3}$  and  $10^{-6}$  cm. as limits which produce these sharp rings and which, therefore, cannot be accurately distinguished. As the grain still further decreases in size below  $10^{-6}$  cm. into the colloidal range, the interference effects become less perfect as the number of parallel reflecting planes falls below a certain value. This manifests itself as a *broadening* of the diffraction rings, so that a measurement of breadth leads directly to an evaluation of grain sizes of colloidal dimensions, as will be illustrated later.

2. *The Measurement of the Size of Submicroscopic (Colloidal) Crystals.*—Since the x-ray method of evaluating particle size was first applied to submicroscopic or colloidal particles from  $10^{-6}$  to  $10^{-8}$  cm., this range will be considered here first.

Debye and Scherrer were the first to derive an equation connecting particle size with an experimental measurement of the

breadth of interferences at points of half-maximum intensities.

$$B_{\text{Scherrer}} = 2\sqrt{\frac{\ln 2}{\pi}} \cdot \frac{\lambda}{D} \cdot \frac{1}{\cos \frac{\chi}{2}} + b$$

where  $B$  is the breadth of a diffraction interference at points of half-maximum intensity,  $\lambda$  is the wave length,  $D$  is the edge length of the crystal considered as a cube,  $\chi$  is the angle of diffraction, and  $b$  is the natural minimum breadth of the Debye-Scherrer diffraction line which is a constant depending upon the particular apparatus and size and absorption of the specimen. Scherrer first determined  $b$  by plotting measured values of  $B$  against

$\frac{1}{\cos \frac{\chi}{2}}$  for a sample of colloidal gold. The straight line drawn

through the points was then extrapolated to cut the ordinate axis which was the value of  $b_0 = b_r$  where  $r$  is the radius of the camera. This equation served for several years though comparatively little work was done on critical experimental test. Selyakov, by a considerably more straightforward proof, derived the equation

$$B_{\text{Selyakov}} = \frac{2\sqrt{3 \ln 2}}{\pi} \cdot \frac{\lambda}{D} \cdot \frac{1}{\cos \frac{\chi}{2}} + b$$

which differs from the Scherrer equation by less than 2 per cent. W. L. Bragg by remarkably simple reasoning and calculation utilizing the conception simply of  $n$  planes of thickness  $d$  arrived at the equation

$$B_{\text{Bragg}} = 0.89 \frac{\lambda}{D} \cdot \frac{1}{\cos \frac{\chi}{2}} + b.$$

Expressed in the same form,

$$B_{\text{Scherrer}} = 0.94 \frac{\lambda}{D} \cdot \frac{1}{\cos \frac{\chi}{2}} + b.$$

In 1926, Laue deduced from vector analysis a new equation which in its most general form is free from the limitations of the cubic system and permits size evaluation in different directions and thus

shape of a particle. In the simplest rigorous form this equation is

$$\eta = \frac{1}{3.6\pi} \left\{ B \cos \frac{\chi}{2} - \frac{1}{B} \left( \pi \frac{r}{R} \right)^2 \cos^3 \frac{\chi}{2} \right\},$$

where  $\eta$  is a pure number,  $B$  is the measured width of the diffraction maximum at points of half-maximum intensity, in *radians*,  $r$  is the radius of the cylindrical specimen,  $R$  is the value of the camera and film, and  $\chi$  is the diffraction angle. The quantity  $\eta$  is related to the size and shape of the particle by the equation

$$\eta = \frac{\lambda}{4\pi} \sqrt{\sum \left( \frac{b_i G}{m_i} \right)^2}, \quad G = \frac{\sum h_i b_i}{|\sum h_i b_i|},$$

where  $b_i$  is the ground vector of the reciprocal lattice,  $h_i$  are the indices of the reflecting planes, and  $m_i$  are numbers which express how many times the elementary cell measurement is repeated in the direction  $i$ . This reduces to  $\eta = \lambda/4\pi m a_i$  for cubic crystals, where  $m a_i$  is the extension (or size  $D$ ) of the crystal particle in the direction  $a_i$ , or the magnitude to be calculated with all the other factors known or experimentally measurable.

A simplified expression used with singular success by Hengstenberg and Mark in determining the actual size and shape of the colloidal micelles of rubber and cellulose is

$$R\eta = 0.088 \left[ b \cos \frac{\chi}{2} - \left( \frac{1}{b} \right) \pi^2 r^2 \cos^3 \frac{\chi}{2} \right],$$

where  $b = BR$  is the direct linear breadth of the interference. The necessary conditions for the Laue equation are for absorption in the crystal powder which is negligibly small, for completely random orientation, for particles of the same form and size, for undistorted lattices, and for known crystal structures. Patterson extended the theory to the case where the particles have different sizes and showed that the sizes must have a Maxwellian distribution, while Mark favored a symmetrical distribution of the Gauss type. Without information concerning the distribution function, the average particle size cannot be determined. Brill extended the theory to the case of substances opaque to x-rays and derived corrections for absorption and for the overlapping of the  $\alpha$ -doublet interferences. The writer has extended these calculations and derived the following general and rigorous

formula for  $ma_1$ , the extension (or size) of the crystal particle in the direction  $a_1$ :

$$ma_1 = \left[ \frac{3.6\lambda \sin^5 \frac{\chi}{2} \tan \frac{\chi}{2RB}}{4d \left( B + \pi r \sin \chi \sin \frac{\chi}{2} \right) \left( B - \pi r \sin \chi \sin \frac{\chi}{2} \right)} \right],$$

where  $B = b - \frac{\delta}{3}$  ( $b$  = measured width of interferences at points of half-maximum intensity,  $\delta$  = separation of the  $\alpha$ -doublet;  $d$  = lattice constant from known crystal structure; and the other symbols have the same significance as noted before.

The latest and most ingenious advance in particle-size measurement has been made by Brill and Pelzer. The previous methods have all been subject to uncertainties concerning the relation between blackening of the photographic film and the intensity of incident x-rays, and the determination of positions of half-maximum intensity of diffraction interferences by means of the photometer. If the specimen under examination is in the form of a hollow cylinder (and thus is transparent to x-rays and obeys the Laue equations), then over a certain range of particle size each interference will be split into two maxima, the separation of which is a measure of particle size. Instead of measuring breadth at points of half-maximum intensity, the much more direct measurement of the distance between two lines is involved. For such a case the particle size (for the cubic system) must have a value

$$D > \frac{R\lambda\sqrt{2 \cdot 1.8}}{4\eta r \cos^2 \frac{\chi}{2}}.$$

For both large particles yielding sharp interferences, and for very small particles for which these two maxima become broad and overlap, single lines are observed. The simpler equations derived for the particle size involved in the split lines are as follows:

$$\begin{aligned} \text{(Small)} \quad \eta &= \frac{\cos \frac{\chi}{2}}{1.8 \cdot \sqrt{2}} \sqrt{\left( \frac{r}{R} \cos \frac{\chi}{2} \right)^2 - \frac{7}{80} \left( \frac{e}{R} \right)^2}, \\ \text{(Large)} \quad \eta &= \frac{1}{1.8} \frac{1}{2} \sqrt{3} \frac{r}{R} \left[ \cos^2 \frac{\chi}{2} - \left( \frac{e}{4r} \right) \right], \end{aligned}$$

where  $e$  is the linear separation of the two maxima.

The equation for the case of very small particles for which the pairs of lines fuse is

$$\eta = \frac{1}{1.8} \cos \frac{\chi}{2} \sqrt{\left(\frac{B'}{2\pi}\right)^2 - \left(\frac{r}{R} \cos \frac{\chi}{2}\right)^2},$$

where  $B' = \frac{2B}{\cos \frac{\chi}{2}}$  and  $B$  is the breadth of half-maximum

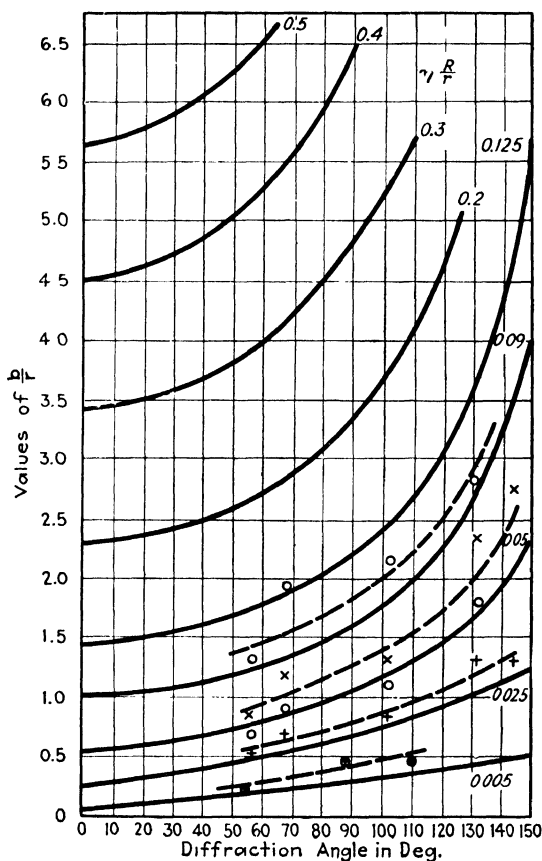


FIG. 150.—Graphical method of determining grain size in the colloidal range. (Brill.)

intensity. Rigorous comparative tests have been made for the new equations derived for hollow cylindrical specimens, with complete agreement for magnesium oxide (Brill and Pelzer) and

even for preparations of colloidal gold, silver, and carbon (Clark and Zimmer).

Brill has performed a useful service in presenting a graphical method for the determination of particle size. The standard curves (shown in Fig. 150) derived from the foregoing formulas show the values of  $\eta \frac{R}{r}$  as they depend

upon  $\frac{b}{r}$  and  $\chi$ . The values  $b$ ,

the interference width,  $r$ , the specimen radius, and  $\chi$ , the diffraction angle, are all determined and the point on the chart for  $\frac{b}{r}$  against  $\chi$  is located.

The value of  $\eta \frac{R}{r}$  corre-

sponding is found by interpolation between the curves of definite value, from which  $\eta$  and then the particle size and shape are calculated.

3. *Examples of X-ray Determination of Submicroscopic Grain Size.*—Some examples of diffraction photographs of colloidal

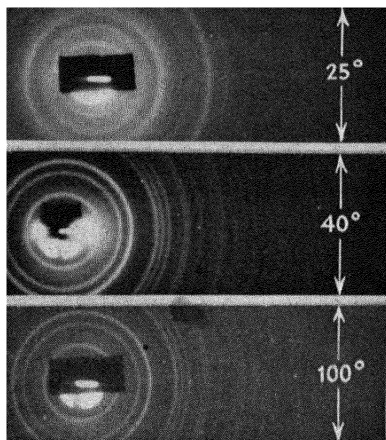


FIG. 151.—Diffraction patterns for cadmium hydroxide, showing smaller particle size (broader lines) the lower the temperature of precipitation.

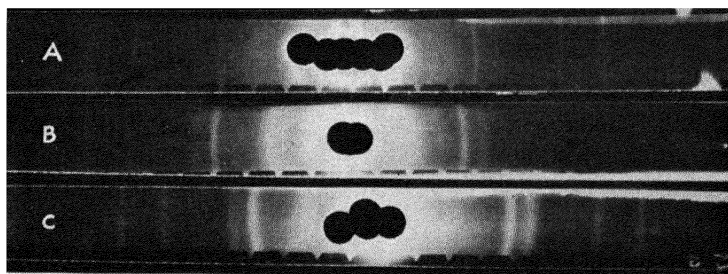


FIG. 152.—Patterns for colloidal metals. A, Silver, particle size  $21 \times 10^{-7}$  cm.; B, gold, particle size  $13 \times 10^{-7}$  cm.; C, gold, particle size  $2.1 \times 10^{-7}$  cm.

materials are shown in Figs. 151, 152, and 153. In Fig. 151 patterns for cadmium hydroxide precipitated at 25°, 40°, and 100° show clearly that the lower the temperature, the smaller the

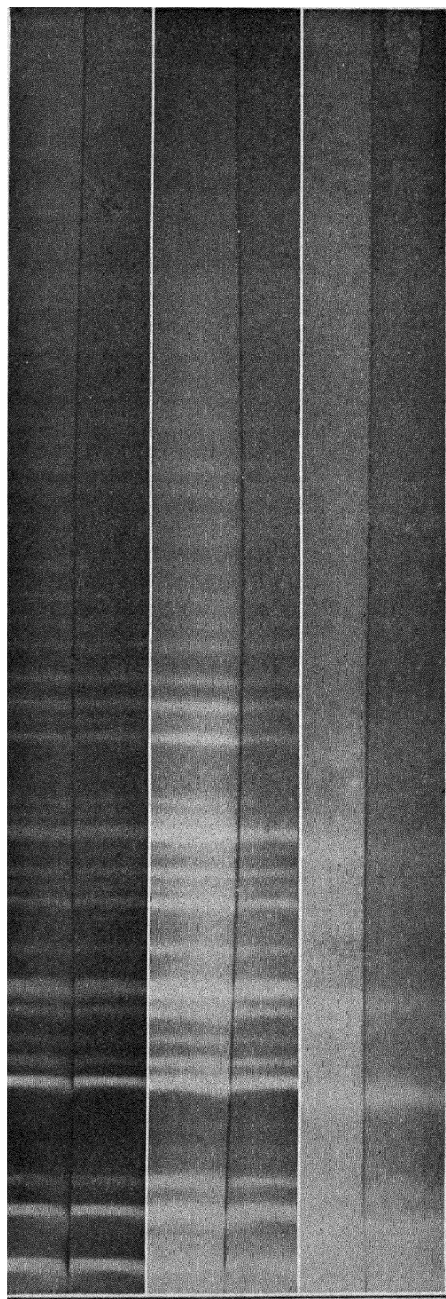


FIG. 153.—Diffraction spectra of three samples of  $\text{SnO}_2$ , showing how particle size affects line width.



particle size and the broader the interferences. In Fig. 152 are presented standard patterns for colloidal gold and silver with the following grain sizes: *A*, silver sol.  $21 \times 10^{-7}$  cm; *B*, gold sol.  $13 \times 10^{-7}$  cm; *C*, gold sol.  $2.1 \times 10^{-7}$  cm. Figure 153 gives a comparison of grain size of three commercial varieties of tin dioxide used as opacifying agent in enamels.

Brill has compared the Scherrer and Laue equations for several samples of iron as follows:

Sample	Scherrer	Laue
Fe from $\text{Fe}_3\text{O}_4$ . . . . .	$2.3 \times 10^{-6}$	$2 \times 10^{-6}$
Heated 10 hr. at $1000^\circ$ . . . . .	$4.2 \times 10^{-6}$	$\infty$
Fe from carbonyl I ( $300^\circ$ ) . . . . .	$7.7 \times 10^{-7}$	$1 \times 10^{-6}$
II . . . . .	$6 \times 10^{-7}$	$9 \times 10^{-7}$
III . . . . .	$1.0 \times 10^{-6}$	$1.1 \times 10^{-6}$
IV . . . . .	$1.2 \times 10^{-6}$	$1.0 \times 10^{-6}$
( $1000^\circ$ ) . . . . .	$3 \times 10^{-6}$	$\infty$
Electrolytic iron	$2.3 \times 10^{-6}$	$2.3 \times 10^{-6}$

There is thus general agreement except for large sizes where the Scherrer equation fails. It is adapted only for small particles in the range and for heavily absorbing substances. Brill has employed lead glass tubes for substances of small absorbing power in order to meet the condition of nearly complete absorption, the diffraction taking place only superficially.

The particle size of martensite has been determined several times, Westgren finding  $10^{-7}$ , Wever  $10^{-6}$ , and Selkjakov  $2 \times 10^{-6}$  cm. Clark and Brugmann in studying the structure of case-hardened steel, which is martensite and troostite very largely, estimated a particle size of  $10^{-7}$ .

One of the most important and interesting applications is that of particle size of metal catalysts. Clark, Asbury, and Wick<sup>1</sup> were the first to make a study of particle size as related to the activity of finely divided catalysts. They measured photometrically the line breadths of diffraction spectra from a number of nickel catalysts with identical crystal lattice type and dimensions, prepared in various ways and differing widely in catalytic activity in hydrogenation and dehydrogenation processes. Most of these catalysts consisted of particles larger than  $10^{-6}$  cm. so that the Scherrer equation did not apply.

<sup>1</sup> *J. Am. Chem. Soc.*, **47**, 2661 (1925).

In general, increase in activity and decrease in particle size did not run parallel as might be expected. There is a more definite relationship for platinized-asbestos catalysts used in the contact sulfuric acid process. Levi<sup>1</sup> has made several measurements of particle size of the platinum family of metals from the photometered x-ray diffraction spectra, with the result that granules of platinum were twelve to twenty-nine times as large on the side as the unit crystal cell; palladium thirteen to twenty-nine, rhodium six, iridium four, ruthenium seven to eight, osmium six (latter two hexagonal).

Some of the most interesting particle-size measurements have been made on such non-metallic substances as carbon-black, pigments, colloidal suspensions, rubber, cellulose, etc. The question is raised as to where the discontinuity between crystalline and amorphous appears, and whether there is any evidence of amorphous metal at grain boundaries, etc. It is reasonable to suppose that diffraction lines may become so broad that they will coalesce and produce the effect of general fogging of the film just as an amorphous material would be expected to do. From the evidence of carbon black an amorphous state may show transition to crystalline as judged by changes in physical or chemical properties, while the x-ray pattern is unchanged at first, simply because the crystalline planes are still too few and too distorted to enable sharp interference. It must be realized that temperature oscillations of atoms in a lattice and also distortion both have the effect upon diffraction lines of broadening them just as small grain size. These factors must be known, therefore, before adequate interpretation is possible. There is no positive x-ray proof of the amorphous cement theory of metal aggregates in spite of numerous attempts. Nor can it be said that the theory has been disproved though it seems unlikely. It has been possible to show that many glasses, always considered "amorphous," do consist of extremely small crystals. For example, vitreous silica consists of cristobalite crystallites of size about  $1.5 \text{ to } 2.0 \times 10^{-7} \text{ cm.}$ <sup>2</sup>

4. *The Shape of Colloidal Particles.*—An important extension of this method is in the determination of the shape of colloidal

<sup>1</sup> *Atti accad. Lincei* (6), **3**, 91 (1926).

<sup>2</sup> RANDALL, ROOKSBY, and COOPER, *Trans. Soc. Glass. Tech.*, **14**, 219 (1930).

CLARK and AMBERG, *ibid.*, **13**, 290 (1929).

particles. If all points for all interferences lie smoothly on the same  $\eta \frac{R}{r}$  curve, then a regular shape, *e.g.*, cubic, is immediately indicated. In studies of colloidal nickel prepared electrolytically in the presence of varying sulfur contents Brill found that the  $b/r$  values for the (200) plane interferences were all too high. The cause of the discrepancy could be determined by assuming various particle shapes and comparing the breadths for (200) interferences with the standard constant (111) interference breadths in the equation for the cubic system

$$\eta = \frac{\lambda}{4\pi a} \sqrt{\frac{(h_1/m_1)^2 + (h_2/m_2)^2 + (h_3/m_3)^2}{h_1^2 + h_2^2 + h_3^2}},$$

where  $h_1, h_2, h_3$  are the usual  $hkl$  indices. Perfect agreement is obtained when calculations are made for a particle built on the octahedral planes and greatly elongated perpendicular to these planes. For the nickel with 5.8 per cent sulfur the following results are obtained by assigning the values  $m_1 = m_2 = 9$  and  $m_3 = 27$ , or the edge lengths actually 45 and 165 A.U.:

Indices	Half value breadth found	Calculated
111	0 66	0 64
200	0 96	0 92
220	1 07	1 10

For the preparation with smallest particle size only the (111) interference appears, simply because only these planes are present in sufficient number in the tenuous elongated particle to produce visible diffraction effects.

The relative variations in intensities and in breadths of interferences for the interferences appearing on a pattern of carbon black, as a series of specimens from different sources is compared, is a means of evaluating the carbon black not only in terms of average particle size but also in shape. In the experience of the author with scores of carbon-black samples, some appear to have nearly cubical or spherical shape and others to have extremely tenuous almost unidimensional shape. The properties of these blacks when incorporated in rubber, for example, are greatly different, the shape of the primary particle being even more important than minimum size.

5. *Particle Size Measurement in the Microscopic Range.*—A method of evaluating grain size to supplement and check microscopic measurement of grains of the order of  $10^{-3}$  to

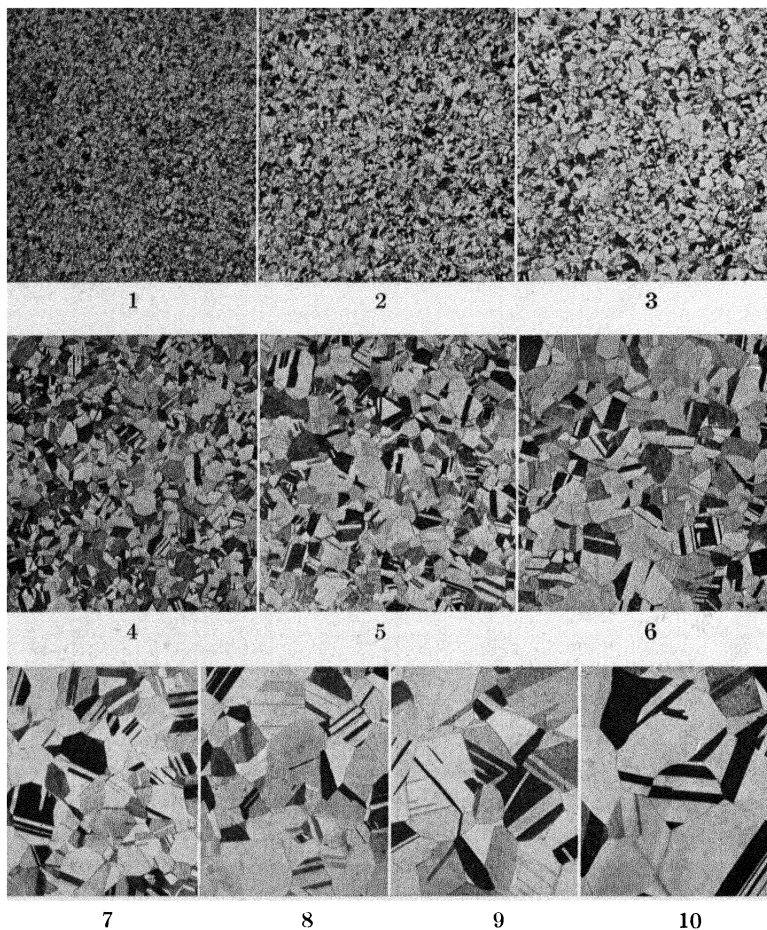


FIG. 154a.—Grain-size standards (A.S.T.M.) for the estimation of the diameter of average grain of annealed materials, particularly non-ferrous alloys such as brass, bronze, and nickel-silver.  $\times 75$ . Average grain diameter as follows:

1 0 010 mm.	6 0 065 mm.
2 0 015 mm.	7 0 090 mm.
3 0 025 mm.	8 0 120 mm.
4 0 035 mm.	9 0 150 mm.
5 0 045 mm.	10 0 200 mm.

$10^{-2}$  cm. in diameter has long been needed, particularly if some information can be obtained about grains below the surface of a polished specimen. X-ray patterns are now filling this require-

ment. It has been demonstrated already that with grain sizes of  $10^{-3}$  cm. or larger, the diffraction interferences are no longer uniform and continuous circles or lines. These interferences show individual spots and as the size increases the Debye-Scherrer

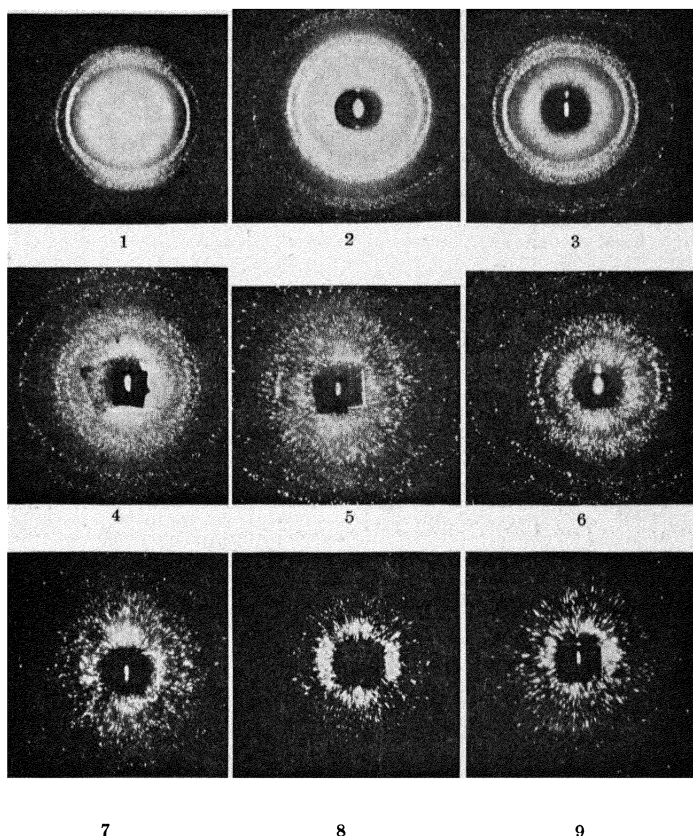


Fig. 154b.—Standard x-ray diffraction patterns for increasing grain size in the microscopic range (compare Fig. 154a).

1 0 009 mm.	4 0 033 mm	7. 0 065 mm.
2 0 012 mm.	5 0 037 mm	8. 0 085 mm.
3. 0 020 mm.	6 0 045 mm.	9. 0.095 mm.

rings disappear and a uniform “peppering appears.” The size of the spots depends upon the divergence of the primary x-ray beam, the size and shape of the focal spot on the target of the x-ray tube, and the extent of the crystal in the plane of the reflecting face. Consequently, the size of the interference

spot on the photographic film from a grain increases with increasing grain size as long as the cross section of the crystal perpendicular to the ray to be reflected is smaller than the cross section of the impinging bundle of rays. Mark and Boss have shown a linear relationship between the size of interference spots for particles between  $10$  and  $100\mu$  ( $10^{-3}$  to  $10^{-2}$  cm.) and the grain size measured microscopically. The slope of the straight lines depends upon the experimental conditions and apparatus but,

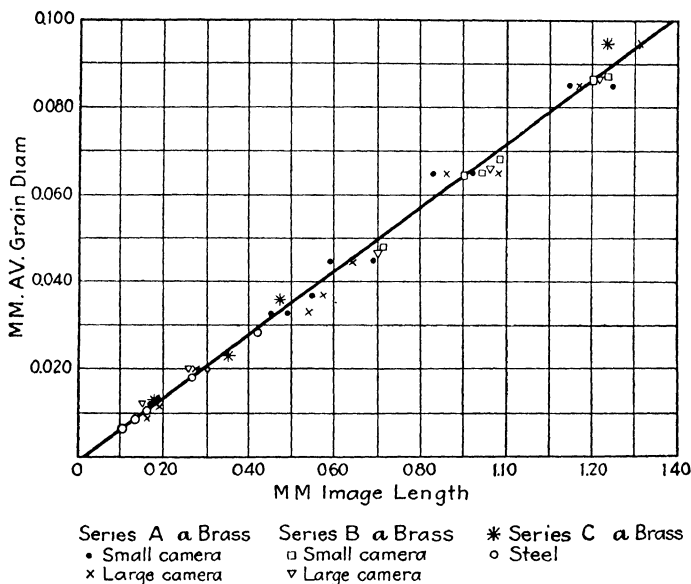


FIG. 155.—Graphical correlation between image lengths of x-ray diffraction interferences and average grain diameters in microscopic range. (Clark and Zimmer.)

once known, grain sizes may be directly read off for any specimen from a measurement of the interference spots.

Clark and Zimmer have greatly extended these results, using the brass samples from which standard A.S.T.M. grain-size photomicrographs were prepared (Fig. 154a). The corresponding standard x-ray patterns photographed in most carefully constructed cylindrical cameras are shown in Fig. 154b. When the microscopic measurements are plotted against the lengths of the x-ray diffraction images, the straight-line plot of Fig. 155 is obtained. The results with two other series of brass samples, steel, carborundum, silica, etc., all lie on this same curve, so

that it undoubtedly represents a universal relationship. It is essential, however, that the annealed metal sample shall not show residual preferred orientation or fibering. It is essential that the grains should have uniform size, since otherwise the x-ray measurement will give the average only of the largest particles, the small particles producing no individual sharp interferences. The effect of size distribution is very clearly demonstrated in Fig. 156. Two specimens of silica with the same average particle size as prepared and measured by Drinker and Hatch at the

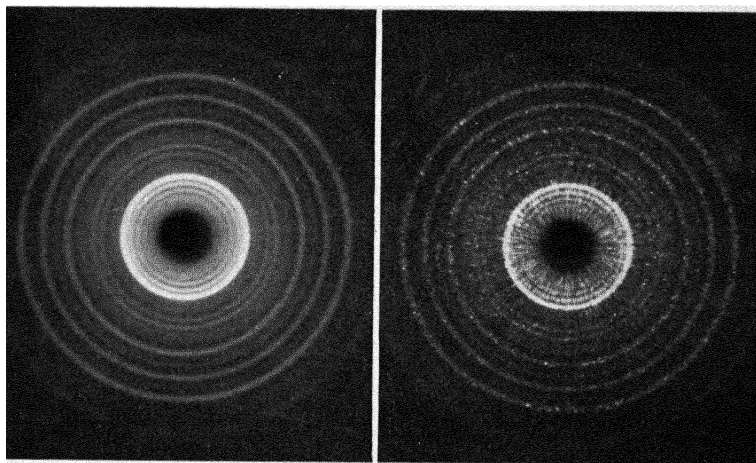


FIG. 156.—Diffraction patterns for two samples of silica with the same average particle size but differing widely in the distribution of sizes. Left, average size  $4.4\mu$ , distribution (standard deviation) 1.341; right,  $4.5\mu$  and 2.166, respectively.

Harvard School of Public Health were subjected to x-ray analysis by Aborn and Davidson. The difference is remarkable. In *a* the deviation from the average was very small, while in *b* it was large. Without a knowledge of the fact that the average particle sizes were the same, and of the distribution, the mistake would be made of assigning a considerably larger particle size to *b* in which the large grains producing individual interferences are balanced by grains too small to produce distinguishable spots. Microphotometric curves are reproduced in Fig. 157 for grain sizes of  $4.4\mu$ , standard deviation 1.34 (Fig. 154*a*); and  $36\mu$ , standard deviation 1.28. These were made by turning the film around an axis so that one of the diffraction circles was continuously registered. It is obvious that there are no equations comparable to those for colloidal particles for calculating particle size of large grains from

a measured quantity such as diffraction interference breadth. Hence the microphotometric curves were measured, including number of peaks per unit length, average height of peaks, area per peak, and the total area under peaks per unit length. When for specimens with nearly the same size distribution the last-named quantities are plotted on log paper against average particle size, the points lie on a straight line. For specimens with widely different distribution but the same average size, the points do not lie on this line. This work on silica is of great

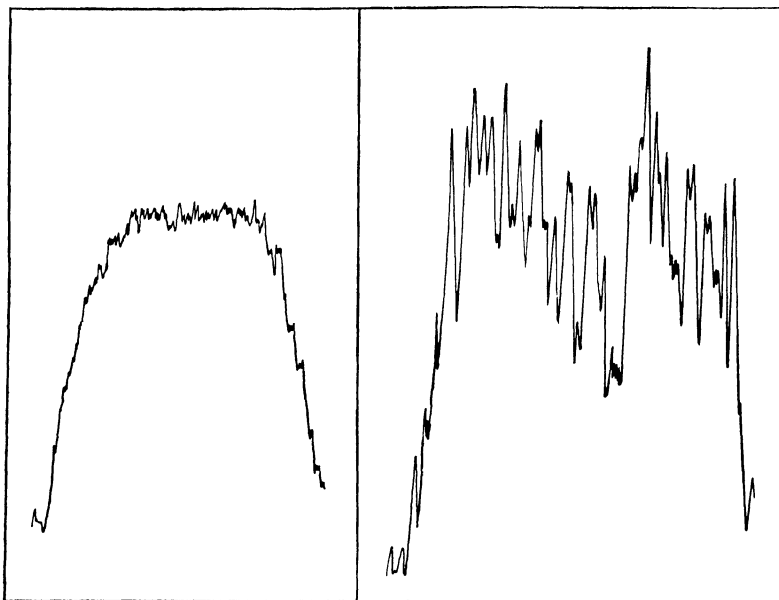


FIG. 157.—Microphotometer curves for diffraction rings of silica samples. *Left*, average size  $4.4\mu$ ; *right*, average size  $36.0\mu$ .

importance in laying the foundation for further work on metal grain sizes. It is evident that considerable care and skill are required in accurately deducing grain size for the region in question.

6. *Examples of Measurement of Size of Microscopic Particles.*—It is needless to point out the very great importance of grain size in terms of practical behavior of commercial materials. Practically all annealing operations following mechanical work involve grain growth. Magnetic permeability and hysteresis loss in electric steels are certainly dependent upon grain size.



The life of electrical contact points is a function of optimum grain size. Even the enameling of steel, corrosion, electrodeposition, and numerous other phenomena depend upon grain size. Many of these will be illustrated in the next chapter, devoted to heat treatment and to practical applications of x-ray methods to commercial metals. The control of grain size in metallurgical products is one of the great achievements of the science. Another typical application has been research on the re-use of plaster of paris molds. These deteriorate very rapidly on re-use, the tensile strength becoming much less on each successive recalcination. X-ray photographs show that the gypsum particles grow larger as strength decreases. The addition of  $\frac{1}{4}$  per cent  $\text{Al}_2\text{O}_3$  increases strength by decreasing grain size.

**Orientation of Grains.**—Many research and practical problems arise in which a knowledge of orientation of crystal planes in a single metal crystal or of single grains in an aggregate are highly desirable. It has been demonstrated previously that the x-ray goniometer is a powerful method of ascertaining orientation. One especially excellent instrument has been devised by Weissenberg for such problems. Single metal crystals are made frequently by cooling a melt in a quartz tube by extremely slow and careful cooling, as first devised by Professor Bridgman. Obviously, no planar faces are developed and recourse must be taken to goniometric establishment of orientation of planes with respect to one direction or another before physical data may be properly interpreted. There are frequent references in the literature to x-ray goniometry of this kind, especially with respect to the presence or absence of twinning. Again, a strip or sheet of metal may be polycrystalline and yet have certain properties dependent upon just how the individual grains (of course, large) are oriented with respect to the surface. This is especially true of electric or magnetic properties, which may differ widely for two specimens, say of silicon steel, with the same apparent grain size and general structure. In this case the Laue method of crystal analysis may be employed. A great service has been performed by M. Majima and S. Togino in making Laue photographs for body-centered and face-centered cubic metals in every possible and known orientation with respect to the x-ray beams. It is necessary, therefore, only to compare a Laue pattern for a grain in a sheet, to the surface of which the x-ray beam is perpendicular, with the standard patterns in order to establish easily the orienta-

tion of the lattice planes of the grain in question with respect to the surface.

Sir William Bragg has indicated another field in which knowledge of orientation is of practical importance. Depending on how jewel bearings for watch movements are cut from original sapphires are the wearing properties. Figure 158 shows Laue patterns for two such bearings with different crystallographic orientations and different resistance to wear.

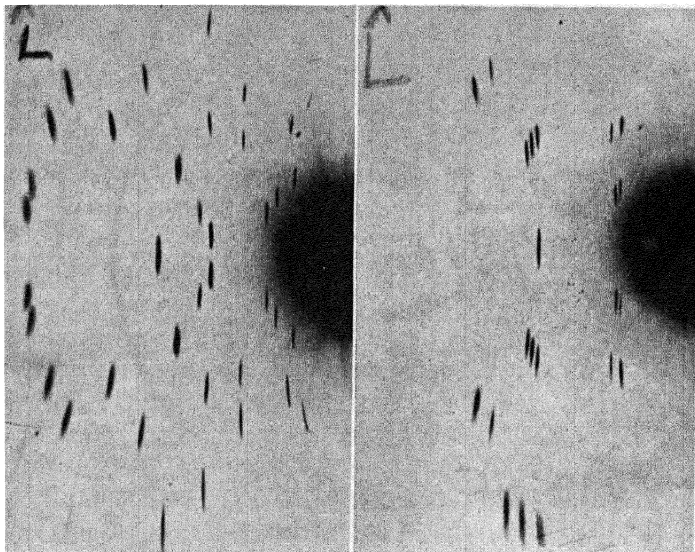


FIG. 158.—Patterns for artificial sapphires used in jewel pivots of watch movements with same structure but different orientations and different wearing properties. (*Sir William Bragg.*)

**Internal Strain.**—Many metal structures fail because of gross defects which may be detected readily by radiographic examination (Part I). But many metal objects may appear radiographically perfectly sound and still fail. The cause here is far more deep-seated and is concerned with residual internal strain or lattice plane distortion. Strain in transparent objects is readily ascertained by interference colors when examined in polarized light. In this manner glass apparatus is tested. Dirigible models of transparent celluloid have been studied under all conditions of stress. The writer has even detected strain in linseed oil and patent leather films in this way. But for opaque

objects such as metals the method is precluded. The use of gage marks for detecting strain in metals is well-known. For example, the diameter of a cylinder of metal is very carefully measured. Successive layers from the inside of the cylinder are then removed on a lathe and the changes in the outside diameter with the relief of strain observed. There are many modifications of this technique which have been widely employed but there are serious objections and limitations. In the first place, the dimensional changes may be too small to measure accurately. Again, the direction of the strain may be such as to be missed entirely

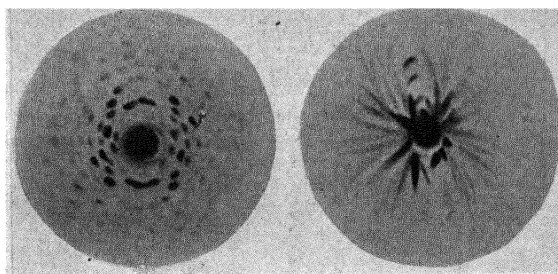


FIG. 159.—Laue patterns of a normal and of a bent crystal of gypsum, illustrating asterism. (Czochralski.)

by the gage-mark method. In all of metallurgy there has been no problem which has so urgently required an adequate method. To the detection and even quantitative estimation of internal strain x-ray diffraction science has made a great contribution, although the application still requires much fundamental research and standardization.

Figure 159 shows what happens to the Laue diffraction pattern of a single crystal (gypsum) when it is bent. The spots are elongated to radial streaks or "asterism striations." Any pattern, even for a polycrystalline material which shows these radial streaks, is an indication of internal strain. The crystal planes are distorted so that reflection takes place as though cylindrical mirrors had replaced plane mirrors. Figure 160 shows how a strain pattern can be synthesized by loading successively a strip of iron while the exposure is made. Even under the elastic limit there is clear evidence of strain; at higher loads slipping on planes occurs and rupture accompanied by fibering of the metal in many cases. Figure 161 shows the strained condition of a block of cast

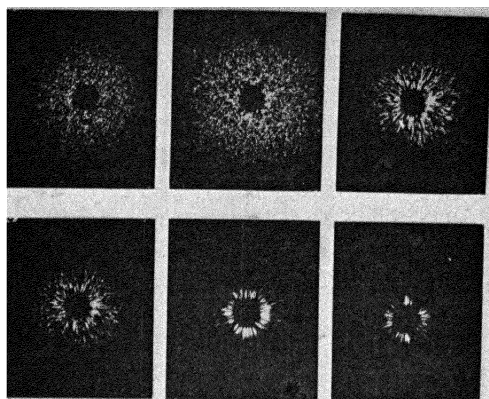


FIG. 160.—Effects upon the pattern of successive loadings of specimen of silicon steel, illustrating asterism striations as evidence of internal strain.

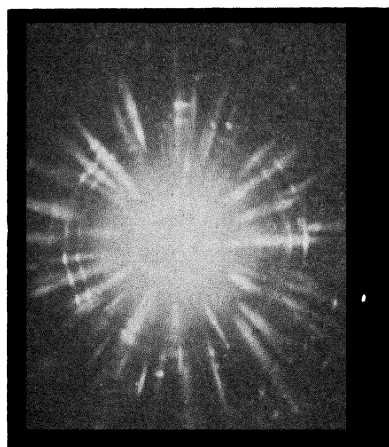


FIG. 161.—Pattern for chilled cast steel showing internal strain.

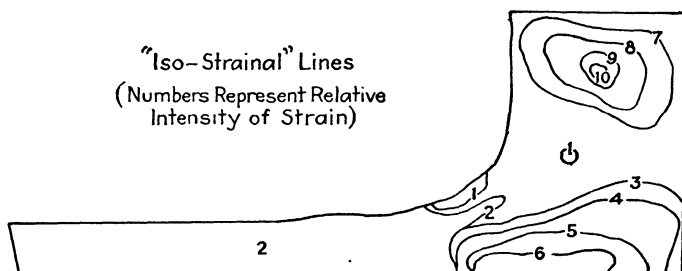


FIG. 162.—Distribution of internal strains in cross section of large steel casting, determined solely from x-ray diffraction patterns.

steel which has been rapidly chilled. The distribution of strains of a large casting determined solely by x-ray patterns is shown in Fig. 162. The world-wide interest in this figure, since its original publication several years ago, is an interesting sidelight upon the

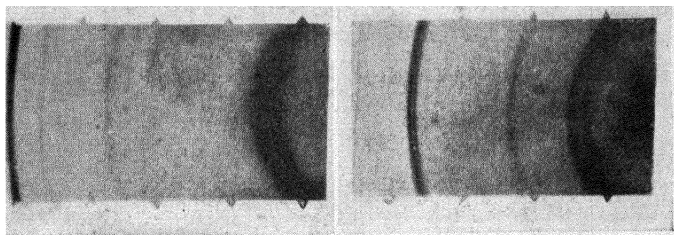


FIG. 163.—Effect of strain in broadening diffraction interferences. Left, strained; right, unstrained.

value of this method in affording information heretofore impossible.

Internal strain also manifests itself by a broadening of the diffraction lines for powder patterns (see Fig. 163). In other

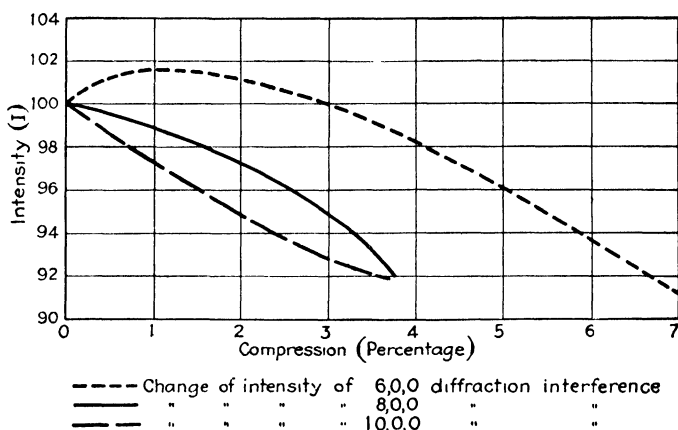


FIG. 164.—Changes in intensity of high-order reflections with deforming force. (Hengstenberg.)

words, interference is less sharp for distorted or bent planes just as is true for a very few planes (colloidal particles). This same phenomenon occurs also at higher temperatures where the thermal vibrations of the atoms cause a departure from planes.

Finally, the newest and most nearly quantitative method of measuring internal strain is concerned with the diminution in intensity of lines particularly at large angles (high orders). Hengstenberg<sup>1</sup> has made an investigation of KCl crystals, with the interesting results shown in Fig. 164 for intensity changes for 6,0,0, 8,0,0, and 10,0,0 reflections. Such relationships have been observed qualitatively also for cold-worked and annealed metals, the ratio  $I_{200}/I_{400}$ , for example, being much greater for the cold-worked specimens.

The exact mechanism involved in strain is still not well understood. It is to be distinguished clearly from the effect of a uniform deforming force which produces slipping on lattice planes. Hengstenberg has calculated for the condition of strain that, for a certain degree of deformation of 4 per cent change in length of an edge parallel to the direction of compression, 3 per cent of the atoms are displaced from their normal positions to a maximum of one-eighth the distance between atoms. Strain must represent a condition of localized failure on the glide planes. In contrast to this irregularly distributed strain, plastic deforming forces on the surfaces of whole glide blocks do not change the lattice constants. The high-order lines remain perfectly sharp, so that the  $K\alpha$ -doublet is perfectly resolved. Consequently, whole blocks of the crystal at least 600 A.U. in dimensions must slip relative to each other, since deviations of the lattice constant of only 0.5 per cent or the formation of glide blocks smaller than 600 A.U. would cause inevitably an increase in breadth of the diffraction lines.

Brill and others have demonstrated also that the intensity of scattered radiation is markedly greater for strained specimens. It is the function of heat treatment, of course, to eliminate such a condition. Strain is usually accompanied by an increase in tensile strength for reasons which are not clear. Strain as it precedes fatigue and failure will be illustrated together with other important examples in Chap. XVIII for metals. The same considerations apply to ceramic materials, glass, bakelite, and similar materials.

Lattice distortion can be produced not only by mechanical deformation but also by the introduction of foreign atoms which form solid solutions. These effects may be expressed quantitatively by the intensity changes as has been done by Hengsten-

<sup>1</sup> "Fortschritte der Röntgenforschung," p. 139, 1931.

berg. The intensity of a mixed crystal reflection according to Laue is  $\Psi^2 \sim (p_1\Psi_1 + p_2\Psi_2)^2$  (pure crystal  $\Psi^2 \sim \Psi_1^2$ ) where  $p$  is the atomic per cent of each component and  $\Psi$  is the scattering power of the atoms which is proportional to the atomic number at reflection angle 0. This expression has been experimentally verified for silver-gold alloys. The fact that all the diffraction interferences varied in intensity in the same way as compared with pure silver proved conclusively that the gold atoms with about the same size as silver atoms had negligible distorting effect in the silver lattice. An opposite effect is characteristic of mixed crystals with lattice distortion, such as duralumin. The intensity data are as follows:

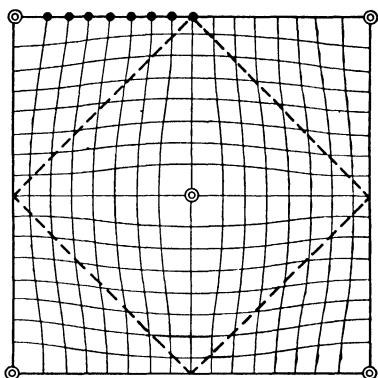
Quenched:  $(p_1\Psi_1 + p_2\Psi_2)^2 = (0.02 \times 29 + 0.98 \times 13)^2 = 177.7$   
(copper 2 atomic per cent)

Tempered:  $(p_1\Psi_1)^2 = (0.949 \times 13)^2 = 161.0$   
( $\text{CuAl}_2$  separated)

The 111 and 200 reflections for the quenched duralumin are actually more intense in the above proportion but with increasing diffraction angle the ratio diminishes and for (420) reflections the intensity is 10 per cent smaller. The explanation is to be found in lattice distortion, as exemplified in Fig. 165, caused by the presence of copper atoms in the aluminum lattice.<sup>1</sup>

## THE X-RAY ANALYSIS OF FIBER DIAGRAMS AS RELATED TO THE FABRICATION OF METALS AND ALLOYS

**1. Fiber Diagrams.**—It is now a familiar fact that metal powders or random aggregates yield pinhole diffraction patterns on flat photographic films consisting of concentric uniformly intense rings. Whenever a piece of drawn wire or thin rolled foil is used as a specimen, perpendicular to the primary beam, the diffraction rings are very intense in localized intensity maxima



● Atoms of dissolving substance  
⊙ Atoms of dissolved substance  
FIG. 165.—Distortion of lattice by introduction of foreign atoms.

<sup>1</sup> The copper atoms are smaller than aluminum; hence Fig. 165 actually represents an opposite case.

as though more crystal grains are contributing reflection effects in certain directions, while in other positions few, if any, crystal grains are available for reflection, and there is little or no blackening on the film. Thus the rings observed for random arrangement of grains become series of symmetrical segments in the case of directed or preferred orientation. This type of pattern for worked metals, generally designated fiber diagrams, has been illustrated in Fig. 121, for aluminum wire, and Fig. 166 for aluminum sheet.

Drawn wires and rolled sheets represent different types of preferred orientation. In wires the same pattern is obtained

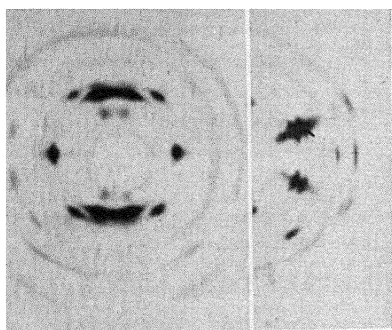


FIG. 166.—Diffraction pattern for cold-rolled aluminum foil showing fibering or preferred orientation. Left, x-ray beam perpendicular to rolling direction; right, beam parallel to rolling direction.

with any orientation as long as the x-ray beam passes perpendicular to the wire axis, while in rolled sheets differently appearing fiber patterns are obtained with the beam perpendicular or parallel to the rolling plane.

These are fiber structures in the same sense that cellulose, stretched rubber, and asbestos are fibers. None of these materials is a single crystal; all are built up of many crystal grains,

but these are arranged so that a definite crystallographic axis is parallel to the axis of the fiber. In an aluminum wire which has not been annealed after drawing, the x-ray pattern demonstrates that the body diagonals, or  $[111]$  direction, in all the grains, each of which is a single crystal built up from unit face-centered cubes, lie parallel to the wire axis. Evidently, therefore, this common orientation has been induced in the process of mechanical working; the particular position is evidently that which will present maximum resistance to further deformation. It will be noted that no other limitation has been put on preferred orientation in an aluminum wire, for example, than that the  $[111]$  direction is parallel to the wire axis, or direction of drawing. Hence any grain may be turned anywhere through  $360^\circ$  around a body diagonal as an axis and still fulfill conditions, and thus the outer form of grains in the wire may appear perfectly irregular with any



kind of a face in the surface. Herein lies the difference in the orientation of grains in a rolled sheet or foil, for in this case a definite crystallographic direction lies parallel to the direction of rolling *and, also*, a definite crystallographic plane in all the crystal grains lies parallel to the plane of rolling. For example, in strongly rolled iron or steel a *face* diagonal [110] direction lies parallel to the direction of rolling, and a cube face parallel to the plane of rolling. On account of this added limitation in rolled structure which does not apply in drawn wires or complete fiber structure, this is called limited fiber structure.

In the foregoing discussion ideal cases of exact arrangements have been implied. In practice these cases are never realized, since the orientations are never perfect, though the greater the deforming force, the more nearly do the grain positions approach the ideal. As will become apparent, it is possible to determine from the x-ray patterns the departures from limiting ideal orientations.

As previously explained, the Laue or monochromatic pin-hole method is almost exclusively used in the study of worked metals, since it affords a pattern 360 deg. in azimuth. It is necessary only to mount a wire or sheet specimen over the outer pinhole so that the beam will pass perpendicular to the wire axis or rolling direction. The pattern is registered on a flat photographic film.

**2. The Interpretation of Complete Fiber Patterns (Drawn Wires).**—Of first concern is the pattern of the Debye-Scherrer rings which defines the particular metal. All the lattice planes with the same lattice spacing  $d$  reflect rays on the same diffraction ring, which is continuous in the case of random orientation or segmented into spots or arcs for fibered materials. It is useful

Body-centered cubic		Face-centered cubic	
Indices	$a_0/d_{hkl} = \sqrt{h^2 + k^2 + l^2}$	Indices	$a_0/d_{hkl} = \sqrt{h^2 + k^2 + l^2}$
(110)	1 41	(111)	1 23
(200)	2 00	(200)	2 00
(112)	2 45	(220)	2 83
(220)	2 83	(113)	3 32
(130)	3 16	(222)	3 46
(222)	3 46	(400)	4 00

to list for the body-centered and face-centered cubic lattices the planar indices corresponding to the rings which appear, passing from the innermost outward.

In this fashion it is possible to determine the planar indices for each ring.

Next to be found are the positions of the intensity maxima upon the rings. One of the sets of parallel reflecting planes may be imagined rotated 360 deg. around an axis perpendicular to the primary x-ray beam. In the course of this rotation it will pass four times through the proper angle for reflection in accordance with Bragg's law and produce upon a photographic plate placed behind the specimen a four-point pattern

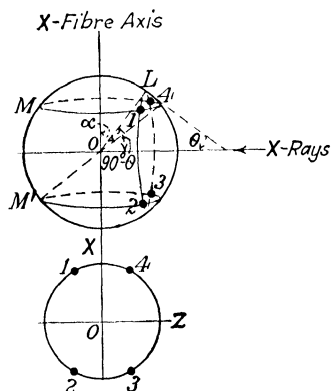


FIG. 167. - Analysis of the ideal four-point fiber diagram, with x-ray beam perpendicular to the fiber axis.

which is symmetrical with respect to a vertical line on the plate parallel to the rotation or fiber axis, and also with respect to a horizontal line. In other words, these maxima are, for example, at the clock hour-hand positions of 1:30, 4:30, 7:30, and 10:30 (see Fig. 167). If this particular reflecting plane in a special case is parallel to the axis of rotation (or fiber axis), then only two spots are produced on the ring on the horizontal line (three and nine o'clock). No reflection occurs, of course, if this plane is exactly perpendicular to the rotation axis. Two spots occur on the vertical line (twelve and six o'clock) if the angle of the reflecting plane with respect to the rotation (fiber) axis is equal to the angle of incidence of the x-ray beam. It is at once clear, therefore, that the positions of intensity maxima on a given ring on the photographic plate may be measured and used directly to deduce the positions of lattice planes in the wire in a very simple manner. If  $\alpha$  is the angle between the normal to the set of reflecting planes and the rotation (fiber) axis, and  $\delta$  is the angle measured on the film between a radius drawn through a particular intensity maximum and the vertical line (which is known to be parallel to the rotation or fiber axis), then

$$\cos \delta = \frac{\cos \alpha}{\cos \Theta},$$

where  $\Theta$  is the angle of incidence. At small reflection angles, such as are true for the most important diffraction circles for metals,  $\cos \Theta$  is approximately 1. Hence  $\delta = \alpha$ . Thus a simple angle measurement on the film is also the value for the angle between the normal to a set of reflecting planes and the fiber axis.

In any cubic lattice the angle between the fiber axis with indices  $uvw$  and a lattice plane  $hkl$  is given by

$$\cos \alpha = \frac{uh + vk + wl}{\sqrt{u^2 + v^2 + w^2} \sqrt{h^2 + k^2 + l^2}}.$$

In aluminum wire the  $[111]$  direction is the fiber axis. The innermost ring registers the reflection from all the octahedral

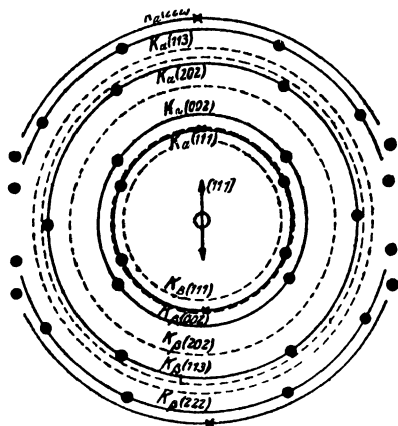


FIG. 168.—Theoretical fiber diagram for aluminum wire with  $[111]$  parallel to wire axis.

planes,  $(111)$ ,  $(\bar{1}11)$ ,  $(1\bar{1}1)$ ,  $(11\bar{1})$ , and the other four parallel to these. Hence  $\alpha$ , and consequently  $\delta$ , on the film will be 0 deg. for  $(111)$ , which means that the  $(111)$  planes are perpendicular to the fiber axis  $[111]$  (as by definition), and cannot reflect. For the others  $\alpha = 71^\circ = \delta$  (see Fig. 168).

Further data for aluminum wire calculated in this way are shown in the table at top of p. 362.

Since there is agreement between the calculated positions and those found experimentally for drawn aluminum (Fig. 121), the assumption of the  $[111]$  fiber axis is correct and the wire structure may be represented as shown in Fig. 169, with the unit crystal

Ring number	Planes	Number cooperating	$\alpha$ , degrees
{1(111) 5(222)	( $\bar{1}11$ )	6	71
	( $1\bar{1}1$ )		
	( $11\bar{1}$ )		
{2(200) 6(400)	(100)	6	55
	(010)		
	(001)		
3(220)	(110)	6	35
	(101)		
	(011)		
4(113)	(110)	6	90
	( $\bar{1}01$ )		
	( $0\bar{1}1$ )	6	30
	113, etc.		
	$\bar{1}13$ , etc.		
	113, etc.		
		12	59
		6	80

cubes oriented with cube diagonals parallel to the wire axis, but at random around these diagonals as axes.

For body-centered cubic wires like iron (Fig. 170) the assumption may be made that the  $[110]$  direction is parallel to the wire axis and this is then tested.

Ring	Planes	Number cooperating	$\alpha$ , degrees
{1(110) 4(220)	(101)	8	60
	(10 $\bar{1}$ )		
	(011)		
	(01 $\bar{1}$ )		
2(200)	(100)	4	45
	(010)		
	(001)	2	90
3(112)	(211), (121), etc.	8	30
	(112), (11 $\bar{2}$ ), etc.	4	55
	( $\bar{2}11$ ), ( $\bar{1}21$ ), etc.	8	73
	( $1\bar{1}2$ ), ( $\bar{1}\bar{1}2$ ), etc.	4	90
	(130), (310), etc.	4	27
5(130)	(301), (031), etc.	4	48
	( $\bar{1}30$ ), ( $3\bar{1}0$ ), etc.	4	63
	(103), (013), etc.	12	77
	(111), (1 $\bar{1}\bar{1}$ )	4	35
6(222)	( $\bar{1}\bar{1}1$ ), ( $1\bar{1}1$ )	4	90

As a matter of fact, the intensity maxima lying on the Debye-Scherrer rings are not sharp spots but are really arcs of 10 deg. in cases of extreme cold work, or more (Fig. 171). This means, of course, that all the crystal grains are not perfectly oriented and that there is a "scattering" in a cone around an average or

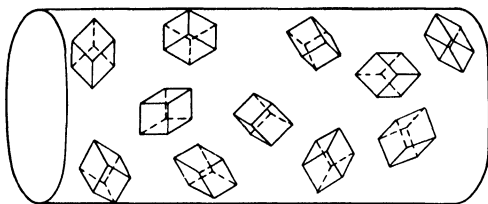


FIG. 169.—Diagram showing unit crystal cubes in aluminum wire with cube diagonals parallel to the axis of the wire, but oriented at random around this axis.

ideal position which is the wire axis itself. The scattering angle or apex of this cone is obviously half of the arc length of the intensity maxima. Every possible gradation of preferred orientation may be practically observed in metal specimens from sharp spots to continuous rings for random arrangement.

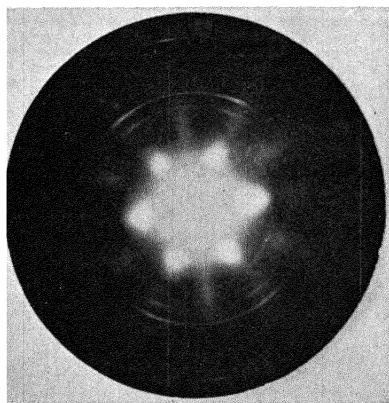


FIG. 170.—Fiber pattern for hard-drawn steel wire.

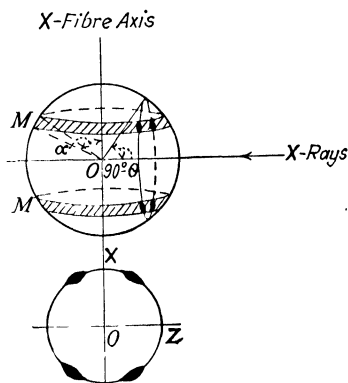


FIG. 171.—Analysis of true fiber diagrams.

The arc lengths of the maxima are, therefore, a measure of the amount of cold work and preferred orientation or fibering in a given specimen, either directly produced or residual after heat treatment.

In many cases of examination of fabricated metals it may be impossible or undesirable to orient the specimen with the fiber

axis perpendicular to the primary x-ray beam. If, then, the specimen is placed at an oblique angle, a pattern is obtained with exactly the same Debye-Scherrer rings as before but the four-point diagram is changed when two of the points move apart on a ring and the other two together, still retaining symmetry with respect to vertical and horizontal lines on the film. Instead of one angle  $\delta$  to be measured for the four spots, there are now two angles,  $\delta_1$  and  $\delta_2$ , evaluated by

$$\cos \delta_2 = \frac{\cos \alpha - \cos \beta \sin \Theta}{\sin \beta \cos \Theta}$$

and

$$\cos \delta_1 = \frac{\cos \alpha - \cos (180^\circ - \beta) \sin \Theta}{\sin (180^\circ - \beta) \cos \Theta},$$

where  $\alpha$  is the same as before,  $\beta$  is the angle between the fiber axis and the direction of the primary beam, and  $\Theta$  is the angle of incidence (Fig. 172).

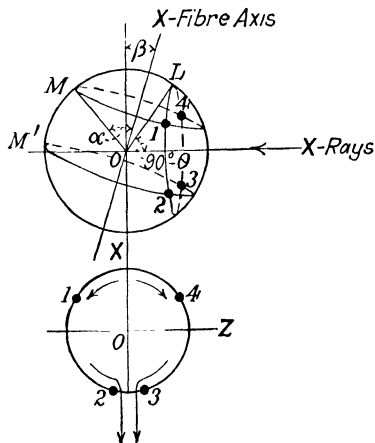


FIG. 172.—Effect upon diffraction pattern of tilting fiber axis at angle  $\beta$ .

liquely oriented fiber axis with a series of values for the angle  $\beta$ . If the crystal lattice plane perpendicular to the fiber axis (Polanyi's diatropic planes) reflect a beam of wave length  $\lambda$  incident at the angle  $\Theta$ , then when  $\beta = 90^\circ - \Theta$ , an intensity maximum will appear at the twelve o'clock position on one of the Debye-Scherrer rings due to  $(hkl)$  planes. For cubic crystals the evaluation of the  $(hkl)$  indices for the ring upon which the intensity maximum appears gives at once  $[hkl]$  the fiber axis, since the normal to these planes is the same as the axis.

For evaluation of the indices of the fiber axis in a drawn metal, two or three methods are available:

a. Trial and failure method by assuming indices, calculating the intensity maxima to be expected on the various rings, as above illustrated for aluminum and iron, and comparing with experimental film.

b. Use of patterns for ob-

c. Sometimes only two or three intensity maxima are necessary to evaluate the fiber axis. Glocker and Kaupp<sup>1</sup> give the example of electrodeposited copper with maxima on the (111) and (200) (or (100), second order) rings. Since

$$\cos \alpha = \frac{uh + vk + lw}{\sqrt{u^2 + v^2 + w^2} \sqrt{h^2 + k^2 + l^2}},$$

where  $[uvw]$  is the fiber axis and  $(hkl)$  a set of planes, then for the (111) and (100) planes, respectively,

$$\cos \alpha_1 = \frac{u + v + w}{\sqrt{3} \sqrt{u^2 + v^2 + w^2}}$$

$$\cos \alpha_2 = \frac{u}{\sqrt{u^2 + v^2 + w^2}}.$$

Intensity maxima appear on both rings at 90 deg.; hence  $\delta_1 = \alpha_1 = \delta_2 = \alpha_2$ ; furthermore, substituting the values of  $\cos \alpha_1$

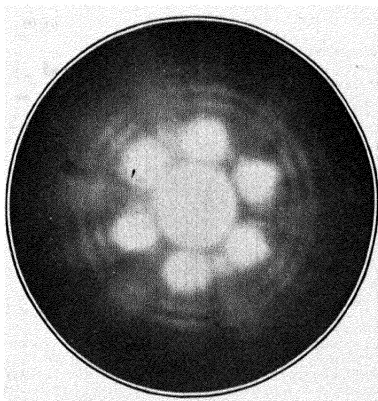


FIG. 173.—Pinhole spectrograms of commercial rolled copper sheet, with rolling direction perpendicular to x-ray beam.

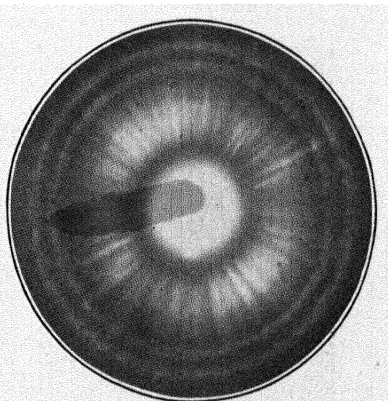


FIG. 174.—Same as Fig. 173 with rolling direction parallel to x-ray beam.

and  $\cos \alpha_2$ ,  $0 = u + v + w$  and  $0 = u$ , or  $v = -w$ . The fiber axis is therefore  $[0\bar{1}1]$ .

X-ray patterns taken with the beam parallel to the fiber axis are characterized by uniform Debye-Scherrer rings indicative of random orientation (Figs. 173, 174, 175, and 176).

**3. Multiple Fiber Structures in Drawn Wires.**—Sometimes more than one preferred orientation is observed as a multiple fiber structure. This is true of face-centered cubic metals in

<sup>1</sup> *Z. Physik.*, **24**, 121 (1924).

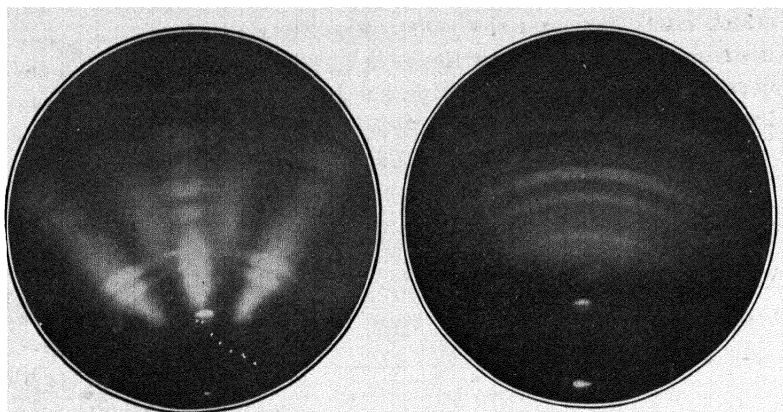
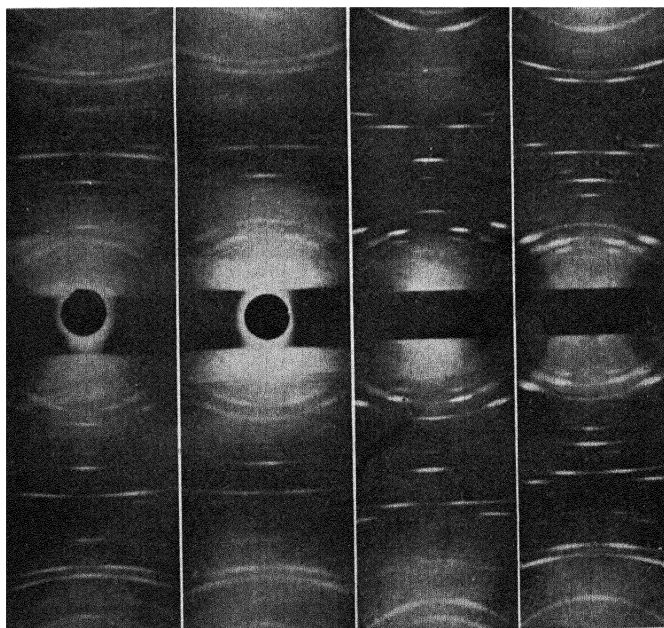


FIG. 175.

FIG. 176.

FIG. 175.—Surface reflection spectrogram of duralumin sheet, with beam impinging on specimen in direction of rolling.

FIG. 176.—Same as Fig. 175 with specimen turned through 90°.



Silver

Gold

Copper

Aluminum

FIG. 177.—Debye-Scherrer patterns for hard-drawn wires. (*Schmid and Wassermann.*)



which both [111] and [100] directions serve as fiber axes. The distribution of grain orientations between these two varies depending on the metal. This has been studied quantitatively by Schmid and Wassermann.<sup>1</sup> Diffraction patterns shown in Fig. 177 were registered on a cylindrical film instead of the usual flat film, so that the layer line diagrams characteristic for fibers are more prominently shown. The data obtained for the percentage of crystals in the [100] and [111] orientations and for the half length of interferences on the (200) ring as a measure of the exactness of fibering are as follows:

Metal wire	Per cent crystals with		Half length of interferences on (200) ring	
	[100]	[111]		
	Parallel to direction of drawing		[100]	[111]
Aluminum . . . .	0	100	.....	3° 30'
Copper . . . .	40	60	7°	3°
Gold . . . .	50	50	8° 30'	4° 30'
Silver . . . .	75	25	7° 30'	3°

The scattering around the [100] preferred orientation is evidently twice as great as around the [111] axis. The presence of a double fiber structure with varying proportions of each and variations in scattering around a fixed position have great practical significance in differentiating drawing, annealing, and physical properties of aluminum, copper, gold, and silver.

**4. The Zonal Structures of Hard-drawn Wires.**—An interesting structural phenomenon in hard-drawn wires is illustrated in Figs. 178*a* and 178*b* for copper wire. A beam of monochromatic x-rays defined by a slit was reflected from the surface of a cold-drawn copper wire about 0.5 mm. in diameter. The pattern in *a* shows a nearly random arrangement of grains in spite of the prediction concerning fibering. The wire was then etched down in successive steps and an x-ray examination made. The structure of the innermost core of the wire in *b* is characterized by extreme fibering. Hence, wires drawn through dies have

<sup>1</sup> *Z. Physik.*, **42**, 779 (1927).

distinctly zonal structures with the grains becoming more perfectly oriented the nearer to the wire axis considered as a line at the exact center. In other words, in the passage through the die, the flow of metal exactly in the direction of drawing occurs only in the middle of the wire, whereas in the walls the

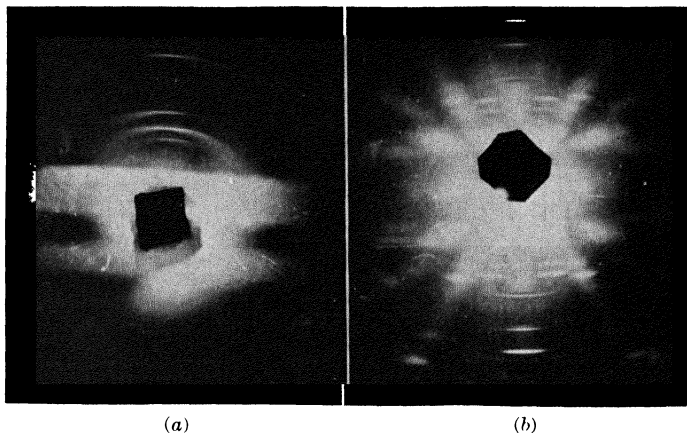


FIG. 178.—Patterns illustrating zonal structure in copper wire. Left, surface; right, innermost core.

metal is flowing inward as well as along the length of the wire and the crystal grains are thus disposed at an angle to the core.

Ordinary powder diffraction spectra (Hull method) also show the zonal structure. Figure 179 (upper) shows the pattern of the

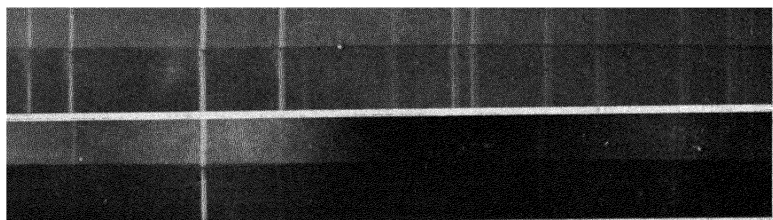


FIG. 179.—Hull diffraction patterns showing zonal structure of copper wire. Upper, outer mantle; lower, core.

original copper wire, which is really the structure of the outer mantle of the wire. The intensities of the various diffraction lines are just about those to be expected from a somewhat random orientation. Figure 179 (lower) is the pattern for the core of this wire after etching down to a diameter of about 0.13 mm. A surprising change has occurred since the (111) line has entirely

disappeared, the (200) line is about the same, the (220) line is about doubled in relative intensity, the (311) line is about half as intense, etc. This illustrates the error which might be made in the interpretation of such patterns if the facts were not known. The phenomena here observed agree with a [100] direction for the fiber axis but not so well with the [111].

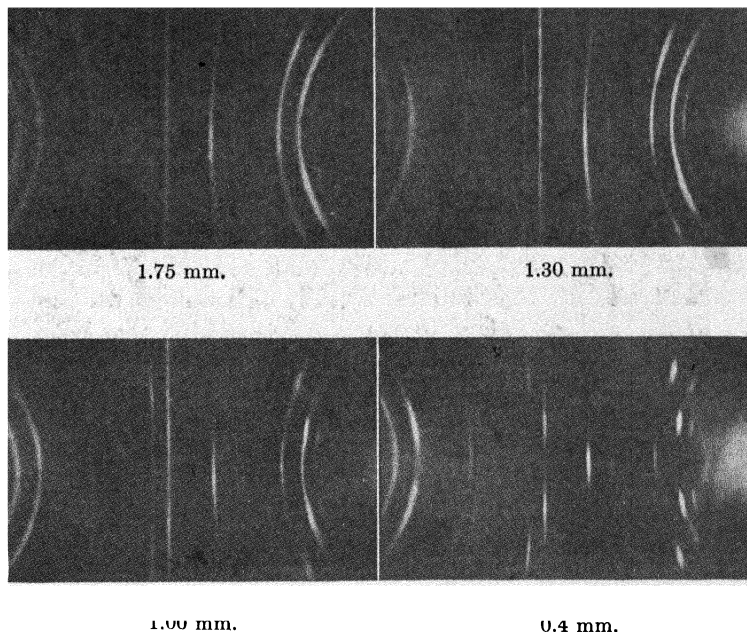


FIG. 180.—Patterns for copper wire showing zonal structure with decreasing diameter. (*Schmid and Wassermann.*)

This condition of a central linear zone and a conical mantle, of course, is of primary importance in affecting the texture of the wire, and in the proper interpretation of diffraction patterns. The zonal structure of wires has also been studied by Schmid and Wassermann.<sup>1</sup> In Fig. 180 are reproduced patterns from their work on copper wire with the diameters 1.75, 1.3, 1.0, and 0.4 mm. Not only does the sharpness of fibering shown by the shorter interference maxima increase as layers are removed, but there is also evidence of unsymmetrical interferences. From these the inclination of the fiber axis [111] to the wire axis in different zones is determined as follows:

<sup>1</sup> *Z. Physik.*, **42**, 779 (1927).

Distance of Layer from Center, Millimeters	Inclination Angle, Degrees
1.75 (outer skin)	<2
1.6	9
1.3	6
0.9	4
0.4	0

This indicates that, in the outermost skin of the wire, the effect of the die has been to keep the grains which are oriented nearly parallel to the direction of drawing, but slightly below this the conical flow is evident. The texture of a hard-drawn wire, therefore,

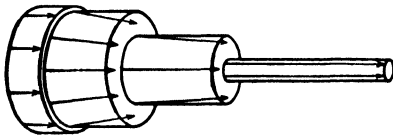


FIG. 181.—Diagram of zonal texture of hard-drawn wires.

may be represented in Fig. 181. Schmid and Wassermann report tests of tensile strengths in kilograms per square millimeter corresponding to zones for two specimens of hard-drawn copper wire, as follows:

	Tensile Strength
1. Original diameter 4.85 mm	38 3
Etched to 3.20 mm	41 3
Drawn to 3.20 mm	45 2
2. Original diameter 1.75 mm	46.1
Etched to 1.00 mm	52 8
Drawn to 1.00 mm	51 0

It is evident that the core zone of a wire has the highest tensile strength in keeping with its parallel preferred orientation. This anisotropic or zonal structure is an inherent property and improvement in the superficial zones is not gained by increasing the amount of cold work.

**5. Summary of X-ray Results on Deformation Structures of Drawn Wires.**—All body-centered cubic metals when drawn are characterized by a [110] direction parallel to the direction of drawing; all face-centered cubic metals have a [111] direction in the wire axis, with a second orientation of [100], the proportion of crystal grains in the various metals varying as explained above. An exception in the case of copper wire recrystallized at 1000° C. has been noted. Only the core of these wires and perhaps the outermost skin approximate these orientations, since in the mantle zones the fiber axis is inclined to the wire axis. In answering

the question why a particular crystallographic direction becomes parallel to the direction of deformation it may be noted that the most thickly populated atomic planes in the body-centered cubic lattice are the (111) planes, with the (100) planes next most densely populated. It is a general drawing phenomenon, therefore, that

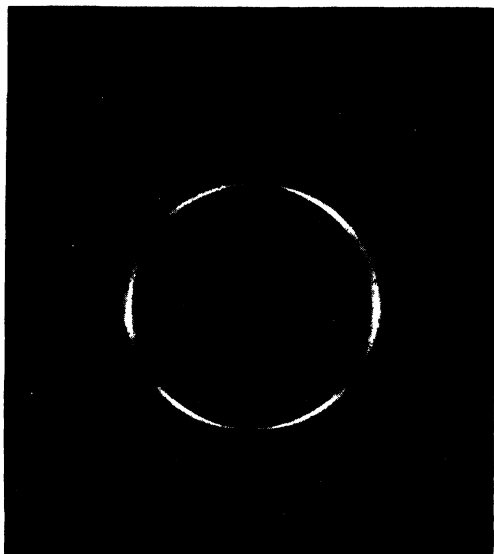


FIG. 182.—Pinhole pattern for rolled sheet metal showing nearly random crystal grains.

the most densely populated planes take up positions perpendicular to the wire axis, and that these orientations are such as to present maximum resistance to further deformation.

**6. Interpretation of Fiber Patterns for Rolled Sheets (Limited Fiber Structure).**—It is possible for cold-rolled sheet metal to

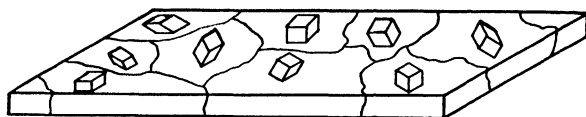


FIG. 183.—Structure of sheet metal with randomly oriented grains.

produce a diffraction pattern indicating nearly random orientation of grains, as in Fig. 182. The structure of the sheet could then be diagrammatically drawn as Fig. 183. But in general, as explained above, crystal grains in a rolled sheet not only take up positions with a certain crystallographic direction parallel

to the direction of rolling but are further limited by having certain crystallographic planes parallel to the plane of rolling and to the transverse direction. Thus the diffraction pattern for rolled sheet steel in Fig. 184 indicates clearly the structure

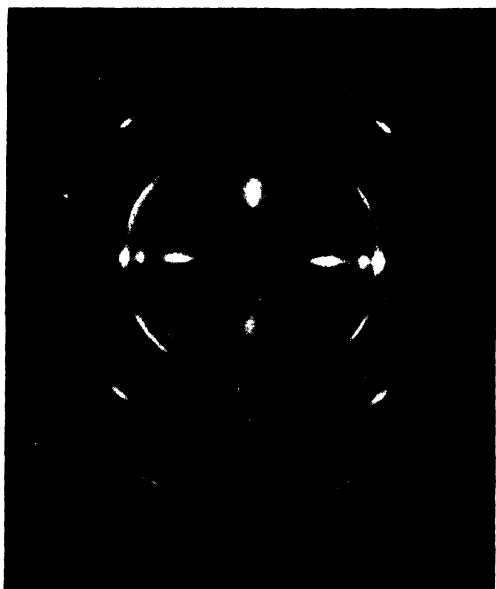


FIG. 184.—Pinhole pattern for rolled sheet steel showing preferred orientation of grains (for complete analysis, see text).

of the sheet with preferred orientation of grains as pictured in Fig. 185. The diffraction patterns enable the evaluation of the indices of these three characteristic directions (*i.e.*, rolling direction, the normal to the rolling plane, and the transverse direction

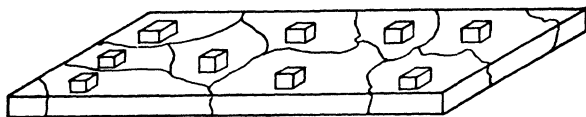


FIG. 185.—Structure of rolled sheet metal (steel) with preferred orientation of grains.

lying in the rolling plane at right angles to the rolling direction), and also with remarkable accuracy the departure or scattering from the theoretically ideal orientation as is always observed in practical cases. The rolling direction may be readily ascertained by the methods outlined under drawing, although all of the

diffraction interferences will not be present on account of the further limitation in rolling. For the determination of the crystallographic indices of the transverse direction and the normal to the plane of rolling, a further step must be taken. The best method is that of Glocker, explained in detail in his book:<sup>1</sup> a single metal crystal is considered to rotate through 360 deg. around the known fiber axis, and the reflection angle  $\Theta$  of the x-ray beam, impinging at right angles to the axis of rotation, on the different lattice planes of the crystal is plotted as a function of the angle of rotation. The result is a series of rotation curves which are extremely useful in interpreting results on rolled sheets or foils. Glocker gives curves for fiber axes [112], [001], and [111], with octahedral (111), cubic (100), dodecahedral (110), and (113) planes for each. He considers in detail the case of rolled silver in which [112] is parallel to the rolling direction and (110) planes are parallel to the rolling plane.

**7. Detailed Analysis of Pattern for Rolled Steel.**—To show in detail how a diffraction pattern of commercial rolled sheet may be completely interpreted, the example of low-carbon sheet steel is selected. The following analysis of a pattern similar to Fig. 184 is carried through in three parts:

- a. Identification of the diffraction rings.
- b. Identification of the type of fiber orientation.
- c. Determination of the type and degree of perfection of further limits of orientation.

The method consists essentially in assuming certain origins, orientations, and limitations and in checking theoretically desired patterns against those experimentally obtained.

*a. Identification of Diffraction Rings.*

If  $\Theta$  = angle of incidence of x-rays with atomic planes,

$D$  = diameter of ring on film,

5 cm. = distance from specimen to film,

then  $\Theta = \frac{1}{2} \tan^{-1} (1/5 \times D/2)$ .

$D$	$D/2$	$\tan 2\Theta$	$2\Theta$	$\Theta$	$\sin \Theta$ (observed)
3.76	1.88	0.376	20° 36'	10° 18'	0.179
5.66	2.84	0.566	29° 30'	14° 45'	0.255
7.28	3.64	0.728	36° 2'	18° 1'	0.309

<sup>1</sup> "Materialprüfung mit Röntgenstrahlen," pp. 312–324, Berlin, 1927.

Calculation of the theoretical values of  $\sin \theta$  assuming these plane families to be the (110), (200), (211):

$d$  = interplanar distances.

$a$  = length of unit cell cube of Fe = 2.87 A.U.

$(hkl)$  = (100), (200), (211).

$$\lambda = 2 d \sin \theta, \sin \theta = \frac{\lambda}{2 d}$$

$\lambda$  for Mo  $K\alpha$  = 0.710 A.U.

$$\text{Hence } \sin \theta = \frac{0.355}{d}, \text{ and } d = \frac{a}{\sqrt{h^2 + k^2 + l^2}}.$$

$hkl$	$d$	Sin $\theta$ (calculated)	Sin $\theta$ (observed)
110	2.03	0.175	0.179
200	1.435	0.247	0.255
211	1.171	0.303	0.309

This is close enough agreement from these rough measurements definitely to establish the identity of these rings.

The inner broad band is caused by the polychromatic or white radiation reflected by the planes of greatest spacing (110). The inner edge is determined by the short wave length of the white radiation, which is determined by the peak voltage across the x-ray tube. The outer edge is caused by an absorption edge due to the silver of the film emulsion, which occurs at a wave length of 0.485 A.U.

To check this outer absorption edge, the following calculation is made:

$$\lambda = 0.485, \sin \theta = \frac{0.485}{2d} = \frac{0.485}{2 \times 2.03} = 0.120.$$

Diameter of outer edge of ring = 2.50 cm.

$$\sin \theta = \sin \frac{1}{2} \tan^{-1} (1/5 \times D/2).$$

$D$	$D/2$	Tan $2\theta$	$2\theta$	$\theta$	Sin $\theta$ (observed)	Sin $\theta$ (calculated)
2.50	1.25	0.25	14° 2'	7° 1'	0.122	0.120

This agreement is also quite close.



The determination of minimum wave length from the diameter of the inside edge of the white radiation band is as follows:

Diameter of inner ring edge = 1.60 cm.

$$\frac{0.80}{5} = 0.16 = \tan 2\theta$$

$$\theta = 4.75^\circ.$$

$$\sin \theta = 0.083.$$

$$\lambda = 2 d \sin \theta = 2 \times 2.03 \times 0.083 = 0.336 \text{ A.U.}$$

Peak voltage =  $V = hc/\lambda e = 12354/\lambda = 36,768$  volts.

*b. Identification of Fiber Orientation.*—Since the reflection of an x-ray beam from an atomic plane must always lie on a plane determined by the beam and a perpendicular to the atomic plane at the point of reflection, the azimuth of the spots appearing on the various rings can be determined by calculating the angle between the perpendicular of the atomic planes being considered and the fiber axis, which is placed perpendicular to the beam. The following notation may be adopted:

$\alpha$  = angle between perpendicular to atomic planes under consideration and fiber axis.

$\delta$  = azimuth angle of spot on film (starting with zero at the twelve o'clock position on the film).

$\theta$  = angle of incidence of the x-ray beam upon atomic plane.

Polanyi gives the relation between these angles as  $\cos \delta = \frac{\cos \alpha}{\cos \theta}$ , but as such small values of  $\theta$  as appear in these diagrams the cosine of  $\theta$  so nearly equals one that it is within limits of accuracy to simplify to  $\cos \delta = \cos \alpha$  or  $\delta = \alpha$ .

Thus the azimuth of an intensity maximum on any ring is directly the angle between the perpendicular to the plane family causing the ring and the fiber axis. This angle between a perpendicular to any family of planes ( $hkl$ ) and any fiber axis ( $uvw$ ) can be given by solid analytical geometry to be:

$$\cos \alpha = \frac{uh + vk + lw}{\sqrt{u^2 + v^2 + w^2} \sqrt{h^2 + k^2 + l^2}}.$$

Since Glocker gives the fiber axis direction in a sheet of iron as  $[110]$ , this orientation will be assumed and the theoretically determined positions of the spots on each ring will be compared

with the actual diagrams. With  $(uvw)$  as  $(110)$ , the equation simplifies to

$$\cos \alpha = \frac{h + k}{\sqrt{2} \sqrt{h^2 + k^2 + l^2}}.$$

Using this equation the theoretical azimuth of spots on the various rings is as follows:

Planes	Azimuth, Degrees
110	0
$\bar{1}10$	90
101	60
100	45
001	90
112	55
$\bar{1}\bar{1}2$	90
121	30
$\bar{1}21$	73

These diagrams should be symmetrical along both a vertical and a horizontal axis, for every spot at angle  $\delta$  on the right there is one at  $\delta$  on the left, and one on the right and left at  $(180^\circ - \delta)$ .

In comparing this theoretical complete fiber diagram with the actual diffraction patterns the fiber axis is assumed to be perpendicular to the x-ray beam which practically may not be exactly true. This will tend in some cases to shift the positions towards one pole or the other and cause fiber spots which originate from planes at high angles from the fiber axis to appear with less rotation than would be expected, as will be discussed in the next section.

In Fig. 184 the following experimental interferences are observed:

INNERMOST SHARP RING (110)	
0°	Present
60°	Missing
90°	Present
SECOND SHARP RING (100)	
45°	Present
90°	Missing
THIRD SHARP RING (211)	
30°	Present
55°	Missing
73°	Present
90°	Missing

The broad band can have the same intensity maxima as the sharp (110) ring:

0°	Present
60°	Missing
90°	Present

Since this orientation takes care of all the spots appearing on the diffraction pattern but calls for spots which do not appear, it is evident that the assumption of a [110] axis is correct, but that there is a further limitation of orientation in a rolled sheet.

*c. Type and Degree of Perfection of Further Limitation.*—It has just been shown that, as was expected, a cube face diagonal lies parallel to the surface of the sheet or nearly so and in the direction of rolling. The other condition of a cube face lying parallel to the surface of a sheet which is usually given will be taken as the zero position and angular rotation about the face diagonal fiber axis necessary to cause the appearance of various spots will be calculated. Then, by the presence or absence of certain spots, the degree of perfection of the fulfillment of this condition can be determined on each film. If this orientation were perfect, only a very few spots would appear on any ring, and the ring itself would be missing.

The calculation of this angle of lateral rocking to one side and the other about the zero position necessary to cause the appearance of each spot is very involved in most cases, and a complete solution of this problem of a cubic lattice rotating about a [110] axis has been worked into the series of rotation curves by R. Glocker, mentioned above. These curves were used in investigating how great an angle of rotation of the cube about the [110] fiber axis from the zero position of the (100) face in the sheet is necessary in order that a diffraction spot may occur by having fulfilled the law specifying the angle of diffraction.

It will be seen that in the special case of any planes containing the x-ray beam the necessary angle of rotation about any axis perpendicular to the beam will directly equal the angle  $\theta$  given in the diffraction equation.

The presence of spots on the two (110) rings at the twelve and six o'clock positions can be explained only by another type of imperfection in orientation. This is a *tipping* of planes which in a perfect orientation would contain the x-ray beam and be perpendicular to the fiber axis, about an axis perpendicular to both

the beam and the fiber axis. This is actually an *inclination of the fiber axis to the surface of the sheet*, and its calculation falls in the special case mentioned in the last paragraph. The angles of rotation necessary for the appearance of the various spots on the several rings arranged in the order of their appearance with increasing rotation were found to be as follows:

Necessary angle of rotation	Ring	Radiation	Azimuth, degrees
4	110	White	90
9	112	$K\alpha$	73
10	110	$K\alpha$	90
18	112	$K\alpha$	30
18	110	$K\alpha$	60
20	100	$K\alpha$	45
22	110	White	60
45	112	$K\alpha$	90
70	112	$K\alpha$	55

The angle of inclination of the fiber axis to the sheet necessary to cause the appearance of spots at the six and twelve o'clock positions on the rings will be calculated. These reflections can only originate from (110) planes, and the inclination is directly equal to the angle of incidence given by the Bragg equation for this set of planes.

Ring	Radiation	Wave length	Inclination angle
(110)	Mo $K\alpha$	0.710 A.U.	10° 18'
(110)	White	0.336	4° 45'

Inclination of the fiber axis to the surface of the sheet in both directions with respect to the direction of the last pass will have the effect of causing the spots to extend over a wider angle on the circles and will cause spots to appear at slightly smaller rotation angles than those calculated to be necessary. If more grains are inclined in one direction than in the other, which in general seems to be the case, the intensity maxima will be displaced in one direction of azimuth and there arises a possibility of the appearance of spots on one side of the equator which have no corresponding spots on the other side.

*d. Experimental Check.*—For the particular specimen considered here the necessary rotation or the degree of imperfection of limitation of the complete fiber diagram caused by rotation around the fiber axis is 35 deg.; the inclination of the fiber axis to the sheet estimated from the relative intensities of the two polar spots to each other and to other interference maxima is small; and the majority of the inclinations of the fiber axes are greater in one direction than in the other with respect to the direction of last pass through the rolls.

### 8. Summary of Experimental Results on Structures of Rolled Foils.

Metal	Lattice type	Treatment	Fiber axis [FA], rolling plane (RP)
Aluminum	F. C. C.	Rolled	I [355] or [112] $\parallel$ FA, (135) or (110) $\parallel$ RP (four positions possible) II [100] $\parallel$ FA, (001) $\parallel$ RP (average reduction)
Silver	F. C. C.	Rolled	[112] $\parallel$ FA, (110) $\parallel$ RP (two mirror image orientations)
		Recrystallized 250 to 800° C	[112] $\parallel$ FA, (113) $\parallel$ RP
Gold...	F. C. C.	Rolled	I [112] $\parallel$ FA, (110) $\parallel$ RP II. [100] $\parallel$ FA, (001) $\parallel$ RP
Copper	F. C. C.	Rolled	[112] $\parallel$ FA, (110) $\parallel$ RP
		Recrystallized 250 to 1050° C	[100] $\parallel$ FA, (001) $\parallel$ RP
$\alpha$ -brass	F. C. C.	Rolled	[112] $\parallel$ FA, (110) $\parallel$ RP
		Recrystallized 300 to 702° C	[112] $\parallel$ FA, (113) $\parallel$ RP
Platinum	F. C. C.	Rolled	I. [112] $\parallel$ FA, (110) $\parallel$ RP II. [100] $\parallel$ FA, (001) $\parallel$ RP
Iron	B. C. C.	Rolled	[110] $\parallel$ FA, (100) $\parallel$ RP
		Recrystallized 600°	[350] $\parallel$ FA, (100) $\parallel$ RP
Tantalum	B. C. C.	Rolled	Same as rolled iron
Tungsten	B. C. C.	Rolled	

**9. Differences in Preferred Orientation in Surfaces of Thicker Sheets of Rolled Face-centered Cubic Metals.**—Although there are numerous statements in the literature to the effect that the preferred orientation assumed upon cold rolling metals having the same crystal structure are identical for the case of very thin foils, recent work has shown that this is not true for face-centered metals at least in the surface layers of fairly thick sheets. Holla- baugh and Davey<sup>1</sup> have investigated the preferred ranges of

<sup>1</sup> *Metals and Alloys*, **2**, No. 4, 256; No. 5, 302 (1931).

the crystal fragments in the surfaces of sheets of aluminum, nickel, copper, and silver for a series of samples of each metal, with consecutively increasing number of passes through the rolls. Instead of the usual transmission method, they used a special reflection method and investigated only the surfaces of comparatively thick sheets. The orientations found for the four metals were similar only in that for each of them one face diagonal of the cube always lies in a plane which is parallel to the direction of rolling and perpendicular to the rolling surface.

Nickel and copper were found to behave identically in that there was one symmetrical preferred range of positions about the *across* axis with symmetrical limits about the *along* axis. Silver was found to differ from nickel and copper in that there are two symmetrical preferred ranges about the *across* axis with no limitation about the *along* axis. The behavior of aluminum was found to be different from that of the three other metals in almost every respect. The limits of the preferred positions were found to vary on rolling instead of remaining unchanged as in the others. Like silver, aluminum shows two ranges of positions about the *across* axis, but unlike silver these ranges are unsymmetrical. Aluminum also shows variable limits around the *along* axis.

Although these metals investigated have the same crystal structure and approximately the same atomic size and lattice parameters, they differ in valence. The authors believe that these differences in the preferred orientation in the surfaces of cold-rolled face-centered metals may be accounted for in terms of the number of valence electrons of the atoms of these metals. They assume that valence electrons in the atoms control the lattice forces and that these differences cause the difference in behavior noted for the four metals discussed.

**10. Plastic Deformation of Zinc and Magnesium.**—Unusual interest has been attached to the x-ray study of the deformation of zinc both as single crystals and as polycrystalline aggregates. The following *résumé* of earlier investigations is quoted from "The Science of Metals" by Jeffries and Archer.

Mark, Polanyi, and Schmid in Germany studied the deformation of single crystals by means of x-ray crystal analysis. They found change of orientation at slip planes produced during the ordinary tensile test in single crystals of zinc. Conditions for maximum elongation of single crystals of zinc were determined. Zinc crystallizes with a

hexagonal space lattice. The plane of easiest slip is the base of the unit hexagonal prism. When this plane makes an angle of approximately 45 deg. with the wire axis, the crystals are very ductile. Single crystal wires broken in tension at room temperature have shown as much as 600 per cent elongation; broken at 205° C., elongations up to 1700 per cent have been obtained. Although zinc is not regarded as very ductile, these values for elongation are the highest of any known metal. Unless the plane of easiest slip is at an opportune angle with respect to the wire axis, the crystal is relatively brittle. Single crystal wires of bismuth were tested at 200° C. and showed up to 300 per cent elongation. In this case also the plane of easiest slip must make an angle with the wire axis of about 45 deg. or the crystal will be brittle when broken in tension. During the process of elongation of the zinc single crystals, the round wire changed into a flat ribbon. The width of the ribbon was at first slightly wider than the original diameter of the wire. Slip occurred in a plane about 45 deg. from the wire axis and extended across the whole cross section of the wire in such a manner that the intersection of each slip plane with the wire surface formed an ellipse. The slight widening of the ribbon was due to the rotation of the elliptical sections. As the elongation increased, the general orientation of the crystal changed, so that the angles of the easiest planes of slip became more nearly parallel with the direction of extension.

The elongation is accompanied by a continued strengthening of the crystal and Polanyi believes that this is due to a bending of slip planes, so that the resistance to slip is increased. The exact mechanism of this strengthening is rather uncertain, but Polanyi assumes that the crystal units themselves undergo inner changes which lead to this result. As a matter of fact, Geiss and von Liempt have concluded from their investigations on single crystals of tungsten that the atoms themselves are deformed by tension, but the only evidence adduced by them for this conclusion is the change in temperature coefficient of resistance.

Mathewson and Phillips have described a new mechanism of deformation of zinc based on the study of large rectangular crystals. One of their conclusions was that deformation produced twinning with a rotation of some of the basal planes into positions 94 deg. removed from their original position, or about the same as that of the prismatic planes before twinning. A second conclusion was that fracture occurred along the basal planes in their new position, and therefore that fractures previously regarded as prismatic were in reality basal. Wilson and Hoyt showed then that cold rolling of polycrystalline zinc strip causes rearrangement of the zinc crystals not by twinning but in accordance with the classical theory of plastic deformation.

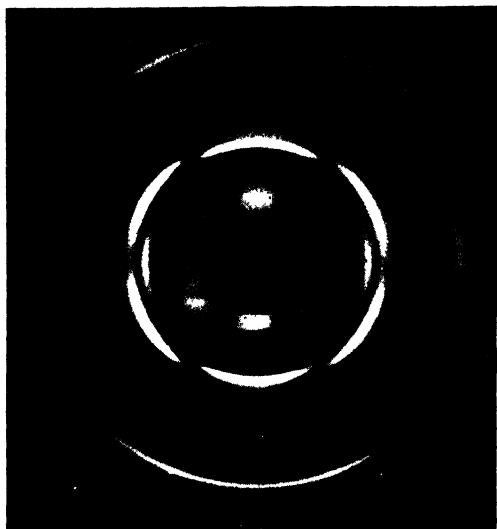


FIG. 186.—Pattern for forged Dowmetal (magnesium alloy).

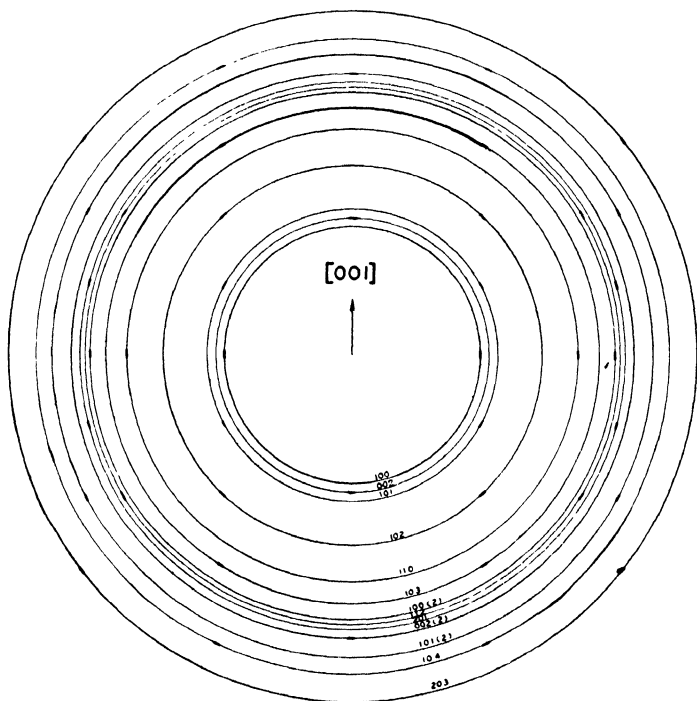


FIG. 187.—Theoretical fiber diagram for  $[001]$  parallel to fiber axis in hexagonal crystals, with which pattern in Fig. 186 agrees.



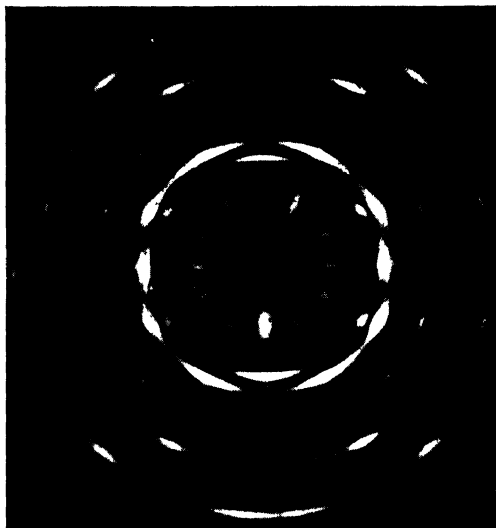


FIG. 188.—Pattern for Dowmetal extruded at ordinary temperatures.

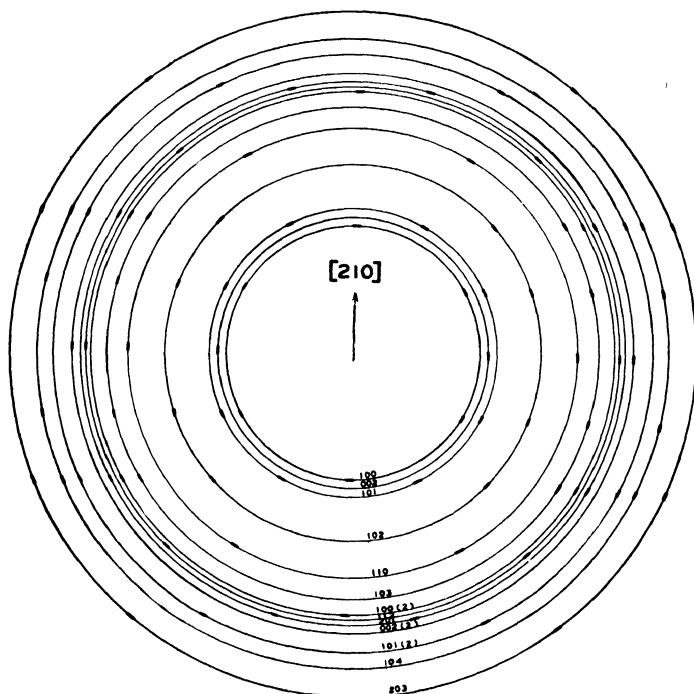


FIG. 189.—Theoretical fiber diagram for  $[210]$  parallel to fiber axis, hexagonal system, with which pattern in Fig. 188 agrees.

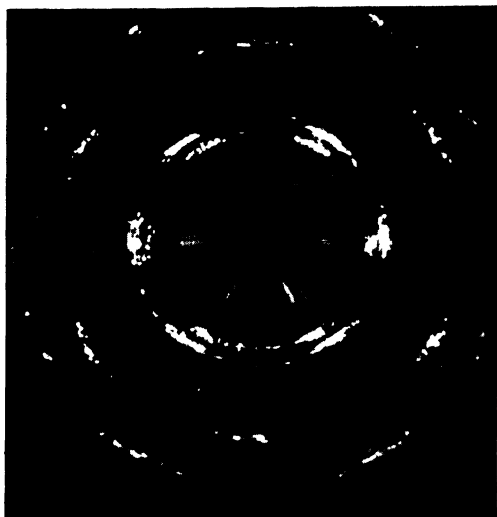


FIG. 190.—Pattern for Dowmetal extruded at high temperatures (compare with Fig. 188 for different orientation and much larger grain size).

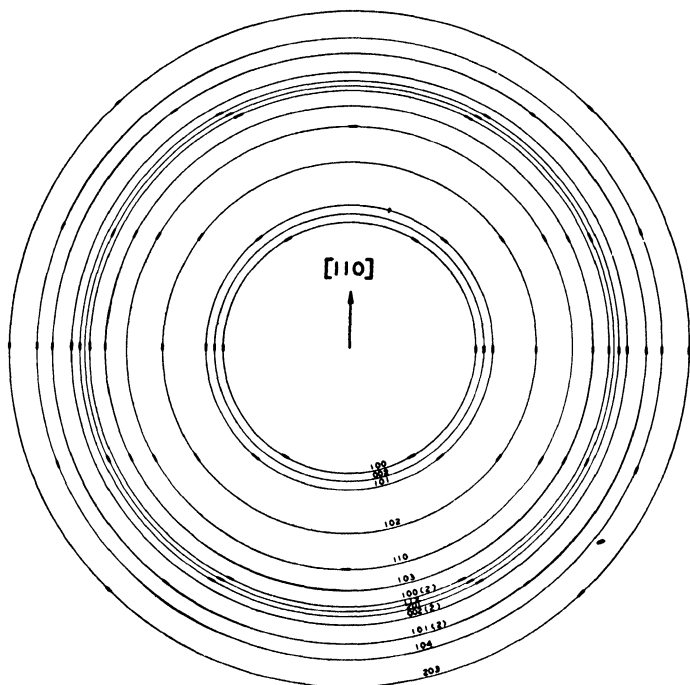


FIG. 191.—Theoretical fiber diagram for  $[110]$  parallel to fiber axis, hexagonal system, with which pattern in Fig. 190 agrees.

Extension of slender zinc single-crystal specimens causes rearrangement of the basal planes in accordance with the classical theory, the single crystal structure being preserved. The formation of the after-elongation thread is accompanied by severe lattice deformation which promotes twinning and fragmentation, though the single-crystal structure seems very permanent. The fracture of a thick zinc crystal occurs as depicted above with twinning present. The fracture of slender zinc crystals under simple tension is prismatic with twinning absent.

The growing industrial importance of magnesium and its alloys also lends particular interest to the mechanism of its deformation. Figures 186 to 191 show diffraction patterns<sup>1</sup> and theoretically calculated diagrams, respectively, for forged and extruded Dowmetal (nearly pure magnesium alloy). The analysis of the patterns proves that the forged magnesium alloy possesses a fiber axis parallel to the [001] direction while the extruded alloy shows a [210] fiber axis in the direction of extrusion at low temperatures and a [110] direction at high temperatures, a curious change in glide direction with temperature. Schmid working with single crystals found translation on the basal planes with the diagonal axis of the first kind as glide direction. Above 225° translation on the pyramid faces occurs with the same glide direction. In many important respects therefore magnesium differs in behavior from zinc and cadmium.

#### **11. Preferred Orientations, in Electrodeposited Metal Sheets.**

In the preceding sections the production of a directed crystal orientation by means of mechanical work has been considered in detail. The question naturally arises as to whether crystals may actually *grow* in such a way as to have a common crystallographic direction parallel to the axis of growth. Experiment proves that electrodeposited metal films show a fiber structure similar to drawn metals, and that the grains grow out parallel to the stream lines of the current or perpendicular to the surface of the electrode. The interpretation of the fiber patterns leading to an evaluation of the indices of the fiber axes proceeds exactly as outlined above. Of course, the fiber axis is parallel to the cross section or thinnest dimension of the deposited sheet. If, then, an x-ray beam impinged at right angles upon the surface of such a sheet, it would pass parallel to the fiber axis. As demonstrated for wires, the pattern is always indicative of

<sup>1</sup> Kindly furnished by Dr. L. G. Morell, Dow Chemical Co.

random orientation, since the crystal units may be oriented anywhere through 360 deg. around the fiber axis. It is necessary, therefore, to have films thick enough to pass the beam perpendicular to the fiber axis or to use the method of inclining the fiber axis at an oblique angle to the primary beam. Bozorth<sup>1</sup> has published curves for graphical analysis of patterns so obtained with the formula

$$\cos \delta = \frac{\cos \alpha - \cos \beta \sin \Theta}{\sin \beta \cos \Theta}.$$

Many excellent papers have been published on detail studies

Element	Lattice	Solution	Current density, amperes per square centimeter	Fiber axis	Observer
Silver	F. C. C.	Cyanide	0 007	Random	Glocker and Kaupp
Silver	F. C. C.	0 1 N AgNO <sub>3</sub>	0 010	[111], [001]	Glocker and Kaupp
Silver	F. C. C.	0 1 N AgNO <sub>3</sub>	0 022	Random	Glocker and Kaupp
Copper	F. C. C.	0 1 N CuSO <sub>4</sub>	0 03	[011]	Glocker and Kaupp
Nickel	F. C. C.	$\begin{cases} \text{Ni}(\text{NH}_4)_4\text{SO}_4 \text{ or} \\ 0 1 N \text{ NiCl}_2 + \\ 0 9 N \text{ NiSO}_4 \end{cases}$	0 005	[001]	Bozorth
Nickel	F. C. C.	NiSO <sub>4</sub> + boric acid	0 10	[001] [011] (on underlying copper)	Clark and Frolich
Nickel	F. C. C.	0 9 N NiCl <sub>2</sub> + 0 1 N NiSO <sub>4</sub>	0 005	[211]	Bozorth
Lead	F. C. C.	Pb(ClO <sub>4</sub> ) <sub>2</sub> or fluosilicate	1 0	[211]	Clark, Frolich and Aborn
Chromium	B. C. C.	Grube		[111]	Glocker and Kaupp
Iron	B. C. C.	10 per cent Fe(NH <sub>4</sub> ) <sub>4</sub> SO <sub>4</sub>	0 001	[111]	Glocker and Kaupp
Iron	B. C. C.	10 per cent Fe(NH <sub>4</sub> ) <sub>4</sub> SO <sub>4</sub>	0 015	Random	Glocker and Kaupp
Iron	B. C. C.	50 per cent FeCl <sub>2</sub>	0 001	[111]	Glocker and Kaupp
Iron	B. C. C.	50 per cent FeCl <sub>2</sub> at 100° C.	0 1	Random	Glocker and Kaupp
Iron	B. C. C.	Same + CaCl <sub>2</sub>	0 1	[112]	Glocker and Kaupp

<sup>1</sup> *Phys. Rev.*, **26**, 310 (1925).

involving effects of electrolytes, current density, temperature, concentration, stirring, orientation as a function of thickness, effect of base electrode metal, recrystallization, presence of small amounts of addition agents, pH, electrode potential, etc. Glocker summarizes the results as shown on page 386.

**12. Deposition of a Metal from Solution by Displacement.**—Metallic silver deposited from a solution of silver nitrate by introducing a small piece of copper has a fibrous structure with the axis [110] which makes an angle of 30 deg. with the direction of growth. The microcrystals show a rotation around this axis with an angle of  $\pm 11$  deg. As the (111) planes of the silver crystals lie parallel to the flat surfaces of the deposited metal, the direction of growth of the deposited silver lies nearly parallel to the [112] axis.<sup>1</sup>

**13. Properties of Mirrors and Sputtered Films.**—Very thin films of metals have been frequently studied. Foils of platinum, nickel and copper 7 to 18 microns thick produced by cathodic sputtering and thermal evaporation show a structure. The support upon which the film is deposited and the presence of gas have a profound effect upon the crystal arrangement.

**14. Growth of Texture of Castings.**—Superficial observation alone discloses the regularity of grain orientations and directions of growth in castings. In both body-centered and face-centered cubic metals the orientation is such that (100) planes lie parallel to the long axis of the crystal grain. In white tin (110), in the hexagonal close-packed metals (Mg, Zn, Cd) (10 $\bar{1}$ 0), with (0001) perpendicular, and in bismuth (111) planes lie parallel to this direction. It is obvious that these preferred arrangements in commercial metal castings are of great significance in determining the possibility of machining operations and the tensile strength. For example, a zinc casting with radially arranged dendritic crystal grains has a modulus of elasticity of 800 kg. mm.<sup>2</sup> and a coefficient of expansion of  $38 \times 10^{-6}$ ; if the crystallization is controlled so that the orientation is parallel to the long dimension of the casting, the modulus of elasticity is 12,000 kg./mm.<sup>2</sup> and the coefficient of expansion is  $14 \times 10^{-6}$ . It is possible therefore by means of x-ray analysis of structures of specimens cut in a certain way from castings prepared by a given technique to ascertain what crystallographic directions correspond to the dimensions of the unit.

<sup>1</sup> *Tsuboi, Kyoto Coll. Sci. Memoirs, 11, 271 (1928).*

## CHAPTER XVIII

### PRACTICAL APPLICATIONS OF X-RAYS TO PROBLEMS OF METALLURGICAL INDUSTRY

In preceding chapters the fundamentals of x-ray metallography have been outlined. The interpretation of diffraction patterns has been presented in terms of the characteristic crystal structures of pure metals and alloys, and in terms of important technical properties such as grain size, internal strain, and effects of mechanical deformation. The immediate practical industrial significance of these fundamental facts has been pointed out in part and other applications are obvious to anyone acquainted with metallurgical problems. It is now the purpose to enumerate briefly some of the actual problems of practical metallurgy, aside from the structure and constitution of alloys, and to illustrate some of the results of approach to these problems by the x-ray method. This list is merely one selected somewhat at random and is in no sense a complete record of achievement. Most of the examples have been selected from among the investigations in the writer's own laboratory.

In general, the x-ray method has been called upon to decide upon the proper method of manufacturing technique, to assure constant properties, and to make a fundamental distinction between metal or alloy commodities with satisfactory and unsatisfactory behavior. For commercial metals the scientific methods of interpretation derived for pure materials as presented in preceding chapters are applied, although every new metal specimen is a new subject for research in itself. Gradually, metallurgical industry is coming to the realization, on the one hand, that there is nothing mysterious in x-rays or magic in the searchings of ultimate structures and, on the other hand, that these rays are not a panacea for all troubles unsolvable by other methods even though a brilliant record of achievement is already written. X-rays enable the observation of the interior of solid objects for gross inhomogeneities, and they extend the scope of fine-structure analysis far beyond the microscope down to the

ultimate architectural pattern of atoms in space. Without undue enthusiasm it may be stated as a fact that the contributions of x-ray research to metallurgical science *over so few years* surpass the record of all other experimental methods. The growing interest and confidence in a great research tool are demonstrated by the number of experimental installations in the research laboratories of metallurgical manufacturers and universities.

**1. The X-ray Analysis and Control of Heat Treatment and Recrystallization of Cold-worked Metals.** *a. The Province of Heat Treatment.*—When metals are worked by rolling or drawing, they become fibered. In other words, aggregates in which the crystal grains have random orientation assume in the process of mechanical deformation a structure in which the grains assume a definite orientation with respect to a common direction—that of rolling or drawing. The analysis of the mechanism from x-ray patterns is given in the preceding chapter. These sheets or wires are now characterized by strongly directional properties and it is the province of heat treatment in general to cause a recrystallization of the grains while retaining the form of the sheet or wire, so that a random, non-directional orientation is again obtained as is absolutely required, for example, in forming steels. Again internal strains introduced by rapid chilling in castings, etc., are relieved by heat treatment. The x-ray method finds powerful practical use in discovering just how completely the fiber structure or the internal strain has been removed. In its sensitiveness as such a control method it far transcends the microscopic or other physical tests.

It is the purpose of the present section to consider in a more quantitative manner the mechanism of recrystallization during heat treatment of single relatively pure metals, principally aluminum, silver, and copper. The information which has been derived from x-ray researches, chiefly by Glocker, Kaupp, and Widmann,<sup>1</sup> on these metals is astonishing in its scope.

*b. Heat Treatment of Cold-rolled Foils.*—There are three possible effects of heat treatment of cold-rolled foils: (1) the directed orientation of grains is completely lost and the new grains are in random arrangement from the outset of recrystallization; (2) between the states of fiber structure and final random arrangement there is an intermediate step consisting of a directed

<sup>1</sup> *Z. Physik.*, **45**, 200 (1927); *Z. Metallkunde*, **17**, 354 (1924); GLOCKER, "Materialprüfung mit Röntgenstrahlen," p. 332, Berlin, 1927.

arrangement different from that produced in rolling, which goes over into the random type of temperatures in the neighborhood of the melting point; (3) the new recrystallization or intermediate directed orientation persists to the melting point.

(1) *Recrystallization of Aluminum Sheet.*—At all degrees of rolling, even up to 98 per cent reduction, aluminum recrystallizes with a random orientation of grains. Heating for 15 min. at  $265^{\circ}\text{C.}$  does not destroy the fiber pattern of the rolled sheet (Fig. 166) but at  $275^{\circ}\text{C.}$ , or above, this is lost. The pattern consists now of concentric rings with a spotted appearance indicative of a random arrangement of larger grains (Fig. 192).

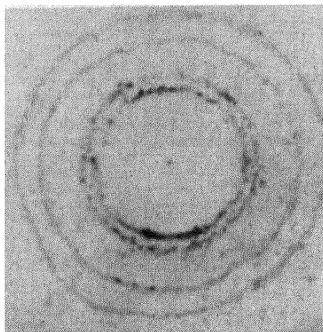


FIG. 192.—Pattern for cold-rolled aluminum foil after annealing, showing recrystallization in random arrangement.

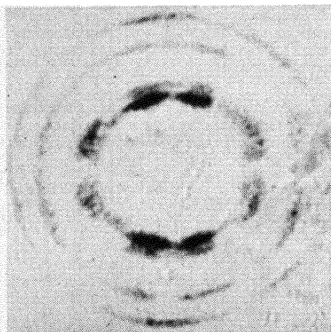


FIG. 193.—Pattern for cold-rolled silver foil after annealing at  $225\text{--}750^{\circ}\text{C.}$ , showing recrystallization in new preferred orientation.

This is the type of structure which might be generally expected, and for all the metals with degrees of rolling below 90 per cent reduction, including silver and copper, this is observed. Aluminum thus represents the first of the above alternatives.

(2) *The Recrystallization of Silver.*—Glocker was the first to observe that with strongly rolled silver (97 per cent) the recrystallization did not take place with chaotic arrangement of grains, but with a new crystallographic orientation (Fig. 193) with the (113) planes in the plane of rolling instead of the (110) planes as in the original rolled structure. This structure is maintained even after 10 days or more of heating at  $300^{\circ}\text{C.}$ , but at higher temperatures (rapidly at  $850$  to  $900^{\circ}$ ) the random orientation results, together with a considerable increase in grain size. These facts illustrate the very important fact that long annealing at low temperatures does not necessarily produce the same effect



as annealing for a short time at high temperatures, as is so often believed and practiced in metallurgical circles.

The sequence of events during recrystallization as interpreted from the x-ray patterns may also be tested and compared with the results of technological tests on tensile strength, elasticity, and grain size. Widmann's data as plotted in Fig. 194 show

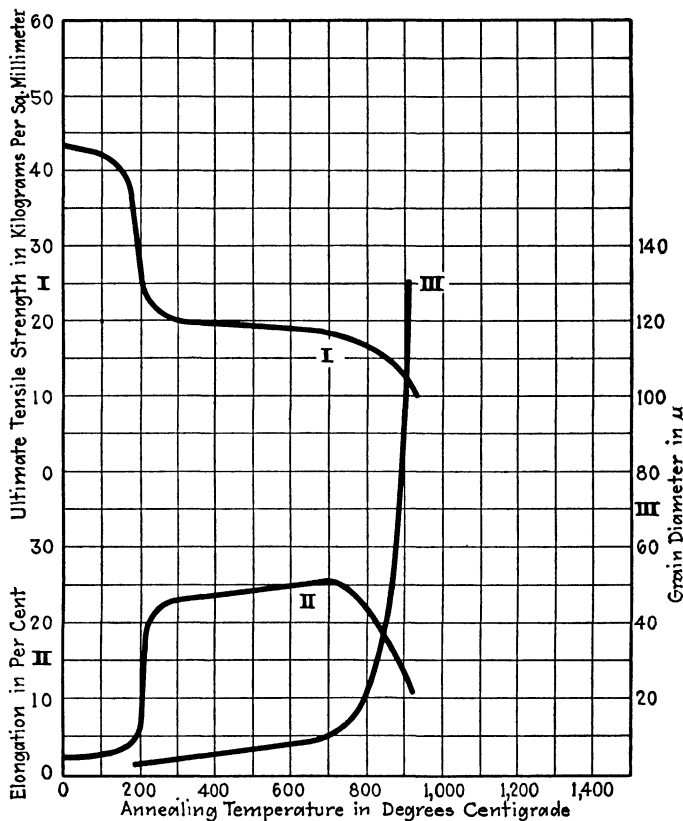


FIG. 194.—Tensile strength, elongation, and grain size of rolled silver sheet as functions of annealing temperature. (Glocker and Widmann.)

distinctly the breaks occurring with the appearance of the new directed position at 200° and with random orientation at 800°.

The very curious fact also was found that if the silver is reduced only partially in one rolling operation, is heated at 700° C., and again rolled down to final thickness, then the properties are distinctly different from those of the silver reduced in one rolling only. In the former case the x-ray patterns indicated that

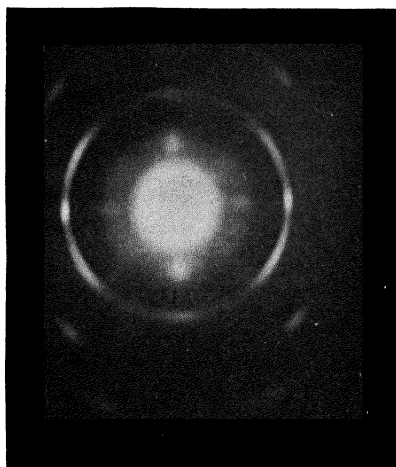
the sheet begins to recrystallize at room temperature. Consequently annealing produces abnormally large grains and loss of tensile strength, the metal is characterized by mixed, very large and very small grains, and is difficult to handle practically.

(3) *Impurities Change Recrystallization Temperature.*—The effects of small amounts of impurities on the recrystallization temperature of silver may be determined far more accurately from the x-ray patterns than from microscopic analysis. Widmann's studies of this subject have been fully substantiated by the present writer. In the following table are listed the data on the effects of impurities.

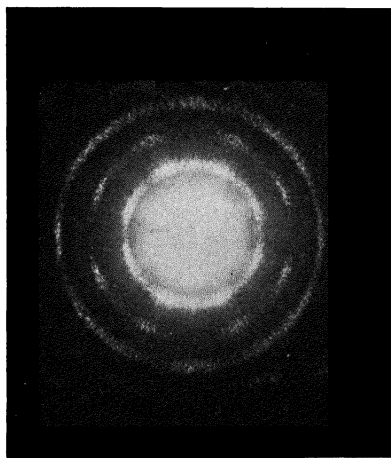
Element	Impurity		Recrystallization temperature, degrees Centigrade
	Weight, per cent	Atomic, per cent	
Pure silver	.	.	150
Copper . . . .	0 303	0 51	230
Copper . . . .	0 12	0 20	200
Copper . . . .	0 073	0 123	175
Aluminum . . .	0 2	0 93	190
Zinc . . . . .	0 119	0 195	145
Lead . . . . .	0 059	0 03	145
Nickel . . . . .	0 1	0 15	137
Gold . . . . .	0 1	0 054	112
Gold . . . . .	0 2	0 11	110
Palladium . . .	0 1	0 10	112
Iron . . . . .	0 035	0 068	110
Iron . . . . .	0 055	0 107	20
Iron . . . . .	0 065	0 126	20

It is clear that copper and aluminum raise the temperature, while all other elements, particularly iron, lower it. Five hundredths of 1 per cent of iron is sufficient to lower the temperature of recrystallization of silver to room temperature. Ancient as is the metallurgy of silver, this fact has been discovered only recently by means of x-rays. It is safe to conclude that silver, except of the highest purity, always has contained at least this trace of iron. Why then has not recrystallization served to ruin, practically speaking, cold-rolled silver articles? The answer is that copper also is universally present and in amounts of 0.1 per cent or less completely compensates for the

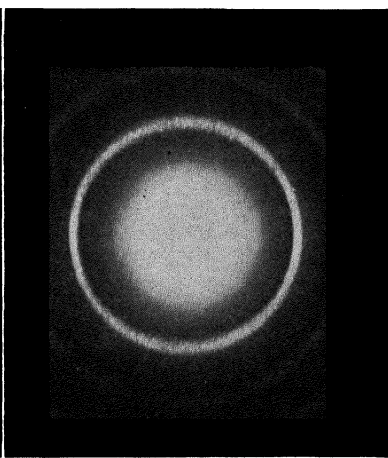
powerful effect of 0.05 per cent iron. In the same way aluminum compensates for gold which also lowers the recrystallization temperature of silver. It is interesting to note, however, that



(a)



(b)



(c)

FIG. 195.—Recrystallization of low carbon steel shim stock. (a) Original rolled structure; (b) recrystallized in new preferred orientation; (c) heated above upper critical point to produce random arrangement of grains.

the temperature of  $150^{\circ}$  for pure silver does not hold for the very purest silver (considerably less than 0.0005 per cent iron and 0.00002 per cent lead) possible to prepare. Very pure silver recrystallizes at room temperature. Copper has little effect on

grain size and on the appearance of the intermediate directed orientations of silver; iron, nickel, and especially lead, increase grain size, and zinc decreases it. The recrystallization positions of grains are not so perfectly directed in the presence of the metals. Thus, for the first time is it possible to have a quantitative idea of the metallurgical importance of very small amounts of impurities. In every case addition of larger amounts has little or no effect as compared with the introduction of the first traces.

(4) *The Recrystallization of Iron.*—Both brass and iron (body-centered cubic) behave somewhat similar to silver when rolled

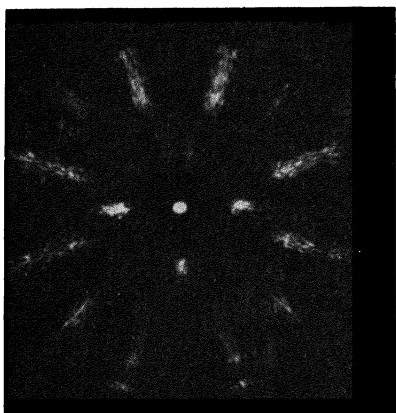


FIG. 196.—Pattern showing very high degree of preferred orientation in recrystallized copper sheet.

and annealed. For iron rolled 97 per cent and heated above  $600^{\circ}$  there is an orientation so that the  $[350]$  direction is parallel to the rolling plane, while the cold-rolled metal is characterized by a  $[110]$  direction. Figure 195 shows a series of patterns for low-carbon steel subjected to various heat treatments; of particular interest are the new recrystallization orientation and the fact that random orientation is obtained only after heating above the

upper critical point. Silver, brass, and iron, therefore, represent the second of the three recrystallization mechanisms.

(5) *The Recrystallization of Copper.*—When strongly rolled copper (99 per cent) is annealed, a new phenomenon is observed. The recrystallization structure shows a new orientation of grains with the cube faces parallel to the rolling plane. Copper of ordinary purity, after complete reduction by cold rolling, tends to recrystallize with a chaotic arrangement of grains; but if a first reduction of 50 per cent is made with hot rolls at  $600^{\circ}$  C., followed by cold rolling, the cubic recrystallization arrangement is so nearly perfect that the x-ray diffraction pattern indicates practically a single crystal (Fig. 196). The further remarkable fact is that this structure persists clear to the melting point. Not only does copper differ from silver (dependent, of

course, on the method of rolling) in an entirely different recrystallization orientation, but also in the fact that this never goes over to the random structure. It follows, therefore, that such a sheet has greatly different properties from one in which the grains are in disordered arrangement.

A comparison of the tensile strength, elasticities, and grain sizes of the two kinds of copper sheet is given in Fig. 197. Both the strength and elasticity of the sheet with cube-face (oriented) grains are smaller than those of the random sheet. Czochralski has found that these properties are minimum in the direction of the cube edge, as is true here, while physical properties of the ordinary sheet are an average (higher) of all directions. The oriented sheet, however, is more resistant to corrosion than the random.

The effects of impurities as ascertained by Widmann from x-ray patterns are as shown in accompanying table.

Element	Impurity		Recrystallization temperature, degrees Centigrade
	Weight, per cent	Atomic, per cent	
Electrolytic copper, unmolten.	.	.	205
Electrolytic copper, melted			250
Tin	0 24	0 129	375
Silver	0 24	0 14	340
Lead.	0 15	0 046	325
Manganese	0 23	0 267	320
Phosphorus	0 36	0 73	325
Cadmium	0 19	0 108	300
Antimony.. . . .	0 06	0 032	280
Sulphur . . . . .	0 21	0 42	275
Arsenic . . . . .	0 14	0 119	250
Nickel. . . . .	0 28	0 302	250
Gold	0 20	0 065	250
Silicon	0 06	0 13	245
Zinc. . . . .	0 33	0 32	220
Bismuth. . . . .	0 027	0 008	200
Iron. . . . .	0 21	0 24	190
Aluminum . . . . .	0 12	0 28	150
Cuprous oxide. . . . .	18 0	8 33	150

(6) *The Recrystallization of Silver-copper Alloy.*—In light of the foregoing results with pure silver and copper, it is interesting

to compare the x-ray results on sheets of an 80:20 silver-copper alloy.<sup>1</sup>

For a strip rolled down to 98 per cent, the tensile strength is 90 kg./mm.<sup>2</sup> as compared with 40 for silver and 50 for copper. After annealing at 800° the strength is only 30. The elongation of the alloy becomes noticeable only above 300° but approaches

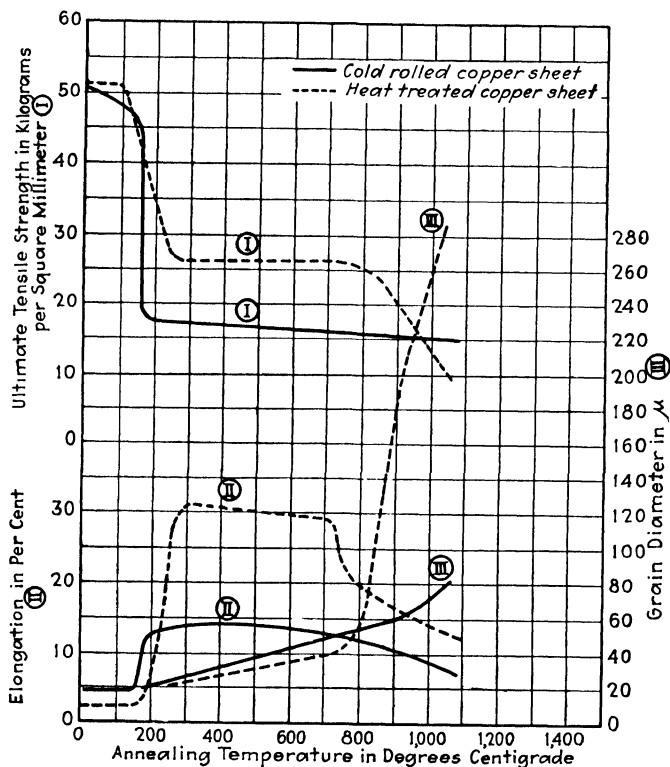


FIG. 197.—Tensile strength, elongation, and grain size of cold-rolled copper sheet (full lines) and of a sheet reduced 50 per cent by hot rolling and 50 per cent by cold rolling (dotted lines) as functions of annealing temperature. (Glocker and Widmann.)

that of silver (20 per cent) after treatment at 800°. While the softening and recrystallization lie in a range of only about 20°, the range in the alloy lies between 200 and 700° C. Mixed crystals, embedded in the eutectic and richer in copper, are brought out when the specimen is heated nearly to the melting point. Even heating for hours at 780° shows only a few of these

<sup>1</sup> GLOCKER and WIDMANN, *Z. Metallkunde*, **20**, 129 (1928).

crystals because the grains are smaller than  $2\mu$ ; at  $800^\circ$  the grains are five times larger but show no preferred orientation. The first evidence of recrystallization in the x-ray photographs appears at  $400^\circ$ , when some diffuse lines become sharply resolved into doublets. Unless the specimen is heated for hours above  $780^\circ$ , x-rays give the typical diagram of rolled silver.

*c. The Recrystallization of Wires.*—The drawing of metals into wires represents also a fibering of the grains but with a different mechanism which is somewhat simpler as previously explained. For all face-centered cubic metals (silver, copper, aluminum, gold, lead, etc.) a [111] direction, or cube-body diagonal, is parallel to the wire axis with every possible orientation of the cubes ( $360^\circ$  deg.) around the diagonal; for body-centered cubic metals ( $\alpha$ -iron, molybdenum, tungsten, etc.) a [110] or cube-face diagonal is parallel to this axis. In general, there are no intermediate new orientations of grains during recrystallization by heat treatment. Instead, the sharply localized intensity maxima in the diffraction patterns for the wires gradually become more indistinct with increasing temperature. The last traces of fibering are remarkably persistent and an entirely random arrangement is attained only after annealing near the melting point.

Sachs and Schiebold<sup>1</sup> have compared the x-ray diagrams and the tensile strength of a cold-drawn aluminum wire (1.18 mm.) after various annealing treatments. The treatments and tensile strengths are as follows:

	Kilograms per Square Millimeter
Original .....	24 4
$150^\circ$ , $\frac{1}{2}$ hr .....	18.7
$200^\circ$ , $\frac{1}{2}$ hr .....	14 3
$250^\circ$ } .....	11 0
$350^\circ$ } $\frac{1}{2}$ hr .....	
$550^\circ$ }	

The x-ray diagrams show a gradual increase in particle size with dots appearing on a continuous background of the diffraction rings at  $250^\circ$  and  $300^\circ$ ; at  $550^\circ$  there appear large spots, far fewer in number but still lying on rings. At  $150^\circ$  the interference maxima broaden, indicating a departure of the oriented particles from perfect alignment, but even after annealing at  $550^\circ$  strong evidences of fiber structure remain.

<sup>1</sup> *Z. Metallkunde*, **17**, 400 (1925).

An exception to the general effect of annealing, however, is observed with very pure aluminum wire.<sup>1</sup> It was been found that on heating hard aluminum wire (0.35 or 0.8 mm. diameter, 99.95 per cent pure) at 600° for 3 hr., recrystallization occurs with perfect unidirectional orientation of the grains with a [111] direction parallel to the wire axis. This orientation is the same as in the original cold-drawn wire, so that aluminum differs from copper in this respect, and, of course, from aluminum of lesser purity. The texture of the wire seems very nearly unchanged by the treatment, but the tensile strength has decreased from 20.6 kg./mm.<sup>2</sup> to 3.5, and the elongation has changed from 1 to 5 per cent (single crystal wires 20 per cent). Here it is clear that the grain orientation is not the only factor governing elastic properties.

For aluminum-silicon alloy wires, the strength decreases from 26.5 to 15.6 kg./mm.<sup>2</sup> after heat treatment, the elongation increases from 2 to 17 per cent, but the grain orientation and texture indicated by the x-ray pattern are unchanged.

The single case of intermediate recrystallization preferred orientation is with deeply drawn copper wire annealed above 1000° C.<sup>2</sup>

The new orientation is with a [112] direction, instead of [111] parallel to the wire axis. This observation is further substantiated by Tammann and Meyer who counted in a cross section the following orientations of faces: (111) 27 per cent, (101) 12 per cent, (100) 61 per cent; whereas theoretically for chaotic arrangement the proportions are respectively 38, 40, and 22 per cent. Such a wire acts as a single crystal as compared with ordinary wires with random orientation. Following are the comparative data:

Treatment	Tensile strength, kilograms per square millimeter	Elasticity, per cent
Original . . . . .	49 3	1
300° . . . . .	24.4	30
800° . . . . .	23.9	23
1000° (3 hr., oriented) . . . . .	21 3	17

<sup>1</sup> SCHMID and WASSERMANN, *Z. tech. Physik.*, **9**, 106 (1928).

<sup>2</sup> SCHMID and WASSERMANN, *Z. Physik.*, **40**, 451 (1926)



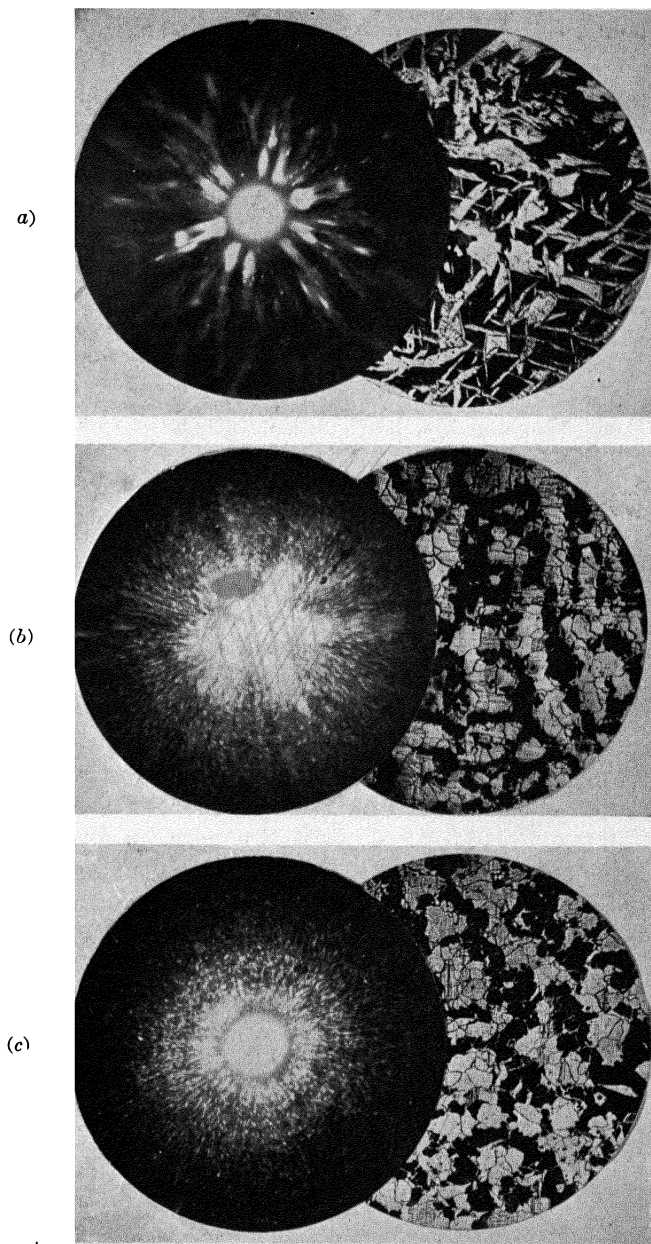


FIG. 198.—Diffraction and microscopic studies of annealing of cast steel. (a) Original structure, as cast, showing internal strain; (b) commercial anneal, showing incomplete removal of detrimental structure; (c) ideal annealed structure of same steel.

In general the x-ray study of wire annealing is not quite so satisfactory as that of rolled foils. Studies on crystalline wires of zinc and tin by Polanyi and his associates prove that often the change in mechanical properties and recrystallization evidence in x-ray patterns do not run parallel, since under certain conditions of original cold working and annealing these crystals may soften without evidence of recrystallization.

**2. Annealing of Cast Steel.**—Figure 198 shows the structures of cast steel as cast with large internal strain, of this steel annealed according to commercial practice, and of the same steel with an ideal structure obtained by the selection of correct temperature and time of heat treatment through the agency of x-ray diffraction patterns. One of the great manufacturers of castings was annealing large steel pieces for 6 hr. at a somewhat indefinite temperature. A short x-ray investigation proved beyond question that the correct temperature of annealing could be determined within  $\pm 10^\circ$ , and that under these conditions a greatly improved structure was obtained not in 6 hr. but in  $\frac{1}{2}$  hr. The economic value of such a single discovery is at once evident in speeding production twelvefold without additional expense. Such examples in this general field of heat treatment for the removal of strains and directional properties might be multiplied many times.

**3. Magnetic Properties as a Function of the Structure of Silicon Electric Steels.**—Figures 199 to 204 reproduce again the first series of pinhole diffraction patterns ever made for silicon steel strips with varying magnetic hysteresis loss as noted. If the grain boundaries have not been unduly thickened by overheating in the annealing furnace, the magnetic loss may be calculated empirically from the number and size of diffraction spots on a given area of the various patterns. Occasionally some strips may be unusually brittle and have unaccountably high loss. In every case an x-ray examination proves that the large single grains have an extraordinary orientation of crystallographic planes with respect to the surface of the sheet due to an uncontrolled factor in the rolling or annealing operation. In the ordinary case it will be remembered that iron grains in a rolled sheet are oriented with a [110] direction parallel to the direction of rolling and (100) planes in the surface of the sheet. The Epstein test for measuring magnetic loss usually employs one hundred or more strips and an average value is, of course, meas-



FIG. 199.—Transformer, steel, hysteresis loss 0.8636 watt/lb.

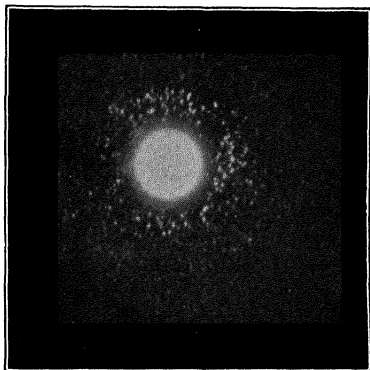


FIG. 200.—Transformer steel, hysteresis loss 0.8181 watt/lb.

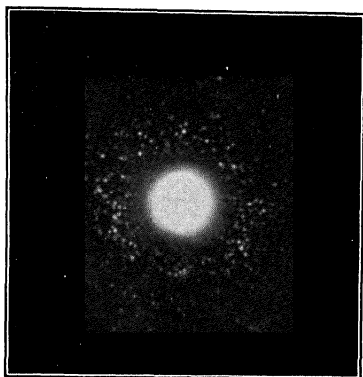


FIG. 201.—Transformer steel, hysteresis loss 0.8068 watt/lb.

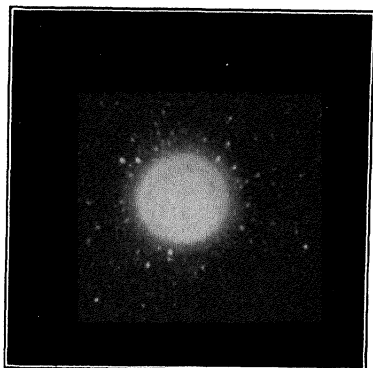


FIG. 202.—Transformer steel, hysteresis loss 0.7727 watt/lb.

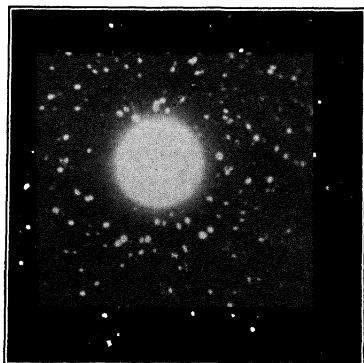


FIG. 203.—Transformer steel, hysteresis loss 0.6331 watt/lb.

ured. On several occasions in the writer's laboratory it has been possible by single patterns to separate a bundle into at



FIG. 204.—Transformer steel, hysteresis loss 0.5535 watt/lb.

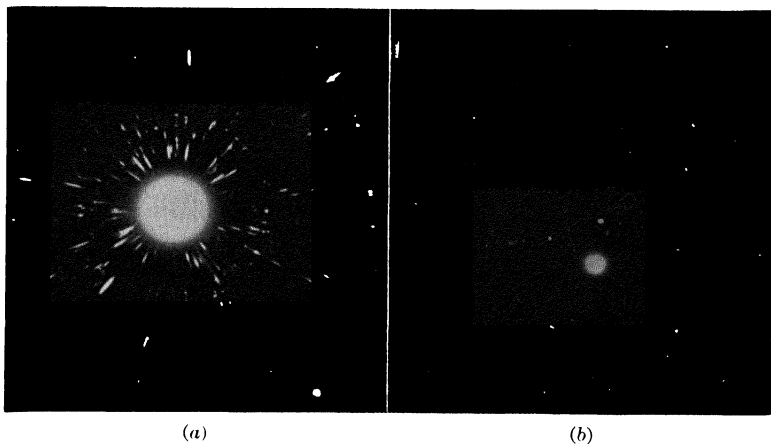


FIG. 205.—Comparison of grain perfection in silicon electric steel. (a) Supposedly superior grade as now produced commercially showing imperfect grains; (b) specimen free from strain produced by simple technique.

least five groups, two with a lower loss, two with a higher, and one with the same average loss of the whole original bundle.

More important from the standpoint of magnetic properties than grain size is grain perfection, *i.e.*, freedom from all strain. This has been amply demonstrated in recent extensive experiments in the writer's laboratory. The x-ray pattern is the only guide to establishment of the correct rolling and heat treatment which will insure grain perfection. Figure 205a shows the pattern of supposedly highest quality silicon steel commercially produced in 1932, while Fig. 205b shows the result of remarkably simple technique, derived with the help of x-ray control, from the same raw material. The magnetic properties of the latter as well as ductility are markedly superior and scientific control of production is easily possible by regulation of the silicon content, percentage cold reduction, without intermediate anneal, time and temperature of annealing, extent of a further pinch pass, and final heat treatment. New mills with small rolls enable cold rolling of the silicon steel successfully for the first time. Since silicon steels represent large-grained aggregates, the x-ray diffraction patterns are characterized by a random peppering of spots rather than definite rings. Hence it would appear to be impossible to discover by ordinary diffraction methods whether there is any tendency toward preferred orientation of these large grains throughout a sheet. Recourse is then taken to the simple device of slowly moving the specimen in its own plane across the pinhole by a suitable mechanical device during the exposure. The resultant pattern is an integration over a large number of grains instead of the few contained in only a certain area traversed by the x-ray beam in the stationary sample. If there is a preponderance of orientations in any one direction, a definite concentration of spots will appear, just as localized intensity maxima indicated preferred orientation on the interference rings for small-grained specimens. The indications are that some such preferred orientation may actually be beneficial for certain magnetic properties.

Further studies will lead undoubtedly to the production and selection of steel for electrical purposes with such lowered magnetic loss and superior permeability that the size of electrical machinery for a given load may be reduced appreciably.

**4. The Stages of Reduction and the Effects of Variables in Commercial Cold Rolling of Sheet Metals.**—The fundamental investigations of the types and degrees of preferred orientation produced in metal sheets by cold rolling have been considered

in the preceding chapter. However, the *course* of changes in crystal fragmentation and orientation during successive stages in the rolling process and the effect of variables in the raw material and in the technique of rolling upon the establishment of the

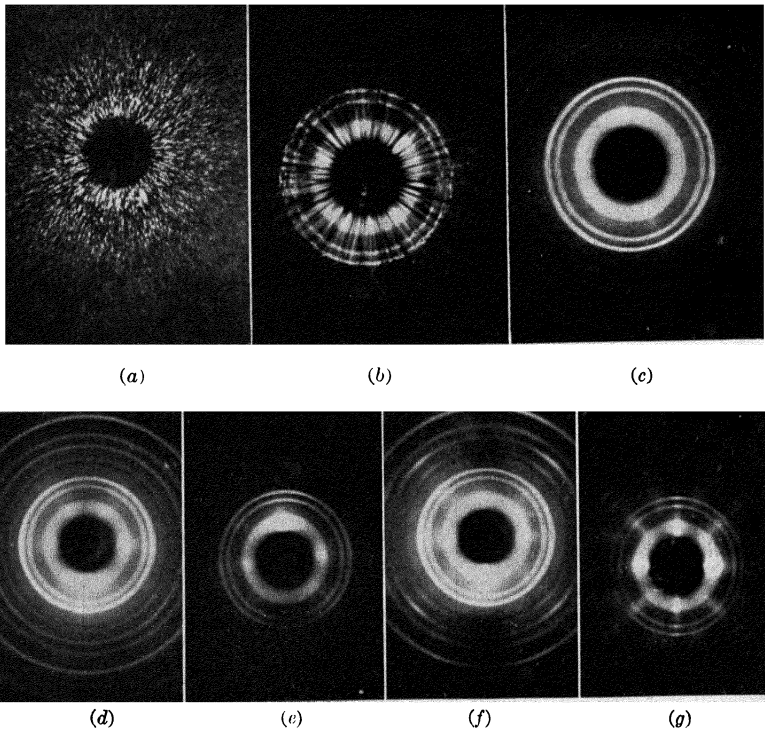


FIG. 206.—Changes in structure with steps in rolling of low-carbon sheet steel. (a) Hot-rolled strip; (b) one pass, 7 per cent reduction; (c) 9 passes, 47 per cent reduction; (d) 14 passes, 71 per cent reduction; (e) 19 passes, 85.5 per cent reduction; (f) 21 passes, 90 per cent reduction; (g) 30 passes, 97 per cent reduction.

ultimately attained preferred orientation are of greater commercial significance. Clark and Sisson have made a long series of studies of these problems for various metals as follows:

A. Percentage reduction and its relation to various factors.

1. Structure.
2. Power requirements.
3. Hardness.
4. Amount of distortion as disclosed by the resolution of the x-ray  $K\alpha$ -doublet.
5. Type and degree of orientation.

**B. Effect of variables in original material on structures.**

1. Grain size.
2. Thickness.
3. Carbon content.

**C. Effect of rolling variables upon structure.**

1. Roll diameter.
2. Speed of deformation.
3. Reversal of strip.
4. Percentage reduction per pass.

**D. Effect of deformation due to combined tension and compression.**

1. Applied tension during rolling.
2. Effect of stretching followed by rolling.
3. Drawing of flat sheets.
4. Rolling of drawn wires.
5. Rolling at various angles.

The scope of these data is obviously far too extensive to permit presentation of results here except for a few points of especial interest.

*A. Structural Changes with Successive Reductions.*—The change in x-ray patterns with successive reductions is best represented by Fig. 206*a* to *g* for low-carbon steel, selected from a series of 84 samples. Here the x-ray beam passed perpendicular to the rolling direction and to the surface of the sheet.

Figure	Pass	Gage, inches	Percentage reduction	Pattern
175 <i>a</i>	0	0.158 (hot-rolled strip)	0	Large random grains
175 <i>b</i>	1	0.1475	7	Fragmentation below 35 $\mu$ and appearance of rings
175 <i>c</i>	9	0.084	47	Nearly complete fragmentation, random
175 <i>d</i>	14	0.046	71	Appearance of six-point fiber pattern characteristic of drawing
175 <i>e</i>	19	0.023	85.5	Passing from six- to four-point pattern
175 <i>f</i>	21	0.0165	90	Typical rolling pattern
175 <i>g</i>	30	0.005	97	Perfected orientation

From a whole series of steel samples the following average results were obtained:

Appearance of	Per Cent Reduction
Continuous rings (fragmentation). . . . .	27
Sharp rings. . . . .	38
Six-point fiber pattern . . . . .	54
Four-point fiber pattern . . . . .	76

Such values, of course, are greatly dependent on type of mills, chemical composition, thickness, grain size, and orientation in the original material.

These results confirm those of Tammann who found that in rolling two clearly defined changes in crystal orientation can be distinguished; the first in which the force due to rotation of the rolls acts as a stretching force (six-point x-ray pattern), and the second in which the action of the rolls is similar to that of simple compression and exerts the greatest influence on the final orientation in cases of large reductions.

*B. Effect of Initial Grain Size.*—Grain size has considerable influence upon the structure of cold-rolled steel during early stages of reduction but after large reductions the effect is lost. The smaller the initial grain size, the less cold work is required to produce fibering (see also topic 16, page 418).

*C. Effect of Initial Strip Thickness.*—The degree of fibering depends not only on the percentage reduction but also on the initial strip thickness. A sample reduced from 0.08 to 0.01 in. does not show the same degree of preferred orientation as one reduced from 0.04 to 0.005 in., although both have received 87.5 per cent reduction.

*D. Effect of Carbon Content.*—Most of the previous work on preferred orientation in cold-rolled sheets has been carried out on pure metals. In steels the pearlite is hard and more brittle than ferrite and concentrates at the junctions of the ferrite grains with the result that when pearlitic steel is cold rolled gliding takes place only in the ferrite. During the rolling process the pearlite is dispersed while the soft ductile ferrite forms a plastic bond which is not oriented, so as to form a straight fiber structure but is curved around the pearlite particles. The x-ray pattern, therefore, gives the appearance of random arrangement for high-carbon steels.

*E. Effect of Rolling Variables.*—(1) The roll diameter has less effect on final structure than the total percentage reduction. The smaller the rolls, the greater is the angular divergence of



the grains laterally in the rolling plane from the ideal preferred direction, while large rolls tend to produce more divergence

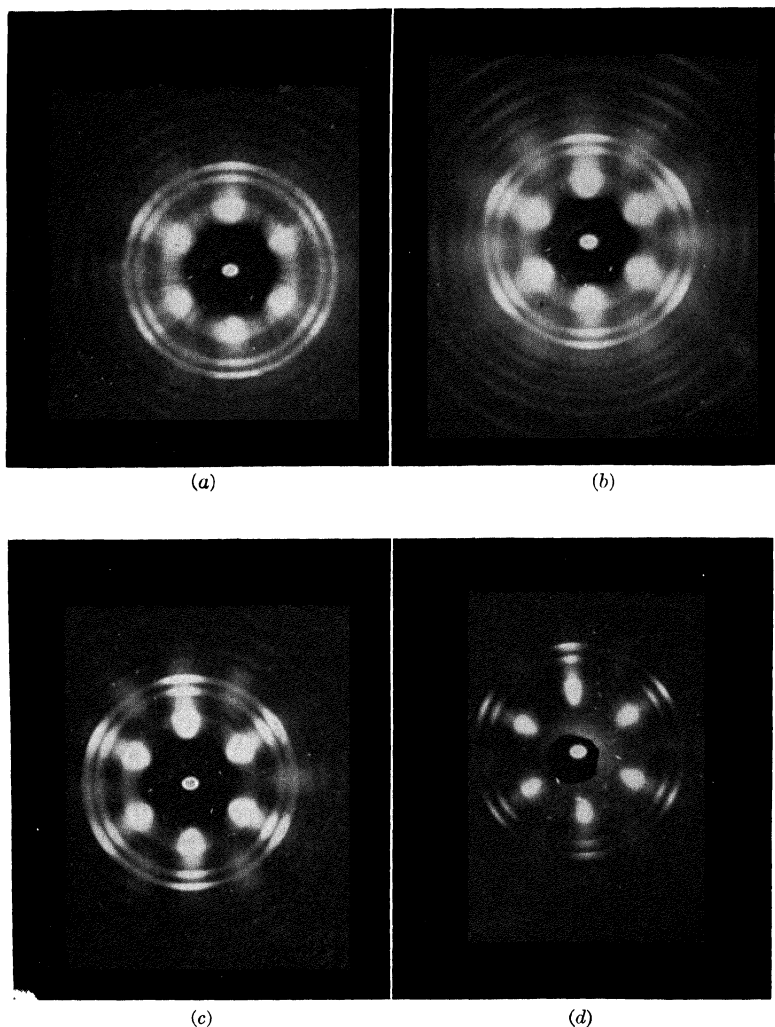


FIG. 207.—Patterns for sheet steel, made with x-ray beam perpendicular to rolling direction and parallel to rolling plane, from which amount of cold work may be calculated. Percentage reductions: (a) 16; (b) 36.5; (c) 53; (d) 85.

normal to the *rolling* plane. Numerous other small differences may also be quantitatively ascertained, particularly for early and intermediate stages of reduction.

(2) With small rolls the same structure is obtained at speeds from 70 to 800 ft. per minute, and with unidirectional or reversed passes through the rolls.

(3) Various combinations of tension and compression of the sheets have been studied in detail, both experimentally and with vector theory. Fiber structures are ultimately obtained but the appearance of the four-point pattern characteristic of compression can be greatly delayed by application of tension.

(4) Interesting results are obtained by rolling metals in all directions (random), at 90 deg. (very perfect fibering), 60 deg. (six-point instead of four-point patterns), etc.

(5) An x-ray method of determining the amount of cold rolling to which a sheet has been subjected. In the usual method of taking x-ray diffraction patterns of cold-rolled sheets, the x-ray beam passes perpendicular to both the rolling direction and the plane of rolling. Preferred orientation may appear only after 60 to 70 per cent reduction, depending on the type of mill and original material variables. If the beam is made to pass through the material perpendicular to the rolling direction and *parallel* to the rolling plane (edge-on of the sheet), evidence of preferred orientation is obtained after 15 to 30 per cent reduction, depending upon the above mentioned variables. This orientation gives a six-point fiber pattern similar to that for cold-drawn wires. Instead of the pattern changing to a fourfold pattern upon further reduction as is the case when the beam is normal to the rolling plane, the type of pattern remains the same. However, as the percentage reduction increases, the intensity maxima become sharper, as illustrated in Fig. 207 for 16, 36.5, 53, and 85 per cent reduction. If the percentage reduction is plotted against the sine of the angle of arc formed by the intensity maxima on the broad inner band of the pattern, a straight line is obtained. For a large number of specimens this relationship has been found accurate within a maximum of 10 per cent.

In certain cases it has been possible even to determine very small amounts of cold work such as roller leveling after annealing, by careful examination of the x-ray patterns (elongation and splitting of interference spots).

**5. Structure of Welds.**—Figure 208 shows the comparison of a weld of the same steel made by the ordinary arc method and by the hydrogen-atmosphere method. The former is char-

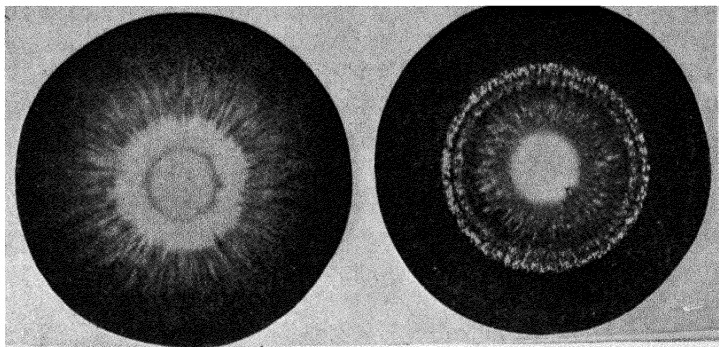


FIG. 208.—Comparison of structures of steel welds. Left, ordinary arc method; right, hydrogen-atmosphere method.

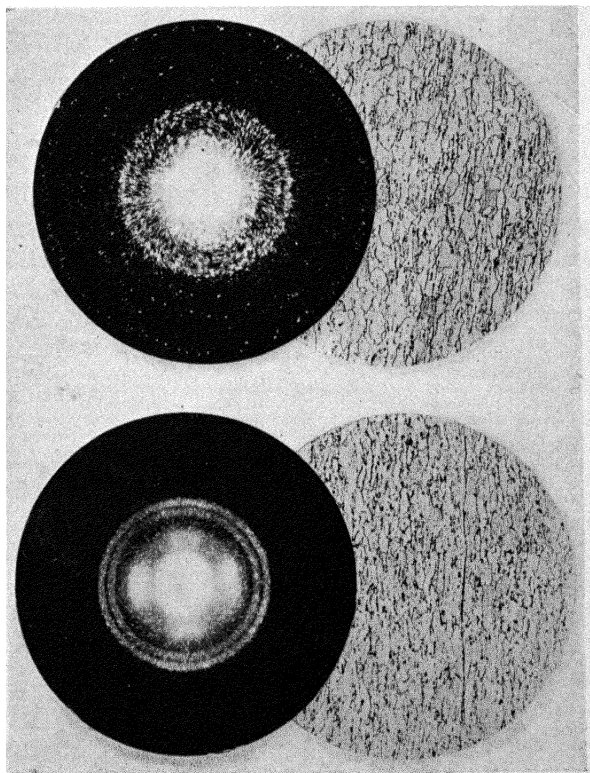


FIG. 209.—Diffraction patterns and photomicrographs for satisfactory (above) and unsatisfactory (below) forming steels. Note residual rolling structure in the latter.

acterized by very small, highly distorted grains (radial striations), and the latter by much larger, random unstrained grains with requisite strength and ductility.

**6. Forming Steels.**—One of the great contributions has been to define specifications in terms of structure for forming steels, especially since unstrained and random properties are essential. Patterns and photomicrographs for supposedly four grades of forming steel, soft, quarter hard, half hard, and hard, demonstrate that there are only two grades essentially. Satisfactory and unsatisfactory forming steels are easily differentiated by the patterns in Fig. 209. The latter retains a residual preferred orientation of grains introduced in the original rolling; hence the annealing has been entirely inadequate and failure in the forming operation can be predicted definitely from such a pattern. Figure 210 demonstrates the structure of a sheet after successful forming and explains why another sheet failed.

**7. Forming Copper.**—Phillips and Edmunds have demonstrated that hard-rolled copper has a pronounced fiber structure with  $[353]$  as the fiber axis, instead of  $[112]$  as found by others, and  $(110)$  planes in the surface. A preferred orientation is found in the annealed sheet which forms ears on cupping, while that which forms without ears has random orientation. The formation of ears in drawn copper is avoided by the limitation of rolling reduction to 65 per cent and annealing at 500 to 600° C.

In general, all sheet metals which fail in forming operations show evidences, by the extremely sensitive diffraction method, of residual fibering which the annealing treatment has not removed, or a new recrystallization orientation, such as is commonly found for copper shown in Fig. 196.

**8. Neumann Bands in Ferrite.**—Mathewson and Edmunds in a remarkable x-ray study by the Laue method have definitely settled the long controversy over the origin of these bands by proof of twinning along planes of the form  $[211]$ .

**9. Passive Metals.**—An interesting application has been the attempt to investigate passive metals upon the assumption that a very thin layer of oxide is the cause. Krüger and Nähring, for example, give results of the x-ray examination of finely powdered passive iron, nickel, and chromium by the Debye-Scherrer and Bohlin-Seemann methods. In no case does the photograph show lines corresponding with a known or unknown oxide of the

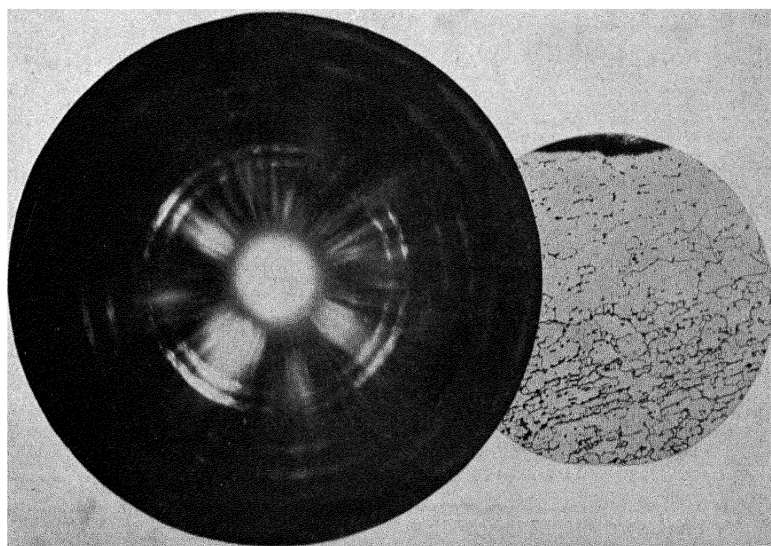
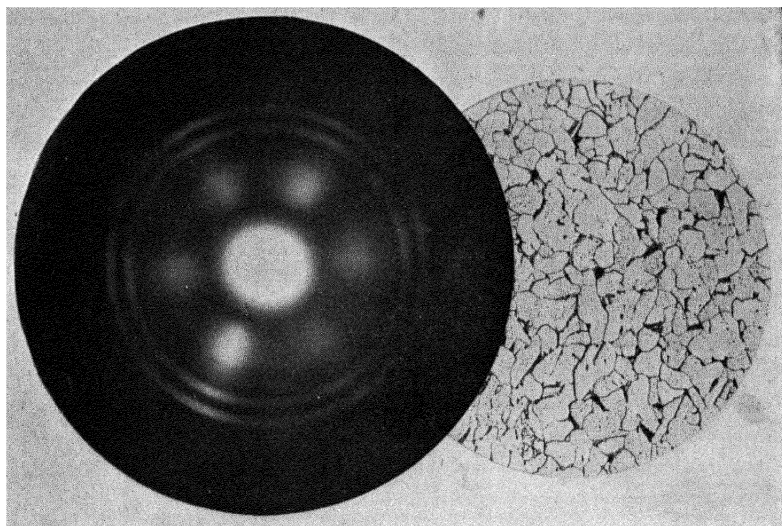
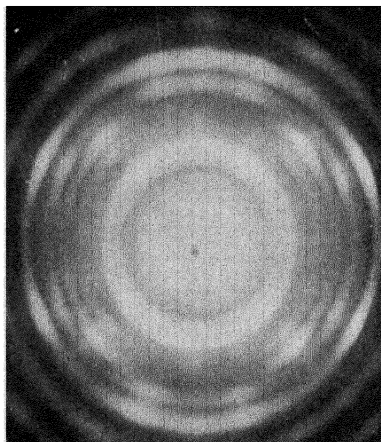
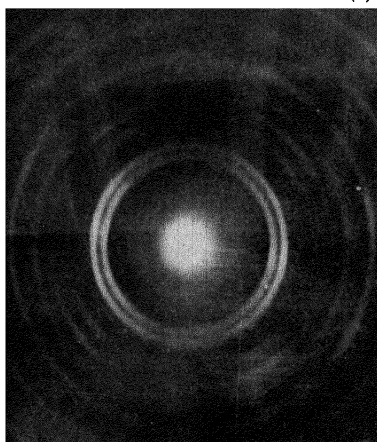


FIG. 210.—Structures of forming steels after forming. Above, satisfactory; below, unsatisfactory.

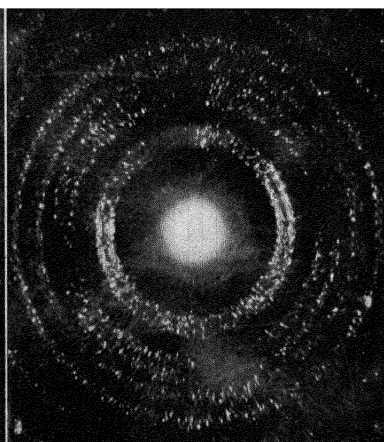
metal, although these should be apparent if the oxide layer  $10^{-7}$  cm. in thickness were present. These results are not in agreement with the view that solid layers of oxide are present on these metals in the passive state. The existence of a molecular layer



(a)



(b)



(c)

FIG. 211.—Patterns for molybdenum ribbon used in electric resistance furnaces. (a) Cold rolled in the United States; (b) cold rolled, German process; (c) ribbon after use in furnace, showing marked grain growth.

of oxygen, which Tammann suggests may cause passivity—the free valencies of the metal at its surface being saturated by oxygen atoms, while the metal lattice remains unchanged—would not be detectable by x-ray examination.

**10. Changes in Electric Furnace Resistor Ribbon.**—Figure 211 shows the patterns of two types of cold-rolled molybdenum ribbon used in resistance furnaces, and another which demonstrates what happens after short usage—a very large growth of grains.

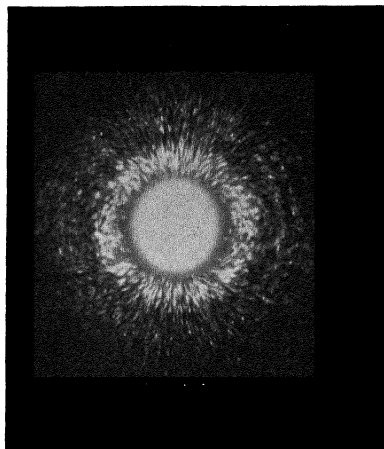
**11. Crystal Structure of White-fractured and Reclaimed Malleable Iron.**—It is well-known that malleable iron suffers embrittlement when quenched from the blue-heat zone, but that this is prevented by quenching from just under the  $A_1$  point. This might be explained as due to changes in structure of the ferrite grains or to grain boundaries. The x-ray diffraction pattern of normal black-fractured malleable shows spotted rings indicating random orientation of fairly large grains, and considerable strain as shown by the radial asterism streaks. Malleable iron embrittled by quenching from  $460^\circ$ , that quenched from  $650$  to  $700^\circ$ , that embrittled by quenching from  $450^\circ$  and reclaimed by quenching from  $700^\circ$ , the same plus an additional quench from  $450^\circ$  which produced no embrittlement, all gave nearly identical diffraction patterns. The explanation of observed properties is evidently related to the grain boundaries which under the experimental conditions were not registered.

**12. Comparison of Effects of Twisting and Bending Steel Wires.** (0.60 per cent carbon, annealed at  $1200^\circ$  F.).—The original structure of the wire is shown in Fig. 212 together with the patterns, respectively, after 38 twists and 10 bends. Grain fragmentation begins with the first twist and reaches a maximum between 3 and 5 twists, followed by a much more gradual effect. After 13 twists the beginning of fibering or preferred orientation is evident, and this is quite marked for the case of 38 twists.

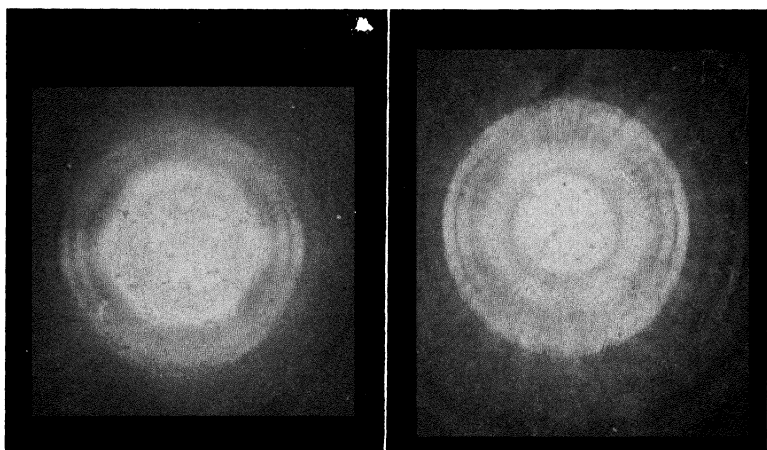
For the bending tests the wire was bent through an angle of  $90^\circ$  and returned to its original position. The next bend was made in the opposite direction, the third like the first, etc. Severe grain fragmentation begins with 1 bend, since the pattern is more diffuse. Two bends were equivalent to 13 twists in this respect; 3 bends introduces preferred orientation which becomes more perfect up to the breaking point. The bending test, therefore, is much more severe.

**13. The Effect of Constitution on the Structure of Wires Drafted and Annealed (Basic Open-hearth and Acid Bessemer Steel).**—Two series of steel wires of the same analysis essentially (carbon 0.10 per cent), except for phosphorus (0.018 (A) and

0.102 (*B*)), were studied. Among many interesting differences in behavior are the following: under identical conditions after drafting 10 per cent and annealing at 1300° F. for 1 hr., recrystallization has begun in *A*, but not at all in *B*; with 15 per cent



(a)



(b)

(c)

FIG. 212.—Patterns showing effects of twisting and bending on steel wire. (a) Original; (b) after 38 twists; (c) after 10 bends.

drafting and annealing at 1100° F. for 1 hr., recrystallization in *A* is nearly complete with very large grains but not perfectly random, while in *B* a very much smaller grain size and larger residual fibering is shown. Both produce random recrystalliza-



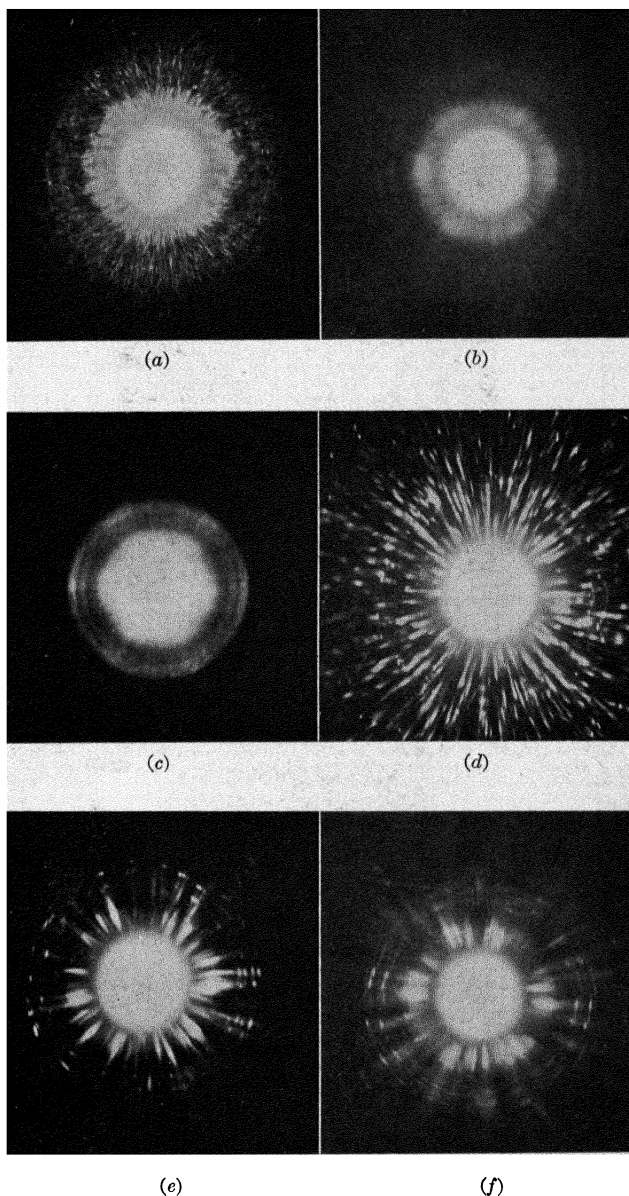


FIG. 213.—Comparison of effects of drawing reduction on steel with small and large initial grains. (a) Original (small grains); (b) after 5 per cent reduction; (c) after 15 per cent reduction; (d) original (large grains); (e) after 5 per cent reduction; (f) after 15 per cent reduction. Compare (a) and (d), (b) and (e), (c) and (f).

tion for 15 per cent drafting and annealing at 1200° F. for 1 hr., but the grain size of *A* is still appreciably greater than that of *B*. After annealing temperatures of 1600° F. complete recrystallization occurs in both with random distribution and freedom from distortion. The impurities in Bessemer wire clearly tend to

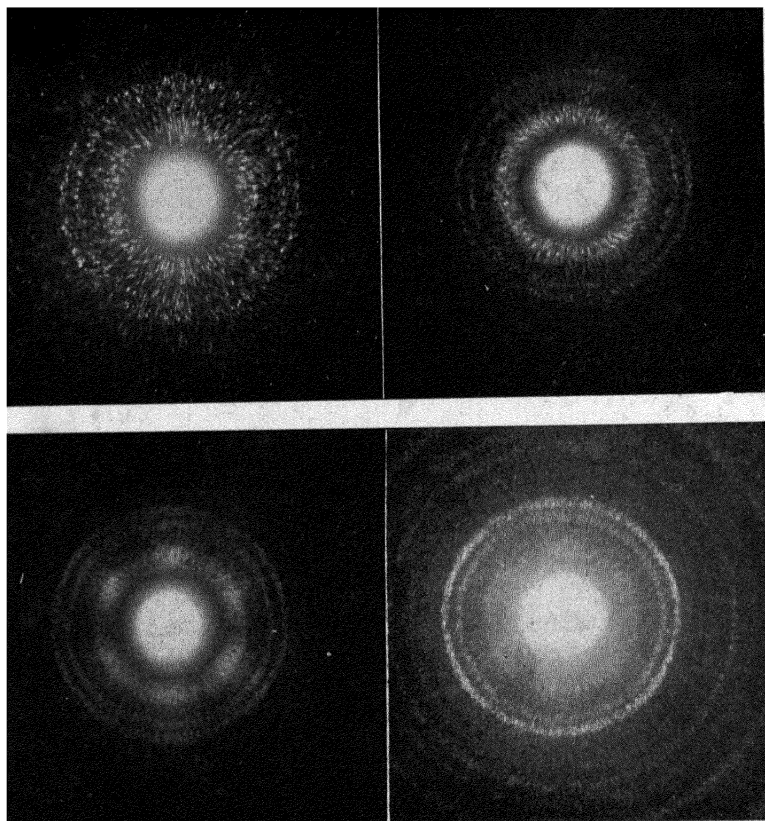


FIG. 214.—Patterns from specimens in same lot of 0.10 per cent carbon Bessemer continuous mill rod, showing non-uniformity of structure.

retard grain growth and to retain directional properties introduced in cold working.

**14. Effect of Carbon Content on Annealing.**—X-ray studies of 0.06, 0.19, and 0.34 per cent carbon steel wires drafted similarly and annealed at the same temperatures for the same length of time prove that increasing carbon increases sluggishness in recrystallization, causes smaller but less distorted grains. In

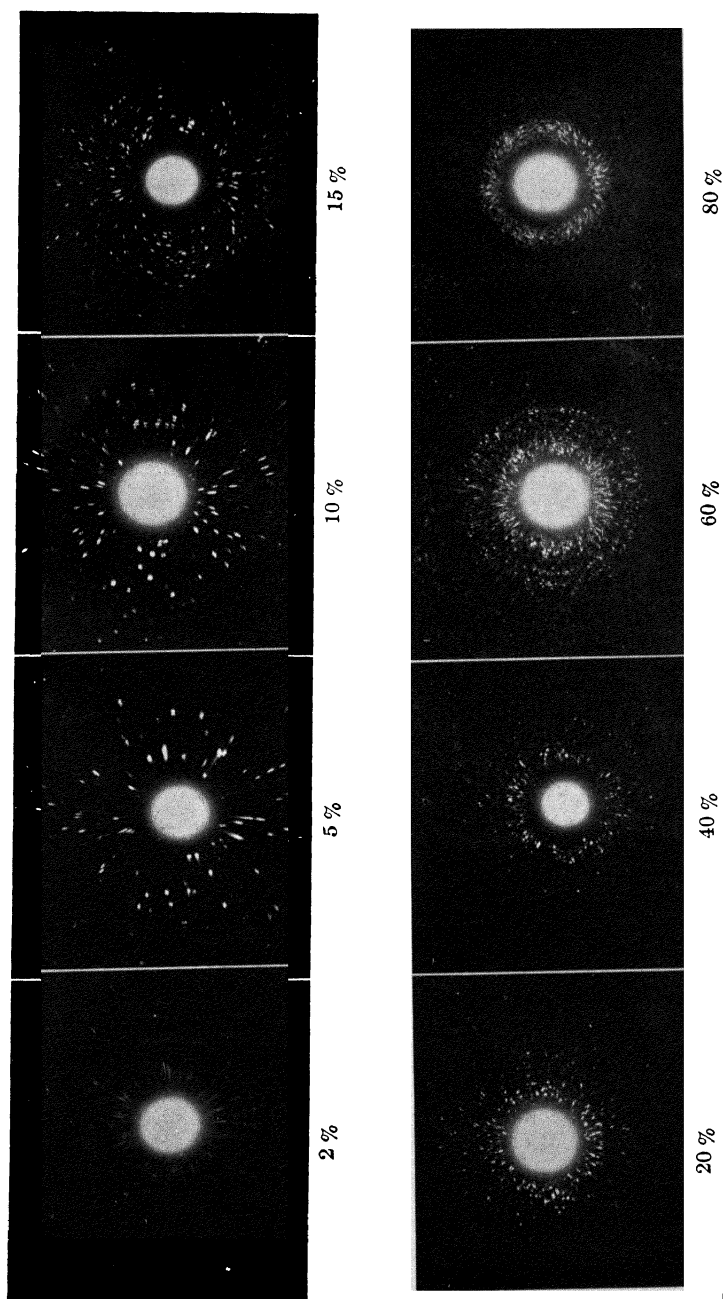


Fig. 215.—Effect of annealing at 1200° F. on low-carbon steel sheet with various reductions by cold work (compare with Fig. 216).

a similar way it has been possible to define in every case the temperature at which recrystallization begins after a given drafting or reduction in area by cold work, the temperature at which good annealing occurs, with removal of strain and directional properties due to original cold work, the grain size resulting from a given treatment, etc.

**15. Effect of Grain Size on Plastic Deformation.**—With ordinary low-carbon basic open-hearth steel wire, a large-grained sample may be drawn as much as 15 per cent without suffering complete grain fragmentation or noticeable preferred orientation, whereas the fine-grained sample will show on its diffraction pattern definite fibering with only 5 per cent reduction. These facts are shown in Fig. 213.

**16. Non-uniformity of Production.**—Many examples of this might be presented. In Fig. 214 are shown the patterns for four samples of Bessemer steel and from the same continuous mill, selected from various coils. The differences require no comment.

**17. The Relation between Reduction, Temperature of Annealing, and Structure.**—Two beautiful series of patterns are reproduced. Figure 215 is for a constant annealing temperature of 1200° F. with successive reduction of low-carbon sheet of 2, 5, 10, 15, 20, 40, 60, and 80 per cent. Figure 216 is for 1500° F. temperature of annealing for the same specimens. These patterns constitute a splendid standard. The most marked effect is the difference between the temperatures of 1200 and 1500° on the specimen reduced in cross-sectional area by 2 per cent. At the lower temperature no recrystallization occurs, while at the higher so great is the change that only a single grain of iron is in the beam.

Relationships between these three variables can best be shown by a three-dimensional diagram such as represented in Fig. 217 which shows readily how research on a given metal can lead to a thorough scientific method of heat treatment rather than an entirely empirical one. In this figure, the variable which may be determined from x-ray data in this case is grain size, though any other property might also serve. It proves that the final annealed structure of a sheet which has been cold-rolled to 90 per cent reduction without intermediate anneals must be different from that of the sheet which has been rolled down in steps with intermediate anneals. Each of these in effect places the specimen back at 0 per cent reduction. The diagram

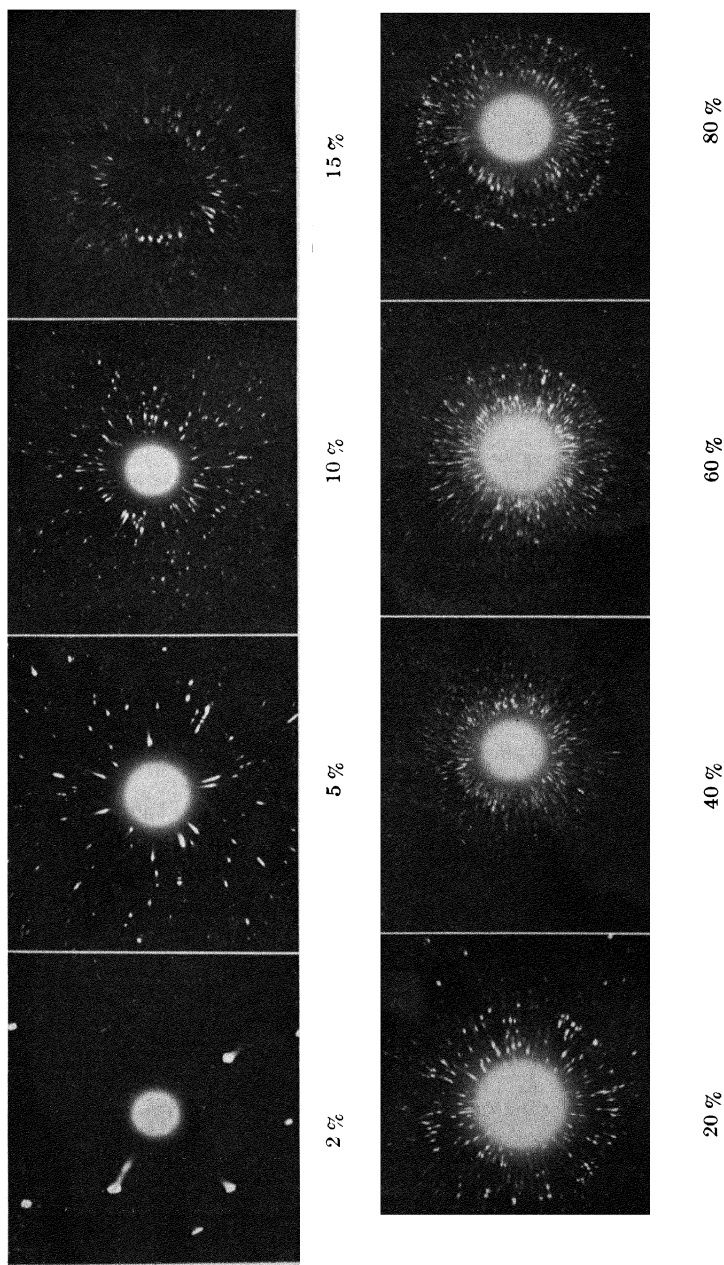


FIG. 216.—Effect of annealing at 1500° F. on low-carbon steel sheet with various reductions by cold work (compare with Fig. 215).

shows also that if very large grains are desired following a complete cold reduction, the specimen is annealed, giving the size characteristic for the reduction at the right of the diagram, then given a pinch pass or very small cold reduction so that the conditions on the left of the diagram are realized, and then again heat-treated.

### 18. Quench and Temper Structures of Carbon Spring Steels.—

Goss<sup>1</sup> has shown by x-ray patterns that these structures are quite independent of each other and that ill effects of distortion due to improper quenching cannot be removed by tempering, which

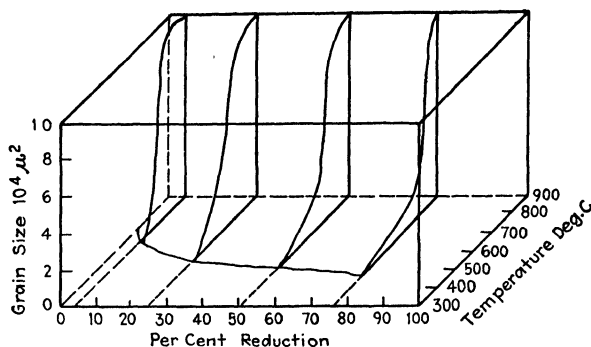


FIG. 217.—Three-dimensional diagram illustrating scientific control of recrystallization of cold-worked metals.

merely facilitates the precipitation of  $\text{Fe}_3\text{C}$  out of solid solution but does not change the as-quenched structure of the  $\alpha$ -iron matrix.

**19. Differentiation between Mechanical and Galvanic Gold Plating.**—The designation of gold-filled and plated objects such as jewelry is often subject to governmental regulation, particularly as to whether the gold layer is rolled or electrolytically deposited. Dehlinger and Glocker<sup>2</sup> have shown that these may be easily distinguished by x-ray diffraction analysis when other tests fail. The rolled filling or plating shows a fiber pattern and the electrolytic deposit a random arrangement of grains. Distinction can be made even after polishing or otherwise working an electrolytic gold layer, or after heat treatment and recrystallization.

**20. Problems of Fatigue of Metals.**—Comprehensive work in combining x-ray research with fatigue tests has not yet been

<sup>1</sup> *Trans. Am. Soc. Steel Treating*, **19**, 182 (1931).

<sup>2</sup> *Z. Metallkunde*, **21**, 325 (1929).

completed, although progress has been made and more should be expected. The chief difficulty has been in providing specimens sufficiently thin for x-ray analysis. As an example of such research some preliminary results are presented in Fig. 218 for steel rails, the diagram in Fig. 219 showing the location of samples. The ideal structure shown by No. 14 may be contrasted with No. 26 for example, which shows strain and actual

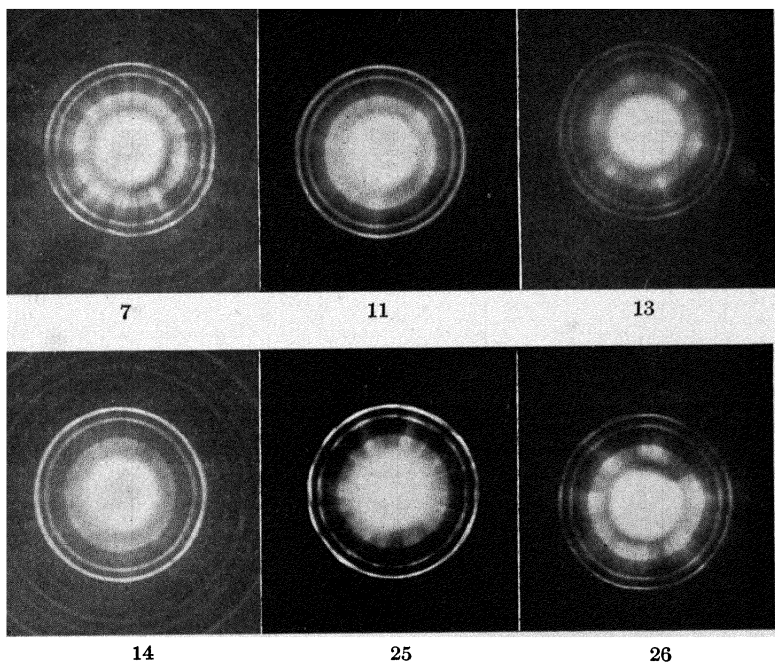


FIG. 218.—X-ray study of structure of steel rails, with numbers referring to location in rail in Fig. 219.

preferred orientation of grains. In such an area fissures usually occur, largely as a result of the varied structure in contiguous portions of the rail.

**21. The Examination of Very Large Specimens by the Back-reflection Method.**—In practically all of the examples cited in this entire book, the x-ray diffraction patterns have been made by transmission through the specimens carefully prepared by etching so as to introduce no spurious effects. But in industrial practice it is frequently desired to know the ultimate crystalline condition of a finished product or of a large specimen which cannot be cut up. For example, in steel rails, in aluminum alloy airplane pro-

pellers, and in very large steel structures such as oil stills where sound structure and freedom from strain are so essential for safety at high temperatures and pressures, such an examination of a fin-

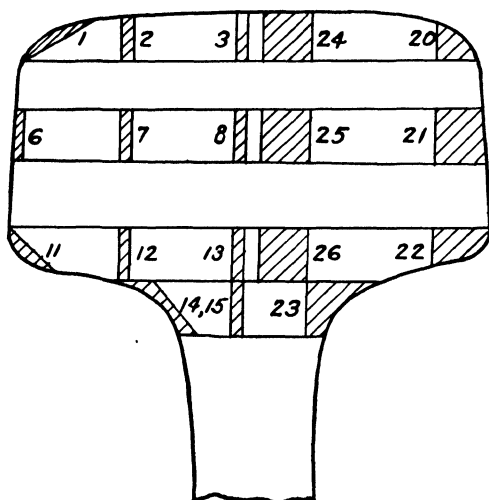


FIG. 219.—Diagram showing location of specimens subjected to x-ray examination for fine structure, some of which are presented in Fig. 218.

ished unit before installation would be invaluable. One method would, of course, consist in making hollow borings, with subse-

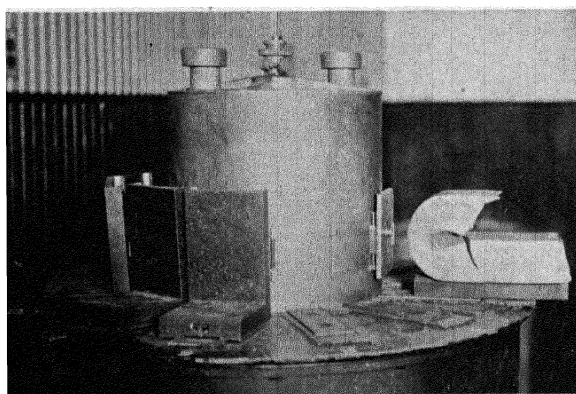


FIG. 220.—Experimental arrangement on General Electric diffraction apparatus for back-reflection method.

quent welding of the holes. However, the writer has deemed it advisable to try and develop a method in which the x-ray beam may be reflected from the surface. The method involving a graz-



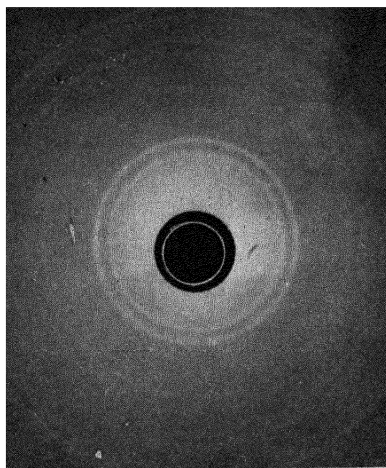


FIG. 221.—Back-reflection pattern from steel rail.

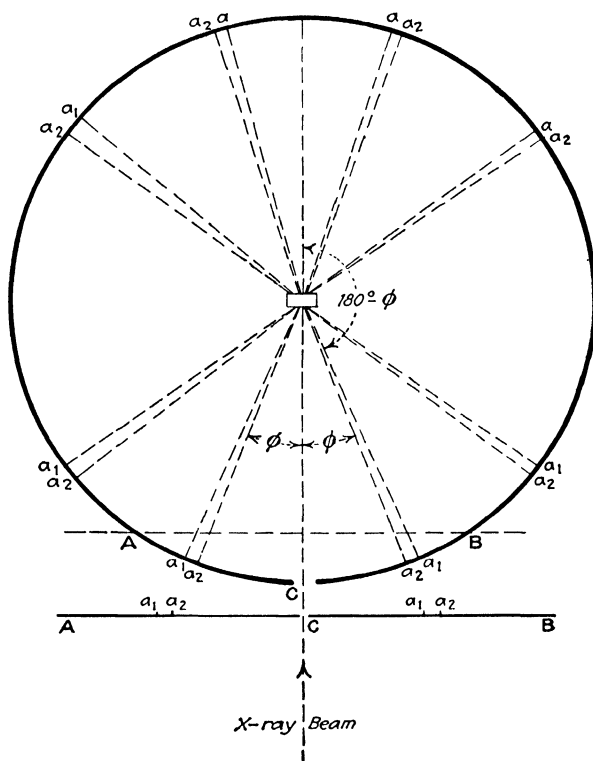


FIG. 222.—Diagram explaining diffraction interferences on film at ABC in back reflection.

ing angle of incidence as in Fig. 99, with such an apparatus as that shown in Fig. 87, is well-known and has been frequently used for fairly small specimens. Utilizing the usual equipment, however, it is necessary to reflect straight back from the surface of very large specimens as shown in Fig. 220. In this case, therefore, the photographic film is mounted *around* the pinhole and registers the patterns of rays diffracted directly back from the surface. A typical pattern from a steel-rail specimen is shown in Fig. 221. The concentric pairs of rings seem at first sight to be very familiar until it is noticed that the less intense line is inside of the stronger line of each pair. If these pairs represent resolution of the  $K\alpha$ -doublet of molybdenum, then in ordinary powder diffraction films, of course, the stronger  $K\alpha_1$  line comes inside the weaker  $K\alpha_2$ . This apparent reversal is, of course, readily explained by a consideration of Fig. 222. The photographic plate is at  $ACB$ . If a cylindrical film, as in the Debye-Scherrer method, were placed coaxial with the specimen, the primary beam passing through the specimen would strike the film at the top of the circle and the diffraction lines would appear as shown. The pattern in Fig. 221 is, therefore, to be read from the *outside in* towards the center, rather than from the center, as would be the case if the film were placed on the opposite side of the circle. These diffraction circles correspond, therefore, to lines appearing at the very end of usual spectra and hence to planes of relatively high indices. The analysis is as follows, the distance from sample to film being 3.5 cm.:

Radius of ring	$\phi$	$\Theta$	$\sin \Theta$	$\frac{h^2 + k^2}{l^2}$	Indices	$d_{hkl}$
1 475	22° 50'	78° 35'	0.98021	62	$\begin{Bmatrix} 3 & 7 & 2 \\ 5 & 6 & 1 \end{Bmatrix}$	0.363 A.U.
3 25	42° 52'	68° 34'	0.9308	56	$\begin{Bmatrix} 6 & 4 & 2 \end{Bmatrix}$	0.383
3 90	48° 6'	65° 57'	0.9132	54	$\begin{Bmatrix} 3 & 6 & 3 \\ 5 & 5 & 2 \end{Bmatrix}$	0.391

The method has the disadvantage, of course, that long exposure is required to develop sufficient intensity for these diffraction effects from sparsely populated but closely spaced planes.

However, large specimens of Armco iron with grains large enough to produce a spotted pattern by direct transmission also gave back-reflection patterns with large spots. On account of the large resolutions of the  $K\alpha$ -doublet the method should be useful for evaluating spacings very accurately and for following small changes due to solid solution.

## CHAPTER XIX

### THE STRUCTURE OF COLLOIDAL AND AMORPHOUS MATERIALS AND OF LIQUIDS

#### **X-ray Diffraction by Crystalline and Amorphous Substances.—**

It is now evident that crystals act as three-dimensional diffraction gratings for x-rays by virtue of the arrangement of the lattice units (atoms, ions, molecules, or groups of these) on sets of equidistant parallel planes. With a beam of monochromatic rays passing through a specimen, a pattern on a photographic plate is obtained, which is absolutely characteristic of the material—whether it is crystalline or amorphous, what are its crystallographic system and space-group defining coordinates in space, and the interplanar spacings, whether it is a single crystal or an aggregate, whether the aggregate has random or preferred orientation of grains, whether it is a single pure substance or is a mixture of two or more individuals or a solid solution, how large the grains or particles are or how thick a film, and whether there is distortion or strain. It follows that an amorphous substance would merely scatter x-rays in all directions and produce a general fogging of the photographic plate without evidence of diffraction interference maxima, whereas any kind of arrangement of ultimate units, even though very imperfect, would produce a diffraction pattern characterized by interference maxima. Even a single diffuse broad diffraction ring indicates at least an elementary tendency toward organization. One of the most remarkable facts from x-ray science is the extreme rarity of the true amorphous state. Repeatedly it has been found that a specimen, which by all ordinary methods of examination appears to be amorphous, produces unmistakable evidence of an organized ultimate structure under the searching scrutiny of radiation with wave lengths only  $1/10,000$  as long as ordinary light, by means of which microscopic examination is made. Even liquids produce diffraction halos indicative of transient arrangement of molecules governed by distances of nearest approach in their thermal agitation and designated by Stewart

as "cybotaxis." And just now results on diffraction halos from gases have given evidence of the true structure of atoms in the sense of the distribution of diffuse wave like negative electricity according to Heisenberg and Compton, instead of sharply corpuscular electrons moving in orbits as depicted by the Bohr theory.

**Diffraction by Colloids.**—A single crystal subjected to analysis by the pinhole method produces a Laue diffraction pattern characterized by a symmetrical array of spots, lying on a series of ellipses. As the size decreases and more individuals lie in the path of the beam, this symmetrical pattern gives way to a random "peppering" of spots. As the size decreases and the number increases still further, these small spots begin to assemble on a series of concentric rings. Finally the spots become so small and numerous that they merge into uniformly intense concentric rings, the so-called "powder" pattern. The maximum range of grain diameter over which these sharp rings are registered is from  $10^{-3}$  to  $10^{-5}$  cm. It is clearly evident that a sharp interference effect can take place only with a certain minimum number of parallel diffracting planes in each particle. As this number falls below the minimum, or, in other words, as the particle size decreases below about  $10^{-5}$  cm., it follows that interference is less perfect and that the diffraction rings (or lines by the Hull-Debye-Scherrer method) will become broader in proportion to decreasing size until in the neighborhood of  $10^{-8}$  cm. atomic dimensions are reached. These will merge and the pattern would be classed as amorphous. A measurement of line breadth in the colloidal range will therefore enable calculation of particle size as was illustrated fully in Chap. XVII. The question arises as to how small a particle can be and still produce a diffraction pattern upon which maxima may be detected. Levi in his study of metallic catalysts reports that particles only about five times as large as the unit crystal cell (in other words 10 or 15 parallel planes) will produce resolved diffraction maxima, even though these are very diffuse.

Now it must be noted that diffuse diffraction maxima must be the consequence of any crystal grating which is imperfect in the sense of having too few parallel planes, or of having these planes, ordinarily sufficient in number, distorted, bent, or imperfectly aligned. In other words, it is conceivable that an assemblage of fairly large colloidal particles might yield very diffuse

patterns simply because molecules which may themselves be very large are not oriented in regular fashion. This condition is observed in the colloidal gels and is particularly interesting in the light of the prediction that simple mechanical stretching might tend to pull these diffracting units into parallel position and thus permit them to act as a diffraction grating.

The question which naturally arises next is whether there is a continuous transition between crystalline and amorphous state. From what has been said concerning continuous broadening of lines till these merge and spread over the entire film, such a process would be indicated. Sir William Bragg quotes the experiment by the present writer on carbon. An activated charcoal producing an essential amorphous pattern had certain characteristic chemical and physical properties which changed over to those of graphite upon brief heating at  $1100^{\circ}\text{C}$ . The x-ray pattern, however, was unchanged since no lines appeared. The great activity of the original charcoal was ascribed to the free valences of disorganized carbon atoms. Upon heating, the solid phase being retained throughout, these began mutually to attach themselves to satisfy these bonds and to form crystal planes of graphite, which were still too few and bent to permit interference of rays, though the properties were typical of graphite. This stage of elementary organization was designated *paracrystalline*. Upon further heating the grains grew in size, and the planes in number and rigidity, so that broad diffraction lines for colloidal dimensions finally sharpened to the typical graphite spectrum.

Another state of affairs, however, is observed with those substances so masterfully studied by Friedel, which display mesomorphic states of matter or liquid crystal phases. Here there are sharp discontinuities between the liquid or so-called amorphous phase (though this yields liquid rings), the nematic (in which the long molecules point in one direction but are not constrained in parallel planes and hence produce no crystal patterns), the smectic (in which the molecules are arranged in parallel planes in one direction, thus giving a crystal interference for one dimension only), and finally the crystalline in which the molecules take up regular marshalling in three dimensions. Undoubtedly, then, transition phenomena must occur in all cases of solidification of a molten substance, but only in the case of certain long organic molecules is the temperature range of each state sufficiently extended to permit detection and examination.

**Results on Colloidal Metals and Inorganic Compounds.—**

Numerous references are to be found in the literature to experimental measurement of particle size for colloids as well as identification of crystallographic system. It is convenient to determine these properties as functions of various methods of preparation of industrial materials. Citation of only a few examples must suffice here.

1. First of all, the identification of the colloidal state as differentiated from the molecular or supercolloid states (not limited to solutions as is the Tyndall cone).

2. Relation in grain size and structure in extremely thin electro-deposited films and colloidal sols, such as those prepared by the Bredig arc method.

3. Catalytic activity, as for nickel hydrogenation and dehydrogenation catalysts, as a function of lattice structure and grain size (work in the writer's laboratory indicating an optimum rather than minimum grain size associated with greatest activity).

4. Structure and grain size of colloidal lead as a function of therapeutic value when injected into tissues subsequently irradiated with x-rays.<sup>1</sup>

5. Structure and grain size as functions of spreading, wetting, obscuring power, stability, gloss, etc., and of method of preparation in pigments (zinc, lead, tin, aluminum, and other oxides).

6. The discovery of the presence of colloidal crystallites in glass, entirely apart from coloring agents added.<sup>2</sup>

7. Grain-size measurements in tungsten for electrical contact points and other metals where grain boundaries are not satisfactorily developed for microscopic counting even for large grains.

8. Studies of possible allotropic forms of colloids produced at various conditions of pH (in all ranges the sphalerite lattice and not the wurtzite is found for colloidal zinc sulfide, contrary to various contentions).

9. Numerous cases of identification of colloiddally dispersed phases in natural and artificial minerals, alloys, including marten-site and troostite, etc., uniformly mixed or at grain boundaries; clear differentiation between solid solution and physical mixtures.

10. Test for presence of invisible colloidal particles, such as

<sup>1</sup> CLARK and PICKETT, *J. Am. Chem. Soc.*, **52**, 465 (1930)

<sup>2</sup> PARMELEE, CLARK, and BADGER, *J. Glass Tech.* **13**, 285 (1929); CLARK and AMBARY, *ibid.*, **13**, 290 (1929); RANDALL, ROOKSBY, and COOPER, *ibid.*, **14**, 219 (1930).

brass or copper in parchment; completeness of filtration and dialysis.

11. Grain size and uniformity (particularly barium), in metal mirrors, in radio tubes, photoelectric cells, etc.

12. Identification of adsorbent films and chemical changes (*e.g.*, mercuric chloride solution adsorbed on charcoal gives the crystal diffraction pattern for colloidal mercurous chloride).

13. Studies of the phenomena involved in dyeing of textiles utilizing metallic sols adsorbed on fibers (sometimes fibered layer, sometimes random).

14. Estimation of crystallinity, dispersion and grain size of excess sulfur in vulcanized rubber.

15. Classification of amorphous carbon, coal, and resins.

Recently a series of papers have appeared from the laboratory of Sir C. V. Raman, which have advanced to a remarkable degree the knowledge of the structure of materials usually classed simply as amorphous. This has been made possible by the observation of an entirely new phenomenon appearing at small angles to the primary beam in the diffraction patterns of all varieties of amorphous carbon, namely, a strong scattering extending to about 7 deg. This corona was first observed in solutions of cane sugar and was definitely attributable to the molecules of the dissolved substance which are distributed at random in the solvent, much in the same way as gaseous molecules.

Krishnamurti<sup>1</sup> has found for samples of sugar, benzene, and naphthalene charcoals and carbon obtained by charring ash-free gelatin with molten sodium, together with colloidal graphite prepared by exploding graphite acid in a vacuum, that all showed the small angle scattering in a marked manner. The patterns displayed two rings in addition to the central scattering, the first and prominent ring corresponding to the (002) reflection of graphite, having a spacing of about 3.8 A.U. as compared to 3.4 A.U. of graphite. The outer ring was fainter and broader and showed a spacing of 2.12 A.U. comparable to the (111) spacing of graphite (2.06 A.U.). The observations accord with the idea that in the amorphous state the carbon atoms join together in clusters, forming highly anisotropic units, essentially two dimensional, the thickness being about one-third the length or breadth. Assuming that the central scattering is due to the dimensions in the plane of the particle, and the first ring to its thickness, a

<sup>1</sup> *Indian J. Physics*, **5**, 473 (1930).



rough calculation gives about sixty atoms of carbon per unit. This picture of the carbon particle agrees with chemical evidence, mainly its oxidation to mellitic acid, and adsorptive properties.

Mahadevan<sup>1</sup> has made an extensive x-ray study of the various varieties of coal, principally vitrain and durain. Vitrain, for example, gives two halos in the position of the two most prominent graphite carbon rings. They are wide and diffuse, suggesting the colloidal nature of the diffracting particles. The halos are due to the complex carbon molecule present in vitrain. The increase of moisture content seems to be accompanied by a finer division of the particles as evidenced by broadening of the rings. The results on durain indicate that it belongs to a colloidal system of the suspensoid type, where vitrain acts as a dispersion medium and the ash and vegetable detritus (with free carbon as end product) as disperse phases. In a study of vitrains of different geological ages, the intensity of the general scattering is seen in the case of the older coals to be approximately proportional to the sum of moisture content and volatile matter. In all cases the sizes of the diffracting particles are found to be of colloidal dimensions. The mineral matter in the ash is also present in a colloidal state. These and related investigations have opened up a whole new series of applications of the x-ray diffraction method by amorphous solids. There has been a further extension to the case of natural and fossil resins<sup>2</sup> and to the changes during heating of ordinary rosin, shellac, and synthetic resins.<sup>3</sup> The importance of these studies can scarcely be overestimated, on account of the much greater amount of information obtained on seemingly hopeless materials and on account of the possibility of solving many difficult problems, particularly in chemistry and geology.

**The Nature of Colloidal Solutions as Revealed by X-ray Diffraction.**—Following the discovery of Krishnamurti<sup>4</sup> that diffraction pattern of aqueous solutions of cane sugar, levulose, and glucose were distinguished by intense scattering at small angles due to the dissolved molecules, it was then possible to undertake the study of colloidal solutions for which the state of molecular aggregation has been the subject of much speculation.

<sup>1</sup> *Ibid.*, **4**, 457; **5**, 525 (1930).

<sup>2</sup> *Ibid.*, **5**, 345 (1930).

<sup>3</sup> *Ibid.*, **4**, 99 (1930).

<sup>4</sup> *Ibid.*, **3**, 209; 307 (1928); **5**, 489 (1930).

The molecular weight of dextrin calculated from the extent of "amorphous" scattering by means of the Bragg formula  $n\lambda = 2d \sin \theta$  comes out 600 and for gelatin, 3000, which are not improbable values. The solution of sodium oleate produced a ring due to the presence of big groups or micelles of sodium oleate in the solution. The extent of the gaseous scattering gave the dimension for the sodium oleate molecule, agreeing with that calculated from molecular weight and density. An excess of scattering directly adjoining the central spot is due to big groups of ionic micelles described by McBain. Aqueous solutions of

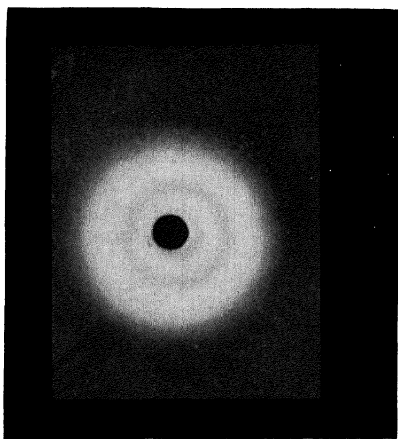


FIG. 223.—Typical pattern for "amorphous" material such as liquids.

starch, tannic acid, and gum arabic showed a further scattering at small angles to the primary beam, due to the dissolved molecules or micelles. The molecular weights calculated from the extents of the coronas were 6200, 3134, and 2810, respectively. Thus, a starch molecule contains about 10 dextrin molecules united together, and a tannin micelle contains 10 simple molecules of the formula  $C_{14}H_{10}O_9$ .

The greater importance of these studies is at once apparent, when it is considered that extremely valuable information should be obtained from biological fluids including blood, filterable virus, etc. In all these cases of amorphous solids, liquids, and solutions, the x-ray patterns are characteristic in showing the presence of one or more diffraction bands, even though these may be ill-defined. The purely amorphous scattering where no maxima are present evidently can exist only in the case of ideal gases. All of these newer investigations are in agreement with the contention by the writer that such a material as amorphous carbon represents an intermediate state, designated as paracrystalline, through which the atoms of carbon have to pass before obtaining the orderly arrangement underlying the graphite structure.

**Diffraction by Liquids.**—It has been known definitely since 1916 that liquids through which x-rays are passed produce

diffraction patterns characterized by one or more halos or interference rings, usually somewhat diffuse (Fig. 223). Approximately eighty papers dealing with this subject theoretically or experimentally have now appeared. It is not possible here to present the historical development but rather to give the status of experimental results as it now stands. An excellent survey of researches up to 1928 is given in a paper by Drucker.<sup>1</sup>

The preponderance of opinion now is that the diffraction effects with liquids indicate orderly spacial arrangements of molecules. The phenomenon is understood qualitatively in the same sense that crystal diffraction is understood. In spite of numerous theoretical attempts to evaluate the phenomena exactly, these have not been so successful as the conception of what Stewart calls "cybotaxis"—a regularity of molecules grouping in liquids. Interference effects might be due to periodicities within the atom (electron distribution), within the molecule (atomic distribution), or between molecules. The first must be true for monatomic substances which were investigated by Debye and Scherrer in 1916. Certain halos for other compounds may be due to atomic distribution, but certainly the third cause is predominating in complex molecules, since the chief diffraction maxima are accounted for by a periodicity in the distribution of molecules. This would be particularly true for asymmetrical molecules. In liquids these would have a certain distance of nearest approach side by side or end to end. According to Stewart,<sup>2</sup>

. . . if x-rays give evidence of periodic molecular grouping it must not be supposed that these groups are large or that the molecules in any one well defined group remain permanently members of that group. At any one instant these small orderly molecular groups might exist at numerous points in the liquid, the regions between them being not so orderly.

This orderly arrangement in groups is called "cybotaxis." There is every evidence, therefore, that the Bragg law  $n\lambda = 2d \sin \theta$  can be applied to liquid diffraction interferences just as truly as to crystalline solids. Scattering centers at random (that is amorphous material) would produce a large scattering near  $0^\circ$ , but such is not the case for liquids any more than it is for crystals. Furthermore, the integrated intensity in the region of the chief

<sup>1</sup> *Physik. Z.*, **29**, 273 (1928).

<sup>2</sup> *Rev. Modern Physics*, **2**, 116 (1930).

diffraction maximum for equal masses per unit area for a solid and liquid show the same values, again indicating distinct coherence.

The principal work on liquid diffraction has been carried out by Stewart and associates at the University of Iowa, who have used the ionization spectrometer, and by Raman and associates at Calcutta, who have used the photographic method. A brief summary of some experimental conclusions must suffice.

1. In diffraction rings of chain molecules such as *n*-alcohols, *n*-fatty acids, *n*-paraffins, etc., there is always a major intensity maximum corresponding to a spacing of 4.6 A.U. which is evidently the effective diameter of the molecule.

2. Branched-chain isomers invariably increase the effective diameters of the chains in characteristic manner.

3. In polar compounds such as *n*-alcohols, etc., a second maximum, whose position depends upon the number of carbon atoms, indicates values of *d* which are twice, or less than twice, the molecular length, indicating a grouping of two polar molecules by attraction of the polar —OH, —COOH, etc., groups. Spacing less than twice molecular length could be accounted for by a tilt with respect to planes, entirely in accord with observations on solid films (see page 319). For isomers in which the polar group is not attached to the end or next to the end carbon atom, doubling does not occur.

4. The carbon atom in these chains occupies a distance of about 1.24 A.U. per atom, indicating probably a zigzag arrangement.

5. Stewart has accomplished simultaneous measurement of more than one diameter in a chain in such compounds as 2-methyl hexane (5.25 and 4.84 A.U.) and *di*-*n*-propyl carbinol (4.85 and 4.5). A third maximum gives the length. This is a powerful support in indicating the actual molecular arrangement.

6. Benzene and cyclohexane give sharp rings, indicating a ring structure with thickness of 4.7 and 5.1 A.U. (Stewart), greater than observed for flat rings in crystals. Para derivatives give least thickness.

7. The effect of temperature on diffraction patterns is precisely that which might be predicted upon the basis of crystal data. The intensity maximum is displaced (expansion), and the maximum is diminished in intensity and increased in width (greater disorder due to thermal agitation).

8. Impurities, particularly containing heavy atoms, have a large effect sometimes upon results. The distinction of purity and isomerism constitutes a very useful application.

9. Some apparent discrepancies among experimenters have been found recently to be due to the fact that, with an x-ray beam which has not been filtered with greatest care in order to render it monochromatic, halos are produced as an interference effect of general radiation. With copper radiation and liquid fatty acids this secondary ring is obtained with specimens thicker than 2 mm., according to Thibeau and Trillat,<sup>1</sup> who further reach the conclusion that inner halos, frequently observed by Stewart and attributed to molecular length, are always due to diffraction of general radiation supposedly by the same spacing as that of the principal halo (cross section). Clark and Stillwell<sup>2</sup> have proved that with molybdenum radiation at a tube voltage of 33 kv. or more the inner ring is produced by diffraction and filtration of general radiation and bears no relation to molecular length while at voltage below 27 kv. the inner ring is characteristic of the liquid under examination.

10. Several interesting researches have shown that in many instances the liquid halos correspond approximately in their positions to the principal diffraction maxima for the same substance as a solid.<sup>3</sup>

11. For totally miscible pairs of organic liquids the pattern exhibits a single major maximum which has an angular position between the maxima for the pure constituents and shifts directly with the concentration.<sup>4</sup> On the other hand, an emulsion or phenol in water produces the interferences for both constituents. Hence in a solution there exists a single type of cybotactic group to which molecules of both constituents contribute, whereas in the emulsion two types of cybotactic groups exist. This constitutes a fundamental differentiation between solutions and non-solutions.

12. Stewart and Edwards<sup>5</sup> have ingeniously shown for a series of 22 octyl alcohols that there is a definite correlation between the coefficient of viscosity and the perfection of grouping

<sup>1</sup> *Z. Physik.*, **61**, 816 (1930).

<sup>2</sup> *Radiology*, **15**, 66 (1930).

<sup>3</sup> KRISHNAMURTI, *Ind. J. Phys.*, **3**, Part II, 225 (1928).

<sup>4</sup> MEYER, *Phys. Rev.*, **38**, 1083 (1931).

<sup>5</sup> *Phys. Rev.*, **38**, 1575 (1931).

in the direction of chain lengths as measured by relative halo intensities. This corresponds with the view that the viscosity within liquid groups is caused by longitudinal slippage. The temperature coefficient of viscosity is negative because the size of groups decreases.

13. An exceptionally careful investigation of water over a range of temperatures has been made both by Meyer,<sup>1</sup> who used a strictly monochromatic x-ray beam obtained by crystal reflection and the photographic method, and by Stewart<sup>2</sup> with his usual ionization method. There is general agreement in finding three interference maxima corresponding to distances 3.13, 2.11, and 1.34 (Meyer), 3.24, 2.11, 1.13 (Stewart). The distance between molecules as scattering centers represented by the most prominent halo decreases with temperature, while the breadth of the halo increases, whereas the distance corresponding to the next most important halo increases. This halo tends to disappear with increasing temperature. There is a quantitative similarity between the periodicities found in the liquid and the three most important periodicities in powdered ice. These results are particularly interesting in the light of theories of molecular association in water. The water diffraction results seem to indicate periodicities of only one kind of molecular grouping, just as the results on ice indicate one kind of crystal structure only. Hence it would appear that the simple explanation of molecular association is the association in cybotactic groups of a relatively large number of molecules and not in complexes such as di- or tri-hydrol. This is different from the type of association found in isomeric alcohols for example. When the polar OH group is on the end or next to the end carbon atom, the association arranges molecules end to end in the same line with two polar groups adjoining, whereas in the case that the OH is elsewhere the associated molecules lie side by side.

14. A comparison of diffraction effects of isotropic liquids and liquid crystals<sup>3</sup> proves that generally these are similar (unless the mesomorphic smectic state, described by Friedel, is observed). Stewart<sup>4</sup> has observed that the intensity of the principal maxi-

<sup>1</sup> *Ann. Physik*, **5**, 701 (1930).

<sup>2</sup> *Phys. Rev.*, **37**, 9 (1931).

<sup>3</sup> For a complete modern survey of the entire subject see *Z. Krist.*, **79**, Heft 1-4 (1931).

<sup>4</sup> *Phys. Rev.*, **38**, 931 (1931).

mum for the anisotropic liquid (117.4 to 134° C.) para-azoxy-anisol is 10 per cent greater than that for the transparent liquid (143° C.). If cybotactic groups exist in the liquids, these "companies" might group together into a large "regiment" responsible for the liquid crystalline phenomena. A marked optical but small x-ray difference is thus to be expected. Ordinary liquids appear perfectly isotropic optically, but, using distances small compared to an optical wave length, the liquid is *never* isotropic but consists of cybotactic groups oriented in all positions and disclosed by x-rays. When these groups enlarge they finally become evident by optical examination.

A logical extension of such researches is the effect of a magnetic field. There has been cited some evidence of orienting effects on liquid molecules of magnetic fields as disclosed by diffraction patterns, but Stewart found none, a result which he ascribed to the smallness of the cybotactic groups. A marked effect, however, is obtained for the liquid crystalline state, explained better by an anisotropic polarization than by a permanent magnetic moment.

In a magnetic field the directed orientation is indicated on the diffraction rings by localized intensity maxima (fiber pattern). The pattern is markedly sharper in passing from the nematic to the smectic phase in the magnetic field as observed by Herrmann and Krummacker. These workers have also proved that, when a melt of a substance which displays mesomorphic phases solidifies in a magnetic field, the crystalline powder is fibered in a direction parallel to the field; the intensity maxima for the pattern correspond in position to those for the liquid crystals in the magnetic field.

Further researches on structural effects in magnetic and electric fields will be awaited with greatest interest.

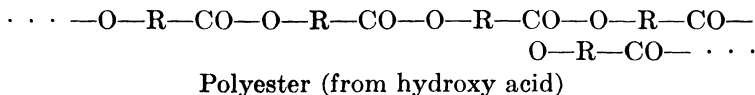
15. Molecular orientation of chain compounds in surface films has been considered in Chap. XVI (page 332). Upon the basis of the Harkins-Langmuir theories, it would be expected that even in liquid films such orientation should be observed. Trillat has obtained evidence of this orientation in diffraction patterns for liquid lead oleate film on mercury drops. This orientation has also been observed repeatedly in the writer's laboratory, although far sharper effects are obtained if these films are cooled to the point of solidification, even of the very thinnest layer on an underlying molten liquid.

## CHAPTER XX

### THE STRUCTURE OF HIGHLY POLYMERIZED ORGANIC SUBSTANCES FOUND IN NATURE

Only a short time ago, very little could have been said upon this subject, not only from the x-ray diffraction point of view but even from that of chemical investigation. The new appearance of a book of more than 250 pages by Meyer and Maer,<sup>1</sup> bearing the title of this chapter, is in itself sufficient evidence of the amazing progress in the study of some of the most familiar natural materials. Impetus to these investigations was given to a large extent by the x-ray analysis of polymerized formaldehyde in the laboratory of Staudinger. The polyoxymethylenes  $\text{—O—CH}_2\text{—O—CH}_2\text{—O—CH}_2\text{—O—}$  are linear and easily produce characteristic x-ray diffraction patterns. Such compounds as these are the basis of the synthetic resins of commerce, of which the best known is *bakelite*, made by condensing formaldehyde with phenol or its derivatives. In these cases the reaction is complicated by the fact that the linear polymers are themselves linked together into a molecular jumble to give a structure of which the textile counterpart is neither yarn nor velvet pile, but a mass of "felted" fibers. These synthetic resins, therefore, yield very diffuse patterns.

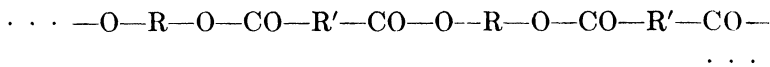
The most illuminating work in the field of synthetic polymers in which x-ray diffraction methods have served as a valuable aid is that of Carothers and his associates.<sup>2</sup> A long series of linear superpolymers (with molecular weights above 10,000) has been prepared by condensation reactions as follows:



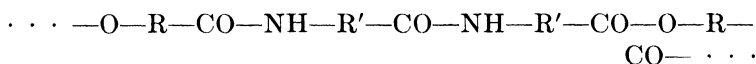
<sup>1</sup> "Der Aufbau der hochpolymeren organischen Naturstoffe," Leipzig, 1930.

<sup>2</sup> *J. Am. Chem. Soc.*, **51**, 2548, 2560 (1929); **52**, 314, 711, 3292; **54**, 1559, 1566, 1569, 1579 (1932).

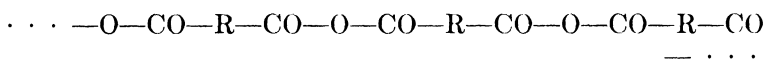




Polyester (from dibasic acid and glycol)

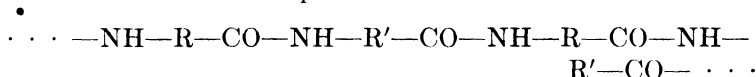


Mixed polyester polyamide

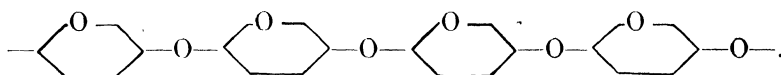


Polyanhydride

With these are to be compared:



Silk (polyamide)



Cellulose (polyacetal)

It was found possible to spin and cold-draw the synthetic superpolymers into beautifully oriented crystalline fibers, as shown by x-ray patterns. A useful degree of strength and pliability in these fibers requires a molecular weight of at least 12,000 and a molecular length not less than 1000 A.U. These results give great support to the interpretation of the structures of natural polymerized materials now generally accepted.

X-ray results on the colloidal polymerized natural products indicate clearly that a common structural plan is utilized for such widely different substances as cellulose, proteins of all kinds, chitin, rubber, gutta percha, balata, and chicle. Long primary valence chains or macromolecules are built up from a relatively simple molecular group (*e.g.*, dehydrated glucose residues in cellulose and isoprene in rubber). A bundle of these chains, which may be 500 A.U. long, is held in position by secondary valence forces and constitutes the colloidal micelle familiar in diffusion and molecular weight experiments.

From usual diffraction patterns, however, very much smaller periodicities and simpler constitution are directly measured. The explanation is found in the fact that the long macromolecules are spiral in character, and one turn in the screw axis is sufficient for a diffraction periodicity, since all other turns are exactly the

same. Within the unit crystal cell, therefore, only a small number of the molecules of the parent monomer are found, instead of one or more of the actual long macromolecules. The information obtainable from diffraction patterns of the crystalline part of these natural products is as follows:

1. Crystallographic system.

2. Dimensions of the unit crystal cell and the number of monomeric molecules in each, from a known density value.

3. Coordinates of atoms within the unit cell which demonstrate molecular shape of simplest chemical unit, and the bonding of these through primary valence bridges into polymerized chains with small periodicities due to screw axis of symmetry. These chains are further indicated by optical anisotropy and by the remarkable persistence during all kinds of chemical treatment, such as oxidation, mercerization, xanthogenation, nitration, acetylation of cellulose, vulcanization of rubber.

4. The length of the macromolecules or in other words of the colloidal micelle, and of the cross section, which is determined by the number of chains in a bundle. These magnitudes are ordinarily calculated from the breadths of the intensity maxima as explained in a previous section. It has been possible, however, in the writer's laboratory to measure these large spacings from direct diffraction interferences when sufficiently long x-ray wave lengths are employed, so that angles of diffraction will be in turn sufficiently large to permit resolution from the undiffracted x-ray beam.

5. The arrangement of the micelles within the substance, whether random or with a preferred orientation with respect to one direction, as in a fiber axis. In the former case a pinhole diffraction pattern shows uniformly intense continuous concentric rings. As definite positions are taken up, intensity increases in certain places and decreases in others. Rings become arcs and then symmetrically arranged spots as the orientation is increasingly more perfect.

6. In terms of all the foregoing types of information, the effects of chemical change, swelling, and mechanical deformation, such as tension, can be followed and, of course, observed properties rationally accounted for.

It is not possible in this chapter to present in detail for this great class of colloids the x-ray data and the steps in interpretation. Rather, these results will be briefly tabulated and particu-

lar attention paid to the practical consequences and predictions from structural models constructed from x-ray data.

TYPICAL X-RAY DATA FOR FOUR IMPORTANT POLYMERIZED ORGANIC NATURAL MATERIALS

Product	System	Unit cell	Dimensions, A U	Number of groups	Space-groups	Micelle size
Cellulose*	Monoclinic	<i>a</i> <i>b</i> <i>c</i> $\beta$	8.3 10.22 7.9 84°	4C <sub>6</sub> H <sub>10</sub> O <sub>5</sub>	C <sub>2</sub> <sup>2</sup>	50 A U cross 600 A U length
Cellulose hydrate (mercerized)	Monoclinic	<i>a</i> <i>b</i> <i>c</i> $\beta$	8.14 10.30 9.14 62°	4C <sub>6</sub> H <sub>10</sub> O <sub>5</sub>	C <sub>2</sub> <sup>2</sup>	Doubtful, chains less parallel
Rubber (stretched)	Orthorhombic	<i>a</i> <i>b</i> <i>c</i>	12.3 9.3 8.1	8C <sub>8</sub> H <sub>8</sub>	V <sub>4</sub>	150 × 500 × > 600
Silk fibroin	Monoclinic	<i>a</i> <i>b</i> <i>c</i> $\beta$	9.68 7.00 8.80 75° 51'	4 alanylglycyl		

\* The data given are those of Meyer and Mark. Sponsler prefers the following.  $a = 10.7$  A U;  $b = 12.2$  A U;  $c = 10.3$  A U. Angles within 2° or 3° of right angles, 8C<sub>6</sub>H<sub>10</sub>O<sub>5</sub> groups per unit cell. The two unit cells are actually very closely related and are merely differently oriented in the same fundamental lattice. Sponsler's *c* dimension is the same as *b* in the table, representing the periodicity along the fiber axis.

**Direct Measurement of Colloidal Particle Sizes.**—The methods of particle-size measurement presented in Chap. XVII obviously involve assumptions and independent methods of evaluation are necessary for their test. The best possible method would, of course, depend upon actual diffraction interference corresponding not to the small unit crystalline cells but to the length and cross section of colloidal particles, for each of which  $d$  may be calculated by the simple Bragg equation. This necessitates a regular arrangement and uniform size of these colloidal particles with respect to each other, so that specimens are limited to organic micellar systems consisting of small elongated particles regularly oriented in a fiber, such as in natural cellulose and in stretched rubber. Another difficulty naturally is that the diffraction interferences corresponding to colloidal dimensions of one or two hundred A.U. will appear at such small angles, that resolution from the primary undiffracted beam will be extremely

difficult or impossible. There are two experimental possibilities: define the beam by extremely fine pinholes or slits, or else utilize x-radiation with a wave length much greater than that usually employed (molybdenum  $K\alpha$ -doublet 0.71 A.U.; copper 1.54 A.U.). By the first method with copper radiation Mark<sup>1</sup> was able to distinguish a broad interference spot very near the primary beam for bamboo and wood cellulose, corresponding to a spacing of between 50 and 100 A.U. and evidently due to reflection from the surfaces of particles of this breadth. Clark and Corrigan<sup>2</sup> have utilized the second method with interesting preliminary results. A combined x-ray tube, pinhole system, and camera was constructed with the target of the tube magnesium ( $K\alpha$  wave length 9.86 A.U.) (Fig. 21, page 38). On account of great absorption of radiation, the entire apparatus was operated at the x-ray tube vacuum, and extremely thin specimens of rubber and cellulose employed. Upon the films appeared a ring for unstretched rubber corresponding to 99.3 A.U. and for cellulose fibers the spacings 85.0 (evidently corresponding to Mark's value for breadth and verified by Thiessen in optical examination with the Spierer lens), 274.1, 168.0, and 156.0 A.U. The micellar sizes, deduced from measurement of interference breadths and calculation by the Laue equation, are approximately  $50 \times 50 \times 600$  A.U. for cellulose and  $150 \times 500 \times > 600$  A.U. for stretched rubber. Further researches by this important direct diffraction method will permit a careful comparison of values and establish the validity of the equations deduced from theoretical considerations, which may then in turn be used with confidence for those colloidal substances in which there is no organized micellar structure.

*The Crystal Structure of Insulin.*—Since the discovery of this important substance for the treatment of diabetes there has been great interest in its composition and structure. It has been known for some time that insulin exhibited certain optical properties of a true crystal. Although numerous attempts have been made by Freudenberg and others, no x-ray diffraction pattern could be obtained beyond the usual ring due to the 3.5 A.U. spacing common to proteins. Work of this kind employing the usual copper  $K\alpha$ -radiation has been carried on in the writer's laboratory for more than two years. In the belief that absence

<sup>1</sup> *Faraday Soc. Mon.*, p. 387 (March, 1929).

<sup>2</sup> *Radiology*, **15**, 117 (1930); *Ind. Eng. Chem.*, **23**, 815 (1931).

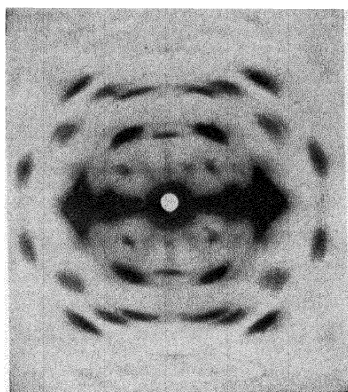


FIG. 224.—Typical pattern for cellulose pattern (ramie).

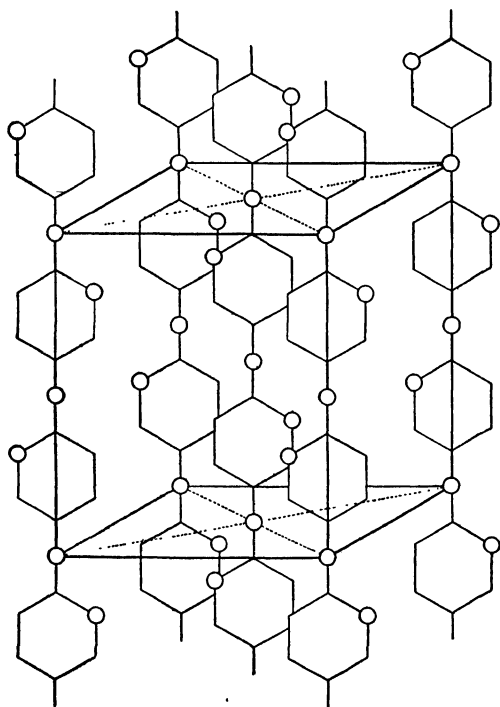


FIG. 225.—The unit crystal cell of cellulose. (*Meyer and Mark.*) The  $C_6H_{10}O_5$  groups (hexagons) are represented as held together by oxygen bridges, each pair forming a cellobiose unit. The dimensions of the monoclinic cell containing four dehydrated glucose groups are  $a = 8.3$  A.U. (horizontal);  $b = 10.22$  A.U. (vertical);  $c = 7.9$  A.U. (perpendicular to plane of paper).

of interference might be due to very large spacings in crystalline insulin, Clark and Corrigan<sup>1</sup> investigated the structure with the long magnesium  $K\alpha$ -radiation by means of the apparatus already described. A crystal pattern was obtained and the unit cell dimensions deduced were  $130 \times 100 \times 80$  A.U., giving an axial ratio of  $\frac{4}{3}:1:\frac{4}{5}$ . With the aid of microscopic data the crystal form was found to be monoclinic, with one angle between  $88$  and  $90^\circ$ , the crystals frequently assuming a pseudo-hexagonal form. The crystals were positive. On the basis of the approximate molecular weight of 35,000 generally accepted, and the density of 1.315, the number of molecules of this highly polymerized complex substance per unit cell is 24. An entirely new field of investigation of very complex natural and synthesized materials is opened up by this application of very soft x-rays.

### Résumé of X-ray Results on Natural Polymerized Materials.

1. *Cellulose*.<sup>2</sup>—*a*. Proof of identity of crystalline part of natural

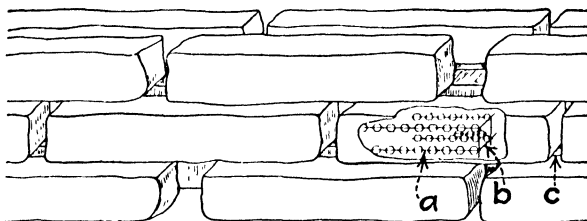


FIG. 226.—Model of structure of cellulose fiber, showing colloidal micelles built up from bundles of long chains of  $C_6H_{10}O_5$  groups. Three kinds of binding forces are involved. *a*, primary valence linkage along molecular chain; *b*, secondary valence forces holding chains in bundle; *c*, tertiary forces between micelles. The principal variation in celluloses from different sources is in the arrangement of the micelles—parallel in nearly perfect fiber as shown here, spiral, random, or brush heap as in cellophane, etc. The micellar dimensions are of the order of 500 A.U. long (also the length of the long-chain molecules) and 50 by 50 A.U. in cross section. The micelle therefore may contain 6,000 to 12,000 glucose groups, or 1,500 to 3,000 unit cells.

varieties of ramie, sisal, jute, hemp, flax, cotton, wood, tunicin (animal cellulose) *ventricosa* B—cellulose (bacterial), *valonia*, etc. (Fig. 224, typical pattern; Fig. 225, unit cell; Fig. 226, model of fiber).

*b*. Rational explanation of properties such as tensile strength and elasticity from arrangement of micelles: the more perfectly parallel to the fiber axis the greater the tensile strength (Fig. 227).

<sup>1</sup> *Phys. Rev.*, **40**, 639 (1932).

<sup>2</sup> See, CLARK, *Ind. Eng. Chem.*, **22**, 474 (1930), for a complete presentation.

c. Differentiation of cellulose fibers in terms of micellar arrangement (parallel to fiber axis in ramie, spiral layers in cotton) and of other substances present.

d. Surest method of identification of true cellulose, which involves *both* constitution and spacial coordinates: esterify unknown, dissolve in proper solvent, spin and regenerate fiber under tension to orient micelles, saponify in solid phase, and

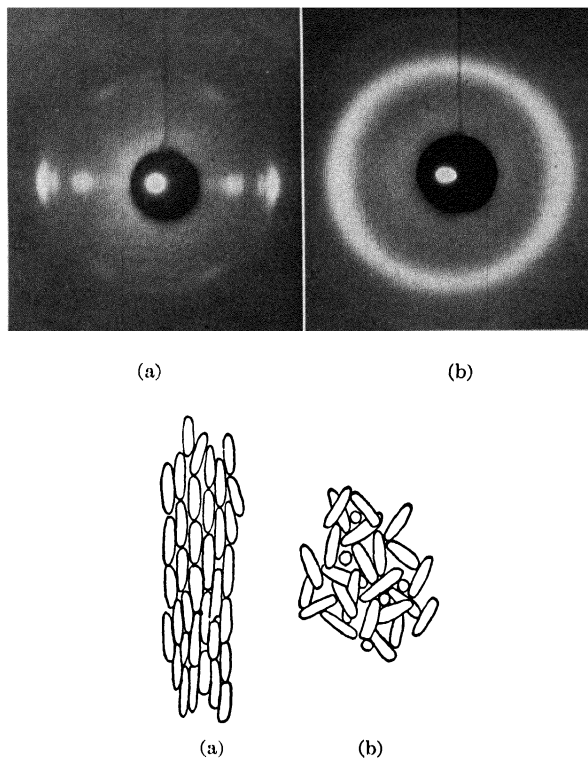


FIG. 227.—Effect of arrangement of colloidal micelles on diffraction patterns of cellulose. (a) Fiber (improved rayon); (b) cellophane sheet.

examine diffraction pattern of fiber suspected to be cellulose. This is the method employed for testing cellulose synthesized from sugars by Hibbert.

e. A remarkable improvement in the quality of rayon from the prediction that tension on plastic fiber during regeneration should pull micelles parallel (x-ray fiber pattern) and greatly increase tensile strength; a structural test of every step in the process to yield optimum structure and properties; assurance that the

manufacturing process has not been so severe as to break primary valence chains in original raw material (wood pulp or cotton linters), as was the case before x-ray research with micellar lengths only half as great as in starting material (Fig. 228).

*f.* Improvements in cellophane manufacture to eliminate directional properties due to slight fibering in sheet when completely random arrangement is desirable. (See Fig. 227.)

*g.* Classification of raw cotton from degree of fibering since ultimate structure is conditioned by growth environment; proof that ancient cottons had a superior fibrous structure not now existent in any cultivated variety (Fig. 229).

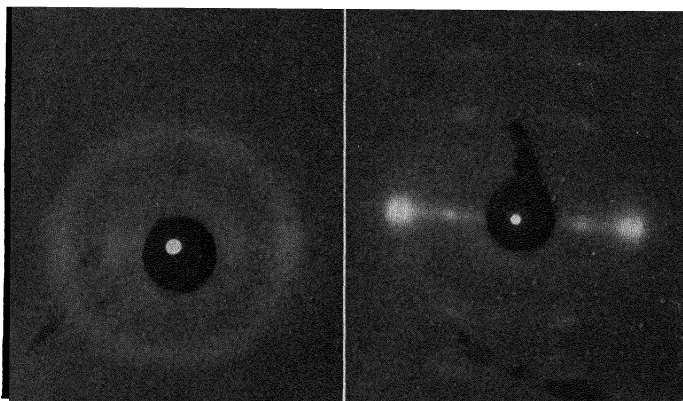


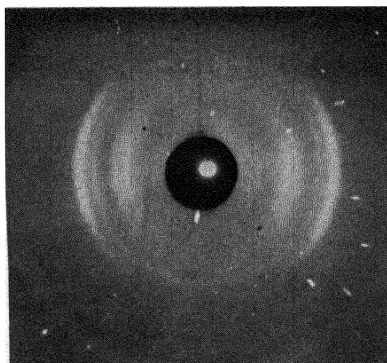
FIG. 228.—Patterns for old (left) and new (right) varieties of rayon, showing great increase in preferred orientation in latter, introduced by tension during coagulation.

*h.* Study of growth of cotton daily from the root hair to mature 50-day fiber; diffraction patterns characterized by gradual increase in organization, decrease in lattice dimensions and hence intermicellar swelling and the sudden appearance of fibering with wall thickening.

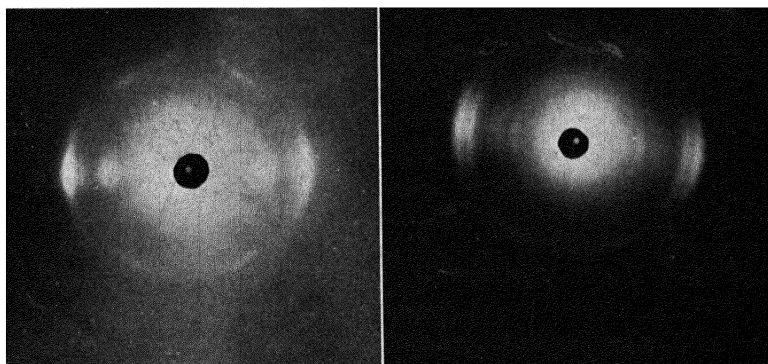
*i.* Classification of kind of wood, angle of fibrils, differentiation of spring and summer wood, and of normal and compression wood (upper and lower side of bough) (Fig. 230).

*j.* A method of proving whether swelling is reversible and inter- or intramicellar; *e.g.*, wood and cotton swell when water penetrates between micelles; other solutions penetrate between chains and produce change in lattice dimensions; new processes for impregnation of wood to avoid swelling and water penetration.





(a)



(b)

(c)

FIG. 229.—Comparison of structures for cotton. (a) Good grade of modern cotton; (b) ancient cotton with much more perfect alignment of micelles parallel to fiber axis; (c) ordinary cotton subjected to chemical swelling and mechanical tension.

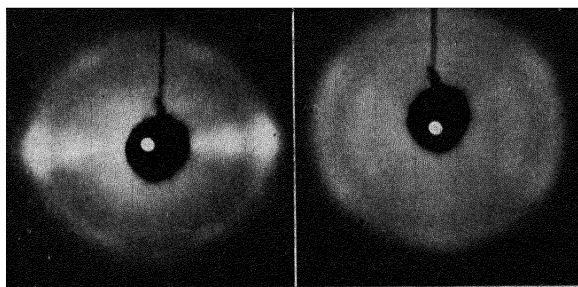


FIG. 230.—Typical patterns for wood, showing variations. Left, high density yellow poplar; right, compression structure on leaning side of tree trunks.

*k.* A new process successfully predicted from cellulose model that cotton may be suitably swollen, maintaining solid form, stretched, and greatly strengthened by virtue of improved orientation of micelles (see Fig. 229c).

*l.* A proof that only the triacetate and trinitrate form definite crystalline substances, since esters of intermediate composition show x-ray interferences for unchanged cellulose and for the tri-ester only; for parts in which all of hydroxyl groups have not reacted, the distortion of the lattice results in no observable sharp interferences. On this account none of the commercial nitrate or acetate films yields more than a very diffuse amorphous pattern, so that variations in manufacturing steps cannot be followed; by plastic stretching of the films molecules are pulled more nearly into alignment, but only a pseudo-crystalline pattern and structure are gained before breakage on account of the interference of amorphous material with completely parallel orientation.

*m.* Discovery of the only method of obtaining native cellulose back from mercerized: two trinitrates are found from x-ray patterns, both produced from either native or mercerized cellulose under controlled conditions. Upon denitration trinitrate I yields native, and II hydrated cellulose only.

*n.* Identifications of various compounds such as Knecht's (with nitric acid) Normann's (copper-alkali-cellulose), copper-amino-cellulose; a rational explanation of observed chemical properties and reactions, oxidation splitting, etc.

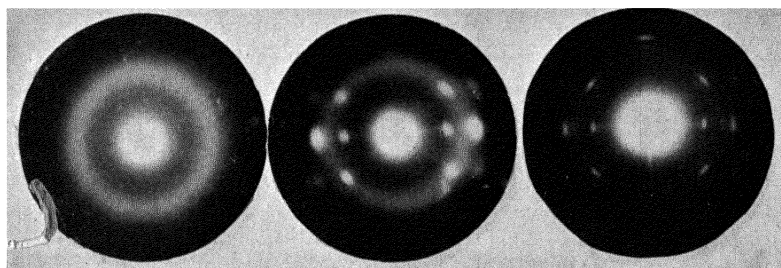
*o.* Conditioning of fiber structure to problems of dyeing, to various types of paper and a control of paper manufacture.

*p.* The proof that celluloid is a double compound of nitro-cellulose and camphor. In a remarkably convincing series of papers,<sup>1</sup> Katz and associates have utilized x-ray patterns correlated with optical anisotropy to show that with small camphor contents (to 10 per cent) unchanged long nitrocellulose micelles and long micelles of the camphor-nitrocellulose compound lie side by side. The first possess strongly positive birefringence with respect to the longest axis, the latter weakly negative. The changes in diffraction patterns clearly indicate such a reaction with camphor, other cyclic ketones, acid amides and esters, aldehydes, and nitriles (all predicted and verified from the

<sup>1</sup> *Z. physik. Chem.*, **149**, 371; **151**, 145, 163, 173 (1930).

observation of  $\text{—C=O}$  combination with nitrocellulose chain) as swelling and gelatinizing agents.

2. *Rubber*.—*a*. Unique proof of micellar structure and parallel orientation of long-chain molecules of  $\text{C}_5\text{H}_8$  when stretched (Fig. 231). Unit cell shown in Fig. 232.



(a)

(b)

(c)

FIG. 231.—Diffraction patterns for rubber. (a) Unstretched; (b) stretched crepe or smoked sheet; (c) stretched vulcanized rubber.

*b*. A fundamental mechanism of elasticity based upon the mutual effects of double bonds in the unsaturated hydrocarbon in coiling up springlike molecules.

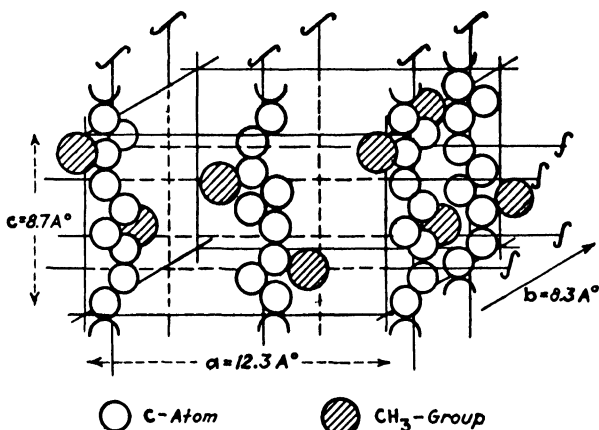


FIG. 232.—Unit crystal cell of stretched rubber.

*c*. A method of racking rubber 10,000 per cent or more, developed largely in the course of x-ray work.

*d*. Discovery that rubber after long standing at cool temperatures “freezes” and produces diffraction interferences for random crystal grains.

e. A "melting curve" for natural rubber determined by von Susich<sup>1</sup> from x-ray patterns. In frozen samples interferences disappear above 35° C., while with increasing degree of stretching the temperatures at which crystalline patterns became amorphous increase up to 90° C. for great elongation.

f. The only exact method of distinguishing natural and synthetic rubbers so far produced, and the criterion of successful synthesis in the future—another indication that the terms rubber, cellulose, etc., imply not only constitution but also spacial structure. Duprene or polymerized chloroprene, obtained by the addition of HCl to vinyl acetylene, is the first synthetic rubber to give a rubber-like fiber pattern upon stretching.<sup>2</sup> That the new product is not identical with natural rubber, however, is shown by a comparison of the *b* spacings (along the ~~free~~ axis) of the stretched specimens:

Rubber. ....	8 39 ± 0 15 A.U.
Chloroprene ..	4 81 ± 0 03
α-Gutta percha. . . . .	8 78 ± 0 12
β-Gutta percha . . . . .	4 87 ± 0 07

g. Sharpening of interferences on vulcanization, indicating sulfur bridge formation between chains though the unit crystal cell is the same; with increasing sulfur content, loss of elasticity as a result of *net* formation of molecules in hard rubber.

h. Cooling of racked rubber with liquid air results in patterns with the appearance of Laue single-crystal diagrams for metals, indicating larger organized lattice units than the usual micelle.

i. Rational explanation of greater tensile strength of stretched samples with greater van der Waals' forces; *e.g.*, unstretched raw rubber (liquid air) 5.4 kg. mm.<sup>2</sup>, stretched 35.1; vulcanized unstretched 5.3, stretched 44.4.

3. *Gutta Percha, Balata, and Chicle*.—There has been a very considerable disagreement concerning the structures of gutta percha and balata which are, like rubber, polymers of isoprene. The discrepancies have at last been explained in the work of Hopff and von Susich<sup>3</sup> and of Stillwell and Clark.<sup>4</sup> These two substances produce diffraction patterns different from rubber,

<sup>1</sup> *Naturwissenschaften*, **44**, 915 (1930).

<sup>2</sup> CAROTHERS, WILLIAMS, COLLINS, and KIRBY, *J. Am. Chem. Soc.*, **53**, 4203 (1931).

<sup>3</sup> *Kautschuk*, **11**, 234 (1930).

<sup>4</sup> *Ind. Eng. Chem.*, **23**, 706 (1931); *Kautschuk*, **5**, 86 (1931)

but probably like each other. There are two modifications, the  $\alpha$  which is stable below 60° C. and  $\beta$  produced by heating above 60° C., giving different patterns in the unstretched as well as the stretched state. Stillwell and Clark have found balata in ordinary commercial form to differ from ordinary gutta percha, in the same way that von Susich's  $\alpha$ -modification differs from  $\beta$ -gutta percha (Fig. 233).

Chicle has been studied by Stillwell and Clark. The hydrocarbon constituent here is identical with gutta percha. The resins, calcium oxalate, and other substances constitute the

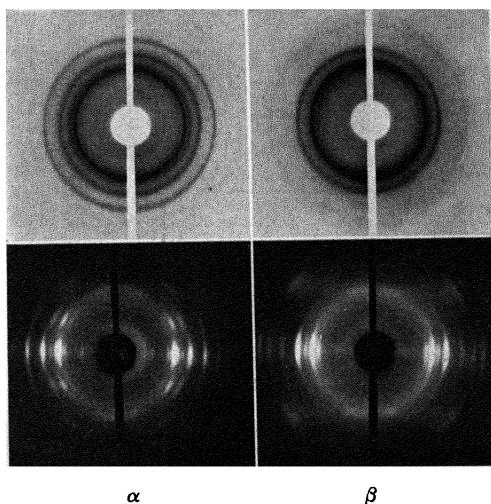


FIG. 233.—Patterns for unstretched and stretched  $\alpha$ -gutta percha (left) and  $\beta$ -gutta percha (right).

remainder of this product. This gutta hydrocarbon may be the explanation of frozen rubber crystals and crystals isolated from rubber by Pummerer and Koch, Bureau of Standards, and others.

Rubber, gutta percha, balata, and chicle all are built from hydrocarbon chains of the same constitution. The difference comes in a *cis* configuration for rubber where the identity period is 8.4 A.U. and a *trans* form in the gutta percha, or zigzag chains with an identity period of 8.8 A.U.

4. *Proteins*.—*a. Silk fibroin*, one of the constituents of natural silk, shows a distinctly crystalline structure (Fig. 234), the analysis of which is given in the table. The chains of amino acid residues are bound in peptide linkage to form long spiral

macromolecules, with four alanyl-glycyl residues per unit cell. The micelles are embedded in a matrix and are perhaps here

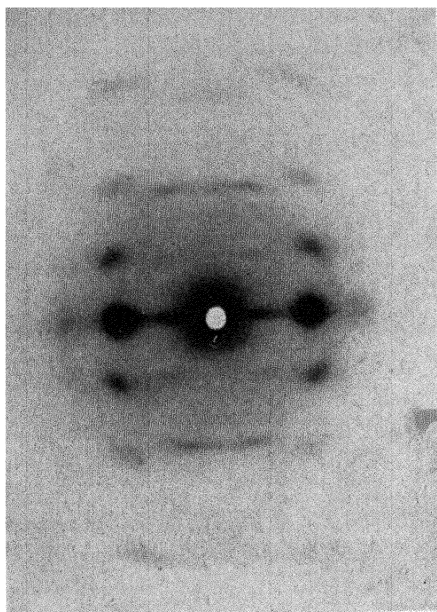


FIG. 234.—Fiber structure of natural silk.

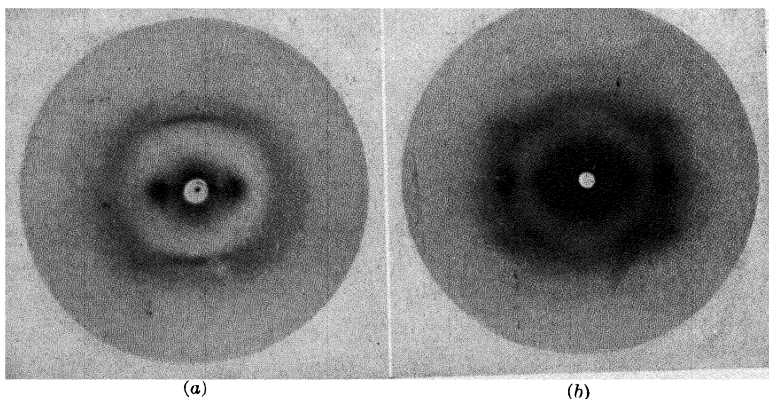


FIG. 235.—Fiber structures of wool and air. (a)  $\alpha$ -form, unstretched; (b)  $\beta$ -form, stretched.

and there chemically bound together. The amorphous part of the silk consists of irregular chains, which may even be bound

into micelles, but without lattice arrangement. Such micelles are termed by Meyer and Mark "mixed micelles" by analogy with "mixed crystals." The great strength of the peptide chains and the bonds holding the micelles together are explained by the high molar cohesion of CONH (10,600), demonstrated by high heat of vaporization, high boiling point, and high dielectric constant. A chain of 100 peptide residues (350 A.U.), as in fibroin, possesses a molar cohesion of over 1,000,000, very nearly the same as in a cellulose chain.

The micelles are resistant like cellulose to swelling media, in the sense of change of lattice dimensions. Swelling is, therefore, intermicellar—a proof that within the micelle no free amide and carboxyl groups exist. Only concentrated acids such as formic and some salt solutions swell the protein to the point of solution. The cobweb spun by the spider gives a pattern practically identical with that of fibroin.

*b. Wool and Hair.*—(1) All untreated wool samples give an x-ray fiber diffraction pattern which is substantially the same for the various varieties of wool as well as for animal hair, human hair, porcupine quills, etc. The most prominent features of this fiber pattern shown in Fig. 235*a* are as follows:

Two sharp spots on either side of the center of the photograph appear on the equator. It is these spots, particularly characteristic of a large interplanar spacing or identity period, which give the marked fiber pattern.

The next most prominent feature is an outer, somewhat diffuse ring which is really a composite of several overlapping reflections. This ring is characterized in most of the wool samples by a sharper arc on the meridian or at the twelve and six o'clock positions. These parts of the pattern are unquestionably due to a crystalline constituent of the wool fiber. There is also present at very small angles, *i.e.*, around the central O spot, a diffuse haze which may be superposed on the sharp spots above noted. This haze is due to the disorganized or non-crystallized material in the fiber. Careful analysis of the best patterns show that there is a spacing of 5.15 A.U. along the axis of the fiber, and dimensions of 27 A.U. and 10.3 A.U. in directions parallel to the fiber axis.

The x-ray pattern is what would be expected from an imperfect crystalline system in which the only sharply defined transition or identity period is that parallel to the fiber axis, suggesting

long, filament-like molecules which cling together sidewise with varying degrees of perfection. The diffuse nature of the pattern, and the possibility of overlapping of several sharp crystalline interferences, prove the existence of very imperfect junctions and mixed crystallization effects. The halo around the center corresponding to disorganized matter is most prominent always in cases where scales are present. This is particularly true in the case of merino wool.

The slight variations in the pattern from one wool to another are concerned with the prominence of this halo, the sharpness of the inner spots, the diffuseness of the outer ring, and the definition of the meridian arc on this ring. These latter properties determine how perfectly lined up the crystalline protein units are with respect to the axis of the fiber. In general the fibers with highest tensile strength and straightest properties are characterized by the highest degree of parallel arrangement.

(2) *Effect of Tension.*—The change in the x-ray diffraction pattern when the wool fibers are stretched 30 per cent or more has been noted independently by Astbury and Street and in the writer's laboratory. The diffraction pattern changes in appearance and measurement show that the dimensions also change (Fig. 235b). A sharp arc noted on the meridian for the unstretched or alpha wool disappears and new strong spots appear on the equator of the outer ring. The spacing for this stretched or beta wool along the axis of the fiber is 6.64 A.U., an increase of 29 per cent over that for unstretched wool. Two other dimensions at right angles are 9.3 and 9.8 A.U.

It has been possible to assure this change more readily for samples stretched wet. It has been impossible to stretch dry wool much beyond 30 per cent without rupture. The definite change, of course, means an actual change in the molecules aligned parallel with the axis of the fiber of which these smaller dimensions represent some repetitional part (Fig. 236). The complete passage from the alpha to the beta form must take place in three stages in view of the fact that wool in cold water may be stretched twice as far and in steam three times as far as perfectly dry wool. The percentage elongation required to bring out the beta pattern varies from one kind of wool to another within a small range and the fact that some of the alpha form remains while the beta form is developing makes it difficult to classify wool on this basis.



Stretching in cold water is reversible under ideal conditions, although in steam a permanent set is obtained upon stretching, this being in accordance with the 29 per cent extension of the change above noted. With constant length maintained stretched wool gradually loses tension and its original power of recovery of its original length is removed. X-ray photographs support

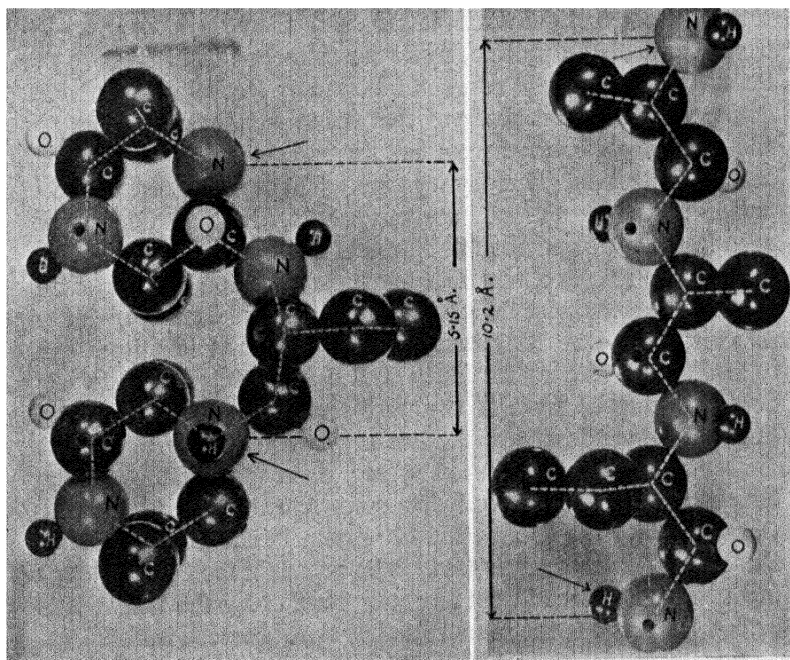


FIG. 236.—Molecular models for fibrous proteins. Left, unstretched or  $\alpha$ -wool; right, stretched or  $\beta$ -wool. (Astbury.)

the idea that in order to repeat a load extension curve up to 30 per cent it is necessary to stretch the fiber quickly and to allow it to rest unstretched in water between successive extensions. This rest period is highly necessary in order that there may be a reversion from the beta to the alpha form. If the loading curve is slow, greater extensions are obtained than with rapid loading. It follows, of course, that the properties of wool in the beta form, however produced and especially if a permanent set has been obtained, must be vastly different from the alpha wool and must be associated with a loss in resilience. Astbury expresses the opinion

that this transformation is the explanation of the "permanent wave."

(3) *Effect of Reagents.*—The alkali sulfides are among the most powerful solvents of wool and it has been established for some time that the change is accompanied by both free  $\text{—S—S—}$  and free  $\text{—SH}$  linkages. The exact nature of the reaction is not known. Stretched wool is far more susceptible to sulfide than unstretched. In the latter case there is a continuous destruction of the protein, while for stretched wool there is an immediate non-solvent reaction followed by a continuous solvent action. Astbury has observed that the most intense x-ray reflection given by stretched wool has the same spacing as the most intense reflection given by cystine. This spacing is at right angles to the sheath axis and may be the half length of the cystine molecule and the full length of the cysteine molecule.

The scale sheath of the fiber remains unaffected by all sodium or potassium sulfides but a very considerable swelling takes place in the cortex, such that the scale sheath is split from end to end. The fact seems fairly well substantiated that in the beta or stretched form of the wool there are molecular chains linked side by side with molecules of cystine or cysteine. These molecular chains are ruptured by treatment with sulfide and the beta structure relieved of tension reverts to the alpha structure. On account of the destruction of protein in the fiber, however, the original orientation is lost. The principal molecular grouping in the unstretched wool repeating itself along the fiber axis is 5.15 A.U., which is the same period as that observed in cellulose.

This seems to suggest that in wool there are long filament-like molecules which are built up by continuous repetition of hexagonal ring systems connected by bridge atoms. Other relationships are also observed which confirm this general idea. A chain of 100 amino acid residues in a protein would possess a length of 350 A.U. and have a molar cohesion of over 1,000,000, a value very similar to that of a cellulose chain.

*c. Tendons, Collagen, Gelatin, and Tissues.*—The protein materials in natural fibrous form also produce fiber diffraction patterns. Stretched gelatin films approach the same structure, though never so perfectly crystalline, evidently because the ends of the micelles are ragged. The identity period for tendon is 8.4 A.U. (Fig. 237), distinctly different from the value 7.0 in silk. A different arrangement of the chains is indicated, as is

found for rubber and gutta percha. All properties indicate that a tendon is constructed similarly to racked rubber; heating causes contraction and disappearance of the fiber patterns. Hence here again are long-chain molecules in parallel orientation in bundles, a structure further verified by lengthwise splitting when frozen in liquid air.

Strength is obtained by such structure as shown by the fact that fresh tendon had a tensile strength of 11 kg./mm.<sup>2</sup>; after contraction at 80° C., 3.0 kg./mm.<sup>2</sup>; and after stretching back to the original length 10.6.

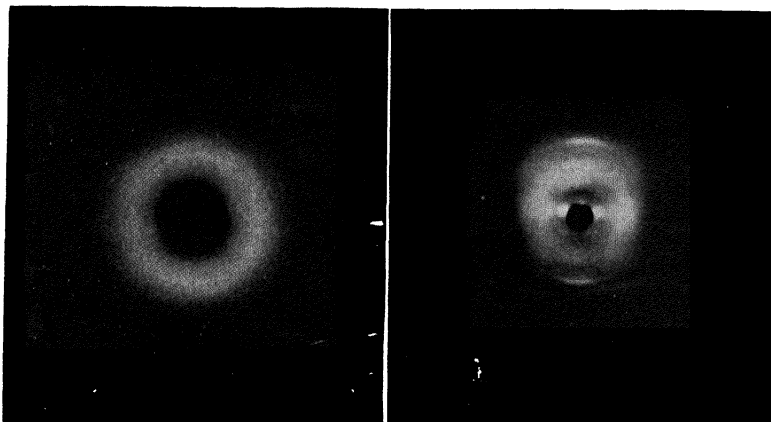


FIG. 237.—Typical diffraction patterns for human tendon. Left, unstretched; right, stretched, showing effect of tension in pulling long protein molecules into parallel orientation.

Botanical tissues are webs spun from long primary valence carbohydrate chains, held by molecular cohesion of unsolvated groups or by chemical bridges. The chains may carry solvated shells on the polar or ionizable groups to account for the familiar freshness. Similarly, animal tissues are webs of protein chains forming cell walls and accounting for combination with water. The most important difference between tissues, animal and plant, lies in the comparative non-elasticity of carbohydrate chains as compared with the pliable protein chain. Seifriz has stated positively, as a result of the study of elasticity, that the last molecular entity of a living substance must possess an elongated form. Fibrous tissues, such as muscles and tendons, have principal valence chains parallel to the fiber axes. Tissue sheets, such as the fascia, have the chains in one plane.

The presence of distinctive larger, regularly arranged bundles of these long chains as micelles seems clearly proved in cellulose, stretched rubber, silk fibroin, etc. In other cases as in unstretched rubber and in tissues, the matter is not altogether settled. Studies of birefringence, of course, prove parallel orientation and these larger complexes can be demonstrated if the dependence of birefringence on imbibition of liquids with different indices of refraction shows a distinct minimum. The separation of birefringence due to the form of rodlike particles, as distinguished from that of single parallel long molecules (or characteristic birefringence), has actually been accomplished. It is not essential to give the name of *crystalline* to these conceptions of oriented long chains which actually diffract x-rays. A much higher degree of arrangement is implied by the term crystalline, since these long molecular chains still possess a rotational degree of freedom and hence are mesocrystalline or mesomorphic. For the first time, however, it is possible to attack the complex problems of chemical structures of chains, their positions in organs, the changes of their forms and position, the relation to each other and to the tissue fluidity. These have already been solved for the simpler fiber sections.

One problem to account for is the fact that many tissues which are insoluble in water still yield considerable quantities of protein to the solvent—a fact which demonstrates that the protein could not have been bound in a chemical network.

Przibram<sup>1</sup> has lately demonstrated by biological methods that the chromatin threads and even genes can be measured in length as  $10^{-4}$  to  $10^{-5}$ . The protein molecule is only one power of ten under the size of these powerful biological units.

Coming then to the behavior of living tissues, it has been demonstrated from mechanical and x-ray investigations that in the extended muscle the principal valence chains are in parallel orientation; in the contracted muscle, not. A muscle stretched and dried produces a fiber diffraction pattern, while a dried contracted muscle is amorphous, in keeping with the fact that the stretched muscle frozen with liquid air splits into shreds parallel with the fiber axis, while the contracted frozen muscle breaks into small clumps. Von Hürthle<sup>2</sup> has shown that the birefringent

<sup>1</sup> PRZIBRAM, p. 238, "Der Aufbau der Hochpolymeren Organischen Naturstoffe," Leipzig.

<sup>2</sup> VON HÜRTHLE, p. 239, "Der Aufbau der Hochpolymeren Organischen Naturstoffe," Leipzig.

part of the muscle fibrils is the actual contractile substance. This birefringence decreases with contraction; consequently the chains in the contracting fibril lose their parallel orientation. Until recently it has been impossible to prove whether or not this mechanism is operative in truly living muscle. Experiments by Boehm and Schotzky<sup>1</sup> and by Clark and Corrigan,<sup>2</sup> utilizing the new high-powered x-ray tubes which permit very rapid exposures, have thrown clear light upon this uncertainty. Diffraction patterns of living, electrically contracted frog muscle (excited by an applied voltage to tetanus contractions), have previously been procurable at a great sacrifice. As each muscle after killing the frog remains sufficiently fresh for only  $1\frac{1}{2}$  min. in the path of an intense x-ray beam, several hundred muscles have been necessary. Diffraction patterns may now be obtained in 2 min. with only six muscles. With the exception that the diffraction ring for water is present, the patterns are the same as for dried muscle. Contracted living muscles show a great decrease in fibering as compared with the muscle at rest (Fig. 238).

A plausible mechanism for muscular action can be deduced in terms of inner molecular forces.<sup>3</sup> Rubber contracts because of double bonds in the long hydrocarbon chains which cause a spring-like coiling. In muscle protein there are many free basic and acid groups in the chains, since glutaminic acid and arginine and lysine may be derived. At the isoelectric point  $\text{COO}^-$  and  $\text{NH}_3^+$  ions may attract and pull the chain into a close spiral.

In acid or alkaline media, however,  $\text{COO}^-$  or  $\text{NH}_3^+$  ions repel each other and straighten out the chain. In confirmation of different chain configurations, casein and hemoglobin form the

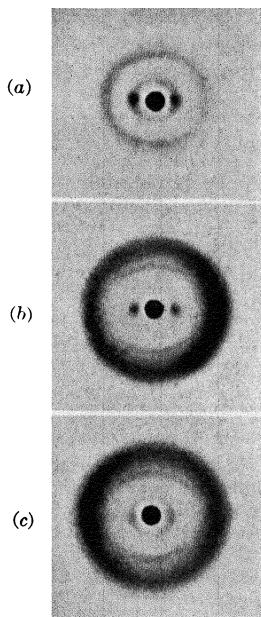


FIG. 238.—Diffraction patterns for frog muscles. (a) Dried muscle; (b) living muscle at rest; (c) living muscle excited to tetanus contraction. (Boehm and Schotzky.)

<sup>1</sup> *Naturwissenschaften*, **18**, 282 (1930).

<sup>2</sup> CLARK and CORRIGAN, *Ind. Eng. Chem.*, **23** (1931).

<sup>3</sup> MEYER and MARK, *loc. cit.*, p. 238.

homogeneous layers in acid or alkaline aqueous solutions 7 or 8 A.U. thick, while globules form only on a neutral surface.

Hence contraction or expansion resides in the ultimate long-chain molecule. Since these are bound together by molecular cohesion or bridges throughout the whole length of the muscle, an inner molecular change with changing pH value produces a contraction or expansion on the macroscopic scale. The physiological and chemical changes relating to production and destruction of acid in the muscle, therefore, lead to direct action on the

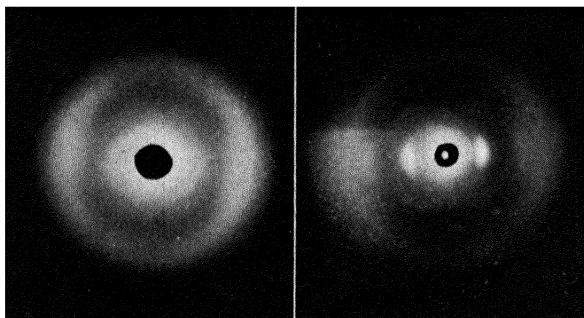


FIG. 239.—Patterns for two specimens of surgical catgut (sheep intestines) ligatures, showing difference in fibering and tensile properties (right, greatly superior).

protein chains and account for the mechanical work. The important conception of change in form of the protein chain as a function of the medium may, therefore, be extended to the behavior of protoplasm and to many physiological problems.

The foregoing account of the new knowledge of natural colloidal protein materials is sufficient to indicate the practical value of such methods of study. The changes in tissues shown by x-ray diffraction throw great light not only on physiological processes but also on pathological developments. A detailed paper from the writers' laboratory shows how cancerous tissue (uterus, breast, bones, etc.) produces characteristically different effects from the normal specimens, which may result in valuable diagnostic progress.<sup>1</sup> A technological application is in the production of improved surgical catgut for ligatures and sutures. Here the process of swelling and tension, referred to so frequently, is highly effective in improving micellar orientation followed

<sup>1</sup> CLARK, BUCHER, and LORENZ, *Radiology*, **17**, 482 (1931).

by the x-ray patterns (Fig. 239), and tensile strength. The dispersion and respinning both of silk and of animal tissues are an accomplished procedure, and any desired properties can be obtained in terms of regulation of the variables. In other words, catgut of an inferior quality can be vastly improved by these steps, just as cotton or rayon can be structurally changed and improved by swelling or dispersion and tension.





## INDEX

### A

Absorption, 91  
     coefficients, 91  
     edges, 66  
     mechanism of, 95  
     practical applications of, 106  
     spectra, 56  
 Acceleration law in Bohr theory, 72  
 Acids, aliphatic, 326  
     dicarboxylic, 329  
 Age-hardening, 302  
 Aircraft parts, testing of, 123  
 Aliphatic chains, 316  
 Allotropic modifications, 152  
 Alloy steels, 303  
 Alloys, 279  
     analogies from, 292  
     classification of systems, 283, 294  
     compound formation in, 280  
     eutectics, 280  
     interstitial arrangement in, 280  
     iron, 295  
     substitutional arrangement in, 279  
     superstructure, 281  
 Aluminum, deformation structures  
     of, 358, 361, 380  
     recrystallization of, 390  
 Amorphous matter, 426  
 Amphiboles, structure of, 274  
 Analysis, chemical, by x-rays, 82,  
     332  
 Annealing, of cast steel, 400  
     effect of carbon content on, 416  
     temperature of, 418  
 Anthracene, crystal structure of, 309  
 Aromatic compounds, 310  
 Asbestos, 254  
 Asterism, 353  
 Atomic radii, 234, 265

Atomic structure, Bohr theory of, 71  
     from intensities of scattering by  
         gases, 100  
         modern theory of, 79  
 Atoms, arrangement of, 211  
     sizes and shapes of, 265  
 Austenite, 297  
 Autoelectronic effect, 23  
 Automotive parts, testing of, 123

### B

Back-reflection diffraction method,  
     421  
 Bacteria, effect of x-rays on, 154  
 Bakelite, structure of, 438  
 Balata, 450  
 Balmer series, 68, 72  
 Barium carbide, 253  
 Battery, high-voltage storage, 40  
 Benzene ring, 309  
 $\beta$ -iron, 299  
 $\beta$ -rays, 98  
 Biological effects of x-rays, 140, 153  
 Bohr orbit, 259  
 Bohr theory, 71, 80  
 Bone, structure and constitution of,  
     255  
 Bragg and Peirce, law of, 93  
 Bragg diffraction law, 180  
 Bragg spectrometer method, 190  
 Bragg spectrum, 222  
 Brass, structures of, 282  
 Bucky diaphragm, 112  
 Bunsen law, 143

### C

Calcite, as standard crystal grating,  
     50  
 Camera, Seemann-Bohlin, 203, 285

- Cancer, 153, 154, 158, 159  
Carbon, crystalline structures of, 307  
Carbon blacks, 344, 428, 430  
Cast steel, 400  
Castings, growth texture of, 387  
    radiographic examination of, 119  
Catalysts, 150, 343  
Catgut, surgical, 460  
Cellophane, 446  
Celluloid, 448  
Cellulose, 444  
Cellulose esters, 448  
Cement, 256  
Cementite, 298  
Ceramic materials, 257  
Chemical analysis by x-rays, 139, 144  
Chemical effects of x-rays, 139, 144  
Chemical reaction mechanism, 142  
Chiele, 450  
Circuits for x-ray machines, 44  
Coal, radiography of, 125  
    structure of, 431  
Cold-rolling, effect on texture of metals, 358, 371, 405  
    effects of variables in, 403  
    stages in reduction by, 403  
Collagen, 456  
Colloidal metals, 429  
Colloidal particles, shape of, 344  
    size of, 336, 441  
Colloids, diffraction by, 427  
    flocculation of, 149  
    nature of, 431  
Coloration by x-rays of glass and minerals, 151  
Combination principle, 70, 78  
Complex formation, 252  
Compounds, of carbon, 246  
    inorganic, 231  
    long-chain, 319  
    organic, 246  
    results of analysis of inorganic, 245  
    of organic, 314  
Compton effect, 96, 131, 132, 134, 162  
Conductivity, effects of x-rays on, 134  
Coolidge tube, 18, 25, 32, 104  
    for quantitative analysis, 88  
Cooling, 19  
Coordination, 264  
Copper, forming, 410  
    recrystallization of, 394  
    wire structure, 367  
Corrosion of alloys, 304  
Cotton, 446  
Counterfeit coins, 107  
Crystal analysis, Bragg method of, 188-190  
    Hull-Debye-Scherrer, 188, 189, 199  
    Laue, 185, 188, 189  
    monochromatic pinhole, 188, 189  
    powder method of, 188-190  
    rotation method of, 188, 189, 195  
    Schiebold-Polanyi, 188, 189, 195  
Crystallography, fundamentals of, 172  
Crystals, classification of, 260, 262  
    spectra from, 49  
    submicroscopic, 336  
    types of, 259  
    and x-ray diffraction, 171, 180  
Cybotaxis, 433
- D
- Debye factor, 215  
Debye-Scherrer method, 201  
    rings, 236  
Deformation, effect of grain size on, 418  
Deformation structures, in drawn wires, 370  
Diamond, 307  
Diffraction, by amorphous substances, 426  
    apparatus, 185  
    by colloids, 427  
    by crystalline substances, 426  
    of electrons, 7  
    by fibers, 357  
    of hydrogen atoms, 7  
    interferences, 208  
    by liquids, 432  
    methods, 188

Diffraction, patterns, 208, 335  
  by powders, 199  
  tubes for, 31  
  of x-rays by crystals, 4  
Diopside, 274  
Diphenyl, 310, 313  
Dosage, measurement of, 160  
Doublets, 70  
Duane and Hunt, law of, 53, 54  
Duane ionization chamber, 164  
Duprene, 450  
Durain, 431  
Dyeing of textiles, 430

## E

Eder's solution, 165  
Effective wave length, 104  
Einstein equivalence law, 147  
Electric steel, 400  
Electrical conductivity, 134  
Electrical precautions, 47  
Electrodeposition of metals, 385  
Electromagnetic waves, 4, 6  
Electrons, back diffusion of, 23  
  dual nature of, 7, 79  
  in x-ray tube, 78  
Elements, crystalline structures of,  
  231  
  discovery of, 69  
Emulsions, diffraction by, 435  
Enamels, 257  
Energy-level diagram, 76  
Erythema, 38, 166  
Esters, 330  
Exposure charts, 113  
Extinction, 216

## F

F curves and values, 214, 311  
Fatigue of metals, 420  
Ferrite, 299  
Fiber diagrams, 357  
  for drawn wires, 359  
  for rolled sheets, 371  
Fiber structure, 365  
Fibers, orientation in, 375  
Filament, line focus, 28  
  spiral, 18

Films, formation of, 331  
  metal, 387  
Filters, 67  
Filtration, 101  
Fluorescence, 136, 138  
Fluorescent characteristic x-rays,  
  95  
Fluorescent screen, 36  
Fluoroscopy, 112  
Focal spot, 19  
Foils, rolled, 379  
  heat treatment of, 389  
Formaldehyde, polymerized, 438  
Fourier series analysis of structure  
  factor, 216  
Frequency law in Bohr theory, 73

## G

Gage, uniformity of, 106  
 $\gamma$ -rays, 6, 129  
Gases, scattering by, 100  
Gelatin, 456  
Gems, 256  
Genetics, and x-rays, 154  
Glass, coloration of, 151  
  structure of, 344, 429  
Goldschmidt law for ionic crystals,  
  268  
Gnomonic projections, 220  
Grains, orientation of, 351  
  size of, 336, 346  
Graphite, 308  
Gratings, 49, 50  
Gutta percha, 450

## H

Hafnium, 69  
Hair, 453  
Hardness, of alloys, 300  
  of crystals, 272  
  of x-rays, 14  
Heat treatment, x-ray analysis of,  
  389  
Heteropolar combination, 262  
Heusler alloys, 304  
Hexamethylbenzene, 311  
Hexamethylenetetramine, 317  
Homopolar combination, 263

Hydrates, identification of, 253  
 Hydrogen atom, diffraction of, 7  
 Hydrogen peroxide, decomposition of, 142

## I

Illinium, 69  
 Indices of lattice planes, 173  
 Industrial diagnosis, 111  
 Inhomogeneity, examination for, 107  
 Inorganic compounds, structures of, 245  
 Insulin, 442  
 Intensifying screens, 116, 138  
 Intensity, measurement of, 160  
     biological method, 166  
     chemical method, 165  
     coloration method, 166  
     fluorescent method, 166  
     heat method, 160  
     ionization method, 161  
     photographic method, 165  
     selenium-cell method, 166  
 Interfaces, molecular orientation at, 332  
 Interplanar spacings, calculation of, 209  
 Ion radii, 265  
 Ionic combination, 262  
 Ionic crystals, law of formation, 268  
 Ionization by x-rays, 131, 161  
 Ionization chambers, 164, 167, 190  
 Ions, sizes and shapes, 265  
 Iron, polymorphism of, 238  
     reclaimed malleable, 413  
     recrystallization of, 394  
     systematization of alloys of, 295  
     white-fractured, 413  
 Isomerism, 331  
 Isomorphism, 271

## J

Jewel bearings, orientation of, 352

## K

K series, 56, 59  
 Kenotron, 42  
 Ketones, 330

## L

L series, 56, 62  
 Lattices, crystal, 52  
     layer, 271  
     space, 176  
 Layer lines, 224  
 Laue method, 185  
 Laue patterns, 138  
     gnomonic projection of, 220  
     interpretation of, 218  
     stereographic projection of, 219  
 Laue spots, 336  
 Lead, colloidal, 429  
     as protection against x-rays, 104  
 Liquid crystals, 436  
 Liquids, diffraction by, 432  
     effect of magnetic fields on, 437  
 Lime, plasticity of, 257  
 Lindemann glass, 34  
 Lorentz factor, 216  
 Lubrication, 332  
 Luminescence, excitation of, 136  
 Lyman series, 68, 72

## M

M series, 63  
 Magnesium, plastic deformation of, 380  
 Magnetic field, molecular orientation in, 437  
 Magnetism, crystal structure and, 304  
 Martensite, 299  
 Masurium, 69  
 Medical diagnosis, 108  
 Mesomorphic states, 428  
 Metal castings, radiographic diagnosis of, 108  
 Metal radiography, 119  
     applications of, 124  
     tubes for, 26  
 Metallic combination, 264, 276, 277  
 Metallurgy, applications of x-rays in, 388  
 Metals, cold working of, 389  
     colloidal, 429  
     control of heat treatment of, 389

Metals, deposition from solution, 387  
  electrodeposited, 385  
  fatigue of, 420  
  passive, 410  
  structure and properties of, 275  
Metastability, effect of x-rays upon, 152  
Methane derivatives, 315, 316  
Mica, 275  
Micelles, 444  
Microphotometer, 116  
Microscope, ultraviolet, 5  
Miller indices, 173  
Mineralogy, applications in, 254  
Minerals, coloration of, by x-rays, 151  
Mixtures, determination of composition, 106  
Molecular form, 330  
Molecular orientation, 332  
Molecular weight, 331  
Molecules, arrangement of, 211  
Momentum law in Bohr theory, 72  
Monochromatic pinhole method, 228  
Monochromatic x-rays, 66  
Morphotropism, 271  
Moseley law, 67, 69, 78  
Multiple-diffraction apparatus, 207  
Muscle, 459

## N

N series, 63  
Naphthalene, crystal structure of, 309, 313  
Nematic state, 428  
Neumann bands in ferrite, 410

## O

Orbits, electron, 73  
Organic compounds, crystal analysis of, 314  
  highly polymerized, 438  
  substituted radicals in, 314  
Orientation, of fibers, 375  
  of grains, 351  
  molecular, 332  
  preferred, in sheets, 379, 385

Orientation, surface film, 332, 437  
Oscillation patterns, 222

## P

Paintings, radiographic examination of, 127  
Paracrystalline state, 428  
Paraffin hydrocarbons, 37, 321  
Paraffin wax, 324  
Particle size, in colloids, 336, 441  
  in microscopic range, 346  
Paschen series, 72  
Pearlite, 298  
Pearls, 256  
Penetrometer, Benoist, 103  
Pentaerythritol, 315  
Permutites, 255  
Phosphate rock, 255  
Photochemistry, 140  
Photographic effect of x-rays, 143  
Photolysis of  $\text{KNO}_3$ , 147  
Photon, 7  
Physical effects of x-rays, 131  
Pigments, 429  
Planck action constant, 7, 73  
Planck-Einstein quantum equation, 53  
Plating, gold, 420  
Point groups, 179  
Polarization, 263  
Polymerized materials, 438  
  results of x-ray investigations on, 444  
Polymorphism, 271, 327, 331  
Porosity, 107  
Potassium nitrate, photolysis of, 147  
Potassium persulfate, decomposition of, 142  
Potentials, critical excitation, 76  
Powder spectra, interpretation of, 226  
Powders, diffraction by, 199  
Properties, prediction of, 272  
  of x-rays, 10  
Protection from x-rays, 104  
Proteins, 451  
  effect of reagents on, 456  
  of tension on, 454  
Purple of Cassius, 253

## Q

Qualitative analysis, 86  
 Quality, measurement of, 103  
 Quantitative analysis, 86  
 Quantum theory, 7, 79

## R

$r$  unit, 163  
 Radii, atomic, 234  
   ionic, 266  
 Radiography, 108  
   applications of, 125  
   cost of, 128  
   industrial diagnosis by, 111  
   medical diagnosis by, 108  
   tubes for, 26  
   use of x-rays in, 129  
 Railroad equipment for x-ray testing, 122  
 Rails, diffraction research on, 421  
 Rayon, 445  
 Rays,  $\beta$ , 98  
   cathode, 3, 9  
   cosmic, 4, 6  
   electric, 6  
    $\gamma$ , 6, 129  
   grenz, 38  
   Hertzian, 6  
   radio, 6  
   Roentgen, 3  
   ultraviolet, 6  
   visible, 6  
 Reactions, chemical, 38, 253, 332  
 Recrystallization, of aluminum sheet, 390  
   change of temperature of, with impurities, 392  
   of copper, 394  
   of iron, 394  
   of silver, 390  
   of silver-copper alloy, 395  
   of wires, 397  
 Rectifiers, 41, 42, 43  
 Refractories, 257  
 Regulator, gas pressure for gas tubes, 17  
 Resistor ribbon, 413

Rhenium, 69  
 Richardson equation, 19  
 Roentgen rays, 3  
 Rolling, effect on texture, 403  
 Rotation method, 195  
 Rotation pattern, 222  
 Rubber, 449  
 Rydberg constant, 68, 70, 75

## S

Scattering of x-rays, 91  
 Shock-proof equipment, 48  
 Silicates, structure of, 273  
 Silk fibroin, 451  
 Silver, recrystallization of, 390  
 Silver-copper alloy, recrystallization of, 395  
 Smectic state, 428  
 Soaps, 330  
 Solid solution, 289  
 Solid state of matter, 171  
 Solutions, colloidal, 431  
 Sorbite, 298  
 Space groups, 179  
 Space lattices, 176  
 Spacings, calculation of, 209  
 Spectra, absorption, 56, 57  
   chemical analysis from, 82  
   continuous, 52  
   crystals for, 49, 50  
   emission, 55, 57, 59  
     K series, 59  
     L series, 62  
     M and N series, 63  
   powder, 226  
   ruled grating, 51  
 Spectrograph, 82  
   Seemann, 84  
   Siegbahn, 87  
   slitless, 197  
   wedge, 197  
 Spectrometer, double, 66  
   ionization, 190  
 Spectroscopy, of soft x-rays, 332  
 Spinels, 254  
 Starch, 432  
 Steel, 296  
   alloy, 303

- Steel, bending of, 413  
  forming of, 410  
  quench structure of, 420  
  rolled, 373  
  silicon, 400  
  temper structure of, 420  
  twisting of, 413
- Stereographic projection, 219
- Storage battery, high voltage, 40  
  structure of plates of, 253
- Strain internal, 352
- Structural formula, testing of, 331
- Structure factor, 100, 211
- Sugar crystal, change of, with heat,  
  37
- Sugars, 318
- Sulfur, conductivity of, 134
- Sulfur trioxide, transformations of,  
  152
- Superstructure alloys, 281
- Surfaces, molecular orientation at,  
  332, 437
- Symmetry, elements of, 100, 211
- T
- Tangent drop method, 320
- Tannin, 432
- Targets, cone, 29  
  magnesium, 38
- Tartaric acids, 317
- Tendons, 456
- Textiles, 444, 451, 453
- Therapy, deep, 157  
  superficial, 38
- Thickness, determination of, 106
- Thiourea, 316
- Tin, single crystal of, 175
- Tissues, 38, 456, 459  
  effect of x-rays on, 155
- Tolerance dose, 105
- Transformers, 41
- Troostite, 298
- Tubes, autofocus, 29  
  Coolidge, 18, 32, 111, 204  
  cross-focus, 33  
  demountable, 34  
  diagnostic, 26  
  diffraction, 31
- Tubes, deep therapy, 20  
  dofok, 27  
  electron, 12, 18  
  gas, 12  
  Hadding-Siegbahn, 14  
  helium filled, 30  
  high intensity, 35  
  ion, 12  
  Lange and Braseh, 25, 53  
  Lauritsen, 25  
  Leiss, 15  
  life of, 21, 23  
  line filament, 28, 33  
  long wave, 38  
  manufacturers of, 13, 20  
  metal radiographic, 26  
  Metalix, 22, 29, 42, 111, 204  
  Müller, 21, 30, 33  
  neon filled, 30  
  Ott-Selmayr, 34  
  Philips, 21  
  rotating anode, 29  
  self-shielding, 29  
  Seemann, 15, 36  
  Shearer, 16  
  Siemens-Pantix, 24  
  special, for very high voltages, 23  
  Tuve, 25  
  Westinghouse gun-type, 31  
  Wyckoff-Lagsdin, 16  
  XP, 29, 30
- Tungsten, contact points, 429  
  filaments, 19
- U
- Ultramarines, 255
- Urea, 316
- V
- Vacuum, Coolidge, 18
- Valence, and x-ray spectra, 64
- Valence electrons in alloys, 292, 294
- Valence forces, 264
- Vegard law of additivity, 280
- Vitrain, 431
- Voltage, measurement of, 46

## W

- Water, association of, 436
  - diffraction by, 436
- Wave lengths, measurements of, 58, 63
- Weissenberg goniometer, 198, 225
- Welds, soundness of, 122
  - structure of, 408
- Wires, deformation structures in, 370
  - effect of constitution on behavior of, 413
  - fiber structure in, 365
  - recrystallization of, 397
  - zonal structure of, 367
- Wood, 446
- Wool, 37, 453

## X

- X-rays, biological effects of, 153
  - chemical effects of, 139
  - effect on tissues, 155
  - generation of, 10
  - and genetics, 154
  - ionization by, 131
  - monochromatic, 66
  - photographic effect of, 143
  - physical effects of, 131
  - properties of, 3, 10
  - protection from, 104
- X-unit, 6

## Z

- Zeolites, 255
- Zinc, plastic deformation of, 380
- Zonal structure in wires, 367







